

g-R.R.R.



THE FRANKLIN INSTITUTE  
RESEARCH LABORATORIES  
Philadelphia, Penna. 19103



58ED-67

AD720454

**PROCEEDINGS**  
of the  
**FIFTH SYMPOSIUM ON**  
**ELECTROEXPLOSIVE DEVICES**

D D C  
RECEIVED  
MAR 25 1971  
A

Held at  
**THE FRANKLIN INSTITUTE**  
**JUNE 13-14, 1967**

Best Available Copy

Unclassified

DISTRIBUTION STATEMENT A  
Approved for public release;  
Distribution Unlimited

Reproduced by  
**NATIONAL TECHNICAL**  
**INFORMATION SERVICE**  
Springfield, Va. 22151

875

[REDACTED]



THE FRANKLIN INSTITUTE  
RESEARCH LABORATORIES

THE BENJAMIN FRANKLIN PARKWAY • PHILADELPHIA, PENNSYLVANIA 19103 • TELEPHONE (215) 448-1000

APPLIED PHYSICS LABORATORY

March 17, 1971

Mr. M. B. Kahn  
Chief, Accessions Division  
Defense Documentation Center  
Cameron Station  
Alexandria, Virginia 22314

[REDACTED]

RE: DDC-TC

Dear Mr. Kahn:

As we agreed in our telephone conversation and you confirmed in your letter of March 5, 1971, I enclose three reports for processing by Defense Documentation Center as follows:

1. A copy of the Proceedings of the Fifth Symposium on Electroexplosive Devices, June 13-14, 1967. This is our last remaining copy. You may accession this and offer it for sale by NTIS without limitation.

Proceedings of the Sixth Symposium on Electroexplosive Devices, July 10, 1967. This copy is intended for announcement purposes only. The volume is available for sale by The Franklin Institute Research Laboratories, Philadelphia, Pennsylvania 19103 at \$100 per copy.

3. About 50 copies of the confidential volume of the proceedings of the Sixth Symposium on Electroexplosive Devices. (The number of copies depends upon how many conveniently fit into the box; the exact number is specified on the receipt.) These copies are for your accession. Distribution is limited by confidentiality and need-to-know. Foreign distribution is not authorized. Please note that the classified proceedings are a price of \$100 printed on the cover thereof, if you wish, or to donate this amount.

I also enclose DDC Form 50. I believe this takes care of all of the items we discussed. Please let me know if I can do anything further.

Sincerely yours,

*Gunther Cohn*  
Gunther Cohn  
Senior Staff Engineer

FORWARDED TO THE DIRECTOR OF THE DEFENSE DOCUMENTATION CENTER

This material contains information affecting the national defense of the United States within the meaning of the espionage laws, Title 18, U.S.C. Secs. 793 and 794, the transmission or revelation of which in any manner to an unauthorized person is prohibited by law.

GC:psg  
Enclosures

Best Available Copy

[REDACTED]



THE FRANKLIN INSTITUTE  
RESEARCH LABORATORIES  
Philadelphia, Penna. 19103

5RED-87

**PROCEEDINGS**  
of the  
**FIFTH SYMPOSIUM ON**  
**ELECTROEXPLOSIVE DEVICES**

*Held at*  
**THE FRANKLIN INSTITUTE**  
**JUNE 13-14, 1967**

Unclassified

Best Available Copy



## PREFACE

In 1967 the 5th Symposium on EED's was attended by 305 people from 28 government agencies and 74 industrial organizations; 78 were government employees including Canadian and British. This year for the first time, the meeting was self-sponsored and supported through registration fees and was unclassified. As usual, Army, Navy, Air Force, NASA, AEC, and the aerospace industry in general were well represented. It appears that the purpose of the meeting, to exchange information and stimulate new ideas among developers, manufacturers and users of EED's, was successfully accomplished.

Thirty-three papers were presented in the two-day meeting. These Proceedings contain a total of 44 papers including a number that were presented "by title only." With few exceptions, the papers contained herein were not solicited but were volunteered by the industry in response to the call for papers issued in February. We feel therefore that these Proceedings represent the state of the art in 1967.

Information about Proceedings of the previous meetings as well as additional sources of information are given in paper 4-4P, "Information Sources for EED's."

### Questionnaire

Attendees at the 5th Symposium on EED's were asked to complete a questionnaire which appears on the next page, filled in with a summary of the responses. Apparently the EED industry wants meetings of this type every other year alternating between Philadelphia and the West Coast. The Franklin Institute Research Laboratories will be pleased to continue to manage these meetings. The majority of the respondees prefer self-supporting (registration fee) meetings and we are happy to report that this appears to be entirely feasible.

### Newsletter

The questionnaire results indicate that the majority are in favor of a newsletter for the EED industry. Subscription orders were distributed at the meeting and a great number have been returned. The Franklin Institute Research Laboratories plan to go ahead with publication of the newsletter and will appreciate newsworthy items and articles on explosives technology and devices including such associated topics as design, safety, circuitry, packaging, specifications, quality assurance, testing, instrumentation, hazards and so on. We also will be happy to

## SUMMARY OF RESULTS

## QUESTIONNAIRE

5th EED SYMPOSIUM

This seems like a wonderful opportunity to find out how the EED industry and technology feels about certain questions of common interest. Will you please take a few moments to consider and answer the following questions? Thank you. You will receive a summary of the results with your copy of the proceedings.

1. How often should EED Symposium be held?

Every year 54 2 years 94 3 years 30

Comments 1 1/2 years 2 4 years 1

2. Do you think the EED industry needs a

Newsletter 96 Magazine 54 Info Center 63?

Comment \_\_\_\_\_

3. How should future EED Symposia be supported?

Single Sponsoring Agency 18

Several Sponsoring Agencies acting jointly 69

Self Supporting (Registration Fee) 82

Comment \_\_\_\_\_

4. Where should future meetings be held?

Philadelphia 66 West Coast 24 Other(specify) \_\_\_\_\_

Comment Rotate 60 Central 5

5. Are you willing to keep us informed of your changes of address? yes 177

6. About how many miles did you travel to this meeting?

Local: 15 50-350: 70 400-1400: 31 1500-2500: 36 West Coast: 27

7. Do you consider questionnaires a bore? yes 36 no 114

Please turn this in at the registration desk. If you forget, mail it to Mr. E. E. Hannum, The Franklin Institute Research Laboratories, Phila., Pa. 19103.

Number of Questionnaires returned 183

have volunteer contributing editors to cover various topics within their fields of specialization. (For more information write to Mr. Gunther Cohn, Editor, The Franklin Institute Research Laboratories, Philadelphia, Penna. 19103.)

In summary, it appears that the 5th Symposium on EED's was successful on all fronts. The papers were carefully prepared, timely, and well presented. The discussion periods were lucid and informative. The entire meeting was well handled and kept on schedule by the able efforts of the several technical chairmen.\* To all of the authors and participants, The Franklin Institute Research Laboratories staff extends their heartfelt thanks. Mr. E. E. Hannum, Manager of the Applied Physics Laboratory, was the general chairman and was capably assisted in planning and arranging of the many details by Gunther Cohn, Senior Staff Engineer, and Arnold W. Caldwell, with support by the entire staff of the Applied Physics Laboratory.

---

\*Session 1, *Earl VanLandingham, NASA Langley Research Center;*  
Session 2, *Dan Waxler, Picatinny Arsenal;* Session 3, *Charles M. Cormack, NAVAIRSYSCOM;* Session 4, *William F. Bell, Space Ordnance Systems, Inc.*



WELCOME TO THE  
**5TH SEED**  
SYMPOSIUM  
JUNE 13-14, 1967  
THE FRANKLIN INSTITUTE  
RESEARCH LABORATORIES





## TABLE OF CONTENTS

Preface. . . . .	111
Summary. . . . .	0-1
<i>E. E. Hannum, Chairman. Manager, Applied Physics Laboratory, The Franklin Institute Research Laboratories</i>	
Welcoming Remarks. . . . .	0-1.4
<i>Dr. Joseph R. Feldmeier, Vice President of The Franklin Institute and Director of the Research Laboratories</i>	

### SESSION ONE - NEW DEVELOPMENTS

(Tuesday Morning, June 13, 1967)

Chairman: *Earl VanLandingham, NASA/Langley Research Center*

Abstracts . . . . .	1-0
1-1 Use of Electroexplosive Devices in the Active Seismic Experiment . . . . .	1-1
<i>Thomas J. Graves, NASA/Manned Spacecraft Center</i>	
1-2 Neutron Radiographic Inspection of Ordnance Components . . . . .	1-2
<i>Harold Berger, Argonne National Laboratory V. W. Drexelius* McDonnell Douglas Corp.</i>	
1-3 Development of a 15-Second Delay Squib . . . . .	1-3
<i>Sidney A. Moses, McDonnell Douglas Corp.</i>	
1-4 The Thermal Stability of RDX in Shaped Charge. . . . .	1-4
<i>N. J. Bowman and E. F. Knippenberg, General Electric Co., RSD</i>	
1-5 Measurement of Explosive Output. . . . .	1-5
<i>M. L. Schimmel and V. W. Drexelius, McDonnell Douglas Corp.</i>	
1-6 Solid State - Timers - Accurate Time Delay for Electroexplosive Devices . .	1-6
<i>Louis J. Caparont, Atlas Chemical Industries Inc.</i>	
1-7 Firing Squibs by Low Voltage Capacitor Discharge for Spacecraft Application.	1-7
<i>J. E. Earnest and A. J. Murphy*, Jet Propulsion Laboratory</i>	
1-8 Laser Energized Explosive Device System. . . . .	1-8
<i>Donald Lewis, Space Ordnance Systems, Inc.</i>	
1-9 The Development of a Water Arm-Air Safe Detonator. . . . .	1-9
<i>Louis J. Montesi, U.S. Naval Ordnance Laboratory, White Oak</i>	
1-10**Application of Neutron Radiography for Non-Destructive Visual Examination. of EED's. . . . .	1-10
<i>Charles Porter, General Electric Co., Pleasanton Frank Burkdoll, Explosive Technology, Inc.</i>	
1-11P Explosive Detonator Shock Testing for Impact Sensors. . . . .	Withdrawn
<i>Robin Klein, General Electric Co., RSD</i>	
1-12P A Radiant Energy Technique to Measure Explosive Output. . . . .	1-12
<i>M. G. Kelly, The Franklin Institute Research Laboratories</i>	

\*Speaker

\*\*A P after the paper number indicates that this paper was presented by title only.

SESSION TWO - PROBLEM AREAS AND FUTURE REQUIREMENTS

(Tuesday Afternoon, June 13, 1967)

Chairman: *Dan Waxler, Picatinny Arsenal*

Abstracts . . . . .	2-0
2-1 Hazards of Electromagnetic Radiation to Ordnance (HERO). . . . .	2-1
<i>R. M. Price, U.S. Naval Weapons Laboratory</i>	
2-2 Radiofrequency-Interference Protection for Pyrotechnic Systems in Manned Spacecraft. . . . .	2-2
<i>R. L. Robinson, NASA/Manned Spacecraft Center</i>	
2-3 Measuring the Electric and Magnetic Components of the Near Field. . . . .	2-3
<i>Robert B. Cowdell, Genisco Technology Corp., Genistron</i>	
2-4 Lightning Surge Current Hazards to Semi-Conductor and Electroexplosive Systems . . . . .	2-4
<i>M. M. Newman, J. D. Robb, and J. R. Stahmann*, Lightning and Transients Research Institute</i>	
2-5 Energy Transfer in Electrostatic Arcs . . . . .	2-5
<i>C. F. Schroeder, Jr., Sandia Corporation</i>	
2-6 Sensitivity of Explosives to Sparks . . . . .	2-6
<i>R. McGirr, Atlas Chemical Industries Inc.</i>	
2-7 Designing Electro-Explosive Devices for Electrostatic Insensitivity . . . . .	2-7
<i>L. D. Pitts, General Precision Inc., Link Group</i>	
2-8P RF Protected EED's Utilizing Miniature RLC Networks . . . . .	2-8
<i>Joseph E. Sidoti, Micro Precision Products, Inc.</i>	
2-9P Effects of Radio Frequency Stimuli on Electroexplosive Devices . . . . .	2-9
<i>P. F. Mohrbach and R. F. Wood, The Franklin Institute Research Laboratories</i>	
2-10P Miniaturization of Out-Of-Line Explosive Safety Systems . . . . .	2-10
<i>R. Stresau and R. Degner, R. Stresau Laboratory, Inc.</i>	
2-11P R. F. Bonding . . . . .	2-11
<i>W. C. Reisner, The Franklin Institute Research Laboratories</i>	

SESSION THREE - INSENSITIVE INITIATORS

(Wednesday Morning, June 14, 1967)

Chairman: *Charles M. Cormack, NAVAIRSYSCOM*

Abstracts . . . . .	3-0
---------------------	-----

A. 1 AMP/WATT

3-1 Temperature Coefficient of Resistivity Effects on 1A/1W No-Fire Initiators .	3-1
<i>D. E. Davenport, General Precision, Inc., Link Group</i>	
3-2 Insensitive Electric Initiators . . . . .	3-2
<i>Vincent J. Menichelli, U. S. Naval Ordnance Laboratory, White Oak</i>	
3-3 Constant Current Ignition of Metal - Metal Oxide Mixtures. . . . .	3-3
<i>James L. Austing,* IIT Research Institute John F. Weber,* Sandia Corporation</i>	

3-4 Electric Detonators for Navy Guided Missile Applications. Experimental Studies of Four Concepts . . . . . 3-4  
*R. Stresau, \* R. Peterson, and D. Chamberlain, R. Stresau Laboratory, Inc.*

3-5 A Microcircuit Bridge for High-Reliability EED's . . . . . 3-5  
*D. N. Griffin, Quantis Industries, Pelmeo Division*

3-6 Electric Detonators with "Markite" Electrically Conductive Plastic Bridge Elements . . . . . 3-6  
*R. H. Stresau and R. L. Peterson\*, R. Stresau Laboratory*  
*S. A. Corren and M. A. Coler, Markite Engineering Company*

3-7P High Temperature Resistant Conductive Priming Mixes . . . . . 3-7  
*Wm. Perkins and Allan Schlack, Frankford Arsenal*

3-8P A Heat Transfer Study of Hot Wire Ignition of Metal - Metal Oxide Mixtures . 3-8  
*J. L. Austing and J. E. Kennedy, IIT Research Institute*  
*D. H. Chamberlain and R. H. Stresau, R. Stresau Laboratory, Inc.*

3-9P Electrical and Thermal Considerations in the Design of Electroexplosive Devices . . . . . 3-9  
*R. H. Stresau, R. Peterson, and D. Chamberlain, R. Stresau Laboratory, Inc.*

B. EBW'S

3-10 Observations on the Initiation of Secondary Explosives by Exploding Wires . 3-10  
*H. S. Leopold, U. S. Naval Ordnance Laboratory, White Oak*

3-11 An Application of a Thermal Explosion Criterion to the Initiation of Explosives by Variable-Current Wires . . . . . 3-11  
*M. H. Friedman and R. L. McCally, \* The Johns Hopkins University, Applied Physics Laboratory*

3-12 EBW Firing Unit and Detonator Compatibility Investigation . . . . . 3-12  
*J. M. Reuter, \* General Laboratory Associates, Inc.*  
*R. G. Amicone, The Franklin Institute Research Laboratories*

3-13 The Initiation of Insensitive Explosives with Metal - Metal Oxides . . . . . Withdrawn  
*James L. Austing, IIT Research Institute*

SESSION FOUR - TOOLS AND TECHNIQUES

(Wednesday Afternoon, June 14, 1967)

Chairman: *William F. Bell, Space Ordnance Systems, Inc.*

Abstracts . . . . . 4-0

A. Testing and Information

4-1 The Outlook for Nondestructive Electrothermal Parametric Measurements on Wire-Bridge EED's . . . . . 4-1  
*J. N. Ayres\*, C. W. Goode, I. Kabik, and L. A. Rosenthal, U. S. Naval Ordnance Laboratory, White Oak*

4-2 Reactivity of Organic Nitro Compounds . . . . . 4-2  
*E. E. DeMaris, General Electric Co., RSD*

4-3P The Design of Sterilizable Pyrotechnic Devices . . . . . 4-3  
*N. J. Bowman and E. F. Knippenberg, General Electric Co., RSD*

4-4P Information Sources for EED's . . . . . 4-4  
*Gunther Cohn, The Franklin Institute Research Laboratories*

4-5P Instrumentation for Research, Evaluation, and Quality Control of Electroexplosives . . . . . 4-5  
*C. T. Davey, W. S. Weiss, and W. J. Dunning, The Franklin Institute Research Laboratories*

B. Statistics

4-6 Comments Relating to Confidence-Reliability Combinations for Small Sample Tests of Aerospace Ordnance Items . . . . . 4-6  
*A. J. Benedict, Jet Propulsion Laboratory*

4-7 Lot to Lot Variations in Explosive Properties and Their Consequences in Explosive Component Development and Production . . . . . 4-7  
*Richard A. Whiting, Honeywell, Inc.; James N. Ayres, U. S. Naval Ordnance Laboratory, White Oak; Richard H. Stresau, R. Stresau Laboratory, Inc.*

4-8 Reliability Assessment of Ordnance Components from Variables Performance Parameters . . . . . 4-8  
*S. Damskey, V. Goldie, and M. West, General Electric Co., RSD*

4-9 A Mathematical Analysis of Ordnance Circuitry to Determine the Susceptibility to Stray RF Fields . . . . . 4-9  
*Jon E. Klima, Martin-Marietta Corp. Denver*

4-10 Experimental Distribution of Brucceton Test Statistics . . . . . 4-10  
*Herbert D. Peckham, Holes Inc.*

Attendance . . . . . a

Distribution . . . . . d

SUMMARY  
E. E. Hannum  
The Franklin Institute Research Laboratories

Many new developments were reported in this symposium that reflect the wide and ever increasing scope of the electroexplosives industry. Most of the new developments discussed at this meeting have evidently taking shape since the last meeting in 1963. The reader is invited to inspect the table of contents in order to appreciate the wide coverage of technical subjects.

It is interesting to note that many of the programs were aimed directly or indirectly at increased safety and reliability. A new method of non-destructive inspection of electroexplosive components (neutron radiography) was described and is apparently refined sufficiently to be available immediately to those who wish to assure themselves of the integrity of the components that they intend to use or sell. Other non-destructive testing methods were described, as were new systems of instrumentation for output measurement as well as research, evaluation and quality control in general.

New statistical tools were described and helpful warnings were discussed concerning lot to lot variations in explosive properties, experimental distributions of Bruceton test statistics and reactivity of organic nitro compounds as consequence of unrecognized impurities.

The first use of a laser beam to initiate explosives for practical application was described at this meeting. We doubt that it will be the only one of its type.

A number of papers presented most useful design data and procedures for such applications as 1 amp 1 watt and insensitive initiators; design of sterilizable pyrotechnic devices and methods of initiating secondary explosives; design of miniature out-of-line safety systems; RF protection; static insensitivity; and lightning protection.

It appears that hazard problems including static electricity, lightning, and radio frequency energy still exist and that they will probably receive additional R&D effort in the immediate future. Electrostatic sensitivity of explosives, pyrotechnics, and electroexplosive devices is still cause for concern and evidently additional factual information is required that can only be obtained through carefully planned and systematically executed R&D programs. There is still a need for means of monitoring RF environments, better instrumentation, better analytical techniques, simple and effective electroexplosive detector-simulators for use in field testing of EED systems or field monitoring. Improved methods of assessing the degree of RF hazard to a particular system in any given environment is desired, but evidently, in the opinion of many people, the problem is far too complex to hope of any immediate breakthrough in this direction.

Measurements of pyrotechnic and explosive output still present problems in spite of the many new and improved methods. It was pointed out that none of the existing methods can tell the user whether his initiator will satisfactorily initiate the explosive train in which it is to be used. The results of the presently available test methods can give him information that he can use to decide for himself whether the probability of success is satisfactory. This is as far as any of the methods go.

The trend toward development and use of insensitive EED's is reflected by the numerous papers on the 1-Amp 1-Watt, insensitive initiators, exploding bridgewire initiators, use of secondary explosives only, and the laser energized device. These are in contrast to the requirements for EED's in long-range spacecraft applications. A round trip to Mars may take as long as 560 days. If very insensitive initiators were to be used on such a mission, the weight penalty would be tremendous. Insensitive initiators in general require comparatively large power supplies and heavier wiring and switching devices. The use of very sensitive EED's and capacitor firing sources becomes quite attractive for

such long term missions. However, firing wire bridge EED's from charged capacitors in optimum fashion involves some interesting complications. One paper on this subject was presented at the meeting. We suspect that this problem will receive considerable attention in the immediate future.

We believe that the reader will find these Proceedings to be a useful reference document.

## WELCOMING REMARKS

Joseph R. Feldmeier  
Vice President and Director  
The Franklin Institute Research Laboratories

The importance of this conference today and tomorrow is best demonstrated by recent discussions of the technology gap. The first reference to this gap was made by Vice President Humphrey on January 25, 1966, when he gave the keynote address before the Panel on Science and Technology of the House Committee on Science and Astronautics. His comments, while brief, started a wide-scale discussion and were again mentioned in the 1967 meeting of the same House Committee when the representative from Norway, Mr. Robert Major, referred to the Vice President's comments and added the following:

"This brings us to the problem of the technological gap, which is now so much debated. There is, no doubt, a gap, but I am not so sure that the basic reason for it is lack of scientific and technological activity in Europe. Many examples can be given where European countries have been leading in science and technology, but nevertheless lost the production race. I think the reasons for the gap is more the difference in mentality and attitude, managerial skill, and markets. I think on this side of the Atlantic you are more dynamic, more geared for the future, and have established a management skill which...has been essential for the creation of big industrial units."

This conference is a part of the dynamic process to which Mr. Major referred and we are pleased that The Franklin Institute has been and continues to be a major contributor to the creation and dissemination of technical information. It is also quite appropriate that this type of meeting should occur here at the national memorial of Benjamin Franklin who, in his day, was also quite a gap-closer.

We hope you find these two days enjoyable and that you will leave with the feeling that much has been accomplished.



## ABSTRACTS SESSION ONE

### 1-1 Use of Electroexplosive Devices in the Active Seismic Experiment

Thomas J. Craves

The use of electroexplosive devices in the Active Seismic Experiment is discussed in this paper. Several unique applications of explosive hardware are found in this experiment which was designed for lunar exploration. Artificial seismic energy is produced by two devices -- the thumper and the mortar package. Basic design, circuitry, and operation are discussed for each of these devices, and testing and safety considerations are detailed on an experiment level.

### 1-2 Neutron Radiographic Inspection of Ordnance Components

Harold Berger  
V. W. Drexelius

Neutron radiographic inspection of ordnance components permits observing the presence, location, density variations, and voids of explosives contained therein. This supplements x-radiography which generally reveals only metal components. Thermal neutron sources most used have been nuclear reactors. X-ray film with conversion screens produce excellent high resolution results which will be shown.

### 1-3 Development of a 15-Second Delay Squib

Sidney A. Moses

The development of a new delay squib is discussed. This "universal" squib initiates three different solid motor igniters used with various models of the Delta Space Vehicle. Douglas-NASA/GSFC philosophy concerning the safety and reliability of electroexplosive devices resulted in a squib specification with unusual requirements. Details are presented. As this specification presented some interesting new concepts, suggestions are made concerning the desirability of standardizing these throughout the industry.

### 1-4 The Thermal Stability of RDX in Shaped Charge

N. J. Bowman  
E. F. Knippenberg

Within recent years flexible linear shaped charge (FLSC) has received widespread acceptance within the aerospace industry and is currently being used in a number of missile and spacecraft systems. Use of FLSC in missile stage separation applications offers several important design advantages. In particular, its use generally results in significantly lighter weight structures as compared to alternate systems. Because of these advantageous features, FLSC separation devices have been developed and successfully employed by the General Electric Company in the Nike-Zeus, TVX, and other re-entry vehicles.

### 1-5 Measurement of Explosive Output

M. L. Schimmel  
V. W. Drexelius

An energy measuring device with calibrated honeycomb as the sensing element is used to quantitate output of a wide spectrum of aerospace ordnance. No electronic instrumentation is required. A description is given of device design and use for evaluating primers, igniters, power cartridges, detonators, and detonating cord.

### 1-6 Solid State - Timers - Accurate Time Delay for Electroexplosive Devices

Louis J. Caparoni

The advantage of using Electroexplosive Devices is further enhanced when they can be triggered with various delay times. A sequence of functions can be performed by Electroexplosive Devices using pre-set time delays. Problems associated with the delay time of Electroexplosive Devices, and in particular, the design of a solid state timer, and the use of a few, can be discussed. The design of a Solid State Timer.

Best Available Copy

1-7 Firing Squibs by Low Voltage Capacitor Discharge for  
Spacecraft Application

J. E. Earnest  
A. J. Murphy

The design of low voltage capacitor discharge circuits for firing hot-bridgewire squibs requires that squib-thermal and circuit-electrical time constants be considered as interrelated. These functional relationships are analyzed by use of an electro-thermal analogy with one composite time constant. The effects of secondary characteristics not considered in the simple analogy are also discussed.

1-8: Laser Energized Explosive Device System

Donald Lewis

A system has been developed which can materially reduce the hazard of ordnance devices from degradation or premature actuation by exposure to various electromagnetic, electro-static and temperature environments. Basically the system consists of a pyrotechnic compound encased in a faraday shield containing an infrared transmitting window which is used in conjunction with a fiber optic. The laser pulse from a small compact laser head is transmitted down the fiber optic and impinges through the window on the ordnance compound, which is in turn, exploded by this incident energy.

1-9 The Development of a Water Arm-Air Safe Detonator

Louis J. Montesi

A Water Arm-Air Safe (WARAS) detonator has been developed that follows closely the design principles embodied in the Stresau-Slie design but modified to meet the standard Navy safety requirements. The detonator will also pass all the Navy environmental tests except MIL-STD-304, the temperature-humidity cycling test. Possible solutions to successful operations after MIL-STD-304 are being actively sought.

The WARAS detonator utilizes a column of the explosive nitroguanidine which is below critical diameter for propagation when surrounded by air but in which detonation will propagate reliably when surrounded by water.

1-10P Application of Neutron Radiography for  
Non Destructive Visual Examination of EED's

Charles Porter  
Frank Burkdoll

Neutron radiography is valuable for routing non destructive examinations of many electro-explosive components. The paper will describe neutron radiography, identify consideration which affect the quality of neutron radiographs of these components, and draw comparasions between information gained from radiography and neutron radiography of identical components.

1-11F Explosive Detonator Shock Testing for Impact Sensors

Robin Klein

Due to inability of present test equipment to duplicate Re-Entry Vehicle impact shocks, a new test method was developed. High energy explosive detonators were used to supply the high shocks (10,000G's) and shock rates (500-1000 G's/microseconds). This new method allowed impact simulation at low cost and good repeatability.

1-12P A Radiant Energy Technique to Measure Explosive Output

M. G. Kelly

A description of the theory, construction, and calibration of a radiation detector to measure the output of explosive devices is presented. The detector, which uses two high speed photomultipliers each having a broad spectral response in a different portion of the 250 to 1200 millimicron portion of the spectrum, is capable of measuring temperature in the range of 100 to 10,000° Kelvin and radiant energy as functions of time as well as integrated radiant energy.

Several experiments are cited which show how the detector may be used to determine the output of the out-out strength, brisance and detonation velocity of various types of explosives including both "hard" and "soft"

## 1-1 USE OF ELECTROEXPLOSIVE DEVICES IN THE ACTIVE SEISMIC EXPERIMENT

Thomas J. Graves

NASA - Manned Spacecraft Center

### ABSTRACT

The use of electroexplosive devices in the Active Seismic Experiment is discussed in this paper. Several unique applications of explosive hardware are found in this experiment which was designed for lunar exploration. Artificial seismic energy is produced by two devices — the thumper and the mortar package. Basic design, circuitry, and operation are discussed for each of these devices, and testing and safety considerations are detailed on an experiment level.

### INTRODUCTION

Several experimental studies requiring unique applications of electro-explosive devices have been proposed for future lunar exploration. One experiment, which makes extensive use of explosive hardware, is the Active Seismic Experiment of the Apollo Lunar Surface Experiments Package. This experiment will require the production of artificial seismic energy at designated points on the lunar surface to accomplish the measurements of the physical properties of the lunar near-surface materials. Two explosive devices will furnish this seismic energy — the thumper and the mortar package.

### THE THUMPER

#### Description

The first of the explosive devices which will be used on the lunar surface is the thumper. Figure 1 shows an outline of the thumper depicted as a

handheld device to be operated by one of the astronauts. Seismic energy is produced by the thumper through the firing of an Apollo standard initiator (ASI) located in the base plate. Figure 2 shows two cutaway views of the thumper base plate. Twenty-one ASI's are located in two rings in the thumper base plate. This plate, in turn, is spring-loaded into an outer shim plate so that the outer plate is in physical contact with the output end of the ASI's. When an ASI is fired, the pressure buildup between the bottom of the base plate and the outer plate forces the outer plate to move away rapidly. The movement of the outer plate against the lunar surface produces a mechanical thump or shock in the surface material. As the gas is exhausted around the outer flanges, the three retaining springs return the outer plate to its original position in contact with the remaining ASI's. This multiple-shot function is a feature of the thumper.

#### Circuitry

Figure 3 is a schematic diagram of the firing circuitry for the thumper. An electrical service and data line is connected between the thumper and a central station electronic package at all times. A charging potential of 24.4 volts is supplied through this line to charge two 350- $\mu$ f capacitors which are used for firing the ASI's. Three switching functions are accomplished by the astronaut prior to the firing of each ASI. A rotary switch on the thumper handle is used to select each ASI. A ganged command and arm switch permits the charging of the firing capacitors, and a firing switch is depressed to fire the ASI. A real-time event circuit is present to relay the instant of seismic energy output. This is accomplished by the momentary closure of a pressure switch located in the thumper base plate.

## Deployment

The deployment and activation of the thumper is connected with the deployment in other portions of the experiment. Figure 4 shows a site layout of the Active Seismic Experiment. After the central station electronics package has been placed in position, the astronaut will walk back toward the lunar module while deploying the seismic detection system, which is stowed on a reel on the thumper handle. This detection system consists of a 310-foot service cable with three geophones tied into the cable at 150-foot intervals. After the deployment and the emplacement of this system on the walkout, the astronaut will fire an ASI at every 15-foot point along a 300-foot line paralleling the geophone line as he walks back to the central station. The seismic energy signals from each geophone, along with the real-time event instant, will be monitored by the Active Seismic Experiment and fed into the Apollo Lunar Surface Experiments Package (ALSEP) telemetry system.

## THE MORTAR PACKAGE

The second seismic energy source is a mortar device which will be deployed by the astronaut prior to the departure from the moon. Figure 5 is a photograph of the mortar package taken during previous flight tests conducted at White Sands Missile Range in New Mexico. This is actuated by and operated by earth commands after the astronauts depart from the moon. The function of the mortar package, which can be activated for up to 1 year from departure, is to reduce the hazard to the astronauts that might result from explosive debris and to preserve the natural lunar environment for other ALSEP experiments.

## Description

The seismic energy produced by the thumper is obviously limited, permitting an investigation of lunar surface material only to a depth of approximately 75 feet. The mortar package will produce seismic energy for a much broader investigation. This package, shown in Fig. 6, consists of the mortar box, an outer shell with two support legs, an electronics card, and a grenade-launch tube assembly consisting of four fiber-glass open-launch tubes and four grenades. The purpose of this device is to individually launch the four grenades (which contain high-explosive charges) to distances of up to 1 mile. The grenades are designed to explode on impact thus producing a large seismic signal.

Figure 7 shows the internal configuration of the grenades. They are square in cross section, approximately 3 inches long at the edge. The outer shell is made of 50-mil (0.05-in.) fiber glass. The rocket motor is located at the bottom of the grenade. Figure 8 is a cross-section view of the rocket motor. A 3-mil (0.003-in.) stainless-steel burst-disk seals the output orifice until motor ignition. A steel screen is used to keep the propellant in the motor case during burning. The propellant chosen for this application is an extrudable fluorocarbon-bound propellant developed and supplied by the Naval Ordnance Test Station, China Lake, California. The composition and performance characteristics of this propellant are classified. The choice of propellant was made on the basis of the thermal and the vacuum stability requirements determined for lunar-environment exposures of up to 1 year. One single bridgewire Apollo standard initiator (SBASI) is used for rocket motor ignition.

Referring again to Fig. 7, a thermal battery and an impact switch, located above the motor, provide power and command signals for detonating the high-explosive charge on impact. The high-explosive detonator is shown above the

motor. For this application, an Apollo end detonator cartridge is being used. The detonator output is physically blocked by a safe-arm slide which is shown above the detonator. This slide is held in place by the launch-tube wall and is ejected by a spring when the grenade leaves the launch tube. The high-explosive charge is shown near the top of the grenade. This high-explosive charge is a plastic-bonded explosive made from HNS-II and Teflon. The bulk plastic-bonded explosive (PBX) is first pressed into a cylindrical shape to a density of approximately 1.7 grams per cubic centimeter and then machined to a rough cubic shape. The PBX was developed, and the finished charges were supplied by the Naval Ordnance Laboratory, White Oak, Maryland. A number of explosives, including Tacot, DATB, TATB, HNS-I, and binders such as Lexan, Nylon, and Viton were investigated prior to the selection of the HNS-II/Teflon combination which was found to be superior in thermal and vacuum stability and impact sensitivity; HNS-II/Teflon is readily available.

The top of the grenade consists of a 200-milliwatt transmitter which relays the instant of explosion to the Active Seismic Experiment electronics at the cutoff of a transmission. The range line, shown on the side of the grenade in Fig. 7, serves as an antenna for the 30-MHz transmitter. The four incorporated grenades are quite similar in configuration, but are designed to travel different distances and to carry different explosive loads.

Table 1 presents some of the interesting differences in these grenades. The largest grenade is designed to travel a range of 5000 feet and carries a high-explosive charge of 1 pound. The other grenades have ranges down to 500 feet, with the smallest grenade carrying a high-explosive charge of 0.1 pound.

## Circuitry

Figure 9 shows the firing circuitry for the grenades. A charging potential is supplied through a frangible circuit board to charge the electric-match firing capacitor. The SBASI rocket motor igniter is then fired from a capacitor source external to the grenade. When the grenade fires, the frangible circuit board is broken. As the grenade leaves the launch tube, the high-explosive safing-slide is ejected permitting a microswitch to close thus discharging the electric-match firing capacitor through the electric match. When the electric match fires, the thermal battery acquires power and begins to charge the high-explosive detonator firing capacitors. The thermal battery also supplies power to the transmitter. Upon impact, the omnidirectional impact switch closes causing the three firing capacitors to discharge through the high-explosive detonator. Detonation of the high-explosive charge destroys the transmitter, thereby relaying the shot instant to the Active Seismic Experiment through a signal cutoff.

## Data acquisition

The accurate measurement of several parameters in the mortar-package system is critical to the ultimate success of the experiment. The range of the grenades will be known to  $\pm 3$  percent. To accomplish this, three ballistic parameters are measured: time of flight, launch velocity, and launch angle.

The time of flight is determined by the cutoff of the transmitter signal from the grenade when it explodes on impact. The launch velocity is calculated from the time of flight measurements made for the first 25 feet of flight outside of the launch tube. This is based on the fact that the velocity of the grenade for the first 25 feet of flight is essentially constant in a vacuum atmosphere. The deviation of actual flight path from theoretical flight path



introduces negligible error. The rocket motors are designed to complete all thrusting while still in the launch tube. The time of flight measurement is accomplished by use of the range line/antenna combination and a gating system in the mortar package. When the grenade leaves the launch tube, it pulls a prewrapped 32-foot stainless-steel wire from the outside of the launch tube. Two break wires are tripped over a 25-foot spacing to give the time of flight over that distance. The initial launch angle is 45 degrees with respect to the mortar-package platform. Orientation of the mortar package with respect to the gravitational field of the moon is measured by two angle-transducers prior to the firing of each grenade. The criteria of any two of these three parameters will enable a calculation of grenade range to be made.

#### TESTING

At the present time, both the thumper and mortar package are undergoing Design Verification Testing at the White Sands Test Facility. Previous system testing of the mortar package at Long Beach, California, and at White Sands Missile Range has been successful in the areas of the rocket motor performance and the detonator high-explosive interface. Performance tests of the thumper in a vacuum environment have been performed at the Manned Spacecraft Center in Houston, Texas. These tests have confirmed the adequacy of the seismic signals and their coupling and injection into the lunar surface for that portion of the experiment.

#### SAFETY

In the designing of the experiment hardware, safety considerations have been paramount. A number of autoinitiation tests of a fully loaded thumper have been conducted. These tests have indicated that autoignition of other ASI's does

not occur when a single ASI is fired. Degradation of the astronaut suit material caused by ejected soil particles from the thumper blast is being investigated.

As previously noted, a safing-slide is present in each grenade which effectively blocks the detonator output from the high-explosive charge. The grenades are retained in the launch tubes by two stainless-steel rods until just before the astronauts depart from the lunar surface. These rods or pins will retain all grenades in their launch tubes, even with an inadvertent motor firing. All rocket-motor igniters and firing capacitors are shorted directly at the mortar box by rotary switches until just prior to astronaut departure from the vicinity. Both the thumper and mortar package are effectively shielded from radio-frequency interference (RFI) by their outer structures, and RF filters are employed in the mortar package. RFI compatibility tests will be conducted on both devices prior to their delivery to Cape Kennedy.

#### PROGRAM MANAGEMENT

Program management for the ALSEP is handled by the Lunar Surface Project Office at the Manned Spacecraft Center in Houston, Texas. The Active Seismic Experiment design is being performed by the ALSEP prime contractor, Bendix Aerospace Systems Division. The grenades and launch tube assemblies are being supplied through a subcontract by Space Ordnance Systems, Inc.

The principal investigator for the Active Seismic Experiment is Dr. Robert Kovach of Stanford University, and the coinvestigator is Dr. Joel Watkins of the Massachusetts Institute of Technology.

NASA-S-67-3094

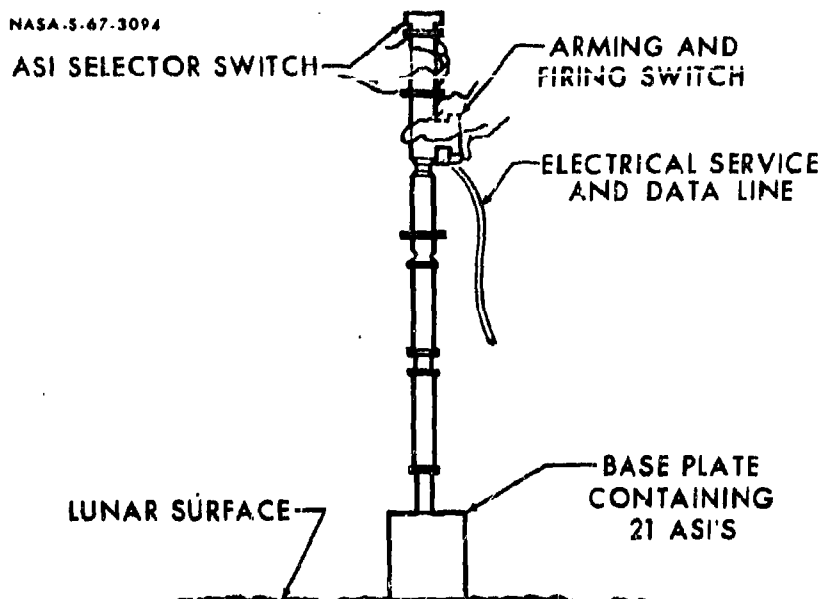


FIGURE 1. THE THUMPER - ACTIVE SEISMIC EXPERIMENT.

NASA-S-67-309F

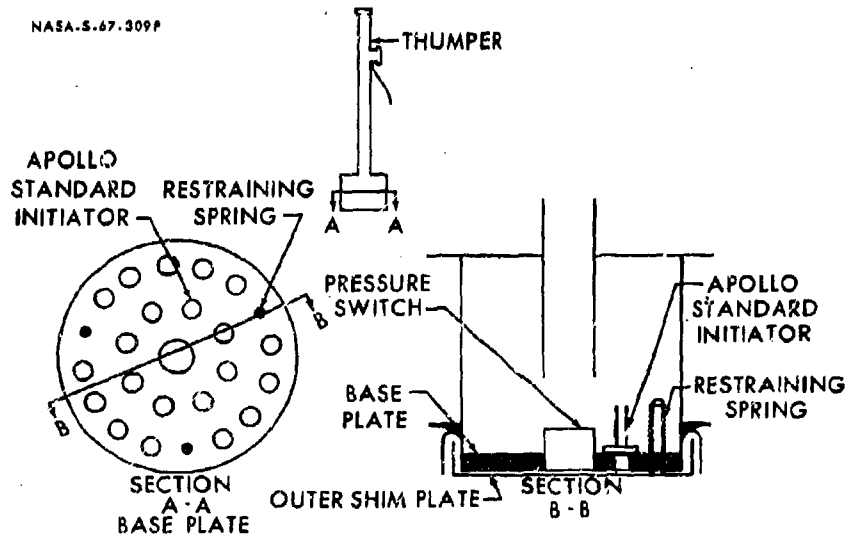


FIGURE 2. CUTAWAY VIEWS OF THUMPER BASE PLATE.

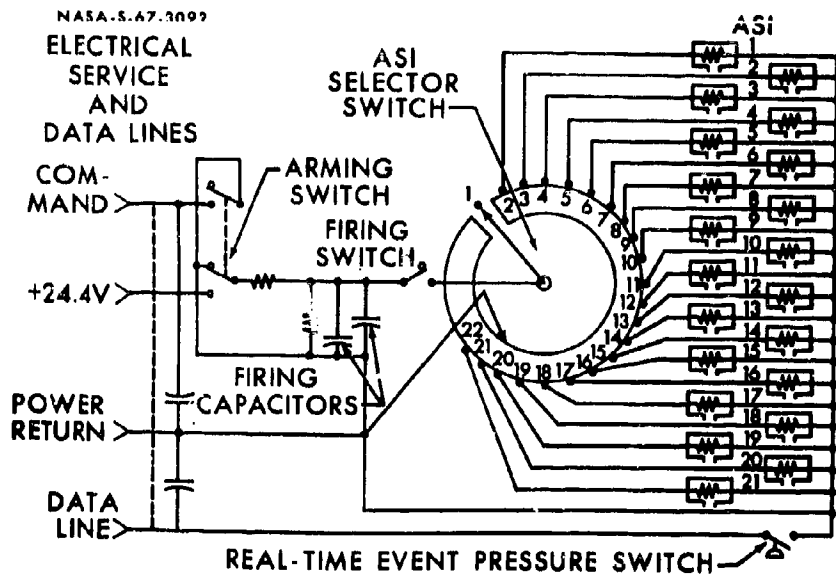


FIGURE 3. SCHEMATIC DIAGRAM OF THE FIRING CIRCUITRY.

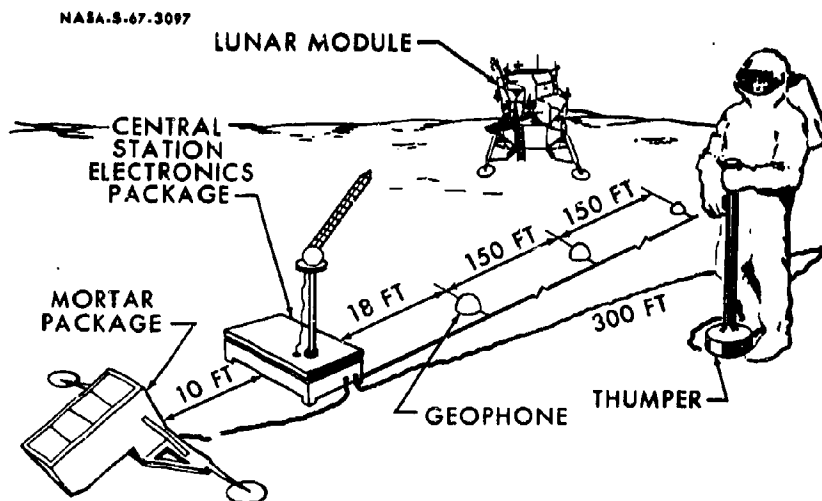


FIGURE 4. SITE LAYOUT OF THE ACTIVE SEISMIC EXPERIMENT.

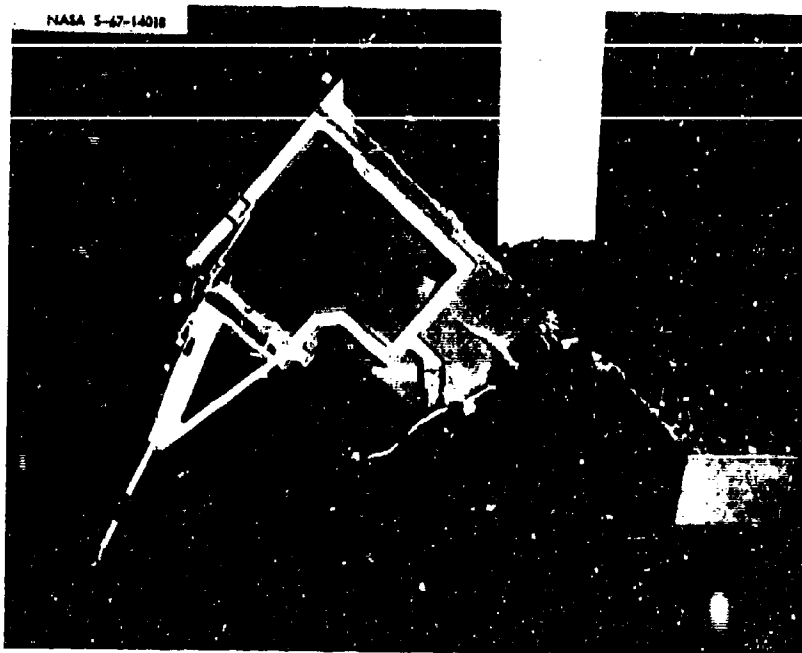


FIGURE 5. THE MORTAR PACKAGE - ACTIVE SEISMIC EXPERIMENT

NASA S-67-3095

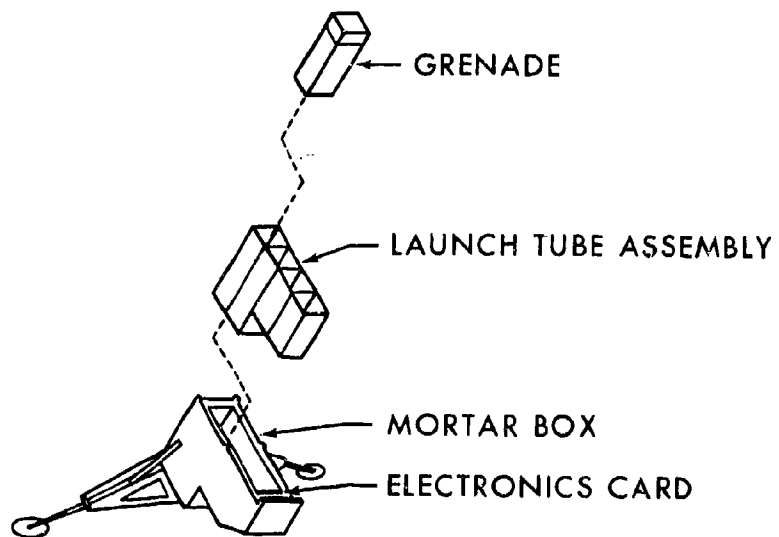


FIGURE 6. THE MORTAR PACKAGE.

NASA-8-67-3093

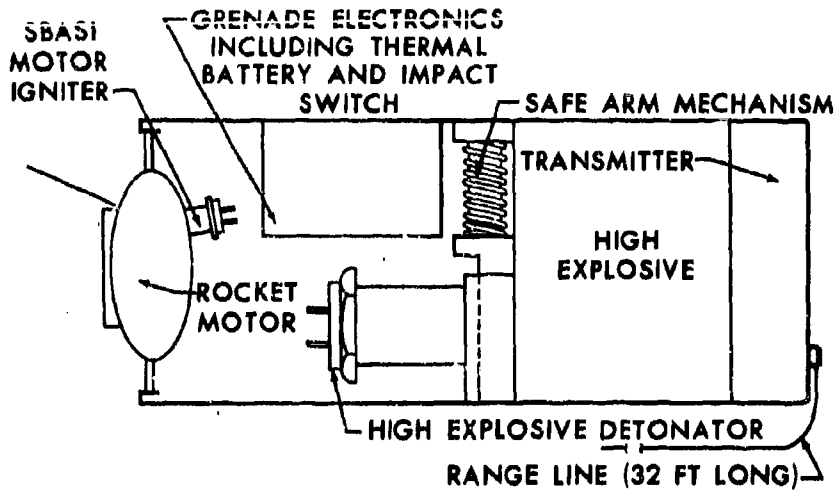


FIGURE 7. INTERNAL CONFIGURATION OF THE GRENADES.

NASA-5-67-3096

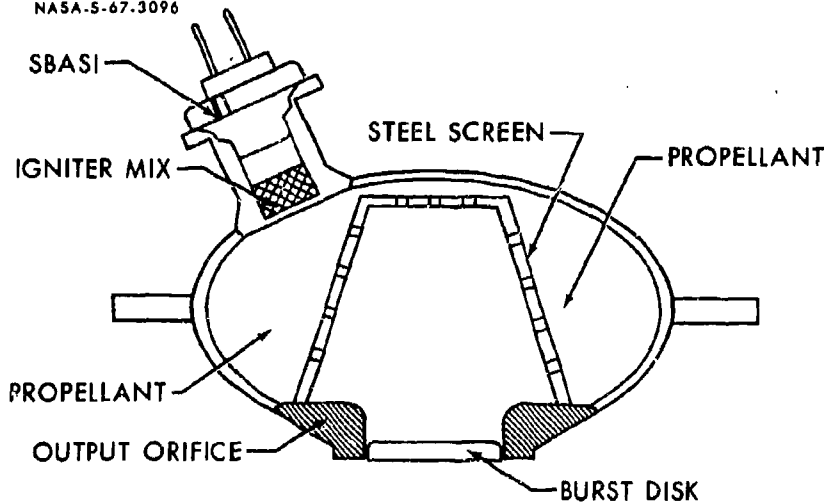


FIGURE 8. CROSS-SECTION VIEW OF THE ROCKET MOTOR.

NASA-S-67-3099

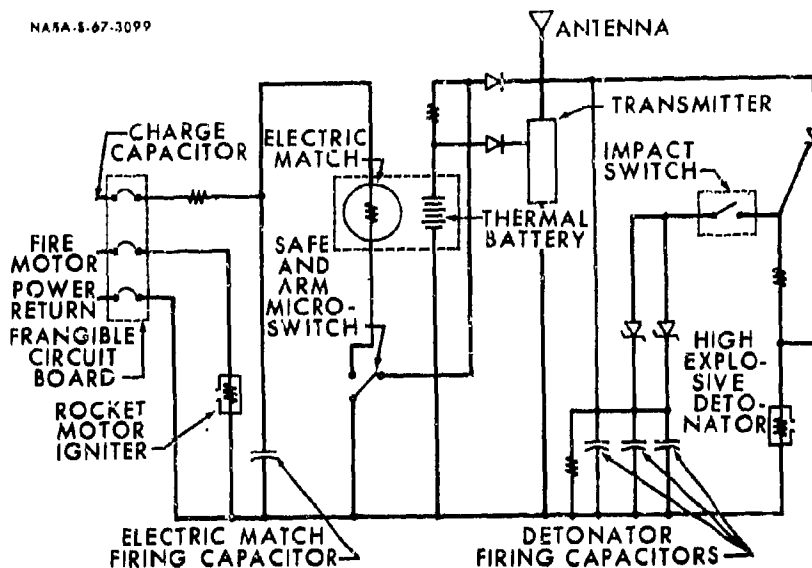


FIGURE 9. FIRING CIRCUITRY FOR THE GRENADES.

NASA-S-67-3140

TABLE 1. GRENADE CHARACTERISTICS  
ACTIVE SEISMIC EXPERIMENT

GRENADE NUMBER	RANGE, FEET	HIGH-EXPLO-SIVE CHARGE, POUNDS	LAUNCH VELOCITY, FT PER SEC	TIME TO IMPACT, SECONDS
1	5000	1.0	164	43.1
2	3000	.6	127	33.3
3	1000	.3	73	19.4
4	500	.1	52	13.6

## DISCUSSION

The seismic experiments are currently scheduled for flight on the fourth manned lunar landing, but it is expected to be moved up to the third manned lunar landing. No launch date has been set as yet.

The grenades use omnidirectional impact switches. There will be a time lapse between the firings of the different grenades to permit the investigator to study the data from the first shot before determining the order of firing of the subsequent grenades. Present plans call for firing the smallest grenade first and the largest one last, but the time interval between firings has not yet been determined.



## 1-2 NEUTRON RADIOGRAPHIC INSPECTION

OF

### ORDNANCE COMPONENTS

Harold Berger, Argonne National Laboratory

V. W. Drexelius, McDonnell Douglas Corporation

#### INTRODUCTION

The aerospace industry utilizes a large number of explosive items to perform a variety of functions, including personnel escape, stage separation, deployment of survival equipment, etc. Generally speaking, the items are relatively small, contain either a high or low explosive, and are hermetically sealed in an enveloping metal container. Once assembled and sealed, the cartridge or explosive item becomes extremely difficult to inspect for presence of the explosive, position of the explosive, defects such as cracks, gaps, or voids, moisture, or other organic sealants that perhaps migrated during assembly. One must therefore utilize radiography to inspect the ordnance item since the integrity of the item must not be disturbed if the reliability is to be achieved. A significant characteristic of most of the more popular explosives is that they are composed of low atomic number materials, containing appreciable amounts of hydrogen.

X-radiographic techniques for the inspection of low atomic number materials are well developed. (1,2,3) Such methods have been successfully applied to inspections of low Z materials such as beryllium, graphite, plastics, biological materials, and explosives. The radiographic inspection of some of these materials, particularly explosives, is frequently complicated by the fact that the low atomic number material is contained within a metallic assembly. Even in cases such as this, X-radiographic techniques can yield excellent results if the steel or other metal-containing walls are not excessively thick, and/or the thickness of the light material itself is sufficiently large to pro-

vide some reasonable attenuation for the penetrating radiation. Concerning such inspections of explosives, the report by Youshaw and Maddy<sup>(4)</sup>, for example, indicates that good quality X-radiographic results could be obtained for the inspections of cast high explosives such as TNT, Comp. B, HEX-1, H-6, and HEX-3, in thicknesses of 3.5 inches or more even with as much as 0.75-inch steel walls on each side of the explosive.

The radiographic problem becomes more difficult in the case of smaller quantities of explosive contained in a metal jacket. Explosive cartridges and small-diameter explosive lines and end boosters, as widely used in the aerospace field, are examples of smaller explosive components which are extremely difficult to X-radiographically inspect.

Since many of the explosive materials contain appreciable amounts of hydrogen, it was recognized that a neutron radiograph would present a much improved radiographic contrast of the explosive material. In 1964 McDonnell Aircraft Corporation, in co-operation with Argonne, initiated exploratory work. The very high attenuation of thermal neutrons by hydrogen would present a significant advantage for the application of neutron radiography with these materials. Figure 1 is a comparison of the mass absorption coefficients of most of the elements for both X-rays (about 120 kilovolt X-rays) and thermal neutrons. The high neutron attenuation by hydrogen and the low neutron attenuation by most metals illustrates that neutrons can provide good contrast for a hydrogenous material within a steel or similar metal jacket. The X-ray plot, on the other hand, illustrates why a similar component is very difficult to X-radiographically inspect. If one provides sufficient X-ray energy to penetrate the metal walls, there is relatively little attenuation in the light explosive material.

In this paper, we shall discuss the neutron radiographic technique, particularly as it applies to the inspection of explosive components.

### THE NEUTRON RADIOGRAPHIC METHOD

Neutron sources most used for neutron radiography<sup>(5)</sup> have been nuclear reactors. Typically, a collimated, essentially parallel thermal neutron beam is obtained from the reactor. The object to be inspected is placed between the neutron source and the radiographic detector. The detection methods which have received the greatest use employ commercially available X-ray film and conversion screens which convert the neutrons into some other radiation which is more readily detected by the film.<sup>(6,7,8,9)</sup> As an example, a cadmium-covered X-ray film is a much better neutron detector than the X-ray film itself; the reason is that the cadmium emits gamma radiation when neutrons are absorbed. The gamma radiation is much more effective on the film than the direct action of the neutrons.

Conversion screens most used include scintillators which provide very fast photographic results, metal screens used directly with film during the neutron exposure in a technique which can provide very high resolution radiographs, and, thirdly, a relatively slow, so-called transfer method in which the neutron image is detected first only by a metallic screen of some material which becomes radioactive easily (indium, gold, silver, etc.). The radioactive metal screen is then placed on film and an autoradiograph reveals the neutron image. The neutron exposures required at the detector for fast film techniques are approximately  $10^5$  neutrons/cm<sup>2</sup> for the scintillator method,  $10^7$  n/cm<sup>2</sup> for a direct metal screen technique, and  $10^8$  n/cm<sup>2</sup> for a fast transfer method exposure.

These numbers can provide an idea of exposure times required. Reactor neutron beams for neutron radiographic applications can provide thermal neutron intensities in the  $10^6$  to  $10^8$  n/cm<sup>2</sup>-second range. Other types of neutron sources can also be used. Small accelerator sources or radioactive neutron sources, supplying fast neutron yields of  $10^{10}$  neutrons/second ( $4\pi$  radiation)

are available. Such sources<sup>(5)</sup> can be moderated and collimated to supply thermal neutron beams having intensities in the order of  $10^4$  n/cm<sup>2</sup> second.

#### INSPECTION RESULTS

The neutron radiographic results shown here were all obtained at Argonne's Juggernaut reactor neutron radiographic facility. This beam provides a collimated neutron beam having an area of 2-1/2 by 4 inches; the neutron intensity is  $2 \times 10^7$  n/cm<sup>2</sup> second. The detection method employed was a direct exposure technique with a single metal conversion screen (0.0005-inch-thick gadolinium) and Kodak Type R X-ray film. Figure 2 shows a schematic view of the setup used. This is a very high resolution detection technique. A typical exposure time with this very slow film was 3 minutes.

Before referring to the explosive component radiographs, it might be best to demonstrate the excellent sensitivity of the neutron inspection technique to hydrogenous material. Figure 3 is a neutron radiographic print (a negative print - black represents high neutron exposure) of a stepped Masonite test object on the source side of a 1-inch-thick piece of steel. The Masonite thicknesses are 0.060, 0.080, and 0.100 inch, left to right. Each step contains three holes, the diameters being equal, two times and four times the step thickness (top to bottom). The actual neutron detectability of a hydrogenous component is, of course, dependent on many factors, including the amount of hydrogen and/or other neutron-absorbing material in the sample, and the type and thickness of surrounding material. However, sensitivity of the neutron technique is well demonstrated by Figure 3. An additional indication of hydrogen sensitivity is available from a reported neutron study<sup>(10)</sup> of hydrogen content in Zircaloy-2 metal samples. Neutron radiographic inspection of a number of these metal samples having varied hydrogen contents indicated that, with these 0.004-inch-thick samples, it was possible to observe hydrogen concentrations of 5000 PPM or more.

Figure 4 shows radiographs of an explosive-loaded cartridge; an X-radiograph (left) and a neutron radiograph (right) are shown. The explosive material is easily imaged on the neutron radiograph but is difficult or impossible to detect on the X-radiograph. In addition to the explosive material itself (the granular material in the upper, metal-threaded region), there are a number of other differences on these two radiographs. The plastic components, for example, are imaged on the neutron radiograph but not on the X-radiograph (the cylindrical components in the center of the cartridge, for example). On the X-radiograph, on the other hand, one can easily observe the shadows of several of the metallic components in the center of the cartridge, components which are masked on the neutron radiograph by the neutron attenuation of the surrounding light materials. Both radiographs together yield a relatively complete radiographic inspection.

Figure 5 is a sketch of a brass cylinder loaded with Dipam at various incremental densities. An X-radiograph of the item shows little detail of the explosive column. The neutron radiograph of the column, Figure 6, reveals the incremental pressings along with density variation within each increment due to direction of pressing. Two densitometer traces of the negative relative to the explosive column and the brass cylinder are shown. These results indicate that techniques for density analysis could be developed for various applications.

Figure 7 shows X-radiograph and neutron radiograph results of an explosive underwater arming device. It is of interest to note the detail as shown on the neutron exposure of the explosive column. The incremental pressings can clearly be observed. The X-radiograph does not reveal any detail with respect to the explosives contained therein.

Figure 8 is a special loaded end tip fabricated to further observe the ability of neutron radiography to detect explosive defects. In this case the explosive core load of the MDF was removed from the last 1/4 inch of the as-

sembly. As anticipated, this defect is clearly observed on the neutron radiograph and not distinguishable on the X-radiograph. The necessity or ability to observe the presence of explosives in metal sheaths is well understood in the ordnance industry.

Another example of the utilization of neutron radiography for small ordnance devices is in the analysis of items after subjection to environmental tests and prior to test firing of same. In this case Figure 9 shows three FLSC end tips that were subjected to vibration and humidity. During vibration the end cap of the center object became loose with subsequent entry of moisture. In addition to the gap, the presence of moisture can clearly be observed.

The aerospace industry is today utilizing new explosive materials having increased temperature capabilities, such as HNS, Dipam, and others. These explosives require relatively high packing densities in order to assure reliability of function and/or propagation. Figure 10 shows a series of specially loaded explosive end booster tips as utilized in a confined explosive stimulus transfer system, and found on aircraft and spacecraft. The series includes typical defects that must not go undetected or failures will result. As many of these systems are associated with personnel escape, it is imperative that failure does not occur.

Some slight residual radioactivity has been observed in the ordnance items after exposure to the neutron beam. This is a low intensity radiation lasting a few minutes. The explosives in the ordnance items are not deteriorated as a result of neutron radiography based on the intensities and exposure times utilized for the results shown herein.

#### CONCLUSIONS

The value of neutron radiography for inspection of explosives contained in small ordnance devices has been clearly established. The neutron radiography

technique permits the observation of voids, cracks, presence of moisture, density variation, plus the ability to ascertain if the item is properly loaded.

With proper development, the technique can be expanded in many instances to provide explosive density values.

Neutron radiography does not replace x-radiography. Both techniques are required in order to observe all aspects of explosive devices.

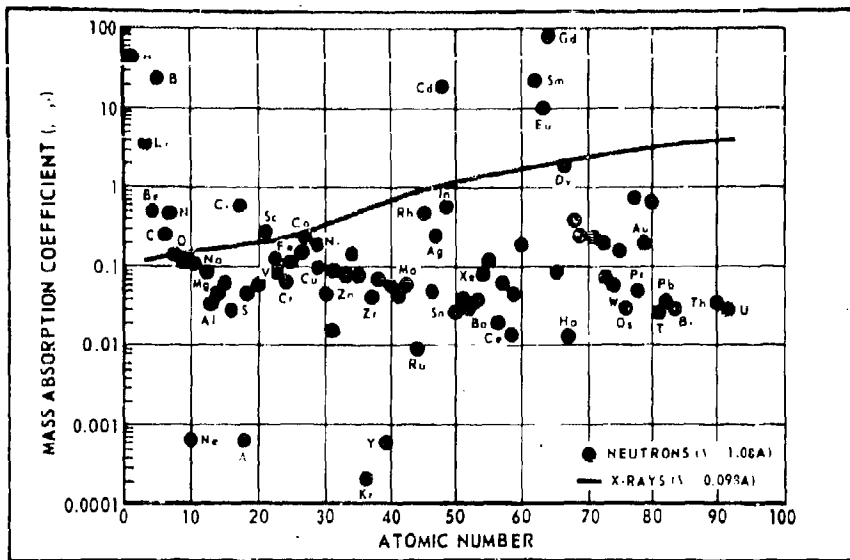
#### ACKNOWLEDGMENTS

The authors would like to thank I. R. Kraska, N. P. Lapinski, B. J. Stralser, and M. L. Schimmel for their assistance with the neutron and x-radiographic work. Portions of this work were performed under the auspices of the United States Atomic Energy Commission

#### REFERENCES

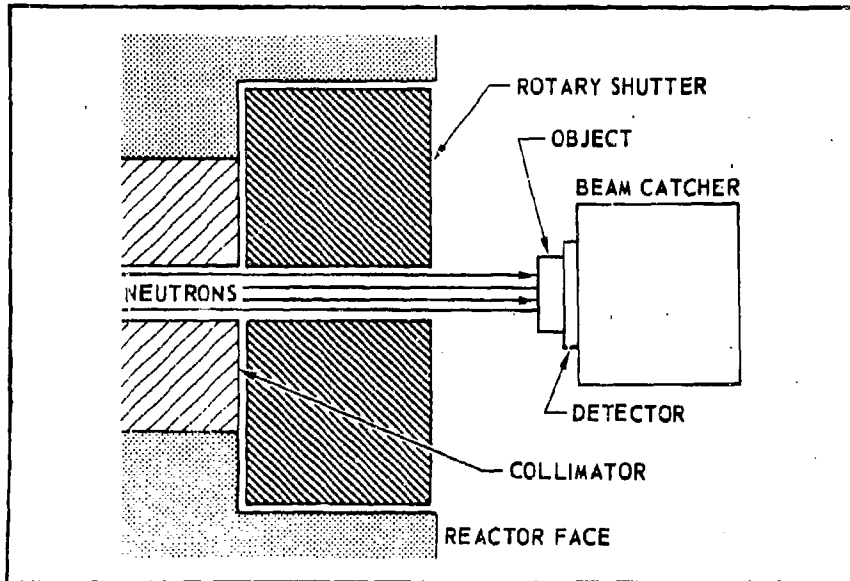
1. D. E. Elliott, J. L. Stokes, and G. H. Tenney, "Radiographic Behavior of Graphite and Beryllium," *Nondestructive Testing*, 20, 161 (1962)
2. H. R. Spletstosser, "Radiography of Beryllium," *Nondestructive Testing*, 20, 98 (1962)
3. R. W. McClung, "Techniques for Low-Voltage Radiography," *Nondestructive Testing*, 20, 248 (1962)
4. R. A. Youshaw and W. R. Maddy, "Radiography of Cast High Explosives," *Nondestructive Testing*, 20, 325 (1962)
5. H. Berger, "Neutron Radiography," Elsevier Publishing Company, Amsterdam/London/New York, 1965
6. H. Kallmann, "Neutron Radiography," *Research*, 1, 254 (1948)
7. J. Thewlis, "Neutron Radiography," *Brit. J. Appl. Phys.*, 7, 345 (1956)
8. H. Berger, "Neutron Radiography," *Scientific American*, 207, 107 (Nov. 1962)
9. H. Berger, "A Comparison of Several Methods for the Photographic Detection of Thermal Neutron Images," *J. Appl. Phys.*, 33, 48 (1962)
10. H. Berger, "A Summary Report on Neutron Radiography," Argonne National Laboratory Report ANL-6846 (1964)

FIGURE 1



**MASS ABSORPTION COEFFICIENTS OF THE ELEMENTS**

FIGURE 2



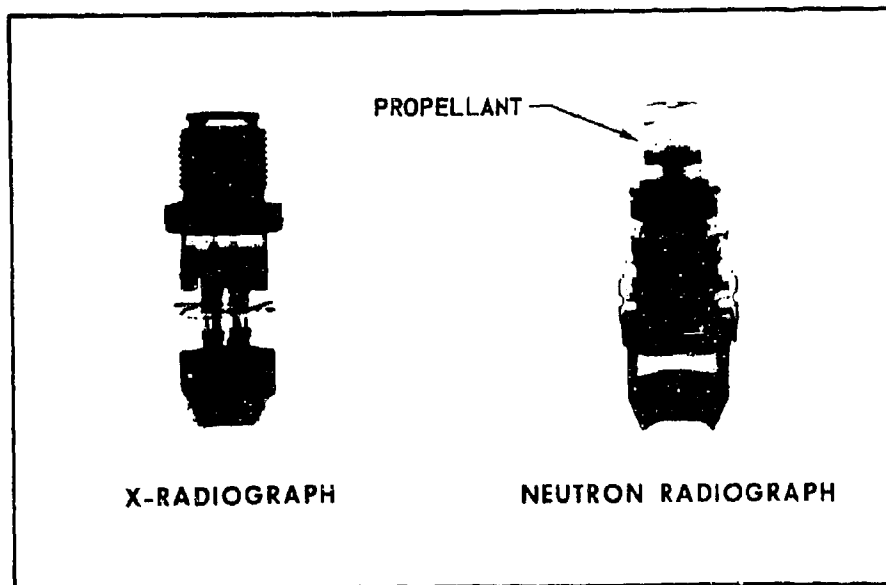
**REACTOR NEUTRON SOURCE SCHEMATIC**





**NEUTRON RADIOGRAPHIC IMAGE  
OF MASONITE  
THROUGH AN INCH OF STEEL**

**FIGURE 4**

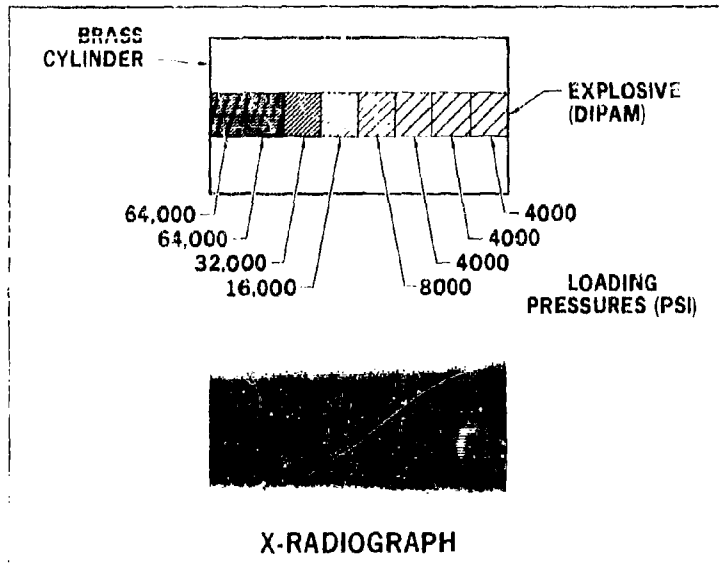


**X-RADIOGRAPH**

**NEUTRON RADIOGRAPH**

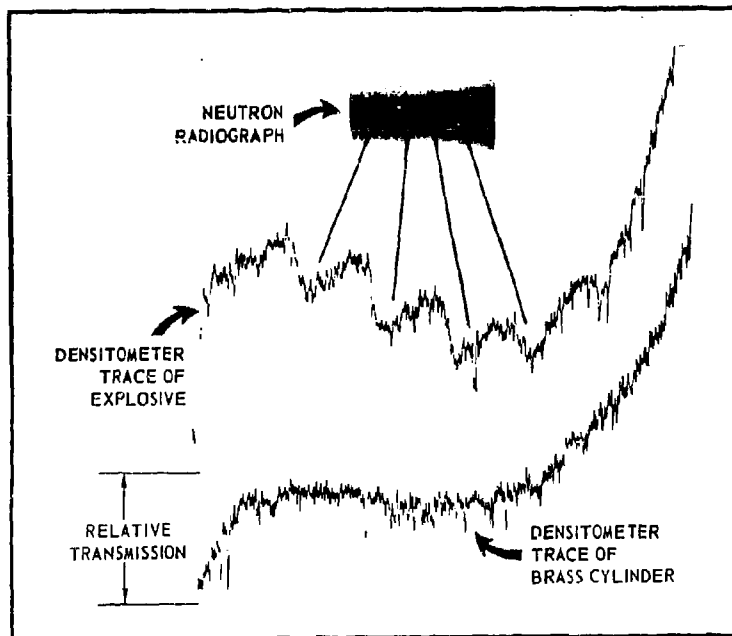
**GEMINI CARTRIDGE**

FIGURE 5



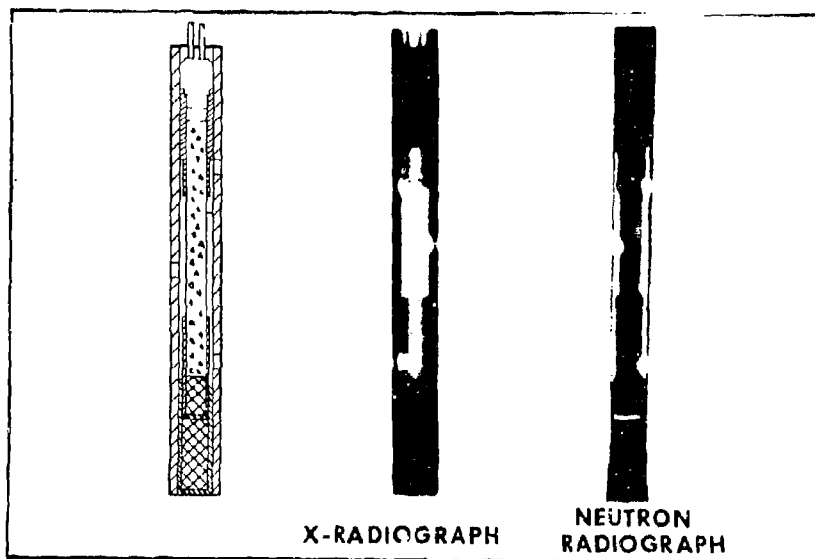
### LAB DEMONSTRATION STEP BLOCK

FIGURE 6



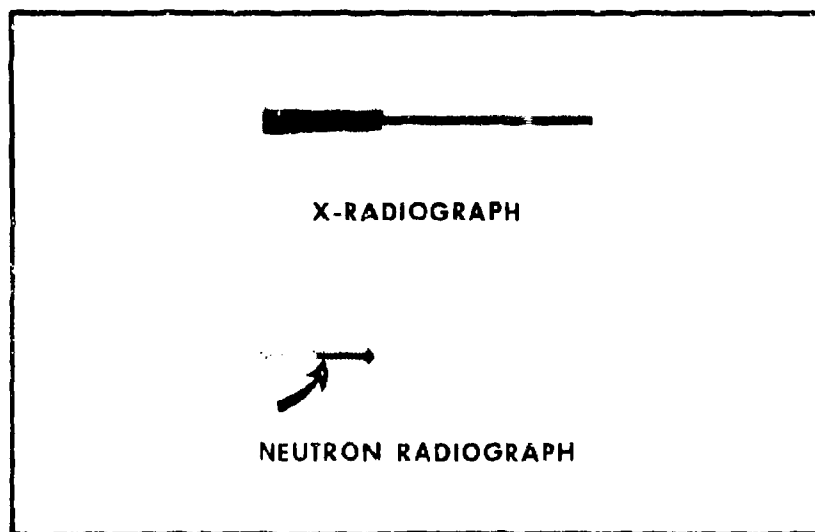
### ANALYSIS OF STEP BLOCK

FIGURE 7



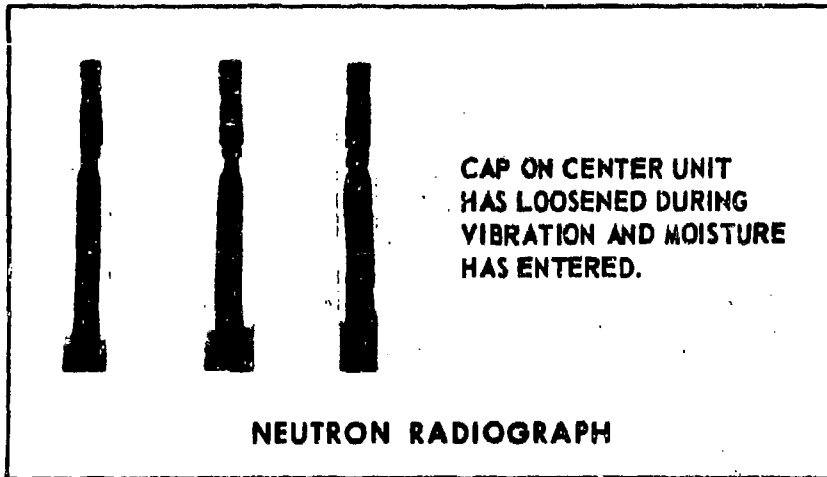
**UNDERWATER ARMING DEVICE**

FIGURE 8



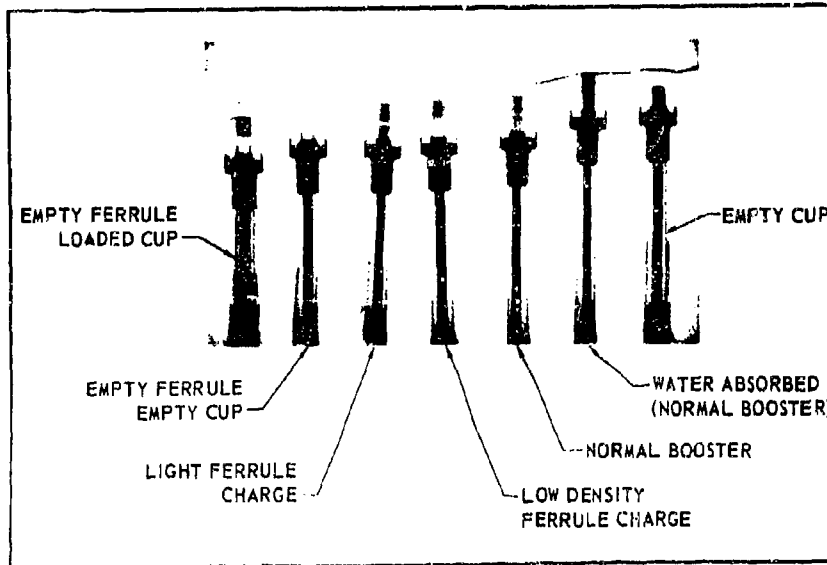
**MILD DETONATING CORD BOOSTER**

FIGURE 9



## FLEXIBLE LINEAR SHAPED CHARGE BOOSTER TIPS

FIGURE 10



## SHIELDED MILD DETONATING CORD END BOOSTERS

## DISCUSSION

The neutron radiographic techniques discussed in the paper have been used primarily as a research tool and are not yet being used on actual production items.

Mr. Burkdoll of Explosive Technology pointed out that his organization has made neutron radiographs and is available to perform such studies for others.

1-3 DEVELOPMENT OF A 15-SECOND DELAY SQUIB

by S. A. Moses  
Douglas Aircraft Company, Inc.

INTRODUCTION

The failure of a Delta Space Vehicle flight in August of 1965 was traced to malfunction of a government furnished delay squib which caused premature ignition of the third stage motor. The National Aeronautics and Space Administration, Goddard Space Flight Center (Goddard), decided to replace it with a new, high reliability device. Douglas Aircraft Company, Missile & Space Systems Division (Douglas) was contracted to prepare a specification for a new squib, to aid in the selection of a vendor and to act in a consulting capacity during the development and qualification program.

The Delta Space Vehicle has a variety of missions and, depending upon the mission, may use any of three different third-stage motors. For this reason, Goddard decided that the new squib should be capable of igniting pellets in the headcap of any of the three motors: the X-258 manufactured by the Allegany Ballistics Laboratory of Hercules Powder Company; the FW-4D manufactured by United Technology Center, and the TE-364 manufactured by Thiokol Chemical Company. Although these headcaps were physically different as shown in figures 1, 2, and 3, each included 1/2-inch thread ports for two squibs and each contained an ignition charge of boron-potassium nitrate pellets. In addition, there was sufficient space around the headcap so that the squib envelope was not critical.

## GODDARD-DOUGLAS PHILOSOPHY

The Goddard-Douglas philosophy concerning the safety and reliability of electroexplosive devices resulted in a squib specification with unusual requirements. Because the program was limited, it was necessary to gain reliability and safety without resorting to large sample-size testing. This was partially achieved by relying on the trustworthy engineering approach of "factors of safety" rather than the more prevalent statistical approach. In addition, reliance was placed on the fact that most vendors of electro-explosive devices have improved their manufacturing and inspection procedures so that the typical EED is, in itself, a more reliable device than was available a few years ago.

As an example, it was decided that the delay squib should be a single circuit device rather than the more conventional two circuit devices which have been popular. This was based on the conviction that the modern EED, having a flush bridgewire and a pressed prime, has virtually eliminated the broken bridgewire problem that plagued the industry during its early years. With a single circuit EED, some weight saving could be achieved in the wiring system and possible circuit-to-circuit problems were eliminated. Ignition reliability was gained by installing two squibs in each headcap.

## SQUIB CHARACTERISTICS

Goddard awarded a contract to McCormick-Selph of Hollister, California, for the development and qualification of this 15-second delay squib\*. A schematic design is shown on figure 4. For this development, McCormick-Selph utilized two interesting proprietary materials: (1) The initiating

\* Contract NAS7-266

explosive around the bridgewire is a high-temperature stable, non-conductive material. It has a melting temperature with decomposition after five minutes at 650°F. Both the material and its residue combustion products are non-conductive. It has a heat of combustion of approximately 1090 cal/grams.

(2) The delay column is a pyrotechnic, prepackaged in a lead tube, which is then drawn to a diameter of less than 0.1 inch. McCormick-Selph calls this Small Column Insulated Delay (SCID). This material has two major advantages over incrementally pressed delays. First, as the tubes are 300 to 1000 feet long after drawing, representative samples can be taken and tested for burning rate uniformity. In addition, the SCID, once mixed and drawn is much less sensitive to manufacturing variations than are incrementally pressed delays. The SCID in the 15-second delay squib is completely gasless and has a deflagration rate of 14 seconds per foot. Based on the Development and Qualification Program, the squib has the following characteristics at 70°F.

A. When calculated at the 95 percent confidence level:

1. At least 99.9 percent of the squibs have a five minute no fire of 1.72 amperes (approximately 2.1 watts) which exceeds the no-fire safety requirement of 1.0 ampere (1.0 watt).
2. No more than one in 10,000 squibs will have a delay of less than 13 seconds which exceeds the reliability requirement that no more than one in 10,000 squibs shall have a delay less than 10 seconds. This is based on the result of 50 firings assuming normal distribution.



3. At least 99.9 percent of the squibs will have a delay of between 14.8 and 16.8 seconds, which is a tighter tolerance than the 13.5 to 18.75 seconds required.

B. When calculated at the 90 percent confidence level:

1. At least 99.9 percent of the squibs require a minimum all-fire current of 3.47 amperes for a 20 ms pulse which exceeds the operational requirement of 4.0 amperes.

2. The squib initiator has a demonstrated reliability of 99.36 percent when fired with a 4.0 ampere, 20 millisecond pulse based on 370 firings. In addition, at 40°F and 8.29 Torr, a single squib will initiate the ignition material in the X-258, FW-4D, and TE-364 headcaps with a demonstrated reliability of 92.7 percent based upon 31 successful firings in each. With two squibs per headcap, the calculated reliability becomes 99.5 percent.

C. The squib will initiate the ignition material in the X-258, FW-4D, or TE-364 headcaps with a demonstrated factor of safety of 1.65 based on the 60 percent firing tests. This exceeds the requirement of a factor of safety of 1.25.

These characteristics are summarized in figure 5.

#### RELIABILITY REQUIREMENTS

If the delay squib had only the above characteristics, it could be termed satisfactory, but not too unusual. However, the specification did impose some unique requirements as discussed below.

Goddard-Douglas considered that the typical delay squib consists of a train of a number of pyrotechnic components as indicated in figure 6. These include a primer mix pressed on the bridgewire, a relatively gasless ignition element on both ends of the pyrotechnic delay and finally an output charge which serves to initiate the headcap pellets. The overall reliability of the delay squib then relates to the reliability of each pyrotechnic component completing its assigned task without damaging the unreacted materials in the pyrotechnic train or the squib itself.

With this in mind, the specification required that test squibs perform in a normal manner when each component of the pyrotechnic train contained only 80 percent of the amount of material to be used in the production squibs. For example, an 80 percent prime charge initiated the gasless ignition element; an 80 percent ignition element set off the delay, etc. In a like manner, test squibs performed in a normal manner when overloaded with 120 percent of the explosive material in each component of the explosive train.

With some delay squib designs, there may be the possibility of a "short" delay because of gas leakage around the delay column. When this condition occurs, flame from the ignited prime material flashes around the delay column, igniting the output charge. To guard against this possibility, the specification required that each squib should be subjected to a pneumatic pressure test after the delay column was installed (but before installation of the primer component or the output charge). The vendor was asked to determine the peak pressure produced by his particular prime when firing into the gasless ignition element above the delay. Having determined this value, each development and production squib was then leak tested at 1 1/2 times

this value. This proved to be a valuable test as leaks were found in some of the early development squibs, which, if uncorrected, might have resulted in short delays.

The ignition characteristics of the delay squib were checked with 60 percent, 80 percent, 100 percent, and 120 percent output loads in each of the three different headcaps. Although it was not feasible to perform a complete Probit type test with each headcap, the B-KNO<sub>3</sub> pellets were successfully ignited by single squibs each containing only 60 percent of the normal output load in 15 tests, five with each type headcap.

#### DEGRADATION TESTS

The usual EED specification requires that the device be subjected to a number of non-destructive tests such as a measure of the bridgewire resistance, the insulation resistance, etc. Although there is no reason to suspect that these tests might degrade the squib in some way, there appeared to be no test data available to demonstrate this fact. Goddard-Douglas decided to gather information on the effect of these non-destructive tests. Therefore, test squibs were subjected to 25 applications of tests measuring insulation resistance, dielectric strength and electrostatic discharge. In addition, test squibs were subjected to a current of 20 milliamperes for a period of 24 hours representing a small leakage through the electrical circuit. None of these tests degraded the firing characteristics of the squib.

Of a more controversial nature was a test subjecting the squibs to 25 applications of the no-fire current of one ampere. Goddard-Douglas believed that if the squib might be exposed to this environment on the launch pads,

the effects of this environment should be determined. Therefore, test squibs were subjected to 25 cycles of the 1.0 ampere no-fire current. After this test, the squibs functioned in a normal manner. In subsequent tests, two initiators were subjected to 52 cycles of the no-fire current for 2 1/2 minutes followed by a five minute cooling period. After this test the initiators were functioned at 4.0 amperes. The bridgewire burnout time of 2.6 milliseconds for the squibs tested is comparable to an average of 2.4 milliseconds for the 72 qualification firings.

#### COMPATIBILITY-STORAGE LIFE TESTS

Typical specifications for EED's require a shelf life of from three to five years. Although it is not unreasonable to believe that an EED is satisfactory after storage for this length of time, or longer, this requirement places the vendor in an unfair position. He can either say that he has no data on the storage capabilities of the materials in the EED, or that based on "engineering judgment" (or some similar ambiguous statement) the squib will meet the requirement, or in the unusual case, that he has this storage information on a "similar" device.

It was the consensus of opinion of the Goddard-Douglas engineers involved, that the five-year shelf life requirement should be validated by an accelerated life test. It was further believed that the pyrotechnic materials, by themselves, would not degrade in storage. Rather, trouble might be expected from the reaction between the contained pyrotechnics and the various goo's and gunks that some manufacturers insist on including in their EED's. It was also believed that any incompatibility between materials would degrade the performance in a relatively short time, especially at elevated temperatures.

As a result, an accelerated storage life test was included in the specification. As there appeared to be no accepted standard for such a test, the vendor was allowed to select three different elevated temperatures and storage times so that, when plotted on a log-log graph of time versus temperature, the three points were on a straight line passing through the 70°F, five year (43,800 hour) point.

McCormick-Selph stored the delay squibs at 160°F for eight hours, 130°F for 72 hours and 112°F for 336 hours. The squibs were then fired in a 10 cc pressure chamber and behaved in a normal manner.

This test is not considered severe and there is certainly no correlation between the test and actual storage conditions. However, a standardized test of this nature is necessary if the vendor is to be held responsible for assuring that his products meet storage requirements.

#### STABILIZATION OF DELAY MATERIALS

In the Aerospace Ordnance Handbook (Prentice-Hall, 1966), Weingarten points out problems concerning the poor storage characteristics of some delay materials. More frequently than not after a period of storage, delay squibs will show an increased burning time. Because of this, many (but, unfortunately, not all) vendors will pre-mix batches of delay powders and use them only after the mixed materials have been stored in intimate contact for a number of months or stabilized at an elevated temperature.

The squib specification attempted to provide for this by requiring that the delay materials be "suitably stabilized before use in accordance with best manufacturing practice". The prepared SCID used in production squibs was

aged approximately six months after being drawn to the proper diameter. It is still too soon to determine whether long term storage will result in an increased delay time. However, the burning rate did not change during this six months storage period. From this it is reasoned that no significant changes will occur during normal storage.

#### EVALUATION OF FLASH PATTERN

In addition to the typical pressure-bomb tests, this specification required photographing the flash pattern of a number of squibs. Although this might not be called a quantitative scientific test, it did provide information on the uniformity and size of the flash pattern. Interestingly, the pattern from this particular squib showed few coruscating particles although these hot sparks are normally believed to be necessary for reliable ignition of boron-potassium nitrate pellets. This is not meant to imply that the ignition characteristics of the squib wouldn't have been improved if the hot particles had been produced. Only that without these incandescent particles the squib successfully ignited the B-KNO<sub>3</sub> pellets with a 60 percent output charge.

#### ELECTROSTATIC PROTECTION

Because of a previous lethal accident caused by static electricity, Goddard-Douglas was acutely aware of this potential hazard. It was decided to take extra precautions in making this squib safe from electrostatic discharges (ESD). A review of ESD protection devices indicated that a preferential air gap between the electrical lead-in pins of the squib and the metal case appeared to offer the best protection available. This allows an electrostatic spark to jump across a small air gap without passing through the explosive primer material around the bridgewire. In the production squib, this air gap was controlled to break down between 1000 and 3500 volts dc.

A preferential air gap is protection only if it can be determined that it is preferential. That is, the primer material around the bridgewire must be insulated so that breakdown does not occur through this material. It is possible to completely insulate this explosive against any voltage likely to be encountered. However, to function properly the flame from this primer must initiate the next component in the pyrotechnic delay train. This requires an opening in the primer cavity for the flame to pass through and this, in turn, limits the amount of insulation that is practical.

Again, the concept of "factor of safety" was used in determining the relationship between the preferential gap and the insulation of the primer cavity. With development squibs, breakdown of the primer cavity did not occur at 10,000 vdc providing a factor of safety of at least 3:1 over the maximum breakdown of the preferential gap.

Production squibs of the same design were subjected to 25 discharges from a 500 picofarad capacitor charged to 25,000 volts between the pins and case. Following this test, they functioned in a normal manner.

#### RF SENSITIVITY

As part of the development program, 270 initiators were sent to Franklin Institute for RF sensitivity tests.

Of major interest was whether the non-conductive primer material used by McCormick-Selph in this squib was more or less susceptible to RF at various pulsed frequencies than conventional conducting mixes. Unfortunately, comparative data were not available at the time this report was prepared.

As an additional safeguard against RF, a Douglas lossy line (skin effect) filter is installed on the squib in the spacecraft. This filter is similar to one described by Warner and Klant at the Second Hero Congress in 1963\*. It provides from 10 to 80 db protection over the frequency range from 0.1 to 10,000 MHz.

During transportation and storage, the squib is provided with an RF tight, Faraday cage-type protective cap over the connector end.

#### CONCLUDING REMARKS

The Goddard-Douglas specification produced several concepts that are worthy of consideration by others in the industry.

For example, the techniques of underload and overload testing of the pyrotechnic components resulted in a design in which an engineer can place a great deal of confidence. This was achieved with a test program that required far less units than typical statistical testing.

The concept of pressure testing the delay column for possible leaks proved to be valuable and is one that should be considered for other delay devices.

A reasonable method of estimating shelf life should be of interest to all manufacturers of EED's. Whether the test is the one suggested in this paper or some other accelerated aging test is of little concern. However, it is desirable to reference a standardized government procedure for determining shelf life. Therefore, it is suggested that a specification outlining such a procedure be prepared.

---

\* Skin Effect Filter-Attenuator for Electroexplosive Device RF Protection, by H. B. Warner and R. H. Klant, Douglas Aircraft Company, Inc., presented to the Second HERO Congress, April 30--May 2, 1963.



And lastly, industry-wide standards are needed for determining the electrostatic sensitivity of EED's. This potential hazard is largely neglected by the industry. A better understanding of the dangers from static electricity and how to eliminate these dangers should receive the same attention that has been given to the RF hazard.

FIGURE 1

M2-1713

### TEST CHAMBER FOR X-258 HEAD CAP TESTS

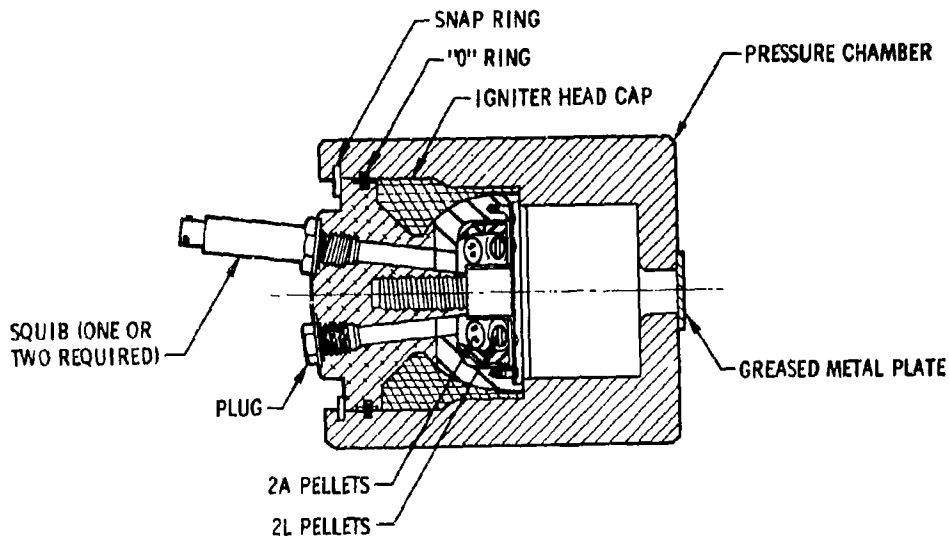


FIGURE 2

M2-1716

### TEST CHAMBER FOR FW-4 HEAD CAP TESTS

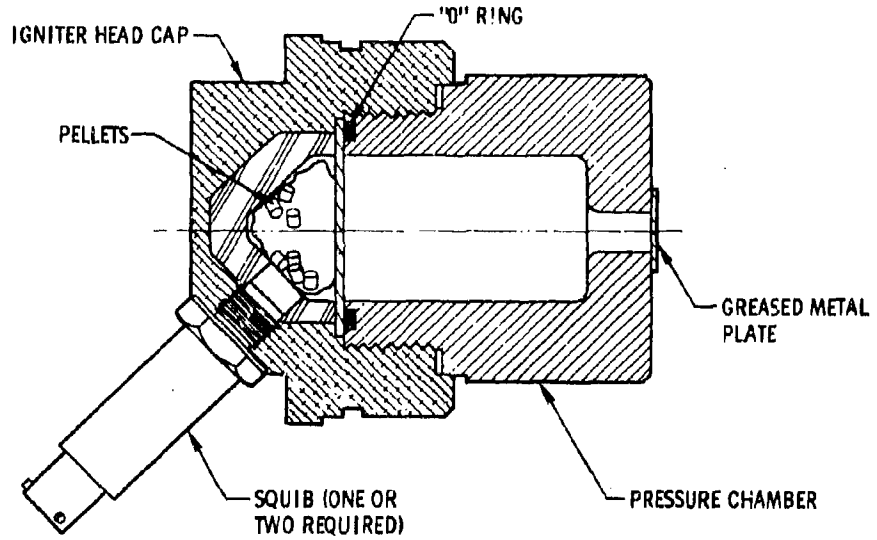
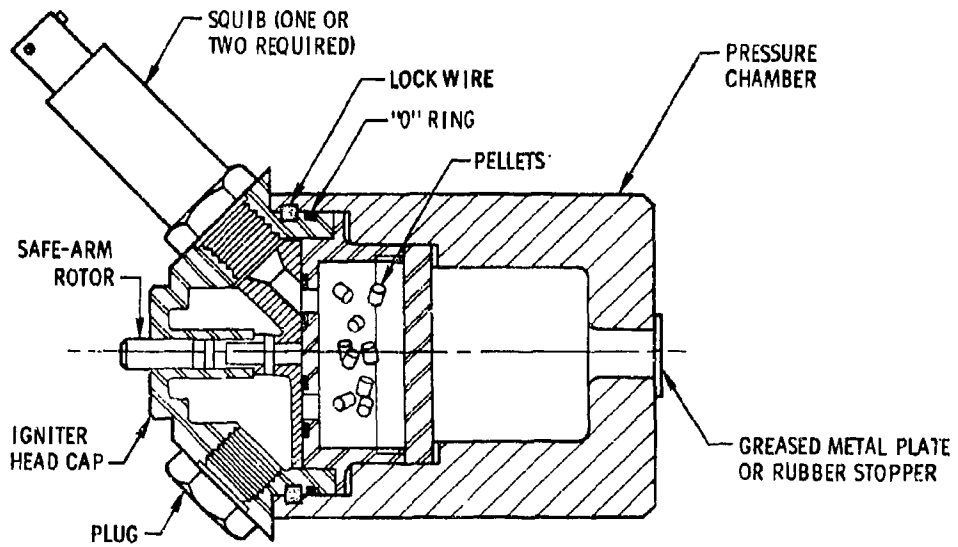


FIGURE 3

M2-1715

### TEST CHAMBER FOR TE-364 HEAD CAP TESTS



M2-1717

FIGURE 4

**15-SECOND  
DELAY SQUIB**

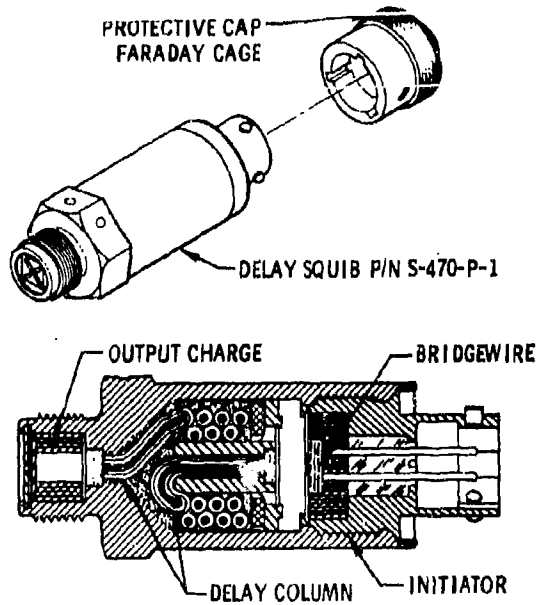


FIGURE 5

M2-1714

**DELAY SQUIB, COMPARISON OF SPECIFICATION  
REQUIREMENTS AND DETERMINED VALUE**

SQUIB CHARACTERISTIC	SPECIFICATION REQUIREMENT	DETERMINED VALUE
NO-FIRE	1.0 AMP, 5 MIN.	1.72 AMP, 5 MIN
ALL-FIRE	4.0 AMP, 20MS	3.47 AMP, 20MS
DELAY TOLERANCE	13.5 - 18.75 SEC	14.8 - 16.8 SEC
MIN. DELAY	10 SEC	13.0 SEC
INITIATION FACTOR	1.25	1.67
PRIMER RELIABILITY	—	99.36%R, 90%C
INITIATION RELIABILITY	—	SINGLE: 92.7%R, 90%C DOUBLE: 99.5%R, 90%C

FIGURE 6

M2-1718

**SCHEMATIC OF DELAY SQUIB PYROTECHNIC TRAIN**

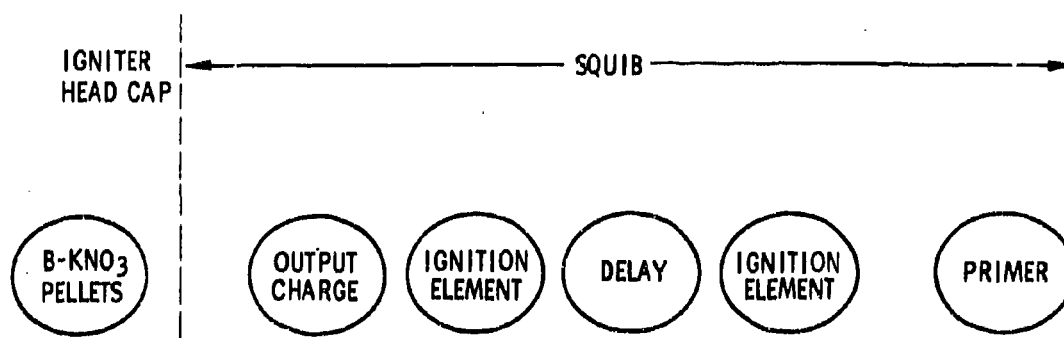


FIGURE 7

M2-1757

**CONSTANT CURRENT BRUCETON TESTS**

VALUE (1)	FRANKLIN	MC CORMICK SELPH
ALL-FIRE (AMPS)	4.05	3.47
50% (AMPS)	2.31	2.40
NO-FIRE (AMPS)	1.32	1.72
NO-FIRE (WATTS)	2.01	2.10

(1) CALCULATED AT 99.9% R, 95% C

FIGURE 8

M2-1758

**RF SEARCH TESTS**

FREQUENCY (MHz)	TYPE OF POWER	PIN-TO-PIN		PIN-TO-CASE	
		NO-FIRE (WATTS)	FIRST-FIRE (WATTS)	NO-FIRE (WATTS)	FIRST-FIRE (WATTS)
1.5	CW	2.75	3.0	2.8	-
10	CW	8.5	9.3	2.0	-
243	CW	5.0	7.5	3.0	-
2700	CW	31.0	-	22.0	-
9000	CW	20.0	25.0	25.0	-
2700	P	1.5	-	2.5	-
5400	P	1.5	2.0	2.0	2.5
9000	P	2.0	2.5	1.5	2.0

FIGURE 9

M2-1759

**RF BRUCETON AND PROBIT TESTS (1)**

TEST TYPE	FREQUENCY (MHz)	MODE	NO-FIRE (WATTS)	50% (WATTS)	ALL-FIRE (WATTS)
BRUCETON	1.5 CW	P-P	1.50	3.92	10.3
PROBIT	5400 P	P-P	1.08	2.66	6.54
PROBIT	9000 P	P-C	0.75	2.13	6.09

(1) CALCULATED AT 99.9% R, 95% C

## DISCUSSION

The investigating committee that studied the failure of the delay squib which led to the development discussed in this paper determined that the failure occurred because there was a gap between the delay column and the sleeve within which it was held. This gap could be attributed to an out-of-round ferrule. Some of the output charge was apparently pressed into this gap so that, when the squib was initiated, the flame propagated through the primary mix and up through the gap passing around the delay mix and igniting the output charge. As a result, the squib fired instantaneously rather than with a 12 second delay.

Mr. Lipnick of the Harry Diamond Laboratories pointed out that all too often people in industry and government make use of an explosive component in a current design without performing a proper statistical evaluation of the potential performance of the component in the design in which it is to be used. It is common, for example, to use an explosive component in a new design that was actually developed for a completely different purpose without adequate testing and evaluation of its possible behavior in the new and unintended application. It is often necessary to enter into a large development program to develop an item which is intended for the purpose for which one wishes to use it. Mr. Lipnick then reiterated the need for any industry or agency of the government to avoid attempts to make use of something for which it was not intended and not properly evaluated.

Mr. Lipnick made the further point that while Mr. Moses indicated in his development program that heavy dependence was placed on engineering judgment, but that his data indicated that considerable testing was done and that, in his opinion, sampling from the lot and proper statistical testing was absolutely necessary. Mr. Moses confirmed this view.

In answer to a subsequent question Mr. Moses pointed out that the term "initiation factor" which appears in Figure 5 pertains to the percentage underload which ignited the ignition pellets. An initiation factor of 1.25 is a 80% underload; an initiation factor of 1.67 is a 60% underload.

Mr. Demskey of General Electric - RSD made the point that using redundant squibs as was planned could affect the reliability estimate with respect to the delay time specifications because, if either of the two redundant units functioned prior to the shortest acceptable delay time, the function must be considered a failure. On the other hand, if either unit functioned prior to the longest acceptable delay time, the result is a success. While both Mr. Moses and Mr. Demsky essentially agreed that this effect, resulting from a redundant system, should affect the standard deviation and therefore the estimate of failure or success against specific specification limits, they were unable to agree on whether or not the mean time would shift in a redundant system.

Mr. Lipnick commented on the practical aspects of 5 year storage life tests, pointing out that his customers frequently could not find the components after 5 years.

In answer to a final question, Mr. Moses stated that the all-fire Bruceton test, the results of which are shown in Figure 5, was conducted at 70°F.

1-4 THE THERMAL STABILITY OF RDX IN SHAPED CHARGE

by

Dr. M.J. Bowman, Consulting Engineer, and  
E.F. Knippenberg, Development Engineer (1)

Within recent years flexible linear shaped charge (FLSC) has received widespread acceptance within the aerospace industry and is currently being used in a number of missile and spacecraft systems. Use of FLSC in missile stage separation applications offers several important design advantages. In particular, its use generally results in significantly lighter weight structures as compared to alternate systems. Because of these advantageous features, FLSC separation devices have been developed and successfully employed by the General Electric Company in the Nike-Zeus, TVX, and other re-entry vehicles.

FLSC contains a continuous core of high explosive encased in a thin metal sheath. Almost all FLSC manufactured and utilized to date consists of an RDX explosive core in a lead alloy sheath. Originally FLSC was fabricated with a cardioid cross-sectional shape. More recently a chevron shape has been employed, as it was found to give significantly improved cutting performance. While the chevron shape is optimum from an explosives performance standpoint, it is somewhat fragile from a mechanical point of view. In particular the thin metal sheath of this configuration has been found to be easily distorted by internal gas pressure generated during storage or

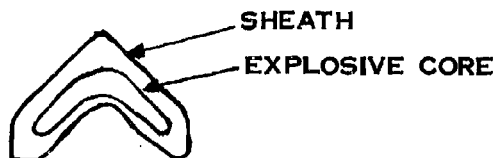
---

(1) Re-entry Systems Department, General Electric Company,  
3198 Chestnut Street, Philadelphia, Pennsylvania.

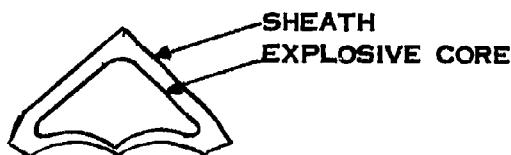


testing at elevated temperatures. When subjected to increasing internal pressure, the chevron shape has been found to gradually deform into a shape approaching a triangle as shown below. With the loss of the chevron shape, the cutting ability drastically degrades.

In actual applications the shaped charge is provided with end-seals to prevent moisture from being absorbed into the RDX core since this can destroy the detonating properties of RDX. Thus, any chemical instabilities of the FLSC constituents, or of the end seal materials, result in the generation of gases which will gradually distort the chevron shape and degrade its cutting properties. Therefore, it is essential that the ingredients and sealing materials used in the FLSC possess a high degree of chemical stability at elevated temperatures.



STANDARD FLSC



FULLY BALLOONED FLSC

CROSS SECTION OF NORMAL AND BALLOONED SHAPED CHARGE

The General Electric Company first observed deformation of shaped charge during the high temperature conditioning portion of a qualification test program on a separation subsystem. As a part of an extensive investigation to correct this deficiency, it was conclusively established that the

chevron shaped FLSC then available, even if provided with leak tight end seals, was not stable at higher temperature levels. Ballooning of FLSC was consistently observed at temperatures as low as 180°C. In various tests it appeared that part of the instability of the FLSC assemblies was due to incompatibilities of the RDX with the materials used as end seals. It was also determined that the use of an external mechanical support to restrain the FLSC sheath greatly increased the resistance to deformation. As a result of this latter finding, continuous external supports were incorporated into the designs of several separation assemblies, which were then successfully qualified.

This approach avoided rather than solved the basic problem which is to remove the cause of the instability. We therefore began a program, which was funded by AFBSD, to determine and eliminate the basic cause of the instability of RDX as used in shaped charge material.

In order to study the variables involved in thermal stability of RDX, two samples of this explosive were obtained from the Canadian Arsenal Ltd. The first sample was designated as Type B indicating that it was made by the Bachman process which utilizes acetic anhydride as the nitration medium. This results in the formation of from 8 to 10% of HMX as a bi-product.

The second sample, normally referred to as Type A RDX, was made by the British process which uses only nitric acid and results in less than 1% of HMX being formed.

Both samples were specially purified by the Canadian Arsenal for this program. Type B was recrystallized twice from hot acetone without the use of water or other solvents (a true organic recrystallization) and the Type A

was extracted with toluene (to remove the beeswax with which it had been coated) and then recrystallized once from cyclohexanone and once from acetone. The twice recrystallized RDX was obtained to eliminate the possibility of small amounts of impurities decomposing and obscuring the results from the RDX itself. Type C RDX is the unrecrystallized material made by the Bachman process.

The apparatus chosen for the study was a modified isoteniscope as shown in Figure 1. This consisted of a 4-inch diameter by 6-inch high aluminum block with several holes drilled in it to the depth of 4 inches. One hole was of sufficient diameter to hold a test tube and the others were smaller for thermometers and thermocouples. The entire block is heated from below by the electric heater which is controlled by an automatic temperature controller through a thermocouple in the block.

The test tube is placed in the hole and connected at the top to a gas measuring device by means of a rubber stopper and a section of capillary tubing. The gas measuring device is essentially an inverted burette with a stopcock at the top and connected at the bottom to a mercury reservoir and leveling bulb. The test tube with the sample at the bottom is filled with fine glass beads to reduce the free volume and obtain greater accuracy and sensitivity. It was found that if this was not done, temperature fluctuations of a few degrees led to changes in the level of mercury indicating a change in volume in the order of half a cubic centimeter.

About 60 tests were made using this apparatus (mostly at 250°F). Various materials were added to the RDX sample in the test tube before addition of the glass beads. Gas evolution was measured over a period of hours to weeks as the case demanded. Data obtained is summarized in Figures 2 through 7.

Unless otherwise specified, tests were conducted with the twice recrystallized RDX obtained from the Canadian Arsenal. (All RDX used during this program originated from Canadian Arsenal Lot C905.) Samples A and B were dried to less than 0.2% water as it has previously been found that if the RDX contained more than this percent of water, it led to sufficient pressure at 250°F to produce ballooning from this cause itself. Unless otherwise specified, the RDX used is that made by the Bachman process and contains about 8% of HMX as impurity.

There were a wide variety of theories as to the cause of the instability found in shaped charge made from RDX. Space prevents discussion of these, but they can be divided into classes and each was studied experimentally and most of them eliminated. The general classes are as follows:

1. Sheath material and/or moisture. The usual material for shaped charge sheath is antimonial lead but pure lead and aluminum have also been used. Moisture may enter into the reaction postulated between RDX and the sheath material.
2. Additives
3. Materials used in making adequate end-seals in shaped charge systems.
4. Impurities in the RDX.

#### EXPERIMENTAL RESULTS

##### Sheath Materials

First studied was the effect of varying the percentages of lead and of water on the stability of the purified RDX. Figure 2 shows the effect of increasing the amount of water from 0.75% to 2.5%. As can be seen, the

gas evolution increased from 0.6 cc to 4.8 cc in a period of 200 hours. Next, the percentage of lead (as a fine powder) was increased from 50% of the RDX weight to 1000%. In this case 12 cc of gas was evolved in the first 40 hours after which gas evolution appeared to cease. These experiments showed that both the amount of water and of lead affect the rate of gas evolution from pure RDX.

Gas analyses on similar experiments conducted at the Advanced Technology Laboratory of the General Electric Company, showed that in most cases small amounts of formaldehyde and oxides of nitrogen were formed. This indicates that a small amount of thermal decomposition of the RDX itself occurred. This, in so far as is known, is the only reaction that leads to the formation of formaldehyde. No amines were found in these samples which were relatively small. Therefore, a 100 cc sample was prepared and analyzed. In this case traces of both mono and trimethylamine were found. This confirms qualitative observations that upon opening ballooned shaped charge an odor of amines is often detected. However, the fact that it took a large sample to yield traces in the mass spectrographic analysis indicates that the hydrogen formed by the lead-water reaction does not reduce the RDX to any extent and so does not contribute significantly to the overall ballooning. This was confirmed by tests where the RDX was run under an atmosphere of hydrogen (instead of air) and the analysis indicated that there were no amines whatever formed.

These data taken together, support the general theory of a lead-water-RDX interaction but do not tell much about the mechanism. All that can be said is that there is a small amount of spontaneous decomposition of RDX

itself which may be catalyzed by the oxides of nitrogen and the lead oxide which is formed by the lead-water reaction. If the water level does not exceed that normally present in commercial shaped charge (about 0.4%), this reaction is not rapid enough to account for the ballooning phenomena, which, with commercial charge, has been experimentally found to occur in 2 hours at 250°F. It would take roughly 50 hours to develop enough gas from the lead-water-RDX interaction to cause ballooning.

Several attempts were made to determine if the antimony-lead couple was a factor. The only antimonial lead obtainable was the regular shaped charge sheath material. This was fairly hard and was filed to give a powder, which was however, coarser than the commercial lead powder used previously. It was impossible to find any discernible difference between the pure lead and the antimonial lead.

Aluminum was tested in the form of filings taken from the actual sheath of aluminum jacketed shaped charge. It was only tested with water contents below 0.25%. Under these conditions, zero gas evolution was found over a period of several days.

#### Additives

There are at least two materials commonly added to RDX in preparation of shaped charge. The first is Duponol which is an antistatic agent and which improves the working properties of the RDX during fabrication. The percentage of this is less than 0.05%. There is also a trace of rhodamine dye added to give color to the material as an aid in identification. Both of these materials were investigated to determine if they had a detrimental catalyst. Samples containing only rhodamine and only Duponol were prepared

from the recrystallized material. Only the sample containing Duponol showed any effect whatever and it was on the borderline of experimental accuracy. It was therefore concluded that if the amount of Duponol and rhodamine did not exceed that normally present, their effect was negligible. Duponol in gross amounts was known from earlier experiments to lead to rapid gas evolution. It was, however, decided to recommend that neither of these materials be used in new specifications for thermally stable shaped charges.

#### Materials Used In End-Seals

Five different end seal materials were tested for their effect on RDX in isoteniscope tests. These are epoxy resins and are used to fabricate a moisture tight seal at the ends of the shaped charge as it is made into assemblies. Since rubber grommets and metal caps are also used in making the seal, the epoxy resin theoretically never comes in direct contact with the RDX. Faulty fabrication, or use of too much amine curing agent can result in physical contact. The end seal material in use up to the present time by General Electric Co. has been M and P-100. This uses an amine known as TETA (triethylene tetra amine) as curing agent. It has been discovered (as mentioned in the introduction) that if any free TETA comes in contact with RDX it leads to rapid gas evolution and, at elevated temperatures, to deflagration. The M and P was mixed, allowed to cure overnight and then ground up. A volume of the mixture equal to approximately that of the half gram sample was mixed directly with the sample of RDX in one test and separated from the sample by a small plug of glass wool in another test. When recrystallized RDX was used, no effect was found when the two were separated by glass wool. When mixed directly, the gas evolution followed the curve in

Figure 3. The same two experiments were also performed on crude RDX. In this case, even when separated by glass wool, a slow but steady evolution of gas resulted. When mixed directly a rapid decomposition of RDX occurred as illustrated in the lower curve of Figure 3. With freshly prepared material it was found that the RDX deflagrated when mixed directly.

After confirming the fact that the end seal material in current use could lead to gas evolution, four other epoxy resins were tried. These were tested with Type B RDX and mixed directly, rather than being separated by glass wool. The results are summarized in Figure 4. CONAP was found to be the best with the next best being Scotchcast No. 10. Metagrip and Armstrong C7 were better than the M and P-100 but still considerably poorer than the other two materials. Metagrip was tried freshly mixed and used immediately. In this case a deflagration occurred within 5 minutes at 250°F. Metagrip is an amine catalyzed epoxy somewhat similar to M and P-100 so that this is not a surprising result. CONAP, while the best from a stability standpoint, has poorer physical properties (particularly flexibility) than the Scotchcast No. 10. It was therefore decided to recommend Scotchcast No. 10.

Two rubber materials used in fabrication of shaped charge devices were tested. These were Q2-0046 silicone rubber and grommet rubber. In both cases some absorption rather than evolution was found. As before, the samples were in direct contact with the RDX.



### Impurities in the RDX

A theory had been advanced that the HMX was the cause of the instability of the RDX. While this seemed very unlikely because of the superior stability of HMX compared to RDX, it was tested. Type B RDX made by the Bachman process, contains up to 10% HMX as impurity. Type A, made by the English process, contains none of this material. Gas evolution tests were made on both types under several sets of identical conditions and no difference could be found in their behavior thus eliminating the HMX theory from consideration.

At this point, it appeared that a substantial part of the instability of RDX was due to the impurities that were removed by recrystallization from acetone. Figure 6 shows how the purified material compared with the crude (Type C) material. Some of the crude RDX was recrystallized and the acetone filtrate taken and evaporated to obtain a fraction with concentrated impurities. As had been expected, gas was evolved at a very rapid rate as shown in Figure 7. This establishes the fact that the impurities in the RDX are the most important factor in gas evolution leading to ballooning of shaped charge.

It would be desirable to have a qualitative means for measuring the degree of instability of various types of RDX. The isotherm-gas evolution method appeared promising to fit this need. At 250°F the rate of gas evolution, while considerably different, is too slow to be practical. Accordingly the temperature was raised, first to 275°F and then to 300°F. At 300°F, the difference in rate becomes pronounced as shown in Figure 5.

It was of interest to determine how many recrystallizations are required to obtain material of satisfactory stability. Figure 8 shows the effect of one, two and three crystallizations from acetone. The crude material is off scale at the right of this figure. We see that even one recrystallization improves the material drastically. It should be emphasized that recrystallization is used in the true chemical sense. It means that the RDX is completely dissolved in boiling acetone then cooled in an ice bath and permitted to crystallize slowly. It is filtered rapidly and no water or other solvent is used at any step in the process.

#### STABLE SHAPED CHARGE AND FORCED BALLOONING TESTS

The Ensign Bickford Co. prepared a sample of "stable" shaped charge, for our experiments, made from RDX which had been recrystallized three times by the Canadian Arsenal. Duponol and rhodamine were not used in this lot. This "stable" shaped charge was tested and compared with the regular commercial material in forced ballooning tests as described in subsequent paragraphs.

The ballooning of the shaped charge depends both on time and on temperature. In order to determine the limits of storability of shaped charge, artificial ballooning tests were performed by sealing the ends of a short length, placing it in an oven with accurate temperature control, and inspecting it periodically. By use of a range test temperatures in separate experiments, a curve was plotted. Extrapolation of this curve gives the life at any temperature below the minimum temperature at which it was tested.

Difficulty was experienced in making adequate seals on the ends. The best method found was to insert the end of the piece of shaped charge into an aluminum cap. The cap is then filled with glass wool and about half of the cap and a half inch of the shaped charge sheath covered with a heavy coat of epoxy resin.

The adherence of the epoxy to the lead sheath has been shown to be the place where failure occurs due to inadequate bonding. It is not surprising that reliable plastic-metal bonds cannot be made when it is realized that the bond is subject to some internal gas pressure even at low temperatures and that as the ballooning phenomena is approached, the internal pressure reaches 50 psi with attendant sheath deformation. The preparation of the lead surface is of importance and it should be carefully brushed to remove the lead oxide coating that is always present on metallic lead. In using a stiff brush the natural way to brush shaped charge is lengthwise. If this is done, very fine scratches, that can only be seen under magnification, are made in the metal. These scratches are not completely sealed by the viscous epoxy resin. Lateral brushing, though difficult, was found to give somewhat better bonding between the lead and epoxy. Practically no difference was found among the epoxys from the standpoint of adherence. The final choice of Scotchcast No. 10 was made on the basis of thermal stability and flexibility.

In the artificial ballooning tests, 6 inch pieces of shaped charge were cut and the ends sealed as best as possible by the method described. About 6 such samples were placed in an oven preheated to the desired test temperature. In the tests at lower temperatures they were inspected daily for ballooning. At the higher temperatures they were inspected at shorter inter-

( ) vals (as short as 15 minutes at 350°F). The start of ballooning usually began in several hours at the higher temperature which may well be due to the water vapor. This was defined as a 10% change in the width of the shaped charge. Full ballooning was defined as deformation of a portion of the shaped charge (usually between one half and one inch) to the point where the V-groove was in line with the bottom of the legs of the chevron, thus forming approximately a triangle.

First of all, the behavior of the standard commercial shaped charge was determined. These results are shown in Figure 9. This commercial shaped charge was run as a comparison with the shaped charge made by Ensign Bickford Co. using the purified RDX (the "stable" shaped charge). Similar tests were conducted on the stable shaped charge (results are also shown in Figure 9). With the stable shaped charge ballooning was obtained at various temperatures down to 260°F. Below that temperature ballooning could not be obtained even in extended periods. For this reason, 6 feet of stable shaped charge was cut into 1 inch pieces and placed in the isoteniscope to measure gas evolution. It was found that in over 500 hours at 220°F, about 1.0 cc of absorption took place. At 240°F there was about 0.2 cc of evolution in the first 7 hours and then slow absorption took place. In over 600 hours there was about 0.3 cc absorbed.

This corresponds to the results found in the oven tests at 240°F. It was found that the shaped charge began to balloon in about 3 hours, stopped after it was approximately 25% ballooned, and did not balloon further in several hundred hours. Examination upon completion of the oven test indicated that several shaped charges had developed leaks. However, several were still

intact and should have developed ballooning if they were going to. Calculation showed that the moisture content (which was out of specification being 0.4% rather than the 0.2% requested) was sufficient to produce partial ballooning due to the vapor pressure of the water alone. Previous tests have established that it takes between 50 and 100 psi to produce ballooning. A water content of 0.4% is just sufficient to produce an internal pressure at the lower end of this range (due to the vapor pressure of the water alone at 240°F).

Samples of the stable shaped charge were run in the isoteniscope at 250°F and at 300°F for the purpose of giving a correlation with the behavior at lower temperatures. It was found by this method that between 0.3 and 0.4 cc of gas per foot of shaped charge are evolved in the time in which the oven test had indicated full ballooning had taken place at these temperatures. This gives a quantity of gas to expect for full ballooning. Since 6 feet of stable shaped charge were used in the lower temperature isoteniscope tests, it would have been expected that about 2.0 cc of gas would be evolved for complete ballooning. As stated, slight absorption at the lower temperatures was actually found.

It is therefore concluded that, IF THE MOISTURE CONTENT IS HELD BELOW 0.2% the stable shaped charge is good indefinitely at 240°F. At 220°F (even with the higher percentage of water), it is stable indefinitely since the vapor pressure is insufficient to produce an internal pressure above 40 psi.

#### IV. CONCLUSIONS

Based on the above experimental data certain conclusions have been reached, which are summarized as follows:

1. The lead-water-RDX interaction does lead to the evolution of gas, but at a very slow rate. The ballooning of shaped charge cannot be explained on the basis of this reaction alone. The following was also found:
  - a. An increase in the percentage of lead (surface area of contact) causes an increase in the rate of gas evolution.
  - b. An increase in the percentage of water leads to an increase in the rate of gas evolution
2. Hydrogen, even if formed by the reaction of lead and water, does not react with RDX appreciably to form volatile amines.
3. The presence of aluminum of the type used in sheath materials, does not lead to evolution of gas. Aluminum is several times as strong as lead (tensile strength roughly ten times as high) and it was not possible to get ballooning even at 350°F as the end seals consistently failed first. It is therefore concluded that, with aluminum sheathed shaped charge, ballooning will not occur until a high internal pressure has been generated. It is probable that the seals will fail before this necessary pressure is reached.

4. Any PbO formed by the reaction of water and lead does not act to accelerate the decomposition of RDX.
5. The presence of HMX has no effect on the stability of RDX.
6. Duponol (an antistatic agent) in the amounts usually present causes only a slight increase in gas evolution. Duponol in gross amounts is known to lead to thermal instability.
7. Rhodamine (a dye) in the amounts usually present in shaped charge does not affect thermal stability of RDX.
8. No fibers were found in the raw RDX upon microscopic examination of the two samples that were available. From this it has been concluded that raw RDX is thermally unstable even in the absence of fibers, although undoubtedly it is less stable if cellulose fibers are present (as has been reported).
9. M and P-100 (the epoxy resin presently used in Mark-6 shaped charge assemblies) will cause rapid gas evolution IF IT COMES IN CONTACT WITH THE RDX CORE. This may occur through faulty preparation of the assemblies. Vapor contact is to be avoided particularly with over catalyzed M and P-100 which will contain free TETA.
10. Other epoxys tested as replacements for the M and P include: Metagrip, CONAP, Armstrong C7 and Scotchcast No. 10. CONAP, even in direct contact with RDX, evolved only a small amount

of gas. However, its physical properties (flexibility particularly) make it undesirable for use. The second best from a gas evolution standpoint was Scotchcast No. 10. It has acceptable physical properties and its use is recommended.

11. The largest part of the thermal instability of "raw" RDX comes from the impurities which it contains. There are at least 50 of them and it is impossible to identify any particular ones that are detrimental. The chances are that many of the possible impurities have poorer stability than the RDX itself. There are others, notably HMX, which are more stable.

It has been shown, both by isoteniscope-gas evolution tests and forced ballooning tests on shaped charge itself, that these impurities can be removed by recrystallization from acetone. It is important to note that a TRUE RECRYSTALLIZATION is required using differential solubility and no water in any form. The term recrystallization is used in the explosives industry to include a variety of processes in which water is added while cooling or evaporating.

12. It is necessary to dry the RDX at elevated temperatures (65°C to 80°C) under reduced pressure with a stream of DRY air flowing over the surface or through it. This is required for two reasons. First calculations have shown that if the water content is above 0.2%, ballooning of the 15 grain, lead sheathed shaped charge may occur due to the vapor pressure of the water alone. Secondly, if this is not done the RDX may not be dried homogeneously and local concentrations of water several times the average value may be found.



13. By use of highly purified RDX, keeping the water content of the RDX below 0.2%, and using improved and seal materials, shaped charge can be made that is stable indefinitely at temperatures to 240°F.

#### DISCUSSION

All of the questions put to Dr. Bowman are quite adequately answered in the text of the paper so will not be reprinted here.

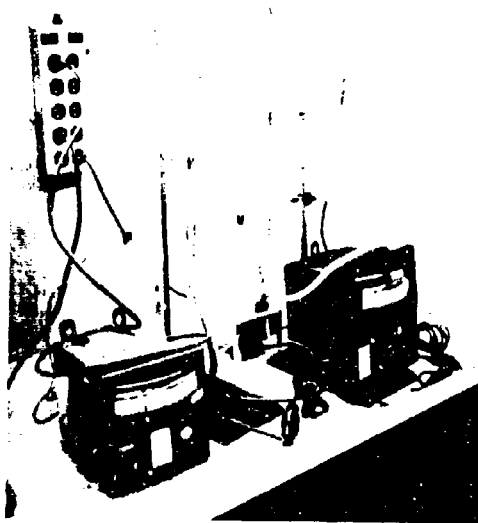
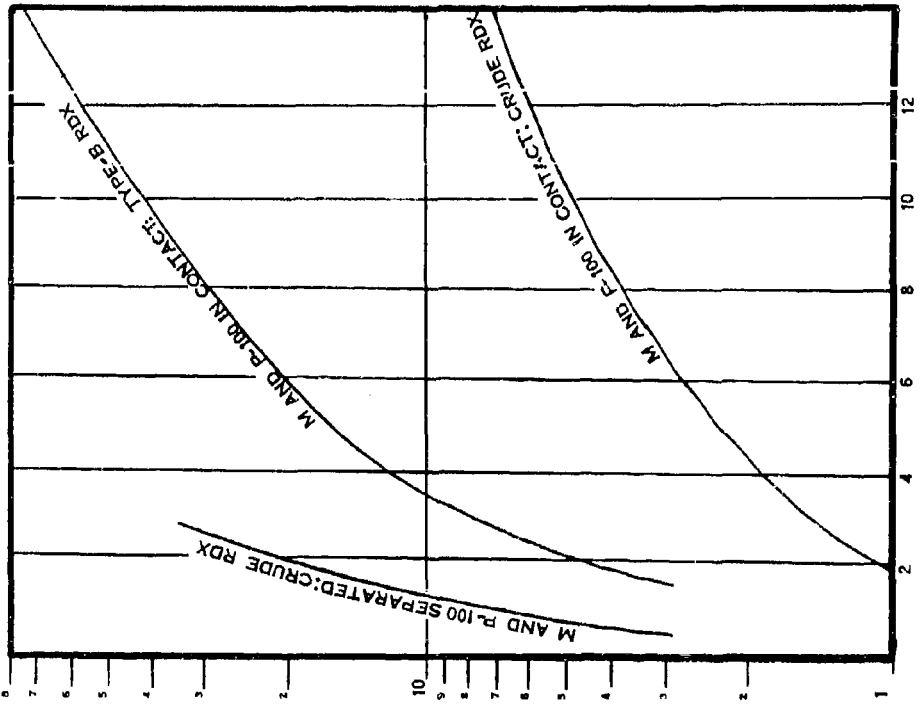


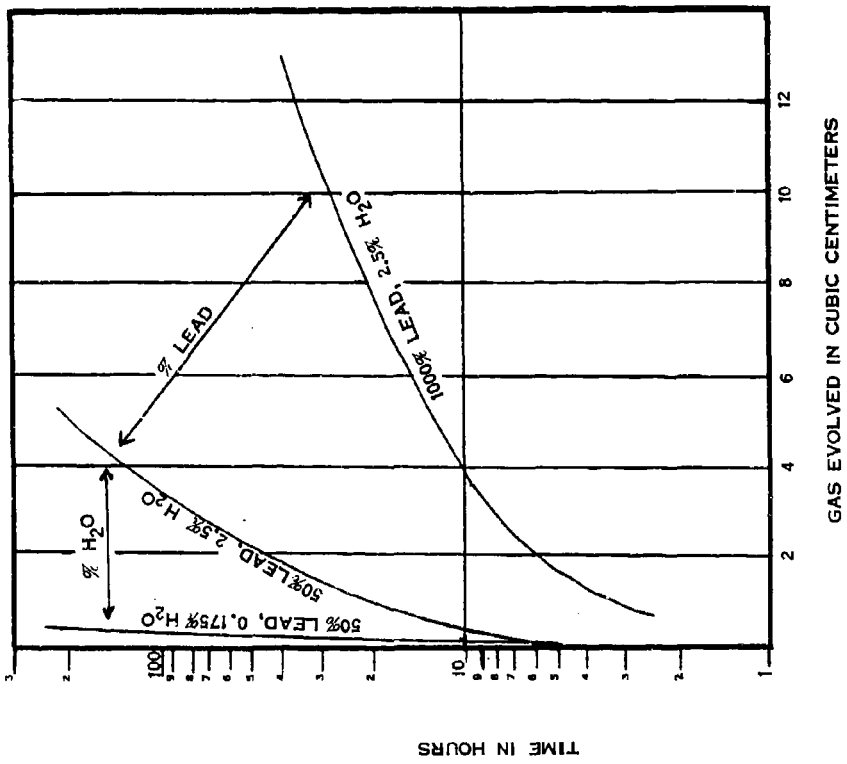
FIG. 1 APPARATUS



GAS EVOLVED IN CUBIC CENTIMETERS

THE EFFECT OF M AND P-100 ON RDX

FIGURE 3



GAS EVOLVED IN CUBIC CENTIMETERS

THE EFFECT OF PERCENTAGE CHANGE OF LEAD AND WATER ON TYPE B RDX

FIGURE 2

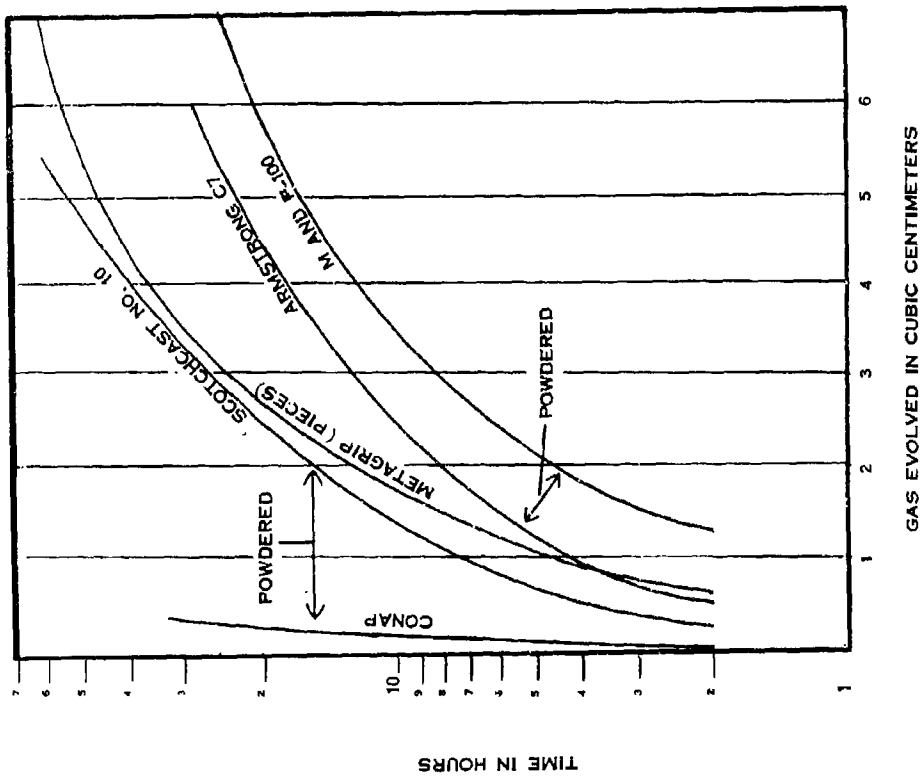


FIGURE 4 COMPARISON OF M AND P-100 WITH OTHER END SEAL MATERIALS

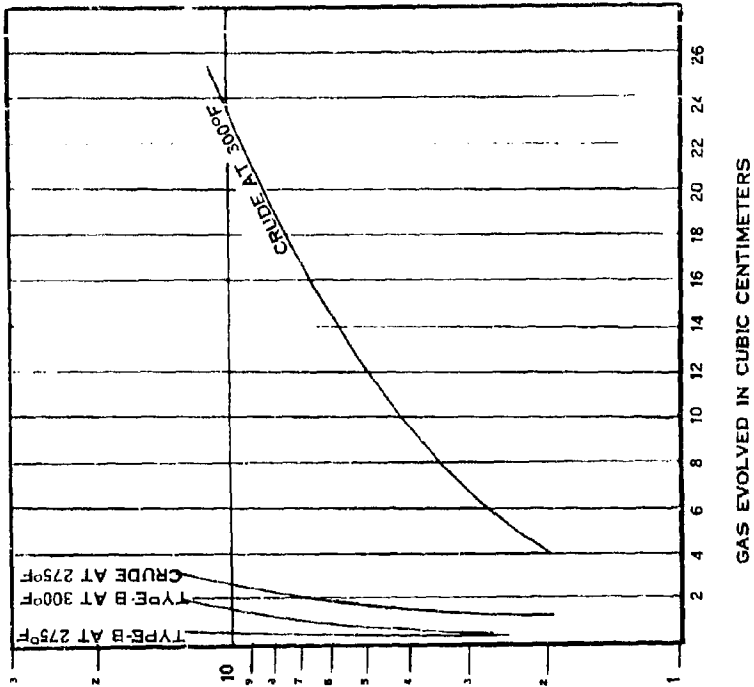


FIGURE 5 USE OF THE ISOTENISCOPE AS A QUALITATIVE MEASURE OF RDX PURITY

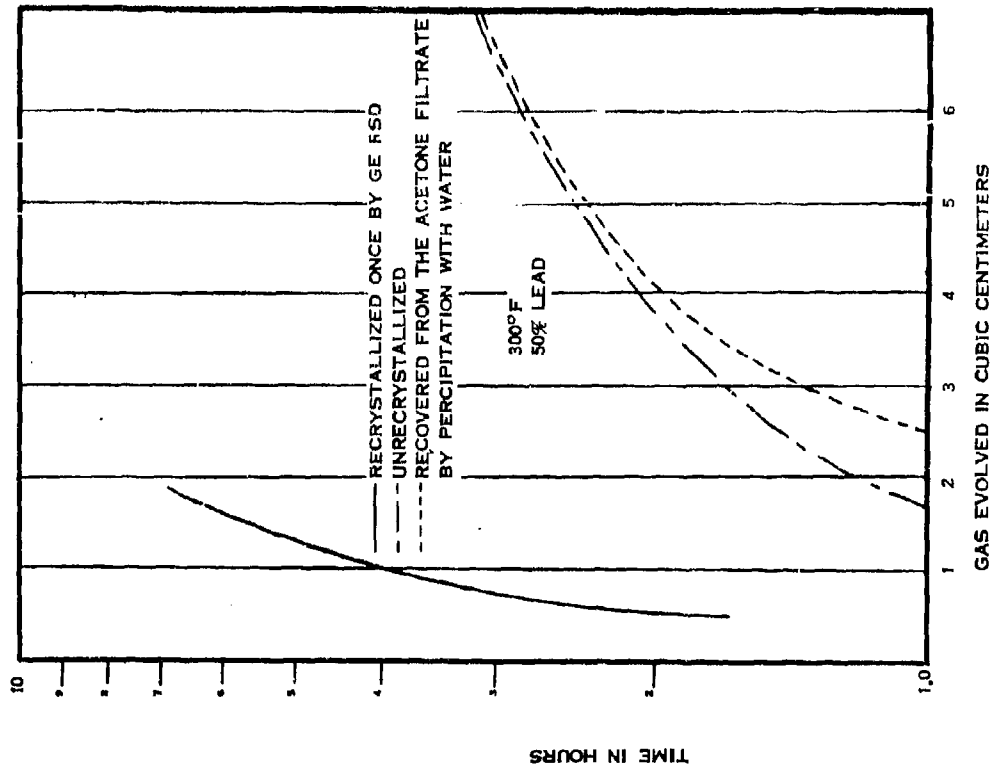


FIGURE 5 COMPARISON OF RDX BEFORE AND AFTER RECRYSTALLIZATION

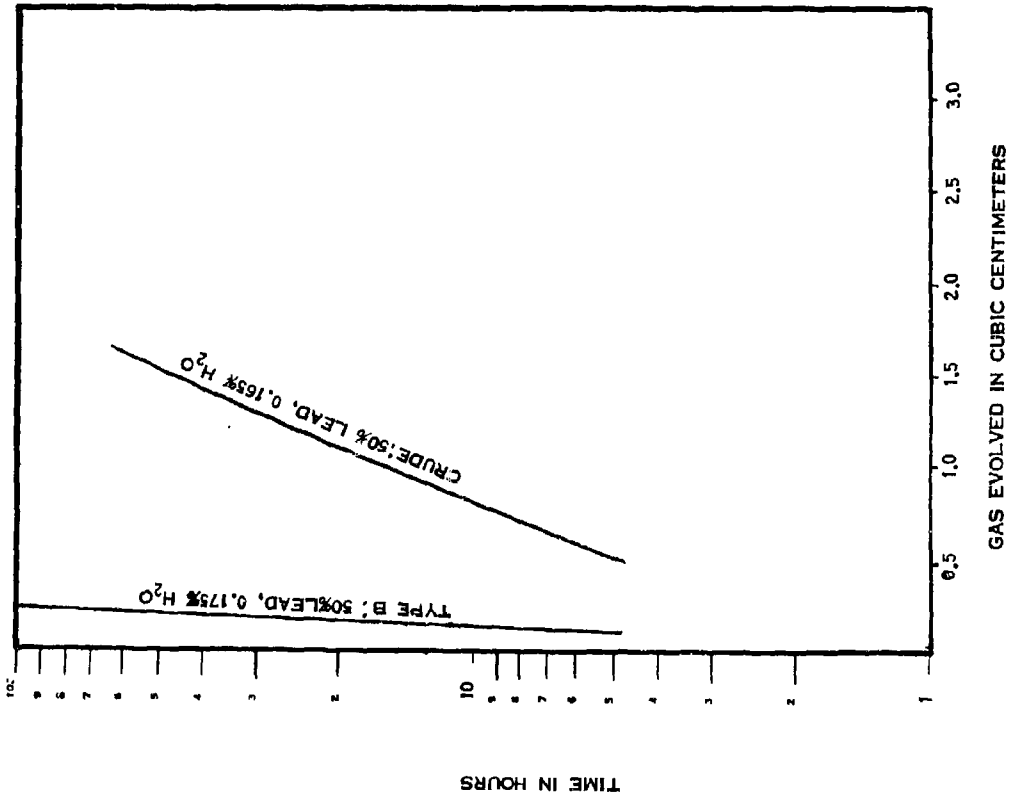


FIGURE 6 COMPARISON OF TYPE B WITH CRUDE RDX

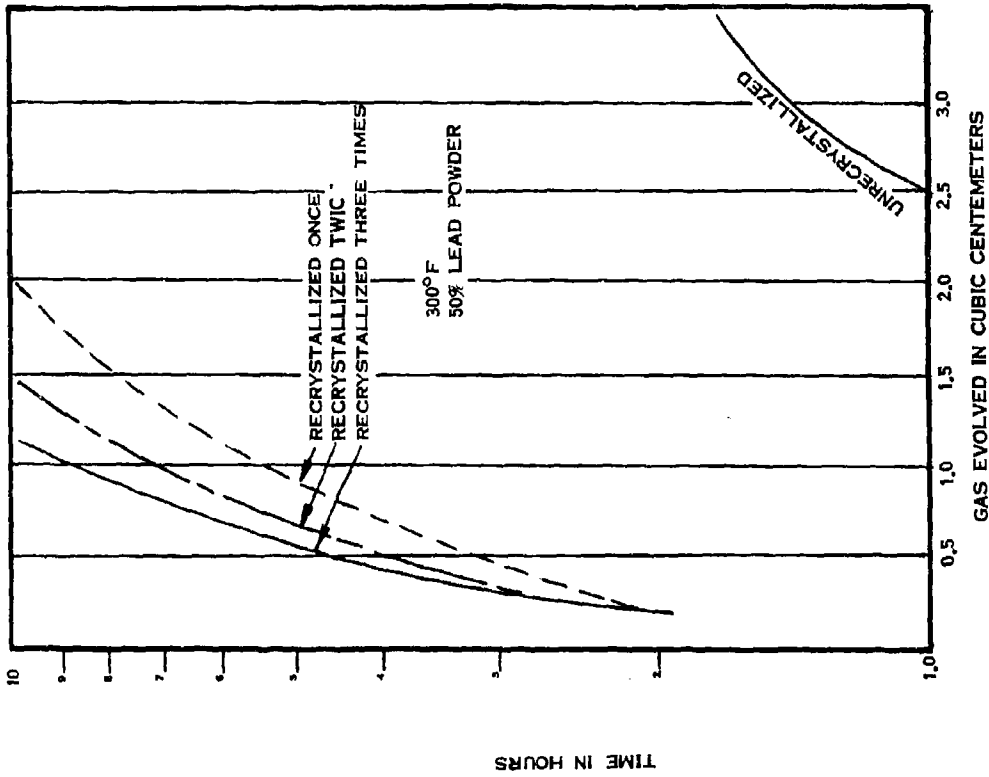


FIGURE 8 EFFECT OF VARIOUS NUMBERS OF RECRYSTALLIZATIONS

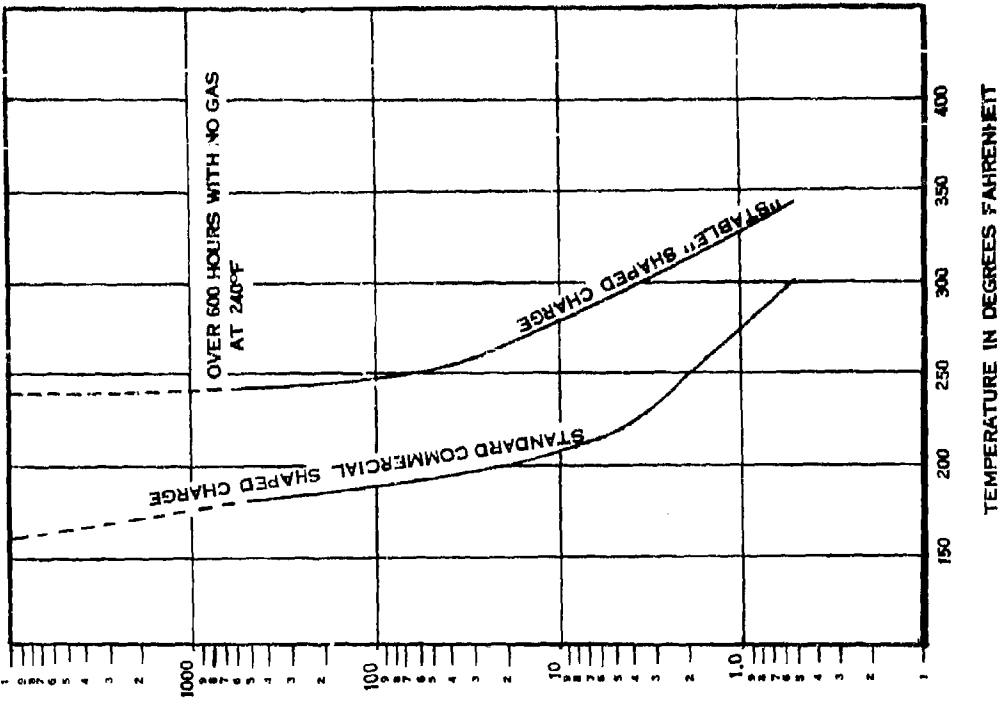


FIGURE 9 TIME FOR COMPLETE BALLOONING

1-5 MEASUREMENT OF EXPLOSIVE OUTPUT

M. L. Schimmel and V. W. Drexelius

McDonnell Douglas Corporation

St. Louis, Missouri

INTRODUCTION

The prime reason for using ordnance devices in aerospace applications is as a lightweight source of energy. Increasing usage has generated a need for a higher degree of precision in determining output in terms of work units rather than comparative methods heretofore available. It was stated most succinctly some ten years ago by Jacobs when he said a perennial question concerning explosives is "How much work can the explosive perform upon its environment when it is detonated?", Reference (1). Three years ago at the most recent Electric Initiator Symposium, Menichelli presented a comprehensive review of explosive output tests in use at that time. These included the Trauzl Lead Block, sand bomb, lead disc, steel dent, gap type and pressure bomb tests, Reference (2).

At McDonnell Douglas Corporation, a device has been developed based on the use of calibrated honeycomb which absorbs energy quantitatively as it is crushed, References (3) and (4). This device offers five advantages:

- 1) It measures the output of a wide spectrum of ordnance devices.
- 2) Each honeycomb sensing element can be accurately calibrated prior to and after use.

3) Output measurements provide an index of the ability of a donor to initiate an acceptor, and the amount of mechanical work a device can perform.

4) For a given strength honeycomb, amount of crush is directly proportional to energy output, and a wide range of outputs can be measured by selecting appropriate honeycomb. Answers are obtained in engineering units (i.e., inch pounds).

5) No electronic instrumentation is required.

The word explosive as used herein includes both detonation and deflagration.

#### DESIGN AND CALIBRATION OF ENERGY SENSOR

##### Design

The Energy Sensor, illustrated in Figure 1, is similar in design to crusher type gauges. The Sensor consists of four parts: a piston, cylinder, end cap, and honeycomb element. The honeycomb has permeated cells which allow air pressure to bleed through the cell walls and out vent holes in the end cap and cylinder.

##### Calibration

Crush strength of each individual honeycomb element is determined prior to use. Figure 2 gives crush characteristics of an element made of 5052 aluminum with 1/8 inch cells, and a density of 8.1 pounds per cubic foot. The foil is 0.002 inches thick and is permeated.

( )

The load - deformation relationship is shown for a one square inch piece, 1.5 inches long. A load of about 900 pounds is required to start crushing; however, once begun, the honeycomb continues to crush uniformly at a load of about 600 pounds, until the element is essentially "bottomed out", at which time the load increases again. The illustrated curve was obtained on a Wiedemann-Baldwin Universal Testing Machine at a crush rate of 0.02 inches per minute. Prior to use in the Energy Sensor, each honeycomb element is pre-crushed .06 inches and then calibrated over the next .04 inches. The length usable in the Sensor is the portion that crushes at a uniform load. For the above element, this length is about one inch. Additional data on energy absorption properties of aluminum honeycomb may be found in Reference (5). A question often arises as to whether essentially static calibration described above is satisfactory for dynamic response to an explosive action. References (6) and (7) describe dynamic testing of crushable material using impact rates as high as 150 feet per second. While these reports do not provide data on aluminum honeycomb, they show that 6.0 pound per cubic foot balsa wood with a static crush value of 4,800 pounds had essentially the same crush strength when impacted at 150 feet per second. Because this rate is more than double that experienced when testing detonating devices, and because the response rate of aluminum honeycomb should be at least as good as that of balsa wood, it is concluded that static calibration is sufficient.



## USE OF THE ENERGY SENSOR

Three different kinds of explosive output have been measured with the Energy Sensor:

- 1) Air and underwater explosive effects
- 2) Detonating cord output
- 3) Output of various initiators and power cartridges

For each of these applications an index of energy output is obtained by multiplying the calibrated strength of the honeycomb by the distance crushed.

### Measurement of Air and Underwater Explosive Effects

Flexible Linear Shaped Charge (FLSC) is used by McDonnell Douglas to accomplish severance of the F-111 Crew Module from the aircraft. The Crew Module is built by McDonnell Douglas Company under contract to General Dynamics Company. Because it is necessary to accomplish severance quite close to the Crew Module, and because personnel escape may be required not only in air but also underwater, it was necessary to determine the effect of the explosive charge on the Crew Module itself. To obtain this information, tests were run using the Energy Sensor both in air and underwater. Figure 3 presents these results for twenty grain per foot RDX FLSC taped to a target plate, and using Sensors mounted at the indicated distances from the shaped charge. It shows that the energy effects on structure 1 inch from FLSC are several hundred times as great underwater as in air. In a similar application, the Energy Sensor was used to measure explosive effects in air from a ten pound spherical explosive charge (Reference 8).

In this series of tests, McDonnell Douglas Sensors and piezoelectric transducers were mounted in pairs at equal distances from the charge. Measurements by the two devices were comparable.

#### Energy Output of Detonating Cord

Mild Detonating Cord (MDC) has been used for some time to perform severance and jettison functions. Figure 4 shows one such application, in cross section, with an assembly composed of a jettisonable door, MDC in a holder, and support structure. The attachment bolts are pre-drilled so as to break at the desired point when MDC is detonated. Such a design was used on the Mercury egress hatch, and also on the Gemini and F-111 Crew Module. For this type of application it is important to know energy output of MDC, as it provides an index to the strength and spacing of bolts that can be broken, as well as door ejection velocity. Figure 5 shows how the Energy Sensor is used for this purpose. MDC is positioned between the Sensor and a weight which is propelled upward by the explosion. The curves show the energy measured by the Sensor, and that imparted to the propelled weight as potential energy, for different weights. It can be seen that the sum of these energies remains relatively constant at about 250 inch pounds for two strands, each 2 inches long, of 5 grain per foot MDC with an RDX coreload. On the F-111 Crew Module extensive use is made of a new high temperature explosive, dipicramide (DIPAM), whose properties have been documented by Kilmer, Reference (9). Figure 6 shows that the energy output of DIPAM by this test is about 140 inch pounds, or 56% that of RDX.

#### Energy Output of Initiators

The primary application of the Energy Sensor has been to measure output of various kinds of initiators, detonators, power cartridges and

primers as shown in Figure 7. A photograph of this apparatus is shown in Figure 8. The initiator is inserted in a massive steel block by means of an adapter. When the initiator fires, the piston in the block is propelled forward and acts against the sensor. Measurement of energy output of the initiator is obtained by the extent of crush of the honeycomb element.

#### Detonating Cord End Boosters

Shielded Mild Detonating Cord (SMDC) end boosters are used on the F-111 Crew Module to provide output in order to function various mechanical devices, and to initiate the severance, ejection and recovery systems. The SMDC explosive train, as shown in Figure 9, consists of  $3\frac{1}{2}$  grains per foot silver sheathed DIPAM, and a ferrule and base charge of hexanitrostilbene (HNS-I). Properties of HNS-I are described in Reference (9). Background on the development of this explosive train at Naval Ordnance Laboratory, White Oak, is given in Reference (10). The end booster cup material is critical from the standpoint of explosive propagation, as described in Reference (11). It is .004 inch stainless steel, and the diameter is .156 inches. The explosive effects from the MDC are completely confined in the stainless steel tubing. The ferrule and cup contain 38 and 65 milligrams, respectively, of HNS-I.

1) End Booster Output for Functioning Mechanical Devices - For several F-111 Crew Module applications, SMDC provides energy to do mechanical work. Figure 10 shows an actuator in which the SMDC end booster propels a piston. An interesting feature of this actuator is that the orifice is used to meter the desired fraction of end booster energy to the piston. A second example is shown in the firing head of Figure 11 in

( ) which redundant end boosters are used to drive a deformable firing pin forward to strike a primer. For both applications, the prime concern is with end booster energy output.

2) End Booster Output for Explosive Propagation - Two different configurations of SMDC end boosters are shown in Figure 12. The figure on the right is the explosive train presently being used. The figure on the left represents an earlier design. It will be noted that the energy output varies quite significantly with compaction pressure and ferrule design. For a base charge compaction of 10,000 psi, the energy output was 130 inch pounds. Increasing the compaction to 32,000 psi increased the output to 185 inch pounds. In the production configuration the ferrule is tapered, such that essentially the entire face of the base charge is initiated, and the energy output averages about 375 inch pounds. These values of energy output provide an index of the ability of end boosters to propagate across air gaps as shown in Figure 13. The first configuration fired across a  $\frac{1}{2}$  inch gap, but failed across a 1 inch gap. For the second, the values were 1 inch and  $1\frac{1}{2}$  inches; for the third, the fire distance is more than 4 inches, and the fail distance somewhat greater than 6 inches. It is postulated that the energy delivered by the end booster is used to generate high velocity particles from the booster output charge cup which initiate the acceptor. This belief is strengthened by findings of Kilmer in Reference (10), in which he showed that for the same explosive train with no cup, the fire point was .040 inches, and the fail point was .160 inches. A detailed study of the mechanism of detonation transfer across air gaps for SMDC

end boosters has shown that energy output of the donor end booster is but one of several factors which must be considered, Reference (11).

#### Energy Sensor Operating Characteristics

Three modes of operation of the Sensor are shown in Figure 14. Even though a single strength of honeycomb is assumed, the pressure required to actuate the Sensor varies when used to measure explosive effects in air, the output of a power cartridge, or that of a detonating end booster. The end booster illustration shows that for 500 pound crush strength honeycomb, over 25,000 psi is required to initiate crushing. An indentation in the steel piston insert, shown in Figure 7, similar to the result of a plate dent test, is obtained for each detonation. However, no reasonable correlation was obtained between either the depth of the dent, or the volume of the dent and the energy output of the boosters. The rate of response of the Energy Sensor to explosive inputs is shown in Figure 15. The curves were obtained by means of high speed motion pictures (5000 frames per second) using a transparent cylinder and photographing the honeycomb compression. It will be noted that for a detonating cord end booster in which the detonation is completed in just a few microseconds, it takes approximately  $1\frac{1}{2}$  milliseconds to complete the crushing action. For the power cartridge which was loaded with double base propellant, compression begins as soon as the chamber pressure reaches the crush pressure of the honeycomb, and continues as long as the propellant burning maintains pressure above this level. When used with a power cartridge, the Energy Sensor

measures only the actual work done on the honeycomb. Almost an equal amount of propellant energy is required to pressurize the test fixture block cavity formed as the piston moves forward. There are also relatively small heat and friction losses.

#### Tabulation of Devices Tested with the Energy Sensor

The wide spectrum of ordnance materials tested and quantitated using the Energy Sensor is tabulated in Figure 16. Included are primary and secondary high explosives, propellants, ignition materials and primer mixes. The major use has been in measuring output of detonating cord end boosters loaded with HNS-I as the base charge. The Energy Sensor is used as part of the SMDC acceptance test procedure in which a minimum energy output is specified. Another interesting use has been in determining energy output of two types of M42 percussion primers. The first was loaded with Picatinny Arsenal 101 mix, and the second with a potassium chlorate, lead sulfocyanate mix. The average output of the PA 101 mix primer is about double that of the latter, namely 100 versus 50 inch pounds. Another application of this kind of measurement is shown in the Figure 17 tabulation of output for eight lead styphnate cartridges. The first group was a control, not exposed to temperature, the second was exposed to 370°F for 8 hours. The average energy output for the two groups is essentially the same, showing that output was not affected by 8 hours exposure at 370°F. These results were used to pinpoint a development test failure as caused by insufficient explosive charge, rather than high temperature degradation.

### CONCLUSIONS

1. An Energy Sensor has been developed which can be used to quantitate explosive output.
2. The Sensor directly measures explosive effects in air and underwater.
3. With appropriate accessories, the Sensor can determine the output of detonating cord, primers, igniters, power cartridges and detonators.
4. Because mechanical work output is measured, results can be directly applied to analysis of explosive devices powered by detonators and cartridges.
5. Results obtained provide an index of the gap jumping ability of detonating end boosters.

### REFERENCES

1. Jacobs, S. J., "The Energy of Detonation", NAVORD Report 4366, 1956.
2. Menichelli, V. J., "A Review of Explosive Output Testing", Electric Initiator Symposium, 1963 (Paper No. 14).
3. Schimmel, M. L., "Measurement of Explosive Output", McDonnell Aircraft Corporation Report E206, 1965.
4. U.S. Patent No. 3,263,489, "Energy Sensor", 2 August 1966.
5. Hexcel Products Inc., "Energy Absorption Properties of Aluminum Wneycomb", TSB-110, 10 January 1960.
6. Brodbeck, F., Cox, G. and Houtman, W., "Dynamic Testing of Crushable Materials for Impact Attenuation Systems", Institute of Environmental Sciences, 1967 Proceedings.
7. Burke, H. D., "Energy Absorption Capability of Materials under Static and Dynamic Loads", McDonnell Company Report E66-10-145, in preparation.

REFERENCES (Continued)

8. Sizemore, J., U.S. Naval Weapons Laboratory, Dahlgren, Va., Unpublished data.
9. Kilmer, E. E., "Annual Report on Investigation of High and Low Temperature Resistant Explosive Devices (U)", NOLTR 66-94, 24 August 1966, Confidential.
10. Kilmer, E. E., "End Booster for Heat Resistant Mild Detonating Fuse (U)", NOLTR 65-98, 6 April 1966, Confidential.
11. Schimmel, M. L. and Kirk, B., "Study of Explosive Propagation across Air Gaps", McDonnell Aircraft Corporation Report B331, 1964.



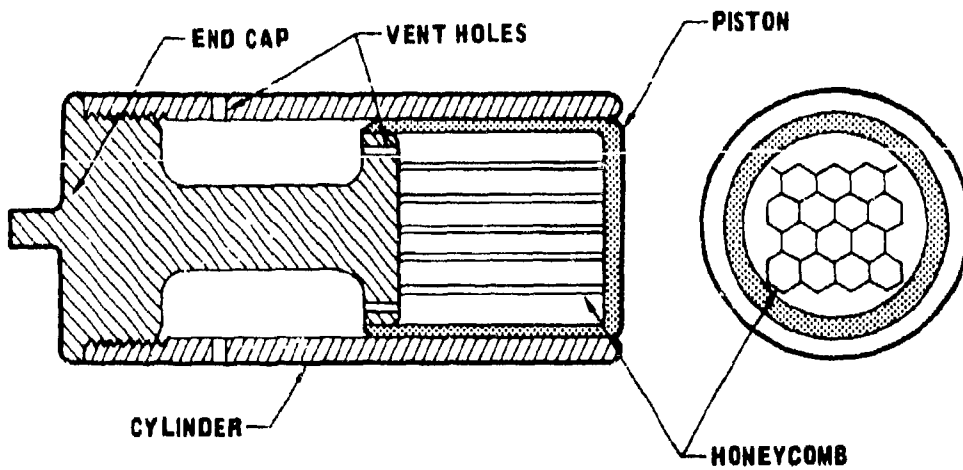


**FIGURE 1 - ENERGY SENSOR**

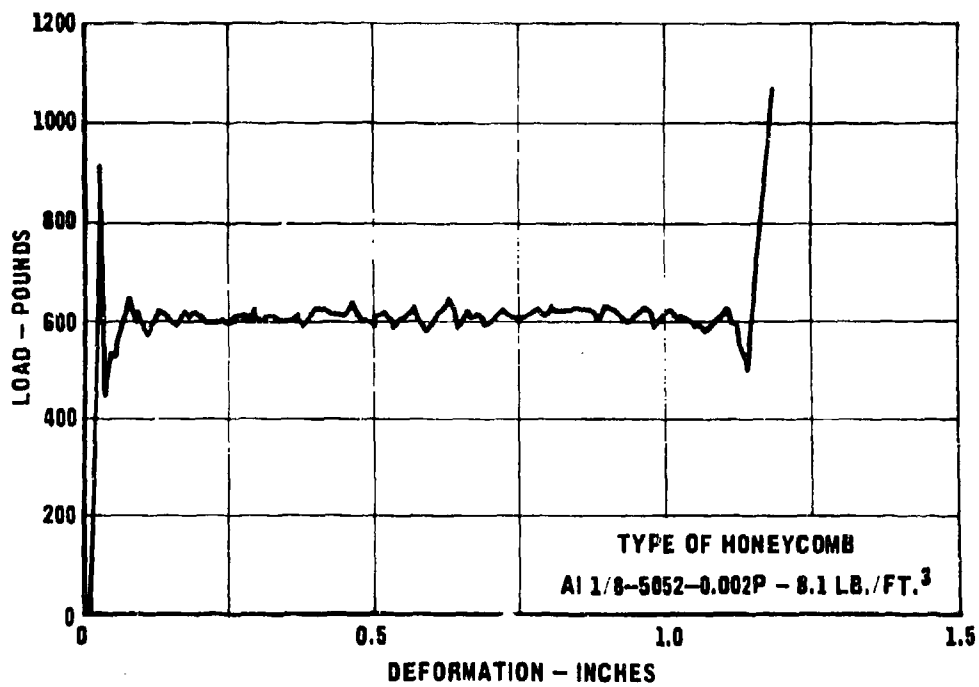


**FIGURE 2 - HONEYCOMB CRUSH CHARACTERISTICS**

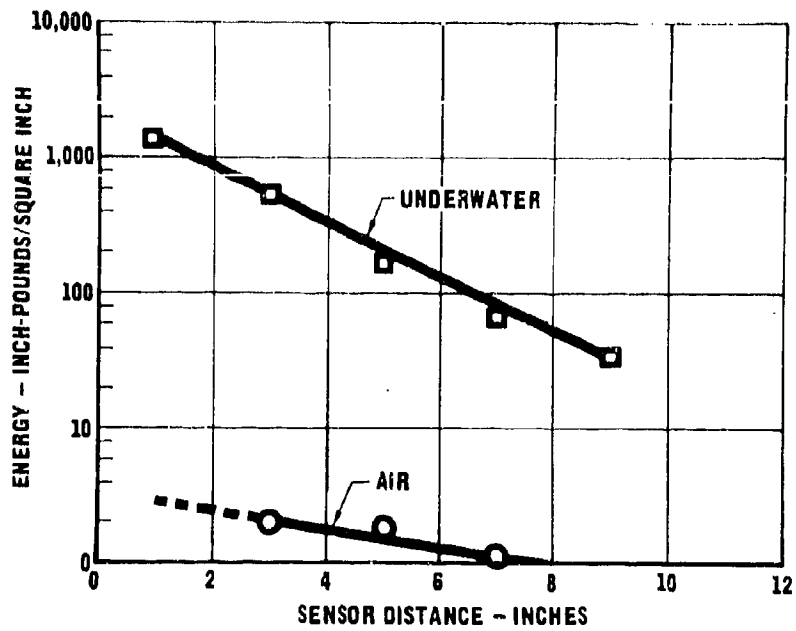


**FIGURE 3 - AIR AND UNDERWATER EFFECTS  
(20 GRAINS/FOOT FLSC)**

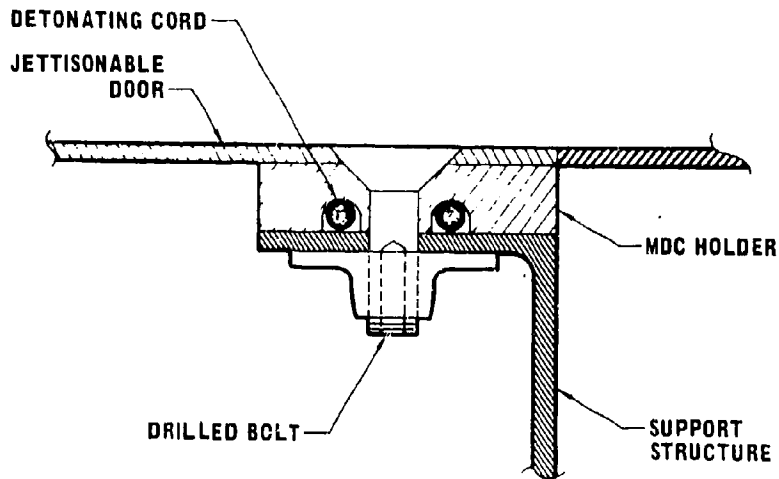


**FIGURE 4 - MDC FOR DOOR JETTISON**

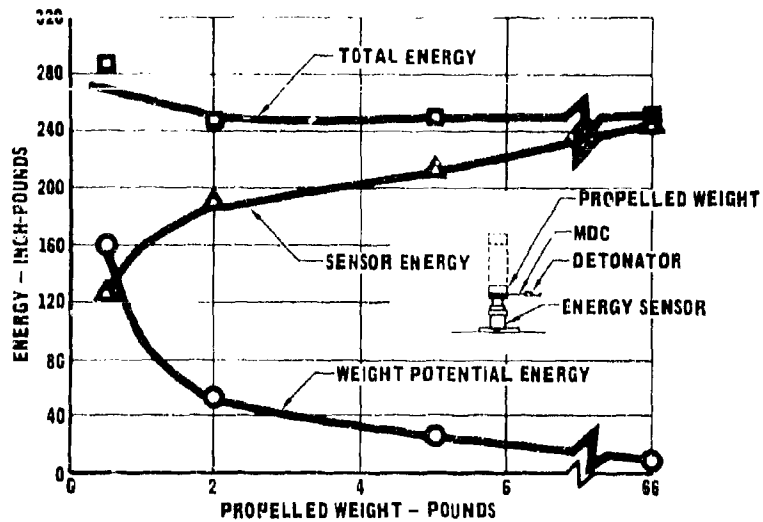


**FIGURE 5 - ENERGY OUTPUT OF DETONATING CORD  
(5 GRAINS/FOOT MDC; TWO STRANDS,  
EACH TWO INCHES LONG)**

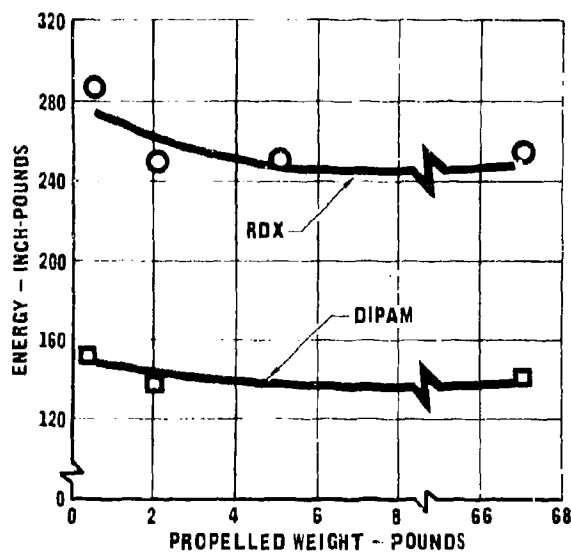


**FIGURE 6 - COMPARISON BETWEEN OUTPUT OF  
RDX AND DIPAM  
(5 GRAINS/FOOT MDC; TWO STRANDS,  
EACH TWO INCHES LONG)**

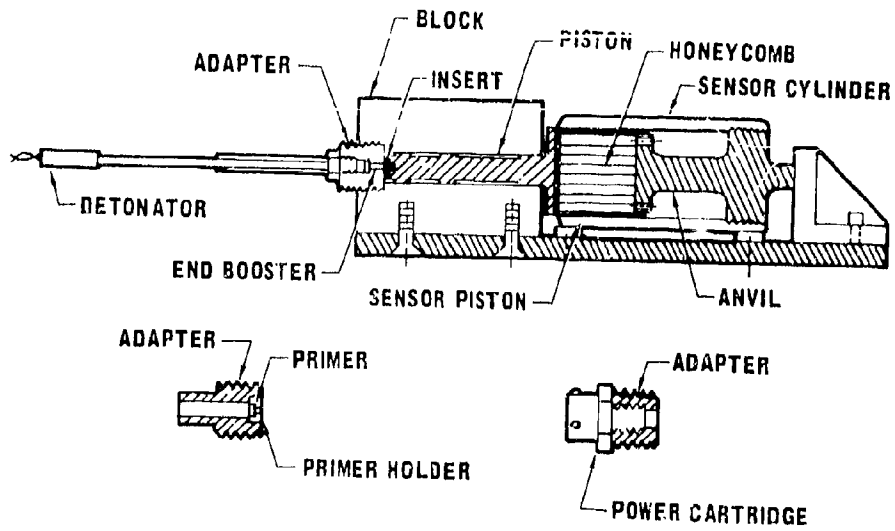
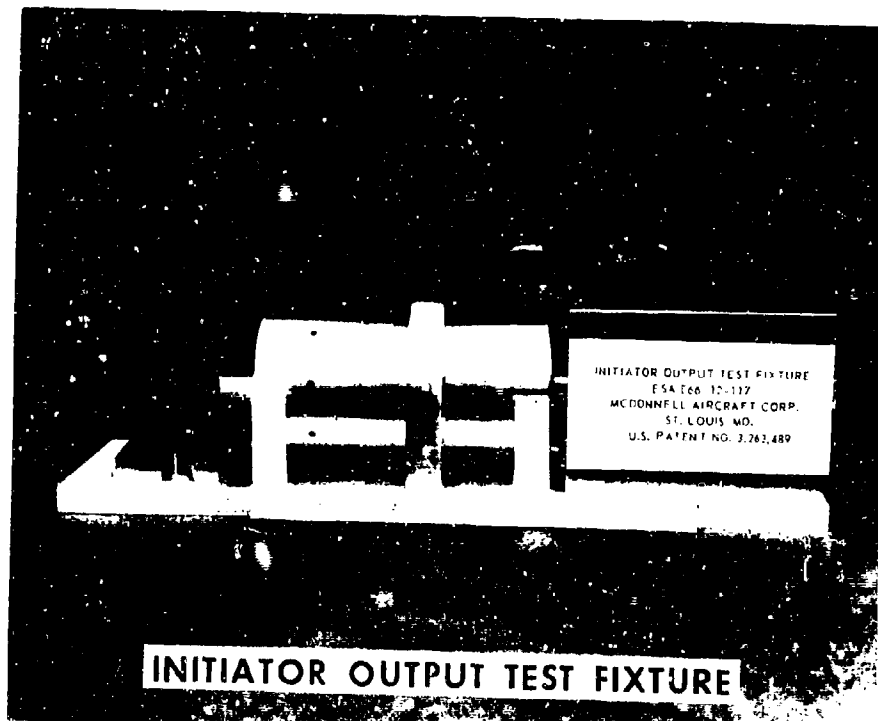


FIGURE 7 - ENERGY OUTPUT OF INITIATORS



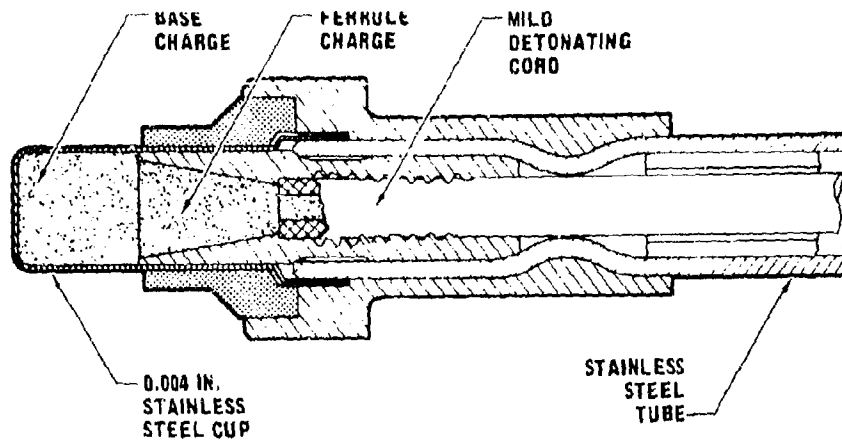


FIGURE 9 - SMDC END BOOSTER

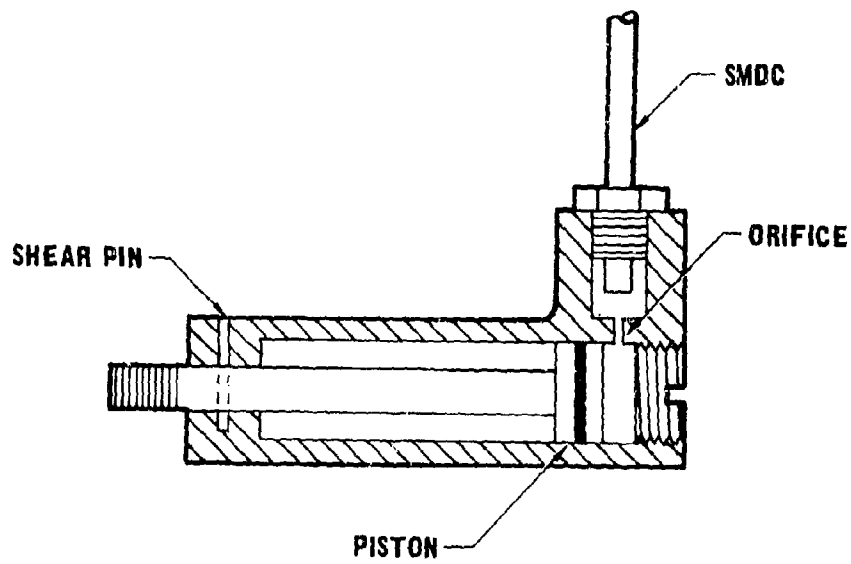
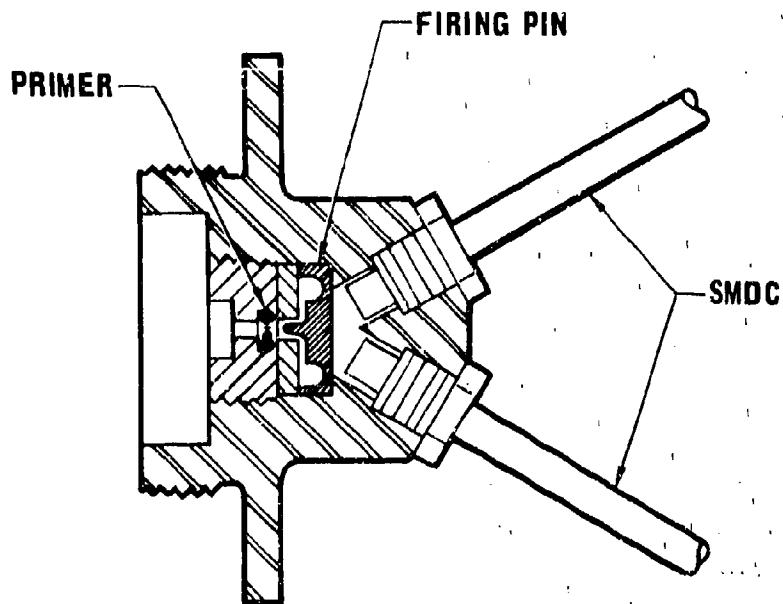
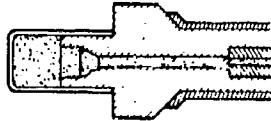
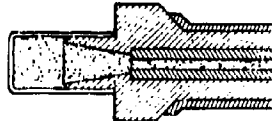


FIGURE 10 - ACTUATOR



**FIGURE 11 - FIRING HEAD**

			
BASE CHARGE COMPACTION (PSI)	10,000	32,000	32,000
ENERGY OUTPUT (INCH-POUNDS)	130	185	375

**FIGURE 12 - EFFECT OF COMPACTION PRESSURE  
AND FERRULE DESIGN ON SMDC OUTPUT**



ENERGY OUTPUT (INCH-POUNDS)	AIR GAP (INCHES)	
	FIRE	NO FIRE
130	0.5	1.0
185	1.0	1.5
375	> 4.0	> 6.0

FIGURE 13 - ENERGY OUTPUT AS AN INDEX OF PROPAGATION ACROSS AIR GAPS

ASSUME: 500 LB. CRUSH STRENGTH HONEYCOMB

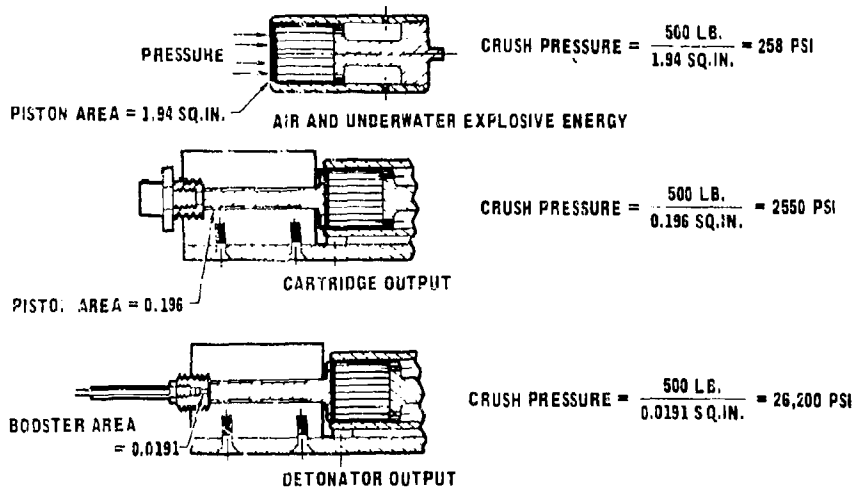


FIGURE 14 - ENERGY SENSOR OPERATING CHARACTERISTICS

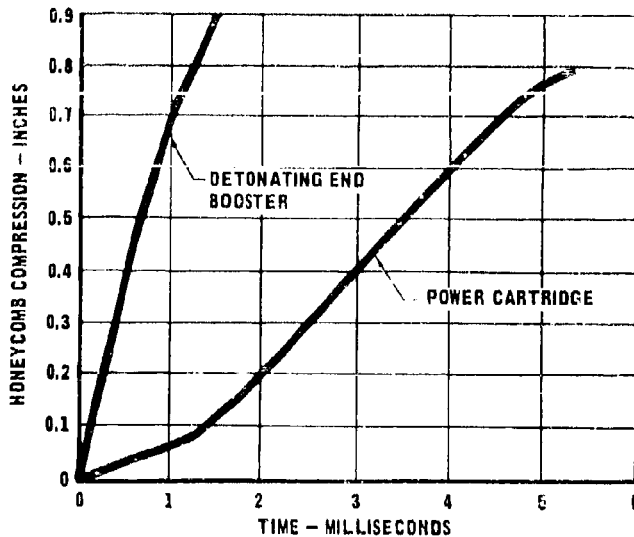


FIGURE 15 - ENERGY SENSOR COMPRESSION RATE

TYPE OF DEVICE	EXPLOSIVE CHARGE	APPROXIMATE NO. OF TESTS
DETONATING CORD END BOOSTER	RDX	20
	DIPAM	100
	HNS	1200
	PICRYL SULFONE	10
POWER CARTRIDGE	LEAD STYPHNATE	20
	LEAD AZIDE	40
	BLACK POWDER	8
	BKNO <sub>3</sub>	5
	IMR6962	14
APOLLO STANDARD INITIATOR	-	20
PERCUSSION PRIMER (M-42)	PA 101	30
	POTASSIUM CHLORATE, LEAD SULFOCYANATE	30

FIGURE 16 - SUMMARY OF DEVICES TESTED WITH ENERGY SENSOR

ENERGY OUTPUT (INCH-POUNDS)	
CONTROL	370°F FOR 8 HOURS
614	490
556	440
402	658
642	617
AVERAGE 553	AVERAGE 551

FIGURE 17 - EFFECT OF HIGH TEMPERATURE EXPOSURE ON ENERGY OUTPUT OF LEAD STYPHNATE



## DISCUSSION

It was pointed out during the question period that the device does not measure gas pressure. The device has been used successfully to measure the output of very low pressure, slow burning items which are nearly gasless in output.

In answer to specific questions from the floor, Mr. Schimmel stated that he was not opposed to the use of pressure bombs nor was he implying that the honeycomb system was necessarily superior to electronic methods of measurement.

Mr. McGirr of Atlas Powder Company made the point that having a measure of the output of a donor did not necessarily give you adequate information to guarantee initiation of the next explosive element. Mr. Schimmel agreed and stated that none of the present output tests can tell if you can propagate across a gap or initiate the next element in the explosive train. The output of the donor is only half of the problem; the other half is the sensitivity characteristic of the acceptor of which the sensitivity of the explosive, the alignment, the metal-explosive interface, the purity of the explosive, the temperature and other parameters were all factors.

Mr. Stresau of the R. Stresau Laboratory added to this discussion by pointing out that the sensitivity of an explosive cannot be expressed in terms of a single variable. As an example he noted that one could have two detonators and two acceptors such that detonator A would initiate acceptor A but not acceptor B while detonator B would initiate acceptor B but not acceptor A. Mr. Schimmel was in full agreement with this comment.

SOLID STATE TIMERS  
ACCURATE TIME DELAYS FOR ELECTROEXPLOSIVE DEVICES

Author: Louis J. Caparoni

Aerospace Components Division Laboratories  
Atlas Chemical Industries, Inc.  
Tamaqua, Penna.

An electroexplosive device will perform its function almost instantaneously when the proper energy is applied to it. The input energy necessary to set off the device can be very small. The high amplification that is possible, very small inputs to trigger large outputs, has resulted in many applications where size or weight are important. Thus we see many functions on aerospace vehicles performed by EED's. A further advantage is that they can be used with time delays: The output occurs some specified time after the input that initiates the action. This flexibility makes it possible to carry out a sequence of functions by using a variety of delay times.

Time delays can be achieved by a variety of methods; mechanical, pyrotechnic (or chemical), electrical, or combinations of these methods. All these approaches depend on some time dependent function: Frequency, either mechanical or electrical; the rate of a chemical reaction; or the rate of flow of a fluid, heat or electrical energy. In the case of frequency-based timers, the desired time is obtained by counting the cycles. In the case of a chemical timer the desired time is obtained by having the

appropriate amount of chemicals in proper configuration. The desired time for timers depending on rate of flow is obtained by having the appropriate flow restrictors, etc.

#### MECHANICAL TIMERS

Mechanical timers may depend on either frequency, or rate of flow. Typical frequency-dependent mechanical timers use gear trains and a clutter or escapement. A source of power, frequently a spring, is used to drive the gears. When the escapement or clutter has cycled an appropriate number of times, a pair of electrical contacts closes, completing the circuit to fire the EED. This type of device can range from inexpensive clutter-controlled units to very precise and costly watch-type mechanisms. While the more precise mechanisms are not temperature sensitive, none of these devices take very kindly to shock and vibration. In addition, they must be protected against contamination and dirt.

Rate of flow mechanical timers usually depend on a volume of fluid, either air or a viscous liquid, being forced through an orifice by a piston. When the piston completes its stroke it closes contacts, thus completing the circuit to fire the EED. Time for these units will vary with the temperature since the viscosity of the fluid will vary with the temperature. They are also sensitive to both contamination and corrosion.

In addition, the smaller the device, the more difficult and costly it is to get uniform timing.

#### PYROTECHNIC AND CHEMICAL TIMERS

The most common timers that depend on the rate of a chemical reaction are pyrotechnic delays, frequently built into EED's. These consist of mixtures of fuels and oxidizers which are fired by the EED initiator and in turn fire the output charge of the device. The desired delay time is obtained by the appropriate column length of mixtures of materials that have known burning rates. They are temperature sensitive: that is, the higher the ambient, the higher the burning rate. They are not sensitive to shock and vibration, but must be protected from moisture.

Other types of timers that depend on chemical reactions are seldom used because of their many problems: Approaches which depend on acid eating through a wire or diaphragm have been used.

#### ELECTRICAL TIMERS

Lumped in this group is a variety of approaches, some of which also require mechanical devices with them. Motor driven timers, for example, usually require gear trains, cams, etc. to open or close electrical contacts. These may be adjustable, and are generally bulky. They may be sensitive to dirty or corrosive environments, and may be sensitive to shock and vibration.

Electronic timers, whether vacuum tube or solid state, can use several approaches: Oscillators which may be feedback, tuning fork or crystal controlled; resistor-capacitor (RC) network; or resistor-inductor (RL) network.

The RC network timer is the most widely used. It is small in size and weight, and can provide uniform times. The timing action is obtained by charging a capacitor through a resistor. When the capacitor becomes charged to the prescribed level, it triggers a solid state switch. This then discharges energy into the EED, firing it. The firing energy can come from the line or a firing capacitor.

The accuracy of such a solid state timer depends on the input voltage, and the stability of the components in the RC network and the various compensating and controlling networks. Higher than nominal voltages to the RC network will charge the capacitor faster, thus giving shorter delay times. Likewise, lower voltages will give longer delay times. The effect of variable supply voltage can be eliminated by a solid state voltage regulating device, regulating at some voltage less than the minimum expected. Since the times obtained by RC networks are a direct function of the values of R and C, it is necessary to use stable components, that is, components whose values change very little over a wide temperature range. Commercial components are available that will maintain a repeatability of  $\pm 2\%$  over a temperature

( ) range from  $-65^{\circ}$  to  $+160^{\circ}\text{F}$ . In order to overcome changes in triggering level of solid state switches with changes in temperature (thus affecting the delay time) it is necessary to interpose a triggering network between the RC network and the switch. Thus, temperature compensation is introduced by applying a fixed bias to a triggering circuit which acts as a buffer stage to the solid state switch. Such a system shows very little temperature sensitivity.

( ) The design of a reliable, precise time delay system for use with EED's presents some interesting problems. The timers must be small, require little power, and yet be capable of transferring fairly high energy pulses rather quickly to the EED's. Conventional transistor circuits are not particularly well adapted for this service. Gain stages and power transistors would be required to handle the output energy. On the other hand, only simple circuitry is necessary with a solid state switch. Low level input pulses (especially good with long delays) will successfully trigger this high gain device to transfer the necessary high energy pulses to fire EED's.

A group of timers were built essentially as described above, with the voltage regulated to the RC network, a temperature compensated triggering network, and a solid state switch. These were used with a charged capacitor to fire a variety of EED's under adverse environments.

Table 1 shows the times obtained (without EED's) with five timers that were vibrated at 30 g's at swept frequencies from 5 to 2000 cps and back, for one hour in each of three mutually perpendicular axes. After the three hours of vibration the greatest deviation from the original time was + 1.25%.

Table 2 shows the results obtained with these same units accelerated at 200 g's for one minute in each of the three axes. The delay times were checked during the acceleration in each plane, as well as afterward. The arrows indicate the direction of the applied force, and the symbols N and S indicate the placement of the unit. Again the time deviation was very small; the greatest deviation was -1.1%.

Table 3 shows the results obtained with 100 g, 11 milliseconds,  $\frac{1}{2}$  sine wave shock pulse. Each unit was tested with three shock pulses in each of three mutually perpendicular planes. Again the times were essentially unchanged. The greatest change from the original time was only + 1.75%. In addition, each unit was shocked while it was timing. No significant change was observed.

Table 4 shows the results of firing 15 Atlas Miniature Switches with A (or 6 ohms) bridges. The firing capacitor was 15 microfarads charged to 15 volts. The nominal delay time was 8 seconds. The delay time at 77°F was 7.9 seconds. The total time spread was -0.4% and + 2.8% with switches fired at -80°F, 77°F and 200°F.

Table 5 shows the results of firing 8 Atlas Miniature Switches having B (or 4.5 ohms) bridges. The firing capacitor was 47 microfarads charged to 15 volts. These nominal 8 second units gave 7.7 seconds at 77°F with a total time spread of -4.1% over a temperature range from -70° to 200°F.

Table 6 shows the results of firing 12 Atlas Miniature Switches with C (or 1.8 ohms) bridges. The firing energy switched by the solid state timer was a 47 microfarad capacitor charged to 15 volts. With a nominal delay time of 8 seconds, the observed time at 77°F was 7.7 seconds. The time spread was -4.0%, + 0.07% over a temperature range from -80° to 200°F.

Table 7 shows the results of firing 11 Atlas 750# Reefing Line Cutters, with B (or 4.5 ohms) bridges, using two 8 second solid state timers. The firing energy switched by the solid state timer was a 47 microfarad capacitor charged to 15 volts. The observed time at 77°F was 7.9 seconds with a time spread of + 3.8% and -2.3% over a temperature range from -65° to 160°F.

#### CONCLUSIONS

As the sophistication of aerospace devices increases, the requirement for more and more precise time delays for EED's will also increase. Solid State Timers offer numerous advantages in this field. They are small and light in weight. They have no



moving parts, they have long life, and they are not significantly affected by vibration, shock, or a wide range of temperatures. Even the poorest results cited above are far better than can be obtained by other techniques in common use.

VIBRATION 5 TO 2000 TO 5 CPS AT 30 G'S  
 TIME DELAY - 8.0 SECONDS  
 SOLID STATE TIMER

UNIT NO.	DELAY TIME IN SECONDS			
	BEFORE VIBRATION	AFTER 1ST HOUR	AFTER 2ND HOUR	AFTER 3RD HOUR
1	7.931	7.908	7.898	7.895
3	7.799	7.897	7.861	7.858
6	7.754	7.744	7.746	7.747
8	7.773	7.722	7.701	7.730
9	7.674	7.680	7.700	7.718

TABLE I

ACCELERATION 200 GS FOR 1 MIN.  
 TIME DELAY — 8.0 SECONDS

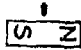


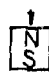


UNIT NO.	BEFORE ACCEL.	DELAY TIME IN SECONDS						AFTER ACCEL.
								
1	7.909	7.905	7.907	7.905	7.911	7.908	7.910	7.913
3	7.917	7.870	7.899	7.905	7.900	7.885	7.893	7.925
6	7.738	7.719	7.723	7.670	7.657	7.681	7.654	7.739
8	7.653	7.639	7.623	7.657	7.669	7.639	7.673	7.678
9	7.741	7.722	7.713	7.709	7.700	7.683	7.692	7.715

TABLE 2

A.C.D. LABORATORY  
 ATLAS CHEMICAL INDUSTRIES, INC.

SHOCK — 100 GS 11 MILLISECONDS  
 1/2 SINE WAVE  
 TIME DELAY — 8.0 SECONDS

UNIT NO.	BEFORE SHOCK	DELAY TIME IN SECONDS		
		AFTER 1ST TEST	AFTER 2ND TEST	AFTER 3RD TEST
1	7.901	7.912	7.916	7.913
3	7.860	7.890	7.895	7.890
6	7.745	7.743	7.728	7.725
8	7.735	7.871	7.697	7.680
9	7.700	7.710	7.698	7.680

TABLE 3

A.C.D. LABORATORY  
 ATLAS CHEMICAL INDUSTRIES, INC.

ELECTRO-EXPLOSIVE DEVICE  
 ATLAS MINIATURE SWITCH  
 ATLAS "A" BRIDGE

TIME DELAY - 8.0 SECONDS  
 SOLID STATE TIMER OUTPUT - 15 V. - 15 MFD.

BRIDGE RES.	DELAY TIME	BRIDGE RES.	DELAY TIME	BRIDGE RES.	DELAY TIME
6.3	8.049	6.0	8.168	5.8	7.970
6.0	8.025	5.7	8.222	6.0	7.970
-80° 5.7	8.030	+200° 6.5	8.111	+77° 5.8	7.979
6.0	8.033	5.9	8.226	5.7	7.976
6.3	8.030	6.0	8.106	5.5	7.977

TABLE 4

A.C.D. LABORATORY  
 ATLAS CHEMICAL INDUSTRIES, INC.

ELECTRO-EXPLOSIVE DEVICE  
 ATLAS MINIATURE SWITCH  
 ATLAS "B" BRIDGE

TIME DELAY - 8.0 SECONDS  
 SOLID STATE TIMER -- OUTPUT - 15 V. - 47 MFD.

BRIDGE RES.	DELAY TIME	BRIDGE RES.	DELAY TIME	BRIDGE RES.	DELAY TIME
+77° 4.9	7.705	+200° 4.5	7.782	-70° 5.0	7.760
4.5	7.694	4.7	7.781	5.3	7.670
4.4	7.689				
4.4	7.707				

TABLE 5

A.C.D. LABORATORY  
 ATLAS CHEMICAL INDUSTRIES, INC.

ELECTRO-EXPLOSIVE DEVICE  
 ATLAS MINIATURE SWITCH  
 ATLAS 'C' BRIDGE

TIME DELAY — 8.0 SECONDS  
 SOLID STATE TIMER — OUTPUT — 15 V — 47 MFD.

BRIDGE RES.	DELAY TIME	BRIDGE RES.	DELAY TIME	BRIDGE RES.	DELAY TIME
+ 200° 1.9	7.775	- 80° 1.8	7.941	+ 77° 1.9	7.700
20	7.788	1.7	7.997	1.9	7.686
20	7.772	1.7	7.970	1.8	7.683
		1.7	8.005	1.8	7.692
		1.8	7.938		

TABLE 6

A.C.D. LABORATORY  
 ATLAS CHEMICAL INDUSTRIES, INC.  
 ELECTRO-EXPLOSIVE DEVICE  
 ATLAS 750# REEFING LINE CUTTER  
 ATLAS 'B' BRIDGE

TIME DELAY — 8.0 SECONDS  
 SOLID STATE TIMER — OUTPUT — 15 V — 47 MFD.

CUTTER SERIAL NO.	TIMER SERIAL NO.	DELAY TIME
9	1	8.298
10	1	8.222
- 65° 2	1	8.305
1	3	8.257
8	3	8.180
+ 77° 4	1	7.929
11	1	7.816
3	1	7.815
+ 160° 7	1	7.814
5	3	7.847
6	3	7.841

TABLE 7

A.C.D. LABORATORY  
 ATLAS CHEMICAL INDUSTRIES, INC.

## DISCUSSION

The size of the 8-second delay was stated to be about  $\frac{1}{2}$  in<sup>3</sup> including the firing switch and capacitor. A buffer stage is used between the trigger and the switch to minimize the effects of temperature on the delay time. This is a uni-junction transistor.

1-7 FIRING SQUIBS BY LOW VOLTAGE CAPACITOR DISCHARGE

FOR SPACECRAFT APPLICATION\*

J. E. Earnest, Jr.

A. J. Murphy

Jet Propulsion Laboratory  
Pasadena, California

ABSTRACT

The design of low voltage capacitor discharge circuits for firing HBW squibs requires that squib-thermal and circuit-electrical time constants be considered as interrelated.

These functional relationships are analyzed by use of an electro-thermal analogy with one composite time constant.

The effects of secondary characteristics not considered in the simple analogy are also discussed.

INTRODUCTION

The use of a capacitor discharge firing circuit to reliably initiate hot-bridgewire type squibs requires among other things that the electrical time constant of the firing circuit be considered in relationship to the thermal time constant of the squib. This paper presents a review of the basic theory,

---

\* This paper presents the results of one phase of research carried out at the Jet Propulsion Laboratory, California Institute of Technology, under Contract No. NAS 7-100, sponsored by the National Aeronautics and Space Administration.

defines the primary electro-thermal parameters and presents a practical example of the design of a capacitor discharge firing circuit. No attempt is made to compare the efficacy of using a capacitor discharge-type firing circuit versus either a constant voltage or constant current power supply. It is presumed that a capacitor discharge-type subsystem has been chosen to initiate HBW squibs. This choice could be required by low power availability (spacecraft solar cells) or other system restraints (direct current isolation from the main battery).

A review is presented of the readily available, commonly used constant current characteristics of HBW squibs, including Bruceton derived All-Fire and No-Fire sensitivity data. The empirical relationship between the constant current into the bridgewire and the time to fire is examined and an analytical solution is defined by means of an electro-thermal analogy. The interrelationship of current, time, energy and power involved in the electrical sensitivity of the squib is examined in the light of the resulting equations.

Test results for a modern 1 amp/1 watt squib at typical conditions of applied power and reliability/confidence are compared with the analytical solution. A capacitor discharge energy supply is then substituted for the constant current power supply in the basic analogy and the subsequent equations examined. An analysis of some of the more important relationships in the capacitor discharge configuration follows and the results are applied in the design of a practical subsystem.

#### TYPICAL CHARACTERISTICS

The majority of present HBW squib firing circuits utilize either constant current or constant voltage power supplies. It is therefore natural that most published data on squib firing sensitivity is related to constant power. The squib engineer, when using a constant current circuit, is concerned with two

basic parameters, i.e., the level of constant current or voltage which must be applied and the time at which the squib will subsequently fire.

A common method employed to determine this reliable initiation level is the Bruceton All-Fire Test. This is a method of statistically analyzing the results of usually fifty or more test firing attempts by calculation of a mean firing level and extrapolation to a specified reliability/confidence level. For example, with a typical 1 amp/1 watt squib a current of 3.40 amperes might result as the .999R/.90C All-Fire level for all other squibs from the same lot as the test units. In the Bruceton All-Fire Test a current pulse is generally used (e.g., 10 to 50 milliseconds). After completion of the tests, the investigator can state, for example, that he is 90% confident that 999 out of 1000 of the squibs from this lot will fire within 10 milliseconds when supplied with 3.40 amperes constant current. The engineer may then place an additional margin on both the current level and the time the current is applied. In our example, he may then require that the firing circuit deliver a minimum constant current of 5.0 amperes for a minimum of 50 milliseconds. Thus, an adequate margin for system reliability is ensured.

It is interesting to note that the nominal firing energy ( $I^2Rt$ ) delivered to a squib with a one-ohm bridgewire is typically from 35 to 80 millijoules and that the power ( $I^2R$ ) delivered is of the order of 25 watts. However, other Bruceton tests may be run for five minute periods and designated as No-Fire Bruceton Tests. The resulting upper current limit at the specified .999R/.90C level (which will be called the Sure-Fire level) is generally 25% less than the 10 ms. pulse All-Fire level. However, in the No-Fire Bruceton the .999R/.90C no fire level is of primary concern. For a 1 amp/1 watt squib this is typically in the range of 1.2 to 1.8 amperes.

If time-to-fire versus current is monitored during both types of Bruceton tests and the results plotted on logarithmic paper the relationship appears



as in Graph 1. The firing time appears to decrease as current increases, and there is a constant power level below which firing never occurs. These Bruceton tests provide an estimate of the constant current All-Fire and No-Fire levels.

This Bruceton data provokes further investigation into the time-to-fire versus current relationship. Graph 2 illustrates the results of 17 firings conducted with a group of 1 amp/1 watt squibs between 2.0 amps and 20.0 amps (in 0.5 ampere increments). If a best fit is drawn through the firing points an empirical relationship between current and time-to-fire is graphically established. As noted, the time-to-fire decreases as the firing current increases and the firing time approaches infinity as the current approaches some real level. Furthermore, the apparent energy required to fire the squib decreases with increasing current and appears to approach a constant value. In this figure, the equivalent current value where the energy approaches a constant value is approximately 7.0 amperes. This indicates a practical constant energy-to-fire region from 8 amperes up to the highest test firing current of 10.0 amperes. The energy here is a calculated 75.0 millijoules. This relationship is more apparent when plotted as in Graph 3, energy-to-fire versus current.

Without an analytical solution to this empirical relationship, practical use of the graphic method can be made. From a lot of squibs intended for flight use, a simple series of test firings in the All-Fire and No-Fire regions can provide good relative test data. For example, above the expected Bruceton All-Fire level, six or so firings at each of three or four current levels can provide a statistical mean and appropriate reliability/confidence limits of the energy-to-fire and yield a good representation of the constant energy and/or transition region. A modified No-Fire Bruceton Test can be conducted in the no-fire region and a 50% firing line (plus appropriate reliability

levels) calculated.

Graph 4 shows the results of this type of testing. By fitting a curve between these two regions, an empirical function with a band width can be established. This relationship can be used for monitoring lot-to-lot uniformity and sensitivity, to measure relative sensitivity degradation of the squibs after abuse, and to provide the ordnance user with a more thorough knowledge of how a particular squib should function.

#### ANALYTICAL CONSIDERATIONS

Analytical solutions to the mechanics of supplying electrical energy to the bridgewire, the heating of the bridgewire and the consequent explosive initiation have been examined previously in published literature.\* However, a brief review will facilitate the interpretation of the capacitor discharge energy delivery mode related to the basic equations.

Electrical energy is supplied to the bridgewire. This energy may be delivered at a constant rate (i.e., constant power) or delivered as a function of time (i.e., power as a function of time). The electrical energy for constant current is simply  $I^2Rt$  (joules). This is the amount of energy delivered to the squib in time  $t$ . This energy is received by the bridgewire, the temperature of which is increased in proportion to the amount received. This bridgewire has a specific heat capacity, i.e., a specific number of joules of energy are required to raise its temperature one degree centigrade. The dimensions of the specific heat capacity used here are joules/ $^{\circ}$ C. The bridgewire also has a specific thermal resistance which unfortunately is not

---

\* See Bibliography.

infinitely large. This factor results in heat loss away from the bridgewire (i.e., through the ceramic, pins, match head, etc.). As the bridgewire temperature increases, a proportionally higher number of joules per second (watts) is lost by heat transfer away from the bridgewire.

Illustration 1a illustrates the typical HBW squib. Illustration 1b indicates a thermal representation of this squib. The bridgewire has an effective thermal capacitance and a thermal resistance. Power into the bridgewire can be considered in joules per second and the thermal potential in degrees centigrade. This thermal circuit is directly analogous to the capacitor/resistor electrical circuit shown in Illustration 1c and is the basic electro-thermal analogy.

This electrical analog of the thermal characteristics of a squib indicates power input (joules/sec) as current (amperes, or coulombs/sec). This energy raises the bridgewire temperature (i.e., charges the capacitor) while also supplying energy to the heat loss paths (i.e., the electrical resistor) in direct proportion to the temperature. The heat loss in watts per degree centigrade is represented as  $\frac{1}{R}$ . Equivalent units are tabulated below.

<u>ELECTRICAL</u>	<u>THERMAL</u>
Amps (coulombs/sec)	Watts (joules/sec)
Volts	$^{\circ}\text{C}$
Ohms (volts/coulombs/sec)	$^{\circ}\text{C}$ per Watt ( $^{\circ}\text{C}/\text{joule/sec}$ )
mhOs	Watts per $^{\circ}\text{C}$

The equations associated with Illustration 1c can be handled as follows:

(Total Current)  $I_T = I_1 + I_2$

(Current to the Capacitor)  $I_1 = \frac{cd\theta}{dt} = c\dot{\theta}$

(Current to the Resistor)

$$I_2 = \frac{\theta}{r}$$

$$I_T = c\dot{\theta} + \frac{\theta}{r}, \quad \dot{\theta} + \frac{\theta}{rc} = \frac{I_T}{c}$$

$$I_T \cong \text{power in}$$

1) 
$$\dot{\theta} + \frac{\theta}{rc} = \frac{P(t)}{c} \quad (\text{The basic equation.})$$

If the power input is considered constant, the equation becomes:

2) 
$$\dot{\theta} + \frac{\theta}{rc} = \frac{I_K^2 R}{c}$$

$I_K$  is the constant current (amperes) delivered to the bridgewire (of resistance R). Upon integration, equation 2) becomes

3) 
$$\theta = I_K^2 Rr (1 - e^{-t/rc})$$

Equation 3) represents the normal curve utilized for squibs upon application of constant current (the effect of the bridgewire temperature coefficient of resistivity is considered later). Examination of this equation as time approaches zero and as time approaches infinity provides the following:

As  $t \rightarrow 0$

4) 
$$\theta = I_K^2 Rt/c, \quad \theta_c = I_K^2 Rt = \text{Energy to fire as } t \rightarrow 0$$

As  $t \rightarrow \infty$

$$5) \quad \theta = I_{\infty}^2 R r \quad \text{or} \quad \theta c = I_{\infty}^2 R r c = E_t \rightarrow 0$$

Equations 3), 4) and 5) represent a simplified solution to the relationship of time-to-fire versus current. If  $\theta_f$  (firing temperature) is assumed to be a relative constant for a lot of squibs and  $t$  is a function of  $I_K$ , the equation identifying this relationship becomes:

$$6) \quad I_K = \left[ \frac{\theta_f}{R r (1 - e^{-t/r c})} \right]^{1/2}$$

This equation, when graphically plotted as time-to-fire versus current, matches the empirically derived function shown in Graph 4 and is the simplified analytical solution. A graphical representation of equation 3) displaying bridgewire temperature as a function of time at several different values of current input is shown in Graph 5. Note that as time approaches zero the temperature becomes a simple linear function of time ( $I_K^2 R t / c$ ); as time approaches infinity the temperature approaches some upper limit ( $I_{\infty}^2 R r$ ).

There are several test techniques that can be applied in order to make practical use of this analysis of a squib's electrical initiation characteristics. But primarily, this is a tool by which the ordnance user can, with a relatively small quantity of test squibs (1) identify the relative sensitivity characteristics of a particular lot of squibs; (2) determine relative firing reliabilities and confidence levels at different constant current inputs; and (3) measure the relative increase or decrease in sensitivity of squibs after subjection to any of several environmental abuse tests. For example, the Sure-Fire level and the energy to fire as  $t \rightarrow \infty$  may be found to increase or

decrease after electro-static discharge or after several short pulses of All-Fire current.

One interesting approach consists of calculating the electro-thermal efficiencies of a particular lot of squibs. Graph 6 shows such a plot of the ratio of time-to-fire to the thermal time constant of a squib versus the the percentage of delivered energy that is heat loss. As an example, it is easily determined that if our typical squib has a thermal time constant of 8.0 milliseconds and a sufficiently high level of constant current is used in firing to achieve a time-to-fire of 2.0 milliseconds, the heat loss away from the bridgewire is approximately 10%. This means that if the current were 5.0 amperes the energy delivered would be 50 millijoules ( $I_K^2 R t$ ). Thus, 45 millijoules would have been expended in increasing the temperature of the bridgewire and 5 millijoules expended in heat losses. Note that as the firing time approaches the thermal time constant the heat loss approaches  $\frac{1}{2.718}$ , or 37%.

Also, the Bruceton All-Fire and No-Fire current bands may be plotted as energy retained within the bridgewire versus time (Graph 7). A typical 1 amp/1 watt squib is used for this example. Several plots of current to the bridgewire from 1.0 ampere to 5.0 amperes are illustrated. The No-Fire band limits of 1.4 ampere No-Fire and 2.6 amperes Sure-Fire are shown. The 2.6 ampere constant current input approaches a limit of 61.0 millijoules. This can be interpreted as the sure fire energy (retained in the bridgewire) to achieve reliable initiation. The thermal time constant of this squib is  $\frac{61.0}{2.6^2}$ , or 9.0 milliseconds.

It should be apparent that there is a correlation between energies derived by the analytical solution and the typical Bruceton test results (at the .999R/.90C All-Fire limits). No correlation is apparent at the 50%

levels or the No-Fire levels. The No-Fire Bruceton data indicates that the sure fire energy within the bridgewire is 61.0 millijoules (2.6 amperes). The 10.0 millisecond Bruceton All-Fire results also indicate an all fire energy within the bridgewire of approximately 61.0 millijoules. An analysis of the energy margin, if the recommended firing current is 5.0 amperes, indicates a margin of  $\frac{150-61.0}{61.0}$  or 146% (within 10.0 milliseconds).

These sensitivity characteristics of a typical 1 amp/1 watt squib, the nominal current levels at which they are fired and the relative reliability margins will be utilized in the practical design of a capacitor discharge firing circuit.

#### CAPACITOR DISCHARGE ANALYSIS

The electro-thermal analogy permitted a definition of the temperature of the bridgewire as a function of the power in. The previous derivations were for constant current into the bridgewire. This equation, however, should be valid for any power input as a function of time.

The instantaneous current from a simple capacitor discharge circuit is:

$$7) \quad i = I_0 e^{-t/RC}$$

The instantaneous power therefore is:

$$8) \quad P(t) = I_0^2 R_s e^{-2t/RC}$$

Substituting this value in equation 1)

$$9) \quad \dot{\theta} + \frac{\theta}{rc} = \frac{I_0^2 R_s e^{-2t/RC}}{c}$$

which upon integration becomes

$$10) \quad \theta = I_0^2 R_s \frac{RC r}{2rc - RC} (e^{-t/rc} - e^{-2t/RC})$$

In this equation the quantity,  $e^{-2t/RC}$ , approximates the fractional energy left after firing (as a charge on the capacitor) and the quantity  $(1 - e^{-t/rc})$  approximates the fraction of energy dissipated as heat losses (away from the bridgewire). Thus, if at some time  $t$ ,  $(e^{-t/rc} - e^{-2t/RC})$  equals, say,  $(0.9 - 0.3)$ , then 30% of the energy originally stored on the capacitor remained undischarged, 10% of the energy delivered was dissipated as heat losses, and  $(0.9 - 0.3)$  or 60% of the stored energy was utilized in heating the bridgewire.

Equation 10) can be differentiated and, by setting  $\frac{d\theta}{dt} = 0$ , the time at maximum possible bridgewire temperature (i.e., the time beyond which the squib will never fire as it is then cooling off) can be obtained.

$$11) \quad t_{\max} = \frac{\ln(2rc/RC)}{\frac{2}{RC} - \frac{1}{rc}}$$

This value,  $t$ , can be utilized when examining the optimum values for a capacitor discharge circuit.

Using a typical 1 amp/1 watt squib as an example, it is interesting to examine and compare the theoretical bridgewire temperature (or bridgewire energy) as a function of time when constant current power and when capacitor discharge power is applied.

Our typical squib exhibits the following characteristics from the Bruceton No-Fire Tests (5 minutes): No-Fire level of .999/.90, 1.40 amperes; mean No-Fire level, 2.00 amperes; and Sure-Fire level of .999/.90, 2.60 amperes. From a practical standpoint this means that all of these squibs will fire when



2.60 amperes constant current is applied for five minutes. Thus, the Sure-Fire power level is 6.76 watts and all of the squibs in this lot will have increasing bridgewire temperatures until initiation (when 2.6 amperes minimum constant current is applied).

When tested with a constant current input higher than the Bruceton All-Fire level (which might be 3.4 amperes) the .999R/.90C energy-to-fire level is 75.0 millijoules at 7.0 amperes. The theoretical thermal time constant of the squib is the energy-to-fire as  $t \rightarrow 0$  divided by the power below which the squib never fires as  $t \rightarrow \infty$ . In this case, this is simply  $75.0/6.76$  or 11.1 milliseconds. The time at which the squib fires with 7.0 amperes is  $75.0/7^2$  or 1.53 milliseconds. Using Graph 7 to calculate efficiency, the ratio  $t/r_c = 1.53/11.1 = .138$  and the heat loss is 6.4%. Therefore, the approximate constant energy as  $t \rightarrow 0$  is  $.936 \times 75$  or 70.0 millijoules. A more exact thermal time constant can now be calculated as  $70.0/6.76 = 10.34$  milliseconds. For calculation purposes  $r_c$  will be taken as .010 seconds, the constant power level as 6.76 watts and the constant energy level as 67.6 millijoules.

This same squib when energized from a capacitor discharge power supply can be examined by utilizing equation 9) and the energy in the bridgewire plotted versus time (Graph 8). The assumptions are made that the minimum initial current ( $I_0$ ) is 15 amperes, the bridgewire resistance ( $R_s$ ) is 1.0 ohms, the total circuit resistance ( $R$ ) is 2.5 ohms, and the thermal time constant ( $r_c$ ) is 10 milliseconds. Four different values of capacitance from 200 microfarads to 600 microfarads are plotted.

The bridgewire temperature (energy) initially increases at a faster rate than with the constant power input. However, unlike the constant power input, it reaches a maximum value and then decreases. It should also be noted that as the electrical time constant ( $RC$ ) is increased the  $\theta_c$  curve becomes flatter

approaching the constant current curves as RC approaches infinity. As a first approximation of the minimum capacitance value used in this example, the basic equation can be set equal to 67.7 millijoules and solved for the capacitance. This results in approximately 285 microfarads. Initiation would occur at 1.25 milliseconds. However, the bridgewire would only be at this energy level instantaneously and then would begin to cool off. It can be seen that the 600 microfarad capacitor would provide an energy margin of 136-68, or 100%.

68

It is hoped that the foregoing discussion will be sufficient to demonstrate how constant current squib parameters might be used for the sizing of capacitor discharge circuits. One typical design approach will be described and the effects of secondary characteristics not considered in the simple analogy briefly discussed.

The practical design of a capacitor discharge firing circuit entails a number of parameters. However, the following exercise indicates one approach wherein the relationship between the electrical and thermal time constants becomes quite apparent. Equations 7) and 11) can be combined to yield:

$$12) \quad \left( \frac{I_f}{I_o} \right)^2 = (\psi) \frac{1}{1-\psi} \quad \text{where } \psi = \frac{RC}{2rc}$$

Equation 12) is plotted in Graph 9 and can be utilized for design solutions.

First, a maximum allowable current to the squib is established. Experience and available test techniques (in our example) suggest limiting this to approximately 22 amperes. For optimum design efficiency a maximum operating voltage consistent with this 22 ampere limit is desired. However,

an upper limit of 150 volts seems advisable to facilitate packaging and preclude high voltage arcing. An examination of high reliability industrial components with optimal size to weight ratios makes tantalum foil capacitors attractive, while 50 volts maximum appears to be a practical upper limit for available hardware. Note that optimum design is predicated upon specific requirements and subsequent tradeoffs, i.e., size, weight, reliability, availability, cost, rated voltage, rated capacity, etc.

The 22 amperes  $I_0$  maximum and 50 volts  $V_0$  maximum indicate a 2.3 ohm R minimum. Allowing an anticipated  $\Delta R$  of  $0.7\Omega$  results in a maximum resistance of 3.0 ohms. This maximum resistance, R, will predicate our worst case. The basic squib characteristics of energy-to-fire as time approaches zero ( $E_0$ ) and constant current required to fire as time approaches infinity ( $I_\infty$ ) are utilized to define the thermal time constant  $\tau_c$ . In our example we find that a 0.999 reliability/90% confidence examination of the squib indicates 0.75 joules ( $E_0$ ) and 2.8 amperes ( $I_\infty$ ). The  $\tau_c$  product is  $E_0/I_\infty^2 R_s$  or  $.075/2.8^2$ , which is 9.6 milliseconds for a 1-ohm squib. Note that the worst case thermal time constant is not the longest thermal time constant possible, but represents that squib requiring the highest energy ( $E_0$ ) and the highest firing current ( $I_\infty$ ).

Graph 9 can be used directly. However, it is convenient to replot now that some parameters have been fixed. Letting  $C = \frac{2\tau_c}{R \text{ max.}}$   $\Psi = \frac{2x.0096}{3}$   $\Psi = .00644$   $\Psi$

and  $V_0 = \frac{i}{\left(\frac{i_f}{I_0}\right)}$   $R = \frac{2.8x3}{\left(\frac{i_f}{I_0}\right)} = \frac{8.4}{\left(\frac{i_f}{I_0}\right)}$ , a replot of minimum capacitance versus

minimum voltage can be established as in Graph 10. At this time, the voltage regulation is examined and the upper voltage set as, say, 50 volts. Thus, a  $\pm 10\%$  regulated voltage would be nominally 45.5 volts or 41.0 volts minimum. From Graph 10 it is determined that a capacitance of 310uf is required. In this example, the capacitors available are reduced to 75% of nominal capacity

at the lowest expected temperature; thus, 413uf (nominal) is required.

The electronic design engineer must observe a number of precautions in the above procedure. Excessive voltage derating on polarized capacitors, for instance, may affect reliability adversely. A solid state switch, such as a silicon controlled rectifier must be represented as a constant voltage drop and a resistance. In this event the  $V_0$  in our equation is reduced by this drop. The equivalent series resistance of the capacitors and other circuit resistance parameters must be known and controlled within limits. The capacitor reliability at peak discharge current must be examined.

One typical spacecraft circuit utilized on the Mariner 1964 spacecraft involved a transformer coupled a.c. input with rectification and limiting resistors to the capacitor charge bank. Silicon controlled rectifiers were utilized for switching and the limiting resistors so sized that even a shorted squib would eventually result in less than the required holding current. Thus, no protection against squib shorts was necessary and the resulting design incorporated a minimum of components. One ohm load resistors were placed in series with each squib to provide isolation and incidentally mechanize the measurement of current.

#### SECONDARY CHARACTERISTICS

Of the parameters not previously considered, the most important appears to be the change of squib resistance with time. The utilization of one composite thermal time constant for the squib instead of multiple time constants appears to be of lesser importance; however, this factor must be remembered in any rigorous handling of the data as time approaches infinity. The thermal analog utilizing multiple time constants is not only cumbersome in its equations, but selection of the proper critical temperature/voltage

element is somewhat open to question.

Consideration of the change of squib resistance ( $\Delta$ ) due to the temperature coefficient of resistivity ( $\alpha$ ) results in the following equations for constant current firings.

$$13) \quad c \dot{\theta} + \frac{\theta}{r} = I_K^2 R_s (1 + \alpha \theta)$$

$$14) \quad \theta_c = \frac{I_K^2 R_s r c}{1 - I_K^2 R_s \alpha r} (1 - e^{-(1 - I_K^2 R_s \alpha r)t/rc})$$

This equation can be examined at the firing temperature ( $\theta_f$ ) at which time  $\alpha \theta = \Delta$ . The quantity,  $\Delta$ , is the fractional change of resistance from ambient to firing and can be obtained from test results. As time approaches infinity equation 14) yields:

$$15) \quad \theta_f c = I_\infty^2 R_s (1 + \Delta) r c$$

Combining the equations 14) and 15) when  $\alpha \theta_f = \Delta$ , the following is obtained.

$$16) \quad \dot{\theta}_f c = t \frac{R_s \left[ \Delta(I_K^2 - I_\infty^2) - I_\infty^2 \right]}{\ln \left[ (1 + \Delta) \left( \frac{1 - I_\infty^2}{I_K^2} \right) \right]}$$

Equation 16) can be relatively useful.  $\Delta$ ,  $t$ ,  $R_s$ , and  $I_K$  are measurable for a given squib.  $I_\infty$  can be obtained from Bruceton test results for a particular squib lot. The corresponding capacitor discharge equation utilizing  $\alpha \theta$  is complicated. The first approximation yields:

$$17) \quad c \dot{\theta} + \frac{\theta}{r} = I_0^2 R_s (1 + \alpha \theta) e^{-2t/RC}$$

$$18) \frac{\theta_c}{I_o^2 R_s} = e^{-\frac{t}{rc} - \frac{I_o^2 R_s}{Z} \text{ or } (1 - e^{-2t/RC})} - \frac{e^{-2t/RC}}{\frac{Z}{RC} - \frac{1}{rc} + \frac{I_o^2 R_s \alpha}{c} e^{-2t/RC}}$$

Equation 17) is not quite correct. It should be:

$$19) c\dot{\theta} + \frac{\theta}{r} = I_o^2 R_s (1 + \alpha\theta) e^{-2t/RC} (1 + \frac{\alpha\theta R_s}{R})$$

As the parameters  $\theta$  and  $t$  both appear in exponential form, no technique for integration occurs. This equation can be examined at the maximum temperature where  $\dot{\theta} = 0$ ,  $\theta \approx \theta_f$ , and  $\alpha\theta_f \approx \Delta$ . However, the resulting equation:

$$20) \left(\frac{I_f}{I_o}\right)^2 = e^{-2t/C(R + \Delta R_s)}$$

is the basic capacitor discharge equation, and, having no boundaries for energy delivered, is not too meaningful.

The effect of  $\alpha$  on our simplified analogy must be examined. In practice, the curve resulting from equation 6) is superimposed on the various constant current firing data derived in testing. Any significant deviation of the data from this idealized curve would indicate second order effects. Equations 16) and 18) could then be used for spot checks.

The simple analogy does appear to be adequate for sizing the typical 1 amp/1 watt squib utilized in this report. This squib does have a resistance change but the equations supply counteracting factors. First, the derivation of  $E_o$  from constant current data neglected the effect of  $\alpha$  and thus gave a value lower than actual. Second, the simplified analogy fails to account for the increasing squib resistance. Thus, although the calculated  $E_o$  may be low,

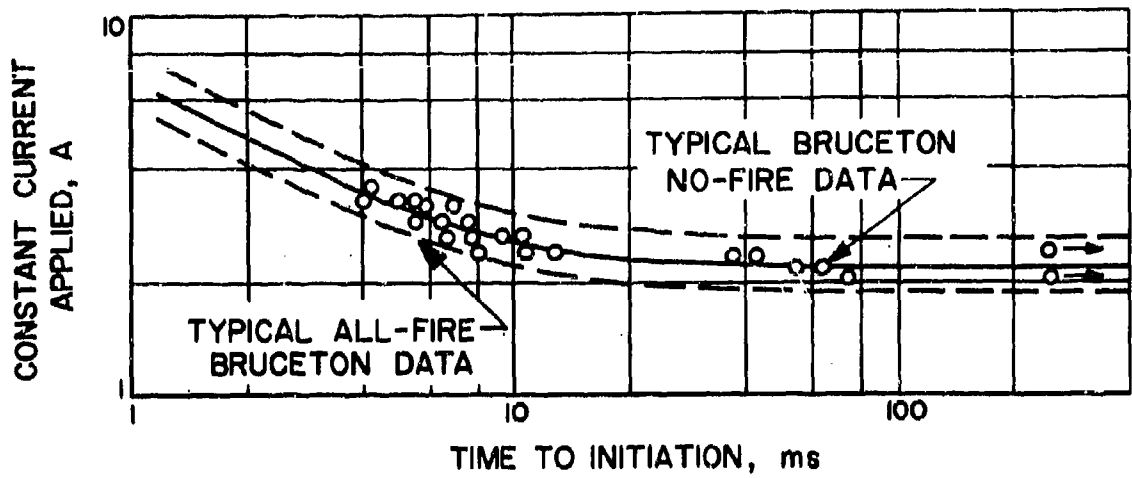
the squib receives more energy than calculated for a given current. This effect is enhanced since the increasing squib resistance not only increases the instantaneous power but also the portion of the available energy which the squib itself receives in the capacitor discharge circuit. A final detrimental factor exists in that the increasing total loop resistance increases the electrical time constant and produces a slower energy delivery thus increasing heat losses.

From the above, it can be seen that the simple analogy has its pitfalls and that test results are required on a given squib before final determination of the applicability of this approach can be made.

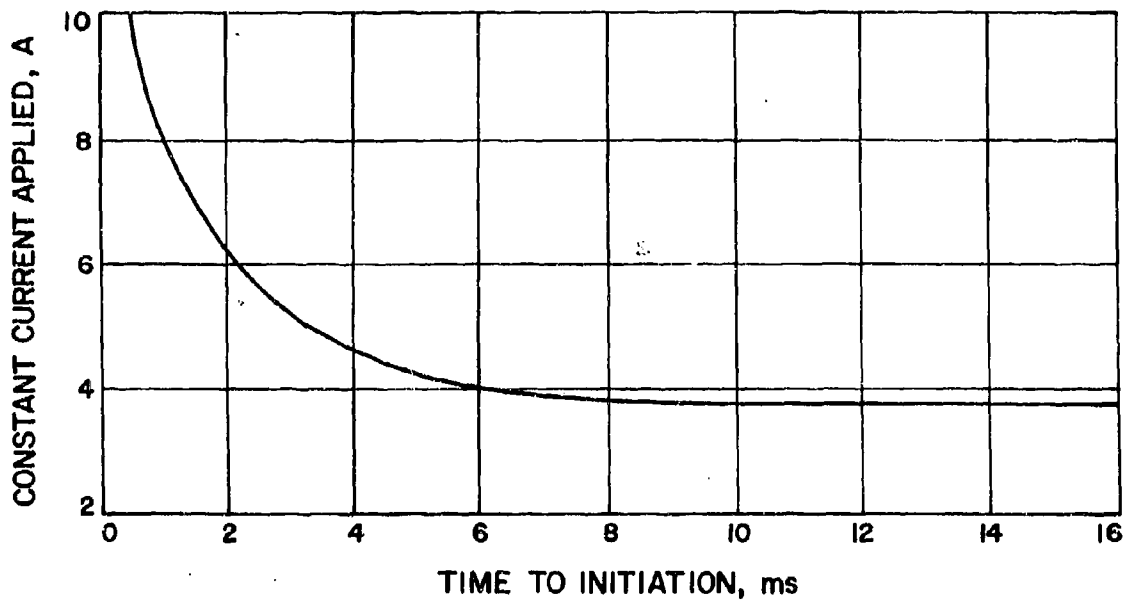
In summary, a short electrical time constant for the circuit is desirable so that the energy being delivered at a fast rate can be most effectively utilized. A long thermal time constant for the squib is desirable so that the initial electrical energy can be utilized primarily for heating the bridgewire, thus minimizing the heat losses. The optimum design of a low voltage capacitor discharge firing circuit requires consideration of these time constants in relation to each other, and considerable awareness of second order effects, only a few of which are discussed here.

#### BIBLIOGRAPHY

1. Benedict, A. G., "Comments on Constant-current Initiation Characteristics of Hot-bridge-wire Squibs, with Particular Reference to Log-current, Log-time Firing Curves," EIS-A2357, Proceedings of the Electric Initiator Symposium, The Franklin Institute, 1963.
2. Kabik, I., Rosenthal, L. A. and Solem, A. D., "The Response of Electro-explosive Devices to Transient Electrical Pulses," NOLTR 61-20, April 17, 1961.
3. Rosenthal, L. A., "Electro-thermal Characterization of Electro-explosive Devices," EIS-A2357, Proceedings of the Electric Initiator Symposium, The Franklin Institute, 1963.
4. Rosenthal, L. A., "Electro-thermal Equations for Electro-explosive Devices (U)," NavOrd Report 6684, August 15, 1959.

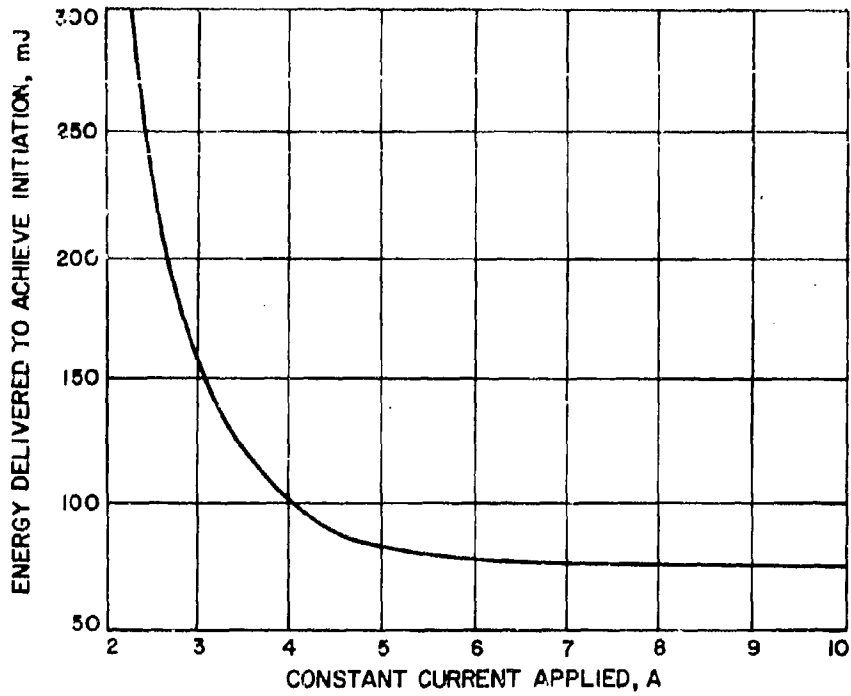


GRAPH NUMBER 1. TYPICAL BRUCETON RESULTS

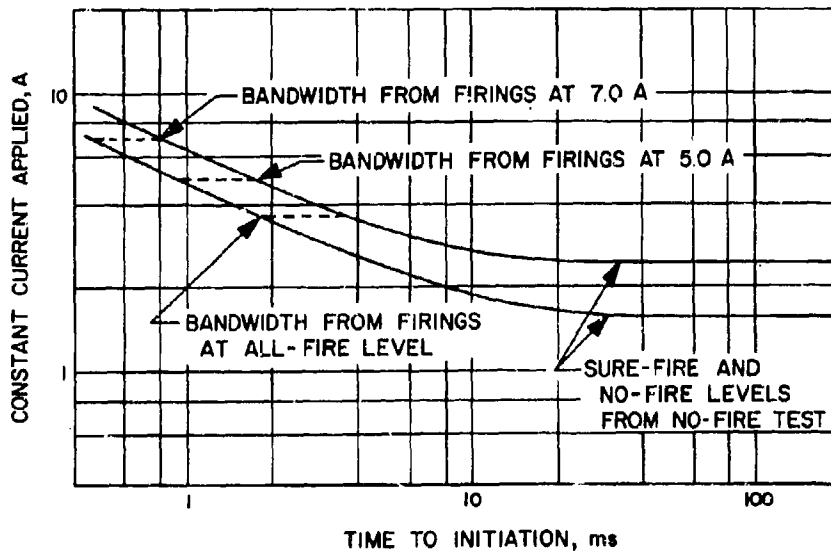


GRAPH NUMBER 2. TIME TO INITIATION VERSUS APPLIED CONSTANT CURRENT

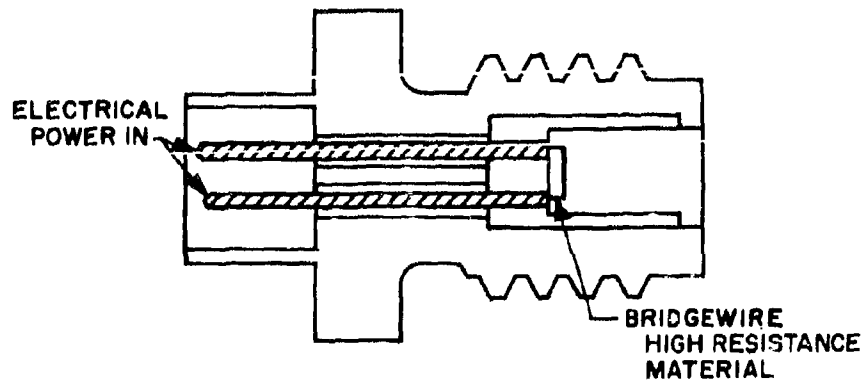




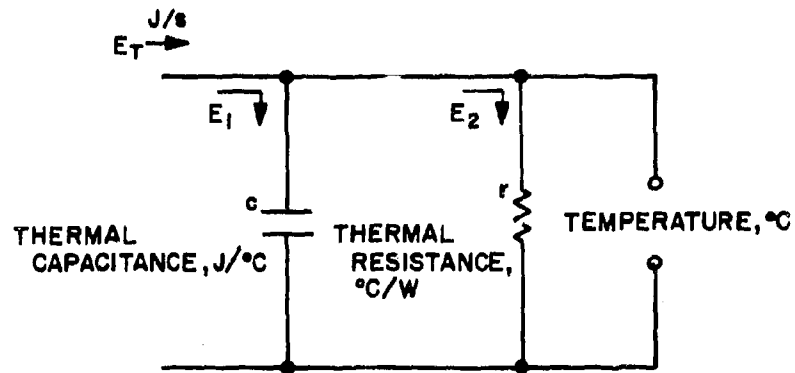
GRAPH NUMBER 3. INITIATION ENERGY VERSUS APPLIED CONSTANT CURRENT



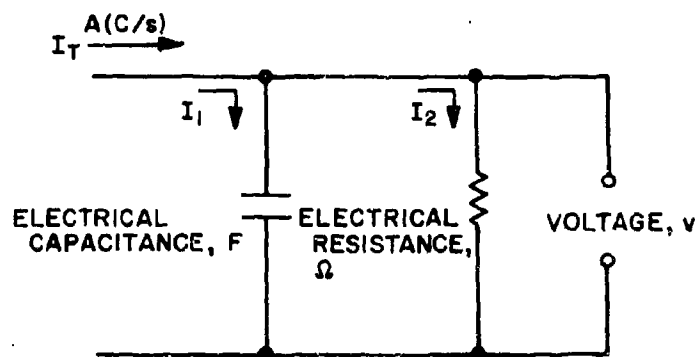
GRAPH NUMBER 4. EMPIRICAL SENSITIVITY CHARACTERISTICS



(a) TYPICAL HBW SQUIB CROSS SECTION

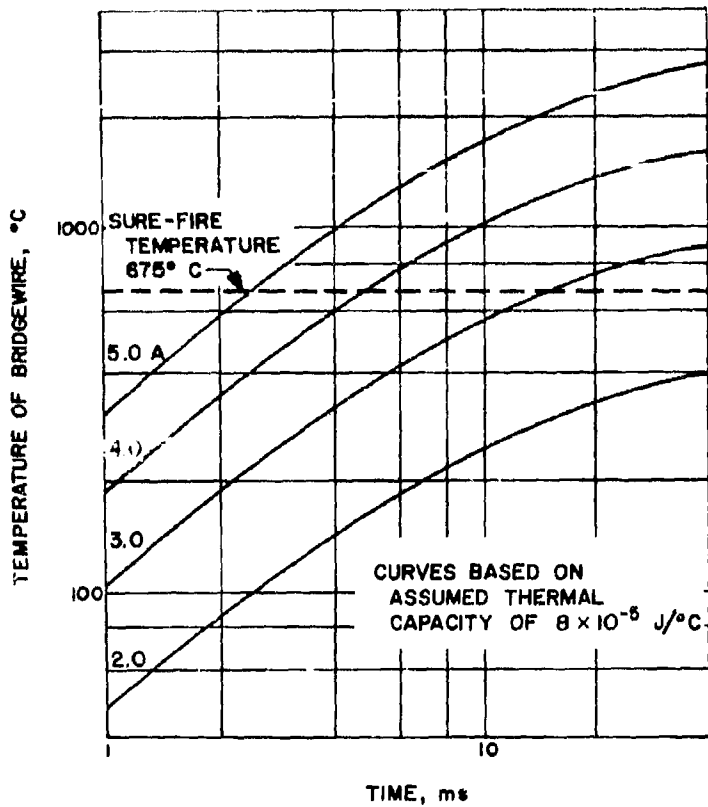


(b) THERMAL CIRCUIT

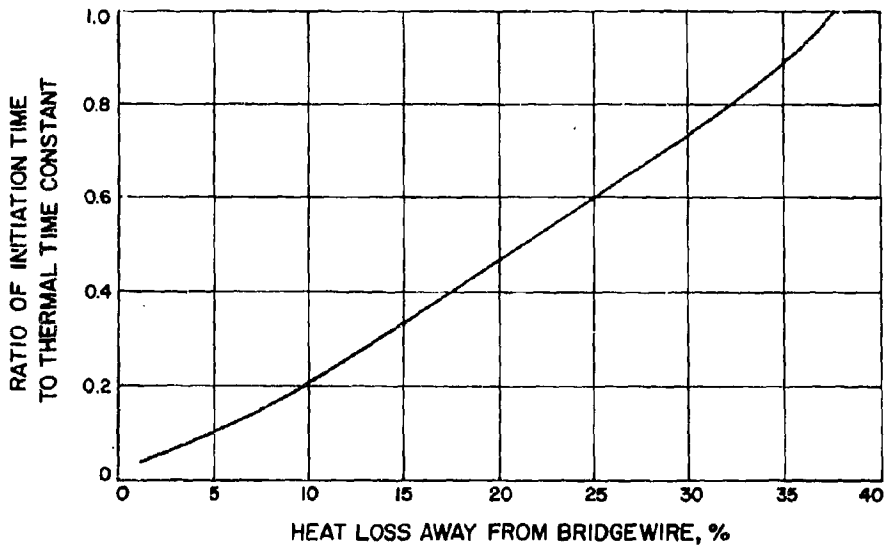


(c) ANALOGOUS ELECTRICAL CIRCUIT

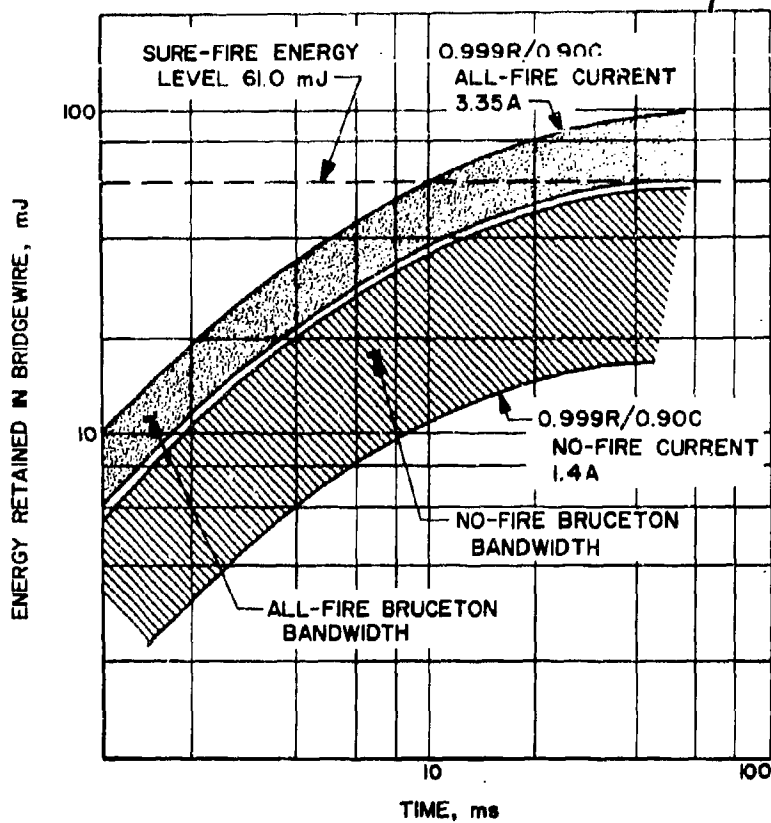
ILLUSTRATION NUMBER 1



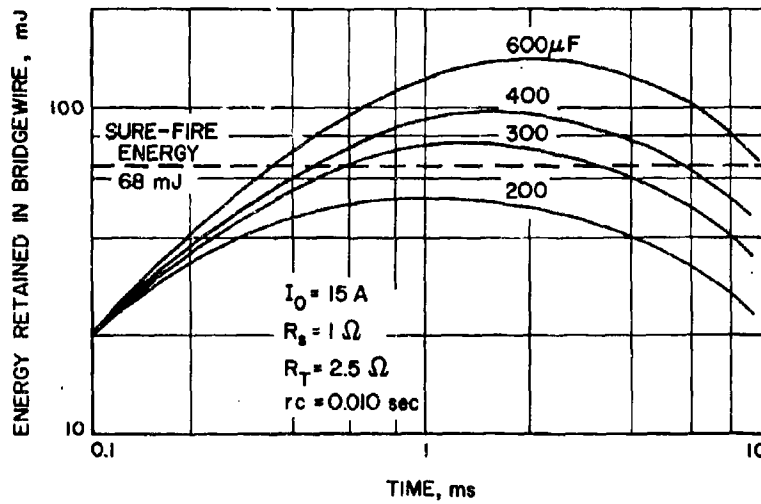
GRAPH NUMBER 5. BRIDGEWIRE TEMPERATURE VERSUS TIME



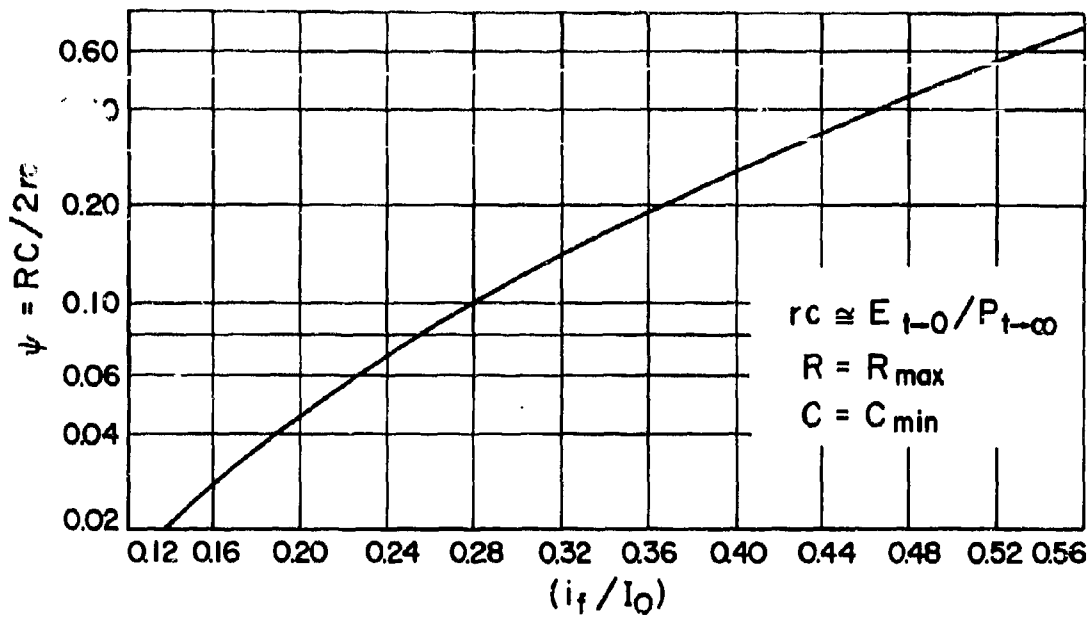
GRAPH NUMBER 6. HEAT LOSS VERSUS RATIO OF INITIATION TIME TO THERMAL TIME CONSTANT



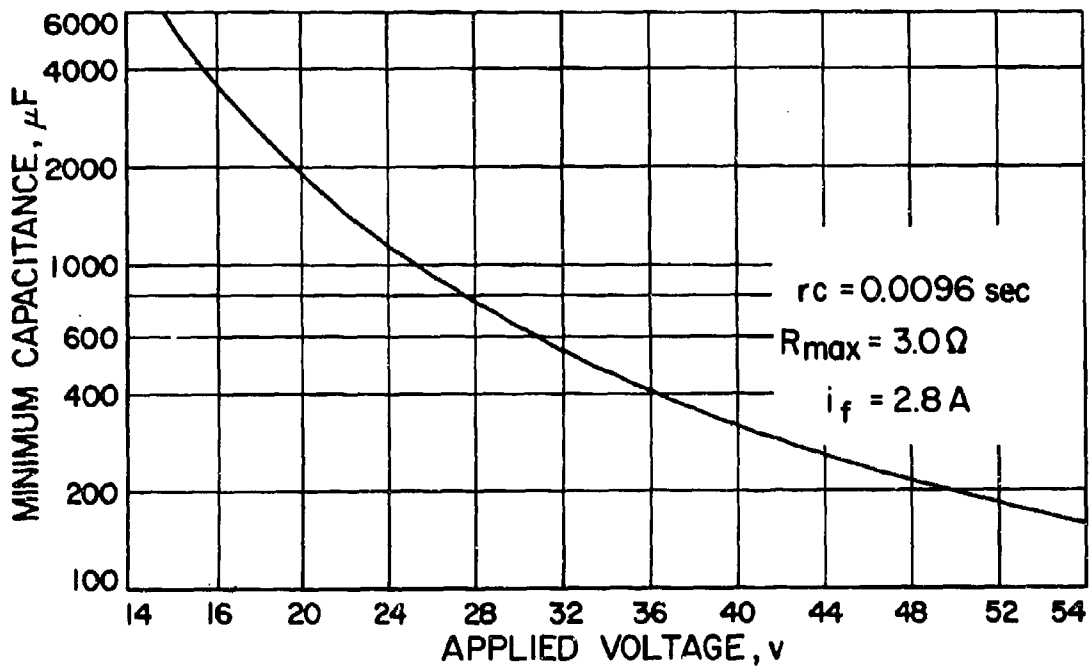
GRAPH NUMBER 7. BRUCETON RESULTS PLOTTED AS BRIDGEWIRE ENERGY VERSUS TIME



GRAPH NUMBER 8. BRIDGEWIRE ENERGY VERSUS TIME



GRAPH NUMBER 9. GENERAL DESIGN PARAMETERS



GRAPH NUMBER 10. SPECIFIC DESIGN PARAMETERS

## DISCUSSION

The C used in this paper for all applications, constant current and capacitor discharge, is the specific heat. The R is the reciprocal of heat loss in °C/watt; this was also used in capacitor discharge and constant current work. This dialogue became lengthy and chairman VanLandingham suggested that the two men get together after the meeting to discuss the work.

1- LASER ENERGIZED EXPLOSIVE DEVICE SYSTEM

Space Ordnance Systems, Inc.,  
122 Penn Street,  
El Segundo, California.

Presented By:

Donald J. Lewis,  
Director of Research.

INTRODUCTION

The LEED System (Laser Energized Explosive Device) operates in a greatly simplified manner and eliminates the use of all connecting metallic lines, bridgewires, spark gaps, ceramic headers, etc. The laser source creates an energy pulse which is transmitted via non-metallic, fiber optic conductors directly to the pyrotechnic compound to produce the required reaction. This system has eliminated the danger of premature actuation or "dudding" of an explosive device in the presence of radio frequency or electrostatic energy. It has also eliminated the problems of premature actuation of pyrotechnic compounds from shock or relatively high temperature.

## HAZARDS AND OPERATIONAL PROBLEMS OF CONVENTIONAL SYSTEMS

The three conventional systems: Hot bridgewire explosively-actuated devices, exploding bridgewire devices, and percussion-actuated devices are all affected to varying degrees by the hazards of RF, electrostatic energy, temperature environments, operational checkout, simultaneity of actuation and remote operation.

### 1. RF Effects on Electro-Explosive Devices

Hot bridgewire and EBW systems are susceptible to RF energies because their bridgewires are coupled to the electrical lead wires used to transmit the energy from the power source to the bridgewire within the explosive device. These components, unless extensively and expensively shielded, constitute an effective antenna to receive the RF energy. Since, in a hot bridgewire device, the bridgewire is specifically designed to actuate the explosive at a relatively low energy level, premature actuation can occur. In an EBW device which is designed to require a high energy level for actuation, the RF energy can be integrated into sufficient thermal energy to "dud" the unit or otherwise degrade its performance. The RF energy may also be rectified within the unit by the electrical discontinuity at the bridgewire interface.

The presence of this high voltage between the bridgewire and case of the unit leads to premature actuation or dudding because of high voltage degradation in a pins-to-case mode.



## 2. Electrostatic Hazards

The electrostatic hazard can be generated in many ways. The following are the most significant. It can be generated by the action of personnel handling devices, due to their body capacitance and mechanical motion. It can also be transmitted from another source such as a vehicle which may become charged due to the turbo-electric charging of the vehicle moving through the air, by antenna rectification, or thermionic emission from large rocket engines. If this energy is in turn transmitted into the initiator via the bridgewire transmission system and/or the initiator grounding system, degradation or premature initiation of the pyrotechnic can occur.

## 3. Temperature Restriction

Most explosives used in both hot bridgewire and EBW systems are limited to temperature extremes of around 350°F. Operation in temperature extremes above these levels requires short term exposure or the result will be degradation of the pyrotechnic function or premature actuation.

## 4. Simultaneity of Actuation

Simultaneity of occurrence is a relative problem, with percussion-actuated devices having the poorest simultaneity capability because of the mechanisms required to actuate these devices. Hot bridgewire devices are somewhat improved over percussion-actuated devices because of the more efficient actuation of the hot bridgewire firing method.

However, this is still limited to the millisecond range. The explosive bridgewire device exhibits the highest simultaneity capability of any of the conventional systems due to the rapid delivery of high energy into the exploding bridgewire interface and the fast reaction of the secondary material.

#### 5. Checkout Capability

The conventional systems are very limited in the ability to determine their operational status. Operational capability is inferred by examinations and tests made prior to the time that actuation is necessary. Also, there is no sound method for establishing if any degradation of the pyrotechnic compound has occurred due to time or other environmental exposure. Also, there are extreme difficulties in evaluating the operational capabilities of the EBW system. The intricate spark gap is difficult to test and this in turn makes it even more difficult to check the presence or integrity of the bridgewire. A confined detonating fuse system which may be employed to transfer the detonation from the EBW detonator to the receptor has no method of operational checkout to determine whether or not it will function properly before actuation is actually attempted.

In summary, it can be seen that designing for, or tolerating, these hazards cause significant compromises to be made in the overall efficiency of a conventional system.

## LEED DEVELOPMENT

On the basis of several preliminary experiments utilizing a laser to initiate explosives, the company decided to fund an in-house investigation of laser-energized systems. The reasons were clear; if explosives could be initiated using coherent light as a source of energy and a means found to transmit it to various components (detonators, initiators, igniters, etc.), one could not only eliminate the RF, electrostatic, and EMI problems, but might possibly arrive at a system that was a great deal simpler in design. The result is the LEED System. Soundness and versatility of the concept have been thoroughly established and the system is now undergoing final development testing.

## THEORY AND OPERATION

### A. Lasers

Lasers (light amplification by stimulated emission of radiation) provide a coherent light output essentially at a single monochromatic frequency. Both ruby and neodymium lasers are currently being used in LEED System. Basically, solid-state lasers work in the same manner. A number of active atoms in a solid-state crystal are raised to a metastable energy level by means of optical pumping. The characteristics of the system are such, that as these atoms fall to lower energy levels, they emit radiation. This radiation stimulates in-phase radiation of other atoms and the output is a highly collimated beam of light of sharply defined frequency.

The following discussion is an extremely simplified version of how lasers operate and is presented only to provide background on the LEED System.

Scattered throughout the ruby crystal, in a typical laser system, are many chromium ions in a ground state or normal energy level (Level 1), see Figure 1 and 2. When the chromium ions are excited above the ground state, they are raised to a high energy semistable (metastable) energy level 3. The energy input to cause this activity is usually derived from a xenon flashlamp. These chromium ions do not, however, return to their ground state in one jump. Some drop (decay) from Level 3 to Level 1 directly, and some drop to Level 2 and remain at that energy level for a short time interval. The rate at which the chromium ions go from Level 3 to Level 2 is greater than the rate of those going directly to Level 1 or from Level 2 to Level 1. In addition, the rate at which the ions go from Level 2 to Level 1 is less than the rate at which they are raised from Level 1 to Level 3. In effect, the chromium ion population level becomes inverted and produces the only condition in which coherent amplified light can be produced. At this point, there are more atoms at Level 2 than at the ground state and stimulated emission is superimposed on any spontaneous emission. This phenomenon occurs because, as the chromium ions drop from Level 2 to Level 1, they emit photons of light at specific wavelengths and frequencies. These photons shower down individually and stimulate further emission of photons from other chromium ions in Level 2.

This activity increases with photon reinforcing photon in a precise phase relationship. As this activity increases, streams of photons bounce back and forth along the axis of the ruby crystal due to the reflectivity of the end mirrors which control the feedback of the optical amplifier system. They build in intensity until they burst from the partially reflecting mirror, and precisely perpendicular to it, in the form of a highly coherent beam of light of about  $6943\text{\AA}$ . The key to the entire process that produces in-step or coherent radiation; is that of an incident photon triggering an ion to emit a photon in-phase with the incident photon.

#### B. Fiber Optics

The techniques of transmitting laser energy through long transparent plastic or glass fibers is relatively new. These fiber optics are produced in many forms and sizes, including single fibers and fiber bundles, either solid or completely flexible. Diameters of glass and plastic fibers may be as small as 4 or 5 microns and as large as desired. Light is propagated through fibers by a series of internal wall-to-wall reflections when the light is induced within the acceptance angle of the fiber to cause these total reflections from the walls. Individual fibers are insulated from one another by a glass "cladding." This cladding must be at least 0.5 micron or one wavelength thick in order to be effective. Some light is lost in its transmission in an optical fiber and this loss is a function of the absorption of the glass or plastic.

In addition, there are losses in the light as it enters and leaves the fibers. Optical fibers may be tapered to concentrate or diffuse a light source and the faces of a bundle of optical fibers may be treated, ground or polished dependent on the results desired.

The maximum angle at which a fiber accepts light is dependent on the indices of refraction of the fiber and the cladding. The behavior of light in different fibers is a function of many variables, fiber configuration, materials, wavelengths, etc. Many types of optical fibers have been investigated in many combinations of core material, cladding materials, end-finishes, diameter and lengths. This investigation resulted in being able to select optimum fibers and a method of treatment to increase their efficiency. These fibers can be produced in long lengths and are completely flexible. They can be tied in knots, dropped, vibrated, and smashed with minimal degradation in their light transmitting properties and can operate in temperature environments of  $-450^{\circ}\text{F}$  up to  $+1200^{\circ}\text{F}$ . They are completely unaffected by E and H fields. Some fibers are also very resistant to high neutron flux fields.

### C. Explosives and Propellants

The high temperatures which can be produced by concentrating the laser light in a very small area, are sufficient to initiate almost any explosive.

( ) Secondary explosives are also detonated. In order to further optimize the LEED system, and reduce the energy and power levels necessary throughout the entire system, we are investigating many propellants and explosive combinations, their chemistry and the optical parameters. The end object is the development of a series (primary and secondary) of explosives insensitive to any damaging environment, but capable of reacting to the laser beam and producing any end-function necessary. In addition, we are investigating absorption spectra of inert compounds in order to produce combinations in which degradation of the pyrotechnic compounds may be discovered by optical means. These compounds are mixed as indicators into the explosive itself.

The coherent light emitted from the laser is transmitted into the optical fiber at an acceptance angle which is optimum for that fiber. These acceptance angles are quite low, on the order of 7 to 9 degrees maximum and produce the highest reflective quantities from the internal walls of the fiber and consequently the best transmission of light. The fibers selected for any system are selected on the basis of the end-function or requirements of the system.

The use of the laser has provided a new and unique approach to the design of initiators, detonators, igniters, and other ordnance devices (see figure 3). The initiator used with the LEED system looks exactly like a normal EBW or hot bridgewire unit on the outside.

It is, however, extremely simple in design. All bridgewires, spark gaps, pins, ceramic headers, insulators, etc., have been totally eliminated and the device simply contains the explosive compound sealed in by means of a glass window. The glass itself is a high quality infrared transmitting glass with tapered conical shaped edges which recollimates the laser beam being received from the optical fiber and loads the window optimally. The windows are designed, and have been tested, to withstand up to 100,000 psi and allow the application of laser light on the explosive compound over a 0.01 in<sup>2</sup> area.

#### Connectors

One of the most interesting features of the LEED System is the ease of connecting the optical fibers to the end-users: detonators, initiators, etc. The system does not require any special methods of optical fiber end-coating, grinding, or special geometry and the optical fiber ends can be cut and mated to the connector in simple fashion. End treating controls are not complex and do not require any sophisticated tooling to achieve. A processing system is under development and will enable this operation to be performed "in the field" with simple hand tools.

The connectors do not have to be water or moisture tight since these environments do not effect the transmission of energy from the donor to the receiving fiber.



No indexing is required since there is no polarity in the common sense of the word. Through bulkhead initiation is accomplished with the simplest of connectors. Instead of the normal explosive donor transmitting a shock wave through the bulkhead to an explosive receiver, a hermetically-sealed window in the bulkhead wall is used to pass the laser energy through the wall and eliminates any shock to the bulkhead itself. The window can be sealed to withstand up to 100,000 psi and 1000<sup>o</sup>F. Connector areas can be significantly reduced since the amount of energy transmitted by the laser system (per unit area) is many times that of an electrical system.

The LEED system is completely insensitive to E and H fields. The only physical connection to a detonator or initiator, or group of these devices, is the series of optical fibers. The coherent light moves, independently of these fields, to the explosive device and causes the pyrotechnic reaction. Since the optical fibers and the ordnance devices are immune to reaction of these fields, (they contain no electrical circuitry or are pure Faraday shields; radiation has no means by which it can produce effects), the system is completely safe and reliable. Tests have been conducted to determine if any electrical phenomena occurs due to the coherent light being transmitted through the fiber. It has been found not to be measurable if even existing.

Accidentally setting off the LEED System by means of extraneous light sources is very nearly, if not totally, impossible for the following reasons:

- a. High intensity non-coherent sources are very nearly non-existent. Tests with output energy as high as 5000 joules, using non-coherent sources, have been focused into the fibers and have not set off any reaction.
- b. Due to the characteristics of the fiber optics, unless the energy it is transmitting is coherent, the phenomenon necessary for pyrotechnic reaction will not be present and since there are no naturally coherent sources, the hazard is eliminated.
- c. The fiber is totally internally reflecting and, hence, is totally externally reflecting. Therefore no energy will be received by the fiber unless it is within the acceptance angle of the fiber which is below 9 degrees.

It can be seen that a very high intensity light (higher than the flux density of the surface of the sun) that is coherent, at the right frequency to transmit efficiently down the fiber, and within the acceptance angle of the fiber must be used. To have all of these parameters occurring and available at a single moment in time at a specific location, is for all practical purposes impossible.

It can be seen that due to the inherent characteristics of the LEED System, electrical tests on the device and its transmitting fibers are totally meaningless, thereby eliminating many MIL Specification tests. Since the device and components are themselves solid-state (solid fibers of glass or plastic, and initiators or detonators which are hollow metal shells) the requirements for tests such as jolt, jumble, sand, dust, fungus, etc., have been greatly reduced.

The laser package itself is nothing more than a firing unit attached to a flash lamp and no new hazards have been introduced by the design of this system. Usually, initiators and detonators with their associated firing leads travel outward from a central location into a more hazardous or exposed environment in an aircraft, missile, or spacecraft. The strains put into the firing package have already been adequately remedied in the development of the present EBW firing control system which is similar in design.

These units have exhibited the capability of operating in all current aerospace environments. There is every confidence that the more simplified firing unit used in the LEED System will easily meet those requirements.

The laser head is designed to be a completely mechanically solid and integrated unit. The emitting rod, whether ruby or neodymium, is mechanically located at one focus of a solid-state ellipse, with the linear flash lamp located at the other foci.

These two components are held in a clear transmitting glass which is supported along its length. The laser head requires no cooling of any type and therefore, the normal susceptibility of cooling equipment to adverse environmental conditions is eliminated.

LEED devices (initiators and detonators) have been placed under water and been fired. Since there are no electrical connections they have been proved to be perfectly safe and totally reliable for underwater operations.

#### Checkout

Most of the current ordnance systems, hot bridgewire, EBW, CDF, etc., are extremely hard to check out reliably. LEED Systems allow visible optical checkout of the entire optical fiber system, the window, and the condition of the propellant or explosive. One mode of checkout is simply to inject light into the optical fiber.

Briefly, the checkout procedure for a LEED System is as follows:

A multiple input is used for all devices, i.e., some fibers are available for transmitting the laser pulse to the reacting pyrotechnic device and a small number of fibers are reserved for checkout purposes. These checkout fibers are routed to a convenient location, where they receive an input of non-coherent light. This light energy reflects down the fiber, through the sealing window in the device and onto the pyrotechnic compound. The pyrotechnic compound then reflects a portion of the light back through the window, through the fibers, to a receiving device.

( ) Depending upon the color (absorption spectra) of the pyrotechnic compound or pyrotechnic compound in combination with various inert indicators, a reflective readout is available at the output end of the return fibers. An analogy might be the use of a Sylvania blue dot flashbulb. If this bulb was placed at the end of a fiber system and one looked down the fiber onto the blue dot, (which would reflect its blue light back through another fiber in the same bundle), a positive indication of the condition of the bulb could be made. If oxidation, moisture, or some other condition occurred, a change in the color of the reflected light would show a "no-go" condition of the system.

1 If the fibers are broken at any point along their routing, we can assess this system failure since we receive no light return. In addition, if an initiator or detonator has not been connected to the fiber, there will be no light return showing a discontinuity in the system.

The use of such a system for checkout allows inspection of the energy carrying capability of the fiber, the transmitting condition of the sealing window, and to a good degree, the chemical state of readiness of the pyrotechnic compound. With this system it is possible to have a non-coherent light source on at all times and know the condition of the pyrotechnic compound and the entire system at any time prior to firing.

When the laser is energized and coherent light is emitted to fire the device, a small light return from the window to the checkout fiber is returned allowing the timing of the actuation of the firing pulse. When the pyrotechnic compound reacts, and emits its characteristic light due to the emission spectra of the various compounds that are burning, a light output at the checkout fibers can be seen, and if applicable, this light can be photographed for later spectrographic analysis to determine sought-after parameters and characteristics of the reaction. After pyrotechnic reaction has occurred, the detection of the darkening or blackening of the windows from oxidation taking place by the pyrotechnic on its surface during the reaction, provides a positive indication that the reaction took place.

#### Explosives and Propellant Characteristics

Many tests on various explosive and propellant combinations have been conducted and a number have been selected for use with the LEED System. These range from the primaries to the secondaries, although from the safety standpoint either type may be used.

Some customer specifications insist upon secondary explosives, and for that reason a number are being tested and qualified with the system, for example, PETN and RDX. The door has been opened by the development of the LEED System for the use of mixes which have special properties and characteristics.

Requirements such as shock, drop, friction, electrostatic input, heating rate, etc., have been set up and these tests are being performed on various new compounds in an effort to develop a material which is tailored to the operating characteristics of the LEED System.

### Firing

The LEED System power supply is adaptable to the normal electrical systems used in aircraft, missiles and spacecraft. The system operates in a similar fashion to an EBW system.

A low voltage source, i.e., DC battery or 400 cycles AC, is used as input energy. This is then stepped up to a higher voltage and charged into a capacitor. The capacitor is then "dumped" into the optical pumping source, which may be a xenon flashlamp, to create the necessary population inversion in the ruby or neodymium rod. Basically, the system is a low voltage, to high voltage step up, to energy storage, and then via an electrical switch, to the flashlamp.

Since simultaneity is not a function of system ready-time, but a function of the relative time of occurrences of the end devices, it is obvious that a laser system which can initiate a large number of devices from the same burst of energy should have an increased advantage in this area.

With an EBW system, a separate firing unit is necessary for each detonator or initiator. Simultaneity of the LEED System is enhanced over an EBW system because of the fact that simultaneity is a measurement of the relative time between any two occurrences. In an EBW system, where a separate firing unit is necessary for each end function, one must take into account not only the variables of the reaction, but the variables of reaction time of the firing units. With the LEED System, since all pyrotechnics are actuated from the same output of coherent light, the only variables are the reaction times of the detonators or initiators themselves.

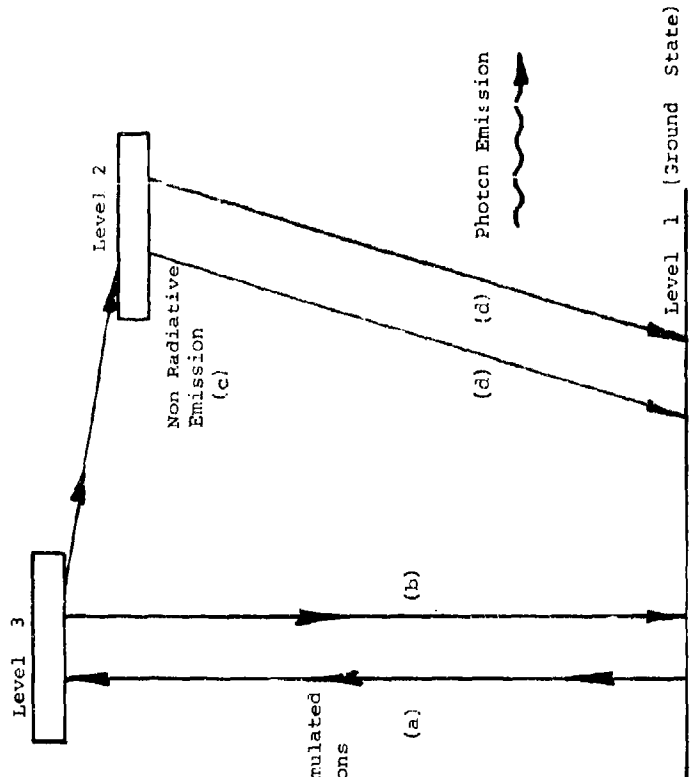
By producing optical fibers of the same length and characteristics, the system is uniform. It is also possible to use fibers of varying length and matched to varying optical properties to produce simultaneity.

#### D. LEED Systems Applications

SOS, Inc., has developed LEED as a systems concept and for the first time ordnance can be handled as a complete integrated system. In the past, for example, with hot bridgewire systems, ordnance was usually a device that was attached to another electrical power system or the distribution capability of another system. This penalized the designer of the ordnance component as well as the use of the component, and did not allow the flexibility of design necessary for optimum performance.



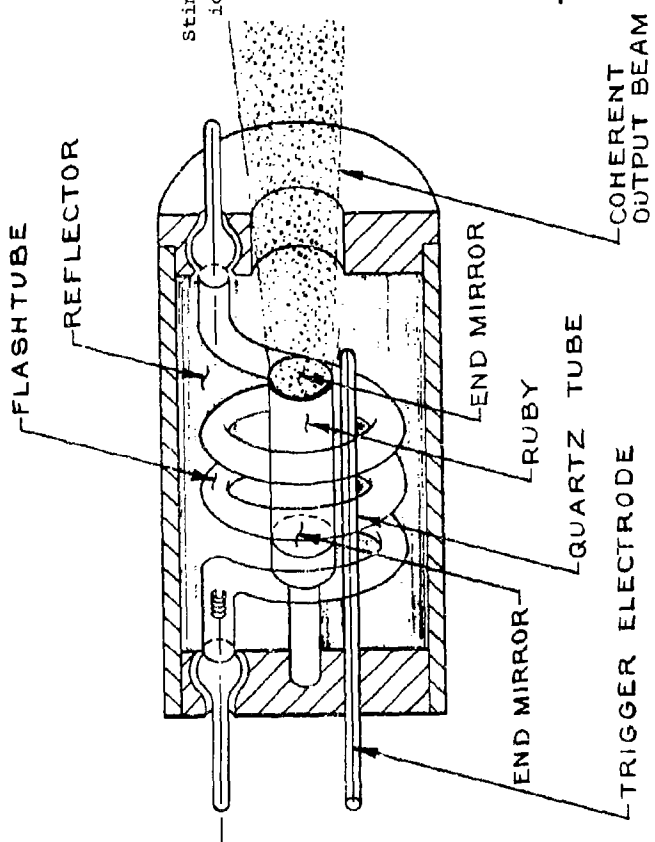
The most important characteristic of the LEED System is its inherent flexibility. Since the laser source is capable of supplying energy for detonators, initiators, igniters, etc., from the same output pulse, it is now possible to connect all of these to a common energy supply line. For example, a multi-branching output fiber bundle may be routed to as many as 50 to 100 leads which may be used for all devices in the system. All of these individual systems are independent of one another and are isolated electrically but programmed from a single source. This capability has been a requirement in the past, but was not available in hot bridgewire or EBW Systems.



SIMPLIFIED ENERGY-LEVEL FOR RUBY LASER

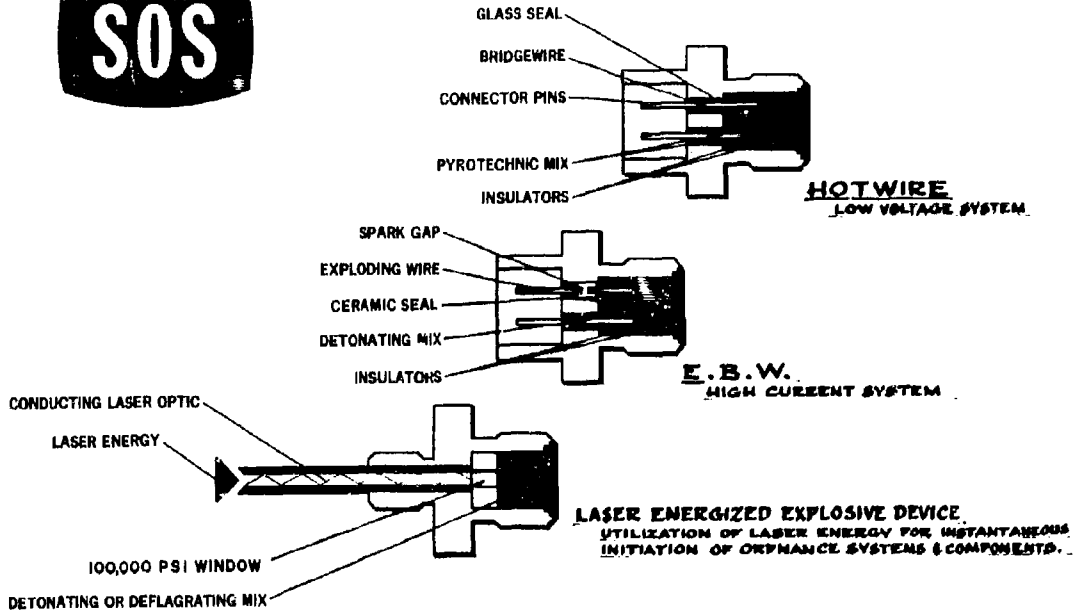
- (a) Chromium ions ( $Cr_2O_3$ ) irradiated.
- (b) Some chromium ions return directly to level 1.
- (c)  $Cr_2O_3$  dropping to level 2 without radiation.
- (d)  $Cr_2O_3$  returning to ground state emitting photons.

FIGURE II



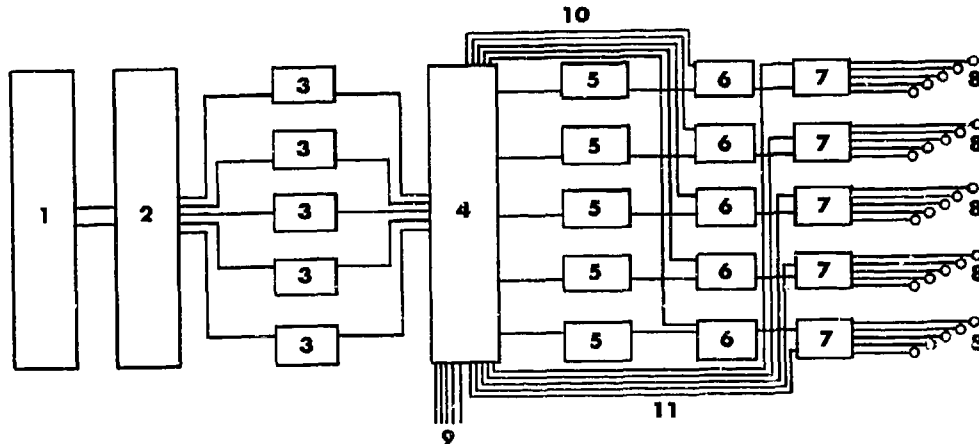
TYPICAL RUBY LASER

FIGURE I



Laser-energized explosive device (bottom) compared with hot-wire and E. B. W. initiators.

FIGURE 3



Integrated laser-energized explosive device system. Legend: 1) electrical power source 2) high-voltage generator and control system, 3) laser-firing energy sources, 4) energy-sequencing system and firing control unit, 5) integrated laser units, 6) safe and arm device, 7) solid-stage optical switch, 8) explosive devices, 9) light-activated remote controls, 10) safe-arm feedback system, 11) optical switch control links.

## DISCUSSION

Coherent light is used to keep energy within the fiber. The free running laser supplies light in discrete pulses to the fiber that serves to bunch the light output and effectively amplify the light in this manner. This feature provides a fuse effect and also prevents sources like xenon lamp flashes or atomic explosions from firing the explosive.

Some pyrotechnics are too transparent to the light from this source. PETN, for example, absorbs energy strongly from light that is below a wavelength of 200 millimicrons but above this the absorption drops from 100% to 12 - 18%. Additives are used with some materials to increase absorption. These additives do not increase the impact sensitivity of the explosive materials appreciably.

Alignment of the fibers and the acceptor is no real problem. The fibers are cut off with a razor blade for demonstration purposes.

Vibration, moisture, and dirt have little effect on the system. Forty-foot drops, 30-caliber machine gun firings or several inches of water have little effect as long as the window is not completely opaque.

1-9 THE DEVELOPMENT OF A WATER ARM-ATR SAFE DETONATOR

Louis J. Montesi  
U. S. Naval Ordnance Laboratory  
White Oak, Silver Spring, Maryland

1. Current Navy design practice for explosive trains is to interrupt the action of the sensitive explosives between the initiator and the input to the lead and/or booster. The explosive action is interrupted to avoid accidents from unintentional initiation of the "sensitive" explosives in the train. This has previously been accomplished by interposition of barriers and/or by misalignment of the train components.
2. A second Navy requirement is that arming, or alignment of the displaced components, for example detonator to lead, be accomplished after launch. In underwater ordnance, such arming is usually accomplished by mechanical means, actuated by either water pressure or movement of the device through water.
3. A third Navy requirement is that any explosive used beyond the interrupter shall be no more sensitive than the Navy standard of tetryl.
4. An appealing approach to the development of systems which are to arm after water entry is to utilize the difference between the confining action of air and of water to control propagation of detonation. Stresau and Slie invented<sup>1</sup> a "Water Confinement Arming Device" using the above differential confinement principle. This is a device which will propagate to detonation only when immersed in water. It does not depend on physical interruption of the column to prevent detonation propagation when in air. The detonator<sup>2</sup>, as further refined by Stresau is shown in Fig. 1.

5. The unique feature of this design is that a lightly confined column of explosive is surrounded by an annular air cavity and, in turn, by a relatively heavy metal tube. The diameter of the column of explosive is chosen so that it is less than the failure diameter when the annular cavity is filled with air, and larger than its failure diameter when this same cavity is filled with water. This change in "failure diameter" is the result of the greater effectiveness of water as a confining medium. This effect is further increased by the reflected shock wave from the surrounding tube.

6. Stresau in his original assessment of safety and reliability used a "no dent criterion" for a detonator failure in air. That is, when his device was initiated in air, explosives could propagate to and through the base charge, but could not produce any measurable dent in a steel witness block used to measure base charge output<sup>3</sup>. However his design when fired in air occasionally permitted complete burning of the base charge explosive.

7. The purpose of this report is to describe work at the Naval Ordnance Laboratory undertaken to further the development of an explosive device of this type. Our work has five facets:

- a. Study feasibility of using higher density nitroguanidine to increase mechanical stability to vibrational forces.
- b. Quench burning action when fired in air.
- c. Verify confinement enhancement effect of steel jacket when in water.
- d. Improve fabrication methods: shorter column, better plastic tubing material.

e. Make item capable of meeting usual surveillance conditions for explosive components, i.e. Mil-Std-304 temperature-humidity cycle.

8. The first tests conducted (on part of the work being reported here) on the water confinement arming device, as refined by Stresau, were to determine the optimum charge density of the nitroguanidine transmission charge. Devices having transmission charge densities from  $0.35 \text{ gm/cm}^3$  to  $1.25 \text{ gm/cm}^3$  were tested in air and water. Table 1 gives the results of these tests. It can be concluded from the results that the nitroguanidine transmission charge density should be less than  $0.80 \text{ gm/cm}^3$  and more than  $0.35 \text{ gm/cm}^3$  for reliable initiation of the base charge in water. As regards safety, or chance initiation of the base charge in air, no high order initiation of the base charge occurred over the entire density range.

9. In addition to these tests the propagation velocity of nitroguanidine at various densities was measured underwater using a 35 mm smear camera. The propagation velocities of nitroguanidine were measured in two test configurations: with and without the outer metal confining sleeve. As earlier stated it was suspected that the shock wave underwater was reinforced by the reflected shock wave from this confining tube. The results of these tests (see Table 2) although inconclusive appear to support this suspicion. It is also evident that the propagation velocity increases as the density of the nitroguanidine transmission charge increases. From the records we noticed that the maximum propagation velocity was always reached prior to a detonation run length of 22.5 mm. For this reason it was felt that the exposed tube

length could be reduced to 22.5 mm without sacrificing the reliability aspects.

10. To determine the feasibility of quenching burning of the base CH-6 charge when the device is in air, and completely detonating the base charge when the device is in water, an aluminum barrier plate was placed between the intermediate CH-6 charge and the base charge. Several other changes were also made based on the propagation velocity studies, see Fig. 2.

11. Tests were conducted to determine the optimum barrier thickness required for reliable detonation transfer in water. The observed probability of initiation through this barrier was studied as a function of the barrier thickness. The data are summarized in Table 3. There were 54 out of 54 successful fires made with barriers ranging in thickness from 40 to 200 mils. Using binomial statistics<sup>4</sup>, we can deduce a reliability of at least 94.6% at 95% confidence for a 40 mil barrier. However, 19 out of 19 fires were observed with a barrier thickness of 150 mils, a thickness nearly four times greater than our intended 40 mil design thickness. These data intuitively indicate a high margin of reliability for the system. The results at 150 mils combined with the observed 2 responses out of 8 trials at 250 mils can be combined to give a quantitative estimate of reliability at 40 mils by the following process.

12. Experience tells us that the probability of detonation transfer\* through solid barriers in small diameter systems such as this increases

---

\*The probability is expressed as a straight line function.



as the logarithm of the reciprocal barrier thickness<sup>5</sup>. We observed 2 responses out of 8 trials at a barrier of 250 mils. Although the observed probability is 0.25, there is at least one chance in twenty that the true probability of firing might be as much as 0.60. At a barrier thickness of 150 mils, 19 successes were observed in 19 trials. The estimate of the true probability of firing at 95% confidence could be as low as 85.4%. Expressing the normalized probability coordinates in probits<sup>6</sup> we can extrapolate a conservative estimate of reliability of greater than 99.91%. Table 4 shows how this extrapolation is made.

13. The safety aspects of the WARAS Device\* tested in air were assessed using the VARICOMP test procedure<sup>7</sup>. This procedure is a method developed by Ayres, et al, and can be used to determine the detonation transfer probability across some explosive interface. Figure 3(a) is a blown up view of the aft end of the WARAS Detonator. When one uses the VARICOMP test procedure to assess safety, an explosive more sensitive than the design explosive is used. The VARICOMP test explosives have been calibrated by the NOL Small Scale Gap Test<sup>8</sup>, Figure 3(b). We wish to prove that detonation will not propagate in air from nitroguanidine to the CH-6 base charge across the 40-mil thick aluminum barrier. We therefore substitute more sensitive explosives--PETN<sup>9</sup> and Calcium Stearate-RDX<sup>9</sup>, (1.65/98.35)--for the CH-6 below the aluminum barrier. It should be noted that only the CH-6 in the base charge is changed.

14. As an additional conservatism we carried out all of the safety tests with a thinner barrier than is intended in the final design, i.e. 25 mils instead of 40 mils.

\*Acronym for Water Arm-Air Safe Detonator

15. The results are shown in Table 5. Three types of quenching were noted; (a) somewhere in the nitroguanidine column leaving some unburned nitroguanidine, (b) somewhere in the intermediate CH-6 charge above the aluminum barrier leaving some unburned CH-6, and (c) quenching at the barrier with all explosives above the barrier being consumed. Only when the latter outcome was observed was there any chance of initiating the VARICOMP explosive. Consequently only line 2 of Table 5 can be used in the VARICOMP safety analysis.

16. Using binomial statistics we can assume that even though we saw no transfers out of 4 trials at 95% confidence there could be as much as 52.7% response with PETN in this configuration. This gives a limit on the drive across this interface of no more than 2.81 DBg. But a very conservative estimate<sup>8</sup> for the firing probability of CH-6 pressed at 10,000 psi in this system is 0.1% at 95% confidence. However, we are using CH-6 at 22,000 psi rather than at 10,000 psi, and CH-6 is known to be considerably more difficult to initiate at the higher loading pressure.

17. Since the safety and reliability aspects of the WARAS Detonator were deemed acceptable with a 40-mil thick aluminum barrier, a number of these units were made and subjected to the standard Navy environmental and surveillance tests with the results shown in Table 6. As can be seen, the WARAS Detonator passed all tests except MIL-Std-304, the temperature and humidity cycling test.

18. Since the device did not pass the temperature-humidity test, we have made a concentrated effort in that direction. In the past a spirally

wound mylar tube, 0.165 ID with a nominal wall thickness of 2 mils was used as the explosive container. The failure of the WARAS detonator to pass Mil-Std-304 was attributed to leakage at the seams between adjacent turns of the mylar. We therefore procured seamless polypropylene and polyethylene tubing (Table 7). Additional units were just made with polyethylene and subjected to Mil-Std-304, but the results were, if anything, worse (Table 8). We believe the problem is to find bonding agents or sealing resins which will adhere to polymer surfaces such as polypropylene or polyethylene. A literature search was made for ways to improve the bonding of these tubes. It was found that the bonding to these tubes could be improved by various surface pretreatment processes<sup>10</sup> such as flaming, corona discharge, dichromating, or exposure to ionized gases.

19. Because treatment with ionized gases was the simplest to conduct, this approach was tested first. Additional WARAS detonators were made using ionized oxygen to prepare the tubing surfaces, and subjected to Mil-Std-304. Two potting compounds were tried in conjunction with the tube materials and surface treatments. However, the end results were discouraging. Failures to fire in water after Mil-Std-304 were still observed. The results are given in Table 9. Leakage was traced to: (a) poor epoxy seals, (b) pin holes in the tube (it seems that it is possible to get pin holes in tubes of 2 mils wall thickness), (c) tube punctures during loading.

20. However, the tests did show that (a) Epoxy A performs better than epoxy B, and (b) the polypropylene tube when treated performs better than polyethylene tubes.

21. From these results it appears essential to either increase the wall thickness of the tubing or have inspection techniques that will preclude the acceptance of tubing having pin holes or other leaks. Since damage to the tubes may occur during the loading process the use of thicker tubes is going to be investigated. Such work is already underway. The use of a thicker tube will necessitate a reconfirmation of the safety and reliability estimates already made.

#### REFERENCES

1. R. H. F. Stresau, Jr., W. M. Slie, Patent 3,169,481 "Water Confinement Arming Device", 16 Feb 1965.
2. R. H. F. Stresau, "An Investigation of the Applicability of the Water Confinement Arming Principle to Naval Underwater Ordnance", R. Stresau Lab Rpt No. 62-11-1, 21 Nov 1962.
3. Mil-Std-316, "Detonator Output Measurement by the Steel Dent Test", 23 Nov 1966.
4. A. Hald, "Statistical Tables and Formulas", Wiley and Sons Inc., Copyright 1952.
5. J. N. Ayres, "Standardization of the Small Scale Gap Test Used to Measure the Sensitivity of Explosives", NAVWEPS 7342, 16 Jun 1961.
6. D. J. Finney, "Probit Analysis", Cambridge University Press, 2nd Edition, 1962.
7. J. N. Ayres, L. D. Hampton, I. Kabik, A. D. Solem, "VARICOMP - A Method for Determining Detonation Transfer Probabilities", NAVWEPS Rpt 7411, 30 Jun 1961.
8. L. J. Montesi, J. N. Ayres, "Detonator to Lead Transfer Studies for the Destructor 115", NOLTR 66-127, 13 Jan 1967, Confidential.
9. J. N. Ayres, C. W. Randall, "RDX/Calcium-Stearate Binary System Explosive Sensitivity Calibration", NOLTR 63-91, 15 May 1963.
10. Modern Plastics - Encyclopedia Issue for 1961, Sep 1966, Vol. 38, No. 1A, Library of Congress File No. TP986.A1M62 V. 38, 1961.

#### DISCUSSION

A possible shallow water limitation was mentioned and acknowledged.

Fig. 1  
**WATER CONFINEMENT ARMING DEVICE**  
**( STRESAU TYPE K160 )**

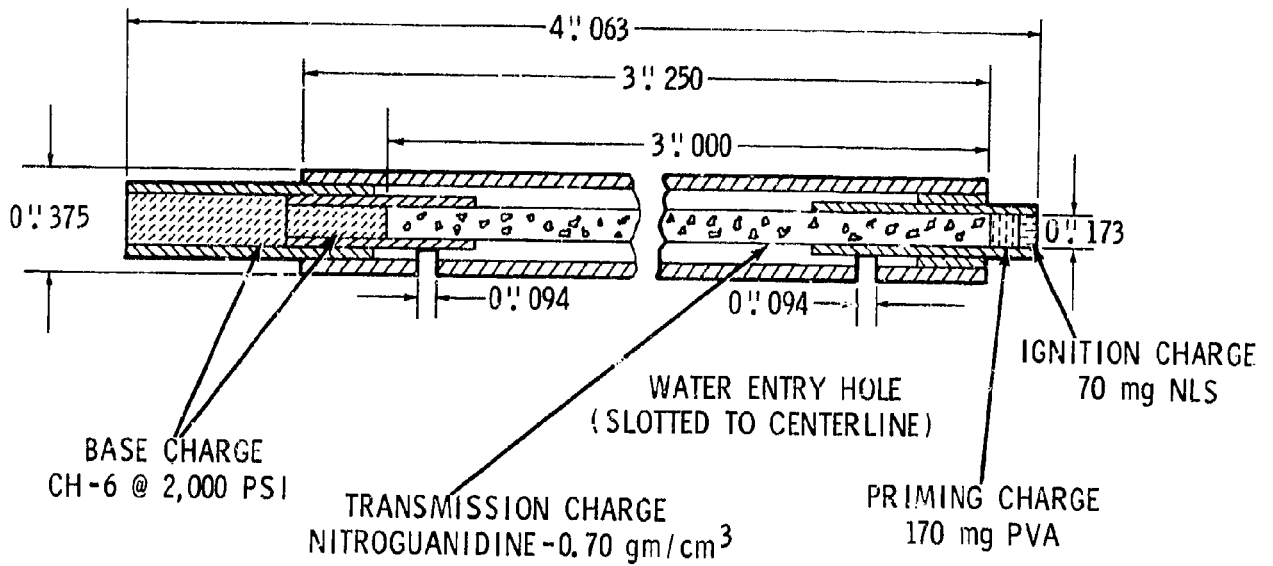


Fig. 2  
**WATER ARMED/AIR SAFE DETONATOR (WARAS DETONATOR)**

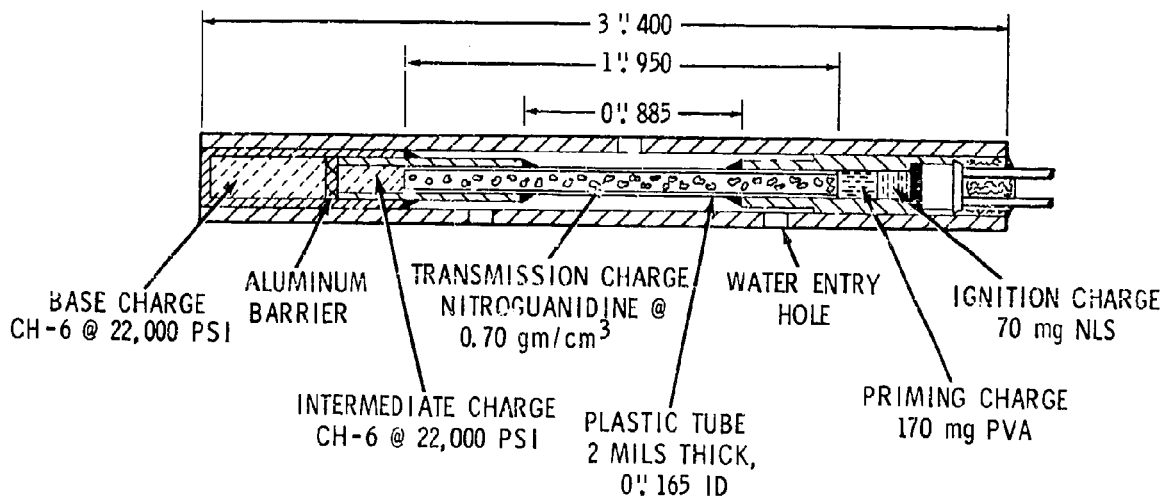


Fig. 3A  
**WARAS EXPLOSIVE DEVICE  
 (AFT END)**

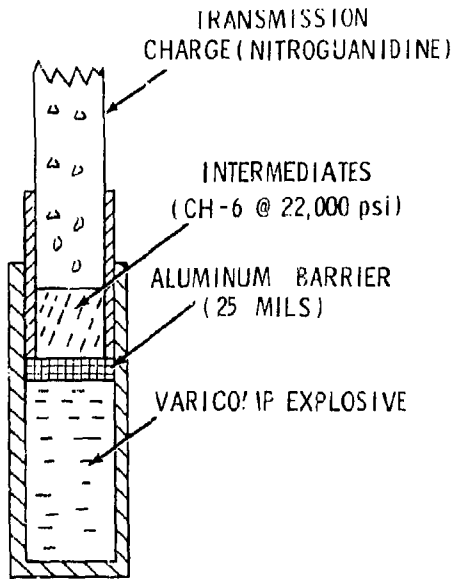


Fig. 3B  
**SMALL SCALE GAP TEST  
 SETUP**

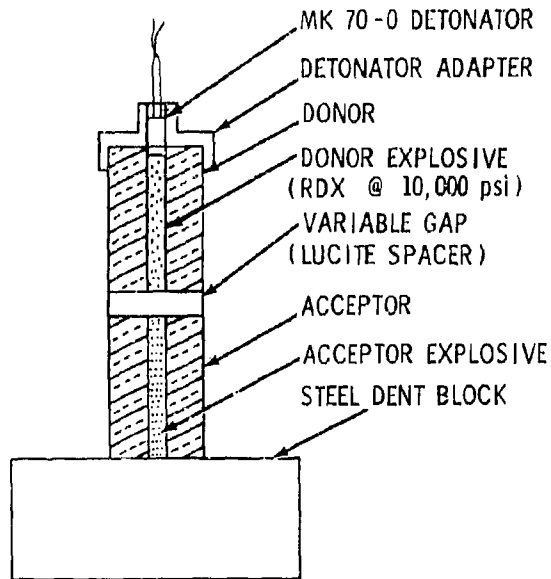


TABLE 1  
**THE EFFECT OF DENSITY OF NITROGUANIDINE  
 ON PERFORMANCE**

NITROGUANIDINE TRANSMISSION CHARGE DENSITY (gm/cm <sup>3</sup> )	TEST ENVIRONMENT	
	WATER*	AIR*
0.35	4/10	0/2
0.40	4/4	0/2
0.45	14/14	0/2
0.50	-	0/5
0.54	-	0/5
0.60	3/3	0/2
0.70	20/20	0/3
0.80	4/5	-
0.90	2/5	0/1
1.00	0/1	0/2
1.25	0/1	0/2

\*RATIO GIVES NUMBER OF HIGH ORDER INITIATIONS (STEEL DENT CRITERION) OBTAINED PER NUMBER TESTED.

TABLE 2  
**PROPAGATION VELOCITY OF NITROGUANIDINE UNDERWATER  
 AT VARIOUS DENSITIES**

TRANSMISSION CHARGE DENSITY (gm/cm <sup>3</sup> )	NITROGUANIDINE PROPAGATION VELOCITY (METERS/SECOND)	
	NO CONFINING SLEEVE	WITH CONFINING SLEEVE
0.45	2600 - 2700	2800 - 2900
0.45	2800 - 2900	2800 - 2900
0.55	2500 - 2800	2800 - 2900
0.70	3000 - 3050	3100 - 3200

TABLE 3  
**ALUMINUM BARRIER THICKNESS TEST  
 RESULTS OF THE WARAS DETONATOR**

NUMBER TESTED	THICKNESS OF ALUMINUM BARRIER (MILS)	RELIABILITY TEST RESULTS*
4	40	4/4
21**	40	21/21
2	50	2/2
2	60	2/2
2	70	2/2
2	80	2/2
1	100	1/1
1	125	1/1
19	150	19/19
1	200	1/1
8	250	2/8

\*RATIO GIVES NUMBER OF HIGH ORDER  
 INITATIONS (STEEL DENT CRITERION)  
 OBTAINED PER NUMBER TESTED.

\*\*UNITS ARE FROM THE ENVIRONMENTAL  
 TESTS (EXCEPT MIL-STD 304)

TABLE 4  
**RELIABILITY TEST RESULTS OF WARAS DETONATOR  
 USING A BARRIER TYPE PENALTY TEST**

ALUMINUM BARRIER (MILS) (c)	OBSERVED RESPONSE (d)	LOGARITHM RECIPROCAL BARRIER THICKNESS (e)	CONSERVATIVE ESTIMATE OF PROBABILITY (f)	PROBIT (g)
250	2/8	0.602	0.600 <sup>(1)</sup>	5.253
150	19/19	0.823	0.854 <sup>(2)</sup>	6.054
40	-	1.397	0.9991	8.134

- (1) UPPER LIMIT OF OBSERVED PROBABILITY FOR 2/8 FIRES, 95% CONFIDENCE  
 (2) LOWER LIMIT OF OBSERVED PROBABILITY FOR 19/19 FIRES, 95% CONFIDENCE

NOTES—

- (a)  $g$  VARIES LINEARLY WITH  $e$ , THEREFORE  $g = me + b$   
 WHERE  $g$  IS THE PROBIT VALUE FOR ESTIMATED PROBABILITY.  
 $e$  IS THE LOGARITHM OF RECIPROCAL GAP.  
 $b$  IS THE Y AXIS INTERCEPT (3.071) CALCULATED BY SUBSTITUTION.  
 $m$  IS THE SLOPE (3.629) CALCULATED FROM THE EQUATION BY SUBSTITUTION.  
 (b) THE VALUE OF  $g$  FOR 40 MILS IS OBTAINED FROM  $m$ ,  $e$ , AND  $b$ .

TABLE 5  
**SAFETY TEST RESULTS OF WARAS DETONATOR  
 USING VARICOMP TEST PROCEDURE**

LINE NO.	NUMBER TESTED	BARRIER THICKNESS (MILS)	BASE CHARGE EXPLOSIVE	CONSOLIDATION PRESSURE (PSI)	SSGT SENSITIVITY (DBG)	FAILURE POINT		
						(a)	(b)	(c)
1	30	25	CH-6	22,000	5.65	0	14	16
2	5	25	PETN	8,000	2.80	1	0	4
3	5	25	1.65% Ca St/RDX.	8,000	3.80	2	3	0

- (a) IN THE NITROQUANIDINE COLUMN  
 (b) IN THE INTERMEDIATE CHARGE COLUMN  
 (c) QUENCHED AT THE ALUMINUM BARRIER



TABLE 6

## WARAS DETONATOR - ENVIRONMENTAL TESTS

ENVIRONMENTAL CONDITIONING	NO. TESTED	RESULTS AFTER CONDITIONING SUCCESSFUL RESPONSES TO NO. TESTED	
		SAFETY*	RELIABILITY
TRANSPORTATION VIBRATION (MIL-STD-353)	10	0/5	5/5
AIRCRAFT VIBRATION (TN 1441-VIA)	10	0/5	5/5
JOLT (MIL-STD-300)**	7	0/3	4/4
JUMBLE (MIL-STD-301)**	7	0/4	3/3
FORTY-FOOT DROP**	3	0/1	2/2
(MIL-STD-302) HORIZ VERTICAL	3	0/1	2/2
TEMPERATURE & HUMIDITY 2 WKS	10	0/2	6/8
CYCLING (MIL-STD-304) 4 WKS	19	0/9	9/10

\*NO EXPLOSIVE BURNED BELOW THE ALUMINUM BARRIER.

\*\*TO MEET THIS TEST SUCCESSFULLY, THE DEVICE NEED NOT BE OPERABLE; BUT NO EXPLOSIVE ELEMENT SHALL EXPLODE OR BE UNSAFE TO HANDLE OR DESTROY. HOWEVER, THE DEVICES APPEARED IN SUCH GOOD CONDITION FOLLOWING THE TEST THEY WERE SUBJECTED TO SAFETY & RELIABILITY TESTING AS WELL.

TABLE 7

## WARAS DETONATOR - DESCRIPTION OF TRANSMISSION CHARGE TUBE

	TUBE 1*	TUBE 2	TUBE 3
MATERIAL	MYLAR	POLYETHYLENE	POLYPROPYLENE
TYPE	SPIRALLY WOUND	SEAMLESS	SEAMLESS
INSIDE DIAMETER (NOMINAL)	0.165	0.167	0.165
WALL THICKNESS (NOMINAL)	0.002	0.006	0.002
TOLERANCE	±0.001	±0.002	+0.002 -0.000

\*TUBING IN THE ORIGINAL WARAS DEVICES WHICH FAILED THE TEMPERATURE-HUMIDITY CYCLE TEST

**TABLE 8**  
**TEST RESULTS OF WARAS DETONATOR**  
**USING POLYETHYLENE TUBES**

TYPE OF TEST	RATIO OF DETONATION TRANSFERS TO NUMBER TESTED
SAFETY	0/5 (CH-6 BASE CHARGE) 0/1 (PETN BASE CHARGE)
RELIABILITY	5/5
MIL-STD 304	28 SUBJECTED 2/12 FUNCTIONED UNDER WATER 16 CUT OPEN FOR INSPECTION

**TABLE 9**  
**RESULTS OF FIRING IN WATER WARAS**  
**DETONATOR CONDITIONED IN MIL-STD-304**

MIL-STD-304 EXPOSURE TIME	EPOXY	TUBE TYPE		
		POLYETHYLENE	POLYPROPYLENE	
		TREATMENT 1 <sup>(a)</sup>	TREATMENT 1 <sup>(a)</sup>	TREATMENT 2 <sup>(b)</sup>
1 WK	A	2/3	3/3	3/3
	B	-	2/2	-
2 WKS	A	1/4	6/7	3/3
	B	0/3	3/4	-
4 WKS	A	2/7	6/9	4/5
	B	0/8	1/4	-

RATIO INDICATES NUMBER OF FIRES TO NUMBER TESTED

(a) TUBES TREATED WITH IONIZED OXYGEN (300 WATTS, 1 HOUR)

(b) TUBES TREATED WITH IONIZED OXYGEN (275 WATTS, 1/2 HOUR)

# 1-10P NONDESTRUCTIVE VISUAL EXAMINATION

## BY NEUTRON RADIOGRAPHY

Charles Porter - General Electric Company  
Vallecitos Atomic Laboratory  
Pleasanton, California

Frank Burkdoll - Explosive Technology, Inc.  
Fairfield, California

### ABSTRACT

Neutron radiography is a valuable tool for routine and special nondestructive examination of many explosive components as well as other devices. With few exceptions, neutron radiography will not totally replace X-ray as a method of nondestructive examination but provides an invaluable augmentation to the present state-of-the-art methods of examination. A technique has been developed and details affecting the quality of neutron radiographs have been identified. For the first time, the ordnance designer has the opportunity to actually see the explosive load in a given device even though the material may be encased in a massive metal container.

### INTRODUCTION

The reliable function of any explosive train is dependent on the presence and proper orientation of one explosive element with respect to the next. The normally applied inspection technique to assure presence of explosive elements in an assembled device are dependent on X-ray photography. The best X-ray techniques available today, however, do not yield the desired degree of clarity or definition. Most explosives used in devices are essentially transparent to X-radiation, while the materials encasing them are relatively opaque.

The presence of explosive material in metal-sheathed detonating cords cannot be ascertained by X-ray directly; it can only be inferred that the apparent cavity in the cords is filled with explosive. Presence of explosive in devices having massive metal cases can neither be detected nor inferred by X-ray examination. Presence of thinly encased explosive can be detected by X-ray, but only with great difficulty and by using densitometric techniques. It is thus evident that the presence of explosive in most devices cannot be determined by X-ray examination, but can only be assumed and an X-ray photograph is not necessary for that assumption. X-ray photographs, however, do provide a valuable method of inspection for presence and proper orientation of all parts fabricated of metal or of materials opaque to X-rays.

Approximately five years ago, Explosive Technology investigated the possibility of inspecting metal-clad detonating cords by using neutron radiography. It was realized immediately that in order to make such radiographs, a neutron flux of a magnitude available only from a nuclear reactor is required. Continuous scanning of metal-clad cords by low-level neutron sources using electronic detectors appeared to not have the required resolving capability.

Explosive Technology, without access to a nuclear reactor, shelved the idea as an interesting possibility for the future. Approximately one year ago, the General Electric Nuclear Test Reactor (NTR) at the Vallecitos Nuclear Center was made available for radiography and a cooperative program was undertaken between ET and General Electric to investigate the possibilities of utilizing this powerful tool to examine explosively loaded devices. The culmination of this cooperative program between General Electric and ET has been the first commercial, large-scale use of neutron radiography and the production of the largest neutron radiograph (14 inches by 17 inches) ever made.

This size radiograph now is made routinely at the GE facility. Doping of explosives to enhance their ability to be detected on neutron radiographs was also investigated and a suitable method has been devised.

#### DISCUSSION

The mechanics of neutron radiography are relatively simple. A beam of well-collimated thermal neutrons is passed around and through an object. The beam behind the object carries in it, via spatial intensity modulation, information about the internal structure and composition of the object. An imaging system is placed behind the object to record the spatial flux variation. This description fits both X-ray and neutron radiography; and the image obtained looks a great deal like an X-ray photograph, with the important exception that the contrast between materials is vastly different from that observed on an X-ray. Also, more detailed study brings out other basic differences.

Essentially, neutrons are atomic particles with no charge. They can, therefore, penetrate relatively substantial objects, and their absorption is a function of the type of material being penetrated. It will be noted that these are exactly the properties that make X-rays useful for the examination of the internal structure of objects. It is logical, therefore, that neutrons can be used in the same manner. Setting aside the methods of production and imaging of the neutrons, what would be the appearance of a neutron radiograph? The appearance of an X-radiograph is easily predictable - thick objects appear lighter than thin objects; dense objects appear lighter than less dense objects; and high atomic number materials appear lighter than low atomic number materials. The first two characteristics are common with neutron radiographs; however, neutron absorption is almost independent of atomic number.

in terms of X-ray attenuation, an equivalent amount of He is more absorbent than H, Li more absorbent than He, Be more absorbent than Li, and so forth up the periodic table. This is because X-ray absorption occurs in the electron shell around the atom and the configuration and the number of these electrons is a function of atomic number. Neutron attenuation is a nuclear interaction and the nuclear properties involved are not a function of atomic number. Therefore, with neutron attenuation, such a systematic behavior does not exist; e.g., He, U-238, Be, Al, Pb, B-11, Li-7, are reasonably transparent, while H, Fe, W, Mo, Mn, are moderately absorbent, and U-235, Pu-239, Ge, Cd, B-10, Li-6, are highly absorbent.

The absorption coefficient for neutrons is a random function of atomic number, whereas the absorption coefficient for X-rays is a monotonically increasing function of atomic number. Table 1 lists a number of elements and their respective absorption coefficients for X-rays and neutrons. Thus, a hydrogen-containing explosive will be relatively opaque to neutrons.

In its most common form, neutron radiography is performed using a well-collimated, thermal neutron beam from an atomic reactor. Other types of neutron sources, electrostatic generators, isotopic sources, etc., have characteristics (primarily intensity) unsuitable for commercial neutron radiography. Indeed, the vast majority of thermal neutron reactors are unsuited for this type of work. The core configuration of the General Electric Nuclear Test Reactor is particularly suitable for the production of the intense, gamma free, large, well-collimated beam, which commercial neutron radiography demands. Standard X-ray film is placed behind the object to record the image of the object and its internal structure. As X-ray film is relatively insensitive to neutrons,

a thin sheet of Gadolinium metal is placed in contact with the x-ray film. This converter screen captures neutrons and emits low-energy gamma rays, which expose the film.

The resolution of the radiographs obtained using the Gadolinium foil technique is a function of the beam-defining aperture and the film grain. These control exposure time. Routine pictures are taken with resolutions better than 4 mils per inch thickness of the object. Higher resolutions are easily obtainable for special application. Resolutions as high as  $2 \times 10^{-5}$  inches are theoretically possible.

The induced radioactivity in samples, caused by neutron bombardment, is very slight and no special handling is required. There are ample data in the literature to indicate that the threshold for damage to explosives caused by irradiation is at least a factor of  $10^8$  above the exposure necessary to make neutron radiographs of the required quality.

Explosive devices are particularly good subjects for neutron radiography. When properly designed and assembled, gas generators, bolts, cable cutters, etc., work reliably. This characteristic is one of the prime reasons for their wide use in the aircraft and aerospace field. But final assembly is done by human beings and the near absolute reliability required of the devices is not possible to assume in this form of manufacture. Explosive sections with gaps, cracks, insufficient density, improper location, or missing altogether, are inherent causes for failure. Also, epoxy glues often used in explosive placement can cause failure if inadvertently allowed between sections of an explosive train. Post-assembly X-ray examination for these defects is generally extremely difficult, if not impossible. The reason for this is the explosive and epoxy sections are made from low density, low-atomic number

materials, while the device housing is steel or aluminum. To penetrate the housing, X-rays of relatively high energies must be used. The low atomic number hydrogenous sections of interest inside are almost transparent to these X-rays. Neutron radiography offers the capability for nondestructive examination for such defects. The hydrogen-containing explosive and epoxy are strong neutron attenuators, slightly stronger than steel and very much stronger than aluminum. These characteristics allow the position and condition of the low-atomic number explosives and epoxies to be established by neutron radiography. Generally, this information cannot be obtained in any other way short of destructive examination.

Let us examine some samples of neutron radiography and compare them to X-ray samples.

Figure 1 shows an X-ray photograph of a common cigarette lighter. We can see that all the metal parts are present and in their proper place, but we can not determine whether cotton and wick have been included. Figure 2 is a neutron radiograph of the same lighter. Here we easily can see most if not all of the components visible in the X-ray, but we also clearly distinguish the cotton stuffing, wick and flint. As a further demonstration, Figure 3 dramatically shows the capability of neutron radiography by showing that the same cigarette lighter has been filled with fluid. The ability to "see" the cotton, wick, and fluid is attributed to the high hydrogen content of these materials. As was pointed out, highly hydrogenous materials are opaque to neutrons. Table 2 lists a number of materials common in the explosive ordnance industry and their X-ray and neutron attenuation coefficients. From Table 2, it is plain that materials such as lead azide and lead styphnate are readily "seen" in X-ray photographs, but not in neutron radiographs, while



materials such as PETN, RDX and smokeless powders will be readily "seen" in neutron radiographs but not in X-rays. Of special interest are epoxy resins and pyrotechnic mixes containing boron. These appear on neutron radiographs as almost completely opaque and on X-rays as almost completely transparent.

Some of the advantages of neutron radiography are evident by examination of Figures 4 through 11.

Figure 4 shows an electrically initiated detonator in both X-ray and neutron radiographs. We immediately note that in the neutron radiograph view the explosive train is pressed in at least five increments. Two increments at the output end are at a higher density than the remaining three increments. It would appear, from the very light area, that the initiating end of the column is a mixture relatively transparent to neutrons. Note that the thin-walled detonator case does not show distinctly on the neutron radiograph, while on the X-ray it is clearly shown but its contents are indistinguishable.

Figure 5 is another electro-explosive device of the gas generating or pressure cartridge type. Comparison of the two images indicate the use of a prime charge cup that is probably made of plastic, since it appears dark on the neutron view and light on the X-ray view. The prime mixture is probably lead azide or lead styphnate since it appears dark on the X-ray and light on the neutron view. Beyond that, nothing more can be ascertained from the X-ray other than that the closure disc is in place. The neutron view, however, indicates that there is a disc separating the prime from the main charge and that this disc is either paper or plastic. The neutron view also reveals the base charge is a granular powder that is loose in the cavity, which is only approximately half-filled. Note also, that one can detect the insulation on the wires in the neutron view.

Figure 6 is another electro-explosive device, and in this case we have views both of a loaded device and the header prior to loading. Evaluation of the X-ray and neutron views reveals that the header consists of a material, probably glass, that is relatively transparent to neutrons. A prime holder is used in the header also and is relatively transparent to both neutron and X-ray, and is probably a ceramic. The prime charge is opaque to X-ray and is relatively transparent to neutrons, indicating that it is probably lead azide or lead styphnate.

The output charge is transparent to X-ray and opaque to neutrons, and is probably one of the more common explosives or double-based propellants. Insulation has been placed over the wire and a plastic sealing compound has been used to seal the back side of the header to effect a seal with the wire insulation. The prime charge holder has been bonded in place using some organic adhesive.

Figure 7 is another electro-explosive device. Three views are shown. Two are neutron radiographs of two different devices; the third is an X-ray of one of the devices. All three are essentially identical.

The X-ray reveals that a primary charge in the device is probably lead azide or lead styphnate, and is properly located. The closure is properly located and intact, and the shorting plug is in place. No information as to quantity or quality of output charge is available.

The two neutron radiographs indicate that in addition to the primary charge, a paper or plastic material over the primary charge is in place. A granular powder, not completely filling the cavity, makes up the output charge. A paper or plastic disc is used also to separate the output charge from the end closure. In one case this paper or plastic disc is properly located.

In the other case, it has relocated itself farther back in the cartridge. Shorting plugs are placed in both devices, but unlike the X-ray, wherein we see only the wires of the shorting plug, the neutron radiograph reveals both the wires and the plastic material making up the shorting plug. Another neutron-revealed difference is worth noting; in one device the cartridge between the shorting plug and the header has been partially filled with what appears to be a plastic material, while in the other device this cartridge is empty.

Figure 8 shows three views of a non-electric explosive device; two of them X-rays and one a neutron radiograph. Studying the neutron radiograph, reveals an explosive train full length of the device. The explosive train is surrounded almost full length by a material transparent to both neutron and X-ray, which is in fact aluminum. In the small end of the device, the explosive train and its aluminum housing are covered by a material more opaque than aluminum; namely, stainless steel. This stainless steel shell is held in place with an epoxy resin. At the large end of the device, the neutron radiograph reveals that the explosive train extends to the end of the device, and that there are two internal parts to the device at this end; one of them is bonded to the aluminum tube surrounding the explosive train, and the other is bonded to the first part. Evaluation of the light X-ray gives no indication of the presence of the explosive train or the aluminum tube that surrounds it. The light X-ray does give good detail of the two internal parts in the large end as well as the outside container of the device, all of which are stainless steel. In order to make an X-ray that shows the very thin stainless steel cup at the end of the device, it is not possible to show any other detail of the device.

Figure 9 shows four shielded mild detonating cord tips, which are built by ET for the F-111 program. Briefly, these tips consist of a silver-sheathed mild detonating cord, a conical transition charge, and a cylindrical output charge. The cylindrical output charge is contained in a 4-mil stainless steel cup. All parts shown, with the exception of the nuts and the silver, are stainless steel. The explosive is HNS. In the first tip, we see an obvious air gap between the transition and the booster charges. In the second tip we see a low-density transition charge. In the third we see low density in both charges and in the fourth, a total absence of explosive in both the transition and booster charges.

Figure 10 gives some idea of some of the things that are possible by doping explosives with materials that are opaque to neutrons, and some idea of the discreet difference that can be detected by this technique. The bar at the top of the figure is a specially prepared length of mild detonating cord having an aluminum sheath. The cord is loaded on the left, or lighter area, with pure RDX, while the right, or darker area, is loaded with the same RDX doped with 1/2% Gadolinium oxide. At the bottom of Figure 10 are four specially prepared pressings of a pyrotechnic material relatively transparent to neutrons. The two samples on the left are as normally prepared, while the two on the right are doped with 1/2% Gadolinium oxide poorly mixed. Of interest, the dark lines at the end of each of the cylinders are nothing more than a piece of masking tape attached to the end of the aluminum cylinder. These radiographs indicate the possibility of using neutrons as inspection technique to establish the degree of dispersion of components in a pyrotechnic mix. In addition, they clearly show that it is possible to design for neutron radiography by adding insignificant amounts of inert materials, thereby making explosive trains or relatively transparent materials, more opaque to neutrons.

Figure 11 shows four aluminum cylinders 3/4 inch in outside diameter with a 1/4 inch diameter hole completely through. The hole is loaded with the same quantity of explosive in each case, pressed in two increments. The explosives are, from left to right, RDX, PETN, Dipam and HNS. Reference to Table 2 indicates that RDX and PETN have neutron attenuation coefficients close to each other, while Dipam and HNS neutron attenuation coefficients are significantly different from those of RDX and PETN. These differences are clearly seen in Figure 11.

Figure 12 dramatically shows the capability of neutron radiography. The three cartridges shown in Figure 12 have revealed in detail that which can be done only by neutron radiography.

#### CONCLUSION

For the first time, the explosive device industry now has available, a technique that allows inspection for the one most important requirement, the presence of explosives. The state-of-the-art in neutron radiography has advanced to the point that its use on a large scale is now practical as an inspection method for ascertaining the presence of explosives in devices.

TABLE 1. MASS ABSORPTION COEFFICIENT ( $\mu/\rho$ )

<u>Element</u>	<u>X-Rays <math>\lambda = 0.098 \text{ \AA}</math></u>	<u>Neutron (Thermal)</u>
H	0.280	48.5
Li	0.125	3.7
Be	0.131	0.5
B	0.138	24.0
C	0.142	0.26
N	0.143	0.48
O	0.144	0.15
Al	0.156	0.036
Ti	0.217	0.119
Fe	0.265	0.141
Mo	0.79	0.055
Cd	1.09	11.2
Gd	2.08	84.0
W	2.88	0.058
Au	3.21	0.2
Pb	3.5	0.034
U	3.9	0.033
U-235	3.9	1.89

TABLE 2. NEUTRON AND X-RAY ATTENUATION COEFFICIENTS

<u>Material</u>	<u>Density</u>	<u>Neutron Attenuation</u>	<u>X-Ray Attenuation</u>
PETN	1.77	2.545	0.255
RDX	1.82	2.894	0.2666
DIPAM	1.8	1.640	0.198
HNS			
Lead Azide	4.8	0.783	12.15
Lead Styphnate	1.5	0.6776	2.442
16% B Boron	2.16	8.588	0.344
84% KNO <sub>3</sub> Potassium-Nitrate			
48% Ti Titanium	3.19	0.569	0.607
52% KClO <sub>4</sub> Potassium Perchlorate			
70/30 57% Zirconium-Nickel	3.97	0.618	1.612
43% KClO <sub>4</sub> Potassium Perchlorate			
Smokeless Powder (Bullseye)	1.6	2.15	0.225
Steel	7.86	1.1	2.1
Lead	11.3	0.39	40.0
Silver	10.5	2.5	11.0
Aluminum	2.7	0.097	0.42
Titanium	4.5	0.54	0.98
Zirconium	6.4	0.31	4.6
Boron	2.65	60.0	0.35
Epoxy - Armstrong C-7/W	1.1	8.38	0.179

---

Transmitted intensity = Incident intensity times  $e^{-\mu X}$

$\mu$  - attenuation coefficient

X - thickness in centimeters

Neutron spectrum - hard thermal

X-Ray energy - 123 Kv

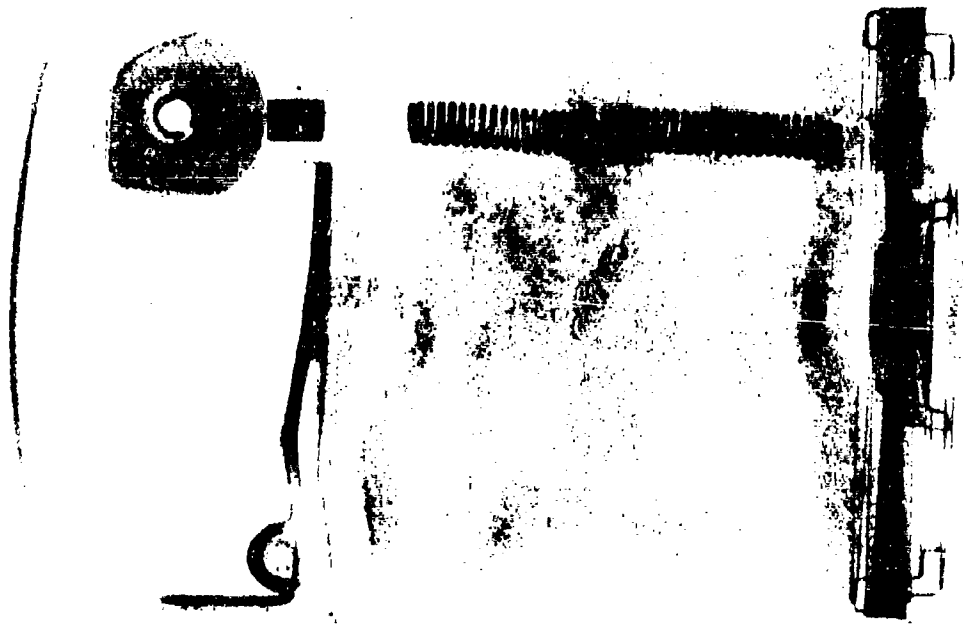


Fig. 2

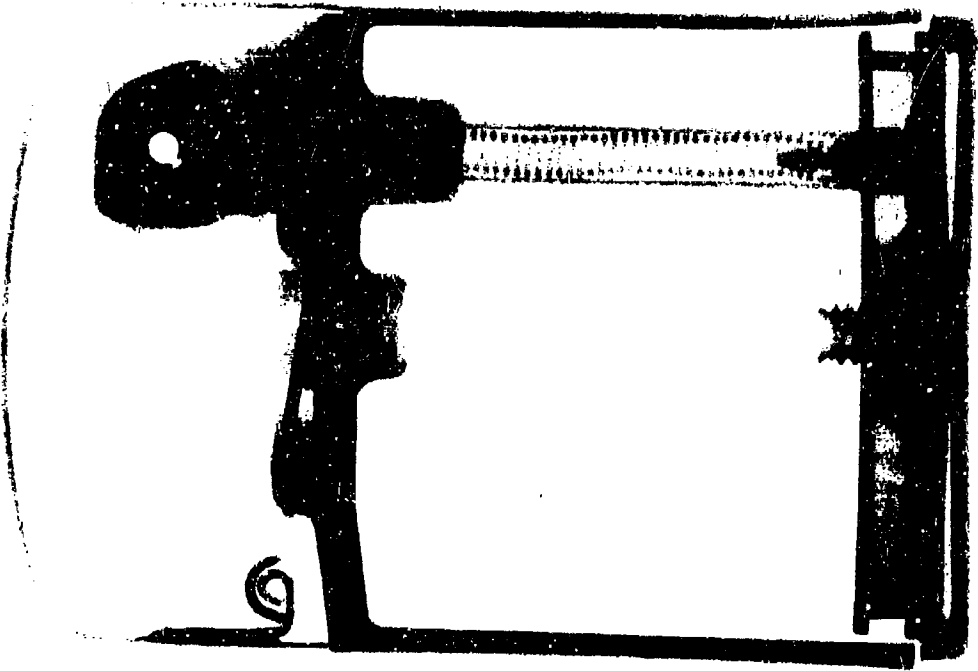


Fig. 3



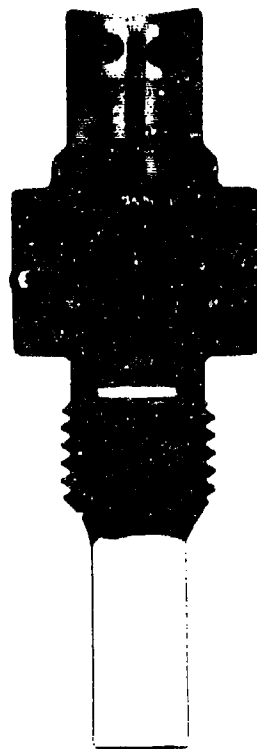
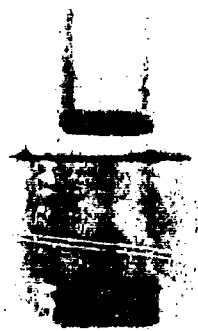


Fig. 4

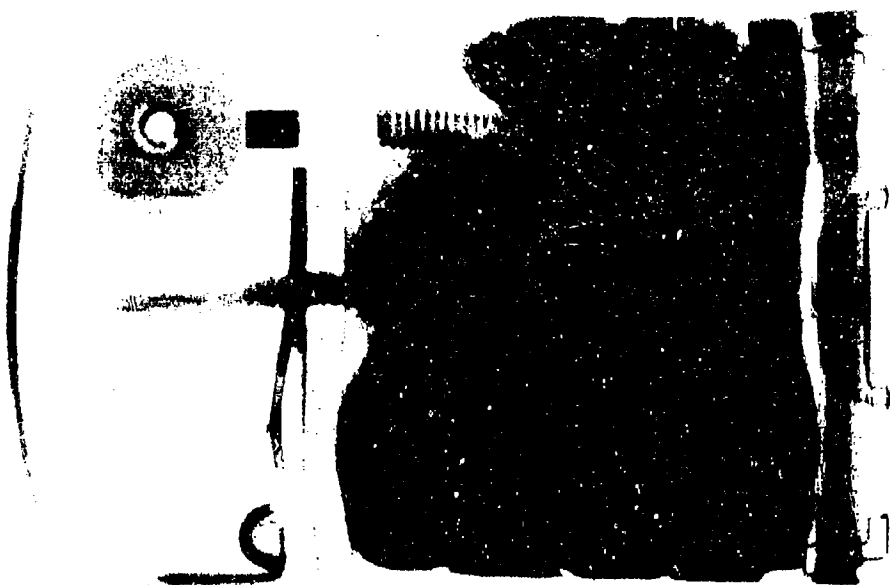


Fig. 3

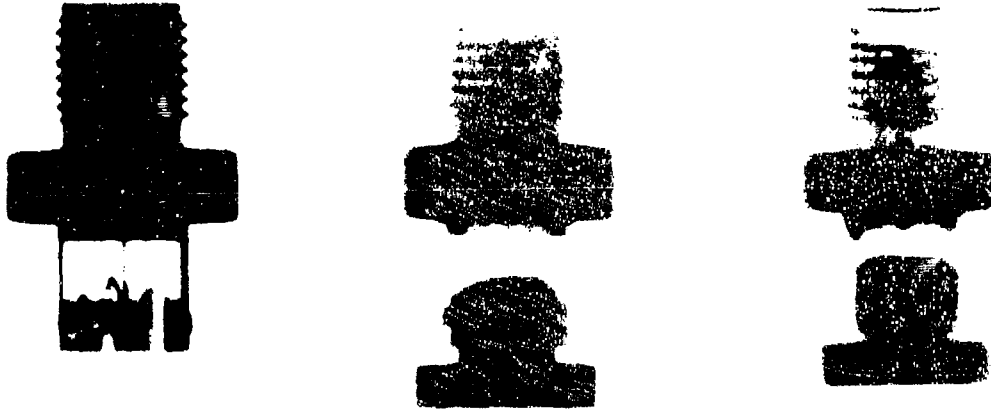


FIG. 6

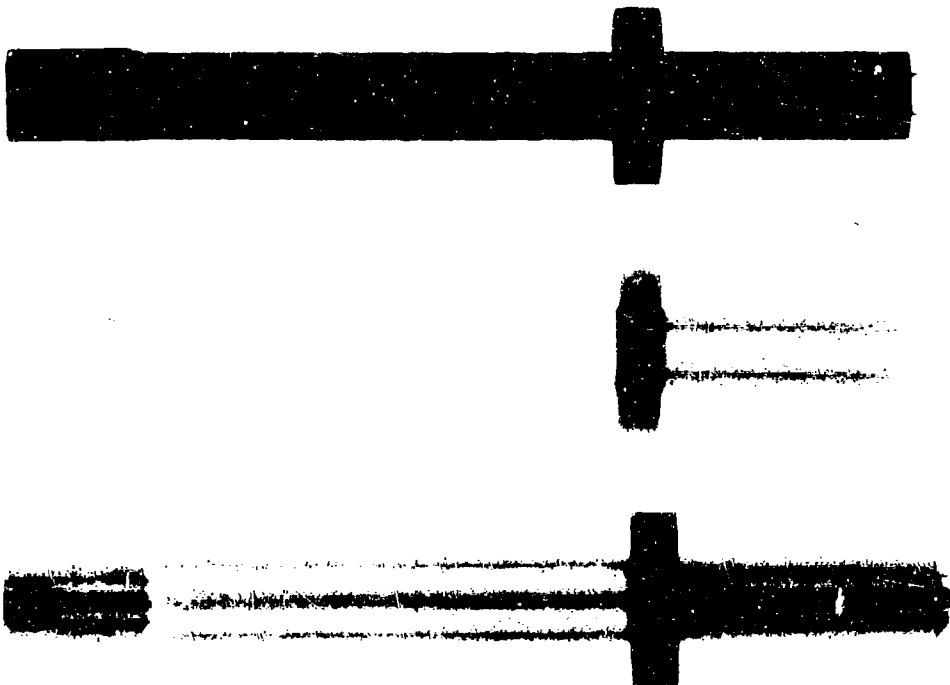


Fig. 7

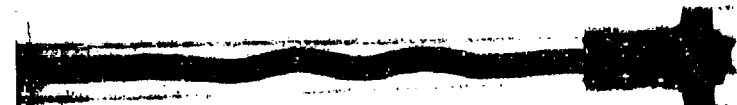
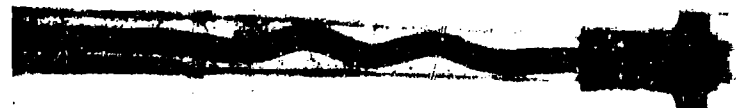
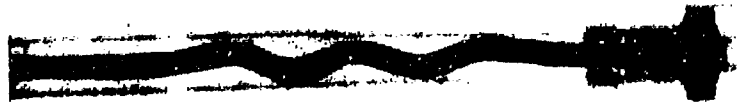


Fig. 8



Fig. 9



Fig. 11

Fig. 10

1-12P A RADIANT ENERGY TECHNIQUE TO MEASURE EXPLOSIVE OUTPUT

by

M. G. Kelly

INTRODUCTION

Our objective has been to develop and test an electro-pyrometric device which can be used to make relative quantitative measurements of the explosive or reactive output of a wide variety of EED's. The need for such a device springs from two problem areas in output testing.

1. Presently used output measuring techniques are very often *time consuming* and *costly*.
2. There is a degree of *uncertainty* associated with conventional output measurement techniques<sup>1,2,3</sup>.

It is well known that the energy output from an EED covers a broad spectrum of radiant as well as the kinetic energy. The radiant energy ranges from dc to radio frequencies. We have chosen to develop instrumentation to observe the radiant energy between 2300 and 12000 Angstroms which encompasses the visible portion of the spectrum. By employing two photomultipliers we are able to determine whether the radiation emitted from an EED is closer to 2300 Angstroms which is at the ultraviolet end of the spectrum or 12000 Angstroms which is at the infrared end of the spectrum. If we combine this qualitative information with the quantitative information given by the magnitude of the radiation emitted from a particular portion of the spectrum, we then have a measurement or series of measurements which we have found useful in estimating the following EED output characteristics:

1. Black or graybody temperature versus time
2. Luminous and radiant intensity versus time

3. Total radiant energy output
4. Relative brisance and output strength
5. Detonation front details

From a practical standpoint these measurements may replace many conventional output testing techniques and, in addition, give a better overall view of the EED output in relation to its job in an explosive train or special application. These measurements are easily and quickly made. If necessary, the output detector (the unit with which all measurements are made) may be located a considerable distance away from the EED. With the addition of some digital instrumentation the output measurement of interest may be displayed in a "go-no-go" fashion for production line work.

The first part of this paper is concerned with the construction of the output detector and its calibration. The second part deals with the experiments on actual EED's which illustrate the various output measurements with the detector.

#### ACKNOWLEDGEMENTS

This work was supported by the Army Material Command under Army Contract Number DA-28-017-AMC-1915(A). Mr. E. Miller of Picatinny Arsenal assisted greatly by preparing special detonators used in this study. Key personnel from the Franklin Institute in this study were E. E. Hannum, Manager, Applied Physics Laboratory and R. G. Amicone, Group Leader. V. W. Goldie, C. T. Davey, B. MacKrell and H. T. Tucker also contributed to these studies.

## 1. CONSTRUCTION OF RADIATION DETECTOR

The radiation output detector consists of two photomultipliers one of which measures intensity of a broad band of light in the ultraviolet region of the spectrum and the other intensity of a broad band of light in the infrared region of the spectrum. The ultraviolet (UV) photomultiplier is an RCA IP28 and the infrared (IR) photomultiplier is an RCA 7102. The typical relative responses of these photomultipliers as used in the output detector are shown together in Figure 1. A sharp cut yellow filter has been used with the 7102 photomultiplier to eliminate a spurious response in the ultraviolet region.

Figure 2 shows the physical layout of the photomultipliers. At the top of the picture we have the output detector housing. At left, center we see the IP28 along with its dynode resistors. At right, center is the 7102 which receives the light through the head of its glass envelope. At the bottom, left is the input filter cell housing which holds protective sapphire windows, diffusers, and "gray" filters. At bottom, right we have the beam splitter which divides the incoming light between the IP28 and 7102. Both photomultipliers are shock mounted and the assembled detector on its tripod is shown in Figure 3 (a heavier housing for the IP28 is shown in this figure).

Figure 4 is a simplified block diagram of the entire detector system. The power supplies are conventional and produce a variable voltage of from 0 to 1200 milliamperes. The dynode voltage dividers are non-indicative and external to the output detector housing to prevent temperature problems (a modification not shown in Figure 2). A Tektronix 551 dual beam oscilloscope with two fast rise preamplifiers is used to monitor the output of each photomultiplier.

## 2. THEORY OF TEMPERATURE MEASUREMENT

We have found that the ability to measure output temperatures is quite useful for the comparison of deflagrating EED outputs and also for the study of detonation front details. Since a large portion of the experimental work with the output detector was concerned with the measurement of these phenomena, a discussion of the manner in which temperature measurements are made is presented below.

The output detector with its two photomultipliers is actually a form of the well known two-color optical pyrometer. To understand the theory of the two-color pyrometer we refer to Planck's equation<sup>4</sup> which expresses the specific intensity of radiation of wavelength radiated by a blackbody at the temperature T:

$$E_{\lambda} = \frac{c_1}{\lambda^5} \left( e^{\frac{c_2}{\lambda T}} - 1 \right)^{-1} \quad (1)$$

where

E = Radiant flux emitted per unit area increment of wavelength,  
watts/cm<sup>2</sup>/cm

c<sub>1</sub> = constant = 2.74 x 10<sup>-12</sup> watts cm<sup>2</sup>

c<sub>2</sub> = constant = 1.438 cm °K

λ = radiation wavelength, cm

e = 2.71828

T = absolute temperature of source, °K

Since there are no perfect blackbodies, emissivity (ε) which



expresses the ratio of radiant flux emitted by a given surface to that emitted by a blackbody surface at the same temperature and wavelength, should be included.

$$E_{\lambda} = \frac{c_1}{\lambda^5} \left( e^{\frac{c_2}{\lambda T}} - 1 \right)^{-1} \quad (2)$$

Emissivity is usually a function of both wavelength and temperature but for now we will assume it is constant over the wavelengths of interest.

Equation (2) may be simplified, if  $\lambda T \ll c_2$  to

$$E_{\lambda} = \frac{\epsilon c_1}{\lambda^5} \left( e^{-\frac{c_2}{\lambda T}} \right)$$

which is known as Wien's Equation and is a good approximation for temperatures below 4000°K and wavelengths in the visible and ultraviolet portion of the spectrum. If we now consider that a measurement of radiant flux E is made at two different wavelengths or wavelength bands then we will arrive at an equation which expresses the ratio's of the flux's

$E_{\lambda_A}$  and  $E_{\lambda_B}$  :

$$R = \frac{E_{\lambda_A}}{E_{\lambda_B}} = \frac{\epsilon c_1 \lambda_A^{-5} \left( e^{-\frac{c_2}{\lambda_A T}} \right)}{\epsilon c_1 \lambda_B^{-5} \left( e^{-\frac{c_2}{\lambda_B T}} \right)} \quad (4)$$

This can be reduced to

$$R = \left( \frac{\lambda_B}{\lambda_A} \right)^5 e^{-\frac{c_2}{T} \left( \frac{1}{\lambda_A} - \frac{1}{\lambda_B} \right)} \quad (5)$$

The emissivity which we have considered to be out constant over the wavelengths of interest has been cancelled out in equation (5) and the ratio R is only a function of temperature T. In actual practice

there are few surfaces or radiation sources which possess an emissivity which is constant at all wavelengths, however, the ratio pyrometer is useful because the emissivity of a surface varies slowly over a range of wavelengths. Thus, if the two measured wavelengths are not too far apart then the ratio of the emissivities will be close to one and equation (5) will be valid. Since only a ratio is being measured the ratio pyrometer is not affected by fluctuations of the radiation source (if the sensors can follow the fluctuation) due to dust, smoke or changes in the source size.

The theory just discussed applies to a two-color optical pyrometer which makes use of the ratio of two narrow bands in the visible or near-visible portion of the spectrum. This type of pyrometer is of limited use in the measurement of sources which exhibit absorption or emission bands. The difficulty occurs when one of the two response bands falls directly on an emission or absorption line. Since the response bands are usually on the order of 100 Angstroms wide or less a false indication of the radiation intensity at the sampling point would be given. The broad band method has the advantage of being relatively unaffected by emission lines, absorption lines, and emissivities which may be dependent upon the wavelength of the radiation.

The radiation detector which we have constructed has the overall response shown in Figure 1. Although the general concept of the two-color pyrometer theory still applies the relationship between temperature and the ratio of two broad response bands such as these cannot be stated simply as in Equation (5). Rather than develop an equation

similar to Equation (5) and use simplifications such as were used in Equation (3) the absolute relationship between blackbody temperature and ratio of photomultiplier outputs was found empirically by multiplying the percentages of radiation emitted by a blackbody at a given wavelength<sup>5</sup> and temperature by the sensitivity of the photomultiplier (s) at the same wavelength to obtain photomultiplier output as a function of wavelength for each temperature. By integrating the area under curves generated by this process, photomultiplier output as a function of blackbody temperature may be obtained. If we then take the ratio of the UV detector output to that of the IR detector output we obtain a curve of UV/IR ratio as a function of the blackbody temperature.

The results of a computer program used to perform these operations are summarized in part by the curve of Figure 5. This curve relates the UV/IR ratio and the blackbody temperature of the source, for a potential of 900 volts on the IP28 and 1200 volts on the 7102 (these voltages are currently being used on output measurements). According to the computer study the useful temperature measuring range of the detector is from about 1700° Kelvin to at least 10,500° Kelvin. The upper limit is probably much higher but our calculations were carried out only to this temperature.

According to Cook the temperatures to be expected from detonations lie in the range of 2000 to 6000° Kelvin. Squib temperatures are probably no lower than 2000° Kelvin, so that the present output detector system seems adequate for the measurement of the temperatures of interest. Should the need arise later to measure reactions of lower temperature a simple substitution of a different photomultiplier in place of the IP28 would fulfill it.

### 3. SENSITIVITY CALIBRATION

In both the experimental stage and in the practical application stage it is important that the sensitivity of the UV/IR output detector be such that readings can easily be reproduced. Factors which may affect the gain or luminous sensitivity of photomultipliers are temperature of the surroundings, fatigue and life characteristics, and supply voltage.

Realizing that the luminous sensitivity of the photomultipliers may not be sufficiently stable over extended periods of time we must provide a source of spectral radiation which will remain constant. This standard must have a spectral distribution which emits light in the portions of the spectrum to which the photomultipliers are sensitive. Thus, a change in the photomultiplier sensitivity which occurs in only a portion of its spectral response curve will be apparent. The standard should be bright enough to equal an EED flash, and its color temperature should be in the 2000° to 6000° Kelvin range.

The standard which we have chosen to satisfy these requirements is an aged 500 watt lamp, made by G. E., with a tungsten filament and frosted T-20 bulb. This type of lamp is recommended for a standard of luminous intensity by the U.S. National Bureau of Standards. We have three such lamps, one of which has been calibrated by a certified agency of the Bureau of Standards. All three lamps are aged so that their intensity is stable. They are bright enough to act as a simulator for an EED. Figure 6 shows the calibrating fixture with the detector in

place. The saddle for the detector is at the far right. To its left is a tube attached to a slotted shield; next is a slotted disc which revolves and "chops" the light to eliminate the effects of background noise; and last in line, the calibrating lamp. The ammeter and voltmeter used in calibrating are shown at the extreme left.

The initial calibration of the output detector is as follows: The output detector is placed on the calibration fixture as shown in Figure 6. The chopper is turned on and the lamp is slowly brought up to 110 volts ac. The current is recorded at this voltage. Various dynode divider voltages ranging from 800 to 1200 volts dc are then applied to the two photomultipliers in the detector and the corresponding photomultiplier currents are read on an oscilloscope at each voltage. These steps are repeated for each of the three lamps so that the accuracy of the calibration is not dependent on a single lamp. Subsequent calibrations simply consist of checking the detector at a few voltages with the lamp operated at the correct current and voltage. If either photomultiplier in the output detector shows a change in gain, due to fatigue for instance, it may be brought back to the original gain by adjusting the dynode divider voltage. On the other hand, if a change in gain is desired it can be accurately set by changing the dynode voltage until current from the photomultiplier is at the proper level.

In general, a major calibration is required only once for each photomultiplier, when it is placed in use, and subsequent checks are made at appropriate intervals. Readings may easily be reproduced within 5% of the major calibration. Actually, the calibrating setup just described is somewhat elaborate. A less elaborate setup would suffice for practical applications and could easily be built into the output detector itself.

#### 4. EXPERIMENTAL STUDIES USING THE UV/IR RADIATION DETECTOR

We have briefly described the construction of our two-channel radiation detector. The overall coverage of the detector extends from about 2300 Angstroms to 12,000 Angstroms. With proper calibration the radiant sensitivity of the detector is reproducible and steady over extended periods of time, and linear over several magnitudes of radiation. The rise-time of the photomultiplier outputs when viewing sharp rise radiation pulse is less than 100 nanoseconds.

In addition to the temperature measurements which may be performed in accordance with the theory and the calibration described in Section 2 and 3, the detector may be used for other output measurements. In the descriptions of the several experiments which follow it will become apparent that the versatility of the detector makes it a suitable tool for many phenomena where radiation is involved. The ease and speed of measurement is especially attractive.

##### 4.1 Measurement of the Temperature History of EED's

It is of general interest and, in cases where deflagrating output and explosive trains are involved, of particular interest to know the approximate temperature history of the EED output. Using the theory and calibration technique described in Sections 2 and 3, and assuming that radiation emitted was fairly rich in background spectra we were able to make estimates of the temperature history of several EED's. The EED's whose radiant outputs were studied are listed in Table 1 along with

some of their properties which are pertinent to this study. Figures 6 and 7 show respectively, typical oscillographs of the photomultiplier outputs produced by the UV and IR radiation from a T24E1 detonator and M1A1 squibs. The oscillograph traces in these figures start at the right and the deflection is in a negative direction since the photomultiplier output signals are negative voltages. These traces are typical and from these we obtain, by graphically dividing the curves, a curve of UV/IR ratio as a function of time. Curves for the EEDs listed in Table 1 are shown in Figure 8. For comparison an output curve is also shown for an exploding Nichrome wire and xenon strobe lamp.

Table 1

PROPERTIES OF EED'S USED IN OUTPUT STUDIES

<u>Name of Device</u>	<u>Base Charge</u>	<u>Case Material</u>
T24E1 Detonator	70 milligrams PETN	Stainless Steel
M51 Detonator (T18E3)	90 milligrams PETN	Stainless Steel
T60 Detonator	50 milligrams PETN	Stainless Steel
M48 Detonator (T18E4)	160 milligrams PETN	Aluminum
T-6 Blasting Cap	870 milligrams RDX	Aluminum
J-2 Blasting Cap	940 milligrams RDX	Copper Alloy
XM3 Squib	?	Aluminum
Mc/S/A Igniter	?	Steel
M2 Squib	Ignition Mix	Plastic
M1A1 Squib	DDNP Ignition Mix	Plastic

## 4.2 Details of the Detonation Front Observed

Having established that the temperature histories of different EED's show characteristic trends our next step was to investigate the possible existence of correlation between output strength and UV/IR ratio as a function of time.. An elementary approach was to measure the average steel plate dent depth of some of the EED's whose UV/IR curves are shown in Figure 8 and check for correlation. Of five EEDs whose average dent depths were measured no striking correlations were found. In another experiment we searched for correlation between the steel plate dent depth produced by a T24E1 detonator and the simultaneously measured UV/IR ratio. No correlation was found but it was felt that the side viewing of the T24E1 which was positioned vertically against the steel block led to unwanted light output variations.

A third technique was tried in which high and low output strength was simulated by varying the length of air gap between a column of high explosives and a detonator-booster charge. Reinforced Primacord (PETN) was used as the "column" of high explosive while a T24E1 detonator was used as the detonator-booster. The series of tests with the PETN-T24E1 combination showed the ability of the radiation output detector to distinguish details of the detonation front via the radiation from the front. A temperature peak of about 5500° Kelvin was observed 200 nano-seconds after the "first light" from the PETN column was detected. Knowing the detonation velocity of the PETN we were able to estimate the width of the temperature peak to be 2 millimeters. It was theorized



that this hot zone represented either the temperature rise produced by the emerging shock wave impinging on the surrounding air or the actual reaction zone of the detonating PETN. The temperature peaks are readily seen in Figure 9 which is a plot of the temperature history of two different types of PETN-T24E1 combinations.

In general, we found that the first 10 or 20 *microseconds* of UV and IR output radiation were suitable for the observation of detonation front details and, perhaps, brisance (see Section 4.5.3 for discussion of brisance in relation to primers). Where a measure of *output strength* is required, however, our experiments indicate that the first 10 or 20 *milliseconds* of radiation must be measured. This period of time includes much of the radiation output from the secondary explosive reactions as well as the initial detonation phenomena.

#### 4.3 Measurement of Output Strength Using Integrated UV and IR Radiation

In view of our findings concerning the total or overall radiation a simple integrating circuit was assembled which, when used with the radiation output detector, would roughly sum the quantity of radiation emitted from the EED over relatively long periods of time. This circuit, diagrammed in Figure 10, consists of a series resistor and a parallel capacitor.

$$\text{If } RC > 15T$$

where

R is resistance in ohms

C is capacitance in farads

T is the period of the observed pulse in seconds

then

$$e_{\text{out}} = \frac{1}{RC} \int e_{\text{in}} dt$$

where

$e$  is the voltage whose waveform is to be observed.

The above criterion ( $RC > 15T$ ) will result in an integrating circuit which will shift an input sinusoid of period  $T$  at least  $89.4^\circ$ . With the circuit of Figure 10 the integration will be very good for pulses having a period of 29 microseconds or less. Pulses of longer duration will be integrated but not with the same accuracy.

To check the validity of our assumption concerning the importance of the total radiation output, a T24E1-RDX explosive train whose output could be varied by changing an air gap in the train was used in two different modes. In the first series of tests the explosive trains were aligned axially with the output detector; in the second series of tests they were viewed from the side while they were being fired on a steel dent block to record dent depth. Still a different setup shown in Figure 11 was used to provide variable explosive output to test the integrating technique. In all three test series the length of the air gap was varied to provide variable output. An oscillograph sweep rate of .5 or 1. milliseconds per centimeter was used for all observations. This allowed the first 10 or 20 milliseconds to be recorded. A set of integrated UV and IR output traces obtained using the radiation detector and the circuits of Figure 10, of the axially viewed T24E1-RDX combination for three different gap sizes is shown in Figure 12. These traces are typical of the T24E1-RDX combination viewed from the front (axially) and

from the side, and the M55-RDX combination shown in Figure 11.

It is apparent from the oscillographic traces that the infrared radiation is influenced most by the variation in output. As the air gap length increases, giving a smaller explosive output, the magnitude of the integrated IR trace increases; this means that the quantity of infrared radiation emitted from a low output simulator is greater than that emitted from a higher output simulator. Also noticeable is the appearance of a "primary" and "secondary" peak on all the integrated IR traces and several of the integrated UV traces. The use of these terms is illustrated in Figure 13. It may be seen moreover, that in both series of simulator firings the "height" (see Figure 13) of the secondary peak in relation to the height of the primary peak increases as the output strength decreases. (As gap length increases output strength decreases). This relationship is most readily seen in the IR traces although it exists also in the UV traces.

Examination of the integrated UV/IR output traces of the M6 blasting cap reveals that the primary and secondary peaks also occur with this EED. Indeed, other systems such as the T24E1-PETN combination (discussed in Section 4.2) and some specially fabricated detonators, later to be discussed, also exhibit the double peak phenomena.

In Figure 14, the ratio of the average heights or magnitudes of the primary to the secondary peaks which occur in the integrated IR traces are plotted as a function of average steel plate dent depth for the T24E1-RDX combination and the M55-RDX combination. The average dent depth were taken from previously obtained data and the ratios of

primary to secondary peaks were averaged from two or more oscillographs obtained from firings at each gap setting. It is readily seen that a definite correlation exists between the ratio of the peaks and the output of depth for both explosive systems.

The occurrence of this phenomena in these systems in the M6 and in other EED systems led us to believe that the study of primary and secondary peaks can lead to a more general way of assessing EED output. A plausible explanation for the primary and secondary peaks is given below.

The appearance of a "primary" and "secondary" peak in the integrated radiation output traces can easily be misinterpreted unless we bear in mind that these traces are the summation of the quantity of radiation emitted from the explosive reaction as time elapses. This fact is best illustrated by examining Figure 15 which shows the un-integrated UV and IR traces obtained from the M6 blasting cap. In this oscillograph the deflection has purposely been made more sensitive than normal to show the secondary period of emission which starts approximately 150 microseconds after the beginning of the traces. The primary emission is so much more intense that the secondary emission that it causes the traces to deflect off scale in Figure 15.

Examination of Figure 15 indicates that there are probably two distinct reactions occurring. The first reaction which causes a rapid intense buildup of radiation intensity lasting about 30 microseconds is undoubtedly caused either directly or indirectly by the

expanding shock and reaction zone. Whether the radiation is emitted from strongly ionized air in the shock front or a reaction zone plasma behind the shock front may be questionable but the rapid rate of buildup and its short duration suggest a plasma-like source of emission.

The second reaction which starts radiation emission at 150 microseconds and lasts for about 600 microseconds appears to be a burning phenomenon. The time of occurrence, the duration, and the random oscillatory nature of the traces during this period all suggest burning. A possible explanation of such a reaction is that after the shock and reaction front has dissipated due to atmospheric attenuation and spherical divergence, the products of detonation enter into secondary reactions in which oxidation and the formation of additional products takes place. Some burning of unreacted explosive may also occur but this will be minimal in high order reactions.

The delay in the appearance of secondary emission may occur because the expanding reaction zone acts as an opaque filter to the radiation produced by secondary products which are found within the detonation head. It is also possible that previous to the dispersion of the detonation front the products of detonation have not mixed with a sufficient quantity of atmospheric gases for secondary reaction.

More difficult to explain is the dependence of the intensity of radiation emitted from the secondary reaction upon the order of the output. The traces of Figure 12 show that the height of the secondary peak, which reflects the quantity of radiation emitted from the secondary reactions, is increased. In other words, there is an increase in the

amount of secondary reaction in the lower order firings. At present we theorize that, in a lower order detonation less explosive material may enter into the production of the shock-reaction front thereby making available more energy-rich products for the secondary reactions. In any case the observations of the ratio of the quantity of radiation from the primary shock reaction (a quantity which remains fairly constant as the order of detonation varies) to that of the secondary reaction results in a measure of output strength which may be conveniently observed with the radiation detector. This measure is common to many, if not all, explosive systems.

There is a difference in the quality and the quantity of the radiation emitted from EED's with different case materials. This effect is often noticeable to the naked eye. To pinpoint this effect and also the effect of different charge materials three types of detonators were specially prepared by Mr. E. Miller of Picatinny Arsenal, Table 2 summarizes the characteristics of these three types as well as those of the XM66E2 detonator which was also used in this test series.

Table 2  
CHARACTERISTICS OF SPECIAL DETONATORS

<u>Item</u>	<u>Lead Charge</u>	<u>Quantity of Charge</u>	<u>Case Material</u>	<u>Configuration</u>
Type A	RDX	230 mg	Stainless Steel	} Identical
Type D	TETRYL	230 mg	Stainless Steel	
Type E	PETN	230 mg	Stainless Steel	
XM66E2	PETN	230 mg	Aluminum	Comparable

This configuration, that is, the physical arrangement of the bridgewire, the plug material, and the various dimensions, is identical for types A, D, E, and comparable to that of the XM66E2.

Some conclusions to be drawn from this brief study of case and charge material are as follows:

- a) Each explosive type (RDX, PETN, and TETRYL) does produce characteristic output traces. The traces are reproducible enough to allow a positive identification of the explosive material if the configuration is held constant.
- b) A large difference exists between the aluminum case output and the stainless steel case output. The aluminum cased items give greater radiation output and exhibit a high, prolonged temperature. Since the boiling point of aluminum is about 2300° Kelvin while the boiling point of stainless steel is close to 3300° Kelvin it is more likely that the cases of aluminum would enter into some of the reactions upon detonations than steel cases. Under heat and pressure aluminum can enter into many heat producing reactions with the elements of the explosive as well as the atmosphere. Cook<sup>6</sup> discusses how certain aluminum oxide products formed in an explosion are capable of buffering

the explosion temperature which may help to explain the relatively stable high temperature observed.

- c) The *integrated* traces appear to be of little value in distinguishing differences in charge material. They may be useful for detecting case material differences.

#### 4.4 Output Tests of M42 Percussion Primer

Thus far, the usefulness of the radiation detector has been discussed mainly with respect to detonating, "hard" output devices. A special series of tests run on the M42 percussion primer serves to illustrate the usefulness of the detector and the various techniques described in the preceding sections for evaluating the "soft" output of devices such as squibs, igniters and primers.

The M42 Percussion Cap (or primer) is a low output device which is initiated by the action of a firing pin which crushes the ignition mix between a tiny self-contained anvil and the primer cup. Its uses are varied but in general it is employed where a heat sensitive reaction must be initiated. The prime purpose of the tests on the M42 percussion caps was to discern qualitative and quantitative differences in outputs of four different lots. The chemical composition of each lot was different so that output differences were expected.

The arrangement of the steel ball drop tester used to initiate the caps and UV/IR radiation output detector is shown in Figure 10. A



3.5 ounce steel ball was used at a drop height of 7.5 inches giving an impact energy of 26.5 inch-pounds. This impact energy is more than enough to insure firing of all four lots of percussion caps. The output parameters which were specifically studied were the energy history, approximate temperature history and brisance.

#### 4.5.1 Energy History of Output

Since the output of the percussion caps is relatively "soft" and the shock output low, most of the energy output can be accounted for by observing the intensity of the emitted radiation. Furthermore, the temperature of output flame and subsequent radiation is low relative to detonation phenomena. For these reasons the energy history of the M42 percussion caps was observed using only the infrared photomultiplier (an RCA 7102). Three distinct types of phenomena were observed in the output of the percussion caps: an initial burst period, an induction period and a burning period. Figure 17 illustrates these three phenomena with an actual radiation trace obtained with the detector.

#### 4.5.2 Approximate Temperature History

For temperature measurements both the infrared and ultraviolet photomultipliers are used. As discussed in Section 2 the temperature of the source may be estimated with a ratio of UV to IR radiation intensity if the source radiation is near blackbody or graybody in nature. Due to the composition of some of the percussion mixes the emitted radiation may not completely fulfill these conditions so that the temperature history presented in Figure 8 is approximate in lieu of further

investigations. The temperature-time curves for each lot are average values for the particular lot. The observed temperature of 2000° to 2700° Kelvin seems to be reasonable for a soft output device such as a percussion cap.

#### 4.5.3 Brisance

When speaking of "soft" output devices such as the M42 percussion cap the term brisance is almost without meaning since the term is a properly identified with the detonation pressure. Since there is some violent action associated with the M42 caps, however, we have tried to make some estimate of the relative brisance or "shattering action" of each lot.

The estimate was made by measuring maximum rate of rise of the oscillograph trace from the infrared photomultiplier by the initial burst radiation. A fast rate of rise in relation to a slower one indicates more brisance. Table 3 lists the average of the maximum measured rise rates for each lot. The actual voltage rise rate as measured on the oscillograph as well as an estimate of the maximum radiant watts per second is given. The latter factor was computed by assuming a 510 ohm load across the RCA 7102 photomultiplier output and an average radiant sensitivity of 4 milliwatts/ampere.

Table 3

MAXIMUM RATE OF RADIATION INCREASE OF  
FOUR LOTS OF M42 PERCUSSION PRIMERS

<u>Lot No.</u>	<u>Maximum Voltage Rate of Rise (volts/milliseconds)</u>	<u>Rate of Increase of Radi- ated Power (watts/secs)</u>
110	.18	.0014
WWC 1-15	4.	.032
WWC 358	10.	.079
PA-101	800.	6.3

4.5.4 General Summary of Four Lots

Enough data were collected with the aid of the radiation detector to define both the apparent and subtle differences between the four lots. In general, the output of Lots WWC 358 and 1-15 seem to be predominately burning in nature while the outputs of Lots PA-101 and 110 show little burning and a tendency towards detonation. One could therefore, select a lot to perform a "soft" or a "hard" initiation task. Table 4 summarizes all radiation tests on the M42 percussion caps on a relative basis.

Table 4

RELATIVE RATING OF FOUR LOTS OF M42 PERCUSSION CAPS

<u>Lot No.</u>	<u>Energy evolved in initial burst (in less than 1 msec)</u>		<u>Energy evolved in burning</u>		
	<u>Relative Peak</u>	<u>Brisance Interpretation</u>	<u>Relative Magnitude</u>	<u>Duration Interpret. (msec)</u>	<u>Relative Amount of Coruscating Particles</u>
110	2	small	1 (neglig)	1 negligible	none
WWC 1-15	10	small	2 (medium)	35 medium	Medium
WWC 358	6	small	3 (large)	110 long	Reg. Pattern Medium
PA-101	400	large	2 (neglig)	4.5 short	Irr. Pattern none

## 5. SUMMARY AND CONCLUSIONS

The primary purpose of this project was to develop an output test which is more meaningful than the presently used conventional tests. What we have developed is a tool and associated techniques which can be used to study, evaluate and monitor most types of EED output.

We have discussed in some detail the construction, theory and calibration of a radiation detector. In this discussion we have shown how the detector can be used for dynamic temperature-measurements in the 1700° to at least 10,000° Kelvin range as well as standardized radiant energy measurements of a wide variety of radiation sources. We have also shown experimentally how the detector may be used to measure several different EED output parameters, in many cases as a function of time. The basic radiation output measurements which can be made with the present detector system are as follows.

1. Blackbody or graybody temperatures as a function of time.

This measurement is made by measuring the intensity ratio of a broad band of ultraviolet radiation to a broad band of infrared radiation. The measured source should be blackbody or graybody in nature but because of the broad detector response it may deviate somewhat.

2. Radiant energy as a function of time.

Since the photomultiplier is basically a detector of radiant energy this measurement can easily be made. With the addition of the proper band pass filters and a routine calibration the detector may be used to make standart luminosity measurements.

3. Time-integrated radiant energy measurements.

With the addition of simple RC integrating networks to each photomultiplier output the total amount of radiant energy emitted in the ultraviolet region and the infrared region of the spectrum over a period of time can be measured.

From these basic measurements a number of important output parameters can be derived. (The technique may be used for deflagrating devices such as squibs as well as non-electrically initiated devices such as stab primers). These measurements along with their implications are given below:

1. Temperature-history.

The temperature as a function of time has been measured for a large variety of EEDs. This measurement seems generally useful for classifying EEDs by type, i.e., squib, igniter, detonator. Case material and composition of the explosive or deflagrating charge are factors which influence the temperature history of the EED.

2. Radiant Energy History.

In "soft" output devices where much of the output is in the form of radiation this measurement of radiant energy as a function of time is very useful for observing induction times, burning times, and the relative merit of the output.

3. Total or integrated radiant energy.

This measurement is extremely useful as an output measurement. For detonating devices the ratio of the primary energy emission to the secondary energy emission occurring during afterburning of the detonation products is an excellent measure of the order or strength of the output. The measurement is especially easy to interpret and a high degree of output resolution is possible. Total radiant energy also has a limited application in studying the effects of case and charge material.

4. Secondary measurement.

Much additional information can be derived by examining various aspects of the first three measurements. Brisance, for instance, can be estimated by measuring the rate of rise of the radiant energy or temperature history curve. Details of the detonation front can be observed also, via the shape of the various curves. Peak temperature is another possible secondary measurement.

In conclusion, we find that the measurement of output radiation from EEDs with the aid of the radiation detector and the proper analysis of the generated data can give a better and in some cases, a heretofore unknown evaluation of output. More experimental work is needed to place some of the empirically proven relationships on a sound theoretical basis but the basic techniques have been presented.

The fact that most of the possible output measurements are of a relative nature does not detract from the usefulness of the system and the techniques, since output information from the photomultipliers is in the form of electrical signals means that many of the output measurements described in this report can be automated so that the final information can be presented as a quality figure or "go-no-go" signal which can be especially useful for production line and quality control testing.

#### BIBLIOGRAPHY

1. V. J. Menichelli, "A Review of Explosive Output Testing", Proceedings of Electric Initiator Symposium - 1963.
2. "Detonator Output Measurement By Lead Disc", MIL-STD 331, Test 302 Paragraph 6.
3. F. A. Baum, et al. "Physics of An Explosion", (A translation of Fizmatgiz, Moscow, 1959) Chapter II, 1963. AD 400151.
4. Max Planck, Theory of Heat, Mamillian 1932, p. 275.
5. A. N. Lowan and G. Blanch, "Tables of Planck's Radiation and Photon Functions", Journal Opt. Spc. Am., p. 70 (1940).
6. M. A. Cook, The Science of High Explosives, Reinhold Publishing Company New York, 1958, pp 300-305.

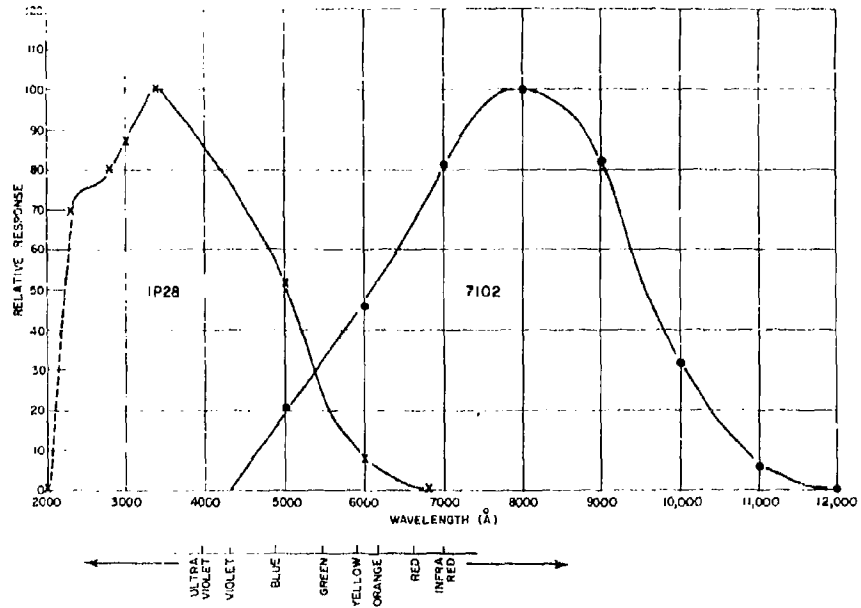


Fig. 1 - Typical Relative Response of Output Detector

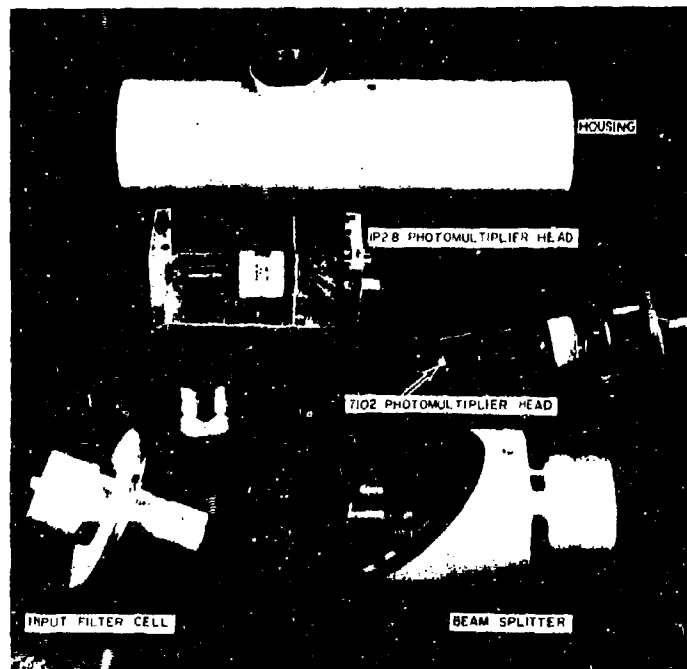


Fig. 2 - Output Detector, Disassembled





Fig. 3 - Assembled Output Detector On Tripod

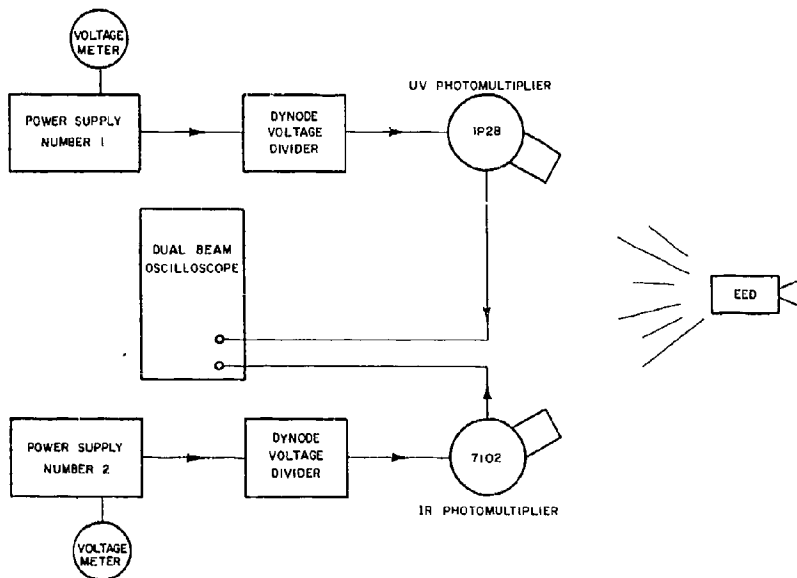


Fig. 4 - Block Diagram of Present Output Detection System

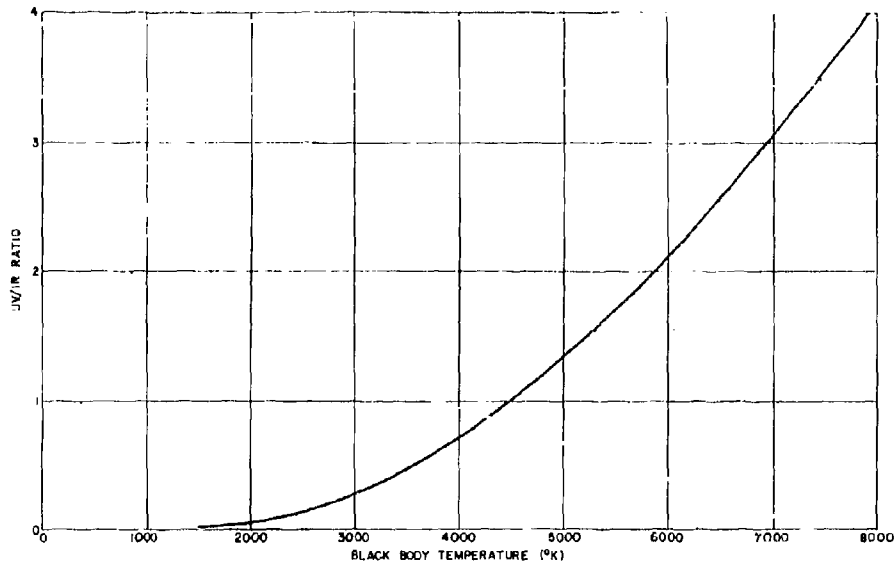


Fig. 5 - UV/IR Ratio As a Function of Blackbody Temperature of Source  
As Predicted by Computer Study

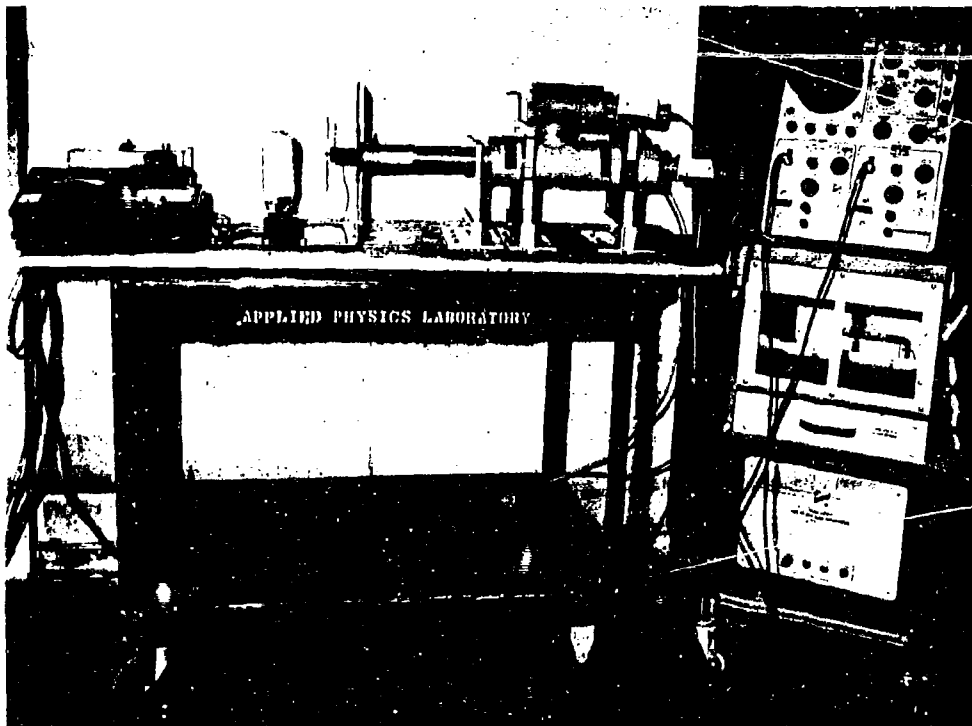


Fig. 6 - Calibration Fixture with Output Detector in Place  
1-12.30

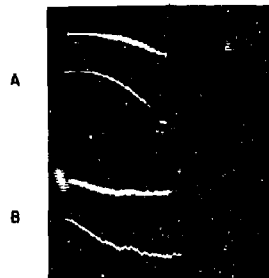
H1080-1



UV (0.2v/div)  
IR (0.5v/div)

BOTH 5 $\mu$ sec/div

UV and IR Output From T24E1 Detonator



A UV (0.05v/div)  
IR (0.1v/div)

B UV (0.05v/div)  
IR (0.1v/div)

ALL 5msec/div

UV and IR Output From Two M2 Squibs

Fig. 7 - Typical Oscillograph Traces of UV and IR Radiation from EEDs

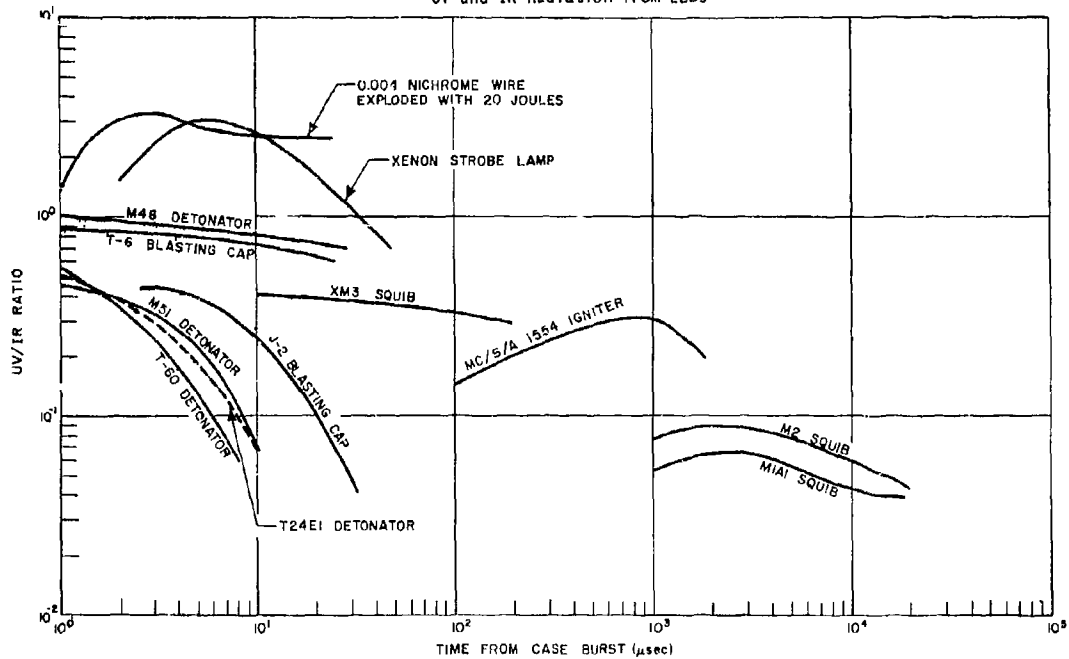


Fig. 8 - Output From Various EEDs

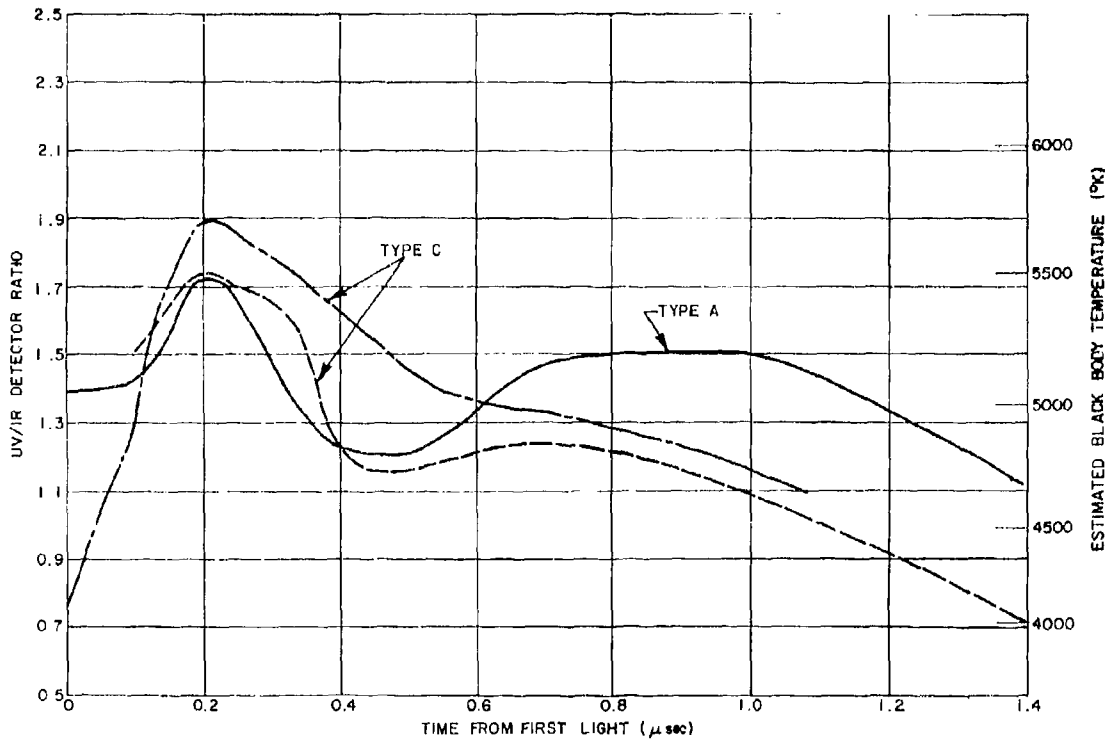


Fig. 9 - Details of the Detonation Front of Two PETN-T24E1 Simulators

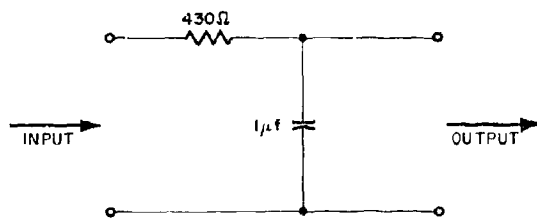


Fig. 10 - Integrating Circuit Used With Radiation Output Detector

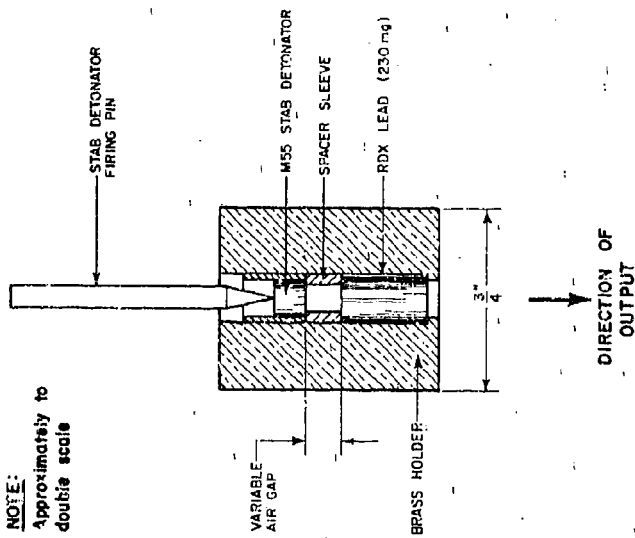


Fig. 11 - Fixture Used for M55-RDX Combination

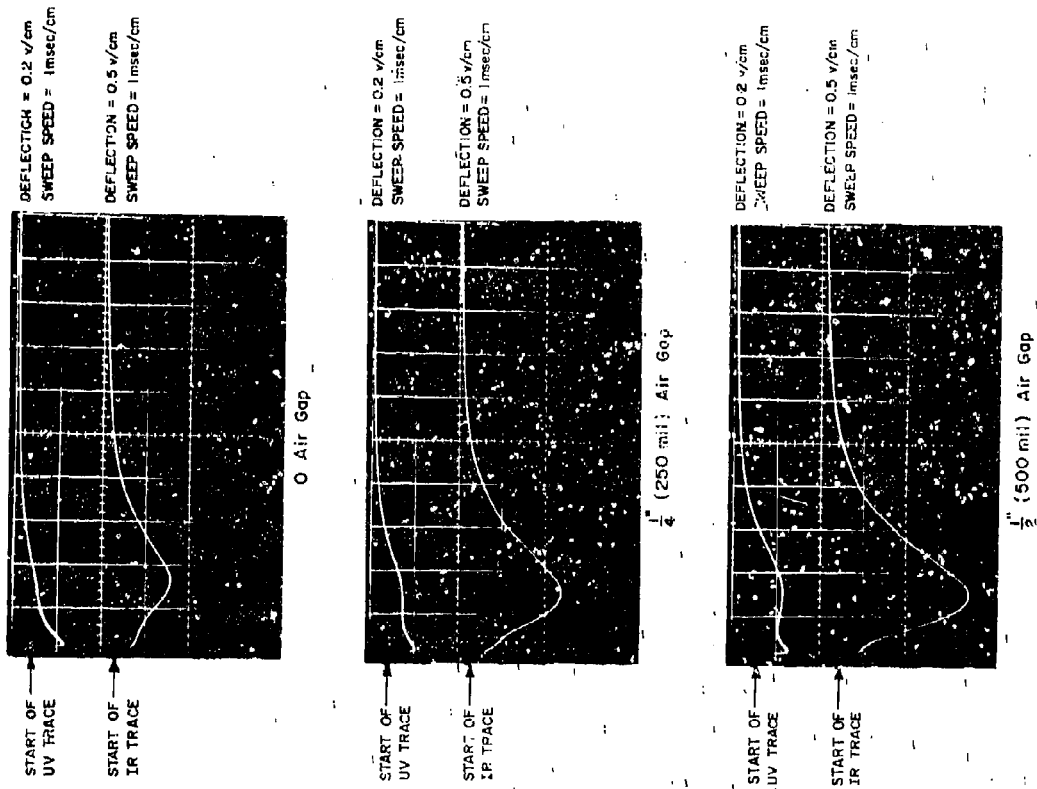


Fig. 12 - Integrated UV & IR Traces of T24E1-RDX Output Simulators

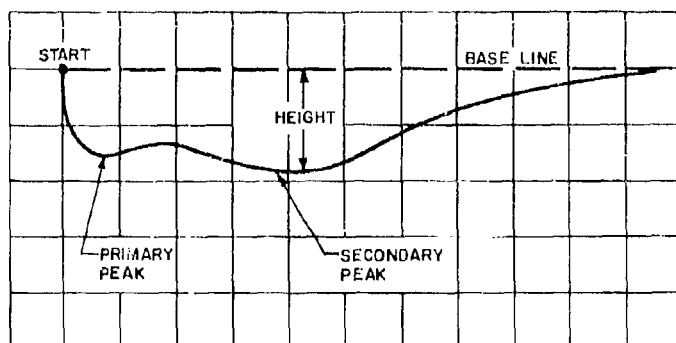


Fig. 13 - Typical Integrated Trace Showing Primary and Secondary Peak

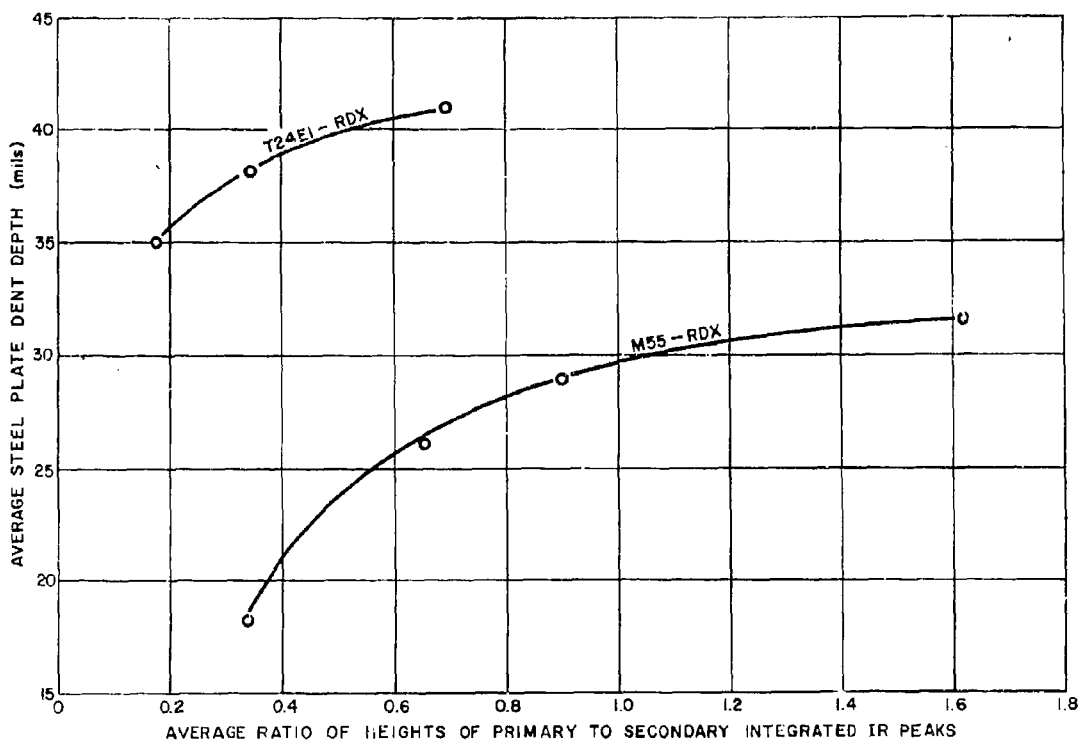


Fig. 14 - Relationship Between Average Dent Depth and IR Peaks Ratio for Two Different Simulator Combinations



Fig. 15 - UV & IR Light Output Traces (Unintegrated) of the M6 Blasting Cap Illustrating the Primary and Secondary Reactions

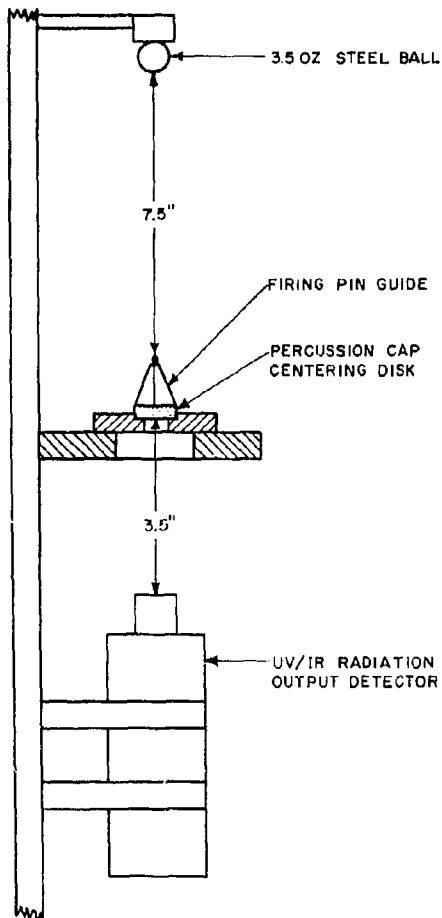


Fig. 16 - Drop Tester and Detector Arrangement For M6 Percussion Caps

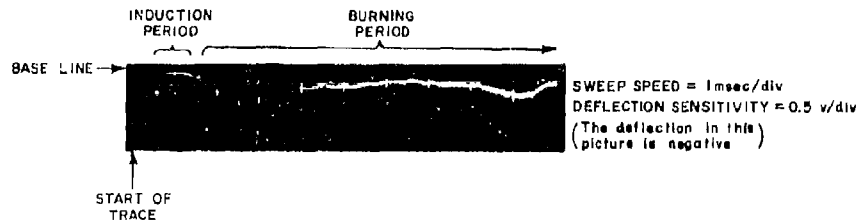


Fig. 17 - Typical Photomultiplier Output Trace for M42 Percussion Cap Showing Various Associated Phenomena

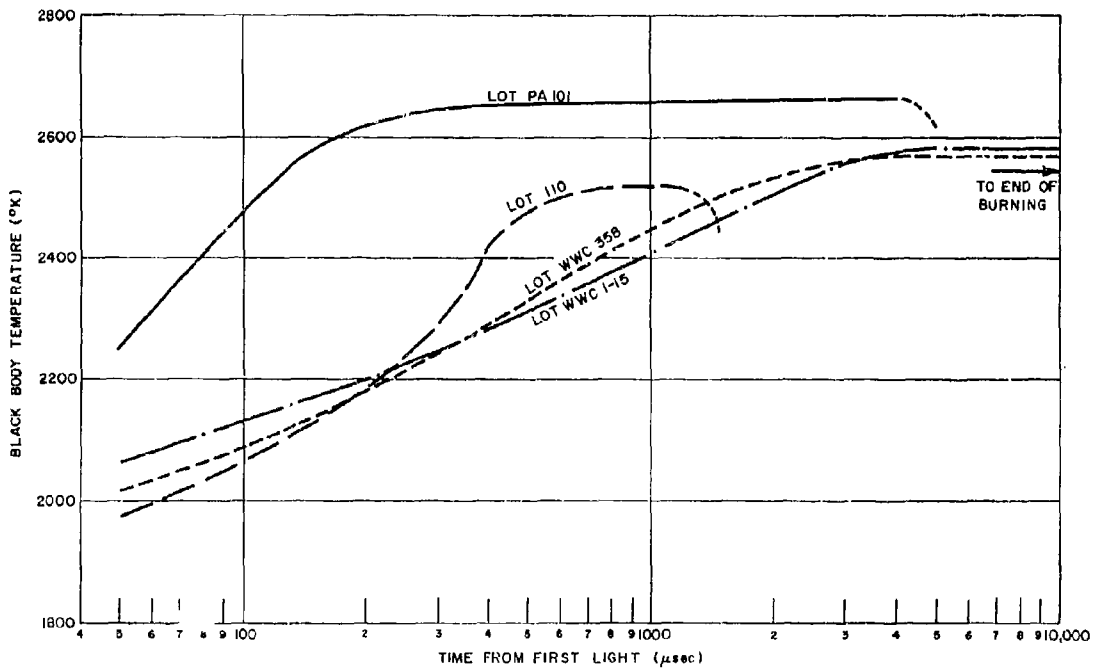


Fig. 18 - Temperature History of M42 Percussion Cap



ABSTRACTS SESSION TWO

2-1 Hazards of Electromagnetic Radiation to Ordnance (HERO) R. M. Price

A brief description of the Navy's Hazards of Electromagnetic Radiation to Ordnance (HERO) program is presented. Included are some of the various objectives such as, the test program for weapon developers, HERO evaluation test information, several basic design approaches for solution of the problem and the consultation services furnished to our weapon designers and developers.

2-2 Radiofrequency-Interference Protection for Pyrotechnic Systems in Manned Spacecraft R.L. Robinson

This presentation describes the technique which the Manned Spacecraft Center proposes to protect an electroexplosive device from potential radiofrequency-interference problems. A typical electroexplosive device and the mechanism by which radiofrequency interference can cause premature ignition are described.

2-3 Measuring the Electric and Magnetic Components of the Near Field Robert B. Cowdell

This paper describes the development of a field intensity meter to measure very high intensity electric and magnetic components of the near field. Intensive tests on existing commercial receivers were conducted to affect a design which could be exposed to high level ambient fields without malfunction. An extensive theoretical study of the near field distribution was conducted to establish a standard field for calibration purposes.

2-4 Lightning Surge Current Hazards to Semi-Conductor and Electro-explosive Systems M. M. Newman  
J. D. Robb  
J. R. Stahmann

Studies of surge coupling into aerospace vehicles indicate a limited spectrum of pulse amplitudes and rise times which can produce significant damaging surges in internal electronic and electro-explosive systems. Most surge coupling arises from openings in the vehicle's conducting outer shell, such as antenna feed throughs and radome systems. Illustrations are given of typical examples of hazards and protective techniques.

2-5 Energy Transfer in Electrostatic Arcs C. F. Schroeder, Jr

The dynamic characteristics of electrostatic arc discharges have been studied with emphasis upon energy dissipation in the arc as a function of circuit parameters. The results are applied to a repeatable pulse test device to study intrinsic explosive sensitivity as well as the safety aspects of electroexplosive devices.

2-6 Quantification of Explosives to Spark A. McGillivray

Quantification of explosives can be measured by two different methods. One method is the use of a spark test which gives a relative measure of the explosive's sensitivity. The other method is the use of a spark test which gives a relative measure of the explosive's sensitivity. The spark test is a relative measure of the explosive's sensitivity. The spark test is a relative measure of the explosive's sensitivity.

2-7 Designing Electro-Explosive Devices for Electrostatic Insensitivity

L. D. Pitts

This paper contains theory and design equations with which the engineer can analyze EED design for capability of withstanding a particular static discharge voltage from pin to case. Included are a general discussion of electric fields, dielectric strength, and resistivity as applied to breakdown voltage calculations and use of such calculations in analysis of general design factors and evaluation of a specific EED design. Also, a method for measuring dielectric strength and resistivity of explosives and pyrotechnics is set forth.

2-8P RF Protected EED's Utilizing Miniature RLC Networks

Joseph E. Sidoti

The use of RLC networks to provide RF protection in EED's has significantly improved their characteristics. Attenuation values can be attained over a considerable frequency range without sacrificing voltage breakdown or insulation resistance. Typical attenuation characteristics of a device 0.179" diameter by 0.379" long, range from 15 db at 100 KC to over 60 db at 10,000 MC. Theoretical and constructional details are discussed.

2-9P Effects of Radio Frequency Stimuli on Electroexplosive Devices

F. F. Mohrbach  
R. F. Wood

Tests conducted on a large number of different types of EED's has given some insight into the general behavior of EED's when exposed to RF signals. This paper describes this general behavior for CW and pulsed signals and for the different functioning modes, (pin-to-pin, pins-to-case and bridgewire-to-bridgewire). In addition these studies have indicated some of the construction fault that lead to increased RF and static sensitivity which may not be revealed by normal testing to standard EED test specifications.

2-10P Miniaturization of Out-Of-Line Explosive Safety Systems

R. Stresau  
R. Degner

Problem areas relating to the miniaturization of fuze explosive systems are discussed. These problems fall in the general areas of policy, design, and fabrication. The two policy problems are the ambiguity of safety policy and the inhibition of innovation which result from standardization policy. A number of solutions to the design and fabrication problem are discussed, one of which has been subjected to an explosive feasibility study. A procedure was devised whereby high reliability can be demonstrated on the basis of the result of a single trial.

2-11P RF Bonding

W. C. Reisener

This paper describes the results of a program currently in progress at the Frankfort Institute to evaluate methods of measuring the RF impedance of commonly used electrical bonds. The ultimate goal of this effort is to provide a means to evaluate the performance of electrical bonds in regards to their ability to conduct high frequency currents and their detrimental effects on surrounding enclosures.

A method for measuring the impedance of a bond at 10 MHz was developed, and a method that will operate around 400 MHz is under development.

2-1 HAZARDS OF ELECTROMAGNETIC RADIATION TO ORDNANCE

R. M. PRICE

U. S. Naval Weapons Laboratory

The Naval Weapons Laboratory, Dahlgren, Virginia is located about 60 miles south of Washington, D. C. on the Potomac River. Research and development programs in support of the U. S. Navy are conducted at Dahlgren. There are over 1800 civilian employees and 150 Navy personnel in our three technical laboratories and support organizations.

Our three technical laboratories are:

1. Computation and Analysis Laboratory which specializes in using large digital computers to solve problems of the Navy. It is the prime agency in the Navy Weapons Establishment in the fields of computation, data processing and exterior ballistics.

2. Warhead and Terminal Ballistics Laboratory which specializes in warhead research and development, terminal ballistics and cartridge actuated devices.

3. Weapons Development and Evaluation Laboratory which conducts research in support of the development of fleet weapons systems. It also develops sub-systems and ordnance components and conducts weapon system evaluations. We in HERO are a part of this laboratory.

Also located at the Naval Weapons Laboratory is a separate command, the Naval Space Surveillance System.

Some of the major programs of the Naval Weapons Laboratory are shown in Figure 1.

The Naval Weapons Laboratory has technical direction of the Navy HERO program. We are charged with the responsibility of determining the degree to which weapons may be susceptible to electromagnetic radiation, of devising means and techniques for rendering weapons safe in radiation fields, and for recommending operational and handling restrictions as a temporary remedy to the problem until permanent methods are available.

We have a film which will present some of the problems we face in the HERO program.

FILM: 9 Min.

Generally the HERO program provides for a systematic attack on the problems with two broad objectives: first, to resolve the HERO problem for current weapons in current environments and second to establish a satisfactory posture with respect to current and future weapons in the more severe environments of the future.

The Electromagnetic Hazards or HERO Division at Dahlgren has approximately 100 people actively engaged in the program.

From the film you have seen what our problem is. The Bureau of Ships, which is now the Ship Systems Command, has specified the magnitudes of the electromagnetic fields on the decks of the ships in both the radio and radar frequencies.

We at Dahlgren must determine the susceptibility of all of the Navy items which contain electroexplosive devices using these fields as the

criteria. To accomplish this, complete weapon systems are exposed to the rf environments in unique facilities. Incidentally, these are the only known facilities of this kind available today.

Figure 2 describes the facility.

This is one of the facilities. It is a steel deck 240 feet long by 100 feet wide designed to simulate an aircraft carrier deck. At one end is a turntable capable of rotating loads up to 25 tons. There are radio and radar transmitters to create the rf fields for the tests. There are three of these ground plane facilities, two of which are at Dahlgren. Our third facility is located at the Naval Air Test Center, Patuxent River, Maryland. We also conduct tests on board the ships of the fleet in the radio frequency environment created by the ships. Our test teams have been on board destroyers, frigates, cruisers, aircraft carriers, and submarines. There have been HERO tests conducted on board more than 80 ships.

Also we have conducted some tests at other Naval Shore Stations plus measurement surveys at various other locations.

When we test, we use the complete weapon system. For an air-launched weapon, this includes the delivering system. The aircraft or launcher to which the weapon is attached and connected will contribute to the rf currents induced into the electroexplosive devices; one reason is by increasing the effective antenna.

The reason for locating our third ground plane facility at Patuxent River was to take advantage of the aircraft located there and to use the airport facilities for flying in fleet aircraft for test purposes.

In our tests we use a weapon which is inert except for live electroexplosive devices for go/no-go tests and we use electroexplosive devices simulators for instrumented tests. Results for our go/no-go tests tell us if there is an actuation or not, but nothing in between. Our instrumented tests tell us how close we are to an actuation.

If we find that a weapon is susceptible, it is then necessary to restrict radio frequency transmissions or retrofit the weapon to make it immune. Of course, the ideal approach is to recognize the possible hazards during the design of the weapon and make provisions to preclude the HERO problem at this time.

There are several basic approaches for solution of the problem.

One approach is illustrated in Figure 3. This approach is to enclose all of the electroexplosive devices and their associated circuits, which includes power sources, transmission lines, and switching and arming devices, within a completely closed conductive shield. The electromagnetic energy which is incident on this conductive surface is attenuated exponentially with respect to the depth of penetration. Thus, this complete shielding approach is an effective solution to the HERO problem. The precautions necessary here are to use proper techniques to assure complete shielding particularly at the joints and seams.

Even though this approach is theoretically sound, it may not be possible to accomplish practically. However, sometimes this approach can be adapted to fit particular situations. Figure 4 illustrates such a case.

Various components can be placed in shielded compartments and interconnected by shielded circuits. Here again the shielding techniques are critical. The circuit shield must be connected to the component shield around the entire periphery of the shield.

Now, even this is not possible in situations where electrical firing signals are required from some source external to the weapon, such as an air launched weapon which receives its firing signal through a cable from the aircraft to the weapon.

Figure 5 illustrates an approach to exclude radio frequency energy in this case. A suppression device, such as a low-pass electric wave filter, is installed in the transmission line and the circuit shielded from the output of the filter through the electroexplosive device.

We have not only the problem of coupling radio frequency energy into the electroexplosive device but also problems caused by radio frequency discharges, sometimes referred to as rf arcs. These occur during interface connections, such as the connection of a weapon cable to the aircraft. The suppression device will not protect against problems caused by the rf discharge because the rf discharges generate low frequency energy similar to that furnished by firing sources.

Figure 6 illustrates one solution to the rf discharge problem. This is simply to open the firing circuit between the point of rf discharge and the electroexplosive device until after the connection is made.

These, then, are three approaches to the solving of the HERO problem:

- (1) Enclose the entire weapon in a continuous shield,

(2) Shield compartments and interconnecting cables of firing circuits, and

(3) Filter the firing circuit, shield from the filter to the electroexplosive device, and make the proper provisions for radio frequency discharges.

In all these three approaches there is only one real principle involved. This is complete and proper shielding. The filter in the third approach is a frequency discriminating device that selectively excludes rf energy from the shielded compartment.

These approaches are described more thoroughly in the HERO Design Guide which has been published under the HERO program. This document has been furnished to provide engineering data and to specify design techniques which will insure radio frequency safety and reliability in weapons. This Design Guide is now available to weapon designers and developers.

Another of our objectives is to furnish a Test Program for Weapon Developers. This is to provide weapon developers with tests for measuring the susceptibility of a weapon to environmental electromagnetic radiation.

If we can furnish test procedures and equipment whereby a weapon designer or developer is able to determine if his methods of making the weapon immune to radio frequency energy are adequate, then this will eliminate the need for costly and time consuming redesign or retrofits.



There are four test requirements. These are:

- (1) Shielding effectiveness of weapon cables
- (2) Shielding effectiveness of enclosures
- (3) Filter effectiveness, and
- (4) Weapon susceptibility to radio frequency discharges.

For the first two requirements we have published a Technical Memorandum describing methods for determining the shielding effectiveness of cables and enclosures for frequencies up to 30 Mc/s.

We also have a statistical program in progress. This is a probability analysis which is to estimate the probability of an accidental actuation of a weapon system under all the combinations of shipboard conditions encountered.

We have a research and development program which is investigating shielding techniques, methods of radio frequency energy suppression, new techniques in explosive train initiation, and new instrumentation techniques. These are programs involving principles and not specific hardware items.

Then we have one other program which is most important to me since this is my particular area of work. This is our consultation service. In this service we will furnish advice to our weapon designers and developers to assure that proper design techniques are incorporated to make the weapon immune to electromagnetic radiation. We have consultants at four other Naval stations, in Pennsylvania, Washington, D. C., and two in California. We furnish service to other Naval installations and their contractors, wherever it is required. The

service is available throughout the complete development even to the assembly line to explain techniques, such as shield terminations.

From three of these programs, the research and development in shielding techniques and radio frequency energy suppression methods, the consultation service, and the test program for weapon developers, we hope to assure that there will be no HERO problem in our future weapons.

This has been a brief description of the HERO program. If there are any questions, we will try to answer them.

Major Programs of the  
Naval Weapons Laboratory

WARFARE ANALYSIS  
ASTRONAUTICS  
EXTERIOR BALLISTICS  
FLEET BALLISTIC MISSILE SYSTEM  
WARHEAD RESEARCH AND  
DEVELOPMENT  
CARTRIDGE ACTUATED DEVICES  
TARGET VULNERABILITY AND DAMAGE  
STUDIES  
HAZARDS OF ELECTROMAGNETIC  
RADIATION TO ORDNANCE  
BIOLOGICAL AND CHEMICAL  
WARFARE  
ELECTROMAGNETIC COMPATIBILITY  
WEAPON SAFETY  
FOUNDATIONAL RESEARCH

**FIGURE 1**

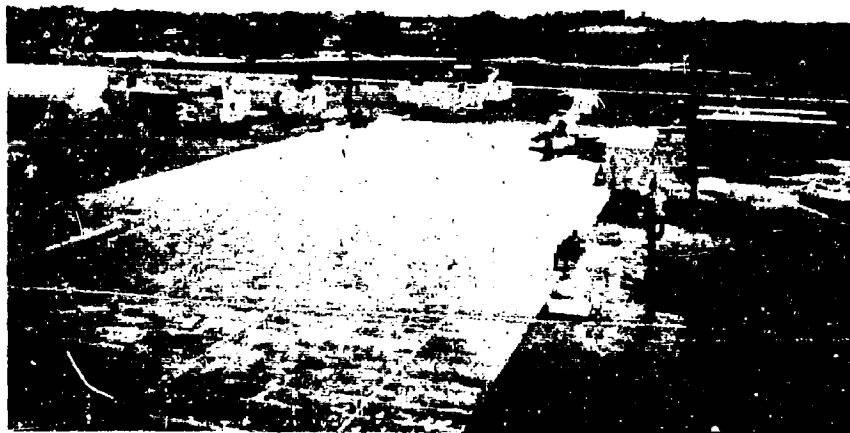


**FIG. 2 HERO TEST FACILITY**

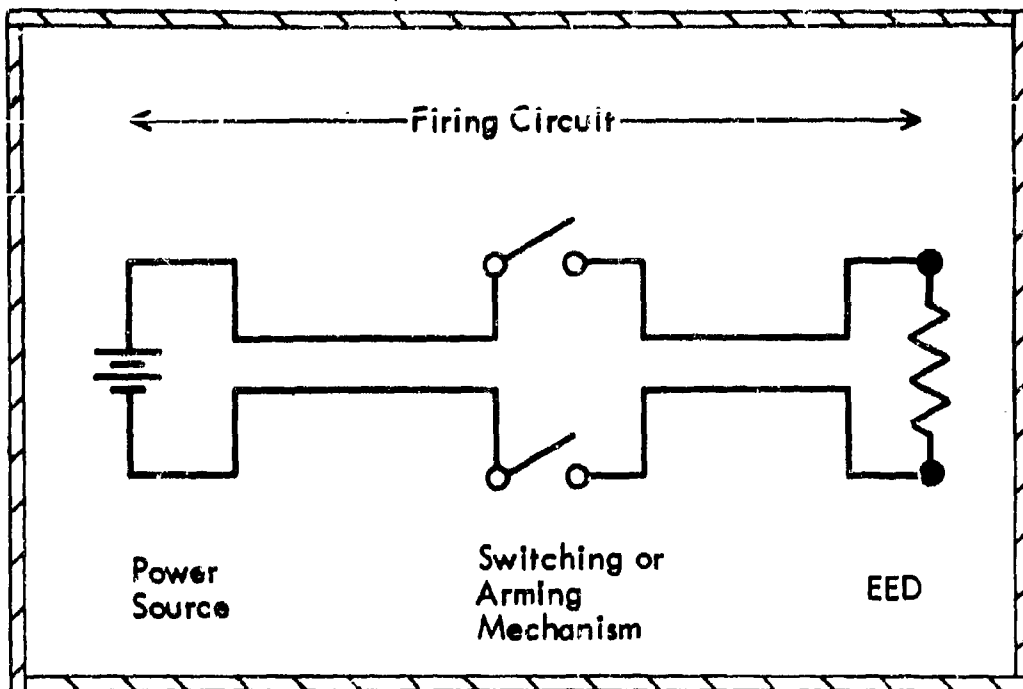


**FIG. 3 THE CONDUCTIVE BOX CONCEPT**

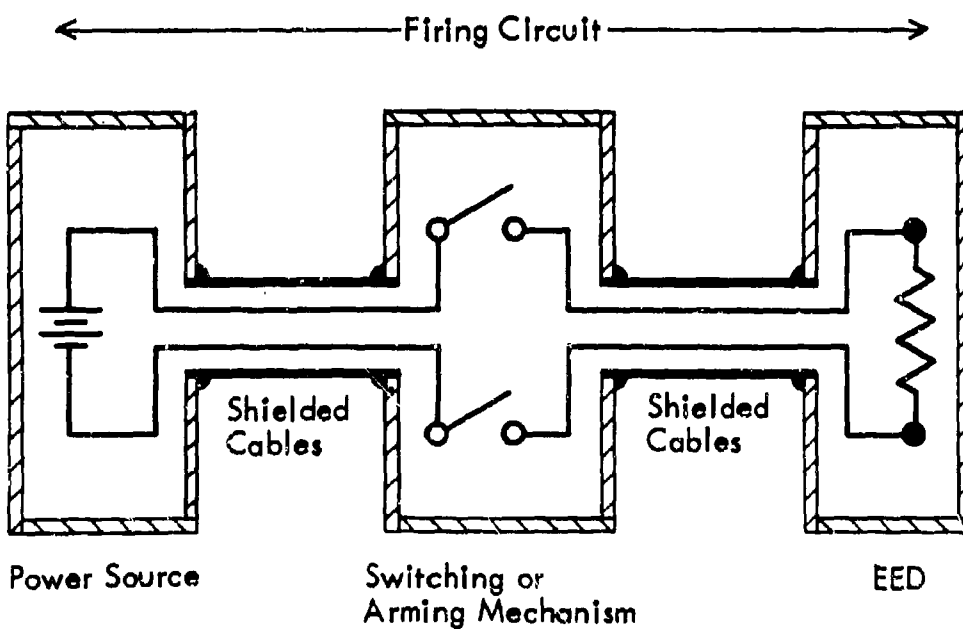


**FIG. 4 COMPARTMENTALIZATION, AND SHIELDING OF COMPARTMENTS AND CONNECTIONS**

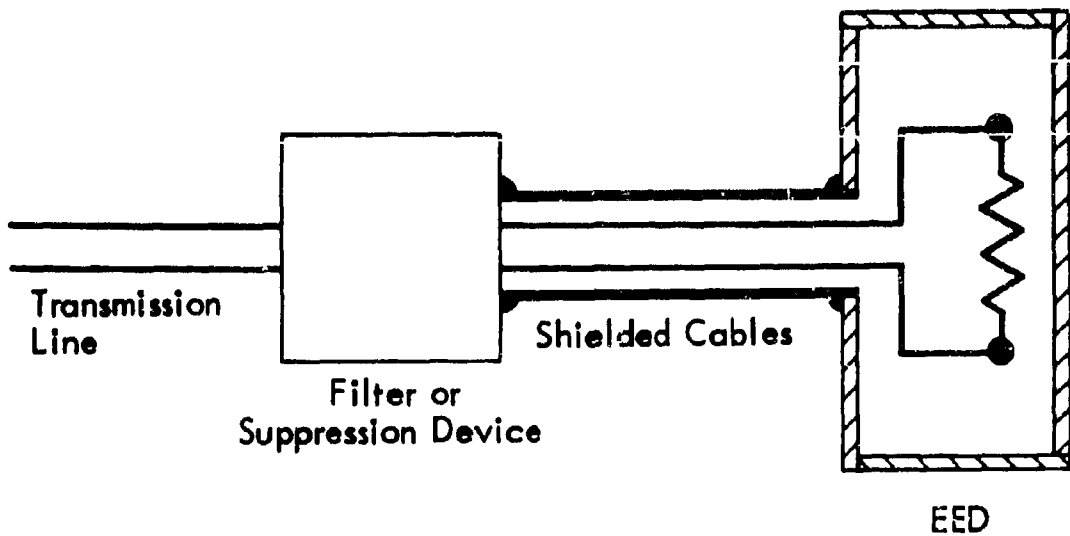


**FIG. 5 USE OF RF FILTER OR SUPPRESSION DEVICE**

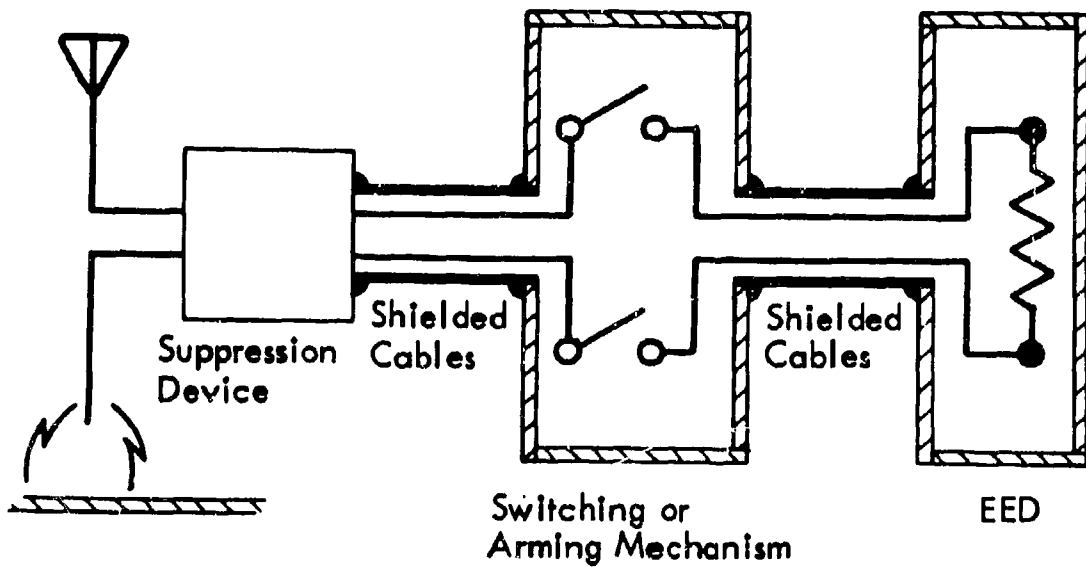


**FIG. 6 A BASIC SOLUTION TO THE ARCING PROBLEM**

## DISCUSSION

Basic instrumentation is a thermocouple of the type developed some time ago by Denver Research Institute. The couple is antimony-bismuth located about 1 to 2 mils from the bridge wire. It is calibrated with direct current. The output of the couple is fed to a recording oscillograph.

Go-no-go testing is only a small part of the work. About 99% is of the instrumented type. Since the beginning of this work in 1959, many initiators have been fired.

2-2 RADIOFREQUENCY-INTERFERENCE PROTECTION  
FOR PYROTECHNIC SYSTEMS IN MANNED SPACECRAFT

By Robert L. Robinson  
NASA Manned Spacecraft Center

ABSTRACT

This presentation describes the technique which the Manned Spacecraft Center proposes to protect an electroexplosive device from potential radiofrequency-interference problems. A typical electroexplosive device and the mechanism by which radiofrequency interference can cause premature ignition are described.

INTRODUCTION

It has been known for several years that electroexplosive devices (EED) are susceptible to premature operation from radiofrequency interference (RFI). Many techniques have been used to reduce this undesirable, and in many applications, dangerous effect.

This presentation describes the methods used by the Manned Spacecraft Center (MSC) to assure that spacecraft pyrotechnic systems are protected from RFI. The sensitivity of EED to RFI and the expected RFI environments will be presented.

## PRESENT SYSTEM CONFIGURATION

The Apollo spacecraft uses a standard EED for the ignition element in all explosive functions. There are two devices: one with a double bridge wire and one with a single bridge wire. In this presentation, only the double bridge wire device will be described. This unit is shown in cross section in Fig. 1(a). The all-fire condition occurs when at least 3.5 amperes are applied through either bridge wire. For the no-fire condition, 1 watt can be dissipated for 5 minutes across each bridge wire, and 9000 volts can be discharged from the 0.0005-microfarad capacitor across the pins to the case without igniting.

The initiator body is made from stainless steel and performs the multiple functions of inner-face and electrical connector. The body also serves as a pressure vessel to contain the pressures produced by the initiator and by the device to which the initiator is attached. The four pins in the header are the connections that bring electrical energy to the bridge wires. The bridge wire is the resistance element which is heated by the input current. Heat from the resistance element ignites the primary charge which burns and initiates the main charge. The primary charge is pressed down into the cup of the header and is covered with isomica insulation discs. The discs, in conjunction with the ceramic header, insulate the initiation charge from the rest of the body material to prevent electrical circuits being made from the body through the charge to the bridge wires.



## Radiofrequency-Interference Environment

Now that the EED has been shown to be sensitive to certain RFI energies, it is appropriate to examine the environment to which a spacecraft will be exposed. Based upon a study made by MSC, the significant radiofrequency (RF) emitting energy sources in a spacecraft mission are those earth-based high-energy transmitting systems shown in Table 1.

TABLE 1. RADIOFREQUENCY SOURCES

Equipment	Frequency, MHz	Field strength, watts/meter <sup>2</sup>
Ground stations	6000	20
Shipboard	4000	80
Emitters onboard spacecraft	3000	30

The first group of emitters is categorized as ground stations and includes commercial, amateur, mobile, and radar stations. Of this group, the radar stations will produce the highest field strength incident on the spacecraft (approximately 20 watts/meter<sup>2</sup>) at a frequency of 6000 megahertz (MHz). The second group of emitters is those energies produced by the powerful shipboard tracking radars used by the Atlantic Missile Range. The radars have a capability of exposing the spacecraft to a power density of 60 watts/meter<sup>2</sup> at a spacecraft frequency of 4000 MHz. The third group is onboard spacecraft emitters, which are the

communications transmitters and the telemetry and tracking beacons. The highest power density produced by these units is approximately 30 watts/meter<sup>2</sup> at a frequency of 3000 MHz.

A simplified envelope of the worst environment for an Apollo mission is shown in Fig. 2. This is a graph of the power density incident on the spacecraft at various frequencies. The figure illustrates that the power density starts to become significant near 100 MHz and peaks at 60 watts/meter<sup>2</sup> at approximately 10,000 MHz. These data consider the location of the spacecraft relative to the various emitters, that is, the distance of the spacecraft from the launch pad and the distance from the emitter to the orbiting spacecraft.

#### Initiator Radiofrequency-Interference Sensitivity

To simplify the discussion on modes of RFI premature ignition, the electrical configuration of the initiator is shown schematically in Fig. 1(b). The dashed lines represent the metal case of the unit. Since the initiator is designed to fire as a result of resistance heating of the bridge wire, RFI currents, as well as the functional direct-current (dc) pulse, can make the initiator fire. Not so apparent is the fact that when a voltage gradient of sufficient magnitude to cause conduction is applied across a metal oxident explosive (the primary ignition material), ignition will occur. In the initiator configuration described, ignition could occur if sufficient voltage were impressed between the pins and the case. Extensive testing has demonstrated that the energy required for this ignition mode (as opposed to bridge-wire heating) is

much less, creating a much greater concern for RFI when these conditions result. The voltage required for this phenomenon is relatively large, although the resultant energy is low. The driving impedance of the spacecraft wiring systems is not conducive to continuous-wave (CW) RFI energy transmission in the high-voltage low-current relationship. This condition does exist with the pulse output modulation now widely used on radar equipment. This RF energy transmission system results in peak voltage levels several orders of magnitude greater than the peak voltage associated with a CW transmission with the same average input power. After testing, the initiator was seen to be most sensitive at 9000 MHz where the no-fire level (1 in 1000 fire) was 89 milliwatts.

#### Protection

From the demonstrated sensitivity of the EED to RFI and environment, it is apparent that provisions must be made in a system design to prevent premature firing. Presently, premature firing is avoided by providing an isolated and shielded system.

The present MSC EED circuitry-design criteria, as related to RFI protection, are shown in Fig. 3. To provide the required isolation from unshielded systems, a separate battery is provided for each EED. The batteries are completely encased within a Faraday-type enclosure. The circuit is balanced with and isolated from the spacecraft structure (with the exception of a high-resistance electrostatic bleed resistance). The total wiring system outside the metallic relay boxes consists of twisted shielded-pair cabling. For complete protection, the shields must not

have any openings. This requirement causes complications in large systems, such as Apollo, and results in a very expensive system in terms of money, weight, and time. Currently, the systems have been able to meet the requirements of 40 decibels (db) of RFI power attenuation (1).

#### RFI FILTER APPROACH

##### Advantages of Filter

A different approach is being taken for the more advanced and longer duration spacecraft missions after the Apollo Spacecraft Program. This approach requires insertion of an RFI filter in the electrical circuitry just ahead of the EED. This method of protection is particularly attractive to spacecraft application because the consequential RFI environment is at the higher frequencies where the smaller lossy-element filters become useful.

In spacecraft used for long-duration missions, the EED electrical system must be powered from the spacecraft's main power system since batteries that permit long mission operation are not available. Also, the present method of circuit isolation (for achieving the required attenuation) cannot be used because the shielding is defeated when the RFI "clean system" is connected into an unshielded "dirty system." Investigations have shown that standard switches and relay contacts must provide the required isolation at high frequencies; therefore, a shield-type interruption cannot be used between the systems. With the RFI filter, the main spacecraft power source can be used for initiation and

still achieve the required circuit isolation at the RFI frequencies involved.

There are several advantages in using a filter in lieu of shielding. For example, a weight saving of more than 100 pounds could have been made by eliminating the shielding system on the Apollo spacecraft and by using a filter. Probably the greatest advantage is that the attenuation of a filter is easily measured. The determination of the attenuation effectiveness of a shielded system requires a costly and involved, full spacecraft system test. This test is usually performed on only one vehicle where many devices are involved; also, data obtained depend greatly on how well the shielding is installed on a particular vehicle. Expensive and heavy connectors are required to penetrate bulkhead structures and provide the required 360° Faraday shielding.

#### Selection Criteria

In the selection of a filter for spacecraft applications, a program to survey industry's on-the-shelf and state-of-the-art inventory was initiated to determine whether a suitable unit existed. The Apollo spacecraft and mission were used as a basis of selection.

The reliability and attenuation of the system were large factors in the selection of a filter. Other factors were the attenuation of the normal EED firing pulse, the power-handling capacity, the voltage breakdown, and the effect of the filter upon monitoring of the EED bridge wire. Weight, cost, and physical size are also large factors in spacecraft systems. For example, in the Apollo spacecraft approximately 150 electro-explosive devices are used to initiate or perform mission functions.

When the Apollo spacecraft is used for the long-duration missions in the Apollo Applications Program (AAP), these filter units must be retrofitted into existing hardware. Therefore, the three factors (weight, cost, and size) become important. The unit must be reliable, to provide the required attenuation and to prevent failure of the system in which it is installed. The device must withstand the initiator firing currents and voltages without failure, either shorted or open.

#### Filter Design

Thirty-two different systems were analyzed in the filter survey. After a program of examination and extensive testing, a hybrid-type filter (shown in Fig. 4(a)) was selected. This filter is actually a combination of two systems. It is an inductance-and-capacitance (LC) filter that uses the standard LC configuration to present the incoming high-frequency signal with a high-impedance path in series and with a low-impedance path in shunt to reject the signal. The normal LC filter has disadvantages that prevent widespread use of this filter only in this application. At certain frequencies, these elements combine (resonance) to give essentially zero attenuation. At the higher frequencies, these elements change their characteristics and become useless. This problem was solved by constructing the LC filter with high-frequency lossy elements (insulated ferrite beads) that dissipate the high-frequency power (area in which the LC filter fails) in the form of heat.

The unit was constructed for an initiator configuration which has two bridge wires and a four-pin connector (Fig. 4(b)). The device

consists of four ferrite and coil assemblies concentrically mounted in a brass grounding ring; the input ends of the ferrite-bead combination are soldered to a solder-mount receptacle connector, and the output ends of the inductor coil are soldered to the pins of a straight plug. The four ferrite and coil assemblies are enclosed in brass tubes which, after encapsulating the assembly with potting compound, are soldered into both connectors, effectively completing the assembly. The four-pin filter with its connectors weighs approximately 65 grams, and is 2-11/16 inches in overall length and 21/32 inch in diameter. The two-pin filter for single bridge-wire initiators weighs approximately 44 grams and is 2-1/4 inches in overall length and 21/32 inch in diameter.

Figure 5 is a plot of the attenuation of the filter in db (logarithmic ratio of input to output power) versus the frequency in MHz. The curve is shown flat above 60 db because this level was the limit of the instrumentation used for the attenuation measurements. The filter provides from 10 to more than 60 db of attenuation at frequencies in excess of 100 kilohertz (kHz). It is important to note that beyond 10 MHz, the attenuation is greater than 60 db and never decreases.

Figure 6 is a plot of the RFI environment, as shown in Fig. 2, and of the same environment attenuated by the filter. As can be seen, the environment is reduced to an insignificant power level.

#### Development Status

Twelve developmental devices have been constructed for preliminary testing. These 12 units have been exposed to sample tests based upon

the mission environments to which the Apollo Standard Initiator will be exposed. The units were also used to fire the initiators at maximum and minimum firing currents. No major problems were found throughout the testing. The only failure that appeared was that of the soldered end closures, and this problem can be corrected by using a weld process to close the end of the units.

Twenty prototype units are now in the process of being manufactured. These filters will be used for testing in a design-verification test program (a condensed qualification program) to verify that the design can survive the test conditions.

#### CONCLUSIONS

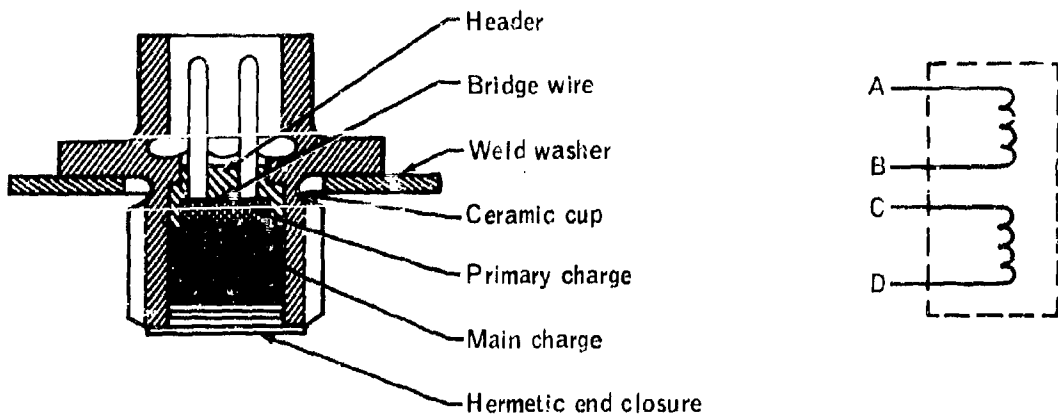
The RFI filter described should satisfy the RFI attenuation, weight, size, and reliability requirements for use in NASA Manned Spacecraft Center programs. The qualification program now being generated will verify whether the design is compatible with these requirements.

The units will probably be used first on the Apollo Applications Program in which the unit will be attached externally to present initiators. Future plans call for filter incorporation directly into the initiator design.

#### REFERENCE

- (1) Anon.: Safety Range Safety Manual. Headquarters Air Force Eastern Test Range, Patrick AFB, Fla., AFETRM 127-1, Nov. 1, 1966.

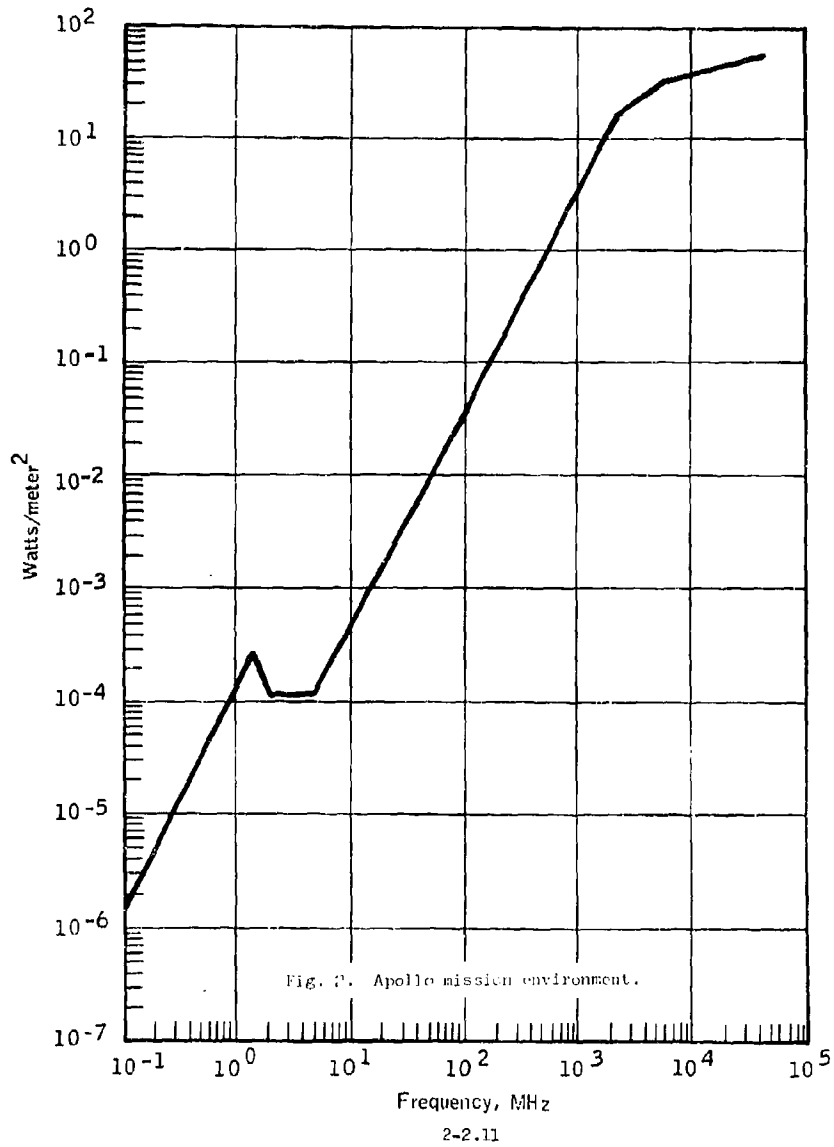




(a) Cross section of the initiator

(b) Schematic diagram of the initiator

Fig. 1. Standard initiator used to initiate all Apollo ordnance events.



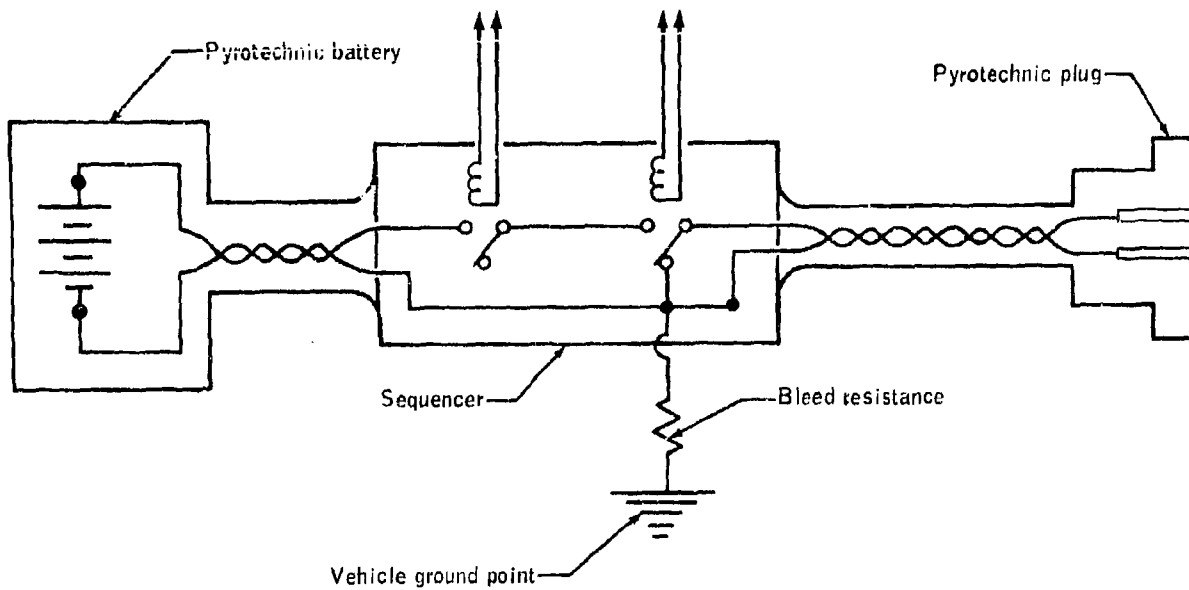
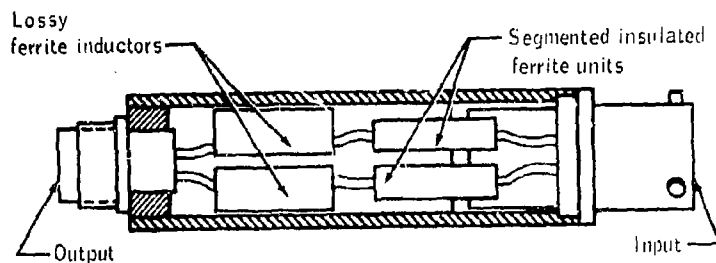
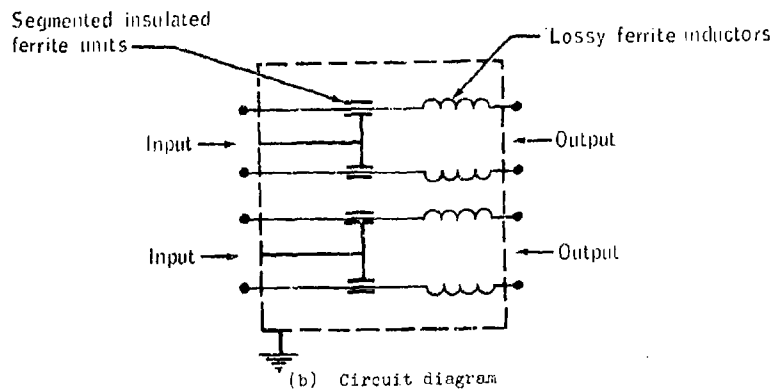


Fig. 3. Spacecraft pyrotechnic circuit shielding.



(a) Inductance and capacitance hybrid filter



(b) Circuit diagram

Fig. 4. Hybrid radiofrequency filter system.

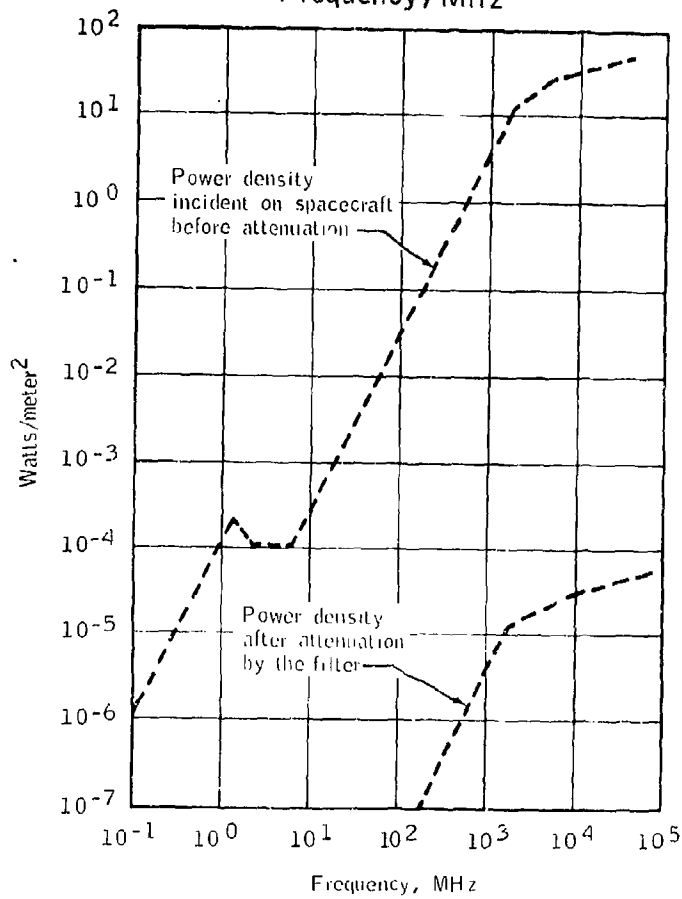
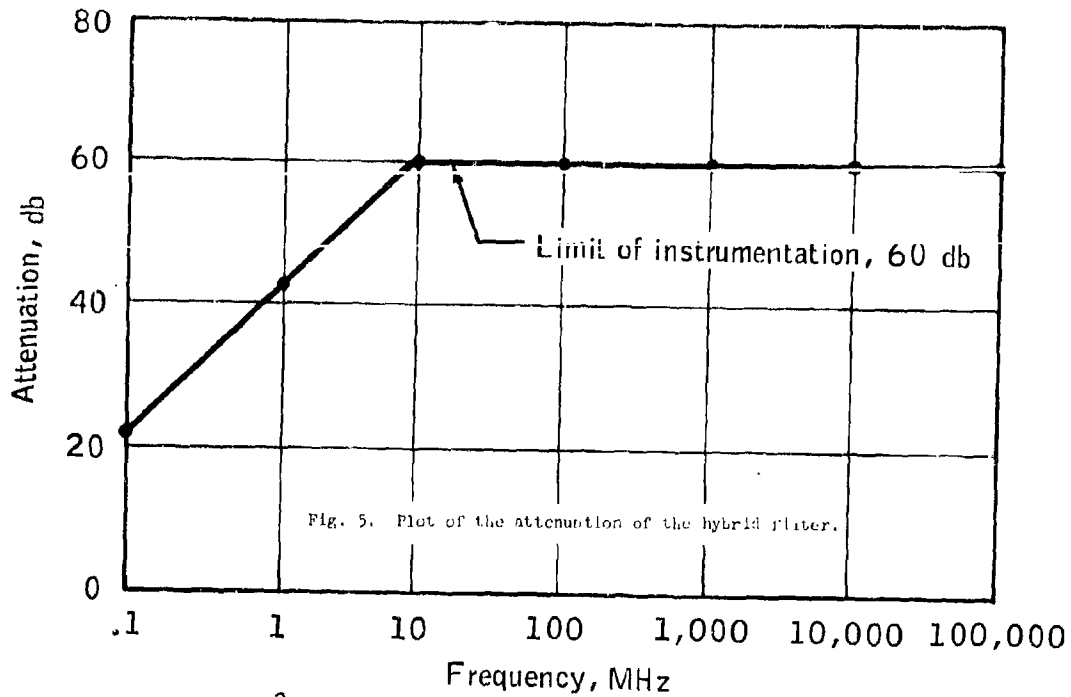


Fig. 6. Power density (Watts/meter<sup>2</sup>) before and after attenuation.

## DISCUSSION

The bridge-wire to bridge-wire mode of initiation is being eliminated by eliminating one of the bridge-wires.

The RF filter mentioned in this paper works for both bridge-wire and pins-to-case modes. The Franklin Institute made this filter and tested it for both modes.

Attenuation measurements are made with normal squib impedance, with a one-ohm carbon resistor and with a load that would be considered worst case. Details of the tests are contained in Franklin Institute reports to NASA/MSC.

The magnitudes of the fields taken for this work were Apollo mission oriented and not taken from other sources. Measurements and calculations are based on a journey from Kennedy Space Center through the lunar mission and back. Some of the orbital fields were surprisingly high, up to 40 watts per square meter and mostly radar frequencies.

A bleeding resistor of 100,000 ohms or more is required; ours is 3 megohms. While the EED's are qualified for 25,000 volts from a 500 picofarad capacitor, these resistors are placed to equalize any stray potentials or currents that may be present.

It was made clear by Mr. Cormack (NAVAIRSYSCOM) that it is indeed difficult to predict the environment with constant movement of shipboard and land-based equipment in secured combat zones. Very high RF environments can be achieved readily under the right set of circumstances and these exist today. These environments can apply to Army and Air Force weapons and equipment just as much as to Navy equipment.

2-3 MEASURING THE ELECTRIC AND MAGNETIC  
COMPONENTS OF THE NEAR FIELD

by

Robert B. Cowdell  
Genisco Technology Corporation, Genistron Division

1.0

INTRODUCTION

In modern weapons complexes it is typical to encounter high levels of power being transmitted in close proximity to weapons systems and personnel. It is generally acknowledged that exposure to excessive levels of power is hazardous and it is desirable to avoid these exposures or protect against them.

In order to accurately define the electromagnetic environment to which systems will be exposed, there is great need for instrumentation that measures accurately the electric and magnetic components of the near field when close to high power radio frequency radiators.

To further the development of such instrumentation, it became necessary to compute a reasonably accurate theoretical description of the near field distribution, and to gather information on the limitations of conventional field intensity meters now in use for near field measurements. The initial goal was to establish a standard field with which to calibrate the instrument and to develop mechanical and circuit design criteria unique for near field measurement.

The remainder of the project consisted in designing the Near Field- Field Intensity (NFFI) meter and subjecting it to rigorous accuracy and susceptibility tests as proof of its ability to perform.

1.1

THEORY OF OPERATION

The unique design of the NFFI meter reflects major developments in measurement philosophy when compared with that of commercially available RI-FI receivers. This instrument is designed to measure radiated levels of electric and magnetic fields directly, in volts per meter or amperes per meter, over the frequency range of 2 MHz to 30 MHz.

The meter is designed to operate in either of two modes. In the wide-band mode the instrument accepts all signals falling in the range of 2 MHz to 30 MHz and indicates the total RMS field present in this frequency region. In the tunable mode the instrument can be set to any frequency in the 2 MHz to 30 MHz range and signals falling within 250 KHz of the selected frequency will be measured (the receiver bandwidth in the tunable mode is nominally 500 KHz). The range of measurement is 2 to 500 volts per meter for electric fields and 5 to 1,500 millamperes per meter for magnetic fields.

The instrument is constructed in two enclosures (Figures 2 and 4). The detector unit contains essentially the receiving circuits (both the wide-band and tunable detectors) and the meter tuning unit contains the reading circuits (the tunable local oscillator and meter). Both units have a rechargeable battery power supply.

#### 1.1.1 SIGNAL RECEPTION IN THE WIDEBAND MODE

The input signal passes through either the electric or magnetic probe (see Figure 1), depending on the type of field being measured. Each probe has its own input filter (which rejects signals outside the 2 to 30 MHz range) four step attenuator, and preamplifier. Signals then proceed into the wide-band amplifier. The three stage (2 to 30 MHz) rf amplifier raises the input signal to a usable level and feeds it into the square law detector. Here the rf signal is rectified. The dc output voltage from the detector is proportional to the input power level (the square of the input rf voltage). The detector output is then fed to a dc amplifier where it is amplified by a factor of 100 and routed through the 60 foot interconnecting cable to the meter-tuning unit where it drives the dc output meter. It is necessary to amplify the detector output in order to drive the dc meter and to insure that signal quality will not be compromised by high levels of rf pickup on the inter-unit cable. The scale of the output meter is calibrated to take the square root of the input voltage. The meter always indicates the true RMS value of any type of input signal.

#### 1.1.2 SIGNAL RECEPTION IN THE TUNABLE MODE

Signals received in the tunable mode pass through the E or H field probe, input filter, attenuator, preamplifier, and wideband amplifier exactly as described in the previous paragraph. The rf signal to be measured (fed from

the wideband amplifier) and the output of the local oscillator (LO) are then coupled directly into the mixer. The tunable LO output is fed from the meter unit through the inter-unit cable. When an rf signal is to be received, the LO is tuned to a frequency 40 MHz above the frequency to be measured. The LO tuning range is from 42 MHz to 70 MHz.

Frequency combination in the mixer occurs in a full wave rectifier. The rectifier output contains many frequency components, including a signal at a frequency which is the difference between the two input signals. This signal is the frequency of interest which is ultimately amplified in the IF section. When it is desired to receive a 2 MHz RF signal, the frequency indicator on the remote dial is set at 2 MHz. This sets the LO at 42 MHz and the 40 MHz difference frequency out of the mixer reflects the amplitude variations of the 2 MHz RF signal being measured. The input RF signal, in effect has simply been translated in frequency.

When a 2 MHz signal is being measured the mixer output will be 2, 38, 40, and 42 MHz. All but the 40 MHz signal will be rejected as they are fed into the highly selective bandpass filter. When the LO is tuned at 42 MHz it is required that the bandpass filter pass the 40 MHz beat frequency and reject the high level 42 MHz LO signal. The bandpass filter provides the necessary selectivity by having greater than 50 DB of rejection at 42 MHz (the lowest frequency of the LO). In the 3 stage, 40 MHz IF amplifier the mixer output from the bandpass filter is amplified to a usable level and fed into the square law detector. The detector output then drives the output meter in the same manner described in paragraph 1.1.1.

## 1.2

### NFFI SYSTEM FREQUENCY RESPONSE

The output of the system calibrator is controlled by a compensating network designed to have a frequency characteristic which is approximately the same as that of the amplifier response. At any frequency where the amplifier response rises, the calibrator output also rises and the calibration procedure requires that the amplifier gain be reduced by means of the "Calibrate B" setting control. The combined effect of the calibrator and amplifier gain control is to produce an almost perfectly flat system frequency response. The effect of the attenuator is to raise or lower the entire system sensitivity by a fixed amount.

The measured system frequency response in the electric field mode is flat within  $\pm 1.3$  DB and the magnetic field response within  $\pm 1.5$  DB for either wideband or tunable sections. The system bandwidth is 500 KHz at all frequencies in the tunable mode.

### 1.3

#### NEAR FIELD PROBES

The modified disccone electric field probe and the shielded loop magnetic field probe (see Figure 4) possess unique properties requisite for near field use. The probe is small when compared to the wavelength of the measured field or to the size of the transmitting antenna. The small size of the probe assures that the field immediately around the probe will not be appreciably disturbed when the probe is inserted into the field for measurements. Although the probe is small it develops sufficient output to drive the meter circuits.

The problems of antenna cable pickup and field distortion are avoided by mounting the probes directly on the face of the detector unit. Use of a grounded cable to connect the probe to its detector would load the transmitter and cause distortion of the normal field distribution. The loading would occur because currents are induced into the ground cable and transmitted energy is dissipated.

### 1.4

#### SHIELDED ENCLOSURES

Extensive susceptibility testing and field intensity measurements established that a minimum of 100 DB of shielding isolation was required between 100 KHz and 10 GHz to isolate meter circuits from high level external fields. Once an adequate metal type and thickness was chosen, control of potential sources of leakage became a critical problem. Important principles of shielded enclosure design are itemized below.

1. No screw or bolt penetration was permitted in the enclosures.  
(See Figure 3)
2. All switches and lights entered the enclosures through single waveguide beyond cutoff openings (Figure 5). The total number of openings were minimized. No electrical leads were routed through the openings. Knob or switch shafts were non-conductive. The length to diameter ratio of each tube is 8 to 1.



3. All meter circuitry is attached to a "shoe box" type of lid (Figure 2) and is taken out of enclosures by removing the entire unit face. The energy leakage path through the seam was designed to be a labyrinth to maximize reflection losses. In addition, a gasket of knitted wire mesh is employed on the top of the seam and finger stock around the sides as an added precaution against energy leakage. The cover is fastened with 8 snap tight catches.
4. To prevent leakage all connectors are the threaded type. Unused connectors are covered with metal caps. Cable shields ground securely around the exterior connector periphery.
5. Cable pickup problems were reduced by minimizing the number and length of cables. Cable shields require high quality grounding to be effective. An inter-unit triaxial cable with insulated shields proved the most effective against cable pickup.
6. The DC meter movement is mounted outside the shielded enclosure (Figure 2) because tests proved it was not susceptible to RF fields. Leads to the movement are filtered where they enter the shielded enclosure.

#### 1.4.1

#### SHIELDING TESTS

During acceptance tests the shielding ability of the enclosures was evaluated. At 5.155 MHz with the NFFI meter placed one meter from the transmitting antenna, a field strength of 425 volts/ meter was recorded. With the probes removed and connectors uncapped, there was no response of the meter. At 9.005 MHz the meter was exposed to 880 milliamps/ meter. With probes removed there was no response from the meter. Also, with the probes removed, the meter could be calibrated normally in the presence of these strong fields.

#### 1.5

#### EASE OF MEASUREMENT

During accuracy tests an average time of 30 seconds was required to calibrate the meter. The meter required recalibration after 15 to 20 minute periods had elapsed. During two days of testing, measurements were recorded

at an average of one reading each 90 seconds.

One great advantage of the NFFI meter over commercial RFI meters is that field strengths are read directly on the meter scale as volts per meter or amps per meter. This eliminates the handling of cable, antenna and other miscellaneous correction factors common to this type of equipment. By directly reading field strengths the transmitter can be adjusted during testing to obtain desired field intensities. These factors should prove to be valuable assets during any test program.

## 2.0 ACCEPTANCE TESTS

Acceptance evaluations consisted primarily of accuracy tests to compare measured and calculated field intensities over the entire frequency range of the meter. In addition, the ability of the broadband section to add two fields at different frequencies was tested. Susceptibility tests evaluated the ability of the meter to operate in the presence of high intensity fields between 2 MHz and 30 MHz as well as the systems immunity to high intensity radar signals.

### 2.1 ACCURACY TESTS

Extensive testing was performed to evaluate the accuracy of the prototype NFFI meter. A serious problem that hampered the completion of testing was that of establishing a standard field for calibration purposes.

Using a 35 foot monopole with a steel ground plane, data measured between 2 MHz and 10 MHz fell within  $\pm 2$  DB of the calculated field. Above 10 MHz the computed field strength could not be used as a basis for comparison because the current distribution along the monopole became non-sinusoidal. (See Paragraph 4.1 for further explanation.) Quarter wave monopole antennas then replaced the original configuration and testing was continued between 10 MHz and 30 MHz. A typical measuring configuration is shown in Figure 6. Figures 7 and 8 are samples of electric and magnetic field accuracy test results.

#### 2.1.1 TEST RESULTS

The average percent deviation between the calculated field intensity and the measured field intensity is presented in Table I. This data was obtained by computing the average difference between the calculated field and the measured field considering all data points recorded at different distances

from the antenna at one frequency.

TABLE I  
AVERAGE DEVIATION BETWEEN MEASURED & CALCULATED  
FIELD INTENSITY IN DECIBELS

<u>FREQUENCY</u> <u>IN MHz</u>	<u>ELECTRIC</u> <u>FIELD</u>	<u>MAGNETIC</u> <u>FIELD</u>
11.064	-0.7	3.5
11.535	1.7	1.3
12.045	0.08	0.8
13.53	.34	0.8
15.595	3.7	1.9
16.06	2.0	1.7
16.3	1.6	2.0
18.036	3.35	1.7
19.27	4.7	1.9
20.05	0.6	1.1
22.91	-3.5	-2.3
23.18	-2.7	-2.8
24.45	-1.9	-0.4
25.575	-0.5	3.4

2.2 ADDITION OF SIGNALS AT DIFFERENT FREQUENCIES

The meter is required to measure the RMS value of the total field present. It was therefore necessary to demonstrate that in the broadband mode the meter will add two signals at different frequencies correctly.

Tests to demonstrate this capability were performed by exciting a parallel plate standard field generator simultaneously at two different frequencies of known amplitudes. The NFFI meter reading was then compared with the calculated RMS value of the total field. Results of these tests were as follows:

Test 1:

<u>Frequency</u>	<u>RMS Field</u>
4 MHz	4.90 v/m
5 MHz	5.50 v/m
Measured RMS total field:	7.50 v/m
Calculated RMS total field:	7.40 v/m
Measurement error:	0.1 DB

Test 2:

<u>Frequency</u>	<u>RMS Field</u>
4 MHz	5.0 v/m
20 MHz	5.1 v/m
Measured RMS total field:	7.30 v/m
Calculated RMS total field:	7.14 v/m
Measurement error:	0.2 DB

The results of these tests indicate extremely good accuracy of overall calibration and flatness of frequency response.

2.3

SUSCEPTIBILITY TESTING

The purpose of susceptibility testing was to establish any susceptibility of the meter to high intensity fields beyond its design frequency range.

The ungrounded NFFI detector unit was mounted on a tripod five feet above the ground plane. Each of several radars was focused on the meter and the power density of each one was measured. While the NFFI meter was exposed to each of the listed radars, measurements were performed with the results shown in Table II. Power densities are in  $\text{mw}/\text{cm}^2$ .

TABLE II  
SUSCEPTIBILITY TEST RESULTS

<u>RADAR BAND</u>	<u>POWER DENSITY</u>	<u>PROBE</u>	<u>IN-BAND MEASURED FIELD</u>	<u>RESULTS, NFFI RESPONSE</u>
P	0.078	none	none	no response
P	0.078	E	170 v/m	no response
P	1.0	E	none	2 v/m
P	1.0	H	25 ma/m	no response
L	1.45	none	none	no response
L	1.45	E	130 v/m	10-DB rise
L	1.45	H	95 ma/m	no response
S	1.20	none	none	no response
S	1.20	E	26 v/m	no response
S	1.20	H	85 ma/m	no response
C	6.3	none	none	no response
C	6.3	E	none	no response
C	6.3	H	160 ma/m	no response
X	1.4	none	none	no response
X	1.4	E	130 v/m	no response
X	1.4	H	35 ma/m	no response

2.3.1

CONCLUSIONS

When exposed to each radar signal the meter gave no indication of susceptibility, nor did the field strength reading change when signal strengths were measured, using the magnetic field probe.

In the electric field mode indications of susceptibility occurred at P-band when the meter was placed ten feet from the transmitting antenna. At L-band, slight susceptibility was also noted as a change in indicated signal while reading field strength at 4.525 MHz.

There was no indication, response or damage when the meter was exposed with the probes removed, and terminals capped.

The electric field susceptibility occurred because signals entered on the electric field probe, were detected, and changed the output meter indication. It is not likely that measurements will be taken in the main beam of a radar transmitting at high power levels due to presence of personnel hazards. Moving the meter a very short distance would enable one to record data while out of the main beam but in high level ambients.

### 3.0 NEAR FIELD INVESTIGATION

The study of the near field distribution achieved its projected goals by obtaining a precise theoretical description of the near field of the 35-foot monopole antenna over an ideal ground plane. A comparison of the theoretical study to field intensity measurements made using commercial meters assisted first in formulating design concepts for a meter to measure in the near field, and second in approaching the problem of generating a standard near field for calibration purposes.

#### 3.1 THEORETICAL STUDY

Equations describing the magnetic and electric (vertical and horizontal) components of the near field were programmed for a digital computer. Data was obtained in graphical and tabulated form for 21 frequencies between 4 MHz and 30 MHz, at 10 heights above ground (0 to 15 feet), and at distances from 1 to 70 meters from the transmitting antenna (a total of 44,100 data points) Figure 9 presents a typical computer graph.

##### 3.1.1 THE ROLE OF ANTENNA CURRENT IN CALCULATED FIELD INTENSITIES

The exact value of the maximum antenna current must be known to calculate either the electric or magnetic components of the near field. Equations describing field strength are based on the assumption that the current distribution on the antenna is sinusoidal, with a node at the free end. The maximum current ( $I_{\max}$ ) occurs at a distance  $\lambda/4$  from the free end. Currents measured at the base of the antenna are only equal to the maximum antenna current when the antenna length is  $\lambda/4$ . When the antenna is longer or shorter than  $\lambda/4$ ,  $I_{\max}$  must be calculated. When the antenna is shorter than  $\lambda/4$   $I_{\max}$  does not occur at any point on the antenna. Nevertheless, the fictitious  $I_{\max}$  must be computed and used to calculate field strengths.

### 3.2

#### FIELD INTENSITY MEASUREMENTS

The measurements survey was conducted on a 100 by 200 foot by 1/4 inch thick steel ground plane using a 35-foot high monopole transmitting antenna. (See Figure 6.) Commercial meters and their antennas as well as the NFFI meter were employed to measure the vertical electric and magnetic components of the near field. Data was recorded at fixed heights above ground and at 8 frequencies between 2 MHz and 30 MHz. Distances from the transmitting antenna ranged between  $.1\lambda$  and  $1\lambda$  in the increments of  $.1\lambda$  of the frequency being transmitted.

### 4.0

#### EVALUATION OF THE NEAR FIELD DISTRIBUTION

The field distribution predicted by the programmed digital computer study differs from the fields actually generated. This does not imply that the theoretical study was inaccurate, but only that the facilities used to generate the fields were physically limited and could not achieve the conditions requisite for generation of the predicted ideal distribution.

The tolerances presented in Table I are those of the entire test system. The test system is composed of the NFFI meter and the reference field. Repeated tests of the NFFI system have proven that its response is well within its prescribed tolerances. The remaining deviation (beyond the  $\pm 1.5$  DB tolerance in the NFFI meter) must originate in the system generating the reference field.

The data reported includes that taken with the 35-foot monopole to a frequency corresponding to approximately 0.42 wavelength, and at all higher frequencies with 0.25 wavelength antennas.

### 4.1

#### ESTABLISHING A STANDARD FIELD USING A MONOPOLE ANTENNA

The calculated nearfield of the 35-foot monopole can be used as a standard field at frequencies below 10 MHz. However, this configuration is not accurate above 10 MHz because the effect of the finite antenna cross section causes the current distribution along the radiator to become non-sinusoidal (see Figure 10) as the length of the antenna approaches  $.47\lambda$  at 10 MHz. Any departure from a sinusoidal current distribution will result in poor agreement between the computed and generated fields. (1) The calculated field has as a prerequisite the sinusoidal current distribution. The problem of computing near field intensities for monopole antennas with nonsinusoidal current distributions is restrictively complex. Additional problems arise when

computing maximum antenna currents for an antenna with an unknown current distribution.

When the cross section of the antenna becomes vanishingly small, its current distribution will approach the simple sinusoid. For antennas of finite thickness that are shorter than  $.47 \lambda$  the current distribution is very nearly described by the simple sinusoid, and the fields can be calculated without excessive difficulty.

#### 4.2 ESTABLISHING A STANDARD FIELD USING A QUARTER WAVE ANTENNA

Above 10 MHz a standard field for calibration was generated by cutting quarter wave antennas from A.W.G. 12 gauge copper wire (diameter .08 inches). The antennas were mounted directly on the ground plane with the antenna current ammeter at the base.

The advantages of this method are:

1. The problem of nonsinusoidal current distribution is minimized by using very thin wire antennas.
2. Location of the ammeter exactly at the antenna base reads the maximum antenna current directly and eliminates maximum current computations.
3. Maintenance of a ratio of antenna length to diameter of 1000 or higher minimizes end effect. (2)
4. Use of quarter wave antennas greatly reduces the complexity of calculating field intensities.

(1) H. Jasik, Antenna Engineering Handbook, 1961, p. 20-9.

(2) Radio Amateurs Handbook, p. 301, Fig. 14-3.



4.3

#### TOLERANCE IN ANTENNA LENGTH

Any deviation in actual length of the quarter wave antenna from the length used in field calculations is reflected primarily as an error in base current measurement. The base current changes very slowly in the vicinity one quarter wavelength from the free end because the current reaches its peak value very slowly. This error is quite small and was estimated at 0.1 to 0.2 DB.

4.4

#### CALIBRATION OF RF AMMETERS

Accurate ammeter calibration is critical to accurate calculation of the standard field because the field intensity is proportional to the maximum current on the antenna. All ammeters were calibrated but no definite statement of accuracy is known. The ammeters were calibrated across their entire scale to insure maximum accuracy. The estimated accuracy of the RF ammeters is  $\pm 5$  per cent of full scale. According to this estimate, the ammeter error could be 0.4 DB.

The location of the ammeter in the antenna circuit was carefully controlled to insure that the current measurement was exactly at the antenna base. Location errors are considered to be negligible.

4.5

#### EFFECT OF ANTENNA BASE HEIGHT

If the antenna base is elevated above the ground plane, the near field distribution will be altered. The 35-foot monopole is elevated because of its large insulator base. At the frequencies and distances used this error is approximately 5 per cent.

The quarter wave antennas were supported with bases very close to the ground plane, thus almost eliminating this source of error.

4.6

#### LOSSES IN SUPPORTS

Some quarter wave antennas were supported by a seasoned wood mast. To check the effects of possible losses in the mast, the same antennas were supported from a spar well away from the mast. The effect of the mast was found to be negligible.

Noticeable perturbations in field distribution appear at the high frequencies. These appear to be related to the location of welded seams in the steel ground plane, and also tended to deviate from the expected distance and height relationship. Several lines of investigation were carried out on these effects.

- (a) A search was made in the technical literature for analytical methods including the effects of magnetic permeability of the ground plane on near field distribution. Several authors recognized the influence of such losses, but made no attempt to analyze the problem. It was recognized as being exceedingly complex even when gross simplifying assumptions were introduced. (3)
  - (b) A professional consultant on antennas was retained to investigate the feasibility of an analytical solution, but the results were negative for the reasons stated above.
  - (c) A simplified solution, based on a plane wave incident on a steel ground plane, was obtained using Genistron's Recomp III computer. This solution confirmed plane wave attenuation by the ground plane, with resulting wave tilt. No suitable modification of results could be found which is applicable in the near field.
  - (d) Two accurate scale models of the ground plane, one of copper and the other of steel were constructed. Frequency scaled quarter wave antennas were installed and comparative measurements of the resulting near fields were performed. This experiment produced the best available estimates of steel ground plane losses as compared to a similar copper ground plane. The experiment indicated a reduction in strength of the near field at 20 megahertz of 0.9 DB and approximately 0.5 DB at 10 megahertz. These numbers are relative to copper and do not account for discontinuities at welded seams which have been observed in some instances to be 1 or 2 DB.
- (3) S.A. Shelkunoff, "Antennas, Theory & Practice", p. 213

#### 4.8

#### EFFECT OF CORONA

Corona discharges occur when a high potential gradient at the top of the antenna causes ionization of the surrounding air, and acceleration of the ionized particles. Movement of these particles constitutes a current flow. Corona is normally only visible in the dark as a blue gas-like glow.

During daylight testing, high intensity corona discharges were, on several occasions, evidenced by burning and melting of the tip of the antenna. The burning could be prevented by carefully filing the end of the antenna until it was round. Thus the corona was reduced so as to not be visible in daylight. Because corona ceased to be visible in daylight does not mean that it ceased to occur, but only that it was reduced in magnitude.

#### 4.9

#### AVAILABILITY OF PRIMARY STANDARDS

Inquiries have been made to determine the availability of primary standards. Although programs were underway to develop an acceptable standard near field for calibration purposes the development was not complete and no estimate was available as to the probability that an accurate standard could be obtained at the time this project was undertaken. Neither could any commitment be obtained regarding the accuracy limitations of a monopole antenna over either a copper or steel ground plane.

In summary, the use of fields generated by a quarter wave monopole over a large, conductive steel ground plane is adequate within  $\pm 3$  to  $\pm 6$  DB, for calibration in the near field.

Other laboratory standards equally as useful and accurate are parallel plates for generation of a standard electric field and a long wire for generation of a standard magnetic field. The distance between plates as well as the plate diameter must be much larger than the system being calibrated. The long line is very susceptible to reflections from metallic objects in its vicinity.

#### 5.0 EVALUATION OF COMMERCIAL RECEIVER PERFORMANCE IN THE NEAR FIELD

Commercial equipment in its off-the-shelf configuration could not be used to measure in the near field when high levels of power were being transmitted. Measured levels were inaccurate (often varying in a random manner and frequently without meaning) even when the meter was placed at great distances from the transmitter. In order to use the standard commercial receiver, it had to be housed in a double screened copper enclosure, placed

inside a second solid steel enclosure, isolated from ground, with its own portable power supply, and with heavy in-line attenuators at the screened enclosure.

The principle source of error, using commercial receivers, was case penetration. Once the receiver was elaborately shielded other inadequacies became apparent. Additional problems arose from grounding the rod antenna counterpoise, the large size of antennas, and long interconnecting cables.

6.0

#### ACKNOWLEDGEMENT

The NFFI meter was developed for the U.S. Naval Weapons Laboratory at Dahlgren, Virginia, under contract N178-8290. The cooperation received from NWL personnel throughout the project is appreciated. Genistron major contributors were James C. Senn and Steven A. Jensen.

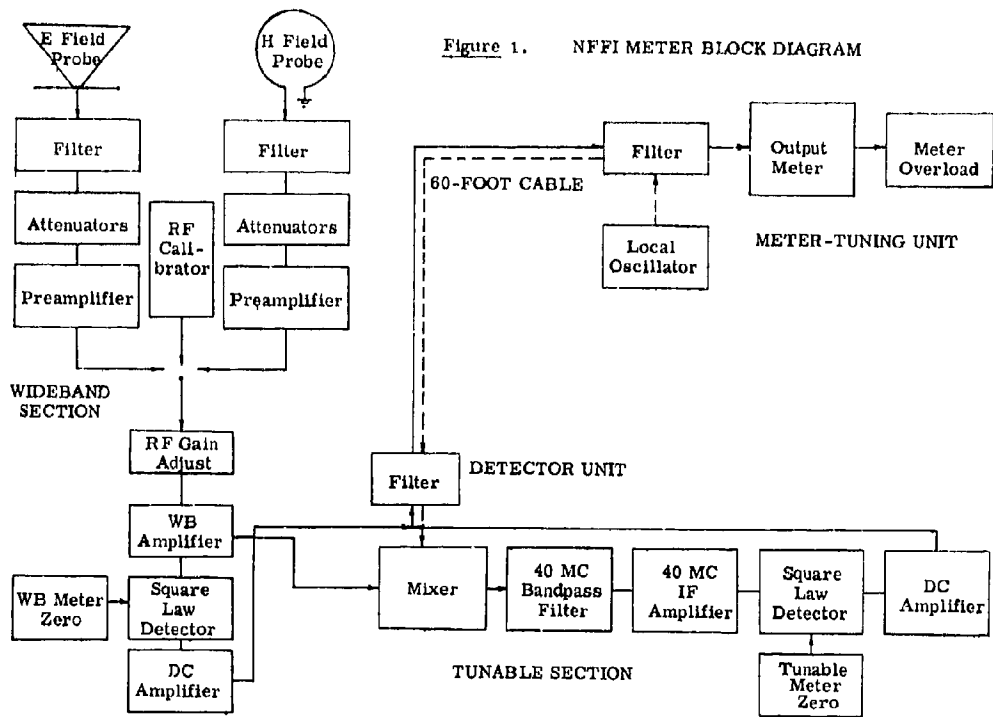


Figure 1. NFFI METER BLOCK DIAGRAM

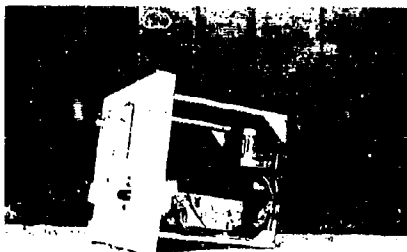


Figure 2: Right of meter unit without enclosure.



Figure 3: Shielded cover (identical for both Meter and Detector Units).

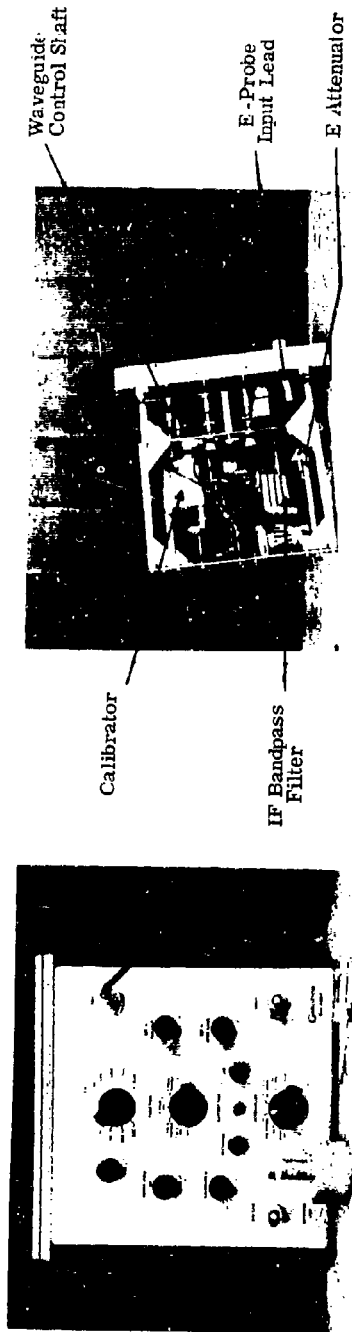


Figure 4: Detector unit with E-field probe at left, H-field probe at right.

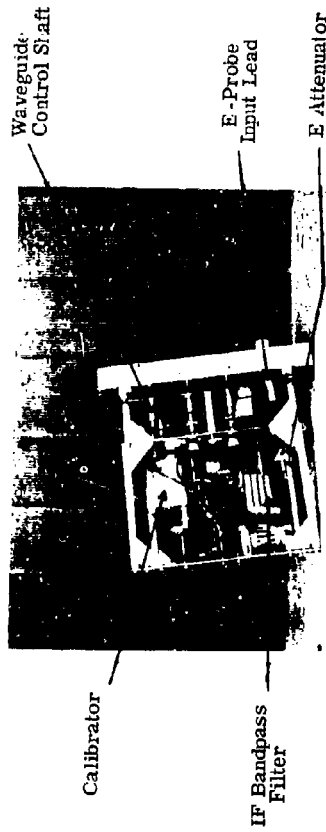


Figure 5: Left side view of detector unit without cover.

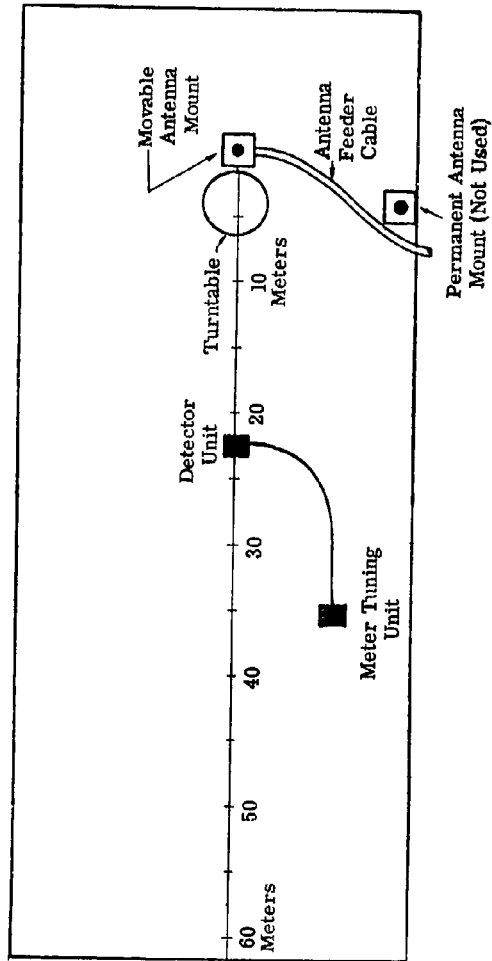


Figure 6: Typical measuring configuration for acceptance tests.

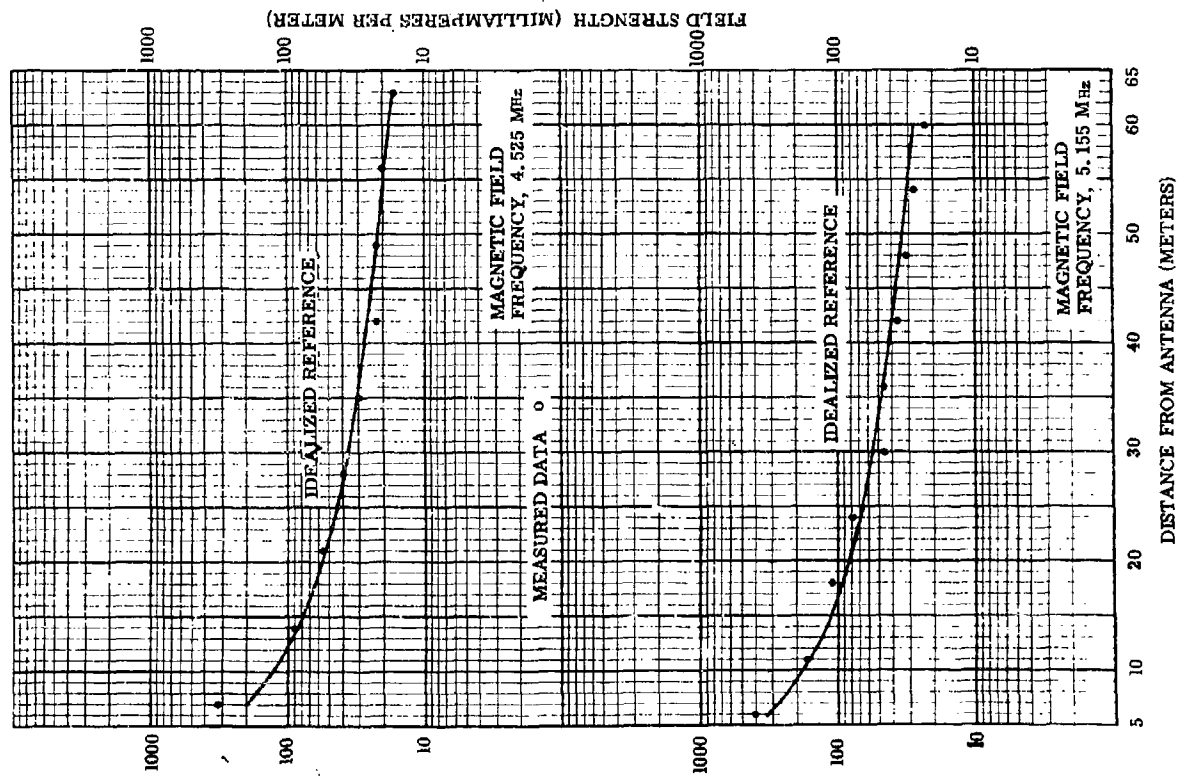


Figure 7: Measured magnetic field strength.

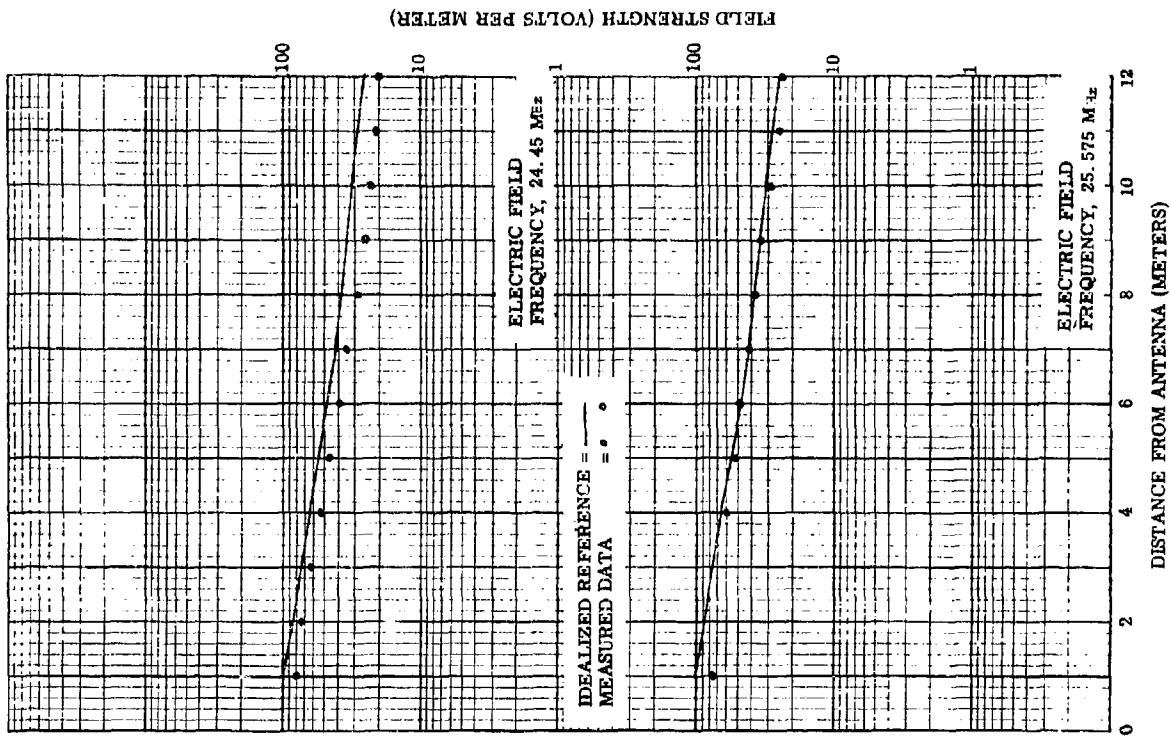


Figure 8: Measured electric field strength.

ELECTRIC FIELD STRENGTH FOR F7

FREQUENCY = 20.05 MHz

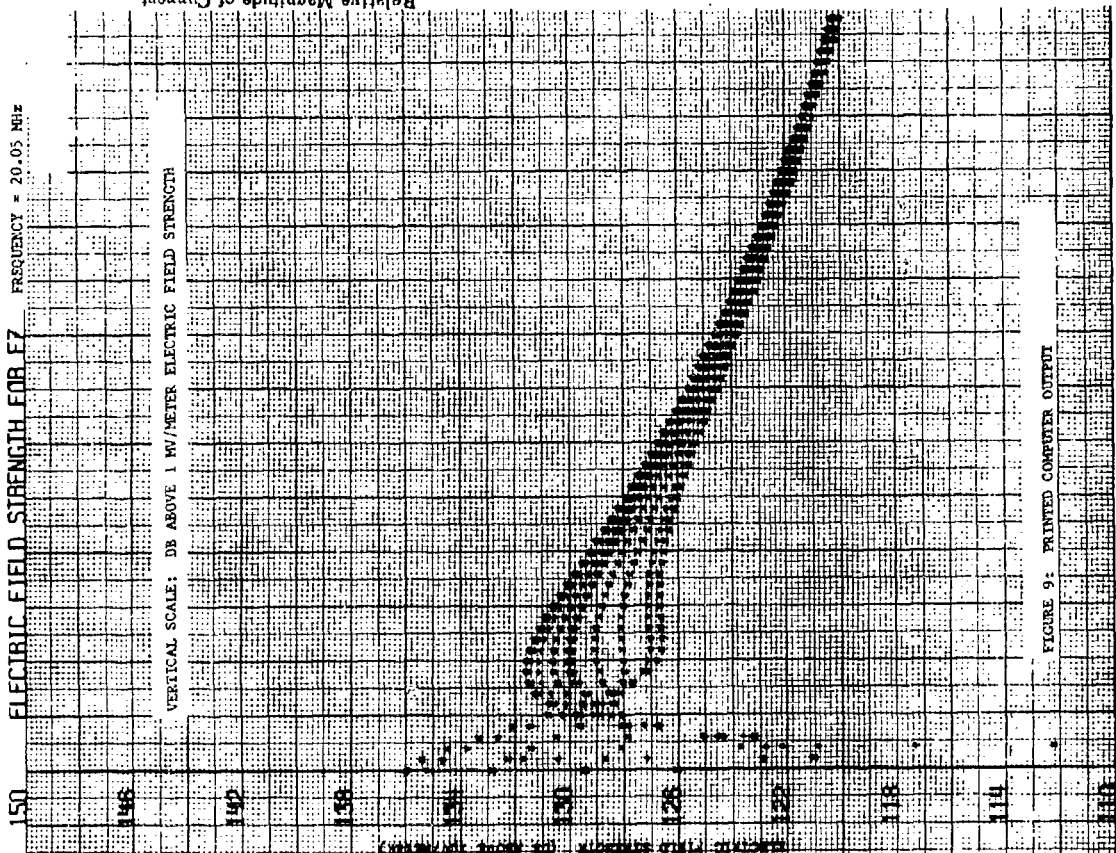


FIGURE 9: PRINTED COMPUTER OUTPUT

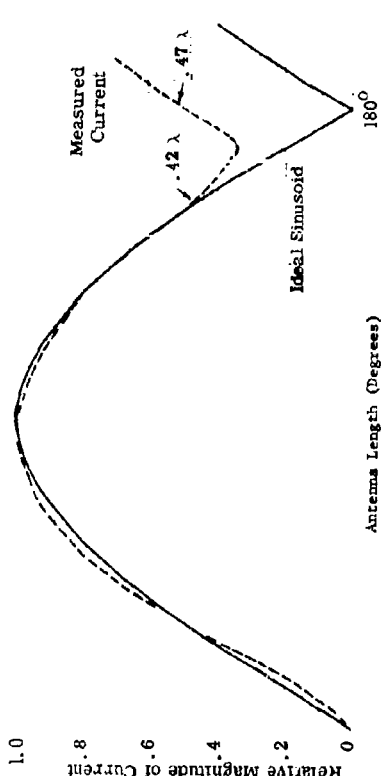


Figure 10a: Current distribution along a 190° vertical tower.

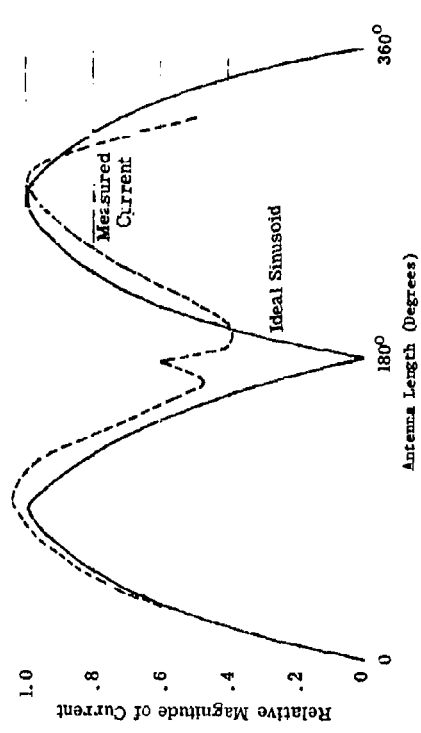


Figure 10b: Current distribution along a 322° sectionalized tower.



## DISCUSSION

Mr. Benedict (JPL): Electromagnetic Hazards to Electroexplosive Systems by G. E. Morgan of the Air Force Avionics Laboratory, W.P.A.F.B., published January, 1967 (AFAL TR 66-354) indicates only the Navy has experienced RF problems. Is NASA spending money for a problem that does not exist?

Mr. Cowdell: The Navy's problem is unique in that its air craft are aboard ships very close to RF radiators and sitting on a good ground plane. NASA encounters similar conditions when tracking space vehicles with high powered radar systems. The proximity to high levels of RF energy determines whether or not there is a problem. The systems used by the Air Force probably do not involve such energy levels.

Mr. Carter (Kentron): Were problems of susceptibility experienced with the interconnector between the two units?

Mr. Cowdell: No. The sensing unit sensed the RF naturally. The RF signal was converted to a DC level within the measuring unit and the cable transmitted DC to drive a meter so that RF pickup on the cable was of no concern.

The first attempt to check our accuracy in a high intensity field startled everyone when the meter was pegged as the transmitter was turned on. The two shields on the triaxial interconnecting cables were both inadvertently shorted to ground. Isolation of the inner shield from ground resolved the difficulty.

The design is not considered optimum. There is a significantly better design which is also considerably more expensive. The project was undertaken with the understanding that there would be two units with an inter-connecting cable. The ideal method would be to use non-conductive cable or another means of transmitting the signal representing RF field intensity or to use telemetry possibly 200 to 300 MHz above the measuring frequency and then telemeter information back to the receiving unit. The latter are expensive and we were forced to go with the cumbersome cable.

## 2-4 LIGHTNING SURGE CURRENT HAZARDS TO SEMI-CONDUCTORS & ELECTROEXPLOSIVE SYSTEMS

J. D. Robb and J. R. Stahmann

Electromagnetic Surge Laboratory and Lightning & Transients Research Institute

### 1. Introduction

A general investigation has been initiated to evaluate the theoretical mechanisms and practical aspects of surge penetration into aerospace vehicles. The theoretical studies have indicated that the principal problem of surge penetration into totally enclosed conducting shells, i. e., those with no openings, would be from high energy pulses with rise times in the range of 0.1 microseconds to 100 microseconds, corresponding to the approximate frequency range of 0.01 to 10 megahertz. For higher frequencies, there is little current penetration because of skin effect and for lower frequencies there are few current sources capable of maintaining the extremely high currents required to produce significant effects inside a conducting shell. In aerospace systems, however, the practical aspect is that most penetration is through openings in the generally excellent conducting shell, such as skin joints, antennas and windows. Typical examples of mechanisms which permit energy coupling into a vehicle interior are given.

### 2. Theoretical Evaluation of Coupling Mechanisms

Studies of possible hazards from electromagnetic surges to electro-explosive systems in aerospace vehicles are underway and the following summary of progress to date along with possible solutions is presented. The possible hazards being evaluated include:

- a. Hazards to EES's from direct natural lightning strikes.
- b. Possible hazards from HF electromagnetic field surges.
- c. Coupling through apertures of transient pulsed microwave energy.
- d. Miscellaneous practical coupling mechanisms.

Studies of these possible modes of energy coupling into the vehicle interior along with measurements of the minimum pulse current magnitudes as time duration required to fire the EES's permit an initial evaluation of the critical problem areas.

A brief theoretical study was carried out of the RF current penetration spectrum (corresponding to pulses with different rise times) for a hypothetical vehicle consisting of an imperfectly conducting cylinder with closed ends. Penetration was calculated for several thicknesses of aluminum skin. The studies showed that the electric field found inside the cylinder would be that due to the IR drop along the interior surface from the small percentage of current which penetrates to the inside surface. (Or more correctly, the voltage drop due to the interior current surface density  $J$  and the interior surface resistivity as determined from skin depth calculations.) A very small magnetic field also would be found inside because of the displacement currents associated with the time rate of change of "E" field but this current flow from displacement currents would in general be very small in any internal circuit loops compared to the direct conduction currents through the interior circuits. A multi-turn loop such as used on MAD equipment could develop significant voltage, however. The calculations of penetration are presented in Appendix I.

The principal internal transient voltage pulses would thus be the residual voltage pulse on the interior skin of the vehicle and, as shown in Figure 2 of Appendix I, this would be quite small. That such interior conduction currents are not negligible is indicated by a recent report of damage to semi-conductors in a jet transport from a nose to tail strike. The basic question which is still unresolved is the degradation of shielding by the vehicle outer skin joints of the various types.

In the evaluation of pulsed electromagnetic field effects on aerospace vehicles, reference is made to the excellent paper\* by Dr. C.W. Harrison of the Sandia Corporation in which dipole antenna theory is used to evaluate RF penetration of imperfectly conducting cylinders. The currents induced on the outer skin are evaluated by antenna theory and at a wavelength corresponding to the dimensions of the vehicle, the lowest impedance to the incident wave would be that of a dipole. Thus the currents coupled to the outer skin through the dipole impedance from the intense thunderstorm fields would be well below those conducted through the vehicle by the extreme driving voltages of natural lightning.

Little information is available of the microwave radiation of natural lightning discharges but this is proposed under future LTRI triggered lightning studies. But it is known that the higher frequencies of the steep front do pass through apertures relatively unattenuated (e.g., aperture antennas) and, that although the total burst pulse energy for a steep wave-front is small, the amplitude can be high and the sensitivity of modern semiconductor devices such as FET's is correspondingly very high.

In reviewing these possible surge penetration mechanisms and in reviewing in-flight damage reports to electrical circuits from surge penetration, the principal problems seem to lie not in direct penetration of the excellent outer skin shielding; however, as outlined in the previous theoretical discussions, but rather in the discontinuities or openings in the skin and the points at which stroke voltages can enter the electrical circuitry to EES's.

These points include the following, as illustrated in the attached figures:

- a. Ground return coupling across bonding or discontinuities  
Bonds of pitot booms, fuel or weapon pods, etc., can build up sufficient reactive potentials with lightning strike currents to couple large voltages into EES circuitry. Peripheral bonding across the boundary to lower the reactance is preferable and in the case of fuel tank access doors, necessary. Coupling across vehicle skin joints remains to be evaluated.
- b. Direct stroke penetration  
Navigation lights permit direct stroke entry into the aircraft circuitry. In a recent strike report, a stroke to an aircraft wingtip light

\*C.W. Harrison, Jr., and R.W.P. King, "Response of a Loaded Electric Dipole in an Imperfectly Conducting Cylinder of Finite Length," Sandia Corporation reprint SCR-148, June 1960.

resulted in a severe explosion of about 6 feet of wingtip. Whether this was due to gas pressures from vaporized wiring or ignition of fuel vapor was not determined as the damaged wing was no longer available for inspection where LTRI personnel could examine it.

c. Induced streamering off components or personnel

Streamering inside plastic enclosures without puncture is quite common as evidenced by frequent fighter pilot reports of electrical shock.

d. Penetration through antennas

Damage to VHF-UHF antennas is nearly as common as damage to HF antennas used to be before the use of lightning arresters. As protection can be easily provided there is no excuse for continued use of older lightning vulnerable VHF-UHF antennas.

e. Inductive coupling of lightning stroke currents into aircraft wiring

A common example is damage to multiple turn coils in MAD equipment from nearby lightning currents. The same coupling can occur to control servo motors, etc., from nearby lightning bonding wires.

The attached figures illustrate the various points. Some examples of many of these problems are also given in a recent report on lightning hazards and protection studies of the F-104 aircraft.\*

Bonding problems are becoming increasingly severe both because of the increased vulnerability of semi-conductors and the more serious concern with fuel systems and this will require a revision of the present bonding specifications which are out of date (for example, Mil 5087). The problem which remains is to develop a specification which can anticipate these new design techniques and this does not appear to be easy. For pylons on fighter aircraft specifications could probably be written but the next question is how could the surge impedance be measured. With conventional laboratory measuring equipment this would be very difficult because of the extremely low impedance. The low cost LTRI artificial lightning generators designed for use by aircraft manufacturers could be used but they require trained personnel for their operation. This training could possibly be handled by LTRI laboratories.

A new bonding specification might require a maximum permissible resistance and reactance between any two possible lightning strike points on the aircraft including external pods or control surfaces. In addition, any wiring entering the aircraft from the outside, e.g., antennas or wing lights, would have to be checked for possible surge coupling. It is again emphasized that it would be a difficult program to implement by specifications and measurement but we strongly feel that some new very serious

\*L&T Report No. 447, "Lightning Hazards and Protection for Lockheed F-104 Aircraft," sponsored by U.S. Air Force and Royal Canadian Air Force, February 1966.

problems are presently being introduced in new aircraft designs and much more sensitive electronic components and that something should be done as soon as possible to prevent costly further retrofit programs on these aircraft. One answer would be to require full scale artificial discharge testing of each new aircraft design as has been done by LTRI on many aircraft such as in the special programs on F-100 and F-104 aircraft. An example is shown in Figure 1 of artificial lightning tests of installed protection on the canopy of a RCAF F-104 aircraft. In line with defense department requirements for greater reliability, we believe that tests of lightning protection (and precipitation-static) for new aircraft will eventually be recognized as necessary on each new aircraft both from the point of view of safety and economics as measured against the cost of retrofit programs or losing even one aircraft. Most of the discussions in this paper have been concerned primarily with aircraft but it should be pointed out that the concepts apply almost equally well to space vehicles exposed to lightning currents or fields.

### 3.0 Concluding Discussion

A general investigation of the mechanisms and the theoretical and practical aspects of surge penetration into aerospace vehicles has shown the following:

a. That the pulse voltages penetrating the continuous outer metal skin of an idealized vehicle would be relatively small for even direct lightning discharges, being equal to the product of the inner surface current density and the metal resistivity, and are smaller yet for impinging electromagnetic waves to which the vehicle presents a relatively high impedance compared with the low impedance for direct conducted lightning strike currents.

b. That the practical aspect of surge penetration is that most penetration is through openings in the vehicle skin such as antennas, navigation lights, plastic sections, windows and possible skin joints.

c. That vehicle skin joints previously evaluated for possible spark-  
ing from lightning discharge currents should again be checked for pulse  
penetration.

Thus the most important aspect of aerospace vehicle protection from surge penetration is surge entry through openings or joints rather than penetration of the generally excellent shielding of the skin. Of recent concern are wet or insulated joints in the outer skin for which little data is available and through which damaging energies could be coupled into the vehicle interior in view of the greater sensitivity of the newer semi-conductor devices and associated EED's.

#### Acknowledgement

This paper is based on studies for the USAF, Avionics Laboratory, Wright Patterson AF Base, Ohio under Contract F 33615-67-C-1475, and studies for the RCAF under whose sponsorship several full-size aircraft have been tested.

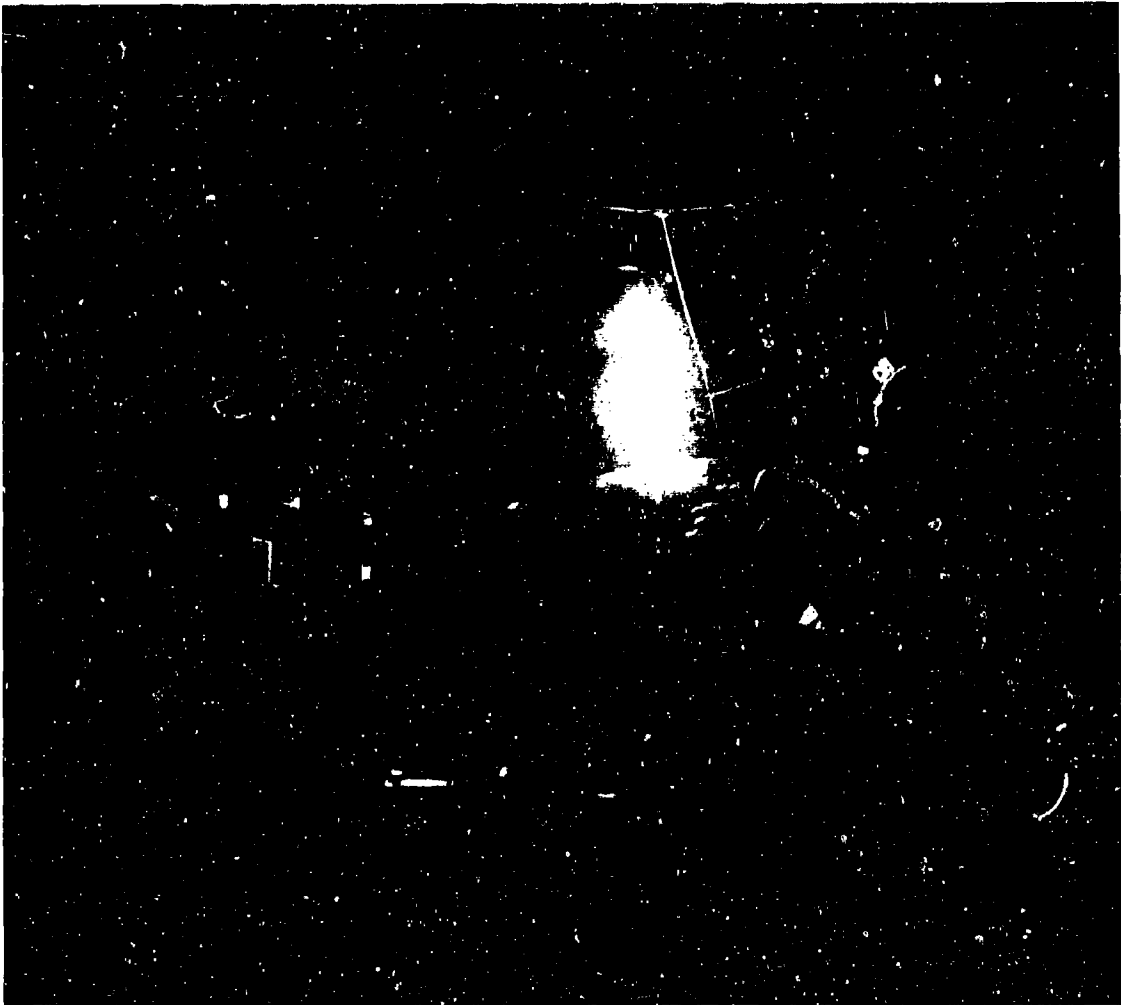
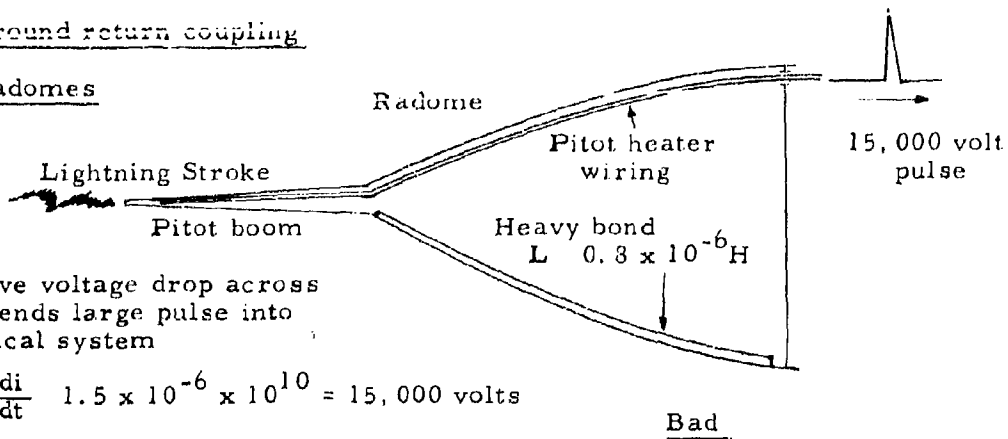


Figure 1. Demonstration of lightning protection for fighter aircraft canopy. Five million volt discharge strikes canopy over protection strip above occupant's head. LTRI Research Vessel "Thunderbolt" on which high voltage generators are located may be seen in background.

Examples of Possible Surge Penetration Mechanism Hazards to EES's

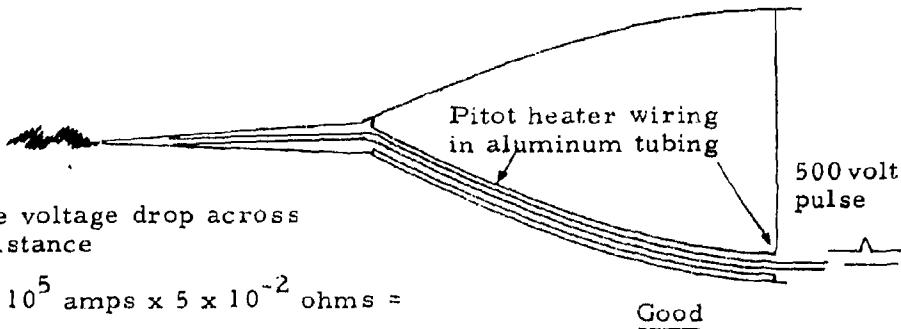
1.0 Ground return coupling

1.1 Radomes



Reactive voltage drop across bond sends large pulse into electrical system

$$V = L \frac{di}{dt} = 1.5 \times 10^{-6} \times 10^{10} = 15,000 \text{ volts}$$



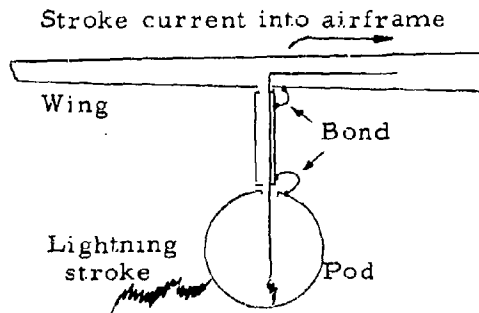
Resistive voltage drop across tube resistance

$$V = IR = 10^5 \text{ amps} \times 5 \times 10^{-2} \text{ ohms} = 500 \text{ volts}$$

1.2 Pylon to wing bonding

Ground return coupled voltage into pod or pylon wiring - of the order of -

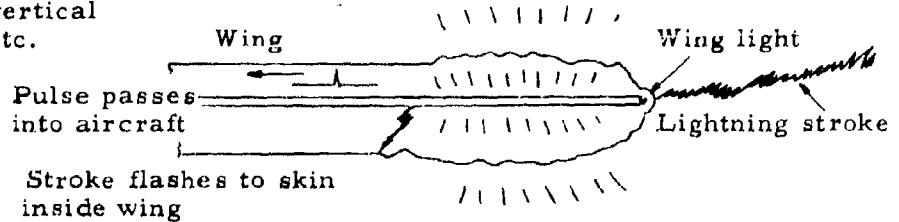
$$V = L \frac{di}{dt} = 0.1 \times 10^{-6} \times 10^{10} = 100 \text{ to } 1000 \text{ volts}$$



## 2.0 Direct Coupling

### 2.1 Navigation light wiring

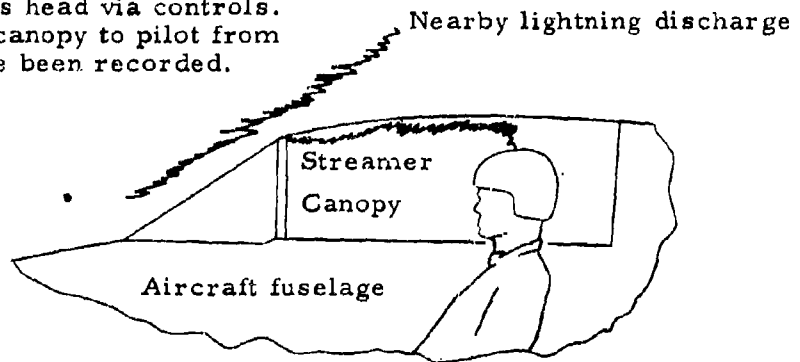
Direct structural hazard to wingtips, vertical stabilizers, etc.



### 3.0 Induced streamering inside plastic housing

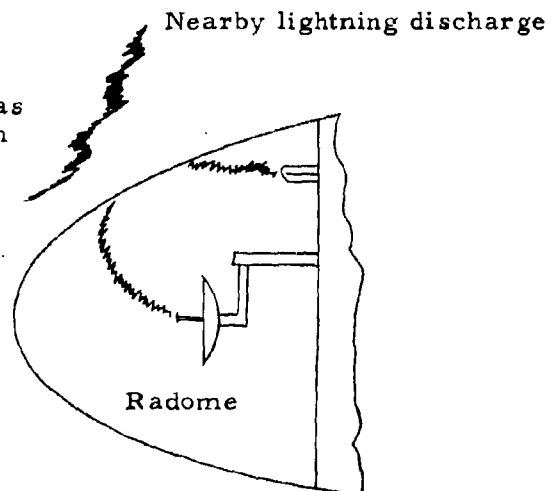
#### 3.1 Canopy enclosures

Nearby lightning discharge induces streamer off pilot's head via controls.  
Note: Puncture<sup>s</sup> of canopy to pilot from direct strokes have been recorded.



#### 3.2 Radomes

Nearby lightning discharge induces streamers off antennas and wiring inside radome with or without puncture.



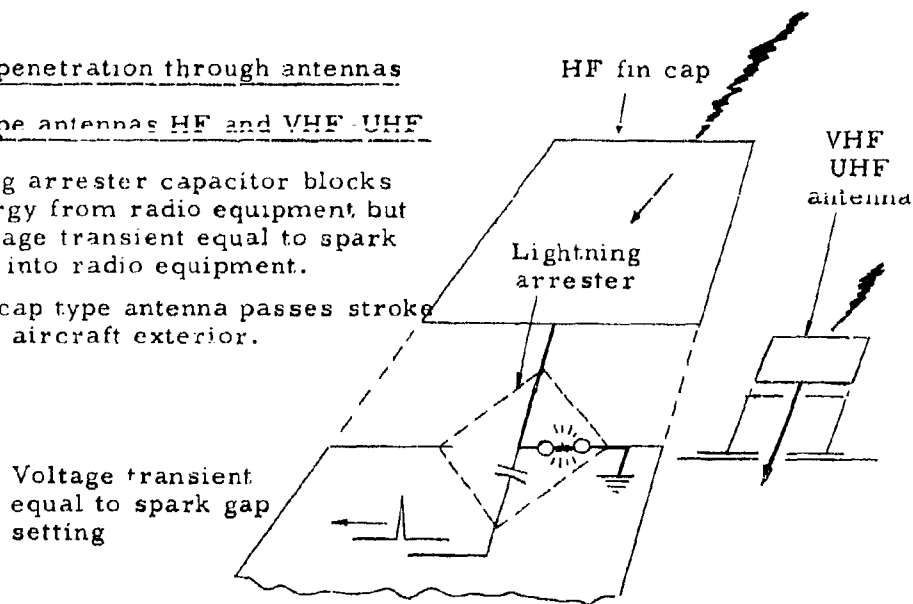


4.0 Surge penetration through antennas

4.1 Cap type antennas HF and VHF-UHF

HF lightning arrester capacitor blocks stroke energy from radio equipment but passes voltage transient equal to spark gap setting.

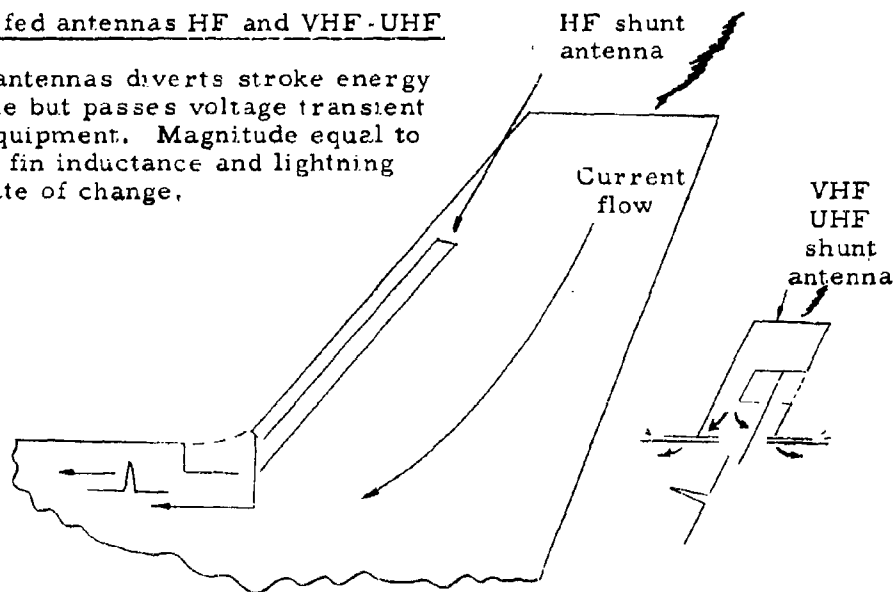
VHF-UHF cap type antenna passes stroke energy into aircraft exterior.



4.2 Shunt fed antennas HF and VHF-UHF

Shunt fed antennas diverts stroke energy to airframe but passes voltage transient to radio equipment. Magnitude equal to product of fin inductance and lightning current rate of change.

$$V = L \frac{di}{dt}$$

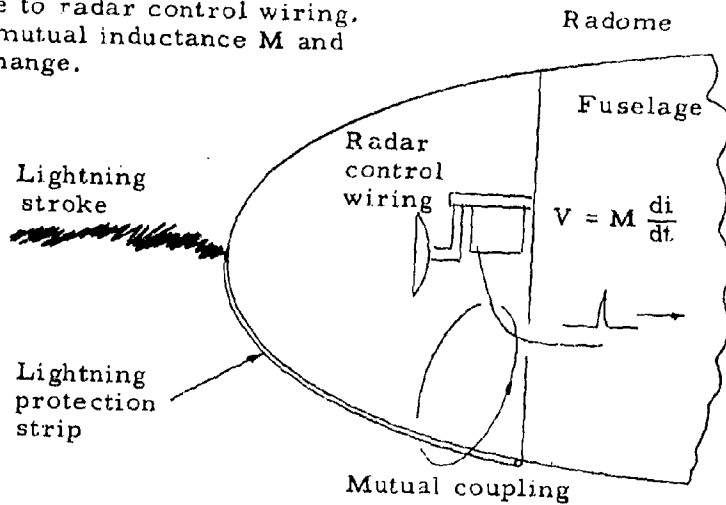


## 5.0 Mutual inductance surge coupling

### 5.1 Radomes

Stroke to radome protection strip couples high voltage pulse to radar control wiring. Voltage equal to mutual inductance  $M$  and current rate of change.

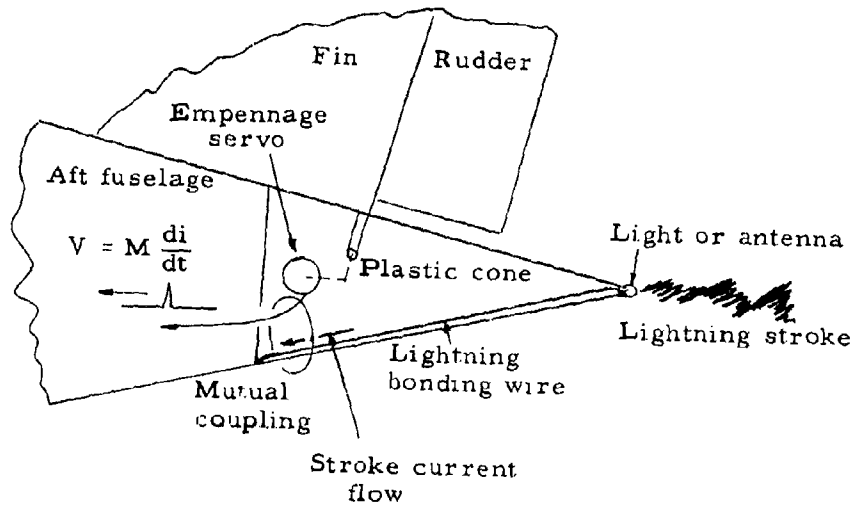
$$V = M \frac{di}{dt}$$



### 5.2 Empennage bonding

Flux coupling to servo motor control wiring product of mutual inductance and current rate of change.

$$V = M \frac{di}{dt}$$



APPENDIX I

Field Penetration Across a Cylindrical Wall

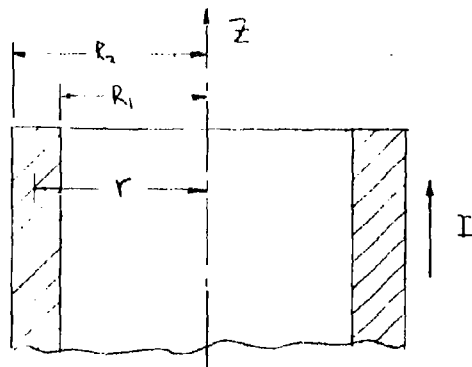


Figure 1.

In Figure 1, consider a current  $I$  (peak value) with frequency  $f$  is flowing in the wall of a cylindrical tube in the axial direction or  $z$  direction. Let

- $R_1$  = Inner radius of the tube
- $R_2$  = Outer radius of the tube
- $\sigma$  = Conductivity of the tube material
- $\delta$  = Skin depth of the tube material
- =  $1/\sqrt{\pi f \mu \sigma}$

In the case that  $R_2, R_1 \gg R_2 - R_1$  (the thickness of the wall is small compared to the radius of the tube). The wall can be treated approximately as a flat surface, the current density across the wall is then given by

$$i_z(r) = i_0 e^{-(1+j)\frac{R_2-r}{\delta}} \quad (1)$$

where  $r$  is the radius distance from the axis.

The constant  $i_0$  can be found by integrating  $i_z(r)$  over the cross section of the tube and equating the result to the total current  $I$ , that is:

$$\int_{R_1}^{R_2} 2\pi r i_0 e^{-(1+j)\frac{R_2-r}{\delta}} dr = I \quad (2)$$

In the case that  $R_2 - R_1 \ll R_1, R_2$  we have

$$\bar{I}_0 = \frac{I(1+j)}{2\pi\delta R(1 + e^{-(1+j)b/\delta})} \quad (3)$$

where  $R$  = mean radius of the tube

$$= (R_1 + R_2) / 2$$

$b$  = thickness of the wall

$$= R_2 - R_1$$

The magnitude of the electrical field at the inside surface of the wall is then:

$$\begin{aligned} E_{in} &= \left| \frac{\bar{I}_z(R_1)}{\sigma} \right| \\ &= \left| \frac{I(1+j)}{2\pi R \sigma \delta} \cdot \frac{e^{-(1+j)b/\delta}}{1 - e^{-(1+j)b/\delta}} \right| \\ &= \frac{I}{2\pi R \sigma \delta} \cdot \frac{\sqrt{2}}{\left\{ e^{2b/\delta} - 2e^{b/\delta} \cos \frac{b}{\delta} + 1 \right\}^{1/2}} \end{aligned}$$

(4)

Figure 2 shows the value of  $E_i$  as a function of frequency  $f$  (note that the skin depth  $\delta$  in Equation (4) is a function of  $f$ ) for copper and aluminum in the case that

$$I = 100,000 \text{ amps}$$

$$R = 3.5 \text{ ft}$$

$$b = 0.03; 0.06; 0.09 \text{ inches}$$

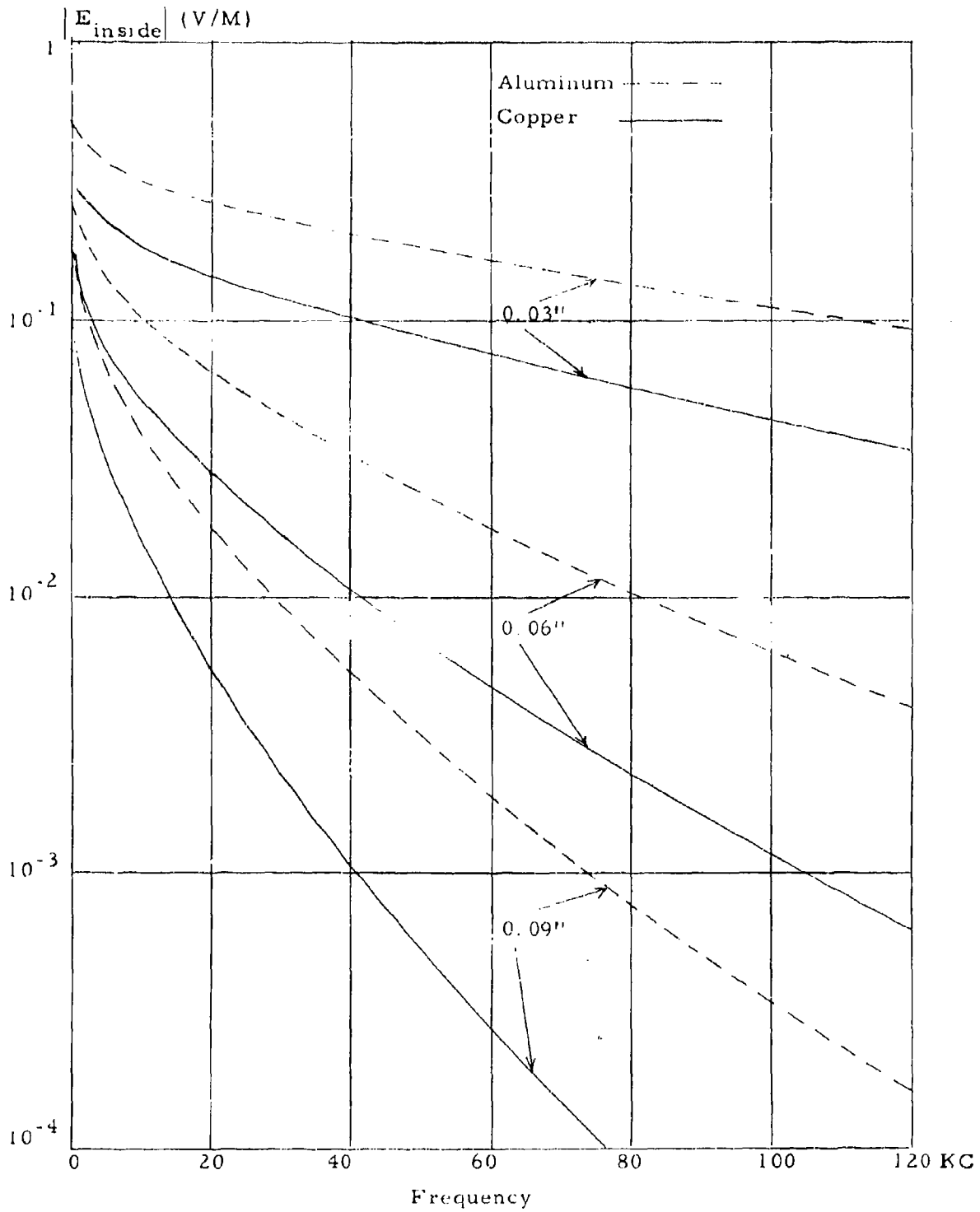


Figure 2. Electric field inside a cylinder carrying 100,000 ampere impulse.

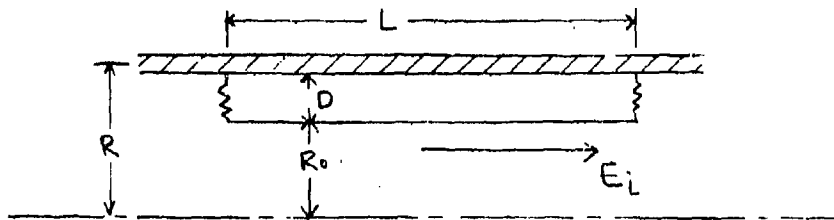


Figure 3.

In Figure 3, consider a conductor with length  $L$  is mounted in the inside of the tube and is parallel to the axis at a distance  $D$  from the wall. We will now find the induced emf due to the change of magnetic field inside the tube.

Assume that the electric field  $E_i$  is uniformly distributed inside the tube. The magnetic field at distance  $r$  from the axis is:

$$\begin{aligned}
 H(r) &= \frac{1}{2\pi r} \int_0^r j\omega E_i \epsilon \cdot 2\pi r dr \\
 &= \frac{j\omega \epsilon E_i}{2} r.
 \end{aligned} \tag{5}$$

The total flux linkage is then:

$$\begin{aligned}
 \Psi &= \int_{R_0}^{R_0+D} \mu H L dr \\
 &= j\omega \mu \epsilon L E_i \left\{ \frac{R_0 D}{2} + \frac{D^2}{4} \right\}
 \end{aligned} \tag{6}$$

The induced emf is then:

$$\begin{aligned} V_{\text{ind.}} &= -j\omega\psi \\ &= \omega^2 \mu \epsilon L E_i \left\{ \frac{R_o D}{2} + \frac{D^2}{4} \right\} \end{aligned} \quad (7)$$

In the case that

$$\begin{aligned} R_o &= 36'' (\cong 1 \text{ meter}) \\ D &= 6'' (\cong 0.15 \text{ meter}) \\ L &= 36'' (\cong 1 \text{ meter}) \end{aligned}$$

we have

$$V_{\text{ind.}} = 3.5 \times 10^{-17} f^2 E_i \quad \text{Volts} \quad (8)$$

A plot of  $V_{\text{ind}}$  as a function of  $f$  is shown in Figure 4.

The current in the conductor is given by:

$$I_c = \frac{E_i L + V_{\text{ind.}}}{Z_c} \quad (9)$$

where  $Z_c$  is the impedance of the conductor and its connections.

A numerical calculation shows that  $E_i L$  is of the order of  $10^{-2}$  volts whereas  $V_{\text{ind}}$  is of the order of  $10^{-6}$  volts. The induced voltage  $V_{\text{ind}}$  in Equation (9) can be neglected and the current is given by

$$I_c = \frac{E_i L}{Z_c} \quad (10)$$

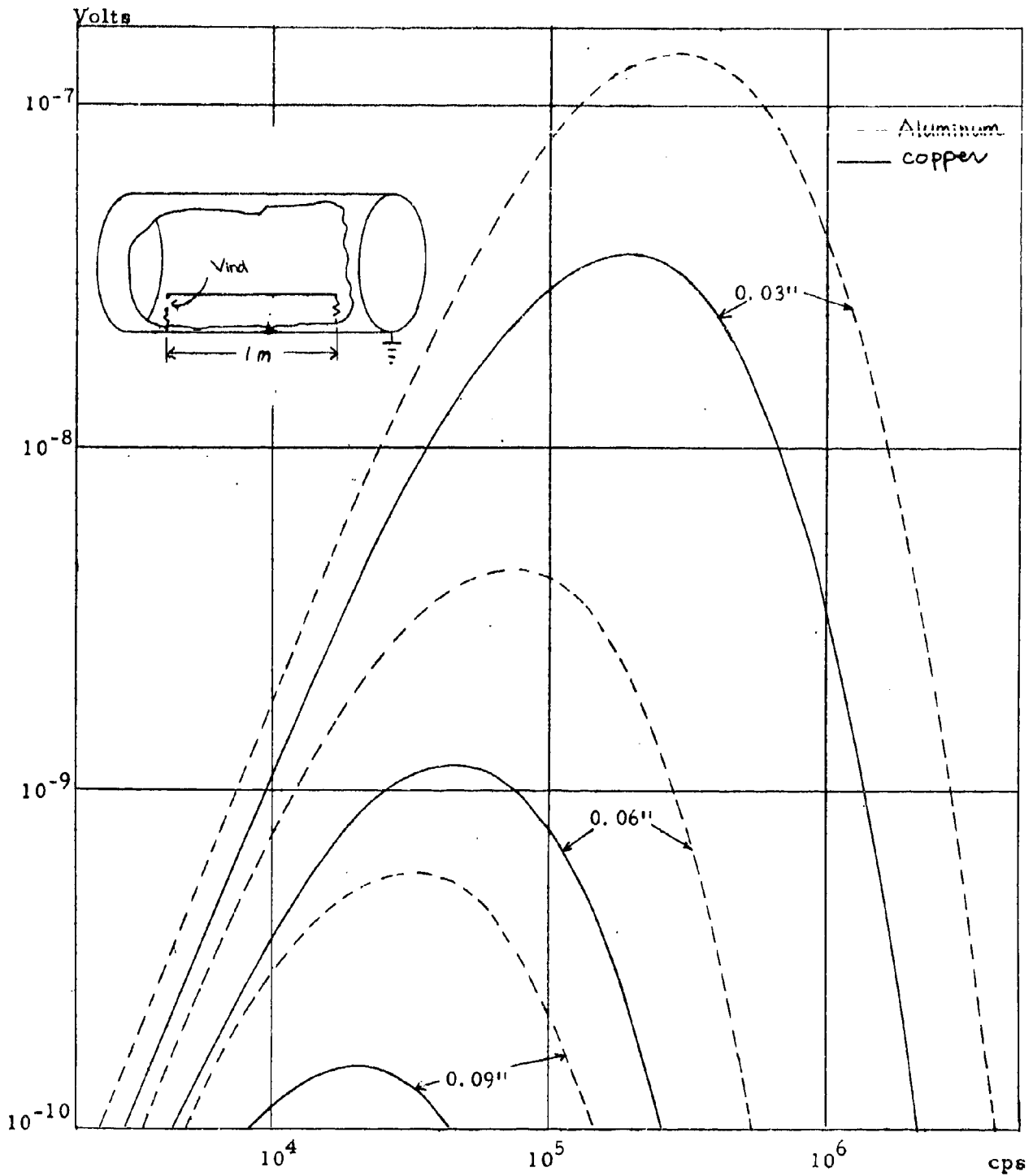


Figure 4. Induced voltage on an axial wire inside a cylinder carrying 100,000 ampere impulse.



## DISCUSSION

In response to a question by M. Tucker of Sandia Corporation, Mr. Stahmann gave the following explanations. During work of a year ago, current profiles recorded on triggered lightning strokes were, as expected, on the order of 1 1/2 microsecond rise time and 50 microseconds to half value. The past summer, strokes had a slow rate of rise, in milliseconds, lasting in the order of tens of milliseconds and components of this nature were repeated as much as 12 times.

Mr. McGirr of Atlas Chemical Industries asked several questions about lightning protection for buildings housing explosives processing operations.

Mr. Stahmann's replies are summarized as follows. There does not appear to be an easy way to eliminate the inductive kick on 440 or 220 lines from a nearby lightning strike. Work by the power companies has been concerned mainly with the breakers kicking out and loss of power but not with pulses that might affect measurements on or storage of EED's. The simple gaps used as lightning arrestors on telephone lines do not work but improvements have been made in the last 2 or 3 years in missile systems and communication lines.

## 2-5 ENERGY TRANSFER IN ELECTROSTATIC ARCS \*

C. F. SCHROEDER, JR.  
SANDIA LABORATORY, ALBUQUERQUE

### INTRODUCTION

Our effort at Sandia Laboratory to gain a better understanding of arc energy phenomena was part of a program whose aims were to develop reliable test instruments and devise meaningful tests for electrostatic sensitivity evaluation of electroexplosive devices. To this end, some basic study of dynamic arc phenomena was mandatory if we expected to be able to use our test data in determining pertinent component characteristics.

I should like to preface my discussion of electrostatic arc energy transfer with a brief summary of pertinent points of test equipment design, and, as an epilogue, to discuss some interesting results of electrostatic sensitivity testing of components.

### TEST EQUIPMENT

Preliminary tests were made to determine the equipment required to produce consistent discharge pulses and to devise a means of interpreting the pulses in terms of their stimulus to explosive materials.

The primary result of the preliminary tests was the definition of the problems to be overcome if the objectives of pulse consistency and effective interpretation were to be met. These problems may be most simply stated as: Stray inductance, stray capacitance, and switching limitations.

Stray inductance, of course, produces ringing and, in general, may be avoided by use of noninductive resistors and reduction of lead lengths

\* This work was supported by the U.S. Atomic Energy Commission.

wherever possible. To this end, a suitable length of RG 213 cable, rather than a storage capacitor, was used in the circuit.

Stray capacitance is significant only in that portion of the circuit which is not charged prior to switching; if, therefore, not held to a minimum value, it can materially reduce the impressed voltage and available energy of the impulse.

The switching problems interact with the capacitance problems in that impulses insufficient in voltage level to insure prompt electrostatic breakdown will charge the stray capacitance and reduce the potential difference across the switch contacts, even to the point of extinction of the switching arc. Eventual discharge of the stray capacitance re-establishes the switching potential and (depending on the switching method utilized) may permit further discharge of the storage capacitance; but the result is multiple discharges - often so spaced in time that they may not be observed by an impulse monitoring device.

While the construction of any real circuit cannot result in zero stray capacitance, and currently available switching devices can all be operated under circumstances which permit multiple striking, the effects may be minimized.

Our construction, which had to provide for operator safety and convenience, as well as a fixed series resistance, included a stray capacitance of about 5 percent of the storage capacitance.

The switch we used is described as a high-voltage spark gap by T. J. Tucker,<sup>1</sup> and consists of an adjustable-length spark gap utilizing a gas dielectric at pressures up to 1000 psi. With nitrogen at 1000 psi as the dielectric, the switch will hold off about 1 kilovolt per thousandth of an inch of gap up to about 30 kilovolts, and permit a clean discharge when the pressure is released.

The test equipment parameters used in electrostatic sensitivity testing are:

Voltage range - 0-50 kilovolts

Storage capacitance - 600 picofarads

Series resistance - 500 ohms

These values agree with those generally in use at Sandia Laboratory for safety testing and have been generally substantiated as representative of body accumulation and discharge parameters by Tucker's work.<sup>2</sup>

#### ENERGY TRANSFER

The same parameters were used as design center values for our studies of dynamic arc characteristics, except that the voltage range was limited to 20 kilovolts.

In the energy studies, repetitive arcs rather than impulses were studied to avoid switching problems, thereby permitting the use of a sampling oscilloscope.

As shown in Figure 1, the circuit capacitance of 600 picofarads consisted of a cable charged slowly to the gap breakdown potential, which was held to very consistent values by irradiation with a beta source; the current was monitored by a low-inductance, fast-rise, current-viewing resistor; and the voltage,  $\phi$ , was monitored by a damped capacitance divider.

Three values of series resistance,  $R$ , were used: nominally 200, 500, and 1000 ohms. The point-to-sphere gap was set to 5 nominal values between 0.050 inch and 0.150 inch. Gases were used as gap materials because of their ability to recover rapidly between successive discharges. Nitrogen, argon, and air were studied. The combination of these parameters required 45 tests in all.

Because the gap length determined the voltage breakdown level, the output voltage level of the power supply determined the spark repetition rate. This rate was adjusted within the range of 20 to 100 arcs per second to permit tracing the oscilloscope outputs on an X-Y plotter at a writing speed of 0.2 to 1 inch per second. The arc phenomena were thus traced at an effective rate of 5 nanoseconds per inch.

Each test was plotted three times consecutively. The plots were then retraced to average small variations in values and to establish initiation points and reference levels of voltage and current. From the tracings, digital values of current and voltage were read at each half-nanosecond time interval from zero to 36 nanoseconds (twice the cable delay time).

The reduction of these data was done by a computer which performed the required operations sequentially on all 45 tests. Consequently, all the calculated values of various pertinent test results were available for evaluation of trends, average behavior, and credibility. As criteria for evaluation, three basic hypotheses were considered:

1. The ability of an explosive device to withstand or be actuated by a given electrostatic discharge would most likely be determined by the rate of energy input to the explosive material and the total energy dissipation in the gap region.<sup>5</sup>
2. Inasmuch as electronic and ionic carriers are required for discharge of the capacitance through the gap, the total gap energy dissipation will be related strongly to the maximum current.
3. The principal gap energy dissipation will occur during the arc current development period,<sup>2</sup> during which time the gap voltage will decay to a virtual zero value.<sup>4</sup>

These hypotheses, and tentative empirical values, aided in the derivation of a computer program which included justifiable correction procedures as well as comprehensive analytical procedures.

The pertinent calculations performed by the computer were:

1. Determination of gap voltage values - as opposed to the plotted values, which were influenced by the passive components in the voltage probe.
2. Determination of the time interval over which significant energy was dissipated in the gap.
3. Summation (in lieu of integration) of the voltage-current-time products to obtain gap energy dissipation.
4. Determination of peak current, breakdown voltage, and total stored energy.
5. Determination of the incremental values of gap resistance.

Correlation of the calculated results was obtained in two areas. First, a comparison of gap energy dissipation to stored energy showed that, at a given circuit resistance, the ratio was well defined, normally distributed, and typified by a standard deviation commensurate with the accuracy aims of the test program. Second, a test of the second hypothesis (relating gap energy to the maximum gap current) produced three distinct, approximately parabolic curves, each associated with a given circuit resistance, as shown in Figure 2.

These modes of data correlation proved mutually corroborative with respect to the relationship between the gap energy and the peak current. However, attempts to define the dependence of the gap energy upon the circuit parameters through curve fitting procedures produced equations involving inexplicable exponents for the circuit parameters.

In order to determine an accountable relationship between gap energy and circuit parameters, a theoretical model was developed defining a cable discharge in which the initial current step was perturbed by the presence of a rapidly descending series resistance.

The model provided an integral equation, explicit in gap energy dissipation, which required postulation of a gap resistance-time relationship for exact solution. However, it was possible to extract dimensioned parameters so that the integrals involved only time-dependent numerical ratios. An examination of the limits of the ratios and the relative values of their integrals justified the use of constants in place of the integrals for a first approximation. Including the time factor in the constants, the first approximation for gap energy was shown to be of the form:

$$E = A^2(k_1 R_s + k_2 Z_0)$$

where

E = Gap energy dissipation

A = Peak current

$R_s$  = Circuit series resistance

$Z_0$  = Characteristic cable impedance

$k_1, k_2$  = Constants (including time)

It is interesting to note that the examination of integral limits and relationships showed that  $k_2$  must be negative; this condition was met by the empirical results. The constants were determined by a weighted regression analysis, and the measured values from the computer program were compared with the values calculated from the empirical equation. It was shown that, within the experimental limits, the gap energy could be predicted with an expected error of about  $\pm 13\%$ .

The calculated values of gap resistance were plotted versus time and compared to various simple functions which might be tested in the theoretical model. A suitable function was found and tested by integrating the model expression; this yielded a new time parameter which showed

close association with the gases under test. When the empirical equation, which included the time parameter, was subjected to weighted regression analysis, no significant reduction resulted in the standard deviation of the measured versus calculated energies.

The conclusions of the experiment are that the gap energy is predictable from the circuit parameters and the peak current and that gap energy dissipation is independent of the arc length and material in the gap.

A pessimistic view of these conclusions would be that the results (and the equation) are valid only over the experimental voltage range of 1500 to 7000 volts. On the optimistic side, extrapolation upon the limited range is not precluded, since the data showed better correlation at the upper end of the range than at the lower end.

#### COMPONENT TESTING

When the test instrument described earlier was utilized in tests of one type of EED, the results of the arc studies were applied as an interpretive aid, leading to some interesting conclusions.

The component involved was a dual bridge-wire detonator designed for a 30,000-erg square wave input per bridge wire. The explosive content was about 30 milligrams of lead azide-lead scyphnate mixture, 100 milligrams of lead azide, plus a secondary booster charge. Electrically, the device afforded a very short gap between the bridge wire and a grounded internal element. An external ring provided shorting of the bridge-wire leads to the case except when the mating connector was in place.

Several tests were performed to evaluate the effectiveness of the grounding ring as well as the consequences of grounding-ring malfunctions. One interesting result occurred where three bridge-wire pins were grounded and the fourth pin received the high-voltage impulse. This



configuration required the pulse to pass through the bridge wire. When the technique of Langlie<sup>5</sup> was applied to determine a voltage threshold of component initiation, a no-fire condition was noted on all tests up to 21.5 kilovolts, and an all-fire condition prevailed at 22.1 kilovolts and above. The calculated bridge-wire energy dissipation was about 12,000 ergs in this voltage range.

For comparison, application of the empirical energy transfer equation showed that an arc initiation at the same energy would require a 10.8-kilovolt impulse.

In other tests of the same component, requiring disabling of the grounding ring and preclusion of external arcs by means of dielectric fluid insulation, an all-fire level was reached at 12.8 kilovolts, with a no-fire level at 11.7 kilovolts or lower to a point which will be discussed later.

The calculated gap energies in the threshold range were 14,000 to 17,000 ergs, comparing rather well with the 12,000-erg bridge-wire threshold. The difference may be attributed to the high velocity of the scattered ions and electrons formed in the arc initiation, compared to the rate of energy loss through thermal conductivity in the bridge-wire detonations.

The fact that the experiment as performed on the component discussed previously revealed a no-fire level below 12 kilovolts is of vital concern in the safety aspects of EED's, at least where similar primary explosives are employed. Again applying the technique of Langlie, the aforementioned threshold range of 11.7 to 12.8 kilovolts seemed established when one test at 6.4 kilovolts (required by the sequence) yielded a detonation where a no-fire was deemed almost a certainty. Continuation of the test sequence resulted in the irrevocable conclusion that the component was capable of being detonated by any pulse as low as 2.5 kilovolts which could bridge the short internal gap. All of these lower level firings were associated with current pulses showing evidence of multiple arc striking.

Without offering a cause for the lower level firings, let me state that the following truths have been established:

1. The voltage did not deviate significantly from the measured values.
2. The capacitance did not deviate significantly from the measured values.
3. The components did detonate.

Since the test equipment described herein was completed only recently, our work has not included testing of EED's with primary explosive materials other than the lead azide-lead styphnate mixture; but the results of our component testing do indicate that a device which does not fire at high or intermediate voltage levels could be hazardous at comparatively low levels. This fact must be kept in mind when establishing standards for electrostatic sensitivity testing.

#### REFERENCES

1. Tucker, T. J., "Square-Wave Generator for the Study of Exploding Wires," Rev. Sci. Instr., 31, 1960, p. 165.
2. Tucker, T. J., "Spark Initiation Requirements of a Secondary Explosive," to be published in the Proceedings of the New York Academy of Sciences, April 1967.
3. Finney, D. J., Probit Analysis, Cambridge University Press, London, 1952.
4. Lewellyn-Jones, Ionization and Breakdown in Gases, John Wiley and Sons, Inc., New York, 1957.
5. Langlie, H. J., A Reliability Test Method for 'One-Shot' Items, Publication No. V-1792 (U), Aeronutronic Division, Ford Motor Co., August 10, 1962.

#### DISCUSSION

Mr. Petrick of NWL asked Mr. Schroeder about jitter in the switching mechanism. In order to reduce the jitter in the switching mechanism, tests are being considered using argon and argon with one percent oxygen to see if a sharper breakdown can be obtained with a reasonable dielectric strength.

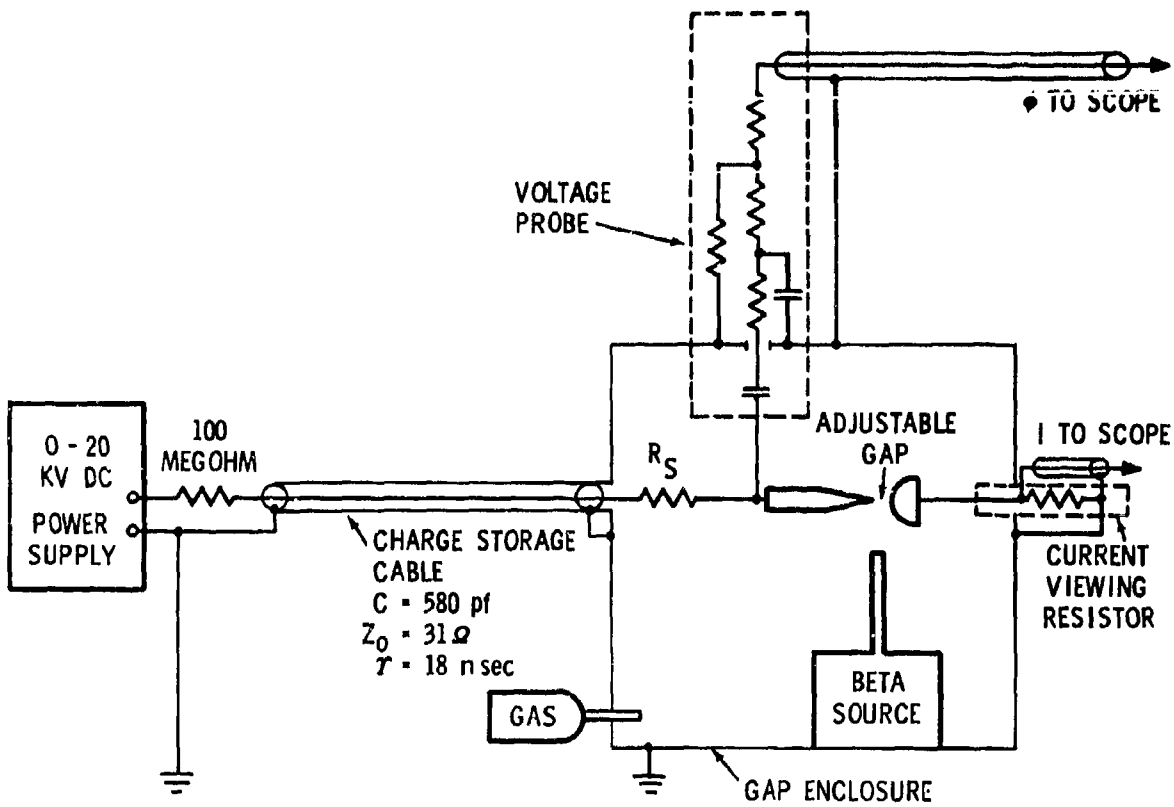


FIGURE 1 EXPERIMENTAL CIRCUIT

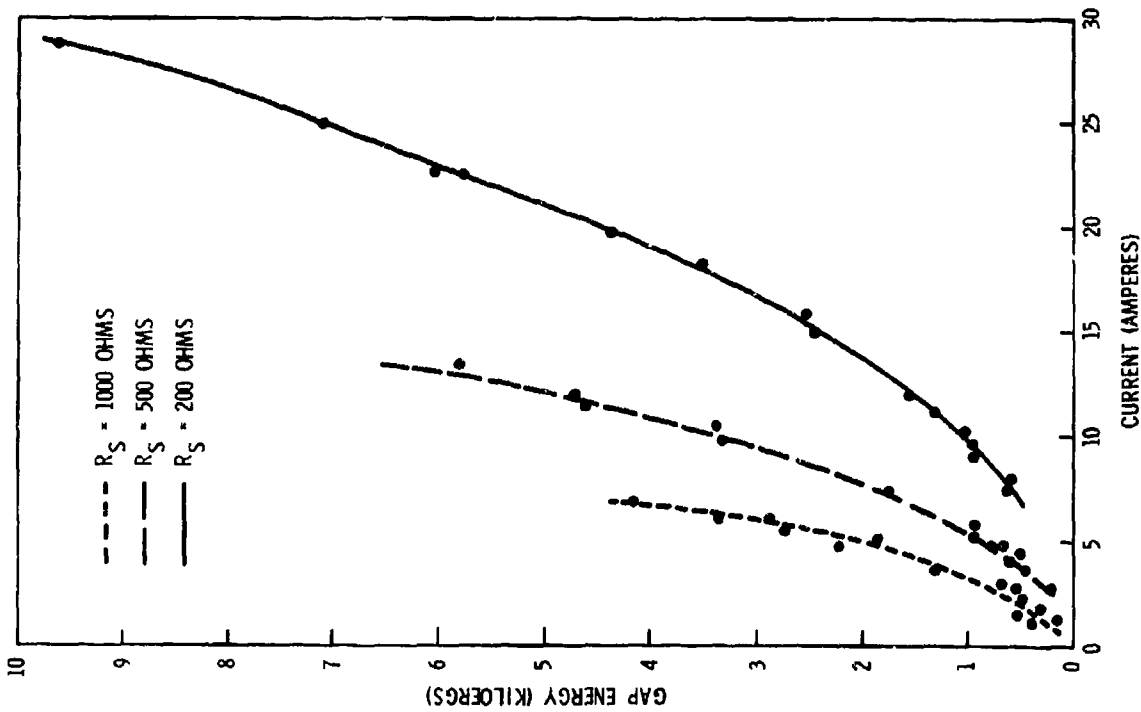


FIGURE 2 GAP ENERGY VS. PEAK CURRENT

2-6 SENSITIVITY OF EXPLOSIVES TO SPARK

Author: R. McGirr

Aerospace Components Division Laboratories  
Atlas Chemical Industries, Inc.  
Tamaqua, Penna.

The Bureau of Mines investigated the spark sensitivity of explosives in 1946 and 1953 and these investigations were reported on in Reports Nos. 3852 and 5002. The technique consisted of exposing a small amount of unconfined or partially confined explosive to a single discharge from a condenser charged to a high voltage. The energy of the spark discharged is varied by changing the capacitance and a plot made of ignition probability vs. energy.

Slide 1 shows the results on explosives with which we are concerned.

Slide 2 shows the same test performed at Reynolds Experimental Laboratory and the results are equal but additional materials of interest were tested.

For these materials a sensitivity rating was arbitrarily assigned and is shown on the left. Lead styphnate is the most sensitive and next in order of sensitivity is lead azide. Note that the dextrinated and polyvinyl are of equal sensitivity.

Another source of data is a report by Moore, Sumner and Wyatt, ERDE, United Kingdom, quoted in Franklin Institute

Report F-B2333 to NASA. It describes a spark gap test using a resistor in series with the capacitor discharge.

Dextrinated lead azide fired with a minimum energy of 70,000 to 280,000 ergs.

Crystalline lead azide fired with a minimum energy of 400 to 18,000 ergs.

This is the first time the purer lead azide was reported on.

For various reasons we had the feeling that this spark gap method is not a true valuation of sensitivity to spark and decided to evaluate these explosives when confined on a carbon bridge.

Slide 3 shows the carbon bridge primer used as a test vehicle.

Slide 4 shows the results of the tests which are performed at 100 volts varying the capacitance. The outstanding point is that the purer lead azides now head the list for sensitivity. This includes the polyvinyl, RD 1333 and colloidal azides. Note that styphnate is no longer the most sensitive. This confirmed our feeling prompted by a series of accidents and incidents when handling these materials or when they were employed as ingredients in finished EED's.

The Bureau of Mines method is limited to high voltage because of the air gap distance. Our method permits the formation

of low energy sparks transmitted through the graphite medium and at the same time gives a truer picture of confined explosive which is again not possible in using the Bureau of Mines method. The unconfined explosive permits some loss of the compression effect of the liquid, solids and gases released as a shock wave and also, the important reflections of the shock waves are lost unconfined. Since the carbon bridge is not efficient below say 60 volts, 100 volts was chosen.

As a 25,000 volt static discharge test is commonplace, when the size of the EED permits, to resist this amount of voltage is a good indication, in view of Chart 3, of the need for good design and care and cleanliness in manufacture.

Slide 4 also is a guide to which materials are suitable for ignition compounds and which are not. It is important to recognize that this knowledge is aimed at the manufacturer of EED's rather than the user as the purer lead azide is more efficient where a space is at a premium; however, it is also very important as the safety of the loading operator comes before all else. When the purer lead azides were introduced generally we were assured that they were not more sensitive than dextrinated. Our experience has always been the opposite and this was confirmed some time ago by an article in "Ordnance" which stated RD 1333 is sensitive enough to require special frictionless loading equipment not required by dextrinated lead azide.

Because the purer lead azides are more efficient, by the same token, the heat and pressure released by the decomposition of the first grain is sufficiently high to set off neighboring grains. Since the pure azides are single crystals they are perhaps more sensitive than the dextrinated azide grains which are multicrystalline grains.

Last, but not least, on Slide 4 it is interesting to note the effect of increasing voltage from 100 to 300 volts on superfine RDX.

STATIC SENSITIVITY 5 KV

RATING	TYPE	ERGS	
		NO ACTION IN 10 TESTS	
2	LEAD AZIDE (DEX)	70,000	
3	TETRACENE	100,000	
1	LEAD STYPHNATE	9,000	
4	PETN - 100	62,000	(DEFLAGRATION)
3	SMOKELESS PWDR. (UNGRAPHITED)	12,000	

REPRINTED FROM BUREAU OF MINES  
REPORT OF INVESTIGATIONS 5002

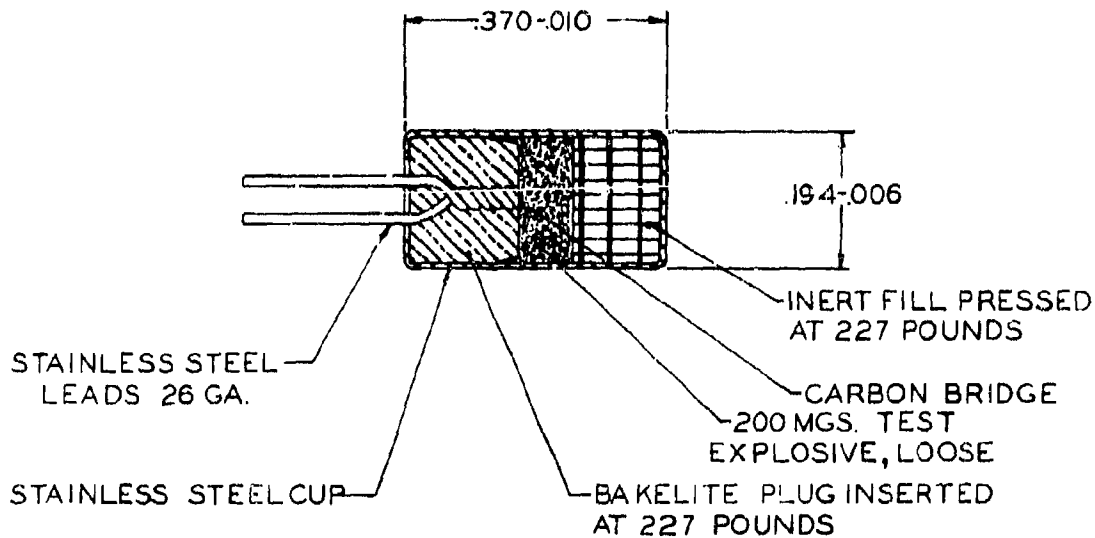
STATIC SENSITIVITY 5 KV  
1/16 INCH AIR GAP

RATING	TYPE	ERGS	
		NO ACTION IN 10 TESTS	SOME ACTION
2	LEAD AZIDE (DEX.)	62,000	75,000
2	LEAD AZIDE (PV)	62,000	75,000
3	TETRACENE	370,000	500,000
2	NOL 130	62,000	75,000
1	LEAD STYPHNATE (BASIC)	4,000 (3 KV)	8,000 (4 KV)
1	LEAD STYPHNATE (NORMAL)	—	4,000 (3 KV)
1	LEAD STYPHNATE (NORMAL MILLED)	—	4,000 (3 KV)
3	LMNR	120,000	250,000
3	LMNR 95% KClO <sub>3</sub> 5%	120,000	370,000

REYNOLDS EXPERIMENTAL LABORATORY  
ATLAS CHEMICAL INDUSTRIES, INC.

2





A. C. D. LABORATORY  
ATLAS CHEMICAL INDUSTRIES, INC

3

SPARK SENSITIVITY OF CONFINED EXPLOSIVES  
100 VOLTS CAPACITOR DISCHARGE

RATING	TYPE	MEAN ERGS	LOWEST
3	LEADAZIDE (DEX)	125	100
1	LEADAZIDE (PV)	6.5 TO 27	2
	TETRACENE		
2	NOL 130	45	40
2	LEAD STYPH. (BASIC)	40	27
2	LEAD STYPH. (NORMAL)	40	20
2	LEAD STYPH. (NORM. MILLED)	75	70
1	LEADAZIDE (RD 1333)	10	2
4	BARIUM STYPH.	2100	400
2	KDNBF	40	35
4	BARIUM PICRATE	7300	2500
	HMX		
10	PETN (MILLED)	—	<500,000
10	RDX (SUPERFINE)	—	<500,000
5	RDX (SUPERFINE)		22,500 AT 300V
1	LEAD AZIDE (COLL)	13	10

A. C. D. LABORATORY  
ATLAS CHEMICAL INDUSTRIES, INC

4

## DISCUSSION

Mr. Lewis (Space Ord. Syst.): In the slide that showed where you converted from the spark gap to determine the electrostatic sensitivity of mixes to the conductive carbon bridge, was the electrostatic energy applied between the carbon bridge and the case or through the carbon bridge?

Mr. McGirr: We applied the energy through the leads and through the carbon bridge. The point is to make the little sparks pass through the intimate particles of explosive. The only way you can do that is to get the carbon bridge to assist it.

Mr. Lewis: The point I was curious about was with the carbon bridge acting as a parallel shunt path of the pyrotechnic compound, how do you know the energy division, if any, that is going through the mix, and the energy that is flowing through the carbon? It seems to me that it might be possible what you are determining here is the thermal sensitivity of the mix, due to the loss across the carbon bridge.

Mr. McGirr: I am not saying just what I am determining, I am saying that the sensitivity of explosive to spark or heat shows that the pure lead azides fall into a pattern that has never been recognized before.

Mr. Petrick (NWL): You mentioned that the spark gap was not a true representation. Why is that so?

Mr. McGirr: The reason I said that was that you lose the effect of confinement, and all these tests neglect confinement. In the Bureau of Mines test, you place the explosive in a loose vial in some kind of a tiny receptacle and then you lower the needle. They had an additional test where they partially confined the explosive. I don't know what the people did at ERDE, I could not make much out of the report synopsis that was available to me, but I presume that the point that is being missed is: if you have 2 particles that are really squashed together, you are going to get a different effect than if they are not.

Mr. Harwood (GE): In determining the sensitivities of various materials, did you consider the effects of moisture or humidity in the materials, and if so, what effect did you observe with increasing moisture?

Mr. McGirr: We know, and I think you will agree, that if you increase the moisture, you are going to get erroneous results. All these explosives were handled with the same relative humidity. The test was performed at constant relative humidity. The explosive, as it came to that locale, was as dry as you would care to handle it. We have a rule at Atlas that we do not go dashing around with bone-dry azide and styphnate. We try to limit it and yet meet the military requirements.

Mr. Harwood: Speaking more specifically, did you notice if there was any increase in sensitivity of the materials as moisture increased, increased conductivity due to moisture, or perhaps a lower discharge voltage due to moisture increasing the sensitivity? (Editor's note: Moisture usually tends to decrease sensitivity. That is why sensitive explosives are handled wet - for safety.)

Mr. McGirr: We didn't run the test to that degree.

Mr. Bendict (JPL): You mentioned a recent Franklin Institute report in which there was a reference to an English paper of about 15 or 20 years ago, showing a curve which looked very much like an impedance matching curve for the sensitivity of explosives to steady discharge as a function of the series resistor. Would either you or Mr. Hannum care to comment on the shape of that curve?

Mr. Hannum: I am not sure I know what curve is meant. Was this the one on the work that the British did showing that there is a critical series resistance for each material? Well, this evidently is a fact, but it is in the test where you have loose explosive and an electrode and a plate. What Bob McGirr did was with a carbon bridge. We did very similar (to Mr. McGirr's) work about 8 years ago and published reports. We found that we had the same results as far as styphnate and azide are concerned.

I think maybe Don Lewis has a point. Are we talking about spark sensitivity or heat sensitivity or what? Apparently the configuration of test fixtures plays a large part in influencing the results.

Mr. Lewis: The reason I made the comment is that we performed a series of tests to determine the effect of electrostatic discharge in confined powders. We made the test as Mr. McGirr did in the bridge mode and we also made the test in pin-to-case mode. We varied the compaction pressure. In the pin-to-case mode test we got data that paralleled the Bureau of Mines as a family of curves, depending upon compaction pressure. When we went to the carbon bridge type test, we got curves much like Mr. McGirr did, which tends to follow a thermal sensitivity curve.

Mr. Ayres (NOL/WO): In the general area of the electrostatic spark sensitivity, Dr. R. M. H. Wyatt came to NOL for a couple of years and built an apparatus which was a Chinese copy of the one he used at ERDE and duplicated the results that he got there. This has been published, unfortunately most of it is classified. Those who have the need to know should get this information. If you will write to NOL, we can at least give you the report numbers, and in some way facilitate your getting Wyatt's reports.

I would like to point out that we should try to make a distinction between the work that Bob McGirr has done with the carbon bridge and a pure spark. I am quite sure that the mechanism whereby the energy is transferred into the explosive is quite different in these two cases. When you are talking about the sensitivity with the carbon bridge as the interchange medium, believe me, this is difficult to figure out just exactly how the carbon bridge operates. I am not arguing against his work. I am saying, as a caution, that you should not say that this is a pure spark discharge mechanism.

Mr. McGirr: In regard to the comment about the mechanism of sparks in a carbon bridge, I think you are glossing over the point that the chart that I put up followed the Bureau of Mines chart in all respects except for one explosive. I don't think this one explosive should be used as an example to upset the apple cart.

2-7 DESIGNING ELECTRO-EXPLOSIVE DEVICES

FOR  
ELECTROSTATIC INSENSITIVITY

By

L. D. Pitts

GENERAL PRECISION, INC.

Link Ordnance Division

ABSTRACT

This paper contains theory and design equations with which the engineer can analyze EED design for capability of withstanding a particular static discharge voltage from pin to case. Included are a general discussion of dielectric strength, resistivity, and dielectric constant as applied to breakdown voltage calculations and use of such calculations in analysis of general design factors and in evaluation of a specific EED design. Measured values of dielectric strength and resistivity for some common explosives and pyrotechnics are presented.

Introduction

Many squibs and detonators used for military and space applications are required to withstand a high voltage discharge from a capacitor without firing (typically 10 or 25 kv from a 500 pf capacitor with sometimes a 5,000 ohm resistor in series). For some commercial uses even such a simple device as a blasting cap must meet such a requirement. The discharge test is intended to simulate the application of the static electric charge which

may be accumulated by a human body or environmental surfaces (Reference 1). The concern with electrostatic sensitivity is well grounded since it is known that many EED's are very easily ignited by static discharge and that this has led to expensive and even fatal "unplanned events" (Reference 2). Much effort is expended to provide protection through safety procedures and external devices, but it is necessary for the EED engineer, whether designer or user, to gain an understanding of design considerations within the EED, for, unless we make the EED itself safe, we shall never have a completely safe system.

#### Difficulties In Designing Insulation Systems

High voltage arcs have been a subject of physical research for hundreds of years; e. g., Ben Franklin's experiment with the lightning discharge in 1752. However, the knowledge of arc mechanics (Reference 3), especially in gases, is not always reliable. Such an authority as Baker says, "It is an indication of the complexity of the problem of producing a satisfactory theory of breakdown that, despite the tremendous advances made, agreement has not yet been reached on the mechanism, even in the simplest of solids, the simple ionic crystals " (Reference 4). Dielectric strength numbers for insulating materials are of limited value since few manufacturers use any sort of standard test, and thus, much data is misleading. Even if breakdown theory and dielectric strength data were perfect, they would be of limited use to an engineer designing an EED or similar complex dielectric system unless he understands the breakdown criteria in such systems. This paper is intended to provide an understanding of the electrical relationships inside multiple dielectric systems, so that the engineer can make rational decisions when

designing EED's for static discharge requirements. It is necessary to begin with fundamentals.

### Single Dielectric

The simplest configuration is the single homogeneous, symmetrical, dielectric block between two plate conductors of Figure 1. With a voltage applied between the plates, a uniform electric field creates the even distribution of equipotential surfaces in the dielectric. For an insulator, at low voltages, the current flow is trivial. When the applied voltage reaches the breakdown voltage,  $V_B$ , the insulator will begin to draw appreciable current. Normally, this consists of an arc in which electrons are pulled from their parent atoms into the arc beam. Presumably, this happens at some critical electric field intensity referred to as the dielectric strength,  $D$ , of the material. Thus, one might expect a linear increase in breakdown voltage with increasing dielectric thickness. For most materials, however, the dielectric strength falls off rapidly with increasing thickness, as indicated in Figure 2. Dielectric strength may decrease by a factor of 10 as thickness varies from 1 to 100 mils. This behavior in solids is due to distance effects on the joule heating of the material by leakage current, according to Eichberger (Reference 5). However, others believe it is a result of statistical probability of avalanching, as in gases (Reference 6).

Other factors strongly influence dielectric strength measurements; electrode and insulator geometry, surface conditions, purity of materials, structural defects, environmental conditions (e.g., temperature, humidity,

and pressure), and method of voltage application. For short time tests (as opposed to life tests) the common test voltages are impulse, ac and dc. Because impulse testing applies voltage stress for the shortest times, it generally produces the highest dielectric strength, often referred to as the intrinsic strength and considered the ultimate dielectric strength of a material. A lower dielectric strength is given by dc voltage, with ac still lower due to heating caused by the reversing motion of the electrons and ions in the changing electric field (Reference 4), or due to creation of space charge (Reference 6). The ac dielectric strength falls still further at high frequencies. However, our tests for dielectric strength of air along an alumina surface indicate that step dc (discharge from a 500 pf capacitor) gives a dielectric strength of only 75% of that for slowly rising dc and peak value 60 Hz ac.

The remainder of this paper assumes that the applied voltage is a fast rising step, like the discharge of a capacitor into a high resistance.

A simple equivalent circuit (Figure 1) may be postulated for this configuration; a high resistance resistor in parallel with a low capacitance capacitor. If we apply a voltage step, the capacitor charges up instantaneously to the input voltage, and leakage current flows through the resistor. One could complicate the circuit by including the equivalent series resistance in the capacitor leg, but it is usually too low to have much effect on charging time of the capacitor.

#### Series Dielectrics

If we place two single dielectrics in contact in series with each other



(Reference 7), we have the case of Figure 3. Looking at the simple equivalent circuit we see that at  $t_0$  the voltage across dielectric 1 prior to break-down will be:

$$V_1 = V \frac{c_2}{c_1 + c_2} = V \frac{\frac{k_2}{d_2}}{\frac{k_1}{d_1} + \frac{k_2}{d_2}} \quad \text{Eqn. 1}$$

where  $k$  is dielectric constant. The remainder of the voltage will be dropped across dielectric 2. This equation is derived from ac laws for capacitance and from the parallel plate capacitor equation.

At long times the voltage division is determined by the resistors to be:

$$V_1 = \frac{V R_1}{R_1 + R_2} = V \frac{r_1 d_1}{r_1 d_1 + r_2 d_2} \quad \text{Eqn. 2}$$

where  $r$  is resistivity. Area cancels out in Equations 1 and 2 since it is the same for both dielectrics.

If the series dielectrics are in parallel with a low resistance path, such as an arc, the capacitances will determine the voltage division since the system decay time will be so short.

Equation 2 illustrates why two 300 vdc capacitors of equal capacitance in series might not stand off 600 volts of dc. That is, the unspecified leakage resistances might be such that practically all the 600 volts was across one capacitor.

For the  $t_0$  case, sufficient criteria for breakdown in  $V_1$  are that the applied voltage be greater than  $V_{B_1}$  for a period like one time constant  $T$  and

that the capacitor  $C_2$  be able to pass large current for this time; similarly, for breakdown in dielectric 2. If the breakdown in one dielectric leaves a sufficiently large voltage across the second dielectric, that may break down too. However, in many cases, one may find evidence of arcing in one dielectric but not the other. For the long time case, after the capacitor is fully charged, if the voltage  $V_1$  is raised above the breakdown voltage for material 1, material 1 will break down. The current is not supplied by the external voltage source since it is current limited by the resistance of material 2; instead, the current is supplied from the discharging of  $C_1$  with the faster time constant of  $\tau = R_{\text{arc}} C_1$ . This discharge is not trivial since a 2 pf capacitor at 1,000 volts stores 10 ergs of energy, enough to set off lead styphnate in some configurations (Reference 8). Also, once the arc starts, the total external voltage is across material 2.

Thus, a criterion for breakdown is that  $V_1$  from equation 1 or 2 exceed the breakdown voltage of material 1. However, for a high-current breakdown, the external voltage must also exceed the breakdown voltage of material 2.

This analysis, which can be extended to any number of series dielectrics, shows that while it is necessary that  $V < V_{B_1} + V_{B_2}$  to prevent breakdown, it is not sufficient.

### Parallel Dielectrics

The case of parallel dielectrics is shown with an equivalent circuit in Figure 4. If you were to test this configuration, you might find an arc at the interface initiated at some voltage below the breakdown voltage of either material, particularly if one of the materials were a gas like air. This is

apparently due to metallic or contaminant islands appearing at the interface and lowering the effective path length for breakdown (Reference 9). Tests at Link Ordnance confirm that this may indeed be a factor in ordnance components. It is at such interfaces that cleanliness of parts is extremely important. If sufficient freedom from contaminants is maintained, the interface effects can be minimized to the point where one may ignore surface breakdown for design purposes. The equivalent circuit is simple, in this case, the same step response for short and long times, a uniform electric field across both dielectrics. When the breakdown voltage of the material with least dielectric strength is reached, the breakdown will occur in that material. But what occurs if the amplitude of the capacitor discharge voltage step is raised above the breakdown voltage of either material? Do both materials break down? Does just the first material break down? Does just the second material break down? If you choose as materials for test two spark gaps such as employed in exploding bridgewire firing units, you will probably find all three answers are correct! Then why do EED's from the simple blasting cap to the most expensive aerospace initiators employ the preferential breakdown concept to prevent an arc through their primers? The criterion for breakdown is application of an over-voltage for some minimum length of time. There is no way in our example to prevent the over-voltage from appearing across dielectric 2. However, if we make the arc resistance through dielectric 1 small enough we can achieve a complete discharge of our voltage source before an arc has had time to form in dielectric 2. The emphasis here is on designing as large a ratio of  $V_{B_2}/V_{B_1}$  as possible, minimizing time  $V$  is greater than  $V_{B_2}$ , and attaining as low an arc resistance in dielectric 1 as possible, by using short gap distances for instance.

### An EED Example

In order to apply the criteria for breakdown of dielectrics to a specific EED design, it would probably be necessary to have better data on dielectric strength, permittivity, and resistivity of insulation materials than is presently available. To make the necessary calculations economically would require a computer program, so presently I suggest the calculation of breakdown voltage across the likely paths in an EED design and use of applicable criteria in analysis of the design.

For instance, Figure 5 shows a hypothetical design of a hot wire detonator. For simplicity, the bridgewire is not shown. First, one computes the breakdown voltage for each possible path.

$$V_{B(AB)} = D_{\text{air}} d_{AB} = (70 \text{ volts/mil}) (25 \text{ mils}) = 1,750 \text{ volts}$$

$$V_{B(AC)} = (250 \times 3) (25) = 18,750 \text{ volts}$$

$$V_{B(AD)} = (90) (20) + (70) (25) = 3,550 \text{ volts}$$

$$V_{B(AE)} = (90) (20) + (2,500) (3) + (110) (25) = 12,050 \text{ volts}$$

$$V_{B(AF)} = (90) (20) + (2,500) (3) + (110) (200) = 31,300 \text{ volts}$$

Dielectric strength values for explosives are taken from Table 1, values for other materials from Appendix A (70 volts/mil is a common approximation) for air. Tabulated value for thick steatite is multiplied by 3 per Appendix A instructions. From the section on series dielectrics, it is obvious we are not strictly correct if we consider only the summation of breakdown voltages across various paths. However, this turns out to be a useful first order approximation.

Let us suppose we are working with a 9,000 volt discharge from a 500 pf capacitor with no series resistor. It is obviously unlikely to arc through the ceramic at AC or, even allowing for decreased dielectric strength of RDX at 200 mils, along path AF. The presence of the teflon disc makes path AE an unlikely breakdown path. Path AB is intended to act as an external air gap to break down preferentially and prevent arcing through the primer. For AD, the dielectric strength of air is employed in the calculation across the top of the cup. Our experiments with a metal disc in place of a primer show that unless an insulator is very carefully glued on the cup with a thick adhesive layer, the dielectric strength will be typical of air. Other experiments show that arcing easily occurs across a surface in air when an insulator is only two mils removed from the surface. Minimum gap distance may be much less.

Path AD is indeed the most likely failure mode for the short cup EED. In this case, of course, with the high spark sensitivity of lead azide, any arc through the primer will be sufficient to cause ignition. The ratio of  $V_{B(AB)} / V_{B(AD)}$  is only 2 to 1 and the ratio of  $d_{AB} / d_{AD}$  less than 2 to 1. Also,  $V_{B(AD)}$  is well below the peak 9,000 volts applied and the arc resistance of AB across 25 mils of air is likely to be somewhat higher than desirable. Thus, one might characterize this as a marginal device, one which would stand off 9 kv, by means of the external gap, but which would likely experience random failures. Filling gap AB with a high dielectric strength potting material would produce 100% failures. The simplest improvements to this design would be an increase in length and breakdown voltage of paths AD and

AE and a decrease in length of path AC, the protective path. If there is a 1,000 volts insulation test required, making it undesirable to shorten the gap, electrode sharpening could be accomplished to encourage faster arc formation.

#### General Considerations in EED Design

There are three general approaches to designing an EED for electrostatic insensitivity.

- 1) Design the insulation system so that internal breakdown voltage is very high, ideally above the maximum specified test voltage by some safety factor.
- 2) Use protective devices (gaps, semiconductive potting, etc.) to prevent arcing through primer.
- 3) Use spark insensitive primer formulations.

In designing for high internal breakdown voltage, the use of tall primer cups and long explosive columns does not offer much help since dielectric strength falls off so rapidly with increasing distance. Our measurements on dielectric strength of explosives indicate that it is unlikely we will find a simple primer capable of standing off 9 kv all by itself. The most likely answer in this region is the judicious and ingenious use of insulators to raise breakdown voltage of the internal paths. Also, one may use the principles outlined for series dielectrics to design for a minimum voltage to appear across the primer mix itself. Ideally, one should check out the EED system for breakdown voltage with actual hardware and all protective devices defeated. The external

gap is easily disabled in many cases by enclosing part of the pins with mylar tape or tubing and filling the gap with a high dielectric strength epoxy adhesive. With inerts in place of the explosive components, one can find the likely internal breakdown paths.

Preferably, protective gaps should be hermetically enclosed in the EED to prevent disabling of the gap by contaminants or mishandling (Reference 10). There are obvious tests to run to determine breakdown voltage and effectiveness of a gap. One may want to set up procedures to assure cleanliness and breakdown repeatability of a gap in production.

I will not discuss the considerations of insensitive mixes except to point out that the conductive mixes will lower internal breakdown voltages, increasing the chances of insulation damage and, in some cases, degradation of the mix.

Obviously, the design engineer will choose whatever combination of the three approaches which seems most likely to be compatible with all the specifications of the particular EED device, including, of course, selling price. It might be mentioned that the customer often can be helpful by allowing larger EED sizes to permit higher internal breakdown voltages and by lowering insulation requirements to permit more effective breakdown protection.

#### Bridgewire Considerations

For the most part, the bridgewire plays a minor role in pin-to-case considerations. One wants to keep sharp corners and exposed points to a minimum, of course. But, bridgewire system design may be very important for certain cases.

Figure 6 shows a bridgewire system and equivalent circuit for a case where the bridgewire is welded well away from the inner edge of the pin. Naively, one assumes that shorting the pins together puts all elements of the pin-bridge system at the same potential, or at least that gaps 1 and 2 break down at the same time, shorting current away from the bridge. However, if the gaps are not designed and tested to insure that both break down at very close to the same time (in the nanosecond range) only one may break down, especially at voltages just above the gap breakdown voltage. Or, one may consider the highly practical case where the voltage is applied to only one pin.

In either case, when only gap 2 breaks down, the sharp leading edge of our applied pulse appears to the system as a very high frequency voltage and skin effect drives the majority of the current to the outside of the pin. In addition, the extremely high currents generated (high enough to set off a thermally sensitive EED if the source is not current limited) cause the voltage drops across the small resistances of CA, AB, EF, and FD to be significant. If these voltage drops are large enough, we are likely to see arcing across gaps 3 and 4; that is, an arc from the inner edge of the pins to the bridgewire. This arcing may have high enough energy to ignite a static sensitive primer adjacent to the bridge. If not, it may still cause a resistance change in the bridgewire by welding the wire to the inner edge of the pin or by eroding away the wire. Such arcing has been observed by us in unloaded units. A decrease in resistance due to the additional welding is the most likely effect. Remedies are to weld bridgewires at inner edges of pins or to design



protective devices so that they shunt current away from the bridge.

#### Dielectric Strength of Explosives

Even a superficial analysis of the internal dielectric system of an EED requires a knowledge of the dielectric strength of explosives. The fixture of Figure 7 was designed to hold explosives for such measurements and permit multiple and inexpensive testing at high consolidation pressures. Mylar\* was chosen for insulation because of its high dielectric and mechanical strength. Drill rod electrodes had flat ends to simplify calculations. The system was proved out with a 20 mil thick sample of epoxy, the entire system standing off 25 kv without any breakdown. Tests were performed with the setup of Figure 8, the voltage source, a charged 500 pf capacitor switched through a Jennings RE 6B high voltage vacuum relay. Breakdown was determined from the stored oscilloscope trace. Incidentally, the storage oscilloscope greatly facilitates a test of many single events. Resistance measurements were also taken and resistivity calculated from the simple formula for constant cross-section resistors. No measurement of dielectric constant was made, though it easily could be in a similar fixture.

The results show that the primary and secondary explosives act like insulators with a dielectric strength in the area of 100 volts per mil (with the exception of HNS). The pyrotechnics fall in three categories. They either evidence similar behavior to explosives, act like a poor conductor, or possess

---

\*Mylar tubing obtained from Stone Paper Tube Co., Washington, D. C.

high resistivity with trivial dielectric strength. Figure 9 shows that the dielectric strength of lead stypmate falls off significantly with increasing column length, as expected. Figure 10 indicates only minor loss of dielectric strength at low densities. Particle size effects may be important, as indicated in Figure 11 for purified  $\text{SiO}_2$ , a convenient material to grind and sieve. The particle size effects are not accounted for in Table 1.

Since air was present in the explosive and pyrotechnic samples, the data of Table 1 should not be taken as necessarily intrinsic to a given material, but they should be valid for design use, where one expects air to be present in the powder. Note that the values are for approximately 20 mil thick samples and should be derated for long columns.

Though the dielectric strength test was not intended as a spark sensitivity test, it is of interest to note that only primary explosives and the  $\text{Zr-KClO}_4$  mix fired in the normal configuration. Some other metal-oxidant mixes fired when an air gap was introduced, concentrating the arc.

The resistivity and dielectric strength tests have been useful at Link Ordnance for development of electric primer mixes. The simple geometry permits one to quantify effects of consolidation pressure, different constituents, etc., so that a better understanding of electric primers may be obtained.

#### Electrostatic Insensitivity Specification

Specifications are inadequately written for electrostatic sensitivity testing of EED's. A typical specification might read, "Shall not fire when 25 kv is applied from either pin to case from 500 pf capacitor through 5,000 ohm

series resistor." Such a loose specification may convince the designer that the customer is not very serious about the requirement and might buy off a lot which had a few test failures.

No tolerances on components or voltages are called out. Switching device and allowable voltage drop across it are unspecified. If a high voltage relay or spark gap is employed for switching, a keep-alive resistor is usually necessary to insure discharging the storage capacitor in a single repeatable pulse. The specification does not allow for this.

Since most EED's breakdown in some manner, the specification should consider high frequency effects. However, there is no specification of rise time, so that a manufacturer's test system may be highly inductive, yielding slow rise time and lower peak currents. With long test leads to the EED, inductance and skin effect may absorb much of the voltage drop in the circuit and radiate a large portion of the energy stored in the capacitor. The customer should require measurement of voltage at the EED if he really intends the test voltage to be there.

Some initiators may be most sensitive with the 5,000 ohm series resistor, but the bridgewire problems will not be tested since the resistor limits peak current to 5 amps. Some EED's may pass a 25 kv test with flying colors, but fire at 5 or 10 kv, voltages they are more likely to see in the field, because the protective gap is less likely to fire first with a lower overvoltage. It would usually be quite simple for the manufacturer to arrange for protective breakdown in his test equipment or output cable. The customer himself usually provides a protective device by specifying a connector that will not stand off the test voltage.

Even if there is no conscious cheating in electrostatic testing, the loose specifications and lack of standardization inevitably lead to confusing and misleading test results. Manufacturers are not going to take electrostatic sensitivity seriously unless forced to by adequate specifications or serious accidents. Until the customer learns to write a complete specification, he is going to continue to buy devices which are unsafe or at least not positively known to be safe.

#### Conclusion

Use of available dielectric strength data permits a first order analysis of any EED for electrostatic insensitivity. Additional data and involved calculations are necessary to include resistive and capacitive factors in analysis.

EED's can be designed rationally to meet electrostatic discharge requirements, and should be.

#### ACKNOWLEDGEMENT

I wish to thank Jerry Blain for performing the dielectric strength and resistivity tests on explosives and pyrotechnics.

TABLE 1  
DATA PRESENTATION  
(at approximately 20 mil thickness)

	Powder	Resistivity ( $\Omega$ -cm)	Dielectric strength (volts / mil)	Density <sup>3</sup> (gm/cm)
Primary Explosive	Normal Unmilled Lead Styphnate	$10^{13}$	140	2.5
	Basic Lead Styphnate	$10^{14}$	100	2.5
	Lead Styphnate with 2% Viton A	$3 \times 10^{12}$	120	2.5
	Lead Azide	$5 \times 10^{10}$	90	3.7
	75% Lead Azide 25% Lead Styphnate	$9 \times 10^{12}$	130	2.5
Secondary Explosive	PETN	$3 \times 10^{12}$	130	1.7
	RDX	$5 \times 10^{13}$	110	1.5
	HMX	$4 \times 10^{10}$	90	1.4
	HNS	$5 \times 10^{13}$	400	1.5
Pyrotechnics & misc. mixes	Bullseye	$4 \times 10^4$	< 5	- -
	Black Powder	$10^6$	< 5	1.6
	BKNO <sub>3</sub> Powder	$3 \times 10^{12}$	70	.95
	80% PETN 20% Graphite	500	< 5	1.5
	PbO <sub>2</sub> - Al mix	$3 \times 10^{10}$	< 9	4.3
	KC10 <sub>4</sub> - Al mix	$3 \times 10^3$	< 5	2.1
	KC10 <sub>4</sub> - Zr mix	$4 \times 10^{10}$	< 5	2.5

## APPENDIX A

### Insulation Properties

Table 1 of Appendix A lists insulation properties of materials culled from manufacturer's literature. Unless otherwise noted, the dielectric strength of the materials listed as header materials and adhesives appear to be for thick samples, while values for the insulation materials are for thin samples. Considering the relationship of dielectric strength vs. thickness (Figure 2), one may arbitrarily raise the header and adhesive dielectric strength values for thin geometries (25 mils or less) by a factor of 3. Values for insulation should probably be reduced by 5 for thick materials (greater than 25 mils).

APPENDIX A

TABLE 1

	Dielectric Strength V/mil		Dielectric Constant	Resistivity Ohm - cm	Source
<u>HEADER MATERIAL</u>					
Alumina 1510 (porous)	50 (1/4" thick)		5.5	$10^{14}$	Carborundum
Alumina 1542 96% (dense)	200 " "		9.2	$10^{14}$	"
Steatite 302	250 " "		5.58	-	Centralab
Boron Nitride	500		-	-	Union Carbide Corp.
Beryllia 7198	258		6.93	$2 \times 10^{14}$	Frenchtown Porcelain
Glass Boro- silicate	1000		4.7	$> 10^{14}$	Corning Glass
<u>INSULATION</u>					
Mylar	4000		3.1	$10^{10}$	DuPont
Kapton	7000 (1 mil thick)		3.5	$10^{13}$	"
Lexan	3910 (1.5 mils thick)		3.17	$2.1 \times 10^{15}$	General Electric
Teflon	2500		2.0	---	Technical Fluoro- carbon
Tedlar PVF film	3500		8.5		" "
Scotchite 3028	1400 (.010" thick)		5.3	$30 \times 10^{14}$	3M Company
Rulon A	400-500 (.080" thick)		2.6	$10^{15}$	Dixon Corp.
<u>ADHESIVES</u>					
Epon 840	400-500		4.6	$5 \times 10^{15}$	Shell Chemical Co.
Scotchcast 504	450		4.33	$12 \times 10^{14}$	3M Company
Scotchcast Resin	450		4.3	$> 10^{14}$	" "
Viton	500		-	$2 \times 10^{13}$	DuPont
Silastic 732 RTV	500		2.8	$1.5 \times 10^{13}$	Dow Corning
Stycast 3070	500		4.2	$2 \times 10^{16}$	Emerson Cumings
Skybond 700	179		4.1	$1.9 \times 10^7$	Monsanto
Eccobond 98	450		4.0	$10^{16}$	Emerson Cumings
Eccoseal W66	500		3.2	$10^{15}$	" "
Polyurethanes	5600		4.3	$10^{16}$	Columbia Technical Corp.
<u>CASES</u>					
Air (1 atm) ball electrode	100	(.100 thick)	1.0	---	Reference Data for Radio Engineers (ITT)
needle electrode	33	(.100 thick)			

## BIBLIOGRAPHY

1. Franklin Institute Monograph 65-1, "Electrostatic Hazard to Electro-Explosive Devices From Personnel - Borne Charges", February 1965.
2. Miller, J. Sam, "Electrostatic Ignition of X248 Rocket Motors", Report No. GM-1934-EZ-1a. Buffalo, New York, March 18, 1965.
3. Penning, F.M. Electrical Discharges in Gases, Phillips Research Laboratories, New York: The McMillan Company, 1957.
4. Baker, W.P. Electrical Insulation Measurements, Chemical Publishing Company, Inc., 1966.
5. Eichberger, Joseph E., "Electrical Failure In Solids", *Electro-Technology Science and Engineering*, May 1966.
6. Sharbaugh, A. Harry and John C. Devins "Electrical Breakdown in Solids and Liquids", *Electro-Technology Science and Engineering*, October 1961.
7. Von Hippel, A., "Dielectrics" (from Handbook of Physics, New York, Toronto, London, McGraw-Hill Book Company, Inc., 1958).
8. Moore, P.W.J., J.F. Sumner, and R.M.H. Wyatt, "The Electrostatic Spark Sensitiveness of Initiators: Part 1: Introduction and Study of Spark Characteristics", *Explosives Research and Development Establishment*, Report No. 4/R/56, Waltham Abbey, Essex, January 10, 1956.
9. Hart, J.E., W.W. Rosenberry, and A. T. McClinton, "Minimum Surface Leakage Distance in D-C Power Systems", *Electrical Engineering*, October 1951, 910-914.
10. Vance, E.F., L.B. Seely and J.E. Nanevicz, "Effects of Vehicle Electrification On Apollo Electro-Explosive Devices", Final Report, Contract NAS 9-3154, Stanford Research Institute, December 1964.



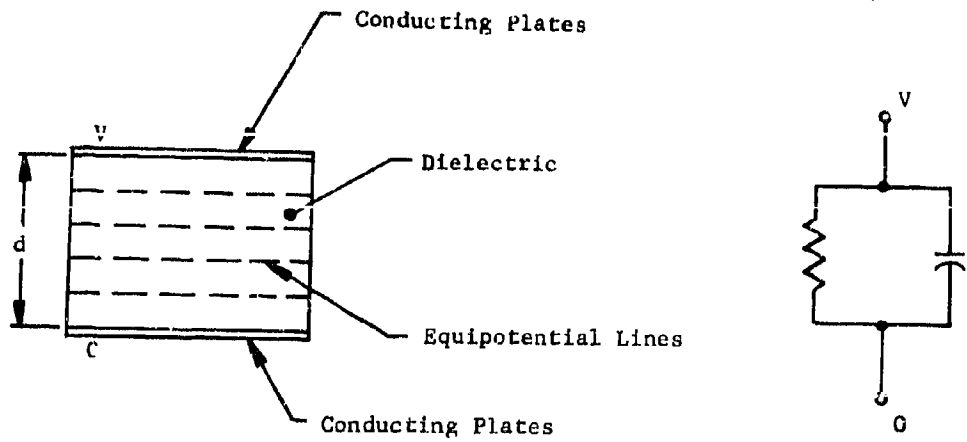


FIG. 1  
SINGLE DIELECTRIC  
SYSTEM

FIG. 2  
GENERALIZED PLOT OF  
DIELECTRIC STRENGTH VS  
DIELECTRIC THICKNESS

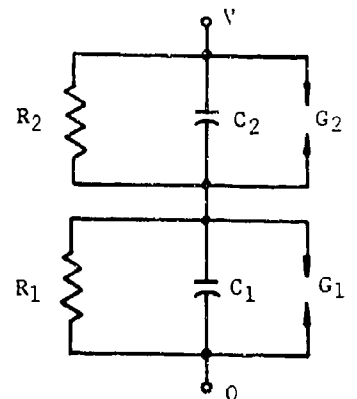
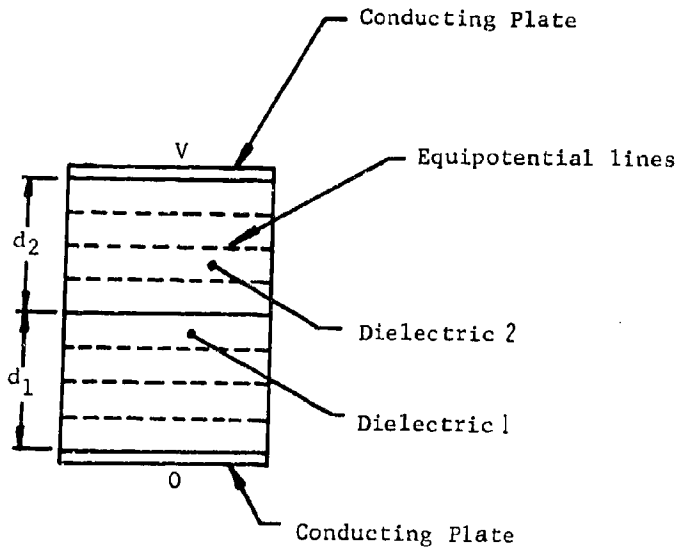
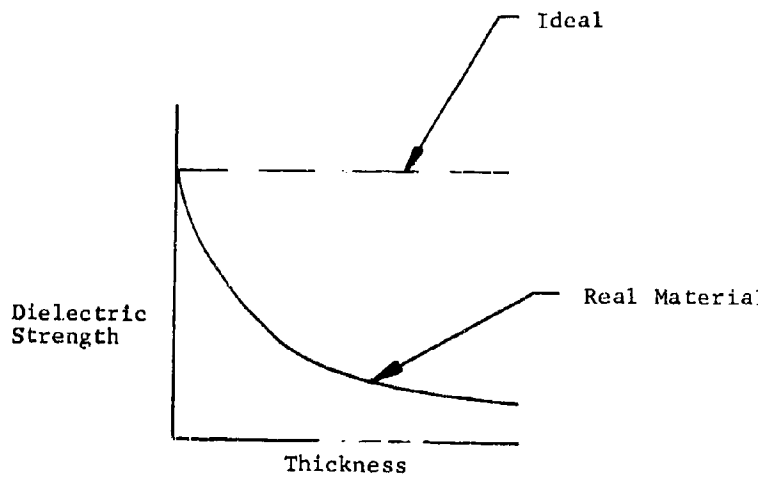


FIG. 3  
TWO DIELECTRIC SERIES SYSTEM

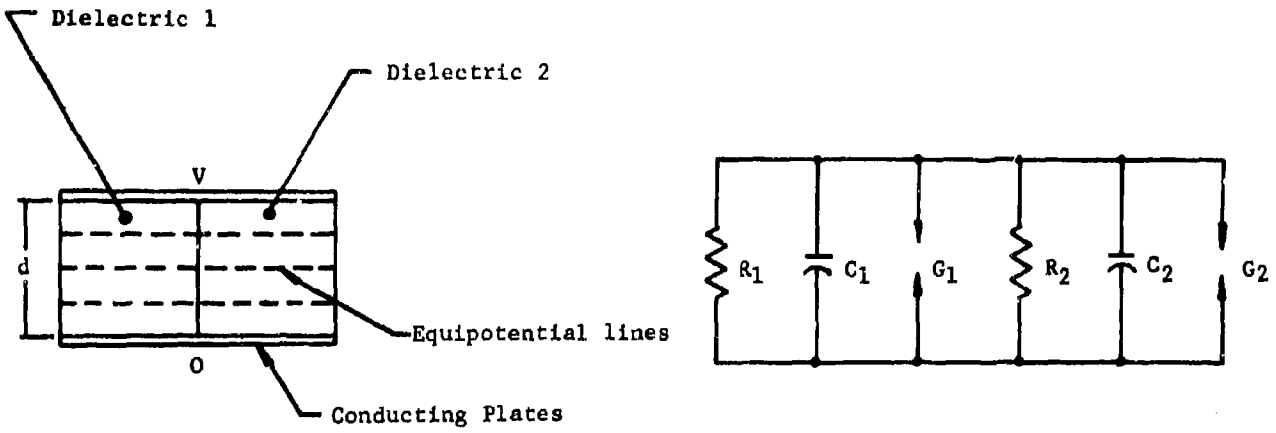


FIG. 4  
TWO DIELECTRIC PARALLEL  
SYSTEM

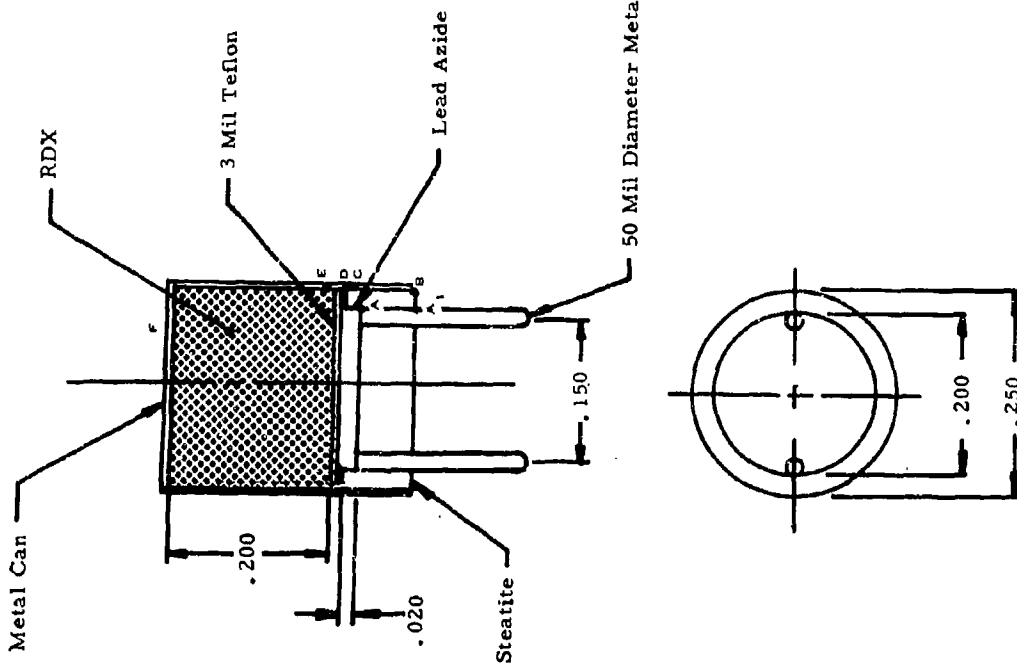
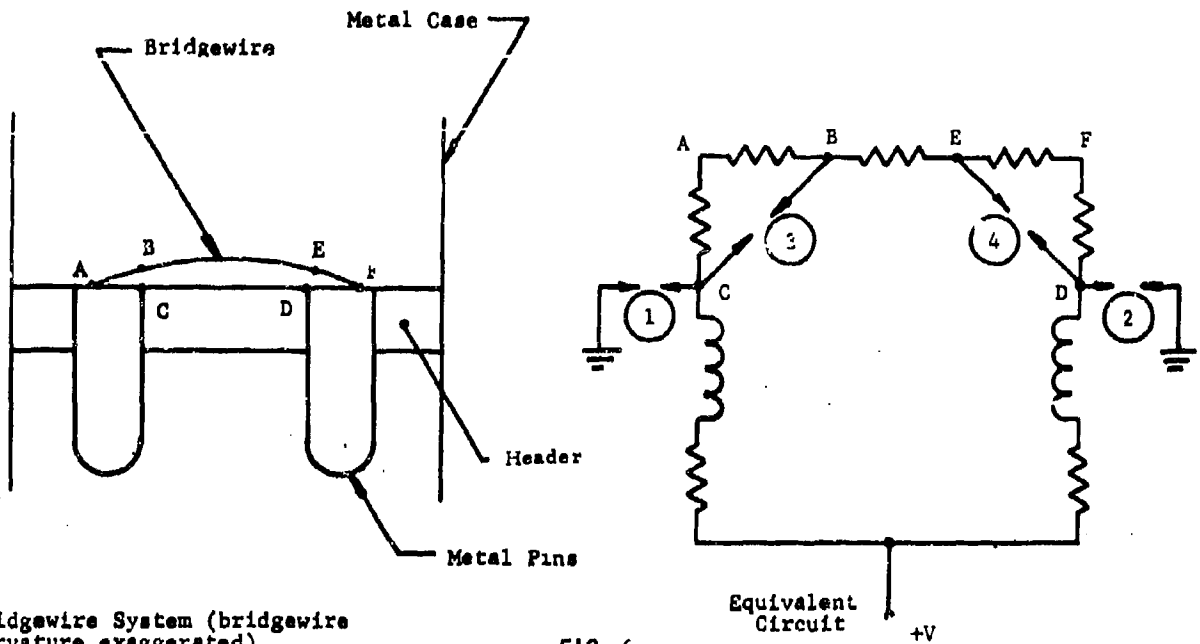


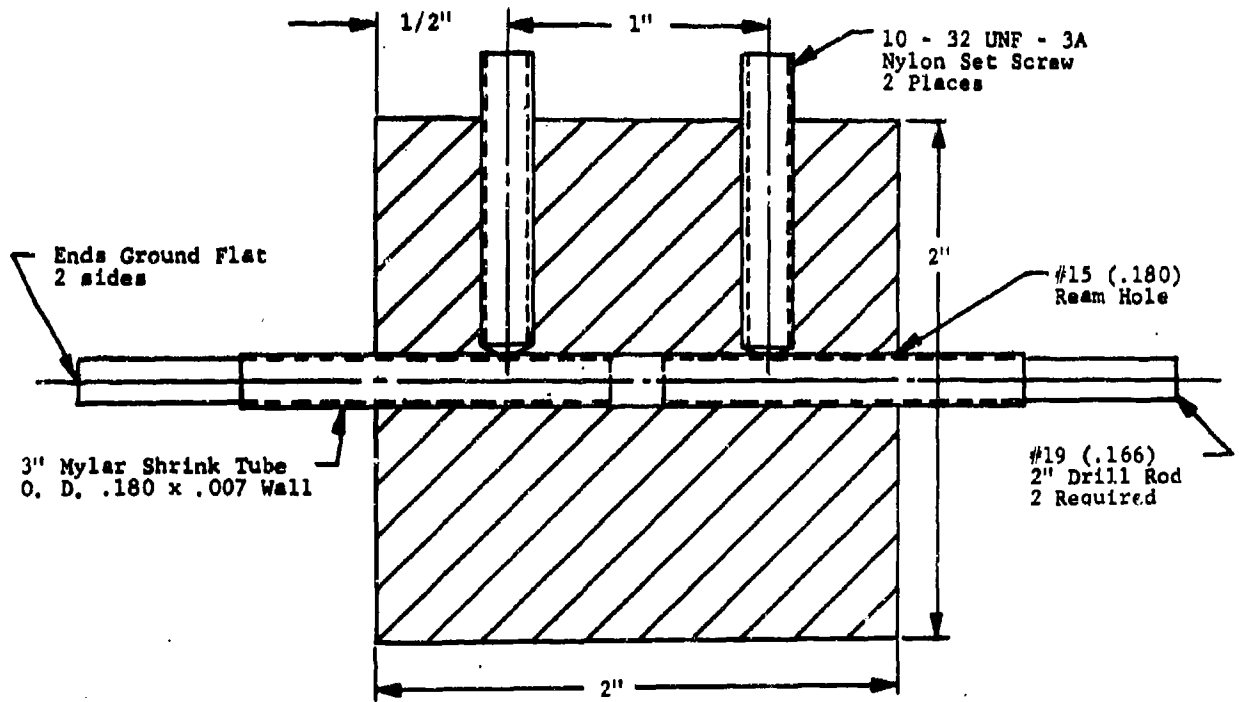
FIG. 5  
HYPOTHETICAL DETONATOR DESIGN



Bridgewire System (bridgewire curvature exaggerated)

FIG. 6

BRIDGEWIRE SYSTEM UNDER STATIC DISCHARGE TEST



TEST FIXTURE FOR DIELECTRIC STRENGTH + RESISTIVITY TESTING OF EXPLOSIVES

FIGURE 7

Instrumentation Setup for  
Measurement of Dielectric Strength  
and Resistivity of Explosives

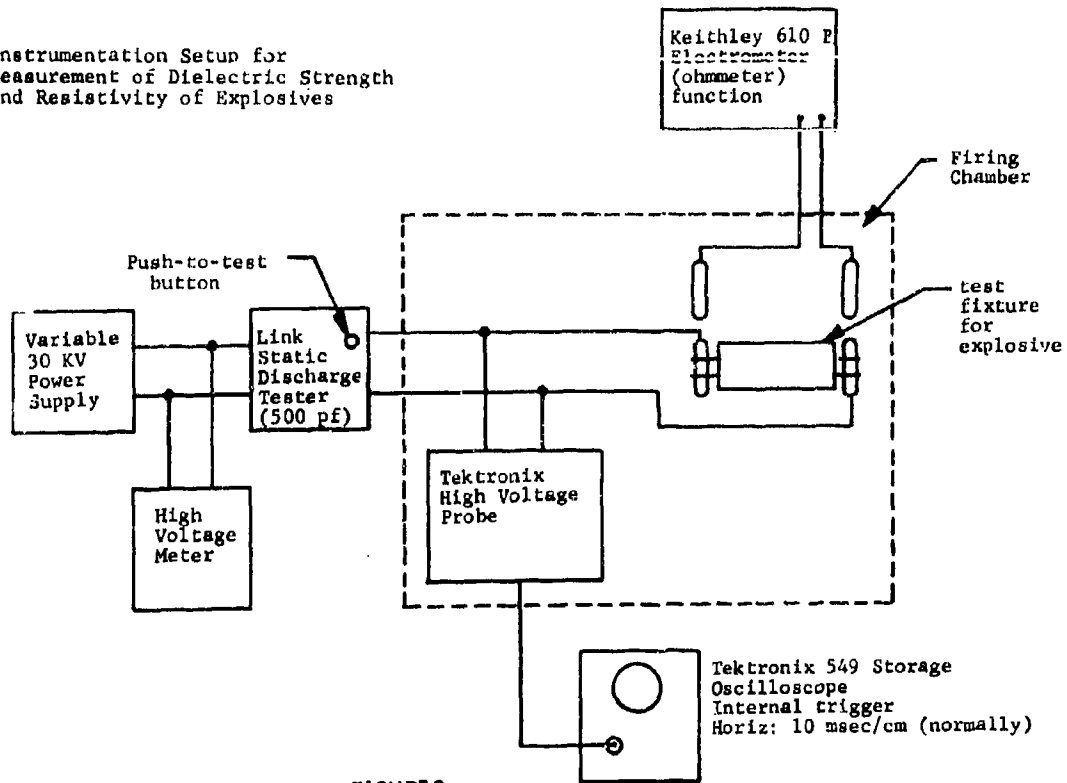


FIGURE 8

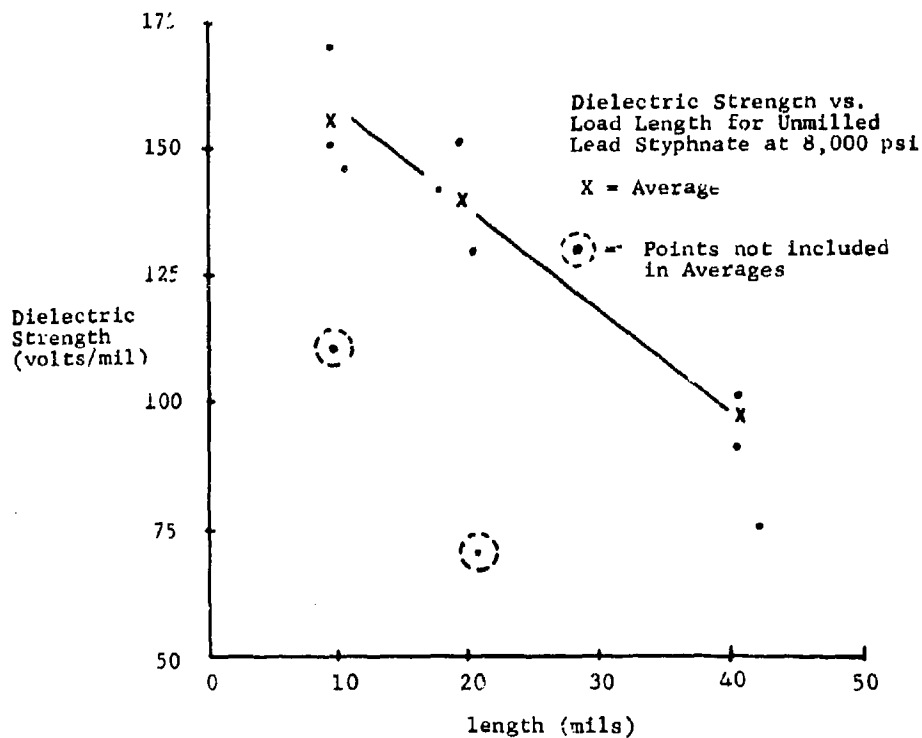


FIGURE 9

Unmilled Lead Styphnate  
Dielectric Strength vs.  
Density for 20 mil length

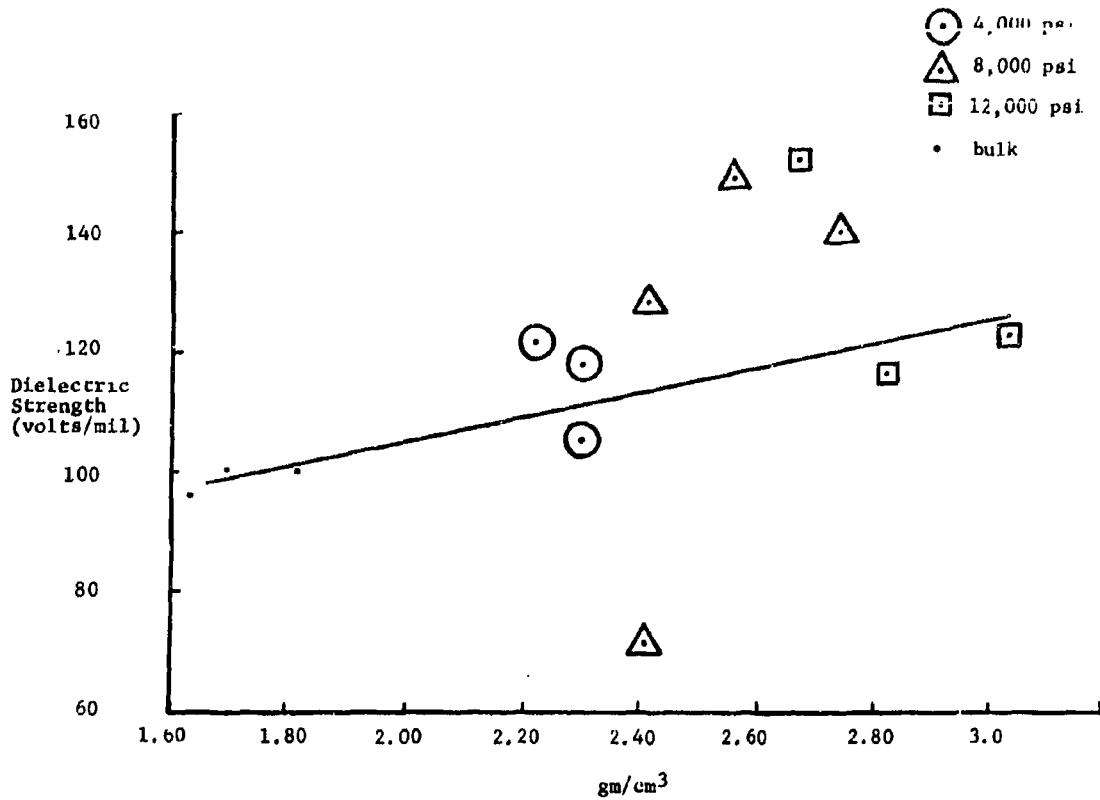
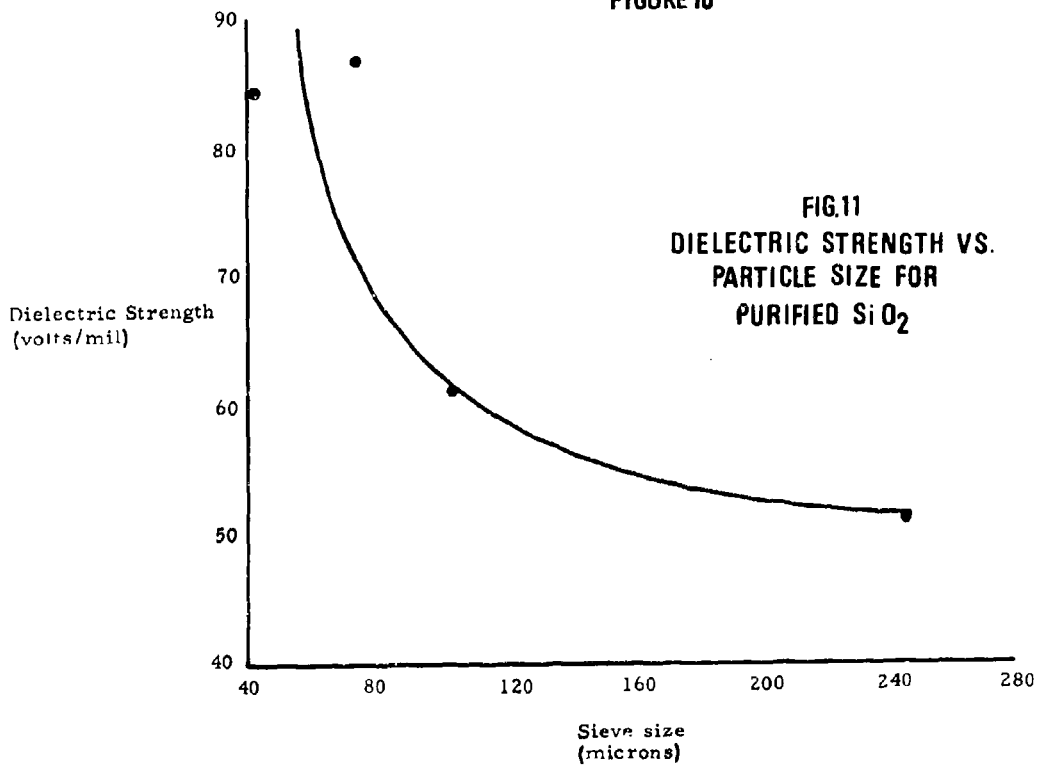


FIGURE 10



2-8P RF PROTECTION IN ELECTRO-EXPLOSIVE DEVICES  
THROUGH THE USE OF  
R-L-C NETWORKS

AUTHOR: JOSEPH E. SIDOTI

COMPANY: MICRO-PRECISION PRODUCTS, INC.

---

The use of ferrites and barium titanate materials in the construction of RF attenuated plugs for electric initiators has resulted in dramatically improved performance over devices heretofore available. Initial attempts at RF attenuation utilizing carbonyl iron with iron phosphate coating, provided some degree of RF protection. The problems that were created, however, were considerable and complex. Voltage breakdown characteristics had to be sacrificed, attenuation was low to moderate at best and practically ineffective below 100 MC; reproducibility in production was difficult, if not impossible to achieve. By the means of incorporation of R-L-C networks, most of these objections were eliminated.

There are a number of parameters involved in the design of such networks and in order that some degree of prediction can be achieved it is essential that the effect of variations in these parameters be established. The following will serve to illustrate the types of circuits which are involved. There are at least three basic types of circuits possible in each of two types of configurations. Almost any desired effect can be provided by the proper arrangement of elements.

At one extreme, for example, would be a filter referred to as a hi-pass filter that would eliminate any DC or AC below a given voltage and frequency. The types of circuits providing this type of attenuation characteristics and their typical response curves are shown in Figure 1.

It is apparent that the DC and low frequency energies would be effectively attenuated in this arrangement, until the cut-off frequency " $f_o$ " is reached. After this point, only the AC component would pass through.

Naturally, the DC flow is necessary if the particular device is to be fired by capacitor discharge techniques, so that at first it would seem that this approach is not feasible. However, it can be shown that as the DC voltage is increased to the point where breakdown occurs across the capacitor, energy would then pass through. This approach has been used as a safeguarding technique generally described as the spark-gap method, which assures that all energy below the frequency " $f_e$ " would be effectively attenuated, including random DC voltages whose potential is lower than the discharge potential.

At the other extreme is the class of filters known as the low-pass filters which are shown schematically together with their typical characteristics curve in Figure 2. As can be seen, it is significantly different from the first group. This type of filter would pass all frequencies including DC up to the cut-off frequency " $f_e$ ". Attenuation would commence at frequency " $f_e$ " with increasing effectiveness at frequencies greater than " $f_e$ ".

To further complicate matters, it is possible to combine any of the previously described circuits thereby achieving some composite type of attenuation characteristic; examples of which are shown in Figure 3.

For the purpose of discussion, if any one type of circuit of all the circuits described were to be selected for investigation, the following would have to be considered:

For example: One R-L-C network adequately suited for an RF attenuated squib plug might be the low-pass filter. Such a device will pass frequencies below a given frequency which we shall call the cut-off frequency, and will attenuate frequencies above that given frequency. The following is a schematic of a simplified "L" section low-pass filter, whose characteristic curve has previously been described. In this circuit the various parameters are labeled and identified. See Figure 4.

In practice however, there are effects which will result in modifications to the described circuits, especially at the higher frequencies. For instance, distributed capacitance, finite resistances of insulation materials and physical means by which components are assembled can convert the relatively simple "L" section network into a more complex circuit. Variations can also occur as a result of the interaction caused by the presence of two leads within the same enclosure, and even this will change as one subjects the frequency to variations ranging from zero (DC) to hi-frequency AC (RF).



Needless to say, a mathematical review would require a considerable number of assumptions before one could proceed in a very elementary manner to attempt to predict final characteristics of any given device.

On the basis of the foregoing, therefore, it seems reasonable to conclude that an empirical evaluation of various parameters would easily provide the most meaningful information. RF attenuation characteristics have been established and effective RF attenuators developed, utilizing a circuit arrangement similar to Figure 2. Attenuation curves for these devices, comparing them to previous state of the art devices are shown in Figure 5.

The following will describe the constructional features of those devices which have been evaluated to date. Figure 6 shows the constructional features of this particular device. Ferrite beads, whose inner and outer diameters have been metallized are soldered to wire leads and to one side of a Barium Titanate capacitor slab. The opposite side of each slab is then soldered in turn to a ground plate. The entire device is then assembled into a metal shell and encapsulated. A shield across the face of the device prevents coax-line type of feed through of high frequency energy.

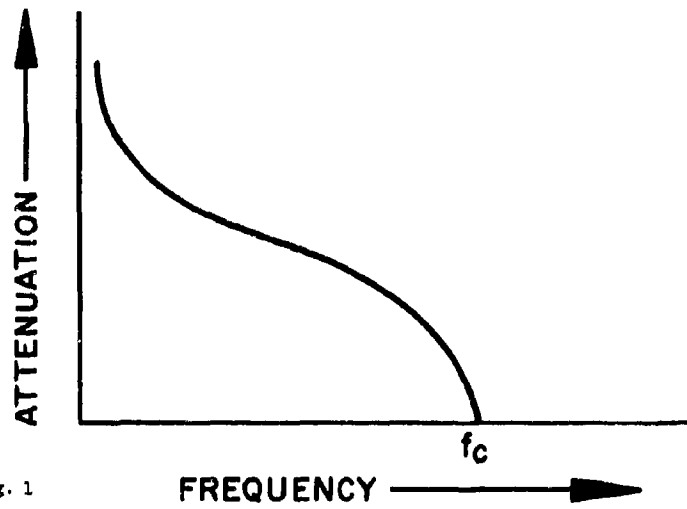
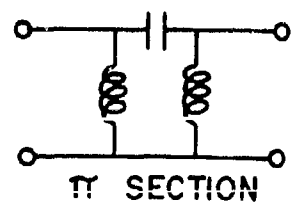
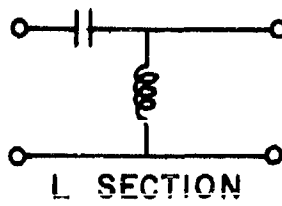
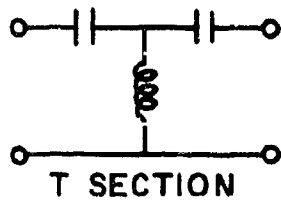


Fig. 1

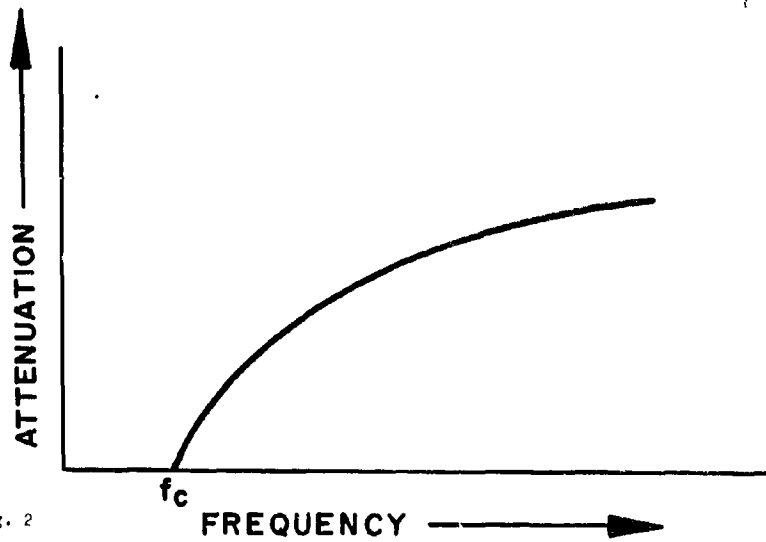
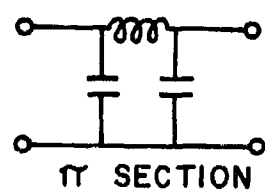
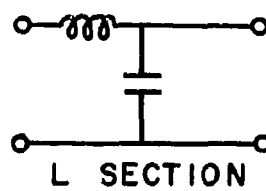
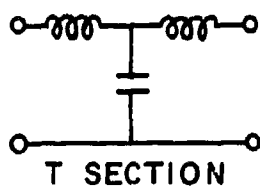


Fig. 2

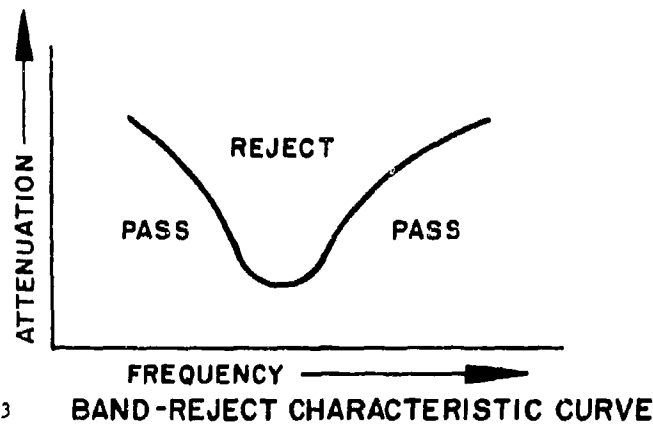
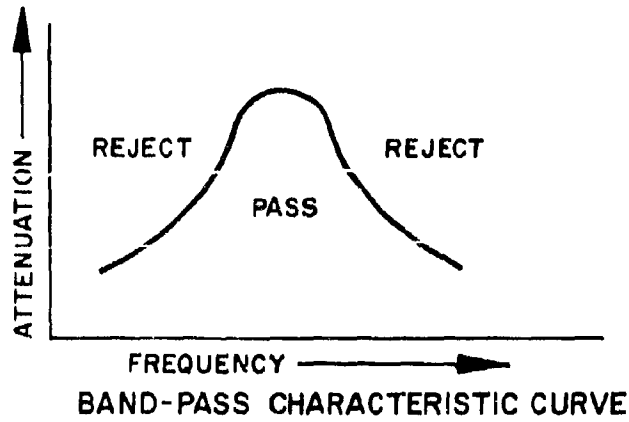
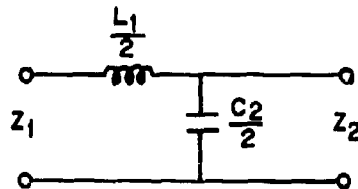


Fig. 3



- |                                  |                           |
|----------------------------------|---------------------------|
| $Z_1$ = INPUT IMPEDANCE          | $L_1$ = INDUCTANCE        |
| $Z_2$ = OUTPUT IMPEDANCE         | $C_2$ = CAPACITANCE       |
| $Z_0$ = CHARACTERISTIC IMPEDANCE | $F_C$ = CUT-OFF FREQUENCY |

THE CUT-OFF FREQUENCY IS SHOWN AS "fc", AND IT CAN BE COMPUTED FROM THE FOLLOWING RELATIONSHIPS:

$$f_c = \frac{1}{\pi \sqrt{L_1 C_2}}$$

THE INTERRELATIONSHIPS OF THE REMAINING PARAMETERS CAN ALSO BE DESCRIBED BY THE FOLLOWING EQUATIONS:

Fig. 4

$$L_1 = \frac{Z_0}{\pi f_c} \qquad C_2 = \frac{1}{2\pi f_c Z_0} \qquad Z = \sqrt{\frac{L_1}{C_2}}$$

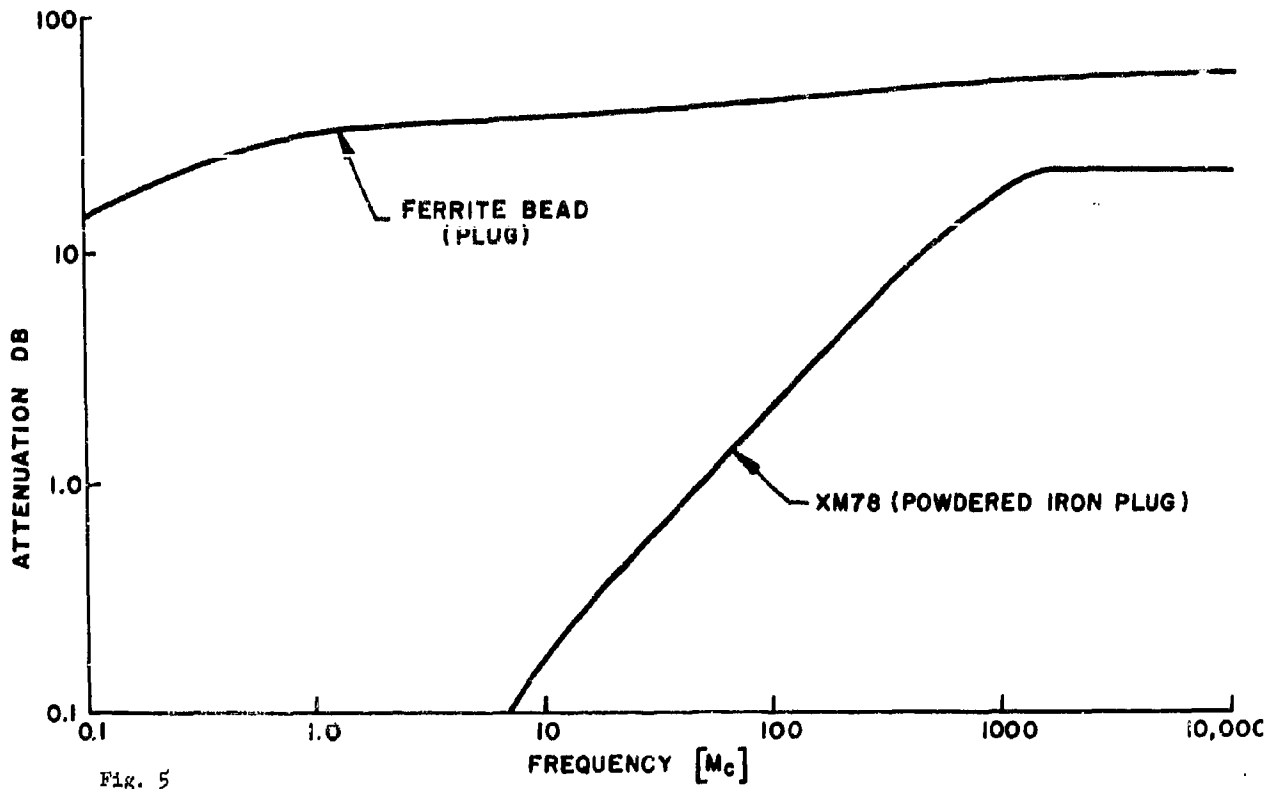


Fig. 5

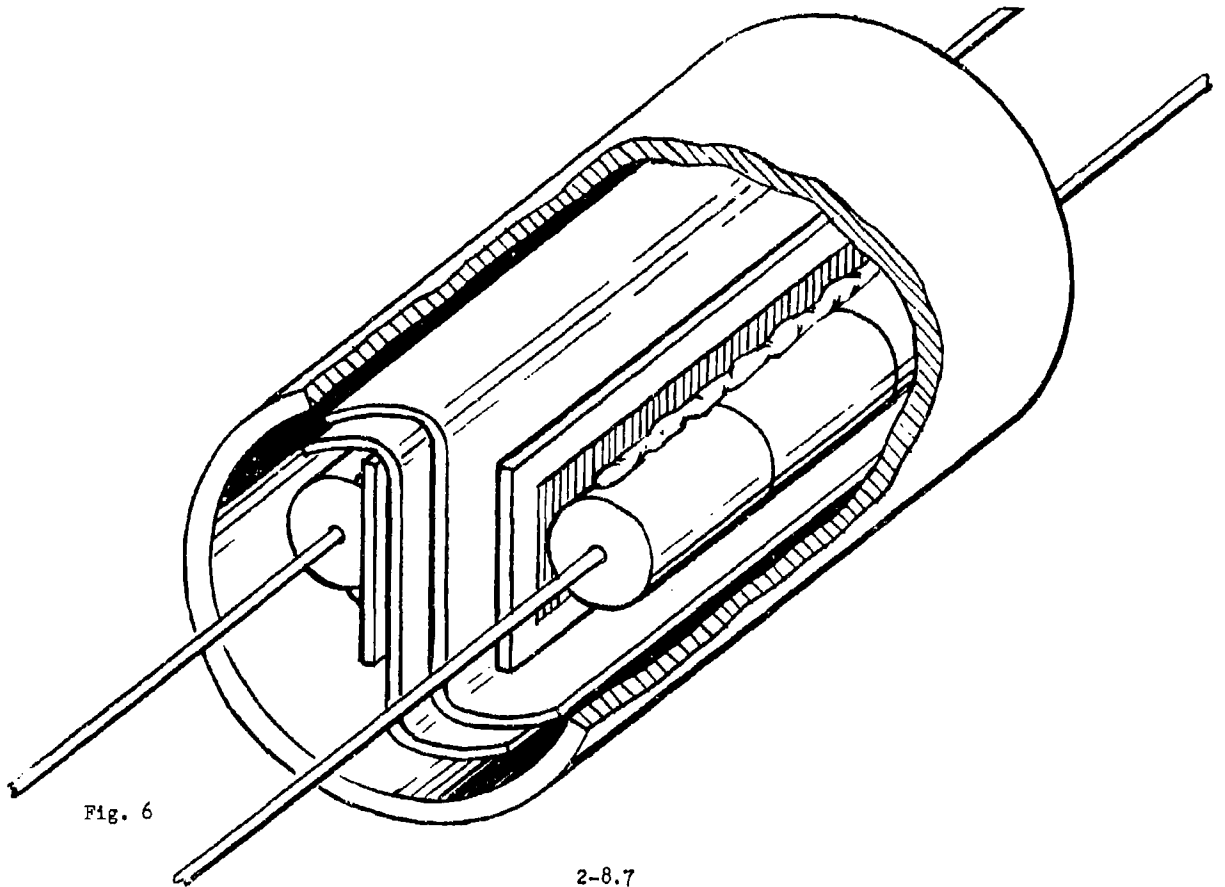


Fig. 6

## 2-9P EFFECTS OF RADIO FREQUENCY STIMULI ON ELECTROEXPLOSIVE DEVICES

By Paul F. Mohrbach and Robert G. Wood  
The Franklin Institute Research Laboratories

### 1. INTRODUCTION

The Franklin Institute Research Laboratories have during the past several years, determined the response of a large number of electro-explosive devices (EEDs) to RF stimuli. These determinations are in terms of magnitude of RF power which must be delivered to the base of an electro-explosive device in order to produce an initiation or a noticeable alteration of characteristics of the EED. In the process of performing these tests and analyzing the results, a number of general trends have been observed both with respect to absolute sensitivity and to the reasons for any pronounced sensitivity. It is the purpose of this paper to present some of these generalizations for the frequency range of 1 to 10,000 MHz, but it is essential to keep in mind that they are generalizations and that there have been exceptions to nearly every one of them. Therefore, the statements made in this paper can be quite successfully used as guide lines for design and planning, but actual testing of the EED must be performed if the specific behaviour of the EED to RF stimuli is to be known.

### 2. HOT WIRE EED'S

The most common type of EED used in modern ordnance and space systems is the hot wire type, hence, the bulk of our studies have been on this type. These EED's contain one or more small lengths of wire (called a bridgewire) connected electrically on the input side to metal pins running to an electrical signal source and connected mechanically on the output side to a pyrotechnic material. Upon application of the proper electrical stimuli to the input leads, the bridgewire is heated sufficiently to initiate the pyrotechnic material.

Unwanted electrical stimuli, such as RF, can also enter on the input pins and in addition, may also appear between the pins and the case

or between the bridgewires in the case of multibridgewire devices. It is convenient to discuss each of these cases separately.

## 2.1 Pin-to-Pin or Bridgewire Behavior

### Response to Continuous Wave (CW) RF Stimuli

Figure 1 shows a typical response curve of a hot wire EED exposed to CW-RF signals in the bridgewire mode. For simplicity, only a single curve is shown which we can consider as the 50% firing level. In actual practice similar statements apply to the 0.1% and 99.9% firing levels. As a general rule, in the range of 1 to 1000 MHz; the RF sensitivity of typical devices in terms of average power is always equal to or less than the dc sensitivity. Therefore, a relatively insensitive device, such as a 1 watt no-fire item, would tend to take more RF power to initiate in the bridgewire mode than would a device with a "no-fire" of 200 milliwatts. Initiation in these cases appears to be mainly a matter of bridgewire heating.

In the frequency range above 1000 MHz no such pattern emerges. At these higher frequencies, initiation phenomena other than simple bridgewire heating occur. Arcing, for example, frequently occurs and may exist between the bridgewire and the case even though the RF stimuli is being applied to the bridgewire. These multiple mechanisms of initiation frequently result in a wide spread in the data such that the 50% firing sensitivity to RF may be less than the comparable dc level but the 0.1% sensitivity may be greater than the dc 0.1% level. The general tendency is for a device to still be less sensitive than the dc level, but any assumptions based on this carries a much larger risk factor.

### Response to Pulsed RF Stimuli

For the most part, pulsed RF sensitivity studies have been conducted only in the frequency range above 1000 MHz. Our standard test conditions use a pulse width of 1.5 microseconds with the pulses repeated every 1000 microseconds (the ideal case is shown in Figure 2). A limited

number of tests in which the pulse widths have been varied from 1.5 to 3.0 microseconds and the pulse repetition rate varied from 500 to 2000 pulses per second have indicated no large variation in sensitivity, in terms of average power, as a result of such parameter changes.

Generally results are similar to those obtained with CW signals except that arcing becomes even more acute resulting, many times, in even greater sensitivity and the phenomena of thermal stacking becomes a factor. Thermal stacking, illustrated in Figure 3, refers to the case where the amount of heat in the bridgewire, and its immediate surroundings, has not been completely dissipated by the time the next pulse arrives. The heat produced by this second pulse is then added to the residual heat from the first pulse. In this manner heat can be built up by successive pulses until initiation temperature is reached or until dudding is produced by a cooking-off or decomposition of the explosive in the immediate vicinity of the bridgewire.

## 2.2 Pins-to-Case Behavior

### Response to Continuous Wave (CW) RF Stimuli

Inadvertent initiation of EED's in this mode appears to be primarily a function of voltage stresses applied between the pins and the case. If an EED is unusually sensitive to static electricity in this mode or if an EED which passes a 500 volt insulation test could not take more than 1000 to 1500 volts from the same type of source without breaking down, it is very probable that it will be sensitive to RF in this mode, at least at selected frequencies. Since the sensitivity is stated in terms of average power, the sensitive condition will occur whenever the pins-to-case impedance is such that large voltages can be produced with small powers. This will occur when the conductance values are very small. For most typical hot wire EEDs this occurs in the vicinity of 1.5 MHz which is the lowest frequency that we normally conduct tests. Unusually sensitive conditions can exist with sensitivity values frequently falling to levels below 100 milliwatts.

### Response to Pulsed RF Stimuli

Pulsed RF and the condition just discussed, represent the most sensitive EED conditions in terms of RF response. Twenty-five to thirty percent of all hot wire EED's tested have shown marked sensitivity to pulsed, pins-to-case applied RF signals. Furthermore, the sensitivity appears to bear no significant relationship to the dc sensitivity. For example, many 1 amp/1 watt devices, especially those that use metal loaded pyrotechnic mixes, have shown pronounced sensitivity to this type of stimuli. Functioning times tend to be relatively long in terms of the normal functioning time of a device, indicating that multiple pulses are frequently required but the power for firing is as much as 18 db below the dc level. Initiation mechanisms are mostly in the theory stages since it is difficult to obtain much meaningful information about the internal impedance at frequencies above 1300 MHz. Power levels below 100 milliwatts are frequently sufficient to produce initiations.

### 2.3 Bridgewire-to-Bridgewire Behavior

The discussion pertaining to pins-to-case behavior applies equally well to bridgewire-to-bridgewire behavior in multiple bridgewire EEDs except that the frequencies at which the proper impedance condition exist are not as consistent as in the pins-to-case instances.

## 3. SPECIAL EED TYPES

Only two types of EEDs, other than hot wire types, have been investigated in sufficient depth to permit any generalizations. These are the exploding bridgewire type and the carbon bridge type.

### 3.1 Exploding Bridgewire

Initiation of this type of device by RF has been a rare occurrence in our studies; however, bridgewires can be burned out with relative ease and, on occasion, explosives in the immediate vicinity of the bridgewire



can be altered. In the case of EBW's which contain a series gap, the gap can become completely ineffective at frequencies above 1000 MHz and major alteration of gap characteristics can occur with RF powers as low as 1 watt average.

### 3.2 Carbon Bridge EED'S

These devices have proven to be extremely sensitive to RF; however, in this case maximum sensitivity occurs in the bridge mode. Pin-to-case sensitivity can be comparable to that of hot wire EED's but sensitivity to RF applied through the bridge can be as low as a few milliwatts. Furthermore, a single high frequency pulse can initiate a carbon bridge EED.

### 4. Causes of RF Sensitivity

Two common reasons for an EED being pins-to-case sensitive arises because of design and manufacturing methods used in their production. The first one, which we call the over-hanging bridgewire, is shown in Figure 4. This figure shows a comparison of an EED in which the bridgewire is carried only halfway across the metal support posts while the other shows the bridgewire overhangs each post. In the evaluation of this item, arcing occurred as evidenced by burn marks at the end of the wire and on the inside of the metal case. The second case, which is shown in Figure 5, shows metal burrs on the bridgewire post. Arcing occurred between the burrs and the case. Microscopic examination of the EED indicated that the burrs on the bridgewire posts appeared to be the results of a grinding operation. When these burrs were examined after RF was applied, the burnt edge of the burr could be distinguished. A burn mark could also be seen in the plastic insert that covers the inside of the case. An inert unit that had power applied for several seconds showed a charred path across the plug face from one of the protruding pieces of metal to the case. To prevent internal arcing careful manufacturing methods must be observed and the design of the EED checked for possible trouble spots.

There is one other situation that can cause extreme pins-to-case or bridgewire-to-bridgewire RF sensitivity. This situation occurs when a conductive mix is used as the pyrotechnic material. The addition of zirconium or aluminum to the explosive charge is normally done to increase the heat transfer characteristics of the EED. These metal particles (insulated from each other by the explosive material) tend to increase the field intensity within the explosive charge which may cause the EED to be extremely sensitive to pulsed RF with its high voltages.

## 5. A SUMMARY AND A WARNING

As indicated in the last section, bridgewires extending over the ends of posts, metal fragments dragged off the ends of posts, addition of metal additives to explosive mixes, poor design from the static electricity standpoint and probably other factors not yet uncovered can all contribute to making EED's sensitive to RF stimuli. This sensitivity can often be much greater than the dc sensitivity, therefore, it is dangerous to use the dc sensitivity as a criterion except for possibly the bridgewire mode in hot wire devices below 1000 MHz.

In general, EBW's are difficult to initiate with RF but can be dudded. The gap in gap type EBWs can be altered by RF. Carbon bridges are extremely sensitive to RF signals, particularly in the bridge mode. The most sensitive conditions for hot wire devices usually occur in the pins-to-case mode. This sensitivity is most likely to occur from a CW stimuli in the vicinity of 1.5 MHz or at some pulsed frequency above 1000 MHz.

It should be noted that these are generalizations and that for any specific EED not yet evaluated only tests will establish the real sensitivity. One of the more sensitive items we have encountered took more than 1 ampere and 1 watt to fire at dc (it was not an official 1 amp/1 watt), and had its most sensitive condition when exposed to pulsed RF in the bridge-wire mode. It initiated at an average power level of 40 milliwatts.

Before closing, one final warning should be offered. We have discussed in general terms the RF response of EED's and what factors contribute to this response. The overall RF/EED vulnerability problem, however, is one that encompasses not only the EED but the circuits that serve to extract the RF energy from incident fields and deliver it to the EED. While one should certainly avoid the use of RF sensitive EED's and initiator designers should strive to use available knowledge to produce less RF sensitive devices, the use of an RF insensitive EED does not guarantee safety. An RF insensitive EED carelessly handled in an RF environment or assembled into a circuit poorly designed from an RF pickup standpoint may be far more dangerous than an RF sensitive EED handled with the proper precautions and assembled into a properly shielded or RF filtered circuit.

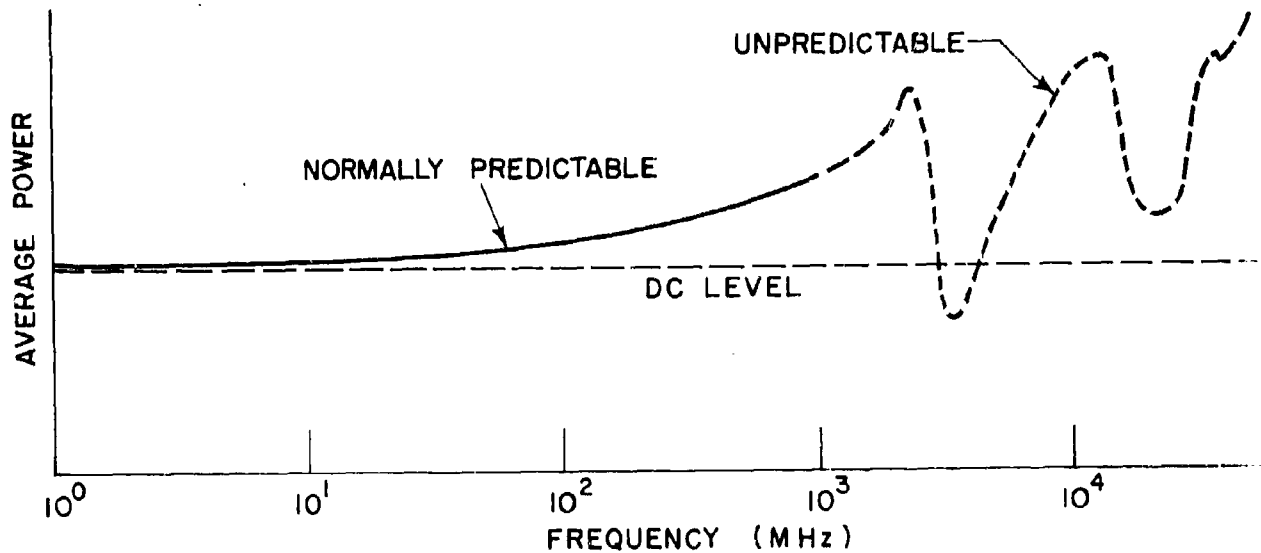


Fig. 1 Typical Response of Hot Wire EED to CW - RF in the Bridgewire Mode

$$P_{avg} = P_{peak} (\text{pulse width} \times \text{repetition rate})$$

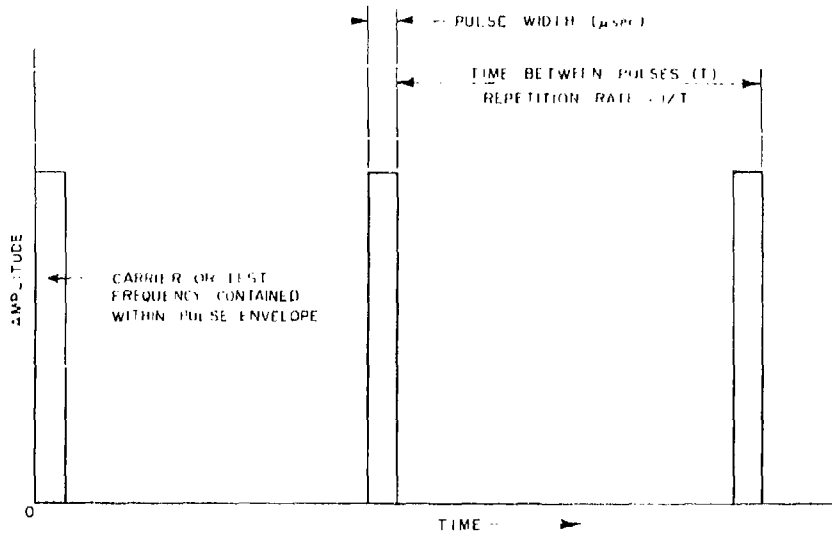


Fig. 2 - Idealized Output from Pulse Modulated Transmitter

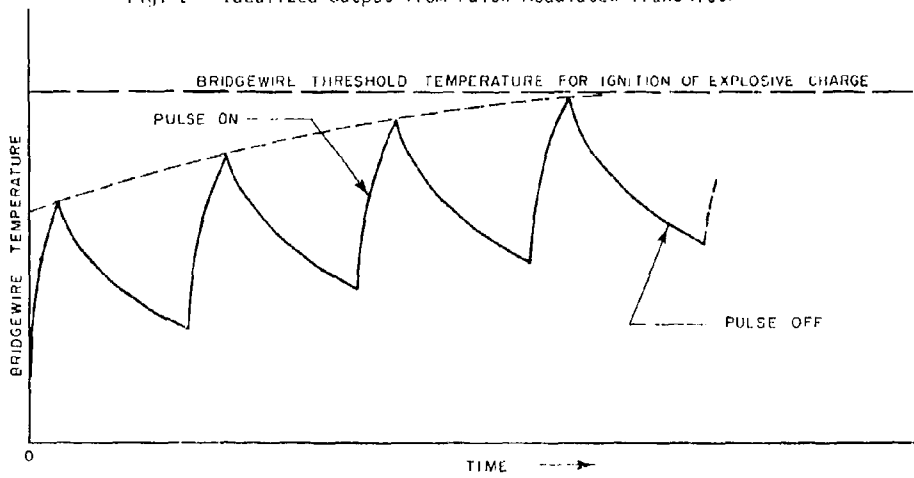


Fig. 3 - Idealized Bridgewire Temperature Versus Time Relationship [Illustrating "Thermal Stacking"]

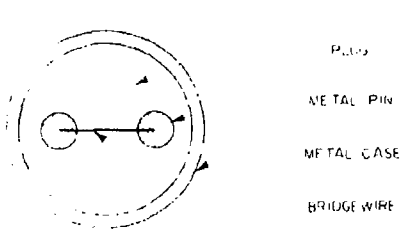


Fig. 4 - Overhanging Bridgewire

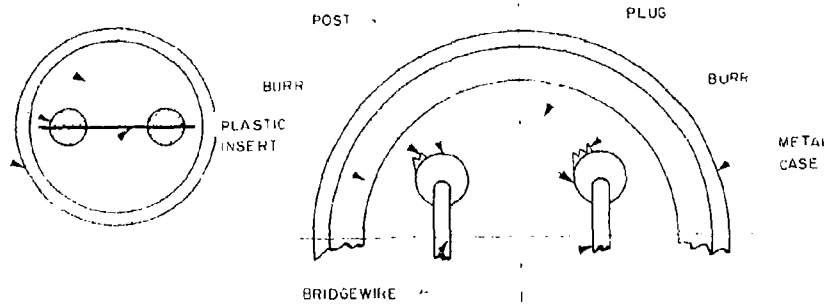


Fig. 5 - Metal Burr on Bridgewire Post

2-10P MINIATURIZATION OF OUT-OF-LINE

EXPLOSIVE SAFETY SYSTEMS\*

By R. Stresau and R. Degner\*\*

R. Stresau Laboratory, Inc. Spooner, Wisconsin

INTRODUCTION

In the usual ordnance explosive devices, the bulk or weight of the safety-and-arming mechanism is reflected in a nearly equivalent reduction of explosive payload. Reduction of dimensions of fuze mechanisms can be expected to lead to increased effectiveness of many weapons. In addition, the availability of smaller safety and arming devices would make it possible to introduce out-of-line safety in auxiliary devices where it is desirable, but where space or weight limitations have eliminated it.

The lower limits of safety and arming device dimensions are related to the dimensions of the smallest explosive components which are available and can be relied upon to initiate subsequent components and charges. The displacement necessary for acceptable safety, the thicknesses of barriers and gaps necessary to isolate explosive components, and the wall

\*Based on work performed for the U.S. Naval Ordnance Laboratory Corona, California under Contract No. NL23(62738)31089A.

\*\*Mr. Degner's present address is University of Wisconsin, Madison.

thicknesses necessary to contain the explosive effects in accordance with safety requirements<sup>1</sup>, are each proportional to the diameter of the detonator. Thus, the volume and hence mass of the explosive train and immediately associated inert assembly is proportional to at least the square (and, to the extent that column lengths can be scaled, perhaps to the cube) of the detonator diameter. At least to some extent, the smaller mass of the moving parts and the shorter distance through which they need be moved (between safe and "armed" positions) should be reflected in similar reduction of bulk and mass of the mechanical components of the safety and arming device. Of course, such potential gains will be realized only after considerable invention, research, and development of mechanical arming systems, which will not be considered in the present discussion.

The smallest detonators and leads in current ordnance use are about 0.1 inch in diameter.<sup>2</sup> Difficulties experienced by both the Army and the Navy with 20 mm fuzes employing detonators of this size have resulted in a widely-held opinion that this size is the smallest compatible with reliable initiation of "booster" type explosives, which are defined by the Navy as no more sensitive than tetryl and by the Army as no more sensitive than RDX. Recent developments, including that of MDF or Missilcord, which, even when loaded with much less sensitive explosives than RDX or tetryl, propagates reliably with charge diameters of a few hundredths of an inch, that of

the "Minidet"<sup>2</sup> and other small detonators by a number of organizations, suggest that this opinion should be reconsidered.

Recent developments, including that of Mild Detonating Fuze\*, suggest that fuze explosive trains and other high explosive systems can be made using explosive components of much smaller dimensions than those currently used in ordnance<sup>2</sup>. Since the total bulk and weight of many such systems is nearly proportional to that of the explosive components used, such smaller components would remove a barrier to miniaturized fuzes and other systems. Such miniaturized fuzes, in turn, could result in improved performance in smaller ordnance by making more space available for main charge explosives, improved reliability in larger ordnance by virtue of increased opportunities for redundancy, and substantial performance gains in ordnance of various types as the result of the more sophisticated systems which are possible.

In most cases where smaller components offer advantages, it is necessary to transfer detonation from such small components to the main charge of a high explosive weapon. Most of the advantages of the smaller components would be lost if safety policy prevented their use in direct communication with

\*Mild Detonating Fuze<sup>1</sup> and MDF are DuPont trademarks for metal jacketed detonating cord with linear explosive densities of one to twenty grains per foot. "Minidet" is also a DuPont Trade Mark. MissileCord is a trade mark of the Ensign-Bickford Co. for metal covered detonating cord.

the main charge. The safety policy of the Navy, as now interpreted (at least by some), precludes the use of explosives more sensitive than tetryl in such direct communication. Explosives which are useable in such positions, but which can be initiated by means of standard fuze explosive components, are referred to as "booster explosives". The booster explosives most commonly used in Naval Ordnance, tetryl and CH-6, will detonate quite reliably in rather small size columns, if well confined, as in MDF. However, the transfer from such small columns to larger charges is not particularly reliable unless it is accomplished quite gradually in a tapered lead or by relatively small stepwise increases.

To attain the full advantage of small explosive components, it should be possible to initiate a booster or relatively large lead directly. On first consideration, it would seem that a booster explosive which can be initiated by a smaller source than can tetryl is a contradiction of terms, since such an explosive would have to be more sensitive than tetryl. If the criterion of sensitivity were the size of source for threshold initiation, this would be unarguable. The criteria which have been used to characterize sensitivity in the application of Navy policy have been impact sensitivity tests, such as those with ERL Type 12 tools<sup>3</sup>, and gap tests, such as the Naval Ordnance Laboratory (White Oak) Small Scale Gap Test (SSGT)<sup>4</sup>. In such tests, the quantity of explosive exposed to the experimental stimulus remains nearly constant, while the



intensity of the stimulus is varied. In contrast, initiation by a small source, such as MDF, involves a stimulus of nearly the same intensity of that delivered by a fuze component of currently used dimensions, but the quantity of explosive exposed to the stimulus is much reduced. Even without consideration of the mechanisms involved, it is reasonable to expect that the susceptibilities of various explosives to initiation by such differing types of impulse should be something other than direct. There is no reason to expect that an explosive which can be reliably initiated by means of smaller MDF than can tetryl would be automatically more sensitive than tetryl in a gap or impact test. Part of the work described herein was the development of an RDX base explosive which, when loaded into explosive components of "standard" dimensions, can be reliably initiated by means of a small source, but which is less sensitive than tetryl according to impact or gap tests.

Several requirements must be met in developing any safety and arming fuze. Chief among these is the policy of the Navy concerning the safety and arming of fuzes which prescribes ". . . a safety-failure rate not in excess of one in one million." (Reference 2). At the same time, reliability in the 99.99% range on a 95% confidence level must be established in the armed position. Practical considerations in developing a safety and arming device would also include an allowance for clearance between the moving parts and a means of preventing the loaded explosives from falling out of the detonator.

Included herein is a report of an experimental feasibility study of a miniaturized safety and arming system utilizing small detonators and SPX-2 boosters which would satisfy the requirements mentioned above.

### **EXPLOSIVES ADAPTED FOR USE IN MINIATURIZED EXPLOSIVE SYSTEMS**

As has been indicated earlier in this paper, an explosive which is capable of detonation when initiated by a very small source adds flexibility in the design of miniaturized explosive systems. Most explosives currently used for leads and boosters impose severe limitations in this respect. An early part of the current study was the development of an explosive (which has been called SPX-2) which is believed to be acceptable as a "booster" explosive according to the usually applied criteria, but which can be initiated by sources of quite small dimensions. More recently, other explosives (notably hexanitrostibilene (HNS)) have been developed which are understood to inherently possess these characteristics. However, since the experimental work to be described was performed using SPX-2, the development of this material is described.

#### **Qualitative Theoretical Considerations**

Detonation has been described as a reactive shock. A more detailed description includes a nonreactive shock followed by a reaction zone of finite thickness. In a stable detonation, the inherent losses associated with shock waves are exactly

compensated by the chemical energy liberated by the reaction.

Stable detonation, where the advancing shock front is a plane surface, so that only movement perpendicular to the shock front need be considered, is referred to as "ideal detonation." Conditions at the end of the reaction zone (usually referred to as the "Chapman-Jouguet point"), as well as the rate of propagation of an ideal detonation, are determined by the density and available chemical energy of the unreacted explosive and the equation of state of the reaction products.

In a "nonideal" detonation, movement in directions other than that of propagation have significant effects. The two common "naturally occurring" situations that result in nonideal detonation are found (1) in a charge so small that the effects of expansion at boundaries are transmitted to the Chapman-Jouguet point at the charge axis, and (2) in the expanding detonation in a larger charge which results when it is initiated by a smaller charge.

Eyring and his associates (Ref. 7) showed that the radial movement in cylindrical charges results in curvature of the detonation front and they related the conditions and stability of such detonation to the ratio of the reaction zone length of the explosive to the radius of this curvature. This relationship of detonation conditions and stability to front curvature, quite obviously also applies (though transiently) to the expanding wave that results when a large charge is

initiated by means of a smaller charge.

Eyring and his associates proposed that the reaction that occurs between the shock front and the Chapman-Jouguet point in a granular explosive is a deflagration at the surfaces of the grains. This "surface-burning theory," which is supported by a wide variety of experimental data (Refs. 8, 9, 10, and 11), implies that reaction zone lengths should be nearly proportional to particle size. It follows that the critical source size for initiation of an explosive should be nearly proportional to its particle size.

The fact that the most effective desensitizers for RDX are waxy materials may, in terms of the experimentally verified "hot spot" theory of initiation published by Bowden and Yoffe (Ref. 12), which is mutually supporting with the Eyring surface-burning model of detonation, be interpreted as an indication that the lubricating properties of these materials inhibit the localized heating at grain boundaries. This lubrication might be expected to have more effect upon the pressure dependence of the reaction zone rate than upon the ideal reaction zone length. It might, then, be expected that waxy desensitizers should have more effect upon gap or impact sensitivity than upon susceptibility to initiation by small high-intensity sources.

The foregoing suggests that RDX of fine particle size should be more susceptible to initiation by sources of small dimensions, and that this property should not be greatly affected by desensitization with waxy substances, such as

stearates. As the experiments described later in this paper have shown, this appears to be correct.

To prepare RDX of fine particle size, the RDX was dissolved in boiling acetone and the solution poured into chilled distilled water while stirring the water vigorously.

The process used to coat the finely precipitated RDX was adapted from that used in the manufacture of CH-6 and the NOL/W Varicomp mixtures. After washing to remove the acetone and removing excess moisture by either decanting or filtering, but without drying, a 100 gram batch of the precipitated RDX was added to a solution of sodium stearate in distilled water and stirred to form a slurry (a small amount of oil soluble red dye had been added to the stearate solution). While continuing to stir, a distilled water solution of calcium chloride was added gradually, precipitating the calcium stearate and leaving a sodium chloride solution which was removed by washing on a filter. (The oil soluble dye, of course, followed the stearate and colored the resulting product pink. The uniformity of the color is visible evidence of the uniformity of the coating.) After filtering, the material was dried in an aluminum pan at about 80°C. Three SPX's (Spooner explosives), listed in Table 1, were made for use in these experiments.

In the determination of the reliability of detonation transfer between small charges and SPX, the same difficulties are encountered which led to the development of the Varicomp<sup>13</sup> method for such determinations with "standard" sized explosive components. To apply the Varicomp technique to small charge-SPX transfers, a series of explosives, similar to SPX except

that larger proportions of stearate were used, was prepared. Designations of these mixtures were SVC-followed by a number indicating the number of parts of sodium stearate used per 100 parts of RDX. The other materials prepared at this laboratory have been included in the following table of the SVC series.

TABLE 1. The SVC Series For Varicomp Methods

SVC No.	Other Designation	Percentage Calcium Stearate <sup>a</sup>
SVC-0	XF-2	0
SVC-1.5	SPX-2 & SPX-2a	1.47
SVC-3	SPX-1	2.88
SVC-6		5.62
SVC-12 & SVC-12a		10.6
SVC-24		19.1

<sup>a</sup> Assuming 100% yields

SVC-12a was made because SVC-12 was somewhat lighter in color and somewhat more sensitive than had been anticipated, indicating that it may have contained somewhat less stearate than intended. SVC-12 was retained as a useful member of the SVC series.

#### Sensitivity Tests of Explosives

The explosives prepared in the course of the work described herein were compared with standard military explosives by means of the "Spoooner Small Scale Gap Test" (SSSGT), which is a "poor man's version" of the Small Scale Gap Test (SSGT) standardized by Ayres<sup>4</sup> at NOL/W, and with respect to their susceptibility to initiation by means of Mild Detonating Fuse. In addition, to simulate an application more closely than does the SSSGT, the "MicroScale Gap Test" (MSGT) was devised for calibration of the SVC series.

Loading Conditions. With one or two exceptions, all of the explosives used in these experiments were loaded at 10,000 pounds per square inch. Increments were measured volumetrically following the general rule that the length-diameter ration of an increment should not exceed one. Because of the low bulk density of the fine particle explosives prepared at this laboratory, increment lengths of these materials were usually much shorter than this.

SSSGT. The setup shown in Figure 2 was used for the SSSGT. A one inch long steel cylinder, one inch O.D. with a 13/64 inch I.D., was loaded with the acceptor explosive. The donor explosive used in all of the SSSGT tests was a 1½ inch length of B100 LJDF (Lead Jacketed Detonating Fuse containing 100 grains of RDX per foot). The length of donor was fit flush in a wooden block and paraffin wax spacers ( in ¼ DBgs step sizes) were used as the variable. The parts of the firing test arrangement were aligned by fitting them in a paper tube as shown in the diagram. Initiation of the donor was accomplished with a blasting cap butted head-on to the MDF with spaghetti tubing.

The "gap Decibang" (DBg) series proposed by Ayres<sup>4</sup> and used in the SSGT is such a series for which the transformation function is

$$X = -10 \log G$$

where

X is the initiation intensity in  
Decibang (DBg) and  
G is the gap in inches

For the SSSGT, the same series of gap lengths was adopted, but, to avoid ambiguities resulting from its differences in detailed

test conditions from the SSGT, the sensitivity Gap Decibang unit is abbreviated DBgs rather than DBg.

MDF Initiation Susceptability. For this test, the explosive being tested was loaded in a steel cylinder (Figure 3), as in the SSSGT tests. The donor explosive was various sizes of Mild Detonating Fuze. Holes of the proper size were drilled in steel blocks and the donor length of MDF fitted flush with the surface of the block. A blasting cap butted head-on to the length of MDF donor served to initiate it. For the MDF Initiation Susceptability Test, the steps used were available sizes of MDF, 1, 2, 5, 10 and 20 grains per foot.

MSGT. A diagram of the firing test arrangement for these tests is shown in Figure 4. The explosive being tested was loaded in 3/8 inch steel cases, 1/2 inch long, with a .132 inch I.D. The correct number of Mylar spacers (.002 inch steps) and the loaded case were then fitted into the wooden location block. A 1 inch length of A5 MDF (5 grains of PETN per foot) was then inserted in the wooden block and cut off flush with the surface of the wood block when it seated on the Mylar spacers. Initiation of the donor MDF was with a blasting cap which was taped to the wooden block in a horizontal position with its side butted against the MDF.

Results of Sensitivity Tests. Experimental results are given in Table 2, which also includes some SSGT and impact sensitivity data, supplied by Ayres (Ref. 4), for comparison of SSSGT and SSGT data.



EXPERIMENTAL FEASIBILITY STUDY OF A  
MINIATURIZED EXPLOSIVE TRAIN

Having developed fabrication techniques for small detonators and an explosive, which though acceptable, at least according to our interpretation of DOD and Navy safety policy, could be initiated by such a small detonator, the combination of these in a miniaturized fuze explosive system seemed to be the next logical step. No specific requirement for such a system had been promulgated probably because the possibilities and dimensions were not known. To obtain data regarding the feasibility of such a system as well as preliminary design data, an experimental study was undertaken. Figure 5, which is a scale drawing of the system which was finally suggested as a result of this study, may also be used as a diagram to illustrate some of the variables which had to be evaluated in order to demonstrate the safety and reliability of the system and to provide design data whereby the safety and reliability could be assured.

#### Reliability Tests

Reliability of the proposed fuze train in the armed position was assessed by means of single-shot, single Varicomp explosive rundown performance tests, adapted from the single-explosive rundown performance test developed by Ayres, Hampton, Kabik, and Solem (Ref. 13). An explosive was needed that would be more insensitive than the design booster explosive (SPX-2) but could be initiated by the design detonator when the fuze train was in

the armed position. SVC-24 was found to have these characteristics. The Spooner small-scale gap test (SSSGT), the micro-scale gap test (MSGT), and the MDF initiation susceptibility test were used to define their relative degrees of sensitivity. By using the standardized Bruceton analysis (Ref. 14) these data were plotted on probability paper to find the maximum stimuli needed to initiate the more sensitive explosive (SPX-2) and the minimum stimuli needed to initiate the more insensitive explosive (SVC-24) at different degrees of reliability (both curves were plotted at the 95% confidence level). The initiation of the booster loaded with SVC-24 by the design detonator indicated a minimum reliability of 5% at a 95% confidence level (1 for 1). This minimum reliability prediction was combined with the curve of the minimum stimulus needed to initiate SVC-24 as a function of reliability to find the minimum value of the stimulus produced by the design detonator. This value was then combined with the plot of the maximum stimulus needed to initiate the design explosive (SPX-2) at various levels of reliability to predict the reliability with which the design detonator will initiate the design booster.

As can be seen from Graph 1, when SSSGT data are used to characterize the sensitivities of SPX-2 and SVC-24, one success in the trial with SVC-24 would be sufficient to predict reliability with SPX-2 of well over 99.99% at the 95% confidence level. This estimate of reliability is a three-step conservative estimate: (1) the plotted response of the less sensitive explosive is the minimum at the 95% confidence level, (2) the plotted stimulus is the minimum at the 95% confidence level that would

produce such a response, and (3) the reliability so determined is the minimum at the 95% confidence level with which this stimulus will initiate the design boosters.

The SPX-2 and SVC-24 response curves shown in Graph 2 are based on 20-shot and 10-shot Bruceton tests, respectively. A logarithmic scale was used as the normalizing function of the MDF sizes, because the step sizes approached a logarithmic progression and also because a logarithmic plot is considerably more conservative than a linear plot. A two-step conservative estimate (used in Ref. 13 for predicting reliability from single explosive rundown performance tests) shows reliability well over 99.99%. A three-step conservative estimate gives reliability of 99.7%.

The plot of SPX-2 response in Graph 3 is based on a 10-shot Bruceton test. The mean was computed to be at 0.019 in. of Mylar barrier, with a standard deviation of 0.00394 in. Unfortunately, the give-grain MDF used in the MSGT did not have sufficient output to initiate SVC-24; therefore, a plot of SVC-24 response was not possible from the MSGT data. However, data from the MDF initiation susceptibility test can be used to show that at a 0.000 inch gap, the maximum reliability with which A5 MDF will initiate SVC-24 is 6% at a 95% confidence level. Also, a response (one-for-one trial) with SVC-24 indicates a minimum reliability of 6% at a 94% confidence level. Using these two estimates, it can be seen from Graph 3 that the minimum reli-

ability from MSGT data in combination with the MDF initiation susceptibility test data is over 99.9%. This prediction is based on a three-step conservative estimate; one at a 94% confidence level and two at a 95% confidence level.

It is recognized that there is likely to be a great deal of skepticism about a test that predicts reliability in the 99.99% range at a 95% confidence level on the basis of one shot. It was for this reason that data from three different tests were used for predicting reliability from single-shot, single Varicomp explosive rundown performance tests. Table 3 shows the reliabilities indicated by the three tests.

TABLE 3. Summary Of Predicted Reliability

Test	Reliability (%)	Basis
SSSGT	Over 99.99	Three-step conservative estimate (each step at 95% confidence level)
MDF	Over 99.99	Two-step conservative estimate (each step at 95% confidence level)
MDF	99.7	Three-step conservative estimate (each step at 95% confidence level)
MSGT-MDF	Over 99.9	Three-step conservative estimate (one step at 94% confidence level, and two steps at 95%)

It is realized that in this type of analysis for predicting reliability a normal distribution and applicability of the tests to the proposed fuze train are assumed. However, these assumptions

are inherent in all statistical extrapolations from small sample data to the reliability and confidence levels generally stipulated in military requirements. From the three different sets of data it may be noted that, with respect to the assumption of normality, the assumptions used in the SSSGT were exactly the ones inherent in the SSGT (Ref. 4). It should also be noted that the normalizing function used in each of the other two tests was that which gave the most conservative estimate of reliability.

With regard to the applicability of the three tests to the proposed fuze train, note that two aspects of sensitivity have been considered. In the SSSGT and MSGT, source intensity was varied and source size remained constant, while in the MDF initiation susceptibility tests, the source size was varied and the intensity remained constant.

In view of the foregoing discussion, it is believed that the reliability estimates from single-shot, single Varicomp explosive rundown performance tests, as used in this program, have more validity than estimates based on 20-, 50-, or even 100-shot tests where a single variable is used. It has been pointed out that each estimate from a test of this kind is based not only on the one test of the proposed system, but on the 200 trials used to characterize the design explosive and the Varicomp explosive.

Firing Arrangement. One basic firing setup was used in all the safety and reliability tests. A  $\frac{1}{4}$ -in.-diameter Delrin rod was

drilled centrally with an 0.050-in.-diameter drill to align the detonator with the center of the  $\frac{1}{4}$ -in.-diameter booster when they were placed in the angle of a steel strap bent to a right angle, as shown in Figure 6. Spring-type clothespins were used to hold the components firmly against the angle during firing. For transverse-displacement tests, the Delrin rod (holding the detonator) was displaced the desired distance by placing a piece of feeler gage stock between it and one side of the angle.

The discharge of a 2.0 uF condenser, charged to 90 volts, was used to initiate the detonators.

Boosters. Three types of booster were used in the experiments. Gilding metal blasting cap casing (0.272 in. O.D., 0.006 in. wall) in  $\frac{1}{8}$ -in.-lengths was loaded with single increments of SPX or SVC explosive for use in the detonator output design tests. Seamless mechanical tubing (0.250 in. O.D., 0.196 in. I.D.) in  $\frac{1}{4}$ -in.-lengths was loaded with SPX-2 at 10 kpsi for use in the barrier safety tests. The results of the barrier safety tests led to the design of the booster shown in Figure 7, which was used in all subsequent experiments. Two procedures were used for loading these boosters. Most were loaded in a single increment (from the large end, of course), but for the last few experiments, the lead was reconsolidated from the small end, and sufficient explosive was added to fill flush.

Detonator Output Design Tests. Early experiments of this project were directed toward the development of design criteria for a

detonator of small dimensions with sufficient output to reliably initiate SPX-2. The criterion used to establish the output of a detonator as sufficient to reliably initiate SPX-2 was the single-shot, single Varicomp (SVC-24) explosive run down test as described above. Dent tests and experiments with other Varicomp explosives of the SVC series were used in some of the earlier detonator design experiments, mainly as indicators of effects of changes in explosive composition, preparation, and loading pressure upon output.

A few preliminary experiments were performed to determine whether the observation reported in Reference 15, that PVA lead azide has its maximum output when pressed at very high pressures, also applies to the general design shown in Figure 1. These, as mentioned in an earlier paragraph, were fabricated using a somewhat different sequence of operations. They also had flash charges of basic lead styphnate or a mixture of lead styphnate and lead azide, which were inserted in the loaded case before the ceramic plug and held under a consolidating pressure of 200 psi during the curing of the resin cement which held the case to the plug. In these experiments, output of detonators loaded at 50 kpsi were more variable in output than those loaded at 15 kpsi and 10 kpsi, which was interpreted as a "dead pressing" effect. Column lengths in these preliminary experiments were varied between 1/16" and 1/4" with no significant effect upon output. In a few, with PVA lead azide intermediate charges and RDX/XF-2 base charges, the effect of RDX upon output, as measured

in dent tests, was negligible. Detonators with milled PVA lead azide (MF-1) were more consistent in dent output and somewhat higher in average output as measured by the dent tests. Some of these, with azide columns only 75 mils long, initiated SVC-6 and SVC-12(a). The results of these preliminary experiments were sufficiently encouraging that the more systematic program described below was undertaken.

On the basis of the preliminary experiments described above, it was decided to standardize loading pressure at 10 kpsi, and to use milled PVA lead azide as the "intermediate" charge in which the transition to detonation is expected. Other experiments showed that the milled PVA lead azide (MF-1) could be reliably initiated by a bridgewire, so the functions of the "flash" and "intermediate" charges could be combined in one charge, which has been referred to as the "flash" charge. All subsequent experiments of the work described herein were performed with detonators loaded at 10 kpsi and with flash charges of PVA, MF-1 lead azide. Data obtained in these experiments are given in Table 4.

In Table 4, a general trend toward increasing effectiveness in the initiation of SVC explosives may be noted as the code numbers of the detonators increase. With the MFTD 5, detonators, scores were 8/10, 7/10, and 2/3 for SVC-24 pressed at 2.5, 5, and 10 kpsi, respectively. Lower limits of reliability (from binomial statistics, see Reference 13) estimated at 95% confidence from these scores are 49%, 39%, and 22% respectively. These



estimates are all appreciably higher than the 5% which can be estimated from a 1/1 score and which was used in the single shot analyses described earlier in this paper and illustrated in Graphs 1, 2, and 3. Using these higher values of reliability for the initiation of SVC-24 in these analyses will lead, of course, to either estimated reliablilities appreciably higher than the 99.99% plus or to higher confidence levels than the three-step 95% confidence of the single-shot analysis. Detonators of this design and loading were used in all subsequent experiments.

Gap Tests with SPX Loaded Boosters. Most of the experiments which had been performed up to this point had been performed with bare ended detonators and leads and with gaps minimized. However, in recognition of the requirement for end closures and clearances in a real S-A device, measurements of the effects of closures, gaps, and their interactions were undertaken.

With bare-ended MFTD 5 detonators, the maximum gap across which boosters loaded with SPX-2 at 10 kpsi could be initiated was 35 mils. A thin coating of epoxy resin on the output end of the detonator increased this to 40 mils, and a heavier epoxy coating raised it to 70 mils. These results, though based on rather few tests, indicated that the closure can be an important factor in transmission of detonation across gaps for miniaturized detonators, as well as for larger charges. Where closures play a role in transmission of detonation, an optimum thickness of any closure material can be anticipated, for which the gap is maximum. Since its thickness can be only qualitatively

controlled, epoxy resin is a rather poor material to use in any investigation of the effects of closure thickness.

A few experiments were performed using aluminum at hand (kitchen-type foils and disposable utensils,) including foils 1.0 mil, 1.5 mils, and 4 mils thick. MFTD 5 detonators with 1- and 1.5-mil aluminum end closures (cemented with contact cement) initiated boosters like those shown in Figure 6 across 0.105 in. air gaps two out of three times in each case. With 4-mil aluminum closures, the same detonators initiated the boosters across 0.035-in. air gaps, but failed when the gap was increased to 0.040 in.

Explosive System Design Tests with Varicomp Explosives. An important motive for the development of the Varicomp concept (Ref. 13) was the complex interaction of the variables in an explosive system. Often the variables interact to result in optimum gaps, barriers, or loading densities for a given combination of other variables. Under such circumstances, an estimate of reliability from tests in which one or another of these variables is used to penalize the system may be quite misleading. The SVC series of Varicomp explosives was used in a series of short experiments to investigate some of these interactions.

Detonation was transmitted to boosters like those shown in Figure 7 (loaded with SVC-12a) through 0.014-in. aluminum barriers four out of five times, but failed with 0.018-in. aluminum barriers. MFTD 5 detonators were used in these tests and the boosters were loaded at 10 kpsi.

In an air-gap test with the components described in the foregoing paragraph and with a 1.5-mil aluminum closure cemented to the detonator, the score for an 0.050-in gap was four out of six.

With the 1.5-mil aluminum end closure cemented in place, the score for initiation of the boosters loaded with SVC-24 at 10 kpsi was only one in three. When the closure disk was pressed against the end of the explosive column at 10 kpsi, the score was improved to five out of seven. With this same detonator (MFTD 5 with an aluminum closure disk contact-cemented in place at 10 kpsi) and the booster shown in Figure 7, loaded with SVC-24 at 10 kpsi, the score with a 3-mil air gap was six out of seven, and with a 6-mil gap, one out of six.

In all previous trials, the booster had been loaded from the output end. When the lead was reconsolidated from the input end, an appreciable increase in sensitivity was apparent. With the same combination of components, mentioned immediately above, for which only one detonation of the booster was observed in six trials, boosters with reconsolidated leads at 10 kpsi were initiated on the first trial at gaps of 0, 6, 10, 20, 25, and 28 mils, and there were no failures in this range. At 30 mils, failures were observed in two consecutive trials. This increase in sensitivity at higher loading density has been observed in other systems where the detonation transfer vehicle is the bottom of a detonator case, or a closure disk or other flying fragments. It may be explained in terms of improved shock or mechanical impedance match between the explosive and the fragments as the density of the explosive is increased.

To the extent that the basic assumptions inherent in any statistical extrapolation of detonation transfer data may be accepted, the foregoing data indicate that a detonator of the MFTD 5 design and loading, with a closure disk of 1.5-mil aluminum applied under pressure, can be expected to reliably initiate the booster shown in Figure 7 (loaded with SPX-2 and reconsolidated from the input end at 10 kpsi) with a reliability better than 99.99% at the 95% confidence level across air gaps ranging from zero to 28 mils.

The choice of Varicomp explosive for the barrier test was somewhat unfortunate in that the SVC-12a is so close to SPX-2 in sensitivity that rather large samples are necessary to establish by the single Varicomp explosive rundown test (Ref. 13) reliabilities and confidence levels that are acceptable for missile systems. The small quantity of data obtained by the analysis described in Reference 13 indicates that, with a 14-mil aluminum barrier, an MFTD 5 detonator will initiate SPX-2 with a reliability of at least 99.8% at the 95% confidence level (two-step estimate). Although this demonstrated reliability is somewhat lower than would be desirable, the 14-mil barrier is much thicker than would be suggested in a miniaturized system.

#### Safety Tests

A safety criterion which has been applied to fuze design is that "the probability of safety failure shall be less than one in a million." When such general criteria have been stated, they are not generally accompanied by definition of "safety failures" or by experimental or analytical procedures whereby such safety is to be demonstrated. We have never heard anyone seriously suggest the firing of the detonators in two million

plus unarmed fuzes which would be necessary to demonstrate such safety at a reasonable confidence level. MIL-STD-315<sup>1</sup> calls for progressing arming tests, using either the Bru ceton or Probit experimental and analytical procedures, but indicates 99% safety as an acceptable level. In this study, a technique has been used (see Graphs 4 and 5) which is believed to be more conservative than either the Bru ceton or Probit method and the results have been used to adjust the design to the "one in a million safety failure probability" level.

Barrier Safety. The barrier safety test was carried out to determine the amount of steel barrier needed between an MFTD 5 and a booster of SPX-2 to assure the required degree of safety from initiation by shock transferred through the booster case. Because the possibility existed that the radial confinement of the case might increase the effective sensitivity of the booster, the charges for this series of experiments were loaded into 1/4-in. lengths of steel tubing, 1/4 in. OD and 0.196 in. ID. All charges were loaded with SPX-2 at 10 kpsi.

MFTD 5 was used to initiate the booster through an annealed spring-steel barrier. In 10 trials with 0.005-in.-thick barriers, all 10 boosters detonated. In 10 trials with 0.010-in. barriers, all boosters were intact. The statistical lever technique outlined earlier in this report was used to determine the barrier thickness needed to meet safety standards. As indicated in Graph 4, a steel barrier 90 mils or more thick is required to assure a safety failure rate of less than one in a million at a 95% confidence level. For a safety test, the

logarithmic normalizing function assumed in this construction is more conservative than a linear function.

The results of the barrier safety test were employed to design a booster that could be used as the output component of a miniaturized system to be used in continued experiments for establishing the safety and reliability of such a system. This booster (Figure 6) was designed before the project technician was aware of the requirement for a safety failure rate of less than one in a million. The 1/32-in. minimum barrier thickness corresponds with 99.9% safety at the 95% confidence level, which is appreciably better than the safety level most frequently mentioned as an objective in one of the most widely quoted references in this area (Ref.9). However, the thickness of the barrier between the deto-nator and the booster explosive when the detonator is in the safe position (as determined by the analysis discussed in the following paragraphs) is well over the 90 mils needed for a safety failure rate of less than one in a million at the 95% confidence level.

"Progressive Armed" Safety Test. A test was performed to determine the amount of transverse displacement from the armed position between an MFTD 5 and the booster shown in Figure 5 that would be needed to attain the required safety failure rate of less than one in a million at the 95% confidence level. In 10 trials at 0.040 in. displacement the booster explosive was unaffected.

These data were plotted in logarithmic probability coordinates (Graph 5), using the statistical lever technique

described previously. The graphical analysis indicates that a safety failure rate of less than one in a million at the 95 % confidence level can be attained with a transverse displacement of 0.110 in. Here, as with the barrier test, the assumption of a logarithmic normalizing function is more conservative than is the assumption of a linear normal distribution function.

#### A Suggested Small-Explosive System Design

Figure 5 shows all the critical dimensions of a miniaturized explosive system in which the data in the preceding section (Results and Discussion) have been applied. In the safe position, the data indicate a safety failure rate appreciably less than one in a million at the 95% confidence level. In the armed position, the reliability of each channel is two-channel redundancy resulting in a failure rate of less than one in a hundred million.

The system shown is only one of a large number that might have been suggested. System configuration is best determined in terms of the mechanical requirements of an S-A device. These experiments have shown that a detonator 1/4 in. long by 1/20 in. in diameter will reliably initiate SPX-2, and that safety in accordance with Navy policy can be attained with the transverse displacement of such a detonator by less than 1/8 in. The experiments have also demonstrated that such reliability and safety is compatible with reasonable design practices with respect to closures, clearances, and manufacturing tolerances. The exploitation of the possibilities demonstrated should be a challenge to the ingenuity of designers of fuzes and S-A devices.

## CONCLUSIONS

The miniaturization of fuze explosive trains offers substantial opportunities for improvement of ordnance. The greatest gains in this respect can be realized by the development of new design criteria, fabrication techniques, and evaluation procedures. Although it is to be anticipated that the effort to develop such criteria, techniques, and procedures will lead to invention, no such invention is necessary to realize very substantial benefits from miniaturization, since all essential concepts exist. The present need is for the detailed data whereby designs may be optimized, evaluation programs outlined, and production standards specified.

An electrically initiated explosive system that meets Navy standards of safety and reliability, has sufficient output to initiate standard booster explosives in current use, and has a total volume less than  $1/2 \text{ cm}^3$  (or  $1/32 \text{ in.}^3$ ) is entirely feasible. The data herein allow appreciably more latitude than would be needed for reasonable design and indicate the existence of several opportunities for improvement of performance not exploited in these experiments, which in turn suggests that further reduction in component dimensions is probably also feasible.

## REFERENCES

1. MIL-STD-315, "Static Detonator Safety Test for Use in Development of Fuzes," Department of Defense, GPO, Washington, D.C.
2. MIL-STD-320, "Terminology, Dimensions, and Materials of Explosive Components for Use in Fuzes."
3. Wenograd, J. "The Correlation of the Impact Sensitivity of Organic High Explosives With Their Thermal Decomposition



Rates." Naval Ordnance Laboratory, White Oak, Maryland, 30 September 1957. NAVORD Report 5730

4. Ayres, J. N. "Standardization of the Small-Scale Gap Test Used to Measure the Sensitivity of Explosives," Naval Ordnance Laboratory, White Oak, Maryland, 16 January 1961. NAVWEPS Report 7342 (also private communications.)
5. Stresau, R. H., "A Theory on the Growth of Detonation From Sources of Subcritical Dimensions," Proceedings of the Electric Initiator Symposium, 1960, sponsored by the Naval Ordnance Laboratory, White Oak, and held at the Franklin Institute, Philadelphia, 29 and 30 November 1960. (Paper 17a)
6. Stresau, R. H., Jr., and L. E. Starr, Jr., "Some Studies of Propagation of Detonation Between Small Confined Explosive Charges," Naval Ordnance Laboratory, White Oak, Silver Springs, Maryland, 15 July 1950. (NOLM 10577)
7. Eyring, H., K. E. Powell, G. H. Duffy, and R. B. Farlin, "The Stability of Detonation," Chem. Rev., Vol. 45, No. 69 (1949).
8. Duff, R. E., and E. E. Houston, "Measurement of the Chapman-Jouguet Pressure and Reaction Zone Length in a Detonating High Explosive," Second ONR Symposium on Detonation, Washington, D. C., February 9-11, 1955. Paper No. 16.
9. Cook, M. A., "The Science of High Explosives," Reinhold Publishing Corporation, New York, 1958.
10. Urizer, M. J., E. James, Jr., and L. C. Smith, "The Detonation Velocity of Pressed TNT," Third Symposium on Detonation, September 26-28, 1960. ONR Symposium Report ACR-53, Vol. 2, p. 327.
11. Sadwin, L. D., R. H. Stresau, and J. Savitt, "Nonideal Detonation of Ammonium Nitrate Fuel Mixtures," Third Symposium on Detonation, September 26-28, 1960. ONR Symposium Report ACR-52, Vol. 1, p. 309.
12. Bowden, F. P., and A. D. Yoffe, "Initiation and Growth of Explosion in Liquids and Solids," Monographs on Physics, Cambridge University Press, Cambridge, England (American Branch, New York).
13. Ayres, J. N., L. D. Hampton, I. Kabik, and A. D. Solem, "Varicomp, a Method for Determining Detonation Transfer Probabilities," Naval Ordnance Laboratory, White Oak, Silver Spring, Maryland, 7 December 1961. (NOLTR 61-134)
14. Statistical Research Group, Princeton University, "Statistical Analysis for a New Procedure in Sensitivity Experiments,"

AMP Report 101.1R, SRG-P No. 40, July 1944. (USRD Report 4040)

15. Stresau, R. F., and M. H. Rowe, "Observations of the Effects of Loading Density on the Initiation and Growth of Detonation in Azides," Naval Ordnance Laboratory, White Oak, Silver Spring, Maryland, 7 December 1961. (NOLTR 61-134)

Further details may be found in the following, of which this paper is a condensation:

16. Stresau, R. H. and Degner, R. L. "SPX-a Booster Explosive Which Can Be Initiated by Sources of Small Dimensions" Naval Ordnance Laboratory, Corona, California, 1 March 1966 (NAVWEPS Report 8837).
17. Degner, R. L. and Stresau, R. H. "Small Explosive Train for Missile Safety and Arming Device" Naval Ordnance Laboratory, Corona, California, 15 May 1966. (NAVWEPS Report 8838)
18. Stresau, R. H. "Miniaturization of Out-of-Line Explosive Safety Systems" Naval Ordnance Laboratory, Corona, California, 15 April 1966. (NAVWEPS Report 8840)

#### ACKNOWLEDGEMENT

The authors wish to express their appreciation of the advice and guidance given by Mr. Robert M. Hillyer of the U. S. Naval Ordnance Laboratory, Corona, California.

TABLE 2. Sensitivity Data

Explosive	Density (g/cm <sup>3</sup> )	Loading Pressure <sup>a</sup> (lb/in. <sup>2</sup> )	NUL/WO SSGT Mean (DBg)	SSSGTa Mean (DBgs)	SSSGTa Std.Dev (DBgs)	MDF Mean <sup>b</sup> Sensitivity (Grains PETN per ft)	MSGT Mean <sup>b</sup> (in. of My- lar Barrier)	Impact (ERL type 12 tools) (cm)
RDX X334	1.62	10,000		5.13	0.19	4.1	0.001	16-35
RDX X189	1.51	10,000	3.28	5.93	0.25	1.2	0.020	
RDX XF-2		10,000						
Tetryl X102	1.58	10,000	3.63	6.30	0.18	5.5		26-50
Tetryl X102		10,000						
SPX-2	1.51	10,000		6.75	0.30	0.7	0.019 <sup>a</sup> 0.020 <sup>c</sup>	26-32
SPX-2		5,000						
CH-6	1.60	10,000		6.80	0.15	15.0		≧ tetryl
CH-6 X255		10,000	3.58					
CH-6 X267		10,000	4.54					
SPX-2 (a)	1.47	5,000		6.90	0.13	0.5	0.019	
SPX-2 (a)	1.52	10,000		7.13	0.28	0.7	0.021	
SPX-1	1.58	10,000		7.55	0.15	2.0	0.012	
SVC-6	1.52	10,000		7.80	0.10	1.7	0.010	
SVC-12	1.51	10,000		7.88	0.25	3.5	0.014	
SVC-12 (a)	1.42	10,000		8.29	0.13	2.9	0.011	
SVC-24	1.53	10,000		9.63	0.25	15.0	0.000	

<sup>a</sup>Based on 20-shot Bruceton tests.

<sup>b</sup>Based on 10-shot Bruceton tests.

<sup>c</sup>Based on 40-shot Bruceton tests.

TABLE 3. Results of Detonator Output Design Tests

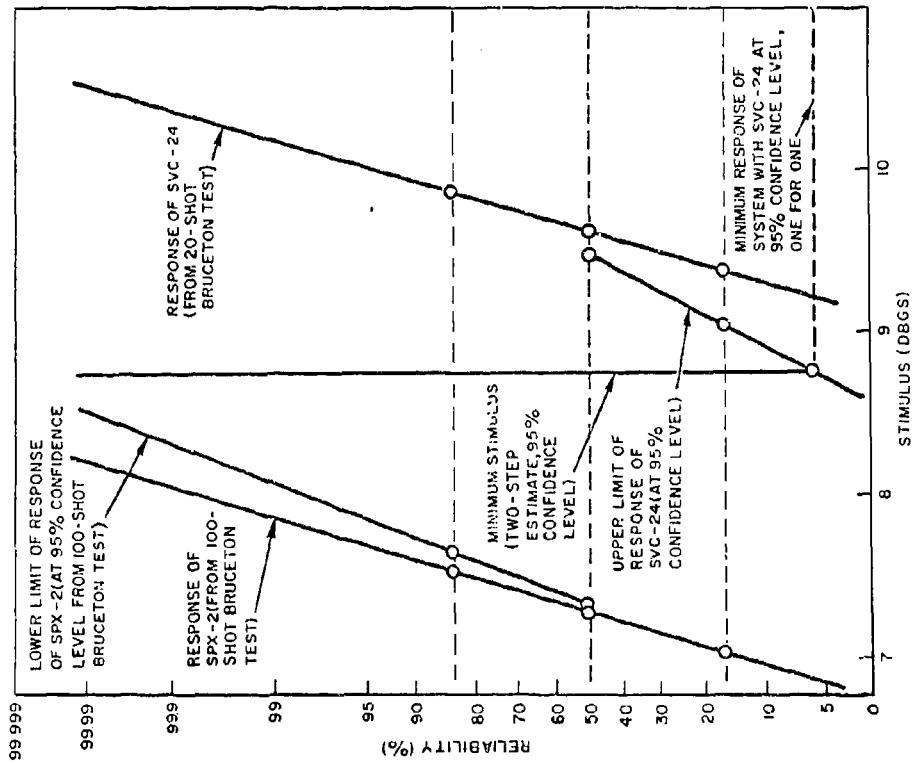
Designation	Flash charge		Base charge		Dent data			SVC pellets			SVC pellets		
	Exp.	Length (in.)	Exp.	Length (in.)	Range	Av.	Shots	Exp.	kpsi	Results	Exp.	kpsi	Results
MFTD 1	MF-1 <sup>a</sup>	0.037	MF-1	0.037	3.1-5.1	3.9	8	6	5	1 for 1	--	--	--
MFTD 2	MF-1	0.125	MF-1	0.125	9.8-15.3	12.5	11	6	10	0 for 2	12	5	0 for 1
					1.8-3.2	2.3	4 <sup>d</sup>	6	5	2 for 2	12 <sup>a</sup>	5	0 for 2
MFTD 3	MF-1	0.125	PVA <sup>b</sup>	0.125	4.5-12.9	6.3	10	--	--	--	--	--	--
MFTD 4	MF-1	0.125	X177 <sup>c</sup>	0.125	--	--	--	6	5	1 for 1	12	5	1 for 1
								24	5	2 for 2	12	10	2 for 2
MFTD 5	MF-1	0.075	X177	0.075	2.6-3.5	3.2	6 <sup>d</sup>	24	5	7 for 10	24	10	2 for 3
													2.5 8 for 10

<sup>a</sup>PVA MF-1 lead azide. (milled)

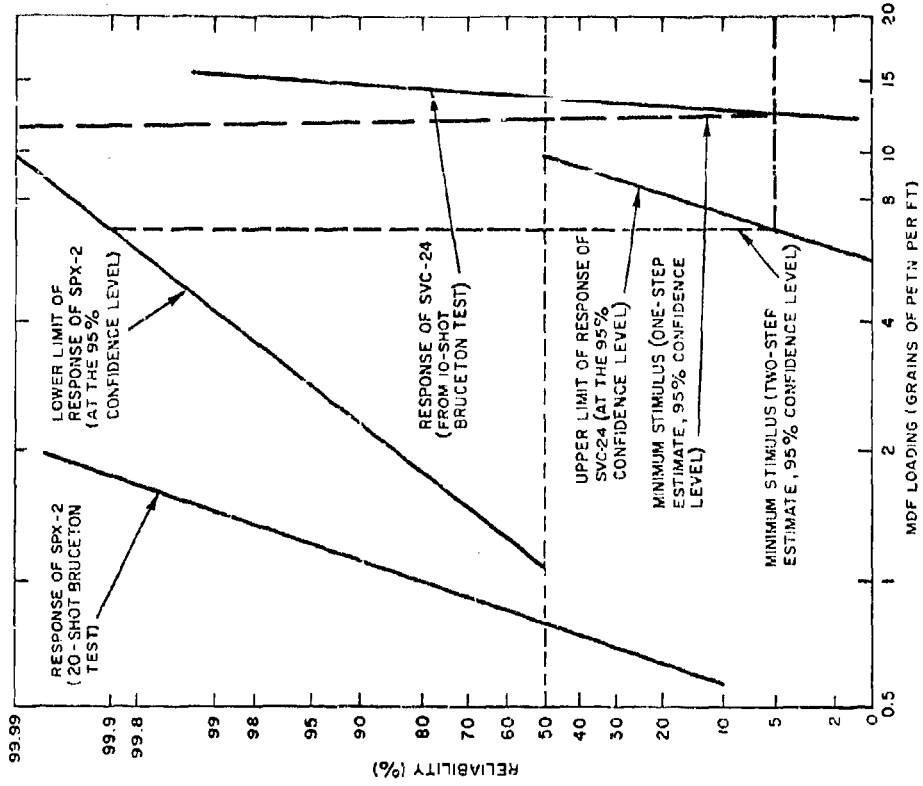
<sup>b</sup>PVA lead azide. (As received)

<sup>c</sup>RDX X177. (44 micron or smaller particle size)

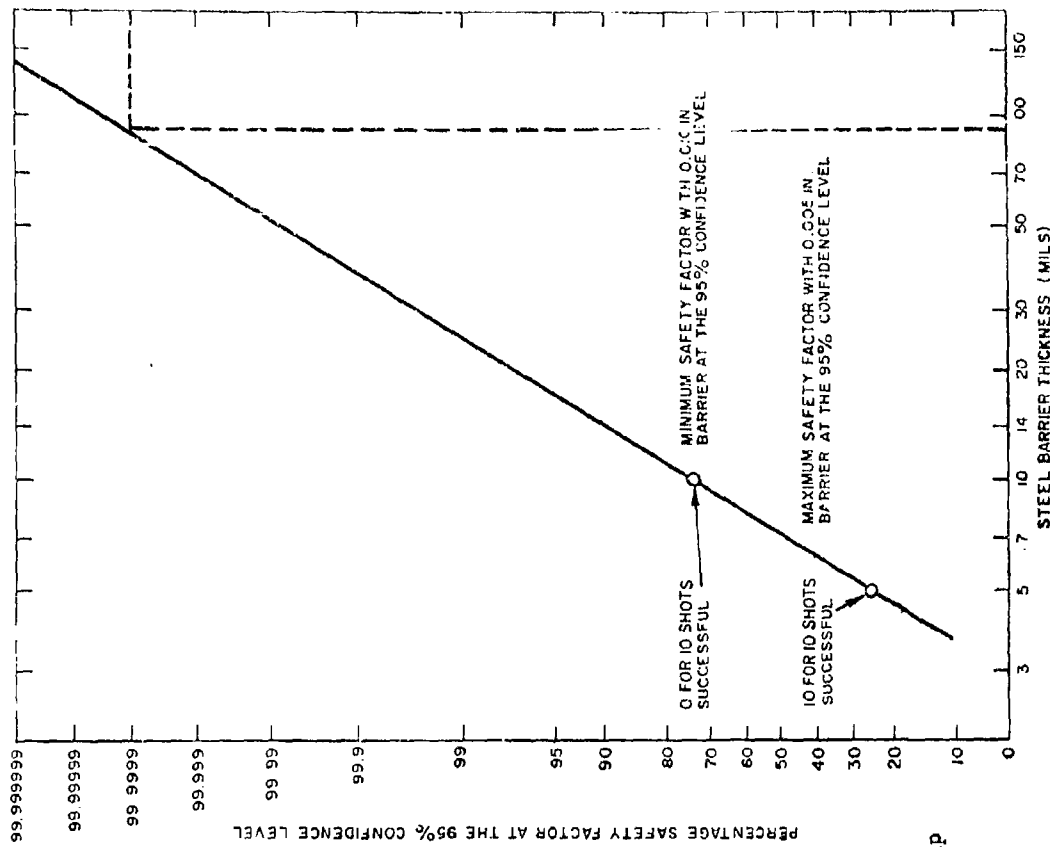
<sup>d</sup>These two dent tests were performed with spring-steel test blocks of Rockwell hardness C 48/51. In all the other dent tests low-carbon, cold-rolled-steel, flat wire (Rockwell B 65/80) was used for test blocks.



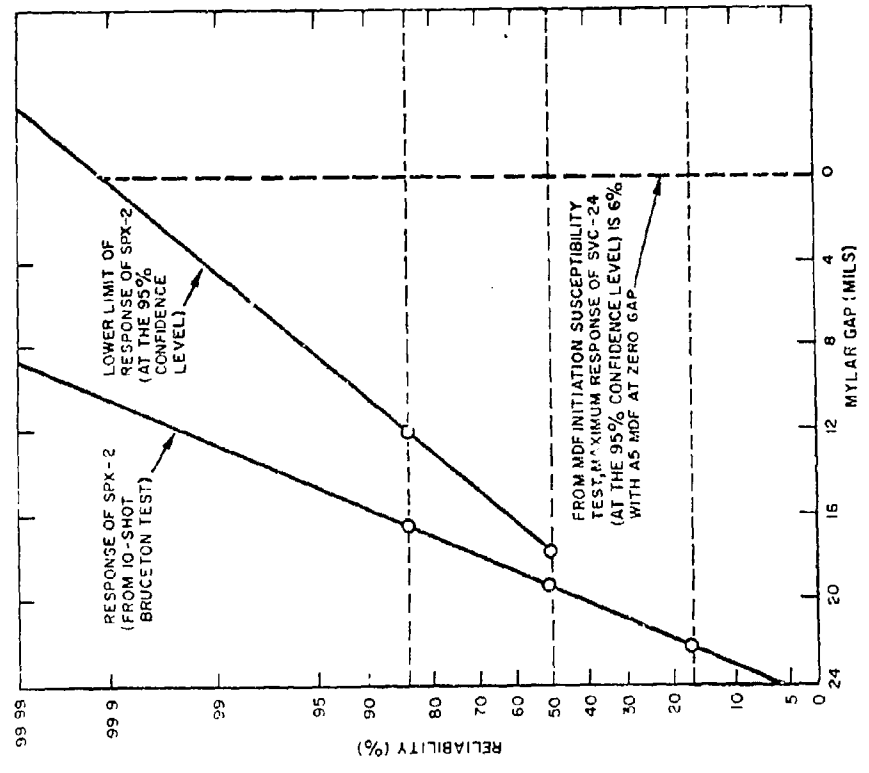
GRAPH 1. Analysis of SSSGT Data for Single-Shot, Single Varicomp Explosive Rundown Test, Using SVC-24 To Establish Reliability of System with SPX-2



GRAPH 2. Analysis of MDF Initiation Susceptibility Test Data for Single-Shot, Single Varicomp Explosive Rundown Test, Using SVC-24 To Establish Reliability of System With SPX-2



GRAPH 4. Interpretation (Statistical Lever Technique) of Data for Predicting the Amount of Steel Barrier Needed in the Unarmored Position for Various Degrees of Safety



GRAPH 3. Analysis of MSGT Data for Single-Shot, Single Varicomp Explosive Rundown Test, Using SVC-24 To Establish Reliability of System With SPX-2

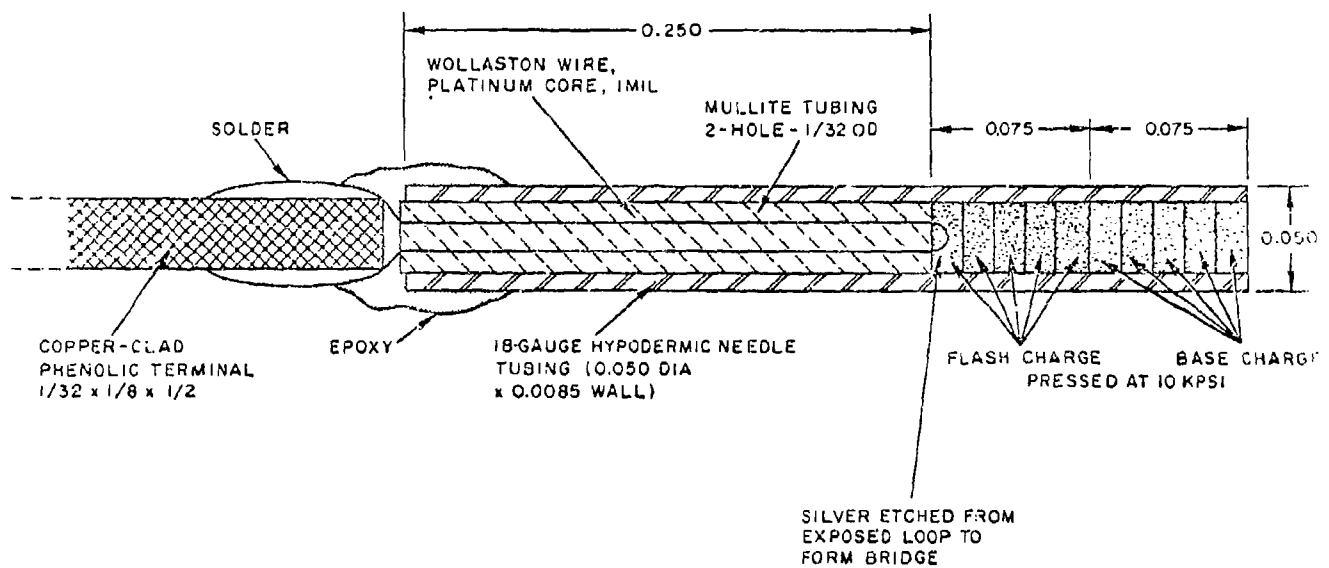
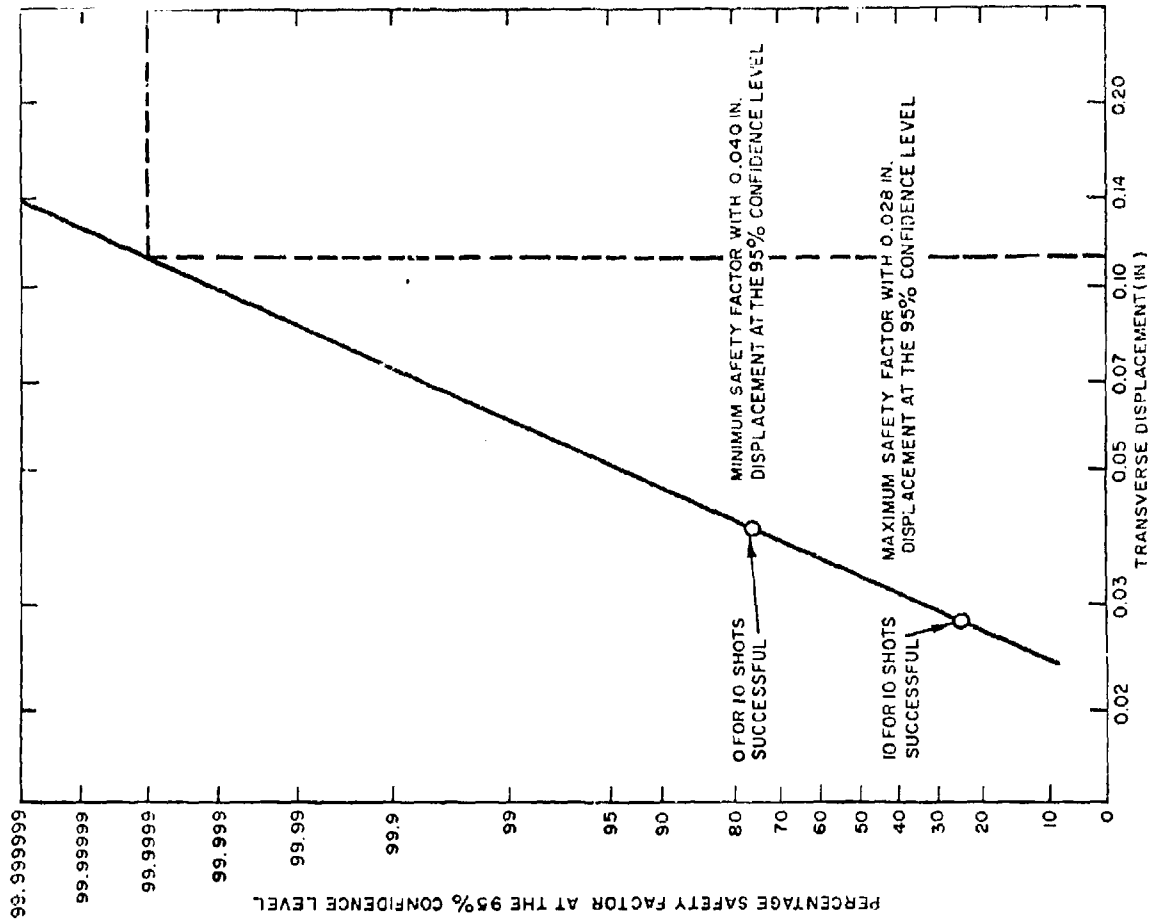


FIGURE 1. Experimental Miniaturized Fuze-Train Detonator



GRAPH 5. Interpretation (Statistical Lever Technique) of Data for Predicting the Amount of Transverse Displacement Needed for a One in a Million Safety Factor

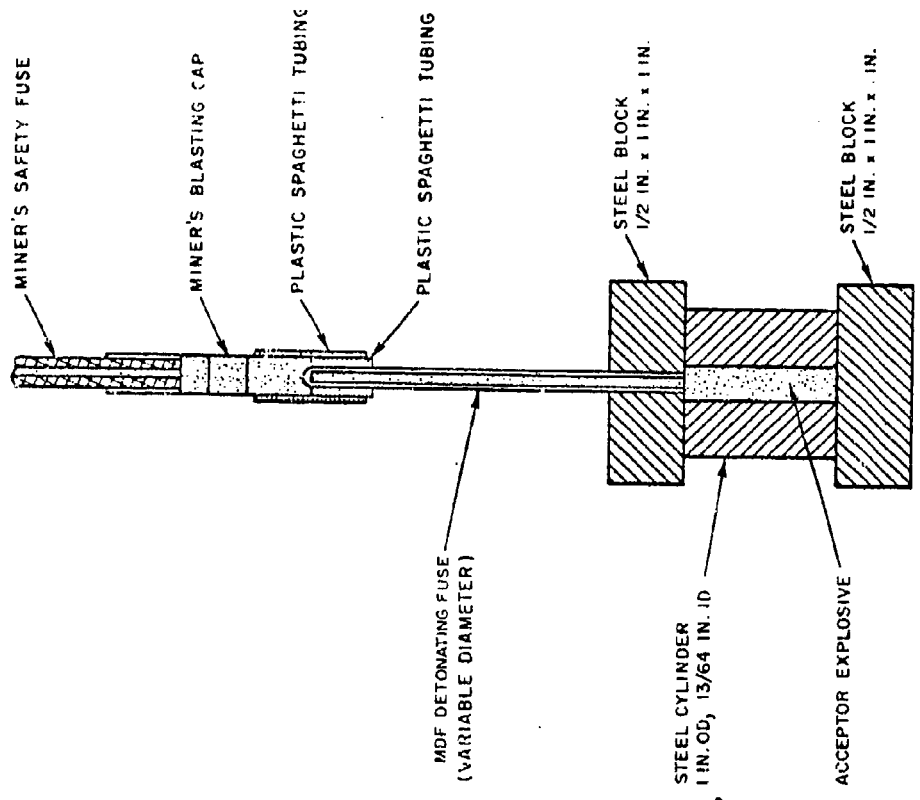


FIGURE 3. Arrangement for MDF Initiation Susceptibility Test

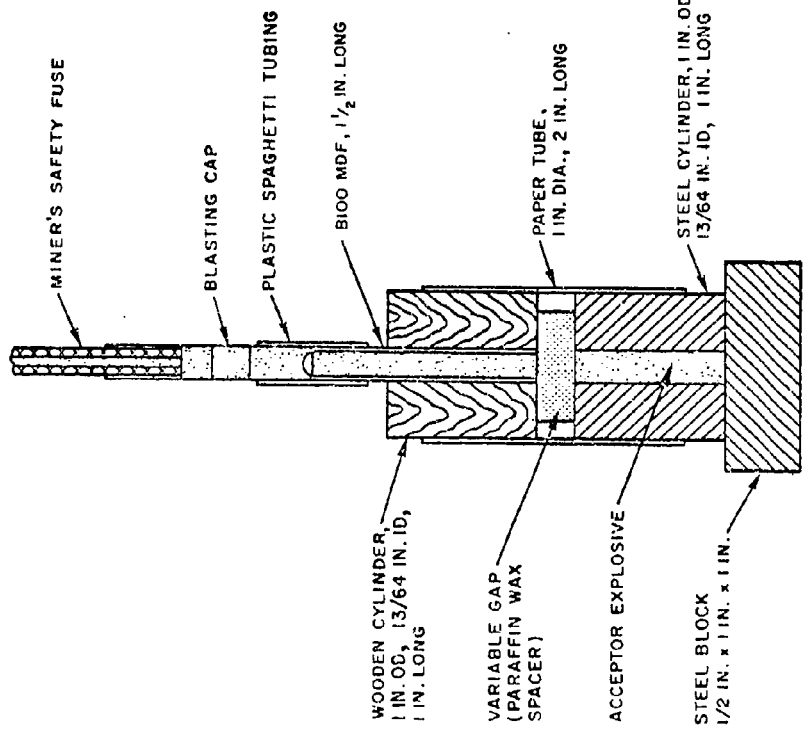


FIGURE 2. Arrangement of SSSGT



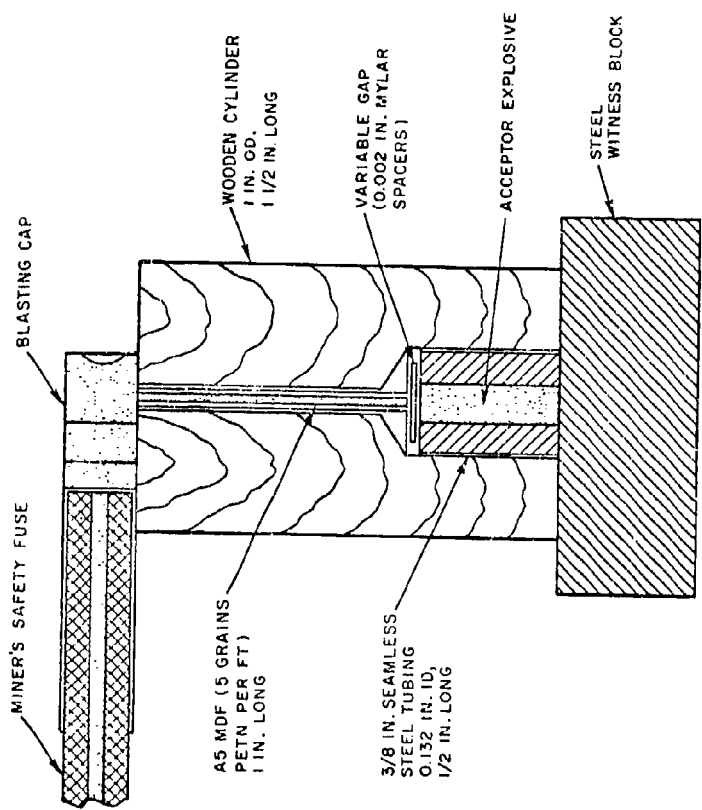
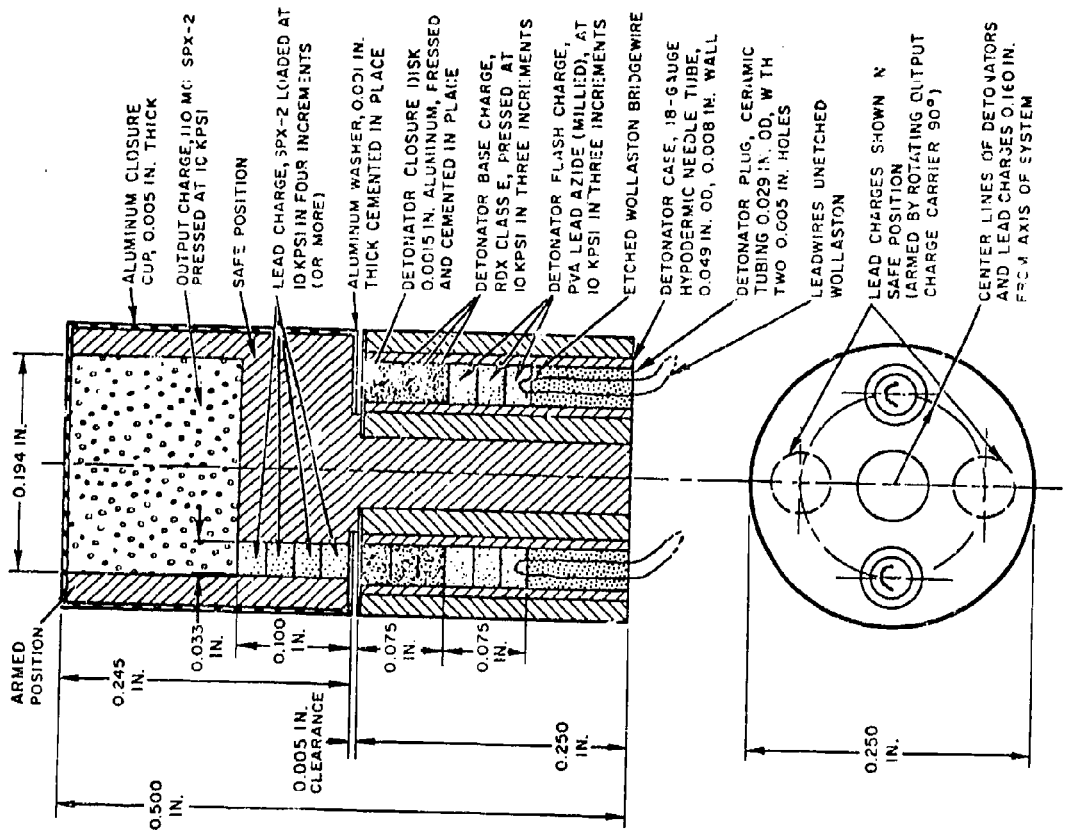


FIGURE 4. Diagram of MSGI Firing Test Arrangement

FIGURE 5. A Suggested Small-Explosive System Design (Scale: 10/1)

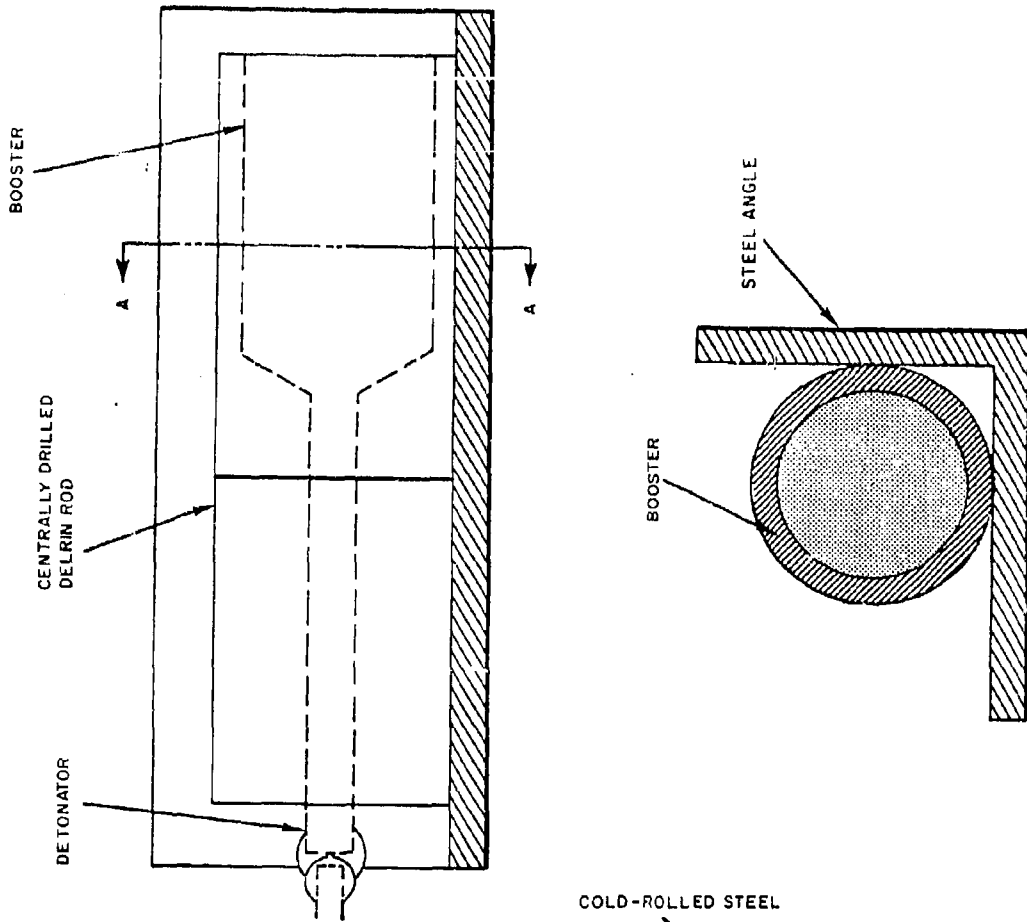


FIGURE 6. Experimental Arrangement Used in Test of Detonation Transfer From Miniaturized Detonators

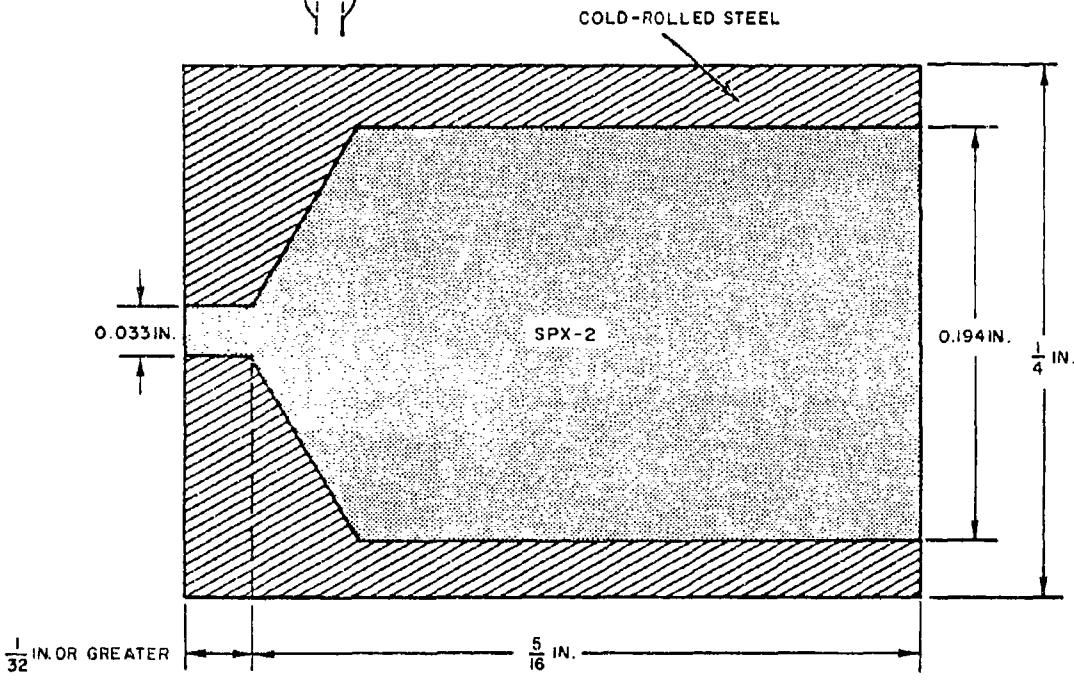


FIGURE 7. Experimental Booster for Miniaturized Fuze Train

2-11P R. F. BONDING

by

W. C. Reisener

The Franklin Institute Research Laboratories

A major cause of radio frequency interference in the past few years has been inadequate electrical bonds on electronic equipment, aircraft and aerospace vehicles. This has been largely a result of the increased complexity and power levels of the electronic systems now in use and can constitute a hazard to systems containing EED's. Standard practice in the past, to determine the adequacy of electrical bonding, has been to measure the dc resistance between various points in a vehicle and require that it be maintained below a prescribed value. However, it has been found that such a procedure does not necessarily eliminate interference problems at communication or radar frequencies. In order to provide a more appropriate procedure for evaluating the performance of bonds at radio frequencies, a program has been underway for the past three years to examine various impedance measuring techniques suitable for this purpose.

During the early phases of the program, bonds of various types were investigated. It was concluded that the only effective way to avoid RF potentials at various points in the system is to provide a continuous ground plane or enclosure with the minimum number of openings. Such bonding techniques as straps are almost worthless at high frequencies and can even accentuate the problems, even though in some cases they are a necessary safety precaution for power frequencies, static charges, etc. Therefore, during the remainder of the program, emphasis was placed on bonds of a continuous nature, such as are used to attach the external skin to aircraft or provide shielded enclosures for electronic instrumentation and ordnance devices. In addition to the structural purpose

2-11.1



of such bonds, they quite often are used to provide the shielding and grounding required for the electrical firing system.

Paralleling the past methods for evaluating the effectiveness of bonds, it was decided to investigate the use of the RF impedance as the criterion, rather than the dc resistance. However, this is now a very localized measure, as opposed to the dc measurement which is influenced by many parallel paths between the two points defining the impedance. The RF impedance must be measured continuously along a bond to insure that isolated areas do not exist that could result in excessive RF voltages or leakage. A poor section of the bond would then be indicated by an excessively high impedance reading.

The primary considerations in comparing various techniques available for impedance measurements were the ability to make connections to the bond conveniently, without introducing additional bonding problems, the sensitivity and stability for measurement of very small impedances, and the ease of measurement for field use by normal maintenance personnel. Furthermore, it was desirable that the instrument did not radiate power over a large area of the bond, resulting in excessive sensitivity to geometry and the adjacent surroundings.

Early work emphasized the lower frequency range, roughly from 100 KHz to 50 MHz. In this area a number of impedance measuring devices are available; however, most require clearly defined terminals and some means of connecting to them (cable connector, clamps, probes, etc.). Since the impedance of the bond is extremely low, (in the milliohm range) and quite often it is not possible to make a metallic contact to the surfaces (due to paint, corrosion, etc.), it was found that the most practical instrument for use at low frequencies was an induction coil. With this device, a flat coil is placed parallel to the surface. Currents are induced on the surface in the vicinity of the coil which are forced to flow through the bond. The impedance of the bond is then determined by its effect on the impedance of the coil. In practice, the coil is first placed over a section of the surface adjacent to the bond. The change

in coil impedance when moving to the bonded section is then measured and interpreted to give the bond impedance.

Two models were built and tested. In these, the induction coil was made part of a parallel resonant circuit which formed one arm of a bridge circuit. This is shown in Fig. 1. The resistor and capacitor,  $R_1$  and  $C_1$ , were first adjusted to balance the bridge over an unbonded section of a metal plate. The coil was then moved over the bond, and the bridge rebalanced. The change in  $R_1$  and  $C_1$  in going from the unbonded to bonded portions of the plate then gave the change in input admittance of the coil. The first experimental model is shown in Fig. 2. This was followed by a second model (Fig. 3) for which the circuitry is given in Fig. 4. The coil itself was etched from copper-clad laminate as drawn in Fig. 5. The base material provided a means for maintaining a constant distance between the plate and coil (5 mils). The coil was backed up by a piece of polyurethane foam to allow the coil to conform to curved surfaces.

The sensitivity of this instrument was quite adequate for measuring typical bond impedances, being able to measure the difference in conductivity between brass and aluminum base plates.

A fairly extensive theoretical study of this technique was made to help clear up several questions about its use and interpretation of the results. An important conclusion of this study was that its use with magnetic plates greatly affects the calibration, and as a result it is more suitable for use with non-magnetic materials. An exact mathematical solution could not be obtained due to the complexity of the geometry; however, by making suitable approximations, the induced current and reflected impedance were calculated with reasonable accuracy as a function of various parameters.

It had been hoped that this method could be used to cover the entire range of frequencies of interest, up to 400 MHz, resulting in a relatively compact, easy to use device, with no problem making contact to the bond. However, after experiments with several designs which

operated at 250 MHz, it was concluded the precision and repeatability were not as high as desirable. A usable device was constructed, but it was too sensitive to physical parameters and difficult to calibrate. Best results were obtained using the coil as part of the resonant circuit of an oscillator. The frequency of oscillation and emitter current of the oscillator provided data to determine the bond impedance.

Several other methods offered promising results at high frequencies. These made use of time domain reflectometer and C. W. transmission line techniques. The pulse reflectometer measurement employs a parallel plate transmission line consisting of the bonded plate as one conductor and a test plate for the other. The discontinuity caused by the bond results in the reflection of a pulse back toward the source. Measurement of the amplitude and shape of this pulse can then be used to describe the impedance of the bond. The sensitivity of such a system is limited primarily by the noise level of the detector circuit (sampling oscilloscope) and by the bandwidth (or time resolution) of the system (both pulse rise time and effective sampling time). The bandwidth limit is particularly important, since the width of the bond is very short compared to practical resolution distances of this type of instrument. A typical time resolution might be on the order of .15 nsec, which for an air dielectric line corresponds to about a 2 inch distance. This is about 40 times the normal width of a bond, resulting in a reduction of the measured reflection coefficient, caused by the bond, by a factor of about 40. Typical noise limited sensitivity limits the resolution to a reflection coefficient of .001. Therefore, the minimum reflection coefficient that could be detected with such a system and typical bonds is about .04.

As an illustration of the effect of this limitation, consider two lines joined together by a short section of line of different characteristic impedance.

For low loss lines and a short bond, the reflection coefficient is approximately equal to

$$\Gamma_1 \approx (\alpha_2 - \alpha_1)l$$

or

$$\Gamma_1 \approx \frac{(R_{S2} - R_{S1})}{R_o} \frac{l}{b} = \frac{(R_{S2} - R_{S1})}{120\pi} \left(\frac{l}{a}\right)$$

where  $l$  is the length of the bond, and  $a$  and  $b$  are the plate separation and width.

Thus, if the length of the bond is about equal to the spacing of the plates, and a minimum reflection coefficient of .04 is required, the difference in surface resistivities must be at least 15 ohms. The surface resistivity of copper is about 5 milliohms at 400 MHz; therefore, the resistivity of the bond would have to be 3000 times as large as that of copper to be detected by this method. Reactive bond impedances may result in higher reflection coefficient, but for a resistive bond of reasonably high conductivity, this method is not sensitive enough.

Laboratory tests were performed using a standard coaxial line, in which was inserted a short section (up to one inch) of high resistance center conductor. In this way much better control was possible of the quality of the line and the characteristics of the simulated bond. The purpose of the tests was primarily to determine if the method could provide adequate sensitivity and to detect any problems which might affect the results.

In none of the tests was it possible to detect any significant reflection from the bond, even though the resistance of the bond was considerably higher than would normally be accepted in practice. There are two major causes of the inadequate sensitivity of the TDR method. These are the limited bandwidth of the device and the reflections caused by purely geometrical discontinuities. The effective rise time of the



reflectometer used for these experiments (HP 1415 A) is about 0.15 ns. This is equivalent to a resolution along the transmission line of about 4.5 cm (1.75 inches). The thickness of most bonds is much less than this (by a factor of 30 or more). This means that the signal reflected back from the bond will be attenuated by this factor, because the reflections from the leading and trailing edges of the bond very nearly cancel each other. Only when the wavelength approaches the dimensions of the bond will a sizable reflection be produced, but this corresponds to frequencies well above the capability of the reflectometer and above the range of interest of this program.

Equally serious is the effect of geometrical discontinuities. Reflections from the normal dimensional variations effectively establish the noise level of the instrument. Only in the case that these geometry variations affect the performance of the surface, such as when it is used as a ground plane for an antenna, does this effect have anything to do with the satisfactoriness of the bond, and generally the variations are small enough so that they can be ignored. In most cases, a change in geometry will not affect the performance of a bond, if the purpose of the bond is to avoid excessive RF voltages on the ground plane or to provide adequate shielding to prevent RF from being induced in a firing circuit. These geometrical discontinuities produce reflections by generating local variations in the wave impedance which may be quite large compared to the variations in surface impedance caused by a poor bond. The inability of the TDR technique to differentiate between these two effects is the prime reason for its poor performance in this application.

It was felt that the limitations imposed by geometric discontinuities in a transmission line approach could be largely eliminated by using a resonant, CW technique in place of the broad band TDR method. The arrangement used for the TDR experiments with the bond in series with one conductor, is equally unsuitable for CW measurements -- to detect the effect of the bond, it is necessary to measure a small change in the standing wave ratio, which for a properly terminated line, is very close to one. A much more sensitive arrangement is possible, in which the line



is terminated by the bond impedance. A perfect bond (zero impedance) then results in a very large vswr, limited only by the line losses. To keep the effect of line losses to a minimum, the vswr should be determined from voltage measurements 1/4 and 1/2 wavelength from the termination. Actually, it is relatively unimportant which maximum is used to determine the maximum voltage, since this value is essentially constant regardless of the distance from the termination, as long as the bond impedance is very small compared to the line impedance. On the other hand, as the distance from the termination is increased, the voltage minima become progressively larger due to the additional line losses that are introduced. It is therefore important to make this measurement as close to the termination as possible. Assuming that the voltage maxima are unaffected by the termination, it is then possible to determine the termination (bond impedance) by measuring the change in voltage minimum and the change in the position of the minimum, when the termination is changed from a solid conductor to the bond. The bond impedance is given in terms of these quantities by

$$Z_B = R_o \left\{ \Delta \left( \frac{1}{r} \right) - j 2\pi \left( \frac{\Delta \ell}{\lambda} \right) \right\}$$

where  $\Delta \left( \frac{1}{r} \right)$  is the change in the reciprocal of the vswr,  $\left( \frac{\Delta v_{\min}}{v_{\max}} \right)$ , and  $\Delta \ell$  is the shift in the position of the minimum.

The line losses are important only since it is necessary to measure a change in the minimum voltage. If the initial voltage is already quite large, it becomes difficult to measure the small difference caused by the bond. If the line were lossless, the change in minimum voltage could be calculated directly from the reflection coefficient of the termination. The vswr in this case would be merely the ratio of the line impedance to the bond resistance. Thus, for a typical example (.05 inch length of Eccobond, operating at a frequency of 250 MHz) a vswr of 2000 is indicated. To be able to measure the effect of the bond, the initial vswr should also be of this order of magnitude. The measured

vswr for the section of GR line was about 48.4 db (vswr = 263). The addition of this .05 inch section of Eccobond would then increase the minimum voltage by 1.1 db. This is within the capability of the instrumentation, indicating that the CW technique does have adequate sensitivity.

For the experimental work, the setup shown in Figure 6 was used. The test line consisted of a length of General Radio type 874 coaxial line, but in this case, a length of Eccobond solder was placed at the end of the center conductor. To this was cemented a brass slug which formed a short circuit termination for the line. The standing wave ratio was measured with a slotted line and probe (General Radio 874-LBA) and an I-F amplifier (General Radio 1216-A).

A set of three samples were tested using this method. All three had the test line terminated with a brass slug (short circuit). The first sample had the brass slug cemented directly to the GR center conductor. The second sample (sample No. 2) had the brass cemented to a 0.7000 inch Eccobond center conductor insert that in turn was cemented to the GR center conductor. The third sample (sample No. 3) was similar to sample No. 2, but it used 1.360 inches of Eccobond for its insert length.

The maximum and minimum voltages for the three test samples were measured for an input power of 0.012 watts to the test samples. This 0.012 watts corresponded to a maximum I-F reading of 46.0 db for all three samples. Minimum I-F readings of -2.4 db were obtained for sample No. 1, zero db for sample No. 2, and +3.0 db for sample No. 3. The maximum and minimum db readings for each sample are averages of three or more readings.

In conjunction with the db readings for each sample, the resistance of the Eccobond portion from each sample was measured with a Keithley Model 502 Milliohmmeter. The Eccobond portion of sample No. 2 (0.7 inch length) had a resistance of 8.1 milliohms, where a comparable length of

brass measured 0.06 milliohms. The Eccobond portion of sample No. 3 (1.36 inch length) measured 15.0 milliohms while a comparable length of brass measured 0.10 milliohms.

Using the values of vswr, the indicated bond impedance for the two cases are

$$R = 50 \left( \frac{1}{202} - \frac{1}{263} \right) = 57.3 \text{ milliohms} \quad (\text{No. 2})$$

$$R = 50 \left( \frac{1}{141} - \frac{1}{263} \right) = 164 \text{ milliohms} \quad (\text{No. 3})$$

These are considerably lower than expected from the assumed resistivity of the Eccobond solder. The factor of 100 estimated for the ratio of resistivity of Eccobond to copper would give resistances at 250 MHz of

$$R = \frac{0.4(0.7)}{2\pi(.125)} = 357 \text{ milliohms} \quad (\text{No. 2})$$

$$R = \frac{0.4(1.36)}{2\pi(.125)} = 693 \text{ milliohms} \quad (\text{No. 3})$$

These are higher by a factor of about 5. Since no reliable data are available on the resistivity of Eccobond at this frequency, it is probable that the actual resistivity is lower than the assumed value.

The initial vswr agrees reasonably well with the theoretical value. Using a value of surface resistivity of 4.0 milliohms for copper, the attenuation constant of the line at 250 MHz is

$$\alpha = \frac{R_s}{2\pi} \left( \frac{1}{r_o} + \frac{1}{r_i} \right)$$

where  $r_o = 0.287$  inch is the radius of the outer conductor, and  $r_i = 0.125$  inch is the radius of the inner conductor. This gives

$$\alpha = 7.31 \cdot 10^{-3} \text{ ohms/inch}$$

If the voltage minimum is measured a half wavelength away from the termination ( $\lambda/2 = 23.6$  in), the value of  $\alpha l$  is 0.173. Thus, the vswr is

$$r = \frac{R_o}{\alpha l} = \frac{50}{.173} = 289$$

The measured value was 263 (9% low). This difference can be accounted for by losses introduced by the connectors and short circuit termination. This relatively good agreement supports the conclusion that the assumed resistivity of the Eccobond solder was too high.

As a result of the encouraging performance of the CW transmission line technique when used with a coaxial line, a parallel plate line was fabricated which would be suitable for field use. Fig. 7 is a photograph of this line, and Fig. 8 is the test setup, showing the appropriate laboratory equipment to be used with it.

Contact between the end of the parallel line and the bonded surface created a problem because of surface irregularities of the bond and the parallel line. This was solved by putting three mil copper shim stock on the ends of the parallel line, for the shim stock tends to compress and fill the microscopic surface irregularities to produce a good contact to the bonded surfaces.

A series of typical bonds were measured at 258 MHz. In all cases the bond produced a repeatable and smaller VSWR than a continuous sheet of copper or aluminum. This indicates that the parallel plate line system has enough resolution to distinguish the difference between good bonds, and hence, can certainly detect a poor bond.

VSWR values for the bonds were reduced from 2% to 68% of those for a copper or aluminum short, depending on the type of bond tested. The copper short showed a VSWR of approximately 115 while the best bond produced a VSWR of 112 and the worst (0.5 ohm dc resistance) a value of 37.

2-11.10

## CONCLUSIONS

The results of this study have shown that it is practical to measure bond impedances in the vhf and uhf ranges for the types of bonds typical of aerospace vehicles and associated electronic equipment. The techniques lend themselves fairly easily to the design of compact, easy to use, field instruments necessary for a practical quality control program. However, before such use can be made of these principles, a great deal of work remains to establish acceptable impedance limits for various applications and to interpret the measured data in terms of its effect on the electronic and control systems. Much of this can only be learned through the use of this type of measurement in actual practice, and correlation of the resulting data with specific interference problems that arise. Eventually, a much more practical and useful method will develop, than is now available, for evaluation of bonding systems and elimination of the RFI problems for electronic equipment and the RF pick-up in ordnance circuits.

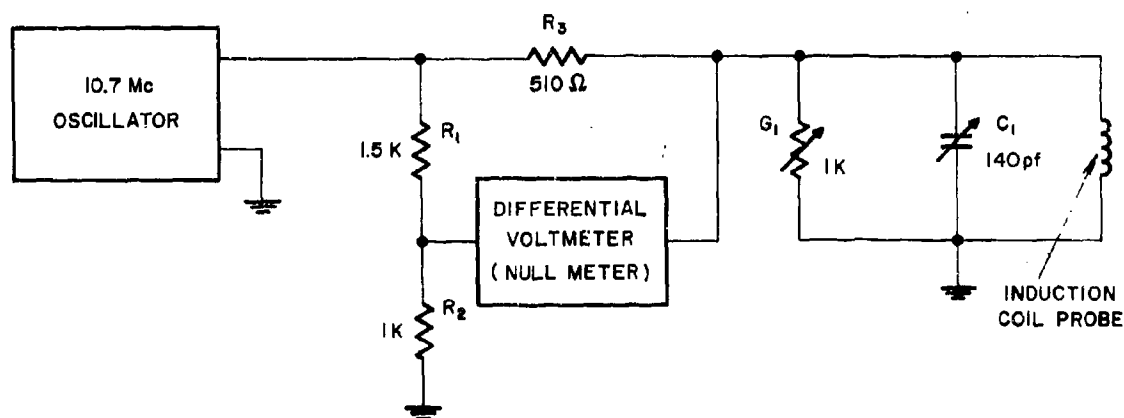


Fig.1 Simplified Diagram of Bond Impedance Meter

2-11,11

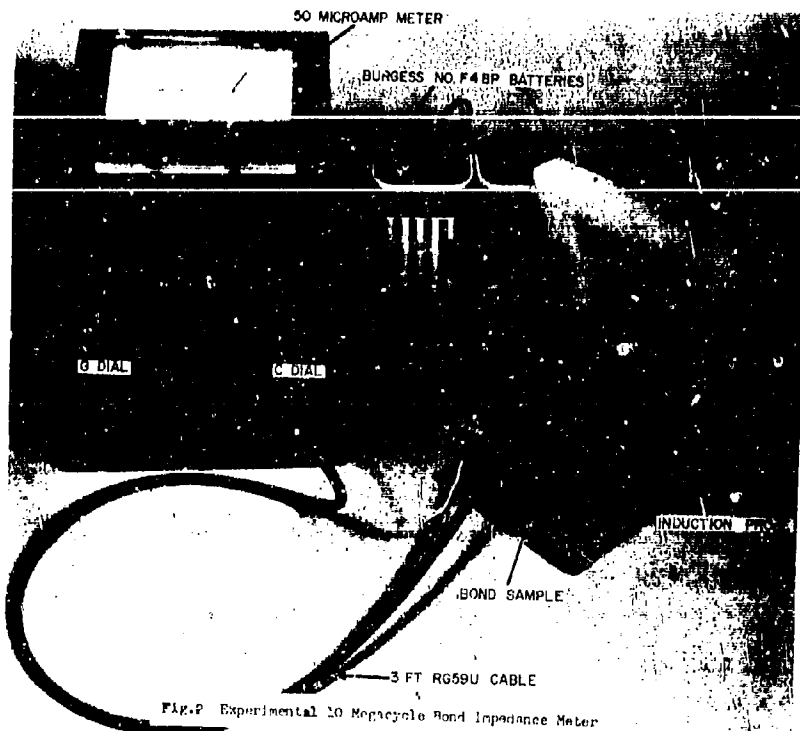


Fig. 2 Experimental 10 Mc/sec Bond Impedance Meter

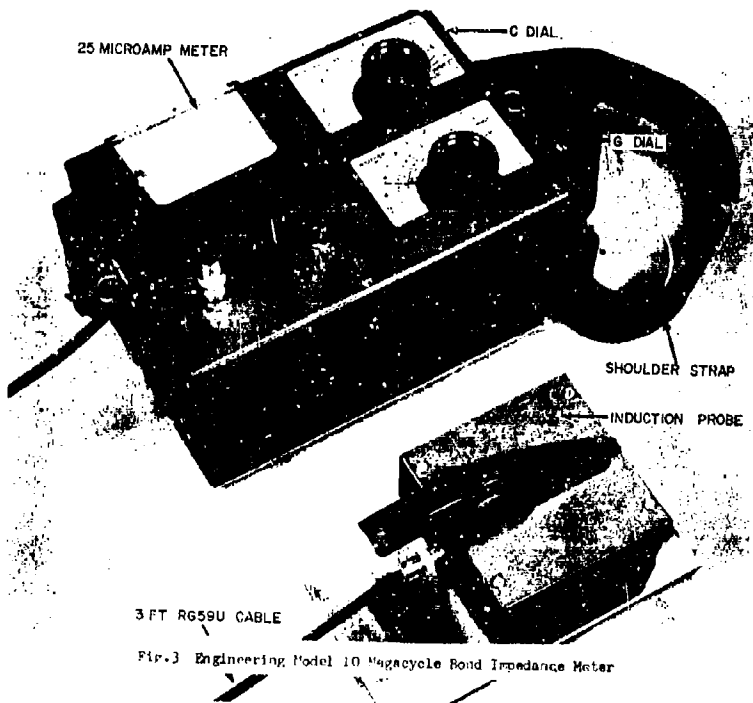


Fig. 3 Engineering Model 10 Mc/sec Bond Impedance Meter

$L_1$  AND  $L_2 = 1.5$  TO  $3.2 \mu\text{h}$   
 J.W. MILLER TYPE 4404  
 $Q_1$  AND  $Q_2 = \text{MOTOROLA } 2N2951$

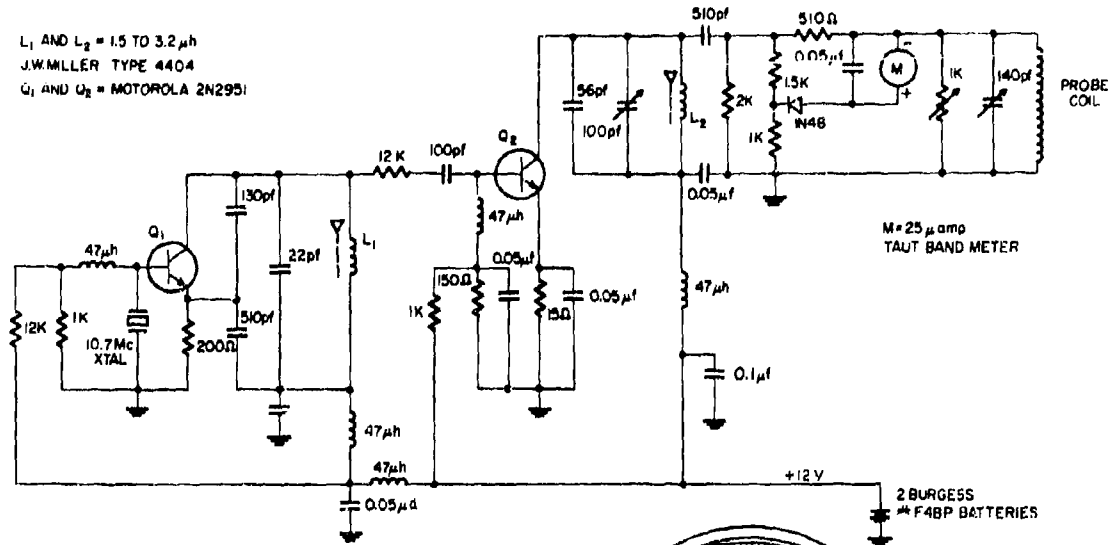


Fig. 4 RF Bond Impedance Meter

Fig. 5 Printed Circuit Induction Coil

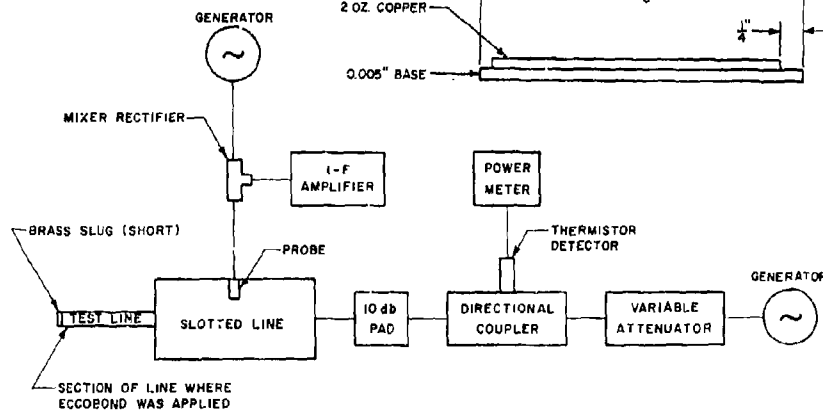
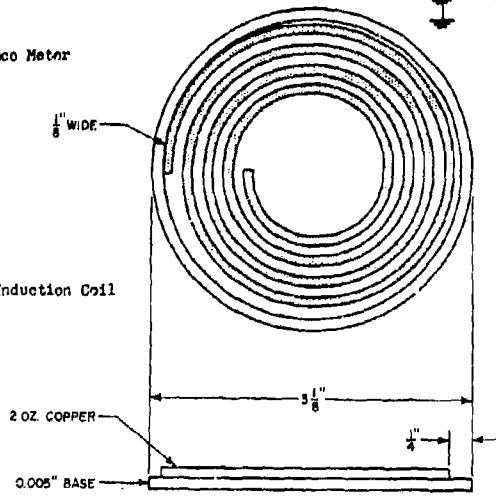


Fig. 6 VSWR INSTRUMENTATION USING A HIGH-GAIN I-F AMPLIFIER

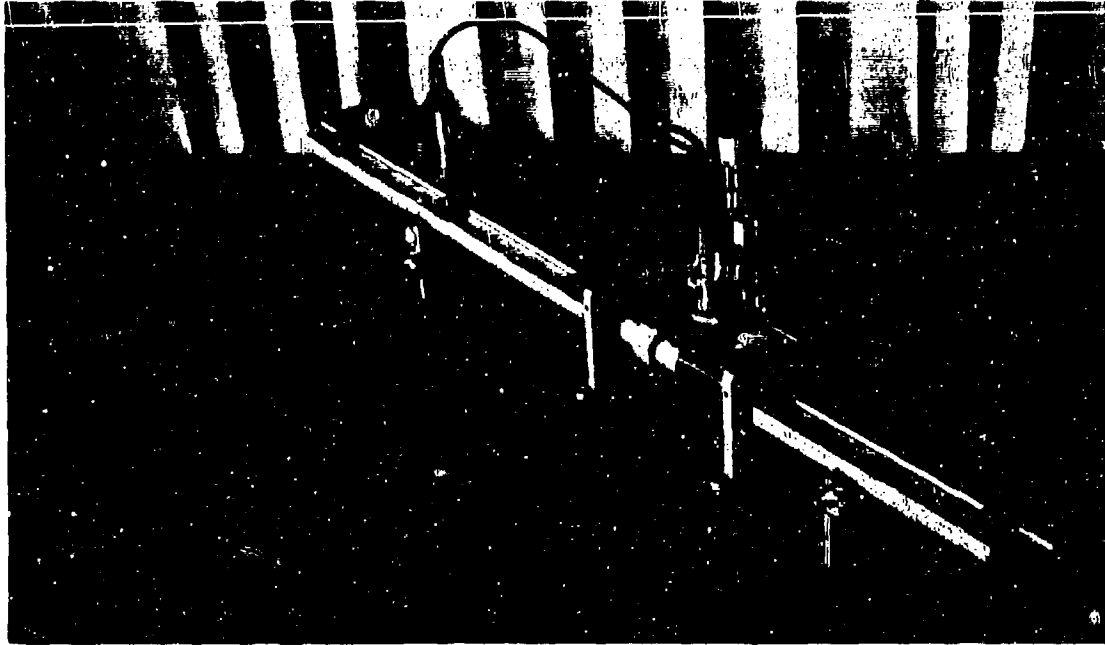


Fig.7 Parallel Plate Line



Fig.8 Instrumentation for Parallel Plate Line



3-1 Temperature Coefficient of Resistivity Effects on 1A/1W  
No-Fire Initiators

D. E. Davenport

A previous paper presented the development of a simple theoretical model for 1A/1W ordnance devices which enable one to predict the design parameters for producing the desired all-fire and no-fire characteristics based upon the heat transfer properties of the various components. This paper used the simplest model with a constant power input to the device for both all-fire and no-fire testing. In this present paper, we have extended the model to the case of the constant current testing, which is so often specified, and have therefore taken into account the effects of the bridgewire resistance on the ordnance device performance.

3-2 Insensitive Electric Initiators

Vincent J. Menichelli

A bridge element design effective for the fabrication of electric initiators capable of passing at least 1-ampere of current and/or absorbing 1-watt of power for 5 minutes without initiating will be described. This objective is accomplished using conventional explosives such as lead azide or lead styphnate, and conventional initiator hardware. Consequently, most existing, relatively sensitive, wire bridge electroexplosive devices can be directly converted to 1-amp, 1-watt no-fire devices by changing only the bridge element in accordance with the described design principles.

3-3 Constant Current Ignition of Metal - Metal  
Oxide MixturesJames L. Austing  
John P. Weber

An experimental study on the ignition of metal - metal oxide mixtures in contact with electrically pulsed bridgewires was performed. The systems that were studied included aluminum - tungstic oxide, aluminum - copper oxide, aluminum - vanadium pentoxide, and aluminum - molybdic oxide. These mixtures are highly exothermic, with reaction temperatures in excess of 2500°K. Metal - metal oxides therefore serve as good ignition sources for a variety of explosive type components. Representative data are presented to show that electric initiators incorporating the proper metal - metal oxide system (1) are capable of withstanding static electric discharge pulses in excess of those generated by the human body, and (2) can be designed to provide a 5-amp, 5-watt no-fire capability.

3-4 Electric Detonators for Navy Guided Missile Applications  
Experimental Studies of Four ConceptsR. Stresau  
R. Peterson  
D. Chamberlain

Feasibility was investigated of four concepts of detonators to meet the one watt, one ampere no-fire criterion while retaining sufficient pulse sensitivity (10,000 ergs "all fire") for use with firing circuits now in service. The four concepts, briefly, are as follows: (I) A bridgewire of low enough resistance to carry one ampere without heating sufficiently to affect the flash charge, with series resistor. (II) A hot bridgewire electric initiator with flash charge of sufficient thermal conductivity to dissipate a watt without firing, (III) An initiator with a conductive plastic bridge element, (IV) An initiator with a film bridge on a thermally conductive substrate.

3-5 A Microcircuit Bridge for High-Reliability EED's

D. N. Griffin

An integrated microcircuit bridge has been developed that provides a higher no-fire capability, and better structural reliability than conventional wire bridge designs. Detailed design and performance data will be given, covering 1 Amp/1 Watt, 2 Amp/3 Watt, and 5 Amp/1.5 Watt No-Fire systems.

3-6 Electric Detonators with "Markite" Electrically Conductive Plastic Bridge Elements

R. H. Stresau  
R. L. Petersen  
S. A. Corren  
M. A. Coler

Detonators with bridge elements of "Markite" conductive plastics were subjected to a preliminary evaluation based on the Military Standard (MIL-STD-322) for the evaluation of electrically initiated explosive devices and the Military Specification (MIL-L-23659(WEP) for the design and evaluation of electric initiators. Additional tests were also performed.

Variations in design parameters achieving miniaturization and other special characteristics are discussed and illustrated. The techniques appear to favor economical mass production of rugged units.

3-7 High Temperature Resistant Conductive Priming Mixes

Wm. Perkins  
Allan Schlack

Because EED's are used in applications where they are exposed to elevated temperatures, it is desirable to design an EED which would function at and after exposure to this environment. Also, EED's are required which can function satisfactorily after being subjected to 1 ampere current and/or 1 watt D.C. power for five minutes. Conductive mix type electric ignition elements were studied which could meet these requirements. Two promising mixtures, evaluated at elevated temperatures, functioned satisfactorily.

3-8P A Heat Transfer Study of Hot Wire Ignition of Metal - Metal Oxide Mixtures

J. L. Austing  
J. E. Kennedy  
D. H. Chamberlain  
R. H. Stresau

The hot wire ignition threshold of metal - metal oxide mixtures is controlled by heat transfer processes in an between the bridgewire and the pressed granular bed of reactive solids. An experimental study has been made of individual parameters affecting ignition, such as the autoignition temperature of the reactive mixtures, the electrothermal heat loss factor of the bridgewire and the thermal conductivity of the reactive mixture. The importance of a convective boundary layer on the bridgewire surface as a barrier to heat transfer to the bed is also discussed.

- 3-9P Electrical and Thermal Considerations in the Design of Electro-Explosive Devices K. H. Stresau  
R. Peterson  
D. Chamberlain

Electrical, and thermal considerations in the design of electro-explosive devices are considered with an emphasis on means of complying with the "one watt, one ampere no-fire" requirement of many recent standards and specifications and yet retaining sufficient pulse energy sensitivity to be fired by guided missile fuze circuitry in current use. Included are discussions of implications of the general, lumped parameter electro-thermal and thermal conductivity, and the control of gross heating of initiators.

- 3-10 Observations on the Initiation of Secondary Explosives by Exploding Wires H. S. Leopold

Photographic, electric, and explosive observations of the conditions necessary for the initiation of PETN and other less sensitive secondary explosives will be discussed. Topics covered include sensitivity, density, and effect of stimulus strength on the growth to detonation characteristics under conditions where propagation depends mainly on the exploding wire stimulus. The effect of changes in wire dimensions on the initiation energy for explosives of varying sensitivity are also shown.

- 3-11 An Application of a Thermal Explosion Criterion to the Initiation of Explosives by Variable-Current Wires M. H. Friedman  
R. L. McCally

An analytic technique has been developed which can be used to predict thermal explosion delays. The only data required are the energy input to the wire as a function of time, and the properties of the wire and surrounding explosive. The procedure is illustrated for EBW operation and is compared to computer solutions.

- 3-12 EBW Firing Unit and Detonator Compatibility Investigation J. M. Reuter  
R. G. Amicone

A study has been performed to determine the compatibility of the EBW Firing Units with the detonators used on Saturn vehicles. This work, at worst case temperature conditions, determined the firing unit peak output current and time to peak current vs. detonator input energy requirements for 99.9% all fire at 95% confidence.

- 3-13 The Initiation of Insensitive Explosives with Metal - Metal Oxides James L. Austing

Temperature-stable and insensitive explosives require initiation systems, which are at least equally stable and insensitive, in order to take full advantage of the improved properties of the main charge. This investigation concerned the feasibility of using selected metal - metal oxides to initiate a detonation in insensitive explosives.

3-1 TEMPERATURE COEFFICIENT

OF

RESISTIVITY EFFECTS

ON

1A/1W NO-FIRE INITIATORS

By

D. E. Davenport

GENERAL PRECISION, INC.

Link Ordnance Division

Introduction

In an earlier paper <sup>(1)</sup>, a theoretical model was developed for the prediction of performance of initiator designs which was based on the thermodissipative characteristic of the design. The model differed from other suggested heat transfer models in that it included the detailed heat transfer property of each of the elements rather than lumped constants, thus making it possible to evaluate the effect of several parameters on all-fire and no-fire characteristics. This also gave the model flexibility to be used as a quality control analysis tool, since one could study the effects of the normal manufacturing tolerances and/or design changes on the performance of the initiator.

This model made possible one of the first 1A/1W no-fire designs which used only primary explosives in the initiation chain, thus providing the stability and long storage life associated with those materials as well as high reliability and short response time of conventional initiators. The model has also been applied to some of the simpler fuel-oxidant mixes that are so often used to achieve 1A/1W no-fire characteristics and has been shown to predict their performance within the uncertainty of the ignition temperatures which can be assigned to these more complex systems.

---

(1) "Theoretical Approach to 1Amp/1 Watt No-Fire Ordnance Designs", D. E. Davenport  
- IEEE Aerospace Technical Conference and Exhibit, June 1965.

The original mathematical model contained several simplifications to make it more readily adaptable to solution. In the interim since the original paper, some of the simplifications have been removed to extend the theory and to make it possible to include temperature coefficient of resistivity effects. This paper will discuss these effects, and some of the experimental techniques which have been developed to use them to non-destructively test initiators.

The original mathematical model was based on a simplified initiator design with cylindrical symmetry as in Figure 1(b).

The simplifications of most serious implication were:

- (1) Assuming a single medium around the bridgewire with properties which were linear averages of those of the insulator and the explosive.
- (2) Assigning an effective linear heat transfer constant,  $H$ , to this medium to calculate radial heat losses rather than using the appropriate Bessel functions or more complex expressions.
- (3) Assuming the complete solution may be made up of two independent solutions; one, a short term transient, which depends only on the bridgewire and its immediate surroundings, and another, which depends on the properties of the remainder of the header assembly.
- (4) Assuming tests were made under constant power conditions so no temperature coefficient of resistivity effects were included.

The first three assumptions led to no noticeable divergence of theory and experiment over a wide range of parameters, but both assumptions (2) and (4)

restrict the information that can be obtained from the model. In this paper we will discuss additional information about all-fire and no-fire conditions which can be obtained when these restrictions are lifted.

### The Original Model

For the all-fire case, elements (3) and (4) of Figure 1 (b) can be considered infinite heat sinks, since their temperature changes very little during the period of interest. The heat flow can then be described <sup>(1)</sup> by the heat balance equation:

$$\rho c (\pi r^2 dx) \frac{d T}{d t} = K \left[ \left( \frac{d T}{d x} \right)_x - \left( \frac{d T}{d x} \right)_{x + dx} \right] \pi r^2 - (2 \pi r dx) \left[ H ( T - T_o ) \right] + \frac{I^2 R dx}{(4.186) (\lambda)} \quad (1)$$

In this equation:

- $\rho$  = density of the bridgewire material, g/cm<sup>3</sup>
- $c$  = heat capacity of the bridgewire material, cal/g/°C
- $r$  = radius of bridgewire, cm
- $x$  = distance along the bridgewire, cm
- $T$  = temperature of the bridgewire, °C
- $t$  = time, in seconds
- $K$  = thermal conductivity of the bridgewire material, cal/cm<sup>2</sup>sec°C/cm
- $H$  = an effective radial heat transfer constant
- $T_o$  = initial temperature of the system, °C
- $I$  = current flow, amperes
- $R$  = bridgewire resistance, ohms

$\lambda$  = length of the bridgewire, cm

In the solution of this equation, the power input,  $I^2 R$ , was considered constant so the equation was written as:

$$\frac{dT}{dt} = H \frac{d^2 T}{dx^2} - v(T - T_0) + a \quad (2)$$

where  $H = \frac{K}{\rho c}$ ,  $v = \frac{2 H}{c r \rho}$ , and  $a = \frac{I^2 R}{4.186 c r^2 \pi \rho \lambda}$

and the solution was shown to be:

$$T = \frac{a}{v} \left[ \frac{1 - \sinh x \sqrt{\frac{v}{H}} + \sinh(\lambda - x) \sqrt{\frac{v}{H}}}{\sinh \lambda \sqrt{\frac{v}{H}}} \right] - \frac{4a}{v\pi} \sum_{n=1}^{\infty} \frac{\lambda^2 \left(\frac{v}{H}\right) \sin\left(\frac{(2n-1)\pi x}{\lambda}\right)}{(2n-1) \left\{ (2n-1)^2 \pi^2 + \lambda^2 \left(\frac{v}{H}\right) \right\}} e^{-ut - t \left[ \frac{H(2n-1)^2 \pi^2}{\lambda^2} \right]}$$

### Temperature Coefficient of Resistivity Effects

In practical cases, however, constant power is seldom used since the resistance of the bridgewire is usually somewhat temperature dependent. The more normal practices are to test the unit under constant current conditions and to use the device under constant voltage conditions. When the bridgewire resistance is not independent of temperature, these practices lead to some marked changes in the time-temperature profiles of the bridge-wire which should be well appreciated by both manufacturers and users of initiators.

These differences can be qualitatively appreciated by the consideration

of what happens to the power level under conditions of constant current and constant voltage firings, when the resistance is written in a temperature dependent form such as  $R = R_0 (1 + \alpha T)$ . Since  $\alpha$  is of the order of  $1 \times 10^{-3}$  to  $4 \times 10^{-3}$  for many common bridgewire materials, it is seen that the resistance level may double as the temperature of the bridgewire rises a few hundred  $^{\circ}\text{C}$  (the initiation temperature of common ignition materials).

When initiator tests are carried out under constant current conditions, the power may be written as:

$$P = I_0^2 R_0 (1 + \alpha T)$$

Thus, the constant current condition of firing is one of rapidly rising power input to the bridgewire. In the case of constant voltage firing the power becomes:

$$P = \frac{E_0^2}{R_0 (1 + \alpha T)}$$

In this case it is seen that the power is a rapidly decreasing function of the bridgewire temperature for most bridge materials and many fall to half or less of the initial power before the initiator fires.

Qualitatively, it can be seen that for the all-fire condition, the initiator should fire much sooner under the constant current condition than under the constant voltage condition assuming the initial power is the same. Thus, a constant current test will be optimistic for a time-to-fire measurement (i. e. predict a shorter time to fire) compared with a constant voltage test. On the other hand, for those multicomponent primer mixes which exhibit failures to fire from bridgewire burnout if the power is too high, the



constant current test will be more effective in detecting this type of failure. This will be seen more graphically in the quantitative calculations to be presented in a later section.

For the no-fire condition, the constant current test is the most conservative since it gives a higher final power application than the equivalent initial voltage. It should be noted that the standard deviation will be smaller on a constant current basis because of this same effect, i. e. the temperature of the bridgewire will vary faster than the square of the current for constant current and slower than the square of the voltage for constant voltage.

### Model Predictions

A quantitative evaluation of the effect of the temperature coefficient on the performance of the initiator at constant current may be obtained by substituting  $R = R_0 (1 + \alpha T)$  into Equation 3 for R and rearranging the equation. It can be seen that this will simply add another term in the first order temperature term and the solution remains the same if the definition of  $\nu$  is changed from:

$$\nu_0 = \frac{2 H}{c r \rho}$$

to:

$$\nu_1 = \frac{2 H}{c r \rho} - \frac{I_0^2 R_0 \alpha}{4.186 c r^2 \pi \rho \lambda} = \nu_0 - a_0 \alpha$$

Thus, the effect of adding a temperature coefficient of resistance,  $\alpha$ , is similar to reducing the value of radial heat leakage constant H. This means it will lead to higher bridgewire temperatures. Note, also, that the effect of  $\alpha$  becomes worse at higher current levels and smaller wire sizes, i. e. greater values of  $a_0$ .

The nature of the temperature increases introduced by the temperature coefficient of resistivity can be seen from calculations which were carried out for the temperature at the mid-point of a 0.1" long bridgewire as a function of time for various values of  $\alpha$ . The results are shown in Figures 2 (a), 2 (b), and 2 (c). It can be seen that for small values of  $\alpha$  the maximum temperature tends to level off with time, but that for larger values of  $\alpha$  the temperature-time curve shows an ever increasing slope. At the highest value of  $\alpha$  the temperature "runs away" and burnout of the bridgewire results in a fraction of a millisecond.

From these examples, one gets a feel for the serious implications of a large temperature coefficient of resistivity on the all-fire conditions of an initiator. Fundamentally, the result is one of limiting the total energy which can be delivered to the system by shortening the time until the bridgewire burns out. Under conditions of no burnout, the bridgewire approaches some high temperature asymptotically and the temperature of the explosive material in contact with the bridgewire approaches the bridgewire temperature over a thicker and thicker annulus until a critical volume for that temperature is heated and ignition is achieved. As the power applied is increased by increasing the initial current level and/or increasing the temperature coefficient of the bridgewire, the bridgewire reaches its melting point and burnout in shorter and shorter times. In the limit, the total energy supplied is just that required to heat the bridgewire to its melting point since the times are so short that there is no significant heat leakage before burnout.

To obtain a better estimate of the amount of explosive which is heated

to the ignition temperature under the various conditions one should calculate the radial temperature distribution about a bridgewire under several conditions and compare the results. The following two sections give the results for two cases; one, the normal all-fire case in which a modest current is applied to bridgewires with various temperature coefficients of resistivity, the second, the high current all-fire condition which is often called out, which results in the bridgewire melting in a very small fraction of a millisecond, the so called "instantaneous" burnout condition in which negligible heat transfer occurs before burnout.

#### Radial Temperature Distribution Calculations

In order to develop quantitative measures of the volume of primer which may be heated by the bridgewire under various conditions, it is desirable to abandon the assumption of a linear radial heat leakage constant,  $H$ , and carry out a more detailed calculation of the radial temperature distribution. In order to do this a computer program was set up using a grid type solution. The bridgewire and the regions about it were divided into annular rings, as in Figure 3, of such size that using small time increments and linear temperature gradients, one can follow the temperature distribution as a function of time. The radial solution was obtained at the center of the bridgewire assuming no longitudinal heat flow along the bridgewire, which is accurate for the very short times involved for the all-fire case. The temperature drop at the explosive - bridgewire interface was assumed to be equivalent to that in a 5 micron thickness of explosives.

Figure 4 shows typical radial temperature distributions in a medium with a thermal conductivity coefficient of  $.001 \text{ cal/cm}^2/\text{sec}/^\circ\text{C}$  which is appropriate

for the most conductive explosives. By assuming this high value one will obtain estimates of the maximum pyrotechnic volumes heated.

The curves indicate that the total annulus heated to a significant temperature is less than 25 microns (1 mil) thick for the best cases before the bridgewire reaches about  $2000^{\circ}\text{C}$  which is above the melting point for many bridgewire materials and may be considered a reasonable burnout temperature. For short times of the order of 1 or 2 milliseconds, it is seen that the annulus, which is above  $200^{\circ}\text{C}$ , is more nearly of the order of 5 - 10 microns and thus, for such short firing times at 4 amperes one must use materials which will initiate from very small volumes.

As  $\alpha$  increases, the bridgewire temperature rises more rapidly, since the effective power is increased. However, at burnout the annular region above the critical temperature becomes narrower. Thus, for  $D = .002$  Figure 4 shows that at  $t = 10$  microseconds for  $\alpha = 0$  about a 30 micron width annulus is heated above  $400^{\circ}\text{C}$  when the bridgewire reaches  $2000^{\circ}\text{C}$  whereas, with  $\alpha = .0035$  burnout is reached in slightly over 1 millisecond and less than 10 microns is heated above  $400^{\circ}\text{C}$ .

The size of these annular regions relative to the particle size of the explosive can be better appreciated from a schematic drawing of this same data such as in Figure 5. In the figure four primer particle sizes (taken to be spherical for simplicity) have been arranged around a 2 mil wire and the annular temperature regions superimposed. The particle sizes shown are those typical of the finest powders normally used (-325 mesh).

One is impressed by the facts that only the lowest indicated temperature range ( $200 - 300^{\circ}\text{C}$ ) includes most of the volume of the largest particles, and that the inter-particle voids are quite large on this scale. This emphasizes

the necessity of using fine particles and making good contact between the particles and the bridgewire if reliable ignition is to be achieved. For pyrotechnics with ignition temperatures above 500°C only the finest particles are entirely heated to the ignition temperature.

From the standpoint of primary explosives which have an ignition temperature around 300°C, the annulus heated to ignition is still quite large since the critical hotspot size is less than 10 microns<sup>(2)</sup>. For a bimolecular reaction however, the critical volume may be expected to be much larger. Thus, successful ignition may occur after burnout as additional heat leaks out from the molten wire. The most severe condition will be "instantaneous" burnout, where only this heat of fusion can contribute to ignition.

#### Instantaneous Burnout of the Bridgewire

If the high temperature coefficient of resistivity (or high current input) leads to essentially instantaneous melting and burnout of the bridgewire, the temperature distributions in the explosive will be of the type shown in Figure 6. In this case, the conductivity assumed ( $K = 10^{-3}$  cal/cm<sup>2</sup> sec °C/cm) is very high for an explosive and very low for a glass header, which will maximize the volume of explosive heated.

It will be observed that there are three vertical scales which depend on the heat content of the bridgewire at the time of burnout, gold and copper being in the lowest range, the stainless steels and nichromes being in the intermediate, and platinum being in the highest group shown.

---

(2) Bowden and Yoffee estimate the critical sphere size as between 0.1 and 10 microns in diameter, Fast Reactions in Solids, Academic Press Inc. 1958

It is to be noted that with the gold and copper alloys an annulus of less than 10 microns width is heated to  $500^{\circ}\text{C}$  for .5 millisecond, but by 1 millisecond, less than a 5 micron annulus is above  $500^{\circ}\text{C}$  and by 1.5 millisecond, the temperature is everywhere below  $500^{\circ}\text{C}$ . Thus, for successful initiation the critical annulus width must be of the order of 5 microns (1/5 mil) or less for 1 millisecond.

For the stainless steel alloys the situation is somewhat improved, but even for the platinum alloys only about a 15 micron annulus remains above  $500^{\circ}\text{C}$  for 1 millisecond. Thus, initiation must be fairly rapid even for the best of these cases, or the temperature will fall below the ignition point.

It is to be noted that if the insulator is ceramic the times on the curves will be less by a factor of 5. Thus, it is easy to see why dudding may occur with pyrotechnic blends on the bridgewire, especially if the bridge wire is made of a gold alloy with a high temperature coefficient of resistance. In this case one may heat only a few tenths of a mil annulus above the ignition point for a few tenths of a millisecond and ignition will be almost impossible to achieve with a pyrotechnic.

#### The Effect of $\alpha$ on Temperature Distribution Along the Wire

The effect of the temperature coefficient of resistivity on the temperature distribution along the wire in the all-fire case is very small because, as we have seen in the previous study, the end leakage effects are negligible in times of the order of milliseconds. Thus, the temperature distributions are essentially flat along the wire until one approaches very close to the ends of the wires (see Figure 7). Of course, the temperature of the wire

is increased significantly since, under constant current conditions, the effective power level is greater as  $\alpha$  increases the resistance of the bridgewire.

In the no-fire case, the effect of the temperature coefficient of resistivity becomes more severe since heat leakage out the ends of the wire in long periods of time extends the temperature gradients further toward the center of the wire. The resulting temperature distribution is magnified as the temperature coefficient of resistivity is increased, tending to make the distribution even more peaked. For this reason, it is preferable to keep the radial heat leakage of the wire large compared to the longitudinal heat leakage so that the power dissipation will remain as uniform as possible for the no-fire case. If the temperature distribution is very flat for the case of no temperature coefficient of resistivity, then a large temperature coefficient of resistance will not change it appreciably.

#### The Effect of $\alpha$ on Local Defects

If there are local defects in the wire such as nicks, reduced diameter, or kinks which tend to result in a hot spot, the effect of the temperature coefficient of resistance is to cause this local heating to increase with time and thus to make the effect of the defect worse. In the no-fire case, this creates an incipient initiation point and in the all-fire case it creates a potential burnout point in the wire. The effect is just as bad whether it is a constant current or constant voltage firing, since it is only a question of relative power of the defect to the rest of the wire.

#### The Use of $\alpha$ as a Quality Control Measure

Although a high temperature coefficient of resistance has been shown

to have some severely degrading effects on the performance of an initiator, a modest temperature coefficient of resistance ( $0.5$  to  $1 \times 10^{-3} / ^\circ\text{C}$ ) can be extremely valuable in allowing one to measure the performance qualities of individual initiators in a nondestructive fashion with a very simple arrangement of a constant current source and an oscilloscope.

Since it was shown earlier <sup>(1)</sup> that  $H$ , the radial heat leakage parameter, affects both the short term and the long term performance of the initiator, a test that measures  $H$  gives a measure of both the no-fire and the all-fire characteristics. One such test is to measure the temperature increase in the bridgewire when a constant current is passed through it for a short period, say 10 milliseconds. The temperature rise can be easily measured if the bridgewire has a significant temperature coefficient of resistivity by using a constant current pulse and measuring the voltage drop across the bridgewire as a function of time.

A time of 10 milliseconds is suggested since in this time the effect of the material within about a 2 mil radius of the wire has contributed to the conductivity and the major temperature rise of the wire has been achieved. From this time on, the temperature rises very slowly and only as a result of heat capacity effects and remote boundaries within the system.

As a further refinement of the technique, it has been customary at Link Ordnance to ignore the first millisecond, since the temperature increase in this time is almost independent of  $H$ . (See Figure 5 and 6 of Reference 1). Only after the bridgewire temperature has reached a temperature such that radial heat loss constitutes a significant fraction of heat



input does the temperature rise become very sensitive to H. Whether or not the first millisecond rise is included will not affect the usefulness of the measurement, but only the absolute size of the numbers one is working with.

Figure 8 shows a circuit designed for the production monitoring of the thermal coupling of bridgewires by measuring the increase in the bridge-wire temperature from 1 to 10 milliseconds after the application of a 1 amp pulse, 10 milliseconds long. The voltage drop across the bridgewire under test is fed through an amplifier that increases the voltage to about 10 volts for convenience in measurement. The pulse is then fed to two peak follower units, one of which follows the pulse for only 1 millisecond and the other for the full pulse length. The outputs of these two units are then fed to a differential amplifier which subtracts the two values and sends the difference to a digital voltmeter which displays the voltage increase (or resistance change) that occurred between 1 and 10 milliseconds.

This gives a fast, reliable, direct reading measurement of the thermal coupling. Since the pulse is short and total energy low, the measurement may be repeated after a few seconds when temperature equilibrium has been reached again. If desired, a Tektronix 549 storage oscilloscope can also be used to monitor the pulse so that one may observe the detailed pulse shape on any anomalous pulses without the cost and bother of taking oscilloscope pictures.

With the use of an evaluation technique such as this, one can monitor production and limit the range of acceptable values of the thermal coupling as close as desired to any level. This can markedly reduce the spread in

both no-fire and all-fire performance values obtained. If it is applied at an early stage in production, just after the primary mix has been loaded into the header, the reject units can be recycled with a minimum loss of manhours or material.

It should be commented that this technique does modify the type of performance distribution which one will have left since the tails of the distribution have been severely limited. This has the affect of making the distribution much narrower than would be indicated by a standard Bruceton test which concentrates its measurements in the center of the distribution which has not been affected.

Link Ordnance has found the TCT measurement an extremely valuable tool from both cost and quality standpoints. As higher and higher reliability levels are imposed, the stray unit which significantly modifies the standard deviation can have disasterous effects on the acceptability of a lot. A non-destructive test which can find and remove such units is a blessing for both suppliers and users.

#### Summary

The effect of a significant temperature coefficient of resistance for bridgewire on the performance of an initiator can be either good or bad, depending on the conditions under which the initiator is used. Under constant voltage firing conditions it allows the temperature to rise rapidly and then lowers the temperature rise rate as the bridgewire burnout temperature is approached. In the case of constant current firings, however, the opposite effect is achieved and the temperature "runs-away" giving bridgewire burnout in undesirably short times.

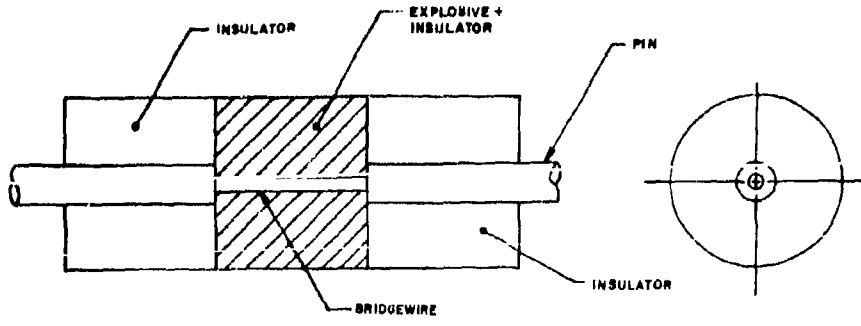
During a normal 4 amp firing pulse, the annulus of explosive around a 2 mil bridgewire that is above ignition temperature is shown to be less than 1 mil before bridgewire burnout with bridgewire materials that have a negligible temperature coefficient of resistivity and less than half of that for materials with a large temperature coefficient of resistivity. Thus, for pyrotechnic materials with larger critical thicknesses for ignition than this, the ignition will occur after bridgewire burnout as the heat from the bridgewire fragments leaks out into the explosive. This indicates the desirability of using materials with small critical volumes for ignition.

Initiators which use high  $\alpha$  bridgewire materials, or which are to be fired with high currents relative to their all-fire levels will function with essentially instantaneous burnout of the bridge. This requires that the primer material be capable of initiating in a fraction of a millisecond and from a hotspot only a few microns thick.

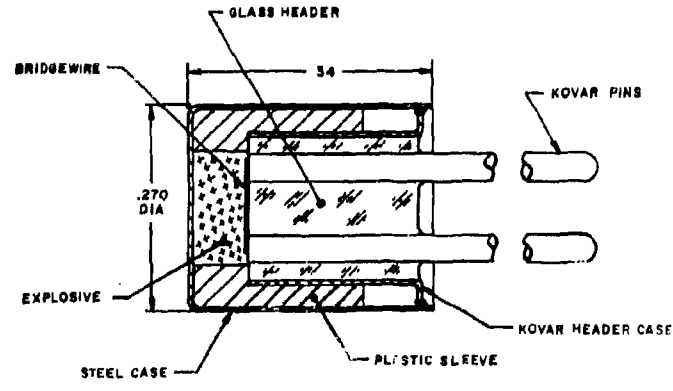
A thermal coupling test (TCT) circuit design has been developed, making use of a small temperature coefficient of resistivity in the bridgewire to monitor the all-fire and no-fire quality of initiators. The simplicity and reliability of the test make a desirable non-destructive test for production monitoring to improve both costs and reliability of units requiring high confidence levels of performance.

#### DISCUSSION

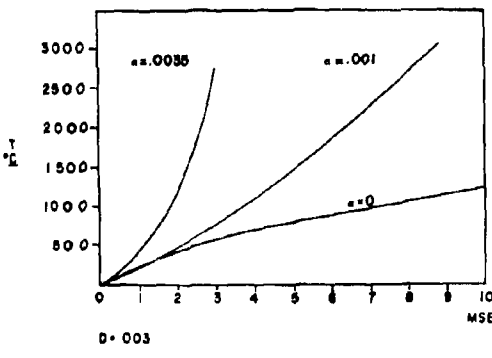
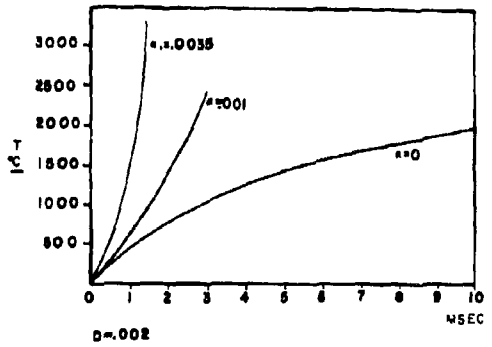
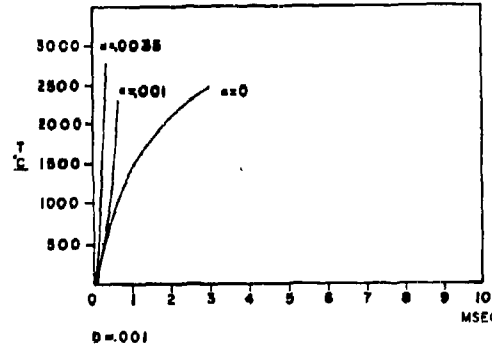
Mr. Parker of Lawrence Radiation Laboratory made the comment that a text by Carslaw and Yeager shows a solution where the resistivity varies linearly in the wire.



IDEALIZED INITIATOR CONFIGURATION FIG. 1B



TYPICAL SMALL INITIATOR DESIGN FIG. 1A



B/W=0.1" LONG  
GLASS HEADER  
CURRENT=4 AMPS  
INITIAL RESISTANCE=10HM

FIG 2

EXAMPLE OF EXPLOSIVE RING DESIGNATION SYSTEM

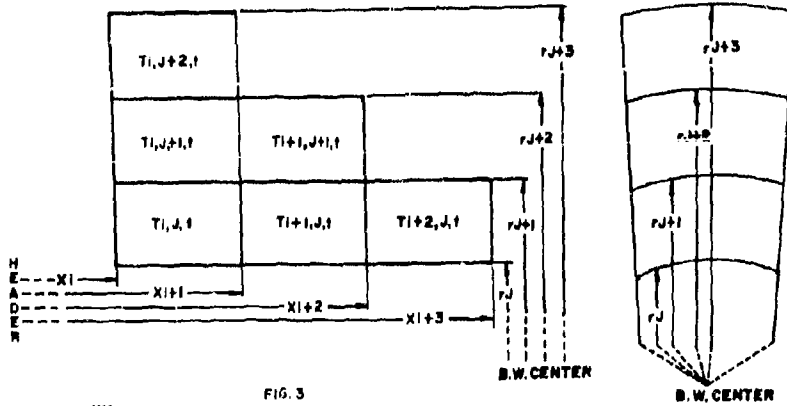


FIG. 3

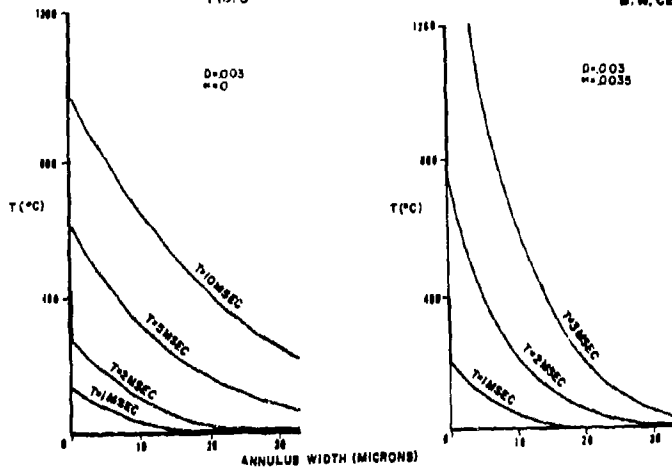


FIG. 4A

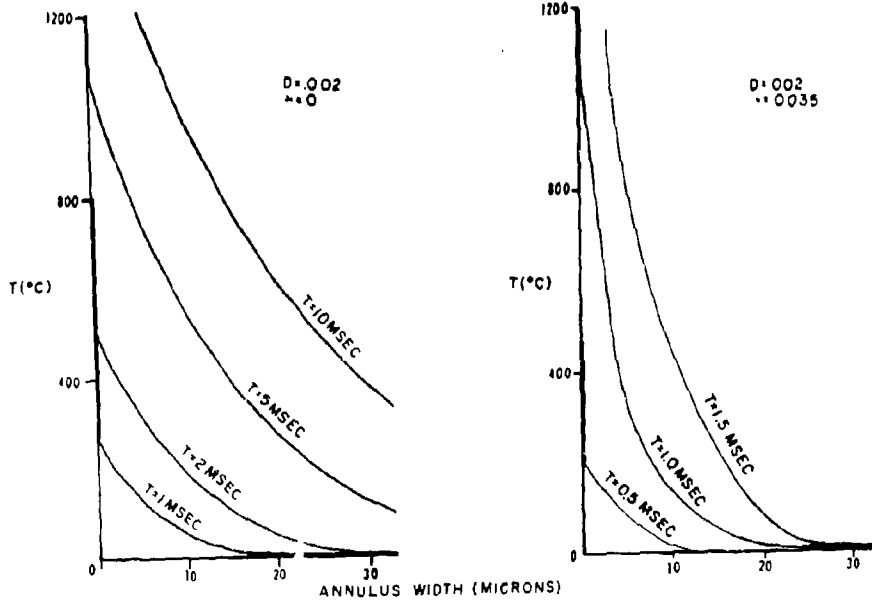
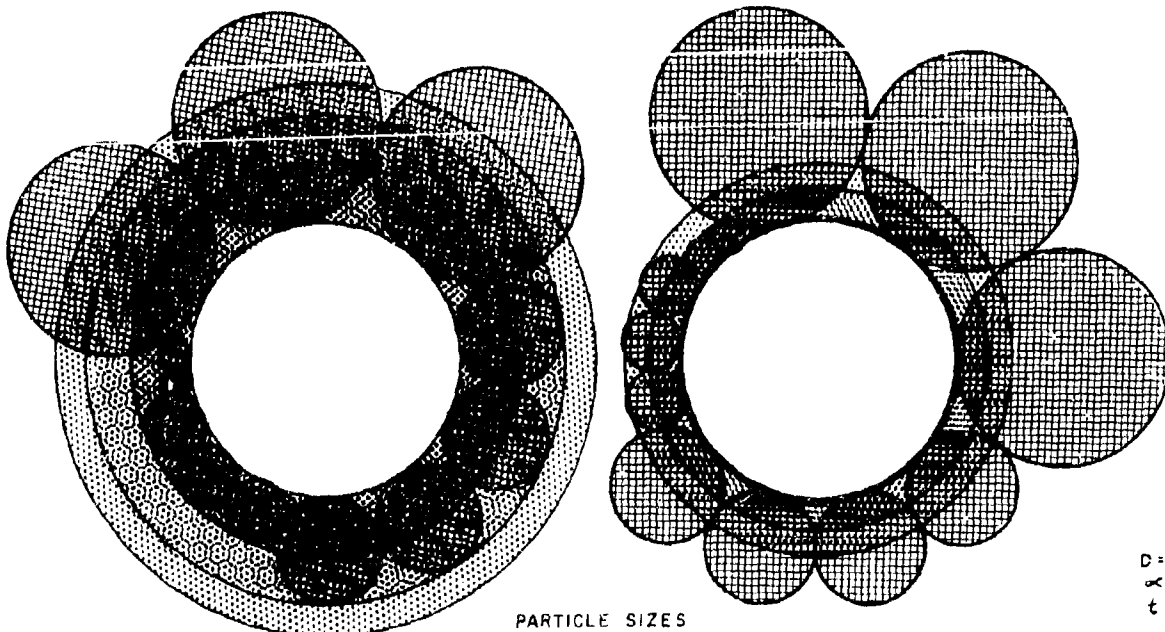




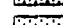
FIG. 4B



D = .002  
 $\lambda = 0$   
 t = 5 MSEC

PARTICLE SIZES  
 40 MICRONS  
 20 MICRONS  
 10 MICRONS  
 5 MICRONS

TEMPERATURE DISTRIBUTION

 500° OR ABOVE  
 300° TO 500°  
 200° TO 300°

D = .002  
 $\lambda = 0$   
 t = 2 MSEC

FIG. 5

INSTANTANEOUS BURN-OUT OF 2 MIL BRIDGEWIRE

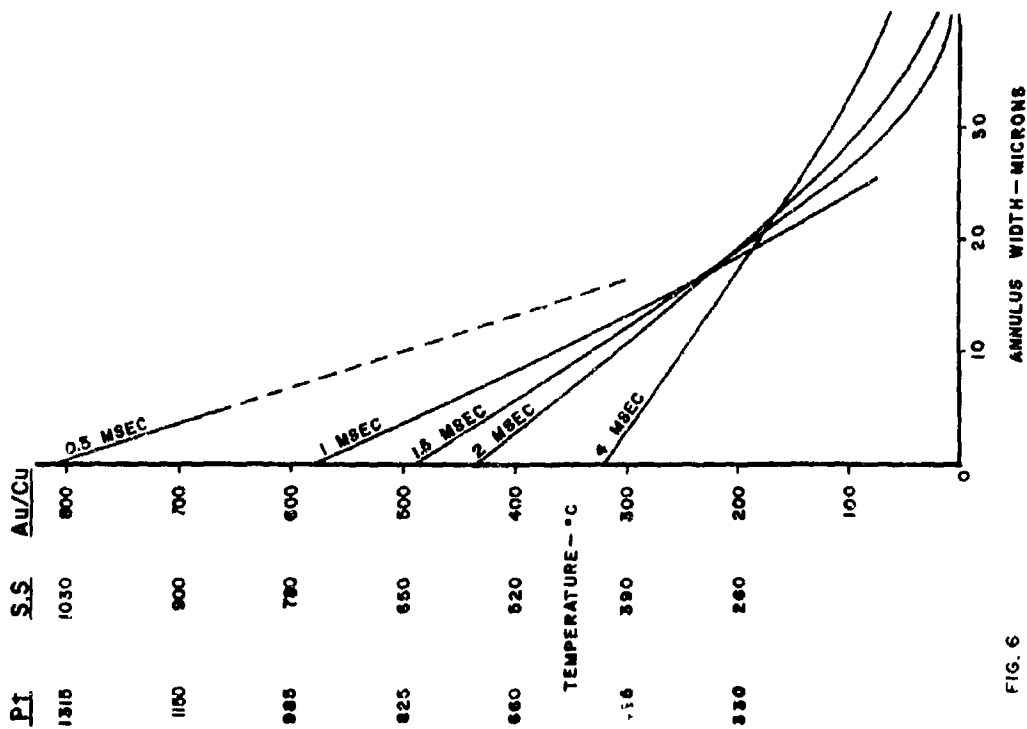


FIG. 6

## 3-2 INSENSITIVE ELECTRIC INITIATORS

Vincent J. Menichelli  
U. S. Naval Ordnance Laboratory  
White Oak, Silver Spring, Maryland

### INTRODUCTION

The electrical initiation of explosives in bridge-wire type electro-explosive devices is a thermal process (exploding bridgewire devices an exception) wherein the temperature of the bridge circuit is raised high enough to cause a sustained reaction in the explosive material in contact with it. The normal mode initiation sensitivity of a given electro-explosive device (EED) depends upon a number of parameters such as the bridge circuit design, the header, and the explosive material in contact with the bridge circuit. EED's can be and have been developed to function over a wide energy range from a few ergs<sup>1</sup> to deci-joules.<sup>2</sup> A number of investigators, as far back as 1872, have devised mathematical models in attempting to describe the electro-thermal conversion and the heat transfer from the bridge circuit to the explosive charge. In general, the models contained a large number of parameters which resulted in equations too

complex for easy solution. In order to reduce the equations to a workable form, large intuitive assumptions had to be made. More recently Korty<sup>3</sup> and Rosenthal<sup>4</sup> have lumped many of the parameters and arrived at a simple set of equations which can be easily handled. Rosenthal has designed and built instrumentation to measure some of the important thermal parameters which are necessary to understand the energy conversion.<sup>5,6,7,8,9</sup>

Rosenthal's basic thermal equation

$$C_p \frac{d\theta}{dt} + \gamma\theta = P(t) \quad (1)$$

where:  $C_p$  = Heat capacity of the bridge system  
(power-time/<sup>o</sup> temperature change)  
 $\gamma$  = Heat loss factor (power/<sup>o</sup> temperature change)  
 $\theta$  = Temperature rise above ambient  
 $P(t)$  = Input power function  
 $t$  = Time

shows that the sensitivity of an EED can be decreased by making  $C_p$  large e.g., increasing the volume of the bridge circuit and/or increasing  $\gamma$ .  $\gamma$  can be altered by controlling bridge element configuration, selection of explosive and other materials in contact with the bridge



element, and by intimacy of contact between explosive and wire. For a fixed bridge circuit, (e.g., header, pin spacing, bridge wire volume, and explosive on the bridge-wire) the sensitivity can be altered by altering the bridge element configuration. By changing the bridge element configuration, an EED was designed which was insensitive enough to pass 1-ampere of current or absorb 1-watt of power for five minutes without initiating, using conventional explosives and hardware.<sup>10</sup>

The theory advanced is that the sensitivity of an EED can be altered by increasing or decreasing the surface area of the bridge element while the bridge element volume remains constant. The bridge element of a conventional EED is usually a conducting metallic wire of a given diameter and length. The heat loss factor, ( $\gamma$ ) is directly related to the surface area of the bridge element. As the surface area increases,  $\gamma$  increases. For a given bridge element (constant volume and length) the surface area can be increased by changing the shape of the cross section. For a constant cross sectional area of approximately 10 square mils, the following table shows the increase in the perimeter (for fixed length, the surface area increase is of course proportional) when the cross section is changed

from a circle to various rectangles.

Configuration (mils)	Cross Sectional Area (square mils)	Perimeter (mils)
3.5 Diameter	9.6	11
1 x 10 Ribbon	10	22
0.5 x 20 Ribbon	10	41

#### EXPERIMENTAL ARRANGEMENT

Hardware of a conventional type presently being used in a number of Navy developed EED's was used to demonstrate that a decrease in sensitivity would occur as the perimeter of the bridge element was increased. It was the intention, if successful, to use this technique to convert existing conventional EED's to the less sensitive 1-amp/1-watt no-fire type with a minimum of redesign. The initiator assembly used is shown in figure 1. It consists of a conventional glass/kovar plug, plastic insulator, and aluminum charge holder. Normal lead styphnate or lead azide was pressed into the charge holder cavity and onto the bridge element. The initiator assembly was then solder-sealed into a metal cup containing a base charge of PETN as shown in figure 2.

Various bridge elements were soldered to the pins of the initiator plug and flush with the surface of the glass. The bridge elements tested, shown in figure 3, are divided into two groups. Group I elements were used to demonstrate that sensitivity could be decreased by increasing the peripheral area of the bridge element (equivalent to increasing  $\gamma$  of Equation 1). Group II elements were used to determine the bridge resistance range which could be obtained and still meet the 1-amp/1-watt no-fire for five minutes criterion. The bridge element material in Group I was Cupron and bridge elements in Group II were fabricated from Cupron, Alchrome, and Evanohm. The compositions of these materials are listed in appendix A. These bridge materials were selected on the basis of their low temperature coefficient of resistivity to minimize thermal feed-back in constant current testing.

#### TEST RESULTS

Heat Loss Study - A series of tests were conducted to determine if in fact the electro-thermal performance was affected as the surface area of the bridge element increased. The tests were conducted using the detonator assembly as shown in figure 2 and the bridge elements of Group I, Figure 3.

Bruceton<sup>11</sup> tests of approximately 50 samples each were conducted on each bridge element configuration in Group I to obtain the mean sensitivity to capacitor discharge, pulsed constant current, and continuous constant current. Table 1 lists the results of this testing. The mean energy to initiate by capacitor discharge (100 microfarads, variable voltage) is approximately constant. This was anticipated because the thermal time constant ( $\tau = \frac{C_p}{\gamma}$ ) is large compared with the discharge time constant of the capacitor<sup>4,12</sup>. Appreciable cooling therefore does not take place during the time of energy input. Because of the adiabatic nature of the heating, the differences in surface areas of the bridge elements are inconsequential. For this adiabatic heating, the temperature rise varies as  $\frac{1}{C_p}$  and  $\gamma$  is ineffective.

The mean pulsed constant current data were obtained by keeping the current constant at 5-amperes and determining the time for which this current had to flow to produce 50% fires. As the perimeter increased, the mean time to fire increased. The results indicate that the heat loss factor ( $\gamma$ ) increased as the peripheral area of the bridge element increased.

Sensitivity to continuous constant current was obtained

in a variable-current Bruceton test. Each current level was maintained constant until firing or for a minimum of 10 seconds, whichever occurred first. If the device did not fire in 10 seconds, it was assumed that an equilibrium temperature below the functioning temperature had been reached. The time to fire for those devices which fired in less than 10 seconds was not recorded, consequently, the energy input to time of firing could not be calculated. Again, as the bridge element surface area increased, the sensitivity decreased. The sensitivity values do not appear to be affected as much by continuous constant current testing as by pulsed (5 ampere) constant current testing. Energy comparisons could not be made because the firing times for the continuous constant current tests were not measured. The fact that the current did not change very much for continuous constant current firing, whereas the energy changed drastically for the pulsed current firing probably occurs from change in the effective heat losses under the two sets of conditions. For the pulsed constant current input the large structural mass of the EED plays no significant role. The effectiveness of the heat sinking is controlled by the leads and the contact between the bridge circuit and the glass substrate. This latter changes rapidly with the bridge geometry. For the relatively long continuous constant current input, the massive structure of the EED probably controls the

heat losses to the surrounding atmosphere. This massive structure remains unchanged by the small changes in bridge circuit - glass substrate geometry.<sup>13</sup>

Bridge Resistance Study - This work was conducted to select bridge element materials and designs which could be put to practical use in existing Navy devices. The method was to load detonators, as shown in figure 2, containing the various bridge elements of Group II, figure 3. The bridge element resistances ranged from 0.1 ohm to 5.0 ohms. Lead azide or normal lead styphnate was loaded on the bridge element. A constant current was allowed to flow through the circuit for a period of 5 minutes or until the device fired, whichever occurred first. If the device fired in less than 5 minutes it was considered a "fire". Not all combinations of bridge circuits and explosive loads were capable of meeting the 1-amp/1-watt for five minutes no-fire criterion. Table 2 shows that for bridge Element "A" only the Cupron material with a bridge resistance of 1.7 ohms met the no-fire criterion with either lead azide or normal lead styphnate. Since only a few samples were tested, it is questionable whether or not the normal lead styphnate loaded items can indeed meet the no-fire criterion.

Table 3 indicates that for bridge element "B" only Cupron with a bridge resistance of 0.7 ohms and with either lead azide or normal lead styphnate on the bridge could meet the no-fire criterion.

In table 4, it is seen that for bridge element "C" all the bridge element materials are capable of meeting the no-fire criterion for both lead azide and normal lead styphnate with the exception of the Evanohm/normal lead styphnate combination. The bridge resistances were 0.4 ohm for Cupron 1.2 ohms for Alchrome, and 1.3 ohms for Evanohm.

For simplicity and ease of fabrication, bridge element "D" was tested. Because of the short bridge element length, the bridge resistance is less than one ohm. Lowering the bridge resistance below one ohm requires that the current value must increase above 1-ampere in order to meet the 1-watt no-fire criterion. Table 5 shows that only Alchrome and Cupron with lead azide on the bridge element could meet the 1-amp/1-watt no-fire criterion.

#### DISCUSSION AND CONCLUSIONS

It has been experimentally demonstrated that the rate of heat loss (and consequently the value of  $\gamma$  in Rosenthal's thermal equations) can be influenced by the geometry of the bridge element. The surface area of the bridge element, through which heat was conducted away, was varied and controlled and for a given bridge element volume and length, the electrical sensitivity decreased as the surface area increased. The

bridge elements used in this investigation are not necessarily the most efficient. It is expected that thinner films such as evaporated metals would be more effective in increasing heat losses. Other investigators have already successfully experimented with evaporated metal films.<sup>14</sup>

Bridge elements made from three different materials were tested to select a design which would be suited for 1-amp/1-watt no-fire devices. Of the three materials, Cupron resulted in a less sensitive system for the same bridge element geometry. It is suspected that thermal conductivity of the materials may be responsible. Thermal conductivities for Evanohm and Cupron were obtained from the Molecu-Wire Corporation, Scobysville, N. J. They are respectively 0.126 and 0.218 watts/cm/°C.<sup>13</sup>

The bridge elements shown in Group II, Figure 3 (except element "D") were fabricated by a photo etching process. The materials were obtained from Driver-Harris Company, Harrison, N. J., in sheet form (1 mil thick) and supplied to the Chem Fab Corp., Donaldson Street, Doylestown, Pa., for photo etching of the elements. This method has proved very successful in producing uniform elements. The other elements described were made by a drawing process.



3-3 CONSTANT CURRENT IGNITION  
OF METAL-METAL OXIDE MIXTURES\*

James L. Austing  
Research Engineer, Chemistry Research Division  
IIT Research Institute  
Chicago, Illinois 60616

John P. Weber  
Staff Member, Component Development Division  
Sandia Corporation  
Albuquerque, New Mexico 87115

INTRODUCTION

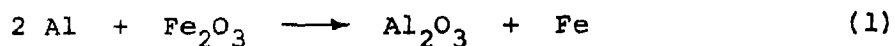
Electroexplosive devices (EED's), or electric initiators as they are frequently called, are used in ordnance systems to convert an electrical pulse into a chemical burning or detonation reaction for purposes of reliably initiating a subsequent propellant or explosive charge. The typical design of the electroexplosive device consists of a suitable electrical bridge element which is in physical contact with an explosive or pyrotechnic flash charge; the electrical pulse heats or explodes the bridge, and this in turn initiates the flash charge. Research and development activities in the area of electroexplosive devices over the last several years have been directed towards improving the safety of these devices, while maintaining their inherent high reliability. Specifications and standards have been drawn up

---

\* Work supported by the U.S. Atomic Energy Commission.

which require that EED's dissipate without functioning input no-fire currents and powers of 1-amp and 1-watt for 5 minutes or 5-amp and 5-watts for 15 minutes. Furthermore, EED's must not be sensitive to electrostatic discharges such as those produced by the human body. By designing EED's to meet these standards, the probability of accidental initiation is significantly reduced. The work described in this paper was part of an overall program to develop electric initiators of improved safety for aerospace applications.

The metal-metal oxide pyrotechnic is a mixture of a metal powder and a metal oxide powder that upon ignition will react in an oxidation-reduction type reaction, with liberation of a large amount of heat, such that the products may be in the liquid or the vapor state, depending on the system of interest. The most familiar of these systems is the thermite reaction,



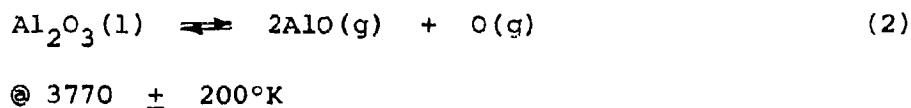
where the product iron is in a molten state. Hence, metal-metal oxides have high reaction temperatures, and can be used as ignition sources for a variety of explosive and ordnance type devices. The thermite reaction itself is somewhat difficult to ignite, but other properly selected combinations can be ignited reliably by the flow of current through a bridge. This paper discusses the experimental efforts related to the development of an electrostatic-insensitive 5-amp, 5-watt no-fire initiator, and the all-fire ignition studies of metal-metal oxides pressed

against 5-mil diameter wire bridges. Subsequent papers in this proceedings will describe the development of an ignitability criterion for a pressed reactive bed in contact with electrically-pulsed bridges (ref. 1), and the initiation of detonation in insensitive explosives by means of metal-metal oxide reactions (ref. 2).

#### THERMOCHEMICAL CALCULATIONS

Table 1 shows calculated thermochemical data for systems of interest. The heat of reaction was calculated from the enthalpies of formation of the compounds as reported by Glassner (ref. 3) and Perry (ref. 4). The reaction temperature was calculated from an enthalpy balance equated to zero for adiabatic and constant pressure conditions by using enthalpies and heat capacities also from Glassner. The final column shows the assumed state of the reaction products at the reaction temperature.

The reaction temperature of all systems except the aluminum-copper oxide system is high enough to bring the product oxide to its boiling point. For the purposes of these calculations, this process takes place as follows (ref. 5):



The reaction temperature of aluminum-copper oxide is much lower, because the product copper boils at 2868°K and thereby provides a heat sink to any further elevation of temperature.

#### DESCRIPTION OF ALUMINUM AND METAL OXIDE POWDERS

Four grades of aluminum powders were evaluated. These included two spherical grades, H-3 and H-5, manufactured by the Valley Metallurgical Company, Essex, Connecticut, and two flaked grades, 28-XD and 40-XD, manufactured by the Reynolds Metals Company, Louisville, Kentucky. The two spherical grades are quoted to be of 3- $\mu$  and 5- $\mu$  average particle size, respectively, in accordance with the designation. The H-5 spherical grade meets the requirements of specification MIL-A-23950 (Wep), while the flaked grades meet the requirements of specification MIL-A-512A.

Two grades of tungstic oxide, TO-2 and TO-3, were used extensively. These were manufactured by the Sylvania Electric Products Corporation, Towanda, Pennsylvania. All Sylvania tungstic oxide is manufactured by roasting tungstic acid. The product is pale yellow in color. The TO-2 grade is a fine powder, with a quoted maximum particle size of 3 $\mu$ , while TO-3 is much coarser, 15 to 20  $\mu$ .

Two suppliers of cupric oxide were located: the Glidden Company, Hammond, Indiana, and Calumet and Hecla, Incorporated, Calumet, Michigan. The products of both companies meet the requirements of specification MIL-C-13600. The Calumet and Hecla powder is somewhat finer than the Glidden powder, according to a comparison of the manufacturers' specifications.

Manufacturer's specifications, when available, showed that all the oxide powders used were of reasonable purity.

Glidden cupric oxide contains at least 95% CuO, and Calumet and Hecla cupric oxide contains at least 98.5% CuO, with the largest impurity in these being cuprous oxide.

The particle size distribution of the above powders was measured by using the IITRI centrifugal disc photosedimentometer. This instrument is described in Reference 6. In this analytical procedure the Stokes diameter distribution of the particles in suspension is deduced from the concentration changes occurring within the settling suspension when the suspension is subjected to centrifugal forces. The size analysis of the powders that were used extensively is shown in Figures 1 and 2. The TO-3 tungstic oxide was not tested, because it was too coarse for the centrifuge, and time did not permit a gravity sedimentation analysis.

#### ENVIRONMENTAL EVALUATIONS

##### Thermal Stability of Metal-Metal Oxides

One method for evaluating the thermal stability of a system is differential thermal analysis (DTA). The sample under study is heated continuously at a controlled rate side by side with a thermally inert reference material. A thermocouple embedded in the sample and in the reference material permits continuous monitoring of the temperature difference between the two as a function of temperature magnitude. As long as no change takes place in the sample, the temperature difference ideally is zero.

If the sample changes phase or reacts endothermically, a thermal arrest occurs. If the sample reacts exothermically, the temperature difference becomes positive, and may be so large that the slope of the curve becomes vertical.

The DTA instrument used was the Fisher model 260 Differential Thermalizer, which consists of three separate units, a furnace, a solid-state programmer, and a sample holder. A Microcord 44 recorder (Photovolt Corporation) completes the instrumentation system.

The procedure for thermal analysis is outlined in Fisher catalogue No. 10-560V1 and was the same for all samples tested. Sample weights were maintained at 100 mg, but some were diluted with alumina to decrease the violence of the reaction should an explosion occur during the heating cycle, and to keep the thermocouple in contact with the material should a reduction in sample volume occur. This method of sample preparation minimized the amount of sample present in the crucible, yet maintained a mass approximately equal to that of the reference crucible. The quantities of sample and reference material should be approximately the same in each crucible to minimize baseline drift in the thermogram.

Thermograms for two metal-metal oxide systems are shown in Figure 3. Similar curves are also presented for the aluminum-potassium perchlorate system, because this system has also been used in the design of initiators with a 5-amp, 5-watt no-fire capability (ref. 7). The peaks which can be readily identified

are the rhombic to cubic transition in  $\text{KClO}_4$  at  $300^\circ\text{C}$ , the decomposition of  $\text{KClO}_4$  at  $500^\circ\text{C}$ , the fusion of product  $\text{KCl}$  at  $770^\circ\text{C}$ , and the fusion of aluminum at  $660^\circ\text{C}$ . In addition, the absence of appreciable exothermic peaks up to temperatures as high as  $800^\circ\text{C}$  suggests that metal-metal oxides have an enhanced thermal stability. These observations are in line with previous work, wherein certain metal-metal oxide mixtures such as  $\text{Al-WO}_3$  were held in  $500^\circ\text{C}$  environments for as long as 60 minutes, during which time no autoignition occurred; upon cooling down, the mixture could be ignited by current flow through a wire bridge with no apparent degradation of performance (ref. 8).

The large exotherm in the  $\text{Al-WO}_3$  trace beginning at approximately  $825^\circ\text{C}$  is believed to be associated with autoignition of the mixture. Accordingly, we have assumed that  $825^\circ\text{C}$  is the autoignition temperature, and have used this value in the development of the ignitability criterion for the  $\text{Al-WO}_3$  system in Reference 1. The fact that propagating reaction was initiated at marginal currents where the calculated bridge temperature was not much in excess of  $825^\circ\text{C}$  suggests that this temperature is a good estimate of the autoignition temperature.

#### Sensitivity to Electrostatic Discharge Pulses

The ability of an electric initiator to withstand electrostatic discharges such as those produced by the human body is an important safety consideration. A number of tests were conducted on initiators loaded with pressed  $\text{Al-CuO}$  and  $\text{Al-KClO}_4$  mixtures.

The initiator is depicted in Figure 4. It consisted of a steel sleeve case assembled to a Kovar-glass header in such a manner as to form a cup approximately 0.540 in. deep. The components were held together by epoxy resin. The Kovar-glass header was bridged with a 5-mil-diameter Evanohm wire each end of which was welded to the pins. The tests were conducted by discharging a 600-pf condenser at a maximum of 25 kv through the metal-metal oxide mixture, that is, from pin to case. No 500-ohm series resistor was used,\* so that effectively the electrostatic discharge was in excess of what can be generated by the human body.

Under the above conditions, it was found that mixtures of H-3 spherical grade aluminum and cupric oxide were not initiated at 25 kv. In fact, a given pressing could dissipate repeated discharges at this voltage without being initiated. Identical results were obtained from mixtures of flaked aluminum and potassium perchlorate. It is conceivable that many other metal-metal oxide systems such as Al-WO<sub>3</sub> subjected to this environment would behave the same way, although these other systems were not tested.

On the basis of these results, a family of electrostatic-insensitive initiators with a 5-amp, 5-watt no-fire capability

---

\*The function of the series resistor, when used, is to simulate the resistance of the human body, which under discharge conditions is approximately 500 ohms.



has been developed for aerospace applications. The basic charge in these initiators is a mixture of flaked aluminum and potassium perchlorate (ref. 7).

### CONSTANT CURRENT IGNITABILITY STUDIES

#### Constant Current Firing Circuit

The ignitability studies of the metal-metal oxides were conducted with a constant current firing circuit, a schematic diagram of which is shown in Figure 5. The basic power supply consists of lead storage batteries connected in series. The operation of the circuit is as follows. The resistance,  $R_1$ , is set equal to the resistance of the initiator under test. The current,  $I_1$ , through  $R_1$  is adjusted to the desired value by moving the rheostat. Then the calibrating circuit switch is opened, and the circuit to the initiator is completed by closing the mercury switch. The initial current through the initiator is equal to the preselected value of  $I_1$ . The switching of resistance,  $R_e$ , into the circuit permits higher currents at a given rheostat setting.

The specification of each component is given in Figure 5. The current,  $I_1$ , was read with a standard ammeter. Alternatively, the current can be adjusted to the desired value by measuring the voltage drop across  $R_1$  with a voltmeter. The variable resistance,  $R_1$ , was constructed from 17-gage (0.045-inch) Nichrome wire about 50 cm long and was suspended along a meter stick graduated to the nearest tenth of a centimeter. Contact between

the circuit and the Nichrome wire was made by means of alligator clips, which permitted adjustment of the value of  $R_1$  by varying the effective length of the Nichrome being used. The mercury switch was a heavy-duty type rated at 15 amp. This switch permitted positive completion of the circuit to the initiator with a minimum of bounce and chatter. The shunt resistor in series with the initiator was also constructed from 17-gage Nichrome wire of such a length as to give a resistance of approximately 0.020 ohms.

All cables in the firing circuit, from the batteries to the initiator, were in the form of long, flat conductors separated by a dielectric. The purpose of this construction was to minimize the rise time to peak current. Stresau and Hillyer (ref. 9) designed an EBW firing circuit based on this principle. Our flat cable, diagrammed in Figure 6, consisted of two soft copper strips, 3/4-in. wide by 0.0108 in. thick, which were separated by 5-mil Teflon tape. These three components were held together by a tight wrapping of Scotch No. 33 electrical tape. Conduit to switches and resistors were constructed in the same manner in order to minimize inductive loops. The inductance and the capacitance of the circuit were measured with a type 1650-A General Radio impedance bridge, and values of 21  $\mu$ henries and 0.009  $\mu$ f were obtained, respectively. Probably most of the inherent inductance was in the wire-wound power rheostat and other resistors.

Oscilloscope studies showed that the rise time to peak current was approximately 10  $\mu$ sec. Selected oscilloscope records at various sweep rates are presented in Figure 7. The oscilloscope was triggered from the applied voltage pulse in Figure 5, and the voltage drop across the shunt resistor was monitored in these tests.

The rise time of 10  $\mu$ sec for the flat cable firing circuit should be compared with that for the previous design of this circuit, in which all conductors were stranded wires. Although the inherent inductance was not measured, the rise time to peak current was 60  $\mu$ sec. These data indicate that the inductance in the latter circuit was higher and that a concentrated effort to minimize inherent inductance where it is undesirable will significantly improve the current-time characteristics of a firing circuit.

#### Formulation and Loading of Powders

The metal-metal oxide formulations were mixed in small batches of 15 to 40 g. Powders were placed in a closed jar and rotated for approximately 10 min on a bench-top roller mill. This rotation resulted in a mixture that visually appeared to be uniform.

The initiator shown in Figure 4 was used for all ignitability studies; this initiator contained the Kovar-glass header bridged with the 5-mil diameter Evanohm wire. The following procedure was used in loading the initiators. A weighed quantity of metal-

metal oxide, 350 to 500 mg, was pressed into the cup of each initiator at a specific, predetermined loading pressure that ranged from 2500 to 20,000 psi. The ram used in the pressings was a drill blank of such a diameter as to have a slip fit inside the initiator. The height of the column of pressed powder was calculated by subtracting the depth of the initiator after loading from the depth prior to loading, both measurements having been made with a depth micrometer.

The density variation at each loading pressure follows a normal probability distribution. This is illustrated in Figure 8, in which the individual densities for  $2/3$  stoichiometric\* H-3 aluminum + TO-2 tungstic oxide at 4800 psi are plotted versus probability coordinates. Similar results were obtained at other loading pressures and for other systems in which a sufficient number of points permitted calculation of standard deviation. The data are summarized in Table 2. There appears to be a general decrease in standard deviation as the loading pressure increases.

#### Instrumentation

The instrumentation included measurement of the resistance of the initiators before and after loading, continuous monitoring of current through and of voltage drop across the initiators during firing, and measurement of overall function time.

---

\* Deficient in aluminum

The system used for measuring initiator resistance consisted of a calibrated circuit that limits the flow of current through the initiator to 1 amp, so that the voltage drop across the initiator in millivolts is numerically equal to its resistance in ohms. An accurate value is obtained by measuring the millivolt drop with a laboratory potentiometer. At the same time, the very low current does not change the characteristics of the initiator.

The performance of the initiators during firing was monitored by a Tektronix type 555 dual-beam oscilloscope equipped with a Polaroid camera. The upper beam was chopped into two channels by means of a type CA dual-trace plug-in unit. Channel A recorded the voltage drop across the shunt resistor in Figure 5. Since the shunt resistor is made from a heavy piece of resistance wire, its resistance changes very little during the milliseconds required for initiator functioning. Hence, this voltage drop is proportional to the current. Channel B recorded the applied voltage drop across both the initiator and the shunt resistor.

The voltage sensitivities on the preamp were set so as to give beam reflections of about 2 cm on each channel. In this way, the simultaneous recording of current through the voltage drop across the initiator provided a continuous picture of initiator resistance during firing. The sweep rate on all shots was slow enough that the chopping frequency of 100 kc did not cause discontinuities in the current and voltage records.

The lower beam of the oscilloscope was used in conjunction with an ion probe system to measure the overall functioning time of the initiator and was equipped with a type L plug-in unit. The ion probe circuitry is shown in Figure 9. The actual ion probe consisted of a Kovar-glass header from which the bridge wire had been removed, and the header was inserted in the end of the loaded initiator. The heat of the metal-metal oxide reaction, as it emerged from the end of the pressed column, caused the air around the probe to ionize and hence to become electrically conductive. When the condenser began to discharge, the voltage drop across the 47-K resistor initially jumped from 0 to 45 v. It then decayed at a rate dictated by the RC time constant, which was 47 msec in this system. In the oscilloscope, therefore, the point at which the jump in voltage occurred was the time interval of interest, the overall function time.

In all the firings the upper beam (two channels) and the lower beam were on separate time bases so that sweep rates could be varied independently. Both beams were triggered from the applied voltage pulse in Figure 5. A typical oscilloscope record is shown in Figure 10. Note that the voltage trace decreases slightly from its initial value. This pattern indicates that the resistance of the initiator decreases during firing. At 37 msec the voltage trace becomes rather erratic, the significance of which is explained below. The lower trace shows that the overall function time of this initiator was 66 msec.

### Determination of Time of Ignition

After firing a number of shots it became apparent that the time at which the voltage trace became erratic was associated with ignition of the metal-metal oxide bed. This result was demonstrated to be a fact in a series of tests in which the height of the metal-metal oxide column was decreased in increments from the test to the next. The burning time, defined as the difference between the overall function time and ignition time, should be a linear function of column height. Furthermore, if the ignition time has been properly selected, an extrapolation to zero column height should show zero burning time. The data are summarized in Table 3, in which the assumed ignition time is the point at which the voltage trace becomes erratic. Plots of the assumed burning time versus column height are shown in Figures 11 through 13, in which the extrapolation is also made. In every case the curve extrapolated to or very near to the origin, thereby confirming the assumption concerning the time of ignition on the oscilloscope records.

### Summary

The constant-current ignitability studies on various combinations of aluminum and metal oxide are summarized in Tables 4 through 9. The data in each table are arranged in the order of decreasing current. Initial currents were varied within a range of 49.6 amp to 7.1 amp, with the majority of the tests being conducted at or near 15 amp, which is the design all-fire current

for the 5-amp, 5-watt no-fire initiator. Most of the evaluations were performed on mixtures containing 2/3 the stoichiometric amount of aluminum, because these mixtures could be ignited more reliably at 15 amp. It was our general experience that ignition became more difficult as the percentage of aluminum was increased and/or the loading pressure was increased. However, some of these systems that are difficult to ignite at 15 amp may be reliably ignited at higher currents.

At the start of the testing the initiator resistance was measured both before and after loading. However, it became apparent that the conductivity of the aluminum-metal oxide bed was low enough that no change in resistance could be detected. Hence, measurements of resistance before loading was discontinued, and only the resistance after loading is reported in the tables.

The resistance at ignition was calculated from the voltage and current traces at the point where the voltage trace became erratic. Most of the records showed a slight, steady decrease in initiator resistance to a value very close to that at ignition. After this decrease the resistance remained essentially constant up to the time of ignition. Calculations presented in Reference 1 show that complete melting of the Evanohm bridgewire occurred well ahead of the ignition. Hence, the decrease in resistance can be explained in part by the possibility that molten Evanohm has a lower resistivity than the solid Evanohm. Another part of the explanation stems from the DTA data in Figure 3. These data showed that melting of aluminum preceded ignition. It is possible



that a layer of molten aluminum developed around the bridge prior to ignition; this occurrence would increase the effective cross-sectional area and thereby decrease the resistance.

The unit burning time in Tables 4 through 9 was calculated by subtracting the ignition time from the overall function time and then dividing this difference by the column height. Overall function time was not reported in the tables in order to conserve space but can be calculated from the following:

$$\begin{aligned} \text{Function time} &= \text{ignition time} + & (3) \\ &(\text{column height}) \times (\text{unit burning time}) \end{aligned}$$

The unit burning time data for several metal-metal oxide systems are plotted in Figures 14 through 19. Unit burning time is the reciprocal of burning rate. Note how well the burning rate correlated with density, particularly in the aluminum-tungstic oxide systems. The scatter in the points for these systems is within the experimental error of the measurements, that is  $\pm 2$  msec in burning time and  $\pm 0.002$  in. in column height. The correlation for the aluminum-cupric oxide systems was not as good, possibly because the pressed columns were inadvertently allowed to exceed one diameter (0.222 in.) in length. This occurrence may have caused excessive density gradients in the column.

Increasing the amount of aluminum caused the mixture to burn more rapidly in all systems. Increasing the density slowed the burning except for H-3 aluminum-Glidden cupric oxide system.

As shown in Figure 18, mixtures that contained a stoichiometric quantity of aluminum or 30% excess aluminum exhibited more rapid burning as the density was increased. However, it is difficult to see such a trend in Figure 19, which shows the results with H-5 aluminum.

The overall function time of an initiator was the sum of the ignition time plus the burning time. Generally changes in the amount of aluminum in the mixtures did not greatly affect overall function time at 15 amp. Most of the overall function times were in the range of 50 to 80 msec depending on the system. Since increasing the amount of aluminum caused the mixtures to burn faster, the conclusion was that these mixtures took longer to ignite. On the other hand, mixtures with decreased aluminum content ignited more quickly but took longer to burn. Our unit burning time data showed fewer points for mixtures with a stoichiometric or greater quantity of aluminum. This resulted because these systems were harder to ignite at 15 amp, and their performance at higher currents was not studied. However, in view of the more rapid burning of these systems, some definite advantages in shortened overall function time might be gained by firing these systems at substantially higher currents.

The data in Tables 4 through 9 show that loading density had a observable effect on ignition time. Generally speaking, at a given current an increase in density caused an increase in ignition time. A possible explanation for this effect is discussed in Reference 1. The implication, of course, is that accurate

control of overall function time of the initiator requires control of metal-metal oxide loading density, particularly for a system such as Al-CuO where not only ignition time but also burning rate varies significantly with density

#### 5-amp, 5-watt No-Fire Experiments

The ability of metal-metal oxide initiators bridged with a 5-mil wire to dissipate a constant 5-amp, 5-watt pulse without functioning or seriously degrading the performance is shown in Table 10. Ten initiators illustrated in Figure 4 were loaded with 2/3 stoichiometric mixtures of either Al-WO<sub>3</sub> or Al-CuO, in the same manner as for the constant current ignition studies. A current of 5 amp was then delivered to the initiator for a period of 15 minutes. The input power at this current was somewhat greater than 5-watts, except for the test where the initiator resistance was less than 0.200 ohm. The initiators became very hot; however none fired under these conditions.

After each initiator cooled to ambient temperature, an attempt was made to fire it at the design all-fire current of 15 amp. The performance at 15 amp is summarized in columns 5 through 8 of Table 10. The ignition times are essentially the same as for initiators which have been tested only at 15 amp, as previously reported in Tables 4 and 8. However, the unit burning times (i.e., burning rate) of the metal-metal oxide was affected somewhat by the 5-amp exposure. The Al-WO<sub>3</sub> system burned more slowly than that studied in Table 4, while the

Al-CuO burned more rapidly than that in Table 8. However, the burning rates under both sets of conditions are of the same order of magnitude, so that the observed differences are of no major concern.

#### ACKNOWLEDGEMENTS

The authors are indebted to all personnel of IIT Research Institute and Sandia Corporation who assisted in the investigation discussed in this paper. IITRI personnel who contributed to the work included: Dr. Brian H. Kaye, who directed the particle size studies; Mr. James A. Erickson, who performed the differential thermal analysis studies; and Messrs. Douglas E. Baker, James E. Daley, Kenneth W. Jones, and Dennis W. Stombaugh, who assisted in the constant current ignition studies. Sandia Corporation personnel who contributed to the work included: Messrs. Paul J. Langdon and William Thompson, who directed the electrostatic sensitivity studies and the development of the 5-amp, 5-watt no-fire initiators.

#### REFERENCES

1. J. L. Austing, J. E. Kennedy, D. H. Chamberlain, and R. H. Stresau, "A Heat Transfer Study of Hot Wire Ignition of Metal-Metal Oxide Mixtures," Paper No. 3-8 This Symposium.
2. Austing, J. L., "The Initiation of Insensitive Explosives with Metal-Metal Oxides," Paper No. 3-13. This Symposium, To be published separately.
3. Glassner, A., "The Thermochemical Properties of the Oxides, Fluorides, and Chlorides to 2500°K." Report No. ANL-5750, U.S. Government Printing Office, 1957.
4. Perry, J. H., Ed., Chemical Engineers' Handbook, Third Ed., McGraw-Hill Book Company, Inc., New York, 1950.
5. Brewer, L. and Searcy, A. W., J.A.C.S., 73, 5308, 1951.
6. Kaye, B. H., Paint and Varnish Production, 55, No. 9, p. 87, September 1965.
7. Langdon, P. J., "High Energy Initiators", AIAA Sounding Rocket Vehicle Technology Conference, February, 1967.
8. Austing, J. L., IIT Research Institute. Unpublished Data.
9. Stresau, R. H. and Hillyer, R. M., Paper No. 5. Proceedings Electric Initiator Symposium-1963, Picatinny Arsenal Report EIS-A2357.

Table 1

## CALCULATED THERMOCHEMICAL PROPERTIES OF METAL-METAL OXIDES

System	Heat of Reaction, $H_{298}^{\circ}$			Reaction Temp., °K	State of Reaction Products
	kcal/mole	kcal/g	kcal/cc		
2Al + WO <sub>3</sub>	-199	-0.70	-3.82	3770	Solid W, molten Al <sub>2</sub> O <sub>3</sub>
2/3 Al + CuO	-97	-0.99	-5.50	2868	Gaseous Cu, molten Al <sub>2</sub> O <sub>3</sub>
10/3 Al + V <sub>2</sub> O <sub>5</sub>	-293	-1.07	-3.33	3770	Molten V, molten Al <sub>2</sub> O <sub>3</sub>
2Al + MoO <sub>3</sub>	-220	-1.11	-4.33	3770	Molten Mo, molten Al <sub>2</sub> O <sub>3</sub>
8/3 Al + KClO <sub>4</sub>	-534	-2.54	-6.55	3770	Gaseous KCl, Gaseous AlO, Oxygen

Table 2

## DENSITY VARIATION OF PRESSED METAL-METAL OXIDE POWDERS

System	Amount of Al	Loading Pressure, psi	Density, g/cc	
			Average	Standard Deviation
H-3 Al + TO-2 WO <sub>3</sub>	2/3 stoich.	4,800	3.42	0.19
H-3 Al + TO-2 WO <sub>3</sub>	2/3 stoich.	20,000	3.81	0.04
H-5 Al + TO-2 WO <sub>3</sub>	2/3 stoich.	4,800	3.59	0.08
H-3 Al + TO-3 WO <sub>3</sub>	2/3 stoich.	4,800	3.84	0.08
H-5 Al + TO-3 WO <sub>3</sub>	2/3 stoich.	4,800	3.83	0.10
H-3 Al + Glidden CuO	2/3 stoich.	4,800	3.16	0.20
H-3 Al + Glidden CuO	2/3 stoich.	20,000	3.14	0.06
H-5 Al + Glidden CuO	2/3 stoich.	4,800	2.98	0.07

Table 3

## COLUMN HEIGHT METHOD FOR DETERMINATION OF IGNITION TIME

System	Shot No.	Density, g/cc	Column Height, in.	Assumed Ignition Time, msec	Overall Function Time, msec	Assumed Burning Time, msec
H-3 Al + TO-2 WO <sub>3</sub>	145	3.81	0.202	26	63	37
	146	4.13	.148	42	70	28
	147	3.84	.118	22	44	22
	148	4.09	.072	26	38	12
	149	3.93	.196	26	65	39
	150	4.07	.150	34	62	28
	152	3.87	.199	30	69	39
	153	4.05	.151	37	66	29
H-5 Al + TO-2 WO <sub>3</sub>	154	3.85	.118	34	54	20
	156	4.04	.073	32	43	11
	141	4.01	.192	33	75	42
	142	4.05	.151	29	62	33
H-3 Al + Glidden CuO	143	3.98	.114	23	47	24
	144	3.9f	.075	20	34	14
	128	3.19	.242	24	60	36
	129	3.11	.198	16	49	33
	130	3.22	.142	25	46	21
	131	3.25	.092	25	39	14
	132	3.26	.042	22	29	7
	137	3.08	.251	16	55	39
	138	3.29	.187	20	54	34
	139	3.13	.146	24	47	23
	140	3.32	0.090	30	47	17

Table 4

## IGNITION OF H-3 ALUMINUM + TO-2 TUNGSTIC OXIDE

Amount of Al	Shot No.	Density g/cc	Resistance, ohms		Initial Current, amp	Ignition Time, msec	Column Height, in.	Unit Burning Time, msec/in.	
			after Loading	at Ignition					
2/3 stoich.	220	3.65	0.228	0.158	37.0	2.5	0.211	183	
	362	3.83	.199	.180	36.2	1	.201	169	
	219	3.58	.222	.164	25.7	5	.215	181	
	361	3.84	.232	.195	21.0	6	.200	170	
	47	3.52	.243	.173	15.7	14	.219	178	
	166	3.60	.268	.170	15.7	14	.214	178	
	150	4.07	.228	.143	15.7	34	.150	187	
	146	4.13	.191	.139	15.7	42	.148	189	
	153	4.05	.205	.140	15.5	37	.151	192	
	167	3.44	.229	.164	15.2	14	.224	165	
	46	3.83	.215	.160	15.2	18	.201	194	
	149	3.93	.217	.158	15.2	26	.196	199	
	145	3.81	.235	.158	14.8	26	.202	183	
	357	3.84	.213	.196	14.8	14	.200	200	
	152	3.87	.216	.158	14.8	30	.199	196	
	48	3.71	.194	.153	14.8	20	.208	186	
	49	3.77	.222	.158	14.8	22	.204	190	
	50	3.67	.231	.149	14.8	27	.199	190	
	51	3.99	.219	.151	14.8	29	.193	192	
	52	3.89	.219	-	14.8	24	.198	197	
	168	3.60	.192	.158	14.2	23	.214	173	
	169	3.56	.221	.169	13.0	29	.217	170	
	358	3.86	.206	.181	12.7	23	.199	196	
	170	3.56	.229	.161	12.2	34	.217	175	
	172	3.72	.203	-	11.3	>180	.207	-	
	173	3.71	.183	No go	10.4 <sup>a</sup>	No go	.208	-	
	Stoich.	313	3.56	.204	.171	23.0	4	.217	111
		41	3.33	.204	.155	15.7	16	.232	99
		45	3.57	.227	.145	15.2	30	.216	111
		42	3.59	.205	.118	15.2	52	.215	107
		44	3.81	.229	No go	15.2 <sup>a</sup>	No go	.202	-
		355	3.58	.211	.156	15.1	24	.215	98
		43	3.40	.264	.161	14.8	20	.227	106
286		3.14	.211	.205	14.5	12	.246	77	
287		3.31	.201	.180	13.2	23	.233	90	
356		3.49	.232	No go	12.9 <sup>a</sup>	No go	.221	-	
288		3.25	.194	No go	11.1 <sup>a</sup>	No go	.237	-	
30% excess		40	3.45	.235	No go	16.1 <sup>a</sup>	No go	.224	-
	39	3.09	.223	.169	15.7	18	.251	72	
	53	3.25	.262	.141	14.8	30	.233	88	
	54	3.29	.211	.135	14.8	29	.235	85	
50% excess	55	3.11	.236	.134	15.2	34	.249	88	
	56	3.17	0.225	No go	14.8 <sup>a</sup>	No go	0.254	-	

<sup>a</sup>One-minute pulse.

Table 5

## IGNITION OF H-5 ALUMINUM + TO-2 TUNGSTEN OXIDE

Amount of Al	Shot No.	Density, g/cc	Resistance, ohms after Loading	Resistance, ohms at Ignition	Initial Current, amp	Ignition Time, msec	Column Height, in.	Unit Burning Time, msec/in.
2/3 stoich.	223	3.57	0.204	0.154	44.4	2	0.216	199
	323	3.85	.211	.190	35.0	2	.200	210
	226	3.58	.202	.158	32.6	3	.215	216
	225	3.50	.237	.157	26.3	5	.220	186
	322	3.79	.208	.187	24.4	4	.203	212
	34	4.01	.207	.154	17.4	19	.192	234
	31	3.69	.217	.150	17.0	13.5	.209	213
	33	3.79	.223	.158	17.0	16	.203	227
	32	3.72	.215	.142	16.3	15	.207	227
	224	3.55	.210	.160	16.1	16	.217	193
	30	3.71	.222	.157	15.2	19	.208	226
	142	4.05	.222	.160	15.2	29	.151	219
	141	4.01	.214	.161	15.0	33	.192	219
	337	3.85	.208	.181	14.5	15	.200	220
104	3.57	.238	.167	12.9	20	.216	208	
338	3.79	.209	.169	12.7	36	.203	226	
105	3.54	.218	.168	11.8	25	.218	206	
106	3.47	.220	.168	11.3	28	.222	198	
339	3.88	.215	.164	11.1	75	.198	227	
108	3.49	.253	.173	10.1	41	.221	195	
109	3.46	.220	.172	9.4	48	.223	197	
340	3.81	.223	No go	9.0 <sup>a</sup>	No go	.202	-	
110	3.50	.248	No go	8.3 <sup>a</sup>	No go	.220	-	
Stoich.	24	3.36	.212	.153	17.4	13	.230	122
	25	3.36	.240	.165	17.0	15	.230	122
	26	3.46	.253	.140	17.0	35	.223	126
	27	3.71	.240	No go	17.0 <sup>a</sup>	No go	.208	-
30% excess	21	3.01	.238	.162	16.9	13	.257	89
	20	3.43	.210	No go	16.5 <sup>a</sup>	No go	.225	-
	23	3.23	0.238	No go	12.2 <sup>a</sup>	No go	0.239	-

<sup>a</sup>One-minute pulse.



Table 6

## IGNITION OF H-3 ALUMINUM + TO-3 TUNGSTIC OXIDE

Amount of Al	Shot No.	Density, g/cc	Resistance, ohms		Initial Current, amp	Ignition Time, msec	Column Height, in.	Unit Burning Time, msec/in.	
			after Loading	at Ignition					
2/3 stoich.	366	3.90	0.223	0.177	42.5	1.5	0.197	226	
	245	3.74	.209	.149	34.1	2.5	.206	211	
	365	4.02	.209	.176	23.7	5	.191	251	
	243	3.98	.220	.160	23.5	6.5	.193	246	
	242	3.75	.209	.160	16.9	12	.205	210	
	69	3.79	.250	.152	15.2	20	.203	226	
	70	3.93	.230	.140	15.3	36	.196	240	
	71	3.95	.211	.134	15.1	36	.195	256	
	72	3.99	.246	.144	15.2	32	.193	243	
	73	4.15	.246	No go	15.4 <sup>a</sup>	No go	.185	-	
	345	4.04	.230	.176	14.5	20	.190	263	
	279	3.83	.212	.165	13.5	24	.201	234	
	346	3.98	.219	No go	12.9 <sup>a</sup>	No go	.193	-	
	277	3.95	.221	.181	12.6	30	.195	246	
	280	3.85	.207	.196	12.1	21	.200	210	
	278	3.88	.213	No go	10.4 <sup>a</sup>	No go	.198	-	
	281	3.86	.210	No go	10.3 <sup>a</sup>	No go	.199	-	
	Stoich.	67	3.64	.232	.151	14.4	16	.212	170
	30% excess	66	3.46	0.213	No go	14.8 <sup>a</sup>	No go	0.223	-

<sup>a</sup>One-minute pulse

Table 7

## IGNITION OF H-5 ALUMINUM + TO-3 TUNGSTIC OXIDE

Amount of Al	Shot No.	Density, g/cc	Resistance, ohms		Initial Current, amp	Ignition Time, msec	Column Height, in.	Unit Burning Time, msec/in.	
			after Loading	at Ignition					
2/3 stoich.	317	3.95	0.235	0.177	36.2	2	0.195	246	
	232	3.75	.229	.161	32.4	3	.205	224	
	231	3.83	.209	.155	24.3	6	.201	229	
	315	4.02	.222	.171	23.2	5	.191	262	
	230	3.85	.200	.148	17.8	12	.200	250	
	35	3.89	.227	.157	15.7	16	.198	248	
	37	4.07	.199	No go	15.7 <sup>a</sup>	No go	.189	-	
	38	3.93	.203	.163	15.4	18	.196	260	
	36	3.99	.230	.171	15.3	20	.193	259	
	111	3.83	.253	.165	15.0	20	.201	244	
	112	3.85	.259	.173	13.7	31	.200	245	
	342	4.02	.206	.165	13.2	44	.191	262	
	165	3.92	.201	No go	12.6 <sup>a</sup>	No go	.196	-	
	343	3.98	.231	No go	10.7 <sup>a</sup>	No go	.193	-	
	Stoich	28	3.67	.211	.141	17.0	21	.210	176
		29	3.64	.215	.147	17.0	17	.212	165
		12	3.85	.234	No go	16.8 <sup>a</sup>	No go	.200	-
	30% excess	11	3.69	0.221	No go	15.8 <sup>a</sup>	No go	0.209	-

<sup>a</sup>One-minute pulse.

Table 8

## IGNITION OF H-3 ALUMINUM + GLIDDEN CUPRIC OXIDE

Amount of Al	Shot No.	Density, g/cc	Resistance, ohms		Initial Current, amp	Ignition Time, msec	Column Height, in.	Unit Burning Time, msec/in.	
			after Loading	at Ignition					
2/3 stoich.	241	2.89	0.202	0.157	33.5	2	0.267	101	
	321	3.07	.219	.196	28.8	3	.252	143	
	320	3.19	.219	.180	21.5	5	.242	153	
	127	3.21	.270	.169	20.3	9	.241	179	
	240	2.94	.225	.163	18.3	11	.263	114	
	138	3.29	.197	.161	16.5	20	.187	182	
	137	3.08	.190	.160	16.3	16	.251	156	
	129	3.11	.244	.166	16.3	16	.198	167	
	135	3.21	.198	.165	16.1	18	.241	170	
	121	3.07	.224	.162	15.7	20	.252	163	
	120	3.10	.200	.165	15.6	21	.250	156	
	86	3.08	.221	.162	15.4	22	.251	191	
	128	3.19	.201	.169	15.4	24	.242	149	
	87	3.04	.200	.163	15.2	19	.255	173	
	89	3.23	.230	.163	15.2	25	.239	213	
	88	3.29	.232	.164	15.2	26	.235	208	
	239	2.82	.201	.162	15.0	14	.274	58	
	119	3.12	.232	.171	14.6	22	.248	169	
	332	3.18	.217	.185	14.5	16	.243	161	
	333	3.17	.210	.182	13.0	26	.244	148	
	334	3.17	.210	.180	11.0	108	.244	156	
	283	2.91	.210	.202	10.6	40	.266	60	
	335	3.10	.211	.180	9.0	220	.249	-	
	336	3.10	.211	No go	7.1 <sup>a</sup>	No go	.249	-	
	Stoich.	85	3.25	.212	.162	15.2	50	.238	80
		83	2.96	.192	.153	15.0	30	.262	99
		84	3.20	.225	.162	15.0	48	.242	87
		82	2.87	0.271	0.167	14.5	20	0.270	126
	30% excess	79	3.16	0.256	0.156	16.1	38	0.245	82
		77	3.06	.241	.151	15.7	36	.253	83
		78	3.06	.245	.154	15.7	51	.253	91
		80	3.02	.249	.159	15.2	30	.256	94
		75	2.86	.192	.143	14.9	26	.271	96
76		2.75	.210	.164	14.8	51	.282	114	
74		2.80	.238	.168	14.8	74	.267	101	
81		3.01	0.241	-	14.4	6 sec	0.257	-	

<sup>a</sup>One-minute pulse.

Table 9

## IGNITION OF H-5 ALUMINUM + GLIDDEN CUPRIC OXIDE

Amount of Al	Shot No.	Density, g/cc	Resistance, ohms		Initial Current, amp	Ignition Time, msec	Column Height, in.	Unit Burning Time, msec/in.	
			after Loading	at Ignition					
2/3 Stoich.	236	2.94	0.207	0.157	49.6	1	0.263	141	
	326	3.15	.213	.180	35.5	2	.245	175	
	235	2.96	.210	.166	35.2	2	.261	103	
	234	2.88	.229	.165	25.2	5	.268	127	
	324	3.15	.203	.173	24.0	4	.245	175	
	174	3.04	.236	.164	15.7	15	.254	150	
	103	3.32	.236	.162	15.5	27	.233	210	
	101	2.93	.216	.167	15.0	21	.264	136	
	328	3.25	.193	.176	15.0	21	.238	198	
	102	3.19	.200	.162	14.2	33	.242	190	
	175	2.95	.190	.161	14.1	30	.262	134	
	176	2.97	.232	.160	13.5	28	.260	127	
	329	3.15	.213	.176	12.5	35	.245	167	
	177	3.04	.226	.171	12.2	50	.254	138	
	330	3.13	.212	.184	10.8	60	.247	162	
	178	3.07	.233	-	10.4	20 sec	.252	-	
	331	3.20	.201	-	9.0	1 sec	.241	-	
	Stoich.	96	2.97	.198	.155	15.5	30	.261	106
		98	3.11	.253	.160	15.1	44	.249	96
		97	3.08	.235	.159	15.0	47	.251	108
99		3.10	.223	.170	15.0	31	.250	116	
100		2.98	.232	.164	14.6	29	.260	127	
30% excess	92	2.96	.229	.155	15.4	49	.262	69	
	91	3.08	.248	.166	15.2	22	.251	88	
	94	2.92	.253	.156	14.8	35	.265	72	
	93	3.06	0.197	No go	14.8 <sup>a</sup>	No go	0.253	-	

<sup>a</sup>One-minute pulse.

Table 10

## SUMMARY OF 5-AMP, 5-WATT NO-FIRE EXPERIMENTS

System	Density, g/cc	Resistance after Loading, ohms	5-amp 15-min Test	Ignition Current, amp.	After Cooling		Unit Burning Time, msec/in.
					Ignition Time, msec.	Column Height, in.	
H-3 Al + TO-2 WO <sub>3</sub> , 2/3 Stoich.	3.65	0.221	No go	15.5	15	0.426	317
	3.72	.221	No go	15.0	16	.419	320
	3.77	.202	No go	14.0	23	.412	286
	3.60	.203	No go	15.0	15	.433	305
	3.61	0.210	No go	15.0	17	0.431	308
H-3 Al + Glidden CuO, 2/3 Stoich.	3.27	0.207	No go	15.0	15	0.381	165
	3.22	.207	No go	15.0	16	.386	161
	3.29	.207	No go	15.0	16	.378	175
	3.13	.193	No go	15.0	16	.398	83
	3.11	0.210	No go	15.0	15	0.400	137

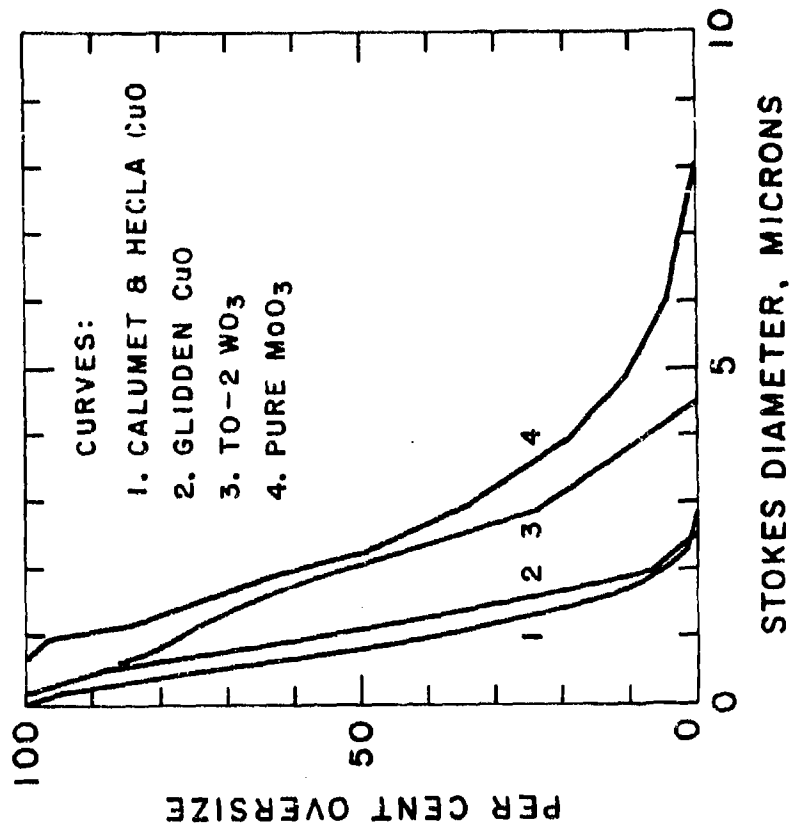


Figure 2  
 PARTICLE SIZE DISTRIBUTION OF  
 METAL OXIDE POWDERS

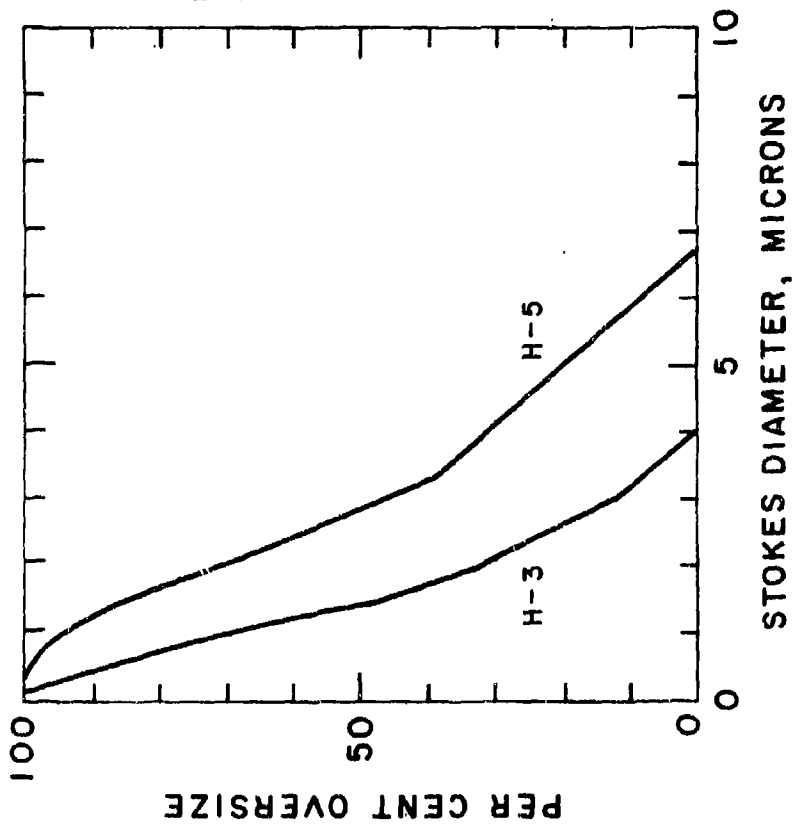


Figure 1  
 PARTICLE SIZE DISTRIBUTION  
 OF SPHERICAL GRADE ALUMINUM POWDERS

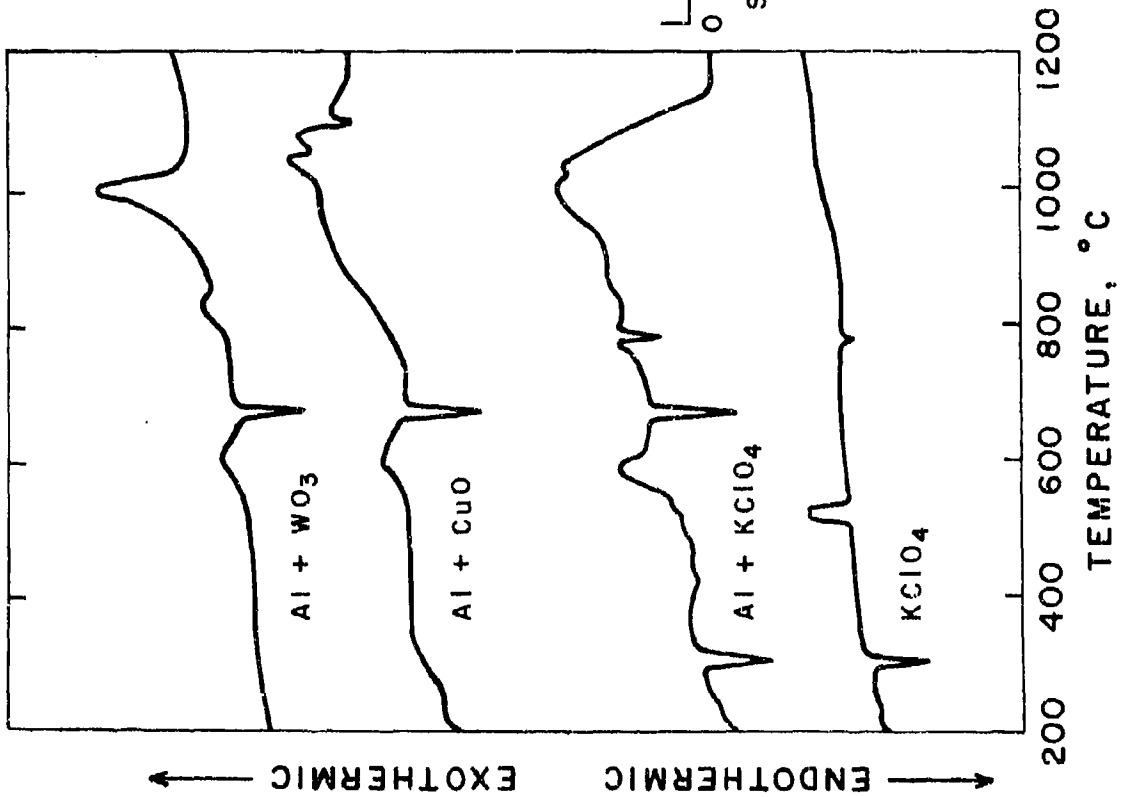


Figure 3

DTA THERMOGRAMS  
(Heating Rate = 10°C/min)

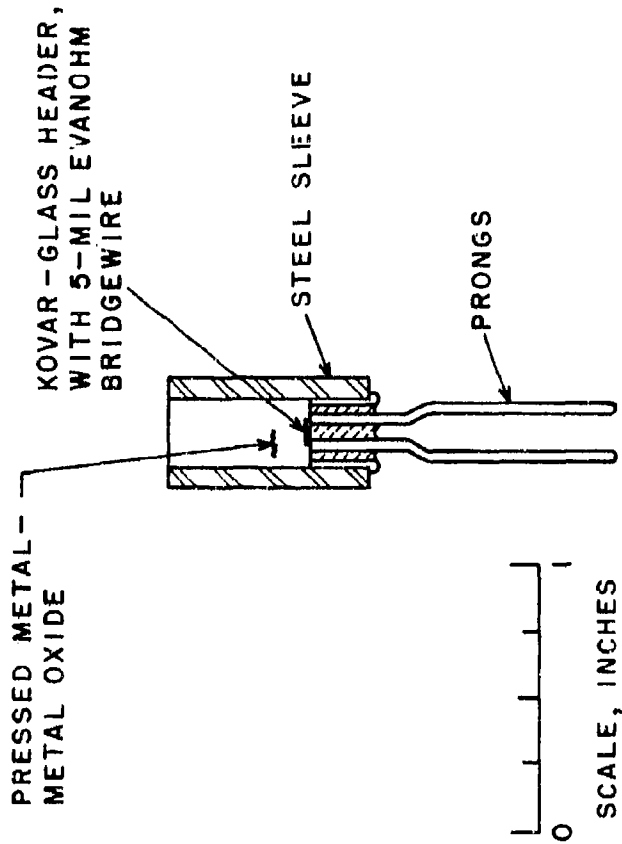


Figure 4

METAL-METAL OXIDE INITIATORS  
(Nominal bridge resistance = 0.20 ohm.  
Inside diameter of sleeve = 0.222 inch.)

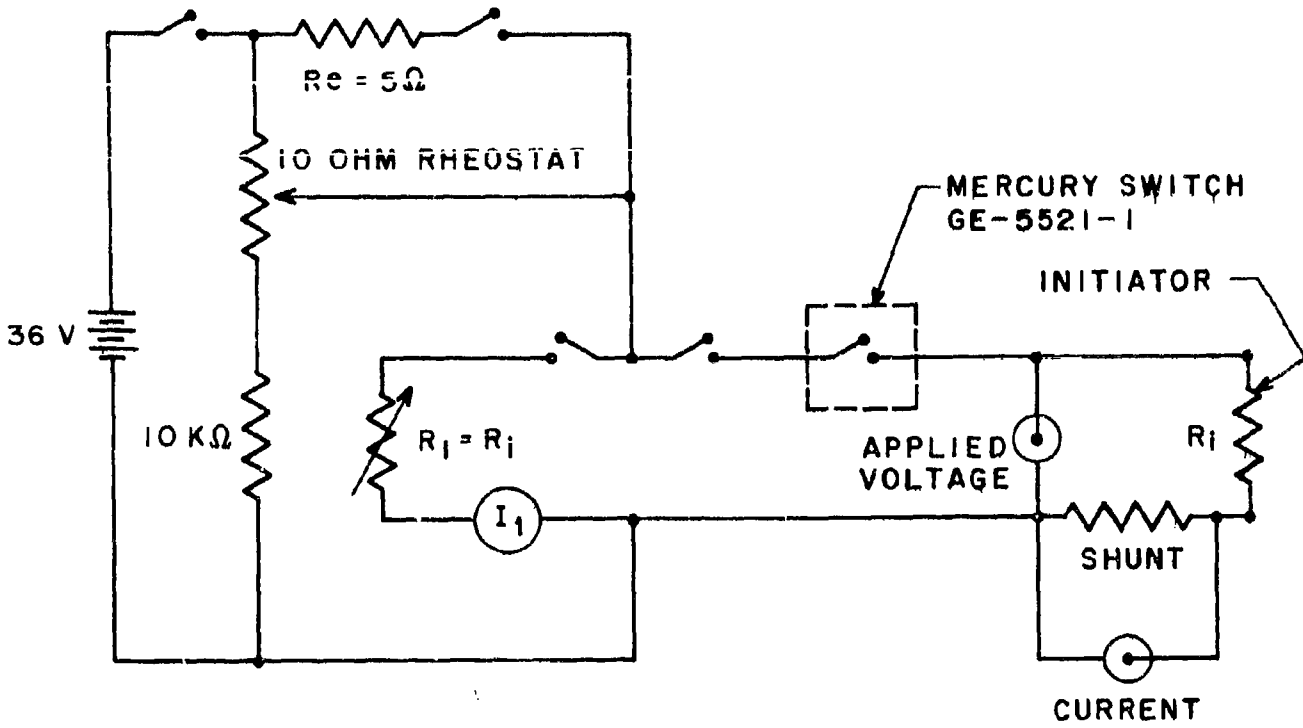


Figure 5  
CONSTANT CURRENT FIRING CIRCUIT

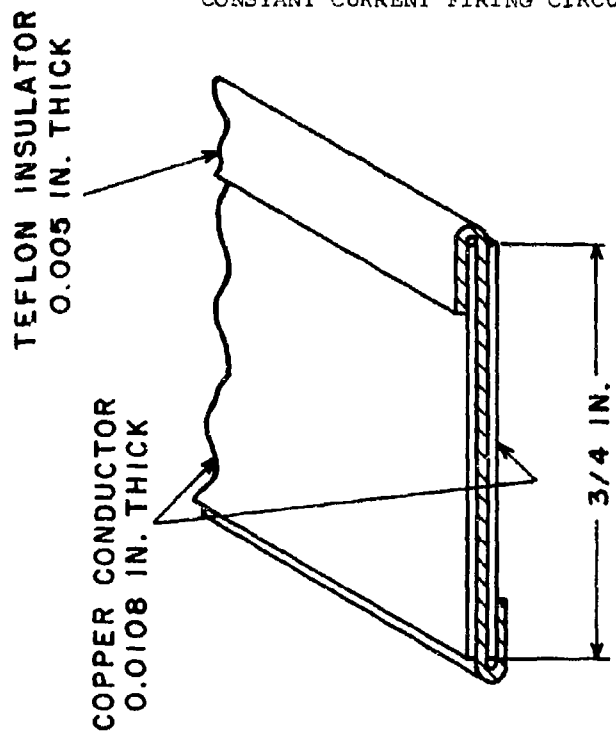


Figure 6  
SCHEMATIC DRAWING OF FLAT CABLE USED  
IN CONSTANT CURRENT FIRING CIRCUIT  
OF FIGURE 5

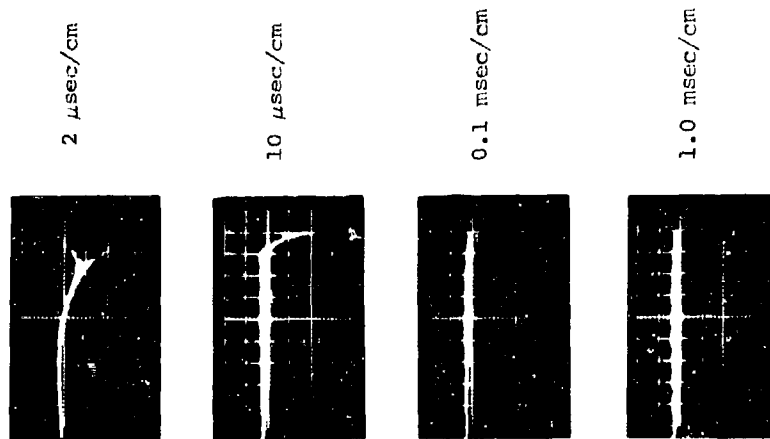


Figure 7

TYPICAL OSCILLOSCOPE RECORDS  
 SHOWING CURRENT RISE IN FLAT CABLE FIRING CIRCUIT  
 (Current = 19.8 amp. Voltage drop  
 across shunt resistor in Figure 5 is monitored)

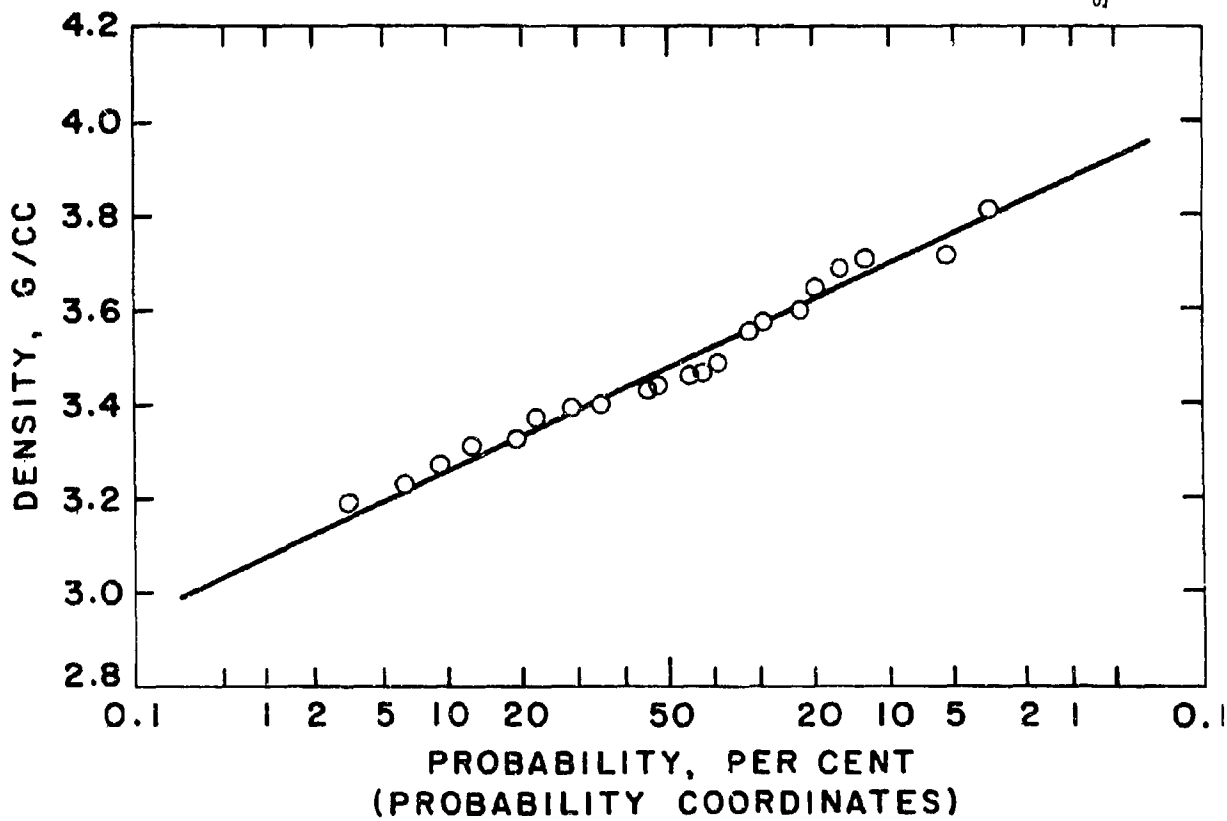


Figure 8

DENSITY DISTRIBUTION FOR H-3 Al + TO-2 WO<sub>3</sub>,  
 2/3 STOICHIOMETRIC, AT 4800 PSI.

TO OSCILLOSCOPE

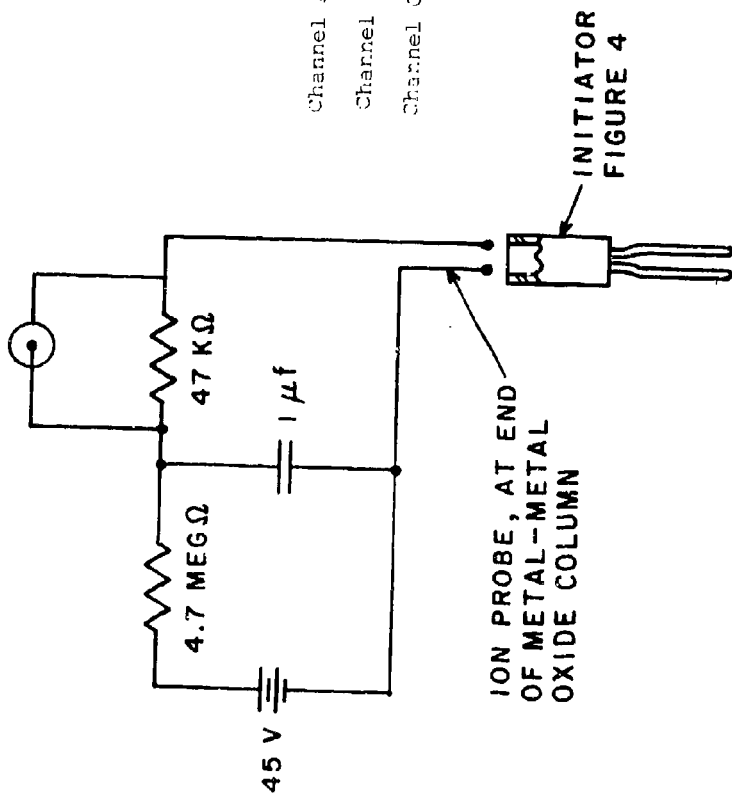


Figure 9

ION PROBE SYSTEM FOR MEASUREMENT OF OVERALL FUNCTION TIME OF INITIATOR

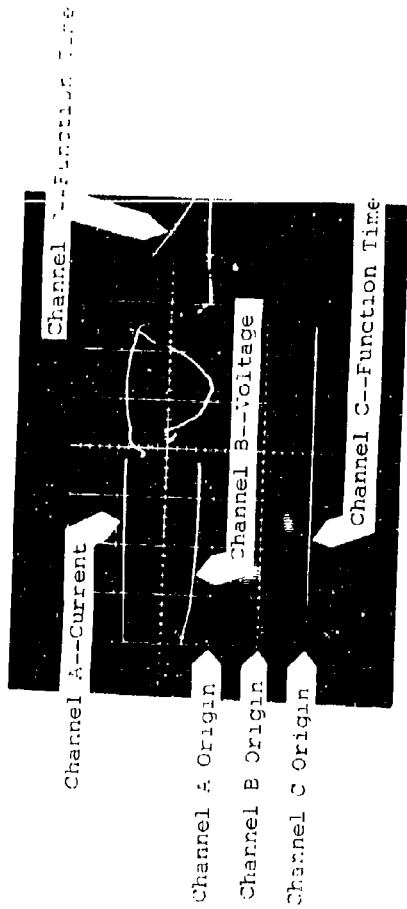


Figure 10

OSCILLOSCOPE RECORD FROM FIRING OF METAL-METAL OXIDE INITIATOR (Shot No. 153, H-3 Al + TO-2 WO<sub>3</sub>). Vertical Sensitivities: A, 0.2 volt/cm; B, 2 volt/cm; C, 10 volt/cm. Sweep Rate on all channels = 10 msec/cm.)



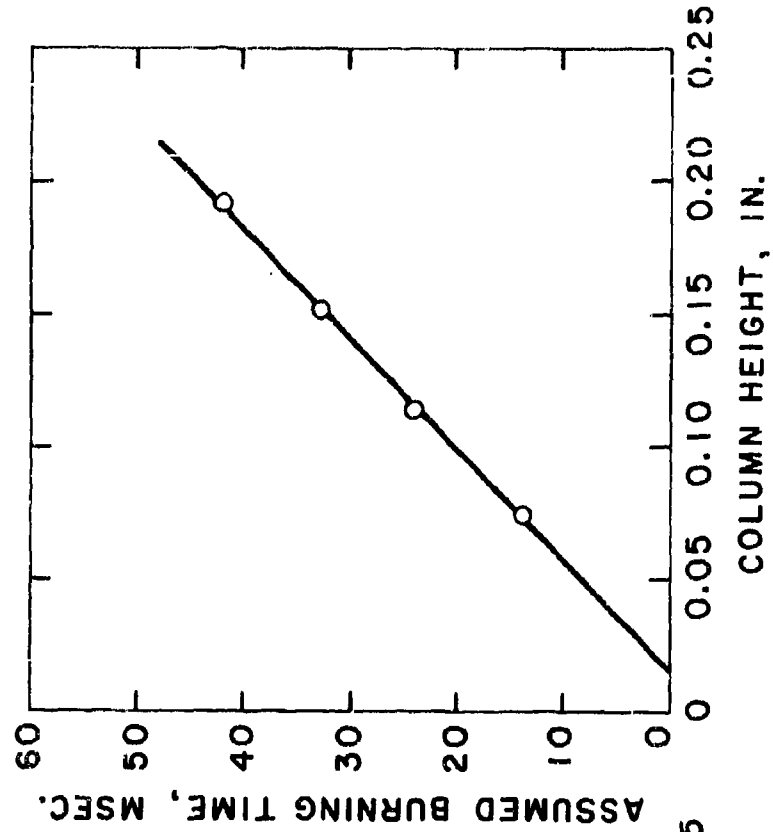


Figure 11

VARIATION OF ASSUMED BURNING TIME  
WITH COLUMN HEIGHT FOR  
H-3 Al + TO-2 WO<sub>3</sub>, 2/3 STOICHIOMETRIC

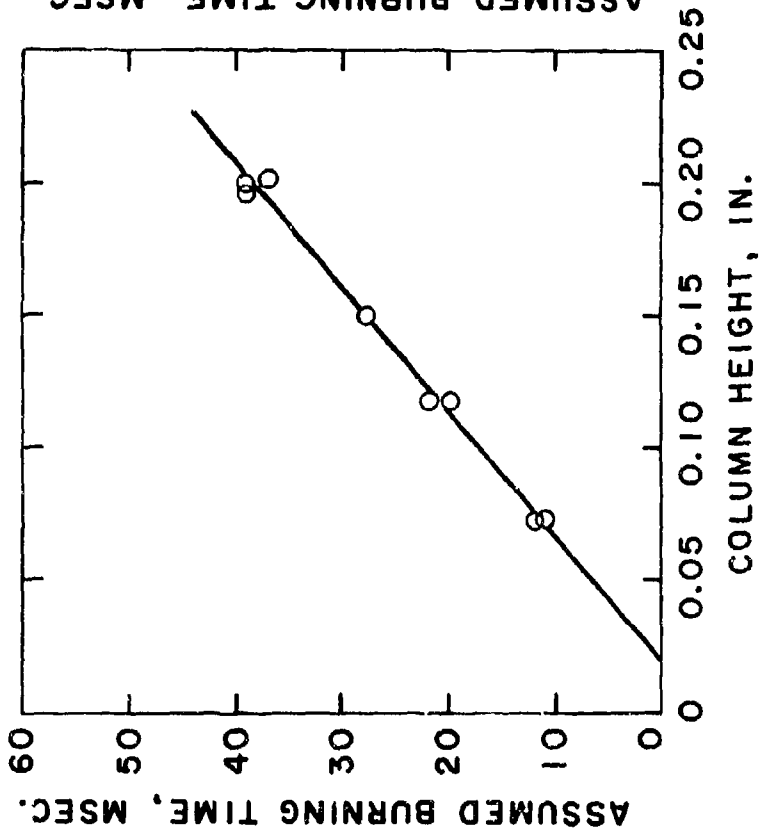


Figure 12

VARIATION OF ASSUMED BURNING TIME  
WITH COLUMN HEIGHT  
FOR H-5 Al + TO-2 WO<sub>3</sub>, 2/3 STOICHIOMETRIC

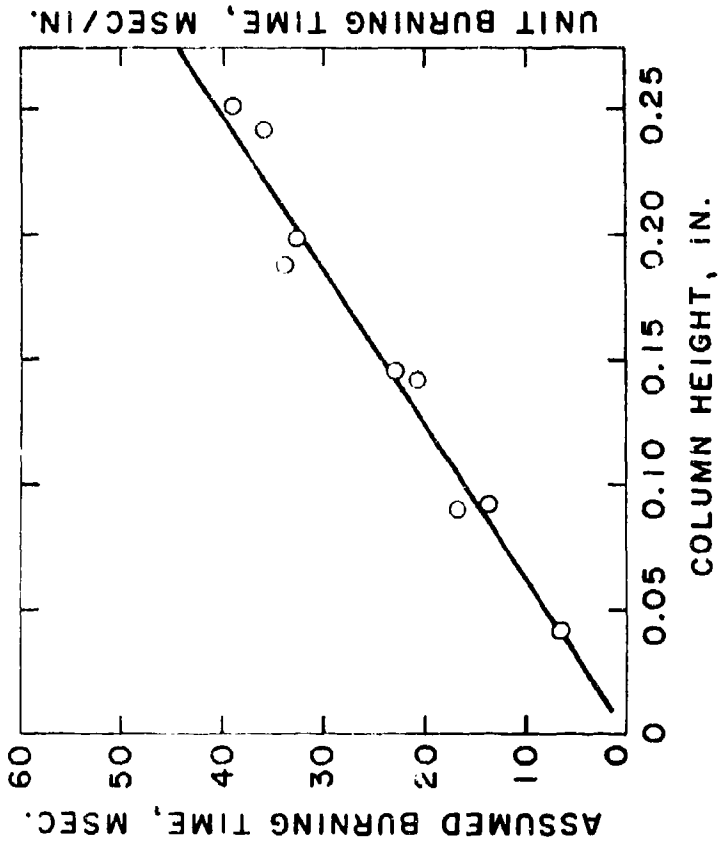


Figure 13  
VARIATION OF ASSUMED BURNING TIME  
WITH COLUMN HEIGHT  
FOR H-3 Al + Gliggen CuO, 2/3 STOICHIOMETRIC

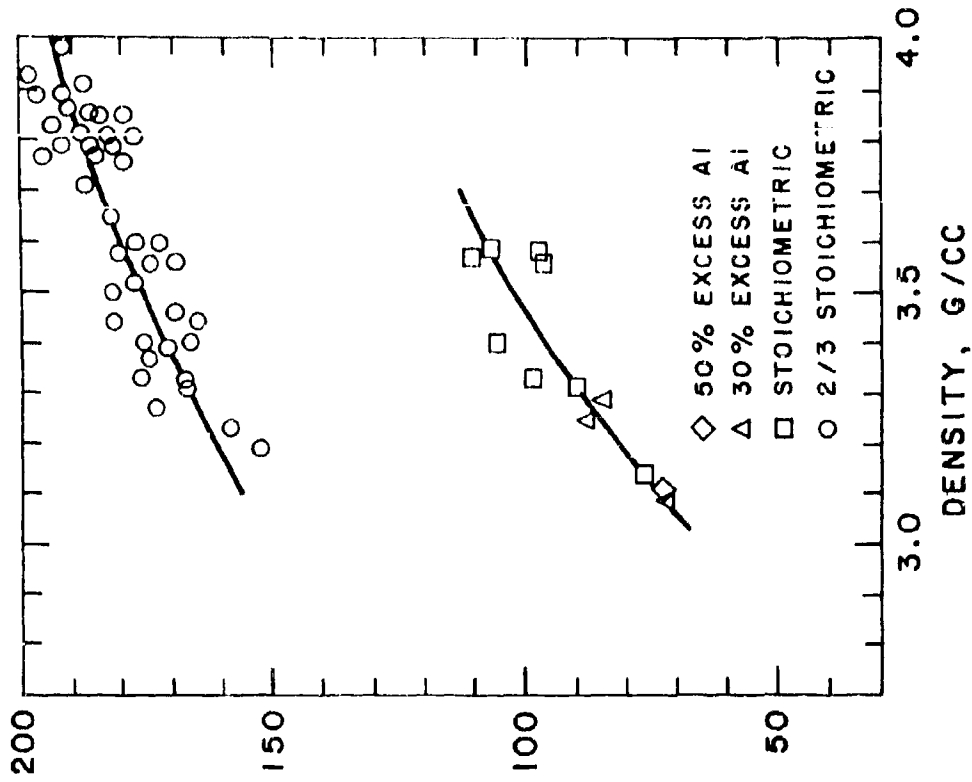


Figure 14  
UNIT BURNING TIME OF H-3 Al + TO-2 WO<sub>3</sub>

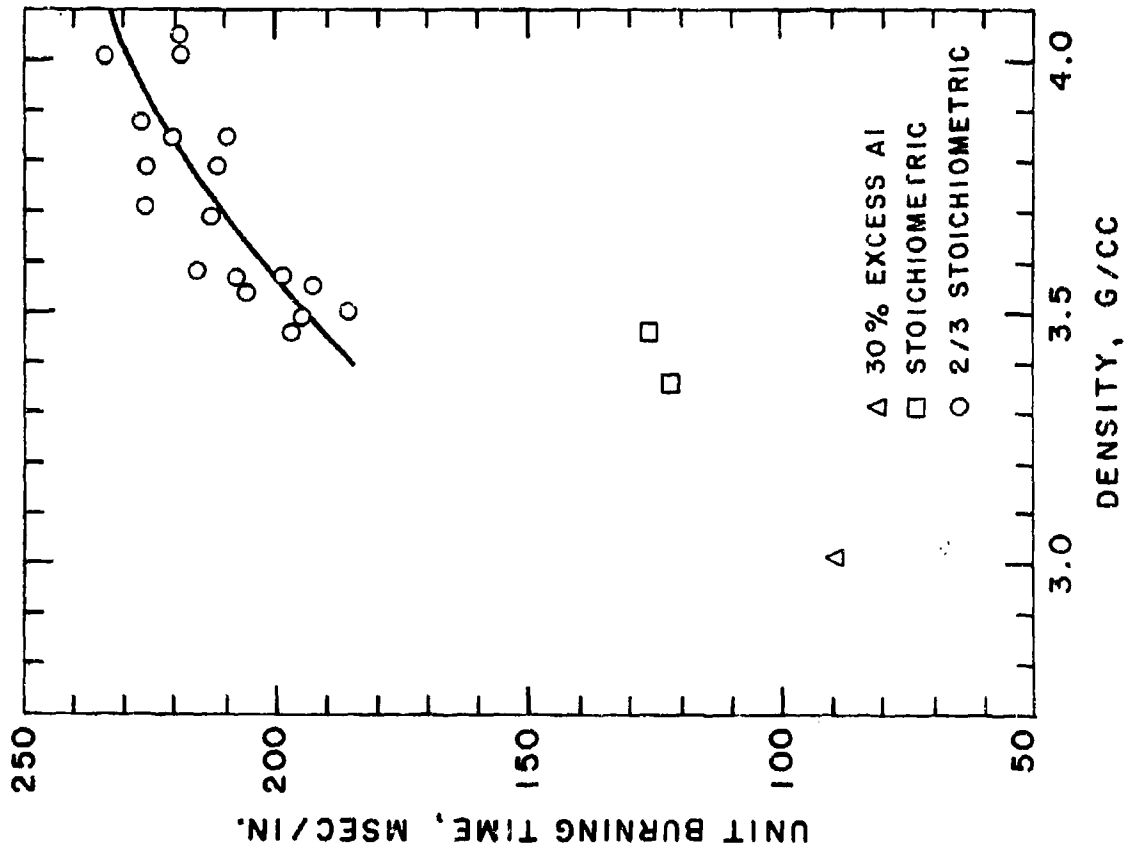


Figure 15

UNIT BURNING TIME OF H-5 Al + TO-2 WO<sub>3</sub>

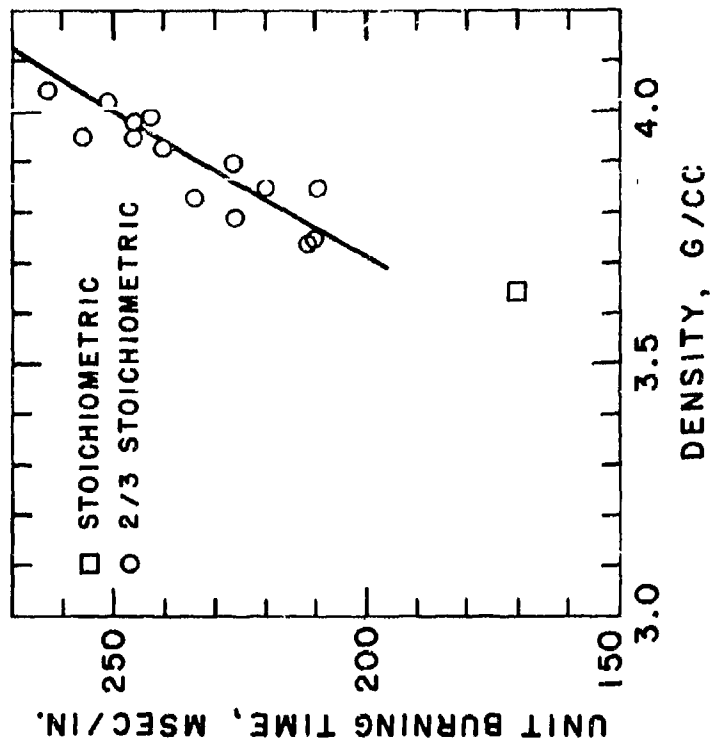


Figure 16

UNIT BURNING TIME OF H-3 Al + TO-3 WO<sub>3</sub>

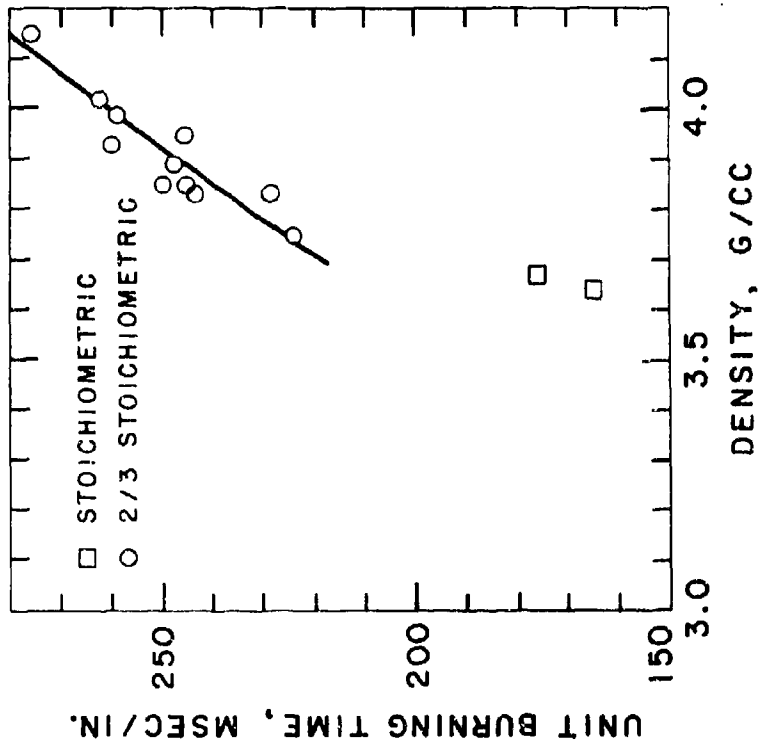


Figure 17  
UNIT BURNING TIME OF H-5 AL + TO-3 WO<sub>3</sub>

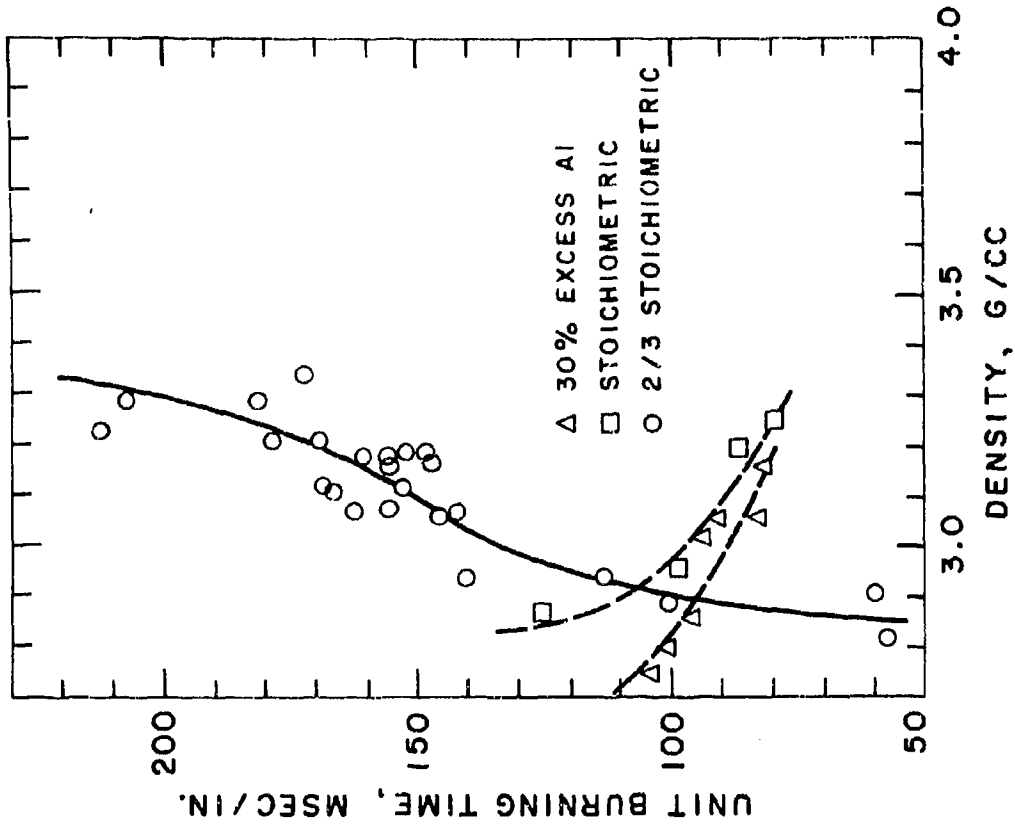


Figure 18  
UNIT BURNING TIME OF H-3 AL + GLIDDEN CUO

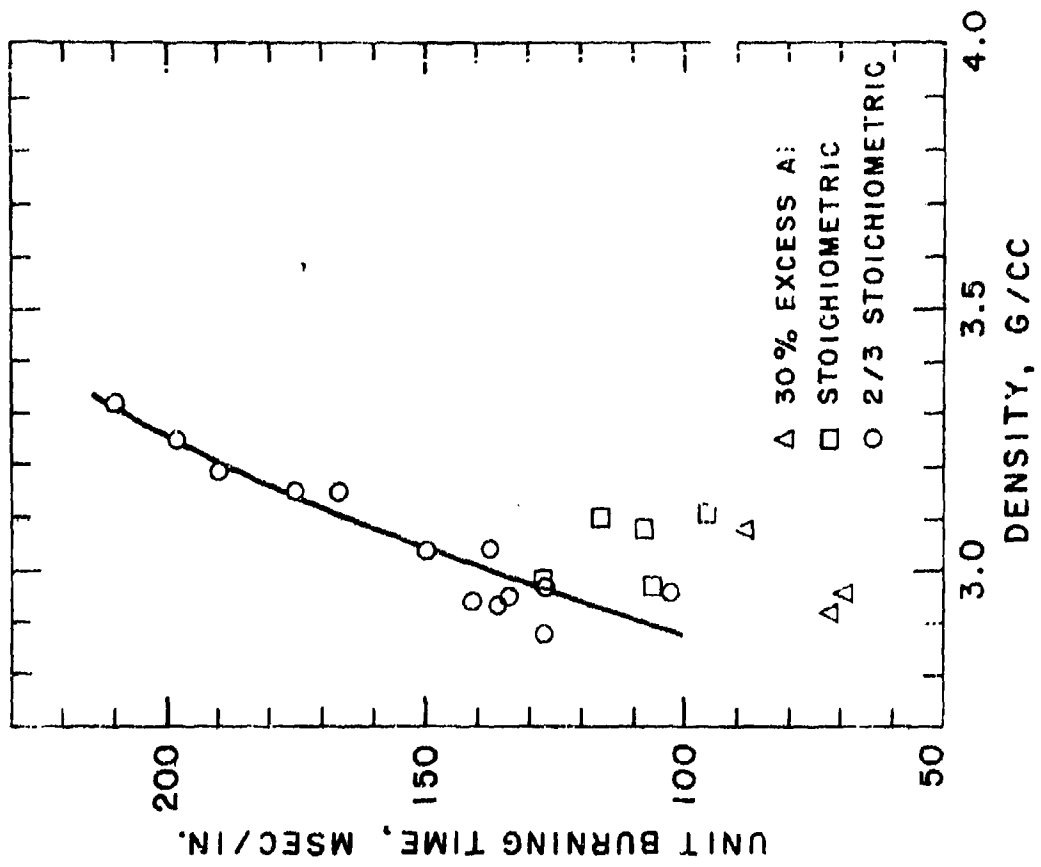


Figure 19  
UNIT BURNING TIME OF H-5 Al - GLIDDEN CAC

## DISCUSSION

Mr. Breslow (NOTS): With respect to all of the non-fire values in the performance requirements, apparently there is no firm specification in terms of tying them together. I would like to ask, after experiencing a no-fire condition, how does this affect the performance as a function of the interval after the no-fire condition?

Mr. Austing: I am going to ask my co-author to answer part of this question, but let me say that this is partly a function of the bridge design. We are currently doing 1-Amp 1-Watt work using some of these mixtures. We find that when we expose them to 1-Amp 1-Watt for 5 minutes and then let them cool down, they perform exactly the same as if they had just been pulsed with 5-Amps all fire. I think this can be handled with the proper bridge design.

John, how does a wire bridge perform under these conditions?

Mr. Weber (Sandia Corporation): Art's question may be related to the mixtures we had. I would like to clarify it a little. The actual 5-Amp 5-Watt system that we are using now is being produced at Mound Laboratories in Dayton with a 5 mil wire. But the only mixture that is currently being used is the aluminum potassium chlorate which meets the resistance after fire requirements nicely.

The work that Jim presented was just part of the overall program. NOTS did part of the work on this; Unidynamics did some other parts. After the 5 amp no-fire exposure, I believe the devices still function for 15 minutes. There is a little shift in the 50% firing point.

3-4 ELECTRIC DETONATORS FOR NAVY GUIDED MISSILE APPLICATIONS-

EXPERIMENTAL STUDIES OF FOUR CONCEPTS\*

By R. Stresau, R. Petersen, and D. Chamberlain  
R. Stresau Laboratory, Inc. Spooner, Wisconsin

INTRODUCTION

Growing concern regarding hazards of premature detonation of electroexplosive devices as the result of induced currents has led to the promulgation of Reference 1, which requires, in part, that "maximum no-fire currents shall be not less than one ampere" and "maximum power shall be not less than one watt per bridge." These requirements eliminate all detonators in current use in Navy guided missiles. In some, (where there is room) it might be possible to attain such characteristics by the use of a large enough bridgewire. However, such an increase in bridge dimensions would result in a detonator requiring more energy, in a pulse, than is available from firing circuits in current guided missile use. Furthermore, the heating time of such a large bridgewire would introduce more delay than is desirable.

As is shown in Reference 2, reliable and prompt initiation by firing circuits in current use is not necessarily incompatible with the requirements of Reference 1. The "one watt, one ampere,

\*Based on work performed for the U.S. Naval Ordnance Laboratory, Corona, California under Contract Nos. N123(62738)31089A  
N123(62738)53830A (X)  
N00123-67-C-0508

no-fire" criterion is attained by designing a bridgewire system of sufficiently high heat loss factor. The pulse energy requirement is proportional to the heat capacity of the bridgewire system. Although for a given configuration and combination of materials, heat capacity tends to increase with heat loss factor (there is at least one exception), a judicious choice of materials and configuration can lead to substantial changes in this relationship. For some general configurations considered in Reference 2, it is possible to control energy requirement and power or current requirement independently over wide ranges by adjustment of dimensions. Reference 2 is a consideration of interactions of materials and configurations in their effect upon thermal properties without more than passing consideration of fabrication problems. The relationships derived in Reference 2 suggest a number of designs which are quite promising (on paper). Two of these were quite adaptable to fabrication by techniques which had been developed at this laboratory for other purposes. A third was essentially a modification of an EED which had previously been developed by the Markite Development Corporation.

The objective of these studies was the development of criteria for the design of an initiator which will:

1. Be unaffected by exposure to a minimum current of one ampere or a minimum power of one watt for at least five minutes.



2. Fire reliably from a pulsed input of 10,000 ergs. (This value was chosen as typical of detonators currently used in guided missiles. It is understood that somewhat more energy can be made available without serious modification of existing firing currents).

3. Function within appreciably less than 100 microseconds after application of an adequate firing signal.

To dissipate a watt without firing or deterioration, the heat loss factor of the bridgewire system should be at least 3 milliwatts per degree centigrade. If the resistance is less than an ohm, the current for one watt must be at least an ampere. On the basis of previous experience that reliable firing from pulses requires about 1000 ergs per cylindrical mil (a cylindrical mil is the volume of a cylinder one mil in diameter by one mil long) of bridgewire volume, this volume should be limited to ten cylindrical mils or less.

The four design concepts considered herein are the following:

I. A bridgewire short enough to conduct sufficient heat through the wire to the terminals to limit its temperature to less than 300°C while carrying a current of at least an ampere, combined with sufficient series resistance to bring the total to more than an ohm.

II. A bridgewire of dimensions similar to those in current use with explosives and inert components of high thermal conductivity.

III. An EED in which the bridge is composed of "Markite" (the trade mark of the Markite Corporation of New York City) electrically conductive plastic molded to a substrate of electrically insulating but thermally conductive plastic.

IV. A flattened bridgewire or film bridge in good thermal contact with a "plug" or header of high thermal conductivity (alumina should be a satisfactory material).<sup>2</sup>

Each of these concepts was investigated using components which could be relatively easily fabricated from commercially available semifabricated materials or with tooling made by modification of tooling at hand. The components tested are not necessarily compatible with designs interchangeable with items in current use such as the MK.71 detonator. However, the data reported herein are believed to demonstrate the feasibility of such components and to provide preliminary criteria for their design.

#### DESIGN CONCEPTS AND EXPERIMENTAL HARDWARE

As stated earlier, the particular design concepts mentioned above were chosen on the basis of availability of materials and techniques for the fabrication of detonators of the desired characteristics (as calculated using equations derived in Reference 2). The first two (which had wire bridges) were made using the selectively etched Wollaston wire technique which had been developed at this laboratory for the fabrication of EBW detonators of special characteristics<sup>3</sup>. The plugs for the Markite detonators were made by the Markite Development Corporation.

##### Selectively Etched Wollaston Wire Bridges

Wollaston wire is a coaxial bimetallic material with a core of platinum or gold and an outer layer of silver. It was originally developed as a means of obtaining wire smaller than can be drawn directly. The Wollaston wire used in most of these detonators, however, has a core size generally larger than the smallest obtainable drawn wire and is used as a means of limiting

effective bridgewire length by selective etching. The process is as follows: (see Figure 1) A "hairpin" of Wollaston wire is inserted in the holes of a short length of double bore ceramic tubing. The protruding ends are soldered to convenient terminals (for most experimental detonators, the two sides of a small strip of copper clad phenolic circuit board are used). The terminals are cemented to the end of the ceramic tube with an epoxy resin which, (if the operation is successful) is drawn through the tube by capillary action to form a nearly flat meniscus flush with the opposite end of the tube. The silver is etched from the exposed loop of Wollaston wire to leave an effective bridgewire of the desired length.

#### Short Bridgewire With Series Resistance

Since the thermal conductivities of metals are hundreds and in some cases thousands of times those of commonly used flash charge explosives, appreciable fractions of heat loss factors of many bridgewire systems are attributable to heat flow along the wire. An interesting possibility is that of designing a bridgewire which will dissipate a watt to the terminals with a temperature rise sufficiently low that the flash charge explosive will be unaffected. Due to the close analogy between thermal and electrical conductivity, as pointed out in Reference 2, the choice of bridgewire materials is the only source of latitude in the otherwise fixed inverse relationship between heat loss factor and electrical resistance, and this latitude is insufficient to result in a design of practical interest.

On the other hand, as shown in reference 2, a bridgewire of 0.1 ohm resistance of almost any metal would have a temperature differential between the center and terminals of less than  $300^{\circ}$  when carrying one ampere. By inserting series resistances in the terminal system sufficient to raise the total resistance to at least one ohm, the power dissipation of the detonator may be raised to one watt. This series resistor, of course, would also dissipate about 90% of the energy of a pulse (the high temperature coefficient of resistivity of a pure metal bridge would decrease this percentage somewhat) so that the bridgewire proper in combination with the flash charge should have an "all fire point" of about 1000 ergs. Based on the rule of thumb given above, it should have a volume of about one cylindrical mil or less. A few simple calculations showed that the most practicable dimensions for a bridgewire of one cylindrical mil volume and 0.1 ohm resistance would result with a metal of low resistivity. In gold, for example, a wire about 0.3 mils diameter and 10 mils long would have these characteristics. Since a few feet of 0.3 mil gold core Wollaston wire were at hand and it seemed at least possible to limit bridgewire lengths to ten mils or less, such items were used in experiments to check the calculations and determine input characteristics of units with such bridgewires.

The concept outlined above is embodied in the design shown in Figure 2. Although detonators of this general design could be made and, as results reported herein will show, would be expected

to have the desired characteristics, the operations involved in applying the series resistors would add to the cost and the resistors themselves would add to the bulk of the detonator. A simpler, more compact, and less expensive design would be one similar to that shown in Figure 1 in which the "leg wires" also act as series resistors. In order to serve this function, the legwires should have a combined resistance of not less than 0.9 ohm and a heat loss factor sufficiently high to limit their temperature rise to fifty degrees or preferably less while dissipating a watt. The design of legwires of such characteristics requires some attention to heat dissipation, but is quite simple technically.

#### Explosives Of High Thermal Conductivity

"Flash charges" which surround the bridgewires of most EED's are essentially very finely divided powders at relatively low loading densities. In this state of aggregation, almost anything is a good thermal insulator. It was hoped, at the outset of these experiments, that lead styphnate, lead azide, or most likely, silver azide, if loaded at high enough densities, might have high enough thermal conductivities to dissipate a watt from a bridgewire of the size needed for the desired pulse sensitivity. Although this hope was thwarted by the results of early experiments, it was found that thermally conductive additives to the flash charge explosive resulted in EED's of the desired input characteristics. Figure 3 shows the arrangement used in these experiments.

## "Markite" Conductive Plastic Bridged Initiators

The Markite Development Corporation is, primarily, a manufacturer of precision potentiometers in which conductive plastics are used as resistance elements. In connection with this work, they have developed techniques for the precise control of properties and dimensions of plastic components in which two or more materials of very different electrical properties are molded together. They have also developed electrically insulating plastics, the thermal conductivity of which can be predetermined over wide limits by composition. The Markite Corporation had developed, as an internal development program, an electric initiator plug which met the one ampere, one watt, no-fire criterion of Reference 1. In this development, however, no effort has been made to minimize firing energy requirement since Markite had not been informed regarding guided missile applications. When consideration of such detonators was assigned to this laboratory, the writer contacted the Markite Corporation and later visited them to discuss the possibility of developing an initiator, based on their materials. The information regarding their capabilities was used as the basis for a tentative schematic design. Markite adapted existing tooling to fabricate items approximately this design for preliminary tests. The results of these tests were sufficiently promising to suggest procurement of a larger quantity of units, which are dimensionally interchangeable with those of Mk. 71 detonators. Most of these plugs have been

incorporated in complete detonators, as per Figure 4, for testing.

#### Gold Leaf Bridges On Alumina Substrates

The fourth concept outlined on Page 3 of this report (that of a bridge element in good thermal contact with a thermally conductive substrate) might be reduced to practice in any of several designs. The "Markite" conductive plastic devices are an embodiment of this concept in the most general sense. Approaches which were considered included bridgewires "mashed" flat, and hopefully into the pores of the substrate sufficiently to give a good thermal bond and chemically, electrochemically, and vacuum deposited films. Of the schemes considered, the first with which promising results were obtained was that in which the bridge consists of gold leaf, applied to the surface of an alumina "plug" or "header" at rather high pressure. Headers for experimental detonators of this kind were made from two hole alumina tubing of the kind made for protection of thermocouple leads. Legwires of platinum, copper, stainless steel, and Ceramvar were cemented into the holes with epoxy resin and Kovar legwires were brazed in place. The gold leaf was pressed onto the surface at pressures from 20,000 to 50,000 pounds per square inch. Most of these had the annular space between the lead-wire and the bore of the tube only partly filled, leaving cracks or grooves which were filled with lead-tin solder at this laboratory. The plugs were loaded and assembled in complete detonators as shown in Figure 5.

## Evaporated Metal Film on Alumina Substrates

In addition to the Gold Leaf bridges, a few bridges were made by the vacuum deposition of metals on alumina headers similar to those shown in Figure 5. This effort has been initiated only recently and considerable effort will be necessary to obtain a combination of header surface preparation and evaporated film material which will perform satisfactorily. The units which have been tested to date had films of aluminum and a proprietary combination of metals which were applied by the G. F. Schjeldahl Company to headers which had been prepared by this laboratory, as described in the preceding paragraph. These were assembled to complete detonators as shown in Figure 5.

## EXPLOSIVES, ADDITIVES, PREPARATION, AND LOADING

Explosive compounds used in these experiments are materials widely used in ordnance with the exception of silver azide, which has been the subject of considerable investigation. Some have been reduced to very fine powders by milling and, for some applications, have been incorporated in mixtures to alter their thermal characteristics. All have been loaded by pressing.

### Explosive Compounds

For "flash charges" in direct contact with bridge elements of initiator, the following were used:

Normal Lead Styphnate. Purchased from the Olin Mathieson Chemical Company in January, 1962 and certified by that company to be in accordance with Military Specification MIL-L-17186 (Bu Ord).

Basic Lead Styphnate. Purchased from the Olin Mathieson Chemical Company in January, 1962 and certified by that company to be in accordance with Military Specification MIL-L-16355 (Bu Ord).



Polyvinyl Alcohol Lead Azide. Purchased from the Olin Mathieson Chemical Company in July 1960 and certified by that company to be in accordance with MIL-L-3055 (dated 30 Sept. 1945) and amendment #1 (dated March 24, 1952) and R. C. O. 23505-S-ANR. Polyvinyl Alcohol Lead Azide, which is also referred to as PVA lead azide, is a patented proprietary preparation of the Olin Mathieson Chemical Company, which has been shown 4,5 to have performance characteristics superior to those of the dextrinated lead azide which was used in most ordnance until relatively recently.

Silver Azide. Supplied by the U. S. Naval Ordnance Laboratory, White Oak, Maryland. Their storage lot X-117, which was made by the Hercules Powder Company.

For intermediate charges in the complete detonators which were made and tested as part of this study, Lead Azide, RD1333, made by Hanley Industries of St. Louis, was used. RD1333, which is made in a carboxy methyl cellulose solution has properties similar to those of PVA lead azide. The principal reason PVA lead azide was used in flash charges was that a quantity sufficient for all lead azide flash charges to be used was milled early in the study, when PVA lead azide was the only lead azide on hand. RD1333 was used for intermediate charges because, by the time complete detonators were made, a larger supply of this material was on hand.

Base charges of complete detonators were RDX furnished by U.S. Naval Ordnance Laboratory, White Oak, Maryland, from their storage lot X-177, which is designated as Holston RDX, 44 micron. It is presumed to meet MIL-R 398C, Type B, Class E.  
Milling

Since the normal lead styphnate and PVA lead azide have particles many times larger than the diameter of the bridgewires which must be used to meet the functioning energy requirements, these materials were ball milled before using as flash charges

or components thereof. Basic lead styphnate and silver azide were fine enough, as received, to be used in the unmilled state.

#### Additives

To increase the thermal conductivities of flash charge explosives (and organic adhesives), they were mixed with several materials of high thermal conductivity including silicon carbide of various granulations, carbonyl iron, and aluminum in both spherical granule and flake form. Of these, the only material which increased the thermal conductivity of explosive mixtures sufficiently to be interesting in this application was the aluminum flake. During most of the experiments described herein, the only flake aluminum at hand was some U.S.P. material purchased from a chemical supply house and bearing a Merck label.

#### Mixing

The additives mentioned in the foregoing, which were all fine powders, were blended with the explosive powders by placing all components (a gram or two total) in a cylindrical container (aluminum tubing, stoppered at both ends) of inside dimensions, one half inch diameter by one and one half inch long which was rotated, end over end, at sixty RPM for one hour. In visual as well as microscopic examination, the mixtures appeared quite uniform.

#### Loading

Explosives were pressed at pressures between 1000 and 100,000 pounds per square inch using hand operated mechanical presses. The force applied was controlled with the help of a calibrated spring scale where the force exceeded 20 or 30

pounds. Below this level, direct dead-loads were used to control the force. Longer charges were loaded by increments which were not allowed to exceed one caliber in length.

#### EXPERIMENTAL ARRANGEMENTS AND PROCEDURES

Experiments of this program were determinations of electrical input characteristics of the various types of initiator described in earlier paragraphs as loaded with the various explosives and mixtures which have been mentioned above. Sensitivity to both condenser discharge pulses and steady current were determined. In addition, measurements were made of functioning times and heat loss factors.

##### Pulse Sensitivity

Pulse sensitivity determinations were made by means of Bruceton tests using a condenser discharge circuit in which the controlled variable was the voltage to which the 0.5 microfarad condenser was charged. Since the circuit included a firing chamber safety interlock which may have introduced a significant loss, it is possible that the true threshold energy requirements may be somewhat lower than those determined from the test data.

##### Functioning Times

Functioning times of the pulse fired units were measured using a Taktronix 517 oscilloscope, which has a very accurate driven sweep with rates ranging (by factors of two or two and a half) from five nanoseconds per centimeter to twenty microseconds per centimeter. The sweep is triggered with the firing pulse and displaced by the closure of a circuit by means of the detonator output. When only the "plugs" with charges loaded into the

"ferrules" are tested, closure is accomplished by the ionized gases of the detonating explosives. The case bottoms of complete detonators close this circuit by metal to metal contact. A variety of probe designs have been used, each adapted to the initiator system with which it was used. For purposes of this report, it should suffice to say that each probe system consisted of a pair of electrodes well within a hundredth of an inch of the output face of the initiator. The delay resulting from this gap combined with that of the oscilloscope circuit (estimated by the makers to be about 0.03 microsecond) may result in a positive error of as much as a tenth of a microsecond, which, as will be seen is negligible compared with the time scatter of even the most reproducible initiators, in this respect, which were tested.

The functioning times at steady currents near the threshold firing level, as might be expected, varied from fractional seconds to nearly the five minutes specified for no-fire in the one ampere, one watt, no-fire criterion. Where long enough, they were measured with a watch. Shorter times were not measured.

#### Steady Current Sensitivity

Threshold steady state conditions were measured in Bruce-ton tests as well as by stepwise increases of current on each initiator until it fired. This latter scheme is not generally recommended in sensitivity testing of electric initiators because it has been found, for some types, that exposure to conditions near but below the threshold condition may alter the sensitivity of an item.

In this case, the justification for testing for steady state threshold conditions by "sneaking up on them" is that the purpose of these tests is to guard against initiation by spurious signals. It should be anticipated that, before an initiator, in service, is subjected to a spurious signal sufficient to fire it, it will, generally be subjected to many weaker signals. Thus this "sneaking up" test is a systematized simulation of real conditions. Of course, it was used because it yields quantitative results from much smaller samples than are necessary for Bruceton or other "go, no-go" tests.

For the steady current sensitivity tests, initiators were placed in "heat sinks", one inch diameter cylinders of aluminum, the length of the initiators, and centrally drilled to as close a fit as possible with standard number size and fractional inch drills. Very small diameter initiators (0.050 to 0.065 inch O.D.), were clamped in copper foil lined "split mold" clamps designed to give nearly complete surface contact. When only initiating elements of detonators were used in the aluminum cylinder heat sinks, thermal contact was augmented by the use of soldering gun thread compound. Complete detonators were slipped into the heat sinks without such heat transfer agent to simulate the least favorable condition to be anticipated in service.

The "constant current" used in these experiments was obtained by the use of a direct current supply and a rheostat.

In each constant current test, both the current through and the voltage drop across the detonator were measured. The

power, of course, is the product of current and voltage and the resistance is the quotient of the voltage by the current. The resistance, and consequently the voltage, often changed quite rapidly immediately preceding firing so these values were quite inaccurate for items which fired. For this reason, constant current sensitivity tests are not particularly useful in assessing steady state power sensitivity. In one watt, one ampere, no-fire tests of units with less than one ohm resistance, the current was increased until the power was one watt and held at that level for five minutes.

#### Temperature and Heat Loss Factor Determinations

Since platinum has such a high and accurately known thermal coefficient of resistivity, it is possible to use its resistance increase as a measure of temperature. Where the resistance of a platinum bridgewire is used to measure its own temperature rise due to electrical power dissipation, the measured temperature rise is, of course, the average of temperatures which vary along the length of the bridgewires. In a bridgewire short enough that axial heat flow in the wire accounts for most of the losses, the temperature rise at the midpoint may be over half again the average. Where losses to the surroundings dominate, the temperature is nearly constant along the wire so the average and the peak are rather close to one another.

The heat loss factor is the slope of a plot of power vs. temperature. Since the resistance coefficient of platinum is nearly constant in the range of interest, the slope of the

power/resistance curve is also proportional to the heat loss factor. Heat loss factors for various platinum bridged items were determined by; (1) measuring voltages for current levels from about a quarter of an ampere up to either the one ampere, one watt level or to the firing point; (2) converting this data to power-resistance terms and plotting; (3) converting the power/resistance slope to a heat loss factor. Heat loss factors so obtained should be referred to as "apparent heat loss factors" because of the axial variation in temperature referred to above, but, used in conjunction with threshold firing temperatures determined by the same means they provide a valid means of predicting threshold firing current and power by means of non-destructive tests.

#### RESULTS

The feasibility of each concept was studied, first, by preliminary experiments to evaluate the pertinence and validity of the concepts and the calculations upon which they were based, followed by tests of large enough quantities to obtain estimates of the sensitivities to steady current and power and to condenser discharge applied pulses. The preliminary tests were designed to answer the specific questions associated with each concept, so they are reported separately. The final feasibility tests were designed to determine the degree to which the experimental items approach the design objectives so the data for various types is comparable and are reported together.

#### Preliminary Experimental Results, Type I Initiators

Type I initiators, for purposes of this discussion, are

defined on page 3 of this report as initiators which depend upon axial flow of heat in the bridgewire augmented by series resistors to provide the required power dissipation. Calculations quoted in Reference 2 show that the threshold firing current should be inversely proportional to bridgewire resistance and that the product of the threshold current and the resistance should be about 0.15 ohm-amperes. Other calculations<sup>2</sup> suggest the use of a gold bridgewire 0.3 mils in diameter by 7 mils long with 0.1 ohm resistance. Bridgewires this short present something of a fabrication problem. The first attempt yielded a group with resistances ranging from 0.125 ohm to 0.28 ohm. Although the calculations of Reference 2 indicated that these would fire on less than an ampere, they did provide a means of testing the calculations and, in particular, the inverse relationship of threshold current to resistance.

A steady current from a six volt storage battery, controlled by a series resistor was passed through the bridgewire until it fired the flash charge or for five minutes (in one test two minutes).

The data indicated that the product of the threshold firing current and the cold resistance is about 0.125 ohm-amperes. A subsequent Bruceton test in which the test variable was the product of the cold resistance and the applied current (for each trial, the current was adjusted on the basis of the resistance of the unit being tested) yielded a mean threshold condition of 0.123 ohm-amperes with a standard deviation of 0.047 log units.



### Preliminary Experimental Results, Type II Initiators

For purposes of this report, Type II initiators are defined as initiators in which the electrical power is dissipated in a "conventional" bridgewire which is surrounded by explosives and structural components of sufficient thermal conductivity to dissipate one watt as heat without temperatures high enough to initiate or permanently change the initiator.

Since laboratory scale fabrication of "plugs" with platinum Wollaston wire is convenient for this laboratory, the use of the platinum bridgewire as its own resistance thermometer was an obvious approach for the preliminary experiments.

Assuming that the primary explosives contemplated for use will survive a 300°C temperature rise, an initiator of one ohm resistance and a heat loss factor of at least 3.33 milliwatts per degree should meet the one watt, one ampere, no-fire criterion. It was calculated that a platinum bridgewire 0.5 mil diameter by about 25 mils long (dimensions appropriate for the desired pulse sensitivity) would have a heat loss factor of only a fraction of a milliwatt per degree if surrounded by lead azide or mercury fulminate. However, these calculations were based on literature values (given in Reference 2) accompanying data regarding state of aggregation. It was suspected that the conductivities given were of loose powder or relatively lightly pressed material so that it was at least possible that, with high enough loading pressures, one or another of the explosives under consideration might be conductive enough to raise the heat loss factor to a satisfactory level. Lacking this, an inert additive of high thermal con-

ductivity might have the desired effect.

None of the primary explosives at hand had high enough thermal conductivity, even when pressed up to pressures at 150,000 pounds per square inch, to even approach the desired "one ampere, one watt, no-fire criterion" of Reference 1 in an initiator with a bridgewire of appropriate size. However, it was found that the addition of flake aluminum (25 or 50% by weight) to either lead or silver azide or lead styphnate increases the thermal conductivity to a point where the "one watt, one ampere, no-fire" is readily attainable. The aluminum was found to have little effect upon the pulse sensitivity of lead styphnate or silver azide loaded initiators. However, the lead azide loaded items had substantially reduced threshold pulse fire energies (which more than doubled with exposure to one watt and one ampere for five minutes) when aluminum was added to the azide. The azide/aluminum mixture showed other somewhat mysterious characteristics so this mixture has been abandoned. The result of this preliminary experimentation was the decision to investigate both lead styphnate/aluminum and silver azide/aluminum mixtures as flash charges.

#### Preliminary Experimental Results, Type III Initiators

Type III initiators for purposes of this report are considered to be those with the "Markite" conductive plastic bridge elements. Since these elements were delivered as complete plugs with no quantitative data regarding either their composition or dimensions, the only preliminary experiments which were performed were the loading and test firing of the initial samples which were submitted. The first sample submitted was

a group of three which had external dimensions of a quarter inch diameter by a quarter inch long and resistances between a half and one ohm. These misfired on 10,000 ergs but fired on 20,000 ergs after surviving one watt and one ampere for five minutes. The results of these experiments were sufficiently encouraging that a larger sample was ordered, tests of which resulted in threshold firing energies of 11,600 ergs as loaded and 11,100 ergs after exposure to one watt and one ampere for five minutes. This type of bridge element had promise, but the plugs were too large to fit into the Mk. 71 envelope and the energy requirement was somewhat higher than desired. An additional order was placed with the Markite Corporation for plugs as shown in Figure 4, which were to be delivered in small quantities at first, followed by larger quantities, either the same or modified depending on results of the preliminary tests. In this manner, the design shown in Figure 4 evolved.

#### Preliminary Experimental Results, Type IV Initiators

Type IV initiators are defined (page 3) as film bridge initiators with substrates of sufficient thermal conductivity to meet the one watt, one ampere, no-fire criterion. A wide variety of substrates and film materials can be suggested for this type of unit. Of those that were tried, the first successfully fabricated at this laboratory was the gold leaf bridge on the alumina substrate. In the initiator tests a group of initiators of both sizes were loaded at 10,000 pounds per square inch, some with milled normal lead styphnate and some with milled PVA lead azide. Some were subjected to stepwise increases in steady current until they fired or burned out. Some were fired at 10,000 ergs (1/2 mfd at 63 volts) and

their functioning times measured and the remainder were subjected to progressively increasing condenser discharge pulses until they fired. Some of the latter were also set up for functioning time measurements. These procedures were used to obtain a maximum of data from the limited number of detonators at some sacrifice of pertinence to probable conditions of use. All of the pulse fired detonators had previously survived five minutes at steady input conditions of at least one ampere and at least one watt. Maximum no-fire currents ranged from 1.22 to 2.66 amperes and maximum no fire powers from 1.5 to 5.09 watts. None fired on one watt or one ampere for five minutes. Pulse firing energies ranged from 1000 to 6250 ergs. The only respect in which a significant difference was noted between azide and styphnate loaded items was in the functioning times on 10,000 ergs (0.5 microfarads at 63 volts). The lead azide loaded items, under these conditions had functioning times between 1.0 and 1.75 microseconds, while those loaded with lead styphnate took 20 to 25 microseconds.

The headers used in the detonator for which data are given above were made from short lengths of alumina thermocouple tubing into which copper legwires were cemented using epoxy resin adhesive. To investigate the effects of legwire materials a group of detonators, consisting of three subgroups with copper, platinum, and stainless steel legwires (providing a 14/1 range of legwires' thermal conductivities) was prepared, loaded, and tested. Stainless steel, which has similar thermal conductivity was used because samples of Kovar or Ceranvar had not yet been received.

Steady state threshold firing conditions were determined by stepwise gradual increase of the current until the detonator fires. Although the possibility that such tests can yield misleading results was recognized, the lack of sufficient sample size for Bruceton or other "go-no-go" tests, left us with little choice. All items were bridged with a double layer of gold leaf applied to a circular area 0.1 inch in diameter, concentric with the face of the "plug" and loaded with lead azide at 40,000 psi. (In three increments, the first of milled PVA lead azide and the other two of "RD-1333"). The results, which are given in Table 1, show no significant trend relating power dissipation to leg-wire thermal properties. Of the three materials used, the platinum was the most consistent regarding both resistance and threshold firing conditions. As consideration makes clear, the reduction of threshold firing power with increasing resistance is to be anticipated, whether it results from breaks in the gold leaf or insulating films on the electrodes. The latter are suspected since unusually high resistance items were lacking with the items with platinum legwires, which, of course, don't have the tendency of the other materials to form films due to atmospheric corrosion.

In addition to its corrosion resistance, platinum differs from the other two metals in its rather close match to alumina in thermal expansion coefficient. It is possible that an effect of the differential expansion in the items with the other leg-wire materials was to increase the susceptibility of the bridge to damage by the high loading pressure used. It may be noted that, of the resistance properties given in (or readily calcu-

lated from) Table I that which correlates best with steady state threshold conditions is the ratio of the initial resistance to that after loading.

The data given in Table I indicates that initiators of the design illustrated in Figure 5, with legwires of copper, platinum, or stainless steel can be expected to meet the one watt, one ampere no-fire criterion if the bridge element is not damaged in loading sufficiently to substantially change its resistance. If the damage noted is attributable to differential thermal expansion, Kovar, or Ceramvar legwires should be better than platinum (which is, perhaps, too expensive). If the high resistances are due to oxide or other films, gold or platinum plating of the electrodes should eliminate it.

The three groups (with the different legwires) were combined for pulse firing tests using a half microfarad capacitor and variable voltage. Threshold firing energies were low enough to indicate high reliability at 10,000 ergs, but were triple by exposure to one ampere and one watt for five minutes. Similar changes with such exposure of lead azide loaded items were observed with "Type III" initiators.

Firing times were measured. Three, fired on 10,000 ergs (without previous testing) in 1.09, 1.15, and 1.26 microseconds.

A few headers, similar to those shown in Figure 5 were bridged with evaporated metal films. No mask was used, so the metal film covered the entire upper surface of each header. Some difficulty was experienced in attaining the desired resistance of one-half to one ohm. Thick enough films to reduce the resistance to this level tended to scale off. Detonators

made with these headers (similar to those shown in Figure 5 but with lead styphnate flash charges) were quite variable in both pulse and steady state sensitivity but most survived over one ampere and one watt and fired on less than 10,000 ergs. The variability has been attributed to the irregularity of the surface (as a substrate for evaporated films). Although data on this approach are too few to form a basis for judgment, they seem to indicate that the feasibility of attaining the desired results with an evaporated film bridge on an alumina header can be demonstrated.

#### Feasibility Evaluation Test Results

After preliminary experiments had established design criteria to the point where fabrication of larger lots seemed justified, large enough lots were made to perform Bruceton tests to determine threshold firing currents and firing energies (the latter both as loaded and after exposure to at least one ampere and at least one watt for five minutes). Results are given in Table 2. If it is assumed that the estimated value is the true value of the standard deviation and that the distribution is "normal" in terms of the chosen function (in this case, the log of the current or energy) the degrees of safety and reliability can be expressed as percentages or failure probabilities. For example a degree of safety or reliability of one indicates safety or reliability of 84%, a degree of reliability of 2.054 corresponds with 98% reliability, and a degree of safety of 6 indicates a safety failure rate of one in ten million. Of course, the estimated standard deviation obtained from a short Bruceton test may be considerably more or less than the true value.

As may be seen in Table 2, units of each type were safe at one ampere and fired on less than 10,000 ergs. Except for Type I initiators, examples of each type also were safe at a one watt power level and fired in times appreciably shorter than 100 microseconds. Since only the low resistance bridge was tested for Type I units, they were not expected to be safe at the one watt level. No time data were obtained for Type I units because, with respect to aspects which affect functioning times, these initiators are so "conventional" as to leave no room for doubt that suitable functioning times will be characteristic.

Perhaps a few remarks regarding each test lot will make the meaning of the data of Table 2 more apparent:

Test Lot 1. This lot was a group of initiating elements similar to what might be used in Type I detonators as illustrated in Figure 1. The basic principle of this type of detonator is that of transmitting the heat resulting from the flow of an ampere through the bridgewire axially through the bridgewire itself. As indicated by the calculations of Reference 2, it is necessary that the bridgewire of such an initiator have a resistance of a tenth of an ohm or less. Although such an initiator should be safe against firing on a current of one ampere, they will fire on a watt or less. The data given for Test Lot 1 was for the initiating elements alone without the series resistors. For this reason, they would be expected to fire on a watt but they would have to fire on less than 1,000 ergs because 90% of the energy delivered to the detonator would be dissipated in the series resistors.

Test Lot 2. It may be noted that these units meet all of the design objectives except the functioning time requirements. They would provide an interesting solution where longer functioning time could be tolerated.



Test Lot 3. Test Lot 3 was similar to Test Lot 2 except for the use of the silver azide mixture. The data indicates that silver azide does combine the virtue of lead styphnate in this application with the short functioning time of lead azide.

Test Lot 4. These are the same data as are reported in Reference 4 for these tests of the conductive plastic bridge initiators.

Test Lot 5. The gold-leaf bridges are the most recently studied type for which data is reported herein and consequently less experimental data has been obtained than for other types. It may be noted that the data indicate that initiators of this type may meet all design objectives.

#### DISCUSSION

Each of the concepts appears to be quite feasible as a means of attaining the design objectives, each will require further development before a detonator can be released for production, and each has its own combination of virtues, potential, and problems. Of course, the experience gained in this feasibility study in combination with other factors which have not been included in the stated design objectives may form the basis for concentration on one of these types or to eliminate one or more, at least until new requirements appear. Some of this experience and other considerations are discussed in the following paragraphs.

##### Type I Initiators

Type I initiators have been defined as those in which the bridge resistance is low enough to carry one ampere without firing the flash charge explosive and series resistance is added to make the item safe when dissipating one watt. The

comparative complexity of this type of design may make such initiators more expensive than other types unless it is permitted to include the series resistance in the lead wires. It is possible that this approach would be disapproved on the basis that the safety could be compromised by cutting up the lead wires. On the other hand, this general approach is one in which the one watt, one ampere, no-fire characteristic may be attainable without dependence upon the fuze body as a heat sink.

#### Type II Initiators

This type of initiator in which the explosive is given a high thermal conductivity by admixture of aluminum flake can provide the basis for the smallest one watt, one ampere, no-fire detonators which have resulted from this study and also those for which the highest reliability is indicated at 10,000 ergs. The concept has been objected to on the basis that the electrical conductivity of the mixture might result in other hazards and on the basis that it might be difficult to assure uniformity of the mixture. As to the uniformity of the mixture and possible segregation of components after mixing, this should be less of a problem with these mixtures than, for instance, with some of the metal-oxidant delay mixtures because of the equal proportions of explosive and aluminum used in these devices and because of the similarity in density of the components of these mixtures as well as the small particle size.

The particular design used in tests of Type II initiators (Figure 3) was chosen for these tests rather largely on the basis of this laboratory's capability in fabricating such items.

The basic principle of this type, that of raising the thermal conductivity of the flash charge mixture to a point where it will dissipate the required amount of power, can, of course, be applied to wire bridge initiators of any of the many designs which have been used provided of course that the inert components surrounding the flash charge are sufficiently good thermal conductors.

#### Type III Initiators

The Markite initiators have been developed farther toward the design objectives than any of the other types which are discussed herein. As data given in Table 2 indicate, then electrical input characteristics are satisfactory. In addition, as reported in Reference 4, they perform satisfactorily after exposure to the 28 day JAN temperature-humidity cycle, 28 day high temperature storage, transportation vibration test, forty-foot drop test, and at 160°F and -65°F.

A somewhat limiting aspect of the units which were tested was the relatively low mechanical strength of the Markite plugs which limited loading pressures to 1,000-2,000 pounds per square inch. At these low loading pressures, about the only explosive which has the necessary pulse sensitivity is lead styphnate. A general disadvantage of lead styphnate as compared with azides is its somewhat slower response. It may be noted that, although the response of these items is appreciably slower than that of the azide loaded items of other types, the functioning times are well within those needed in the present application. Markite personnel have suggested

several approaches to the improvement of structural strength should such improvement prove necessary.

#### Type IV Initiators

The gold-leaf bridges on alumina substrates are quite promising so far as data obtained to date show. In this general type of initiator a number of variants remain to be tested. The particular combination of dimensions and materials used in Test Lot 5 appears to have characteristics in accordance with the design objectives. Very preliminary data indicate that similar results will be obtainable with evaporated metal films.

The Type IV initiators are potentially the most inexpensive of those which have been studied since the bridging process, usually the most expensive of electric initiator fabrication, is essentially a printing operation and since the materials used cost only a small fraction of a cent per unit. The evaporation deposition of metal film bridges should also be very economical in volume production.

A problem associated with thin metallic film bridges is that of economically fabricating headers with alumina-electrode surfaces of the necessary flatness, flushness, stability, and cleanness. The epoxy resin bonded headers with which some of the best results were obtained when gold leaf bridges were applied liberated excessive amounts of gas in the vacuum required for the evaporated films. Headers into which the leg-wires were brazed had the annulus between the wire and the hole in the alumina only partly filled. Several other approaches

are under investigation, but, at the time of this writing, the problem is still to be satisfactorily solved.

#### CONCLUSION

The "one watt, one ampere, no-fire" criterion is entirely compatible with a pulse sensitivity of 10,000 ergs or even appreciably less. Each of the schemes investigated has been shown to be technically feasible. Each has advantages and limitations. For most, further development will be necessary before ordnance items can be released.

If something must be put into production at this time, the Markite, conductive plastic plug, which has reached the highest stage of development would be the surest choice. Given more time, some of the other approaches might have important advantages.

#### ACKNOWLEDGEMENT

Most of the initiators described herein were fabricated and tested by Mr. Donald D. Degner and Mr. William L. Campbell, both of whom have made significant contributions to fabrication and experimental techniques. The conductive plastic bridged plugs were fabricated under the direction of Mr. Sidney Corren of the Markite Development Corporation. Evaporated film application has been performed by Mr. Gary Adams of the G.T. Schjeldahl Company and he and Mr. Donald Hanson of the same organization have made useful suggestions.

## REFERENCES

1. MIL-L-23659 (WEP) "Military Specifications, Initiators, Electric, Design and Evaluation of," March, 1963.
2. Stresau, R., Petersen, R., and Chamberlain, D., "Electrical Detonators For Navy Guided Missile Applications Experimental Studies of Four Concepts" (a paper of this symposium).
- 2a. Stresau, R.H., "Electrical and Thermal Considerations in the Design of Electro-Explosive Devices," R. Stresau Laboratory Report No. 64-11-1 for the U.S. Naval Ordnance Laboratory, Corona, California, Contract No. N123(62738)31089A, dated 23 December 1964.
3. Stresau, R., Hillyer, R., and Degner, D., "Fifty Millijoule Exploding Bridgewire Detonator Feasibility Study and Applied Research", R. Stresau Laboratory Report No. 65-6-2 for the U.S. Naval Ordnance Laboratory, Corona, California, Contract No. N123(62738)31089A, dated 5 August, 1965.
4. Coler, M., Corren, S., Peterson, R., and Stresau, R., "Electrical Detonators With Conductive Plastic Bridge Elements" (a paper of this symposium).
- 4a. Peterson, R.L., and Stresau, R.H., "Preliminary Evaluation of Electric Detonators with "Markite" Electrically Conductive Plastic Bridge Elements", R. Stresau Laboratory Report No. 66-11-1 for the U.S. Naval Ordnance Laboratory, Corona, California, Contract No. N123(62738)53830A (X), dated 9 November, 1966.

Further details may be found in the following, of which this paper is a condensation:

5. Stresau, R. "Electric Detonators for Navy Guided Missile Applications, Experimental Studies of Four Concepts", R. Stresau Laboratory Report No. 66-7-1 for the U.S. Naval Ordnance Laboratory, Corona, California, Contract Nos. N123(62738)31089A, N123(62738)53830A (X), and N00123-67-C-0508, dated 18 October, 1966.

Table 2. Feasibility Evaluation Test Results

Test Lot	1	2	3	4	5
Initiator Type	I	II	II	III	IV
Bridge Element (Mat'l)	Au	Pt	Pt	M	GL
Dia. of thickness (mils)	0.3	0.5	0.5		0.007
Length (mils) (ave.)	7	30			0.1" disc
Resistance (ohms) (ave.)	0.095	0.6	0.75	0.7	0.85
Flash Charge (Mat'l)	BLS	NLS/AL, 1/1	SA/AL, 1/1	NLS	SA
Loading Pressure (psi)	2K	100K	100K	1K	20K
Current Sensitivity	a	a	a	b	b
Mean (amps)	>1	>1.0	>1.0	1.78	2.09
Std. Dev. (log units)				0.036	0.0685
Degree of Safety (@ 1 amp)				6.97	4.75
Power Sensitivity					
Mean (watts)	k	a	a	c	c
Pulse Sen. (as loaded)	<1	>1.0	>1.0	2.22	2.57
Mean (ergs)	b	4300	4250	4630	6350
Std. Dev. (log units)	4728	0.035	s	0.120	0.05
At 10,000 ergs	0.21				
Degree of Rel.	(n)				
Firing time (usec)		10.4	3.4-4.9	2.79	4.08
Pulse Sen. (after 1W, 1A) <sup>m</sup>		160	b	20-49	0.65-1.8
Mean (ergs)		4470	4120	5670	
Std. Dev. (log units)		0.050	s	0.132	
At 10,000 ergs					
Degree of Rel.					
Firing time (usec)		7	3.8-6.2	1.86	16-35

Types I, II, III see page 3

BLS basic lead styphnate

NLS normal lead styphnate

LA lead azide (PVA)

SA silver azide

a none fired on 1A and/or 1W

b Bruceton test

c average of Bruceton misfires

M "Markite" conductive plastic

(n) not applicable  
 k calculated (I<sup>2</sup>R)  
 m except as noted, obtained using 0.50 mfd with variable voltage Bruceton  
 g 1 microfarad  
 d @ 27,500 ergs (X 56)  
 e data combined for det. as loaded & exposed to 1W, 1A  
 s too short for significant Std. Dev.  
 GL two layers of gold leaf

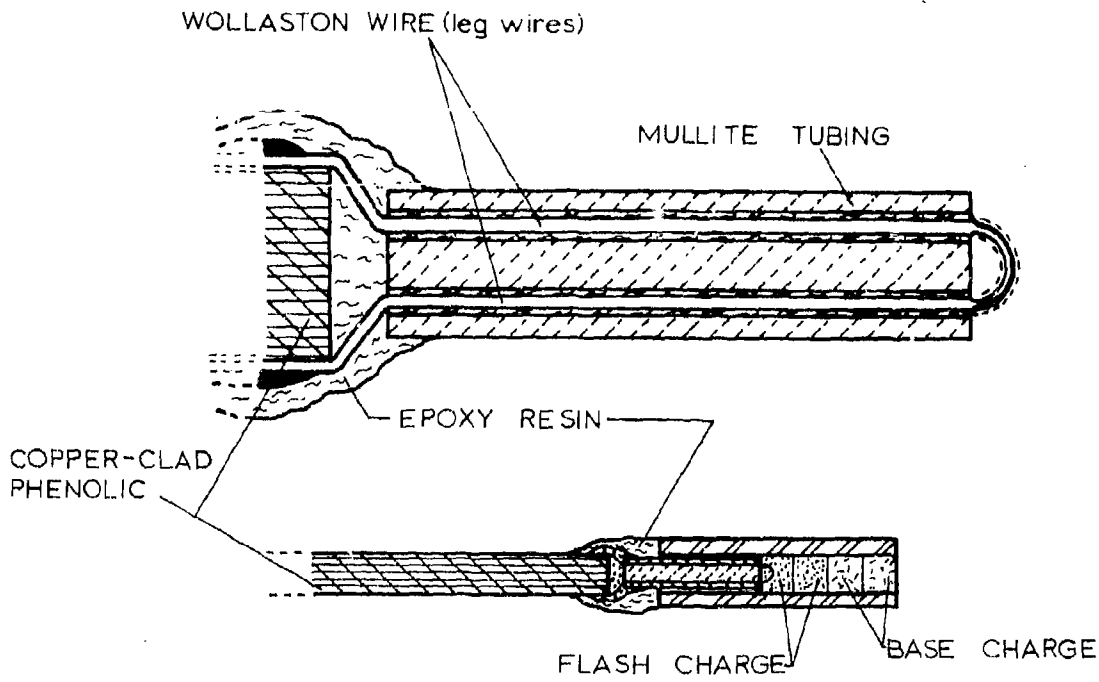


Figure 1. Initiator with Wollaston Wire Bridge as Used in "Short Bridgewire" and "Thermally Conductive Explosive" experiments.

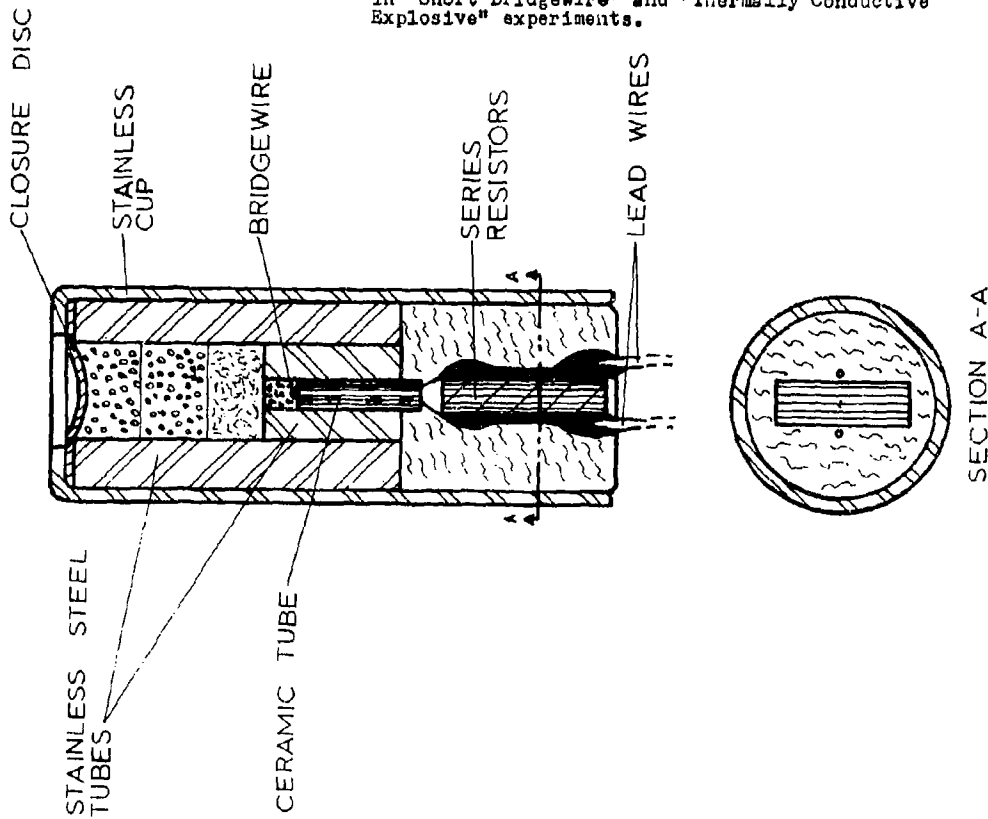


Figure 2. Proposed "One Amp-One Watt No-Fire" Detonator with Low Resistance Bridgewire and Series Resistors. (Type I)



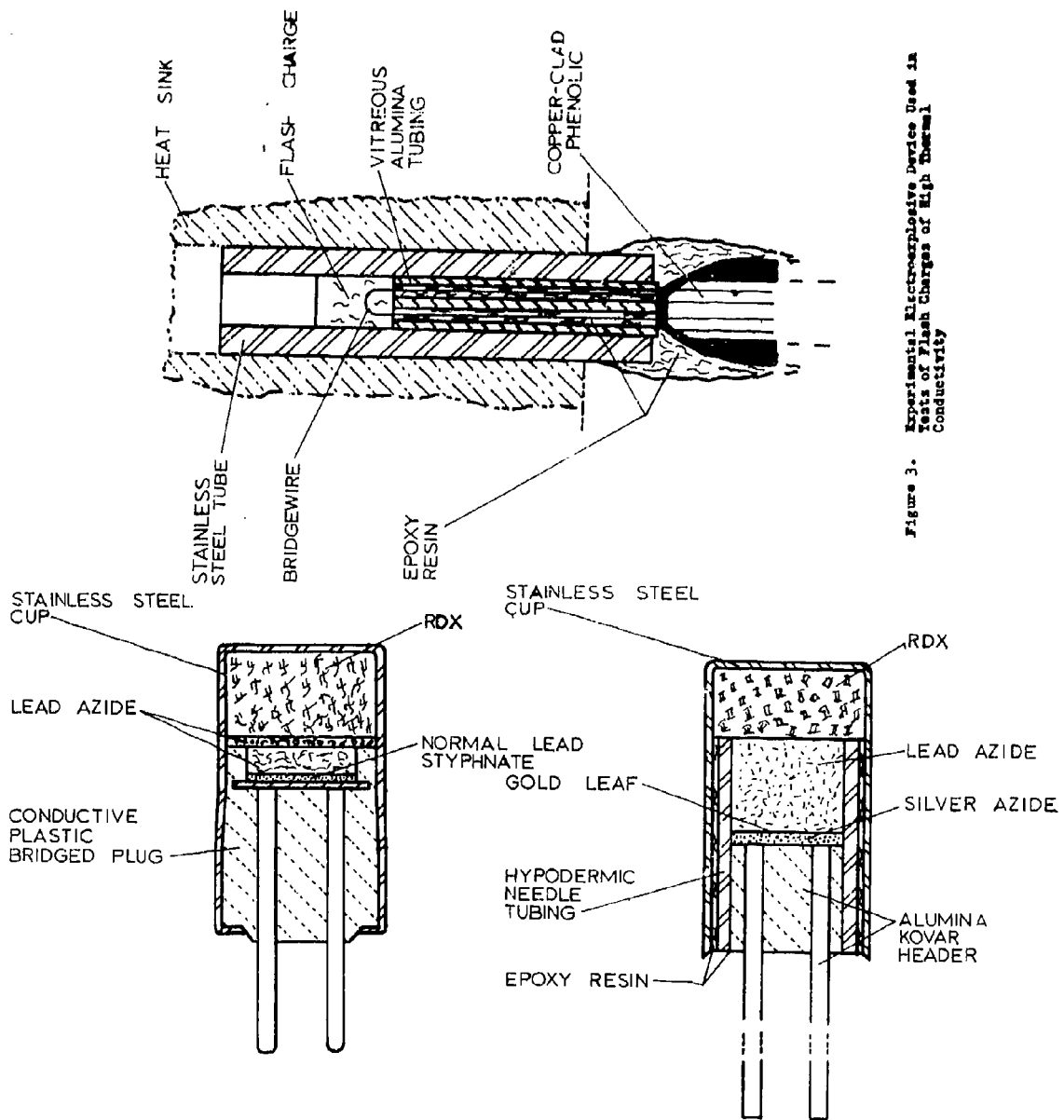


Figure 3. Experimental Electroexplosive Device Used in Tests of Flash Charges of High Thermal Conductivity

Figure 4. Experimental Electric Detonator with Markite, Conductive Plastic Bridged Plug

Figure 5. Experimental Electric Detonator with Alumina-Kovar Header Bridged with Gold Leaf

## DISCUSSION

The use of flake aluminum in the explosive mix to aid in thermal dissipation will increase the hazard to static discharge if used in the conventional design. It was suggested that the initiating element be placed in an electrically insulated assembly. Aluminized epoxy could then be coated on the back end to form a breakdown path.

The plastic bridges discussed in this paper have a very low specific resistance; however, they can be made much higher. This means that there is a possibility of using them in applications where graphite bridges are used.

3-5 A MICROCIRCUIT BRIDGE FOR HIGH-RELIABILITY  
ELECTRO-EXPLOSIVE DEVICES

D. N. GRIFFIN

PELMEC DIVISION  
QUANTIC INDUSTRIES, INC.  
SAN CARLOS, CALIFORNIA

INTRODUCTION

Most electro-explosive devices use a wire bridge for initiation. The bridge wire is delicate, usually only in the order of 0.001 to 0.002 inch in diameter. Also, the wire is attached to its terminal pins by welding or soldering, both of which are manual operations that are highly dependent on the skill of the worker. The bridge-wire concept has not changed significantly for many years and can be considered archaic, both in design and in manufacture, when compared with the advances that have been made in printed circuits and micro-miniaturized electronics. Therefore, an obvious place for improvement of electro-explosive devices is the ignition bridge.

During the past six to eight years, considerable emphasis has been placed on raising the no-fire characteristics of electro-explosive devices. The general approach has been to improve the heat-transfer characteristics of the bridge and the surrounding components so that heat can be effectively dissipated when a no-fire current is applied. Logically, a metal film or printed circuit is the ideal ignition bridge, since the bridge is actually bonded to the supporting insulator, resulting in optimum conditions for heat

transfer. Metal-film bridges have been under investigation for many years, but major problems have been encountered in controlling resistance and dimensional tolerances within practical manufacturing limits. As early as 1955, metal-film ignition bridges were fabricated by the vacuum-deposition process and more recently, several organizations have been active in efforts to develop this process.

Vacuum deposition results in ultra-thin films that normally do not exceed a thickness of about 2000 Angstroms or about 10 millionths of an inch. Films as heavy as 20,000 Angstroms can be produced, although exposure times become very long with a resulting adverse effect on production rates and cost. Because it is so thin, a metal-film bridge fabricated by the vacuum process must be in the form of a wide band or ribbon in order to provide the proper electrical resistance and current-carrying capacity. While production of a given film pattern is relatively easy, precise control over film thickness is also required if uniformity of performance is to be maintained.

About four years ago, work was initiated at Peltec Division of Quantic Industries on the development of a metal-film bridge. Although vacuum deposition was considered, it was concluded that this process would not be economically feasible for routine production of high no-fire electro-explosive devices. Instead Peltec chose to work with the moly-manganese process, which had already been well developed in the vacuum-tube industry for the production of

ceramic-to-metal seals. This process results in a film approximately 1 mil thick, primarily consisting of molybdenum metal sintered and intimately bonded to an alumina substrate. The process is attractive on a cost basis because the bridge can be formed simultaneously with the metalizing operation used in the attachment of the connector pins to the alumina header. The Peltec moly-manganese bridge is not a "metal-film" bridge in the strict sense of the word since it has a cross section about 2 mils wide by 1 mil deep that closely approximates the cross section of a conventional wire bridge. Therefore, to differentiate it from the metal-film bridge produced by the vacuum-deposition process, the Peltec bridge is referred to as a micro-circuit or MC bridge.

The micro-circuit bridge has been fully developed, and over a thousand units have been fabricated and tested in various configurations. These cover a wide range of initiators, detonators, and cartridges, all having substantially higher performance than their wire-bridge counterparts.

#### PROPERTIES OF THE MOLY MANGANESE FILM

##### The Moly-Manganese Process

The moly-manganese process is widely used in the semiconductor and electronics industries for metalizing ceramics and for making ceramic-to-metal seals. In this process, powdered molybdenum and manganese metals and/or their oxides are mixed in the form of a paint or ink which is applied to the ceramic part by brushing,

spraying, or other coating methods. The ceramic part is placed in a hydrogen-atmosphere furnace, where the metal film is bonded to the ceramic by sintering at a temperature above 2000°F. The moly-manganese film is then plated for subsequent soldering or brazing to the metal part. When properly applied, this process provides a hermetic seal having high mechanical and thermal shock resistance.

While there are almost as many formulas for the metalizing paint as there are users of the process, the basic composition is a mixture containing about 60 to 80% molybdenum metal, 5 to 20% manganese metal, and other metals and oxides as minor constituents. The powdered metals and oxides are mixed with a suitable nitro-cellulose lacquer binder to give a paint having approximately 50 to 60% solids by weight.<sup>1</sup>

After sintering, the resulting film is predominantly molybdenum metal, since most of the manganese and other oxides tend to form a glassy interface between the metal film and the ceramic substrate.

#### Electrical Properties

The first step in developing the moly-manganese bridge was determination of the basic electrical and thermal characteristics of the moly-manganese film. Samples were prepared, as shown in Figure 1, with thin lines of the metalizing film deposited on alumina substrates. Various segments of the test strips were marked off, and the physical dimensions (width and thickness) were

determined. By clamping various lengths of segments in the test fixture, also shown in Figure 1, simulated bridges were produced having widely varying resistances and dimensions. From these measurements, the following ambient temperature coefficient of resistivity was obtained:

$$RA = 2.14 \times 10^7, \quad (1)$$

where R = resistance (ohms per inch length),  
 A = cross-sectional area (in.<sup>2</sup>).

The measured coefficient of resistivity is about nine times higher than the reported value for pure molybdenum, apparently because of the non-homogenous nature of the sintered metal and the fact that a portion of the film is non-metallic in composition.

Measurements were made to establish the thermal coefficient of resistance for the bridge material. Utilizing the test fixture shown in Figure 1, test segments were heated in an oven and resistance was measured at various temperatures up to approximately 450°F. Straight-line plots of resistance versus temperature were obtained and from these the following coefficients were derived:

$$\begin{aligned} (R/R_0 - 1) (t - t_0)^{-1} &= 0.00137 \text{ (ohm/ohm/}^\circ\text{F)} \\ &= 0.00246 \text{ (ohm/ohm/}^\circ\text{C)}, \end{aligned} \quad (2)$$

where R = resistance (ohms) at temperature t,

R<sub>0</sub> = resistance at 0°F,

t = temperature,

t<sub>0</sub> = 0°F.

The measured thermal coefficient is about 70% of the reported value for pure molybdenum and is of the same order of magnitude as that of gold and platinum, which are typical bridge-wire materials.

#### Current-Temperature-Time Characteristics

Utilizing the test fixture shown in Figure 1, segments of the test strips were subjected to various applications of direct current, with voltage and current across the bridge being simultaneously recorded on an oscillograph. With suitable corrections for lead resistance, the resistance of the bridge could then be derived at any time on the basis of the recorded voltage and current values. With the bridge resistance ( $R$ ) at any time known, the average bridge temperature was then derived using the thermal coefficient of resistance given in equation 2.

Tests were conducted with ambient temperature bridge resistance varied from 0.52 to 3.05 ohms and with applied current varied from 1 to 10 amperes. A primary battery was used for power supply, and current was regulated by selection of battery voltage and by adjustment of total circuit resistance.

At low currents, the bridge temperature rose rapidly (within a few milliseconds) to a steady-state condition, after which a slow temperature rise occurred due to the gradual heating of the alumina substrate. The rate of this slow temperature rise increased as current, and hence initial temperature, was increased. At higher



currents (depending on physical dimension and resistance of the specimen bridge), bridge burnout occurred.

Because of the increase in bridge resistance with temperature, current decreased with time. At burnout temperature, the current would normally be approximately 60% of initial current. However, power would remain nearly constant, either increasing or decreasing slightly with temperature, depending on the ratio of bridge resistance to total circuit resistance.<sup>2</sup>

Figures 2 and 3 show typical temperature-versus-time plots in which bridge burnout occurred at widely different heating rates. In the tests shown in Figure 2, the average heating rate was about 10 to 20 degrees per millisecond, and burnout occurred in approximately 1 second. Under these conditions, an upward bend in the temperature/time plots occurred just prior to burnout. This upward shift was assumed to have been caused by an increase in bridge resistance due to oxidation of the bridge rather than by a rise in heating rate. Therefore, the reported burnout temperature in these cases is based on an extrapolation of the normal heating curve. When a heating rate of the order of 100 to 200 degrees per millisecond was used, burnout occurred within 10 to 20 milliseconds as shown in Figure 3. When burnout occurred this rapidly, the upward shift did not occur, indicating that the oxidation reaction was too slow to cause any significant change in bridge resistance.

The average of all of the recorded burnout temperatures was 1408° F,

which coincides with the temperature at which rapid oxidation of molybdenum takes place. Molybdenum is a refractory metal having a very high melting point ( $4700^{\circ}\text{F}$ ). However, it is also a reactive metal and is readily oxidized. At low temperatures, the metal is protected by an oxide film ( $\text{MoO}_3$ ). At about  $1400^{\circ}\text{F}$ , the oxide becomes volatile so that the surface protection is lost, and rapid oxidation can occur.<sup>3</sup> The melting point of molybdenum trioxide is  $1463^{\circ}\text{F}$ .<sup>4</sup>

#### Initiation of Lead Styphnate

After the preliminary tests in which the burnout temperature of the moly-manganese bridge was established, test specimens were covered with a small bead (approximately 5 milligrams) of normal lead styphnate bonded with nitro-cellulose lacquer. Tests were again run at different heating rates, and the temperature and time of initiation of the lead styphnate was determined by means of a sudden small spike on the voltage and current traces. This effect was caused by the heat flash produced by the explosion, which instantaneously heated the bridge about 50 degrees, resulting in an increase in resistance and a corresponding shift in the voltage and current across the bridge.

Initiation time for the lead styphnate bead varied from 0.010 to 3.680 seconds. Initiation temperatures varied from  $544$  to  $845^{\circ}\text{F}$ , with the lowest temperatures occurring in conjunction with the shortest initiation times. This is in reasonable agreement with reported thermal-initiation temperatures of  $500$  to  $590^{\circ}\text{F}$  for

lead styphnate.<sup>5</sup> In all cases, the bridge remained intact after initiation of the lead styphnate.

Typical records of temperature versus time for tests in which lead styphnate beads were fired are given in Figures 4 and 5.

#### MICROCIRCUIT BRIDGE DESIGN

Figure 6 shows the basic design configuration that has been used in the Pelmec MC bridge. The bridge consists of three portions: (1) the bridge itself which is the small necked-down portion in the center; (2) the resistance leads from the connector pins to the bridge; (3) the circular ends that form the points of attachment to the pins.

On the basis of the test data described in the previous section, it was estimated that the functioning portion of the bridge should have a cross section of about 2 square mils in order to provide pyrotechnic initiation and burnout in approximately 1 millisecond with a firing current of 4.5 amperes. In early designs, a bridge width of 5 mils was used, since it was assumed that this was the narrowest pattern that could be produced within reasonable tolerance limits. This width in turn required a film thickness of about 0.4 mil in order to maintain the proper cross section. As process techniques were refined, it was possible to reduce the width of the bridge; at present bridge patterns 2 mils wide are being fabricated routinely with a dimensional variation of about 5%. The narrower width allows a thicker film to be used,

which in turn reduces the relative variation in thickness.

The micro-bridge portion controls the functional characteristics of the circuit. However, most of the total circuit resistance is in the resistance leads. Therefore, changes in the length and width of the leads allow circuit resistance to be changed without affecting bridge functioning characteristics. Variation in the total circuit resistance does have an effect on the no-fire level, however, since rate of power dissipation, and hence rate of heat input is proportional to resistance.

The circular ends of the bridge pattern are coated with a nickel oxide paint and the unit is subjected to a second firing in a hydrogen-atmosphere furnace. This procedure reduces the nickel oxide to nickel, which sinters and bonds to the moly-manganese film. Following this operation, the pins are brazed to the ceramic header, simultaneously forming a high-strength seal and the electrical connection to the MC bridge. The pins used are of Kovar, whose coefficient of expansion closely matches that of the alumina header.

The design techniques just described can result in an almost unlimited variety of bridge patterns. Figure 7 shows the various configurations that have actually been built and tested by Peltec. The first bridge made is shown in Figure 7A. This bridge was designed to give a nominal resistance of 1 ohm; and a limited number of Probit-type tests with lead styphnate indicated a no-fire

level of approximately 2 amperes and 4 watts, together with a functioning time of less than 1 millisecond at 4.5 amperes.

Because of the high no-fire capability demonstrated in the initial tests, the bridge shown in Figure 7B was designed with a nominal 1/2-ohm resistance to give 2 watts of power dissipation at 2 amperes. A considerable number of cartridges were built and tested with this bridge configuration.

The bridge shown in Figure 7C was designed for a small initiator having a nominal 1/2-ohm bridge resistance. It was also modified to give a resistance of 0.07 ohm, which resulted in a no-fire capability in excess of 5 amperes and 1.5 watts.

Finally, the configuration shown in Figure 7D represents the most recent MC bridge design. It has a 5-minute dc no-fire capability of better than 1 ampere and 1 watt with a nominal bridge resistance of only 0.4 ohm.

#### PERFORMANCE CAPABILITIES

The following devices have been built utilizing the MC bridge for initiation. They are described in this paper primarily to show some of the performance capabilities of the bridge. Consequently not all of their design or performance details are included.

### Model 1260 Cartridge

The Palmec Model 1260 Cartridge is shown in Figure 8. This design represents a modification of a qualified cartridge which had a conventional bridge wire and lead styphnate as the first element in the pyrotechnic train. Lead styphnate was also used in the Model 1260 Cartridge. However, because of the high heat-transfer characteristic of the MC bridge, a high no-fire capability was obtained in spite of the relatively low thermal stability of lead styphnate.

Typical ambient-temperature Bruceton No-Fire data for the Model 1260 Cartridge are shown in Figure 9. With a bridge resistance of 0.9 ohm, a 5-minute no-fire level of 1.9 amperes or 3.3 watts was obtained. These values were calculated for 99.5% reliability at 95% confidence. Function time was less than 10 milliseconds with a 4.5-ampere firing current.

### 5-Ampere/1.5-Watt Initiator

An initiator for CDF was built as shown in Figure 10 to meet a 5-ampere/1.5 watt/5-minute no-fire requirement. The MC bridge configuration shown in Figure 7C was used. However, the bridge was modified to give a resistance of 0.07 ohm, which provides a power dissipation of 1.8 watts at 5 amperes. A metal/oxidant initiation charge was used, and a limited number of units were subjected to the various performance tests tabulated in Figure 11. As shown in the figure, all of the specified requirements were met or exceeded.

### Model 1353 Initiator

The Peltec Model 1353 Initiator is shown in Figure 12. In this design, the MC bridge is incorporated in an all-ceramic initiator that is heat-sterilizable, and is insensitive to a 25-kv discharge from a 500-picofarad capacitor in all modes. The unit meets the 1-ampere/1-watt/5-minute no-fire requirement with a bridge resistance of only 0.4 ohm. However, a 1-ohm bridge can also be provided if required. The initiator can be used by itself for pyrotechnic ignition or high-explosive initiation. It may also be used in standard 0.280-inch-diameter squibs and detonators as shown in Figure 13.

The Model 1353 Initiator utilizes the bridge configuration shown in Figure 14. After the MC bridge has been formed on the ceramic header, the areas surrounding the pinholes are nickel plated, and the pins are riveted to the header and brazed. Each of these steps is illustrated in the figure. The header assembly is then pressed into the ceramic cup, together with the pyrotechnic charge, and sealed with a high-temperature epoxide resin that is heat cured at 400°F for 1 hour. The end of the ceramic cup is in the form of a 0.010-inch-thick diaphragm that completely pulverizes when subjected to the pressure of explosion of the pyrotechnic load.

Over 500 Model 1353 initiators have been manufactured. The performance data discussed below are based on preliminary evaluation tests of 100 units. A complete evaluation test program is scheduled.

Figure 15 is a summary of the measured performance characteristics of the Model 1353 initiator. The initiator is tentatively rated as meeting a 500°F environment for 1 hour and 600°F for 30 minutes, since no degradation of function time or pressure output was observed after exposure to these conditions. Since the initiator is of an all-ceramic construction, it displays excellent dielectric strength. Also, it will withstand a discharge of 25 kv from a 500-picofarad capacitor in all modes without any special provisions for external shunting. Function time at ambient temperature versus firing current is shown in Figure 16.

A 25-shot constant-current 5-minute no-fire Bruceton test was performed with results as shown in Figure 17. A no-fire current of 1.4 amperes was computed with a reliability of 99% at 95% confidence level. On the basis of ambient-temperature bridge resistance, this represents a no-fire power of only 0.8 watt. However, because of the increase in bridge resistance with temperature, steady-state power dissipation at this current level is actually 1.2 watts, as shown in Figure 18.

During the no-fire tests, voltage and current were continuously recorded, which allowed bridge resistance and power to be derived. Typical plots of power versus time are also given in Figure 18 for a no-fire test at 1.75 amperes and a test at 1.95 amperes in which the unit fired, since these values represent the extreme spread in test conditions. In all of the tests in which the initiator did not fire, the power approached steady-state conditions at a level of 2 to 3 watts. In tests in which the initiator



fired, the power rose continuously, reaching a level of 4 to 6 watts at the time of initiation.

It can be concluded that the no-fire power rating should be established on the basis of a constant-power no-fire test, run in addition to the constant-current test.<sup>2,6</sup> The present military requirements are not consistent on this point, since in some cases the no-fire power test is specified,<sup>7</sup> whereas other requirements specify that the no-fire power level must be computed from the no-fire current and the ambient-temperature bridge resistance.<sup>8</sup> The latter approach is not considered realistic by this author, and it is hoped that this inconsistency will be resolved at the present meeting.

#### REFERENCES

1. Walter H. Kohl, "Materials and Techniques for Electron Tubes", Reinhold Publishing Corporation, New York, N.Y., (1962).
2. J. N. Ayres, "Approximation Method for Firing Wire-Bridge EED's at Constant Power", NOLTR 66-182, U.S. Naval Ordnance Laboratory, 3 February 1967, White Oak, Maryland.
3. "Marks' Mechanical Engineering Handbook," Sixth Edition, McGraw-Hill Book Company, Inc., 1958, page 6-119.
4. "Lange's Handbook of Chemistry," Eighth Edition, Handbook Publishers, Inc., 1952, page 259.
5. W. R. Tomlinson, Jr., "Properties of Explosives of Military Interest," Technical Report No. 1740, Revision 1, Picatinny Arsenal, Dover, N.J., April 1958, page 177.
6. J. N. Ayres, "Interpretation of Electro-Thermal Measurements on Wire Bridge Electro-Explosive Devices (EED's)", NOLTR 66-114, U.S. Naval Ordnance Laboratory, White Oak, Maryland.
7. "General Range Safety Plan", AFMTCP 80-2, 1 October 1963, Volume I, Appendix A, Air Force Missile Test Center, Patrick AFB, Florida.
8. "Initiators, Electric, Design and Evaluation of", MIL-I-23659B(AS), 3 June 1966.

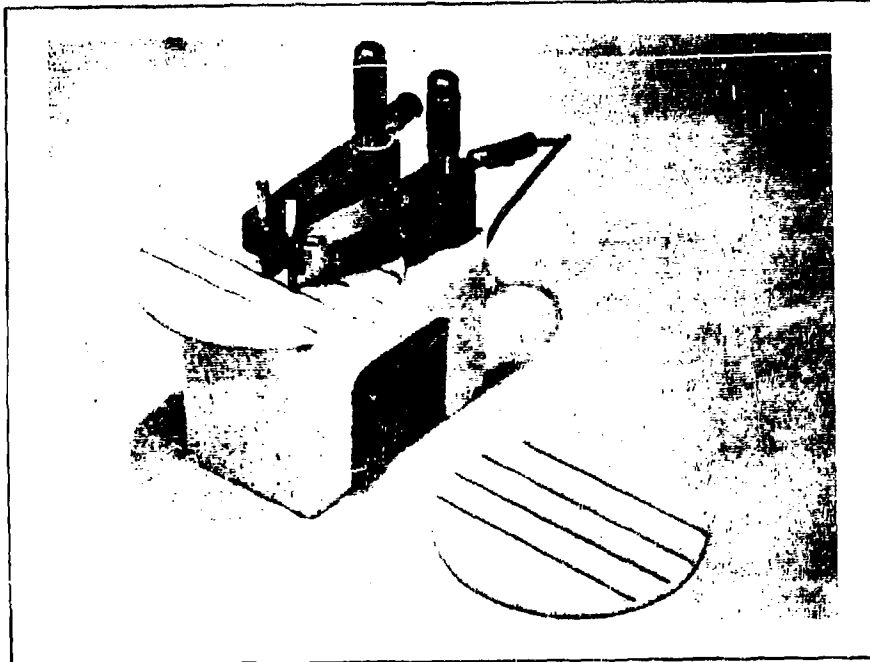


FIGURE 1 - Moly-Manganese Film Bridge Samples and Test Fixture.

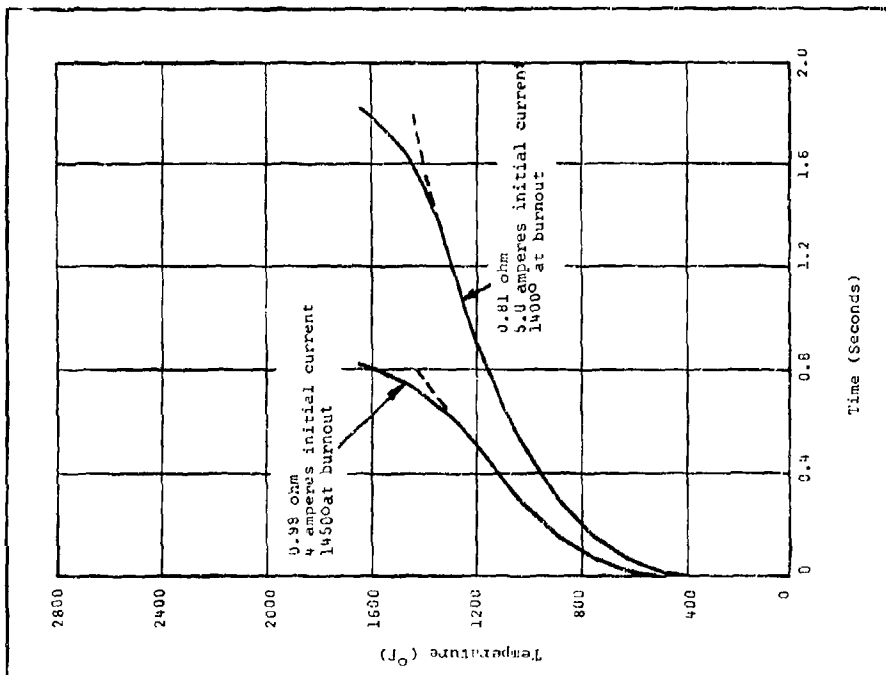


FIGURE 2 - Temperature versus Time for Selected Moly-Manganese Film Bridges.

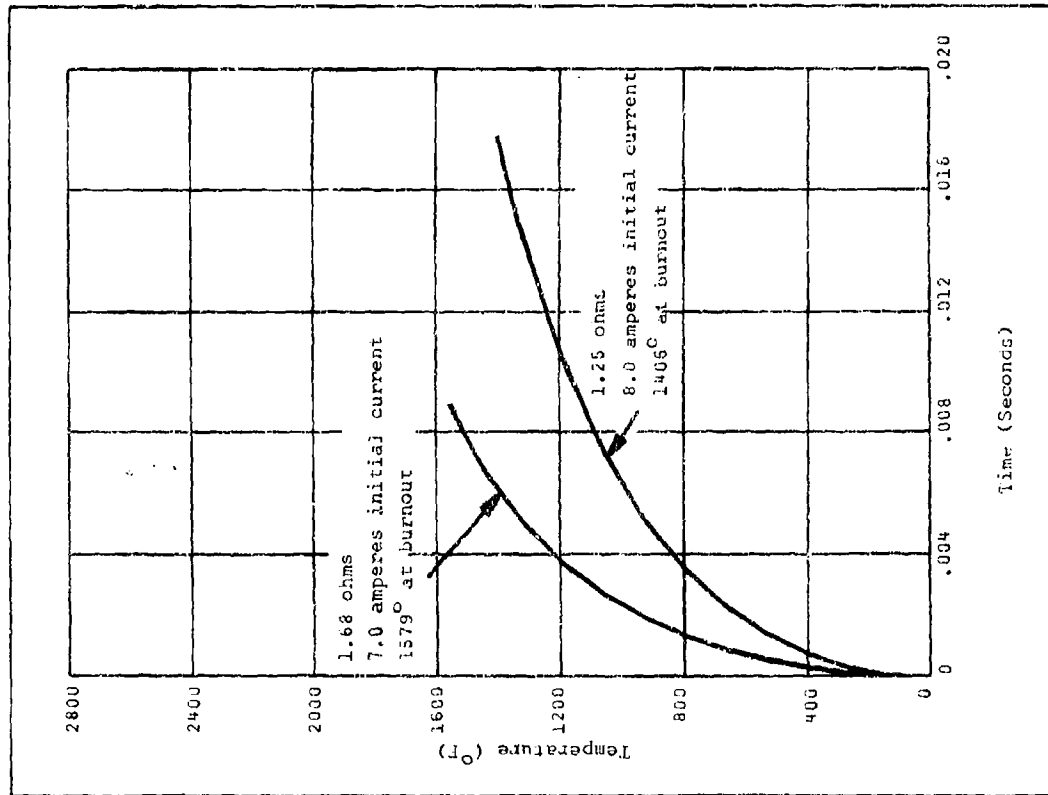


FIGURE 3 - Temperature versus Time for Selected Moly-Manganese Film Bridges.

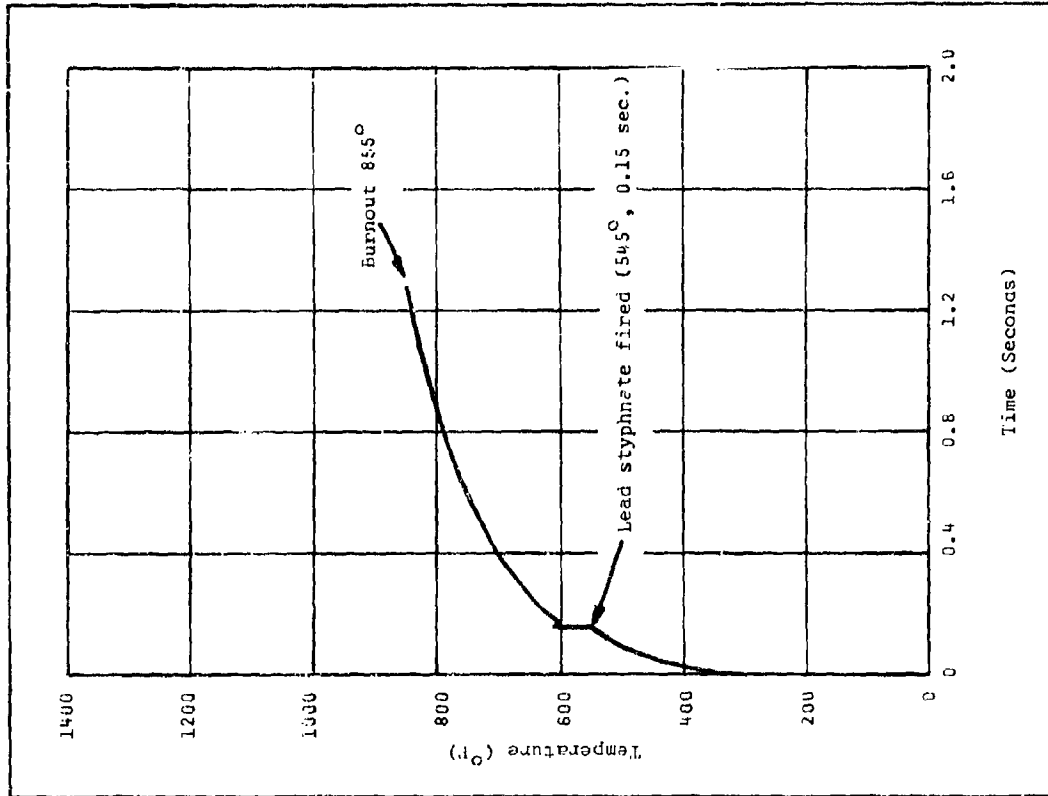


FIGURE 4 - Temperature versus Time for a 1.7-ohm Moly-Manganese Film Bridge with Lead Styphnate Charge Subjected to a 3-ampere Firing Current.

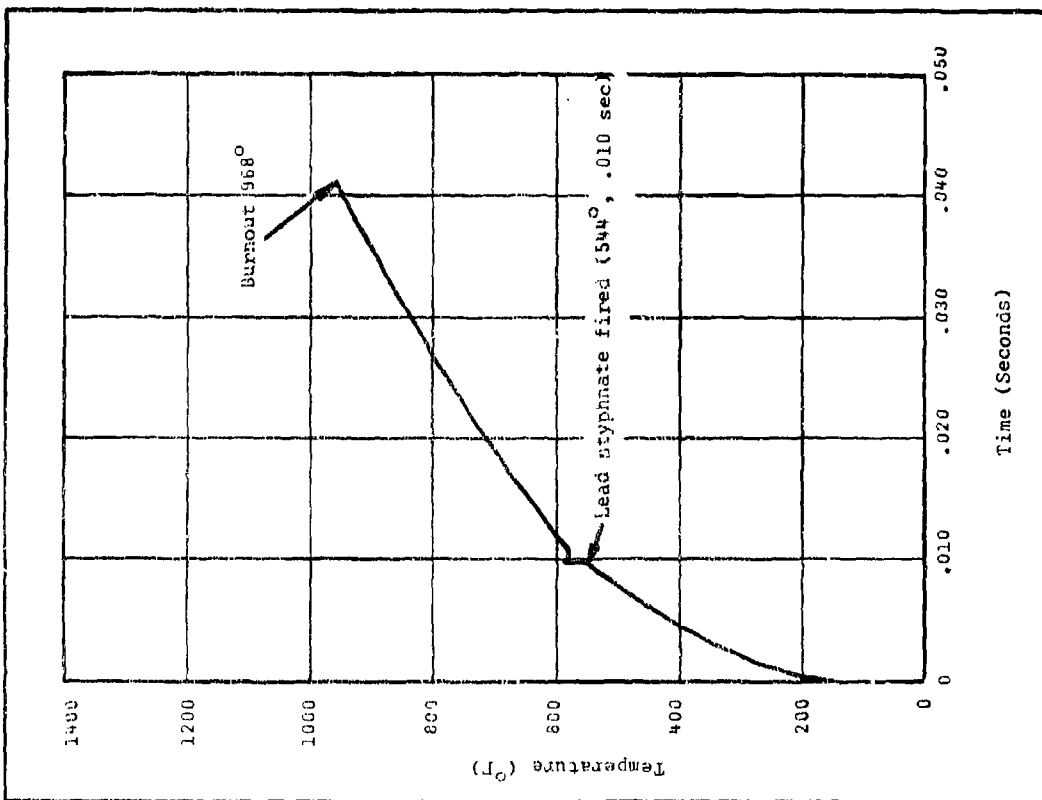


FIGURE 5 - Temperature versus Time for a 1.7-ohm Moly-Manganese Film Bridge with Lead Styphnate Charge Subjected to a 4-ampere Firing Current.

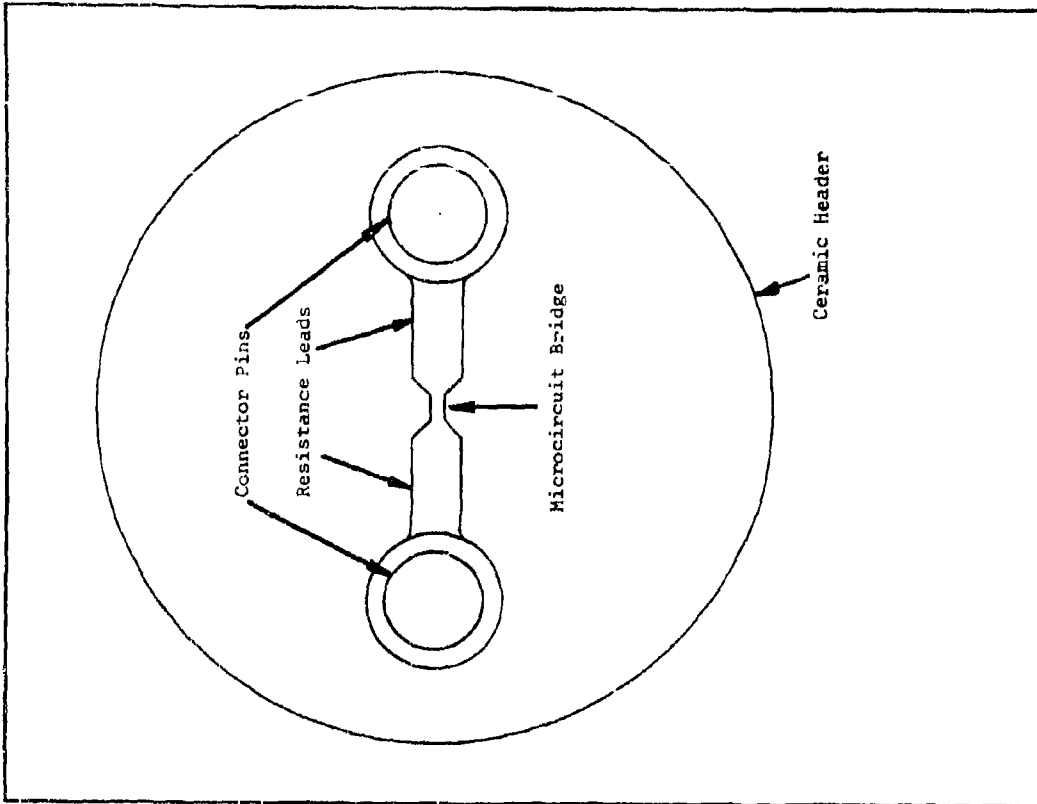


FIGURE 6 - Basic Microcircuit Bridge Design Configuration.

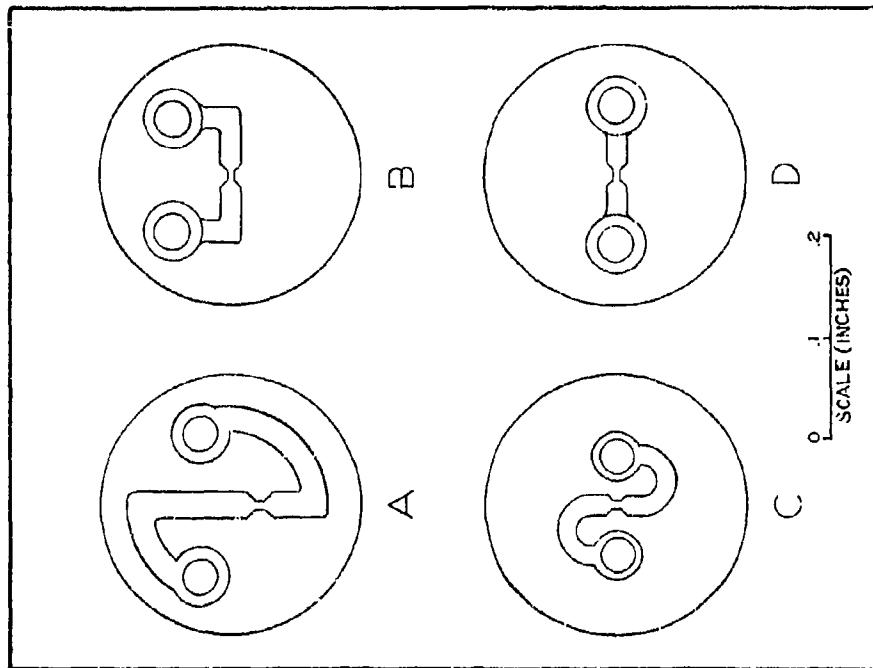


FIGURE 7 - Microcircuit Bridge Designs.

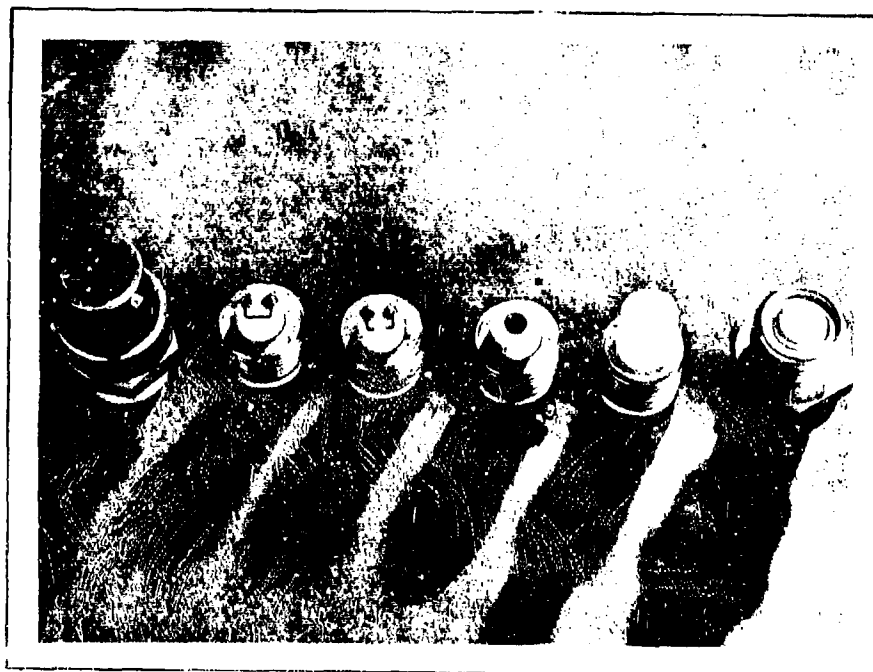


FIGURE 8 - Peltec Model 1260 Cartridge

Current (Amps)	Sample No.																							
	1	2	3	4	5	6	7	8	9	10	11	12	13	14	15	16	17	18	19	20	21	22	23	24
2.50	X		X							X		X				X		X						
2.40		0		X					0		0		X		0		0		X		X			X
2.30					X		X		0						0						0		0	
2.20						0		0																

X = Fire, 0 = No-Fire; Bridge Resistance 0.90 ± 0.05 ohms.

50% Probability Point = 2.36 Amps  
 99.5% No-Fire Probability (95% Confidence) = 1.93 Amps (3.33 watts)  
 99.5% Sure-Fire Probability (95% Confidence) = 2.82 Amps

FIGURE 9 - Bruceton 5-Minute No-Fire Test, Felmeo Model 1260 Cartridge

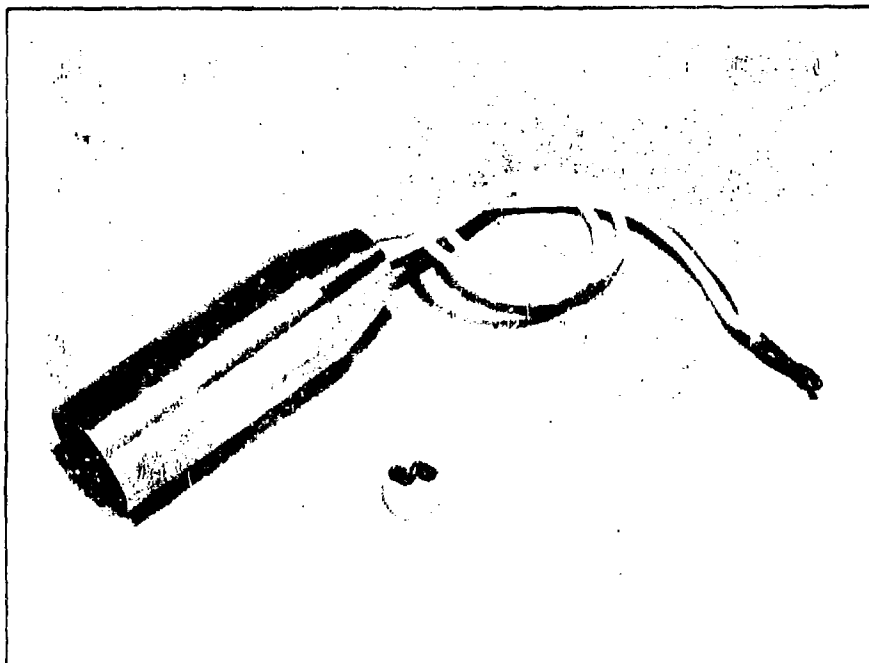


FIGURE 10 - 5-Amp/1.5-Watt Initiator.

<u>TEST</u>	<u>MEASURED PERFORMANCE</u>
Bridge Circuit Resistance:	.07 ohms
DC Dielectric Breakdown (Pin/Case):	>2,500 volts
AC Dielectric Breakdown (Pin/Case):	>1,500 RMS volts, 60 ~
Electrostatic Discharge (Pin/Pin & Pin/Case):	25 kv, DC, 500 MMFD
No-Fire Sensitivity:	>5 ampere/1.5 watt/5-minute
Function Time (15 Ampere Firing Current):	.007 seconds
Post-Firing Resistance (Pin/Pin & Pin/Case):	>5000 ohms

FIGURE 11 - Summary of Measured Performance Capabilities, Pelmeo  
5-Ampere/1.5 Watt HCB Initiator

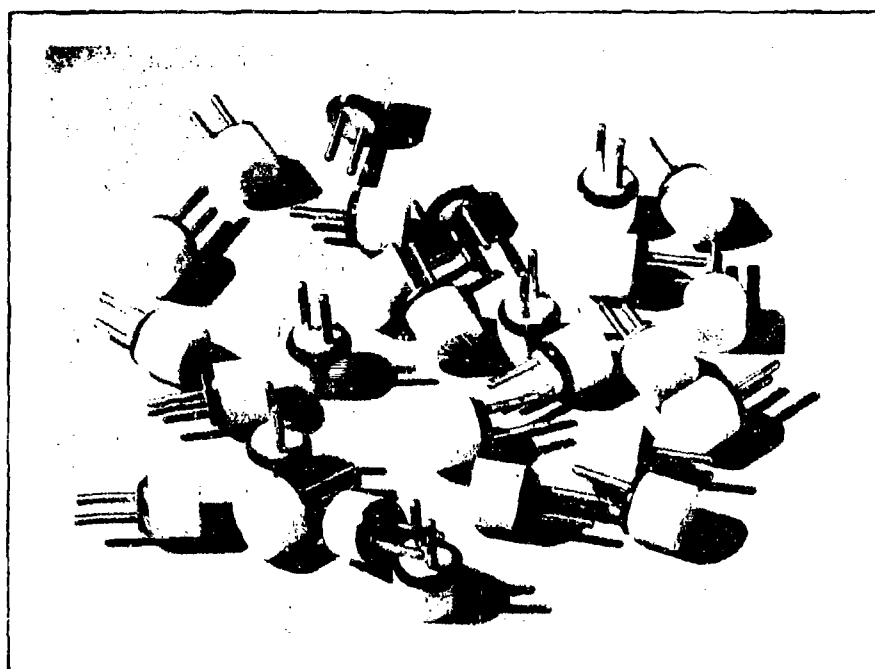


FIGURE 12 - Pelmeo Model 1353 Initiator

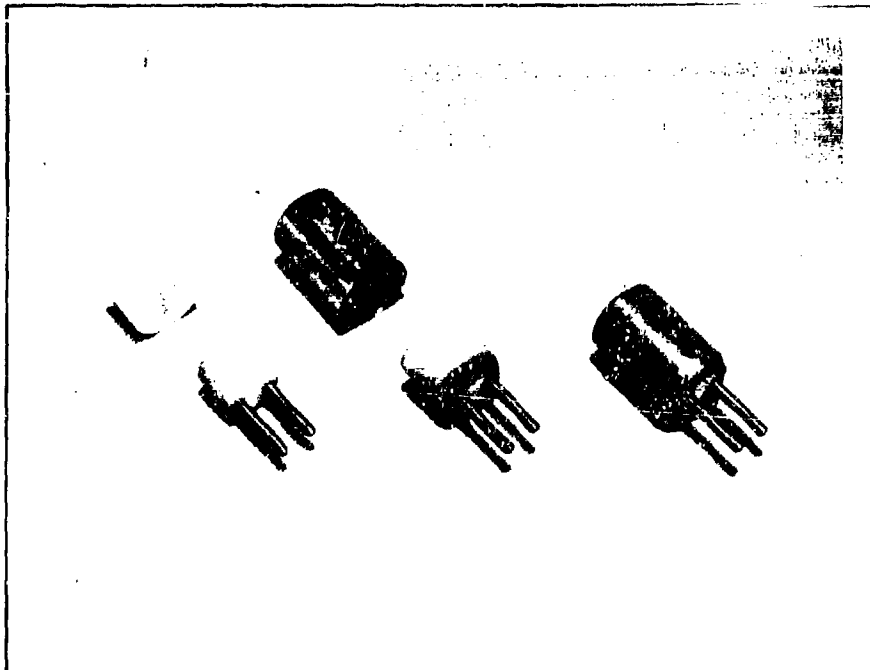


FIGURE 13 - Model 1353 Initiator Incorporated in a 0.280 - Diameter Squib.

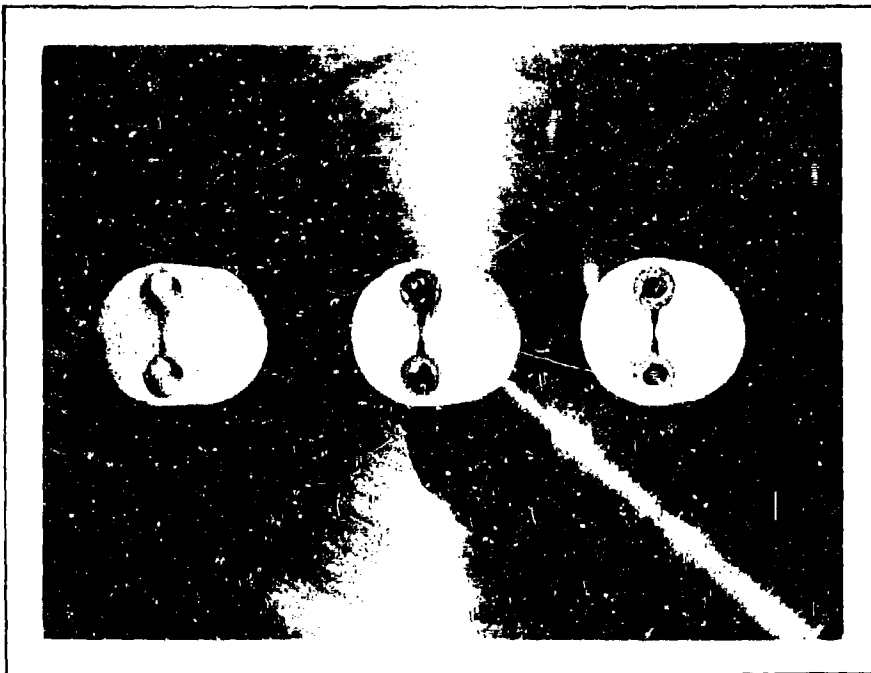


FIGURE 14 - Model 1353 Initiator Header with 0.4-ohm MC Bridge.



<u>TEST</u>	<u>MEASURED PERFORMANCE</u>
Bridge Circuit Resistance:	.38 ± .04 ohms
Insulation Resistance:	> 20 megohms at 2000 vac
DC Dielectric Breakdown (Pin/Case):	> 2,500 volts
AC Dielectric Breakdown (Pin/Case):	> 2,000 RMS volts, 60~
Electrostatic Discharge (Pin/Pin & Pin/Case):	25 kv, DC, 500 MMFD
No-Fire Sensitivity:	> 1 ampere/1 watt/5-minute
High Temperature Stability:	500°F for 1 hour (600°F for 30 minutes)
Autoignition Temperature:	> 800°F
Function Time (Ampere Firing Current):	1 millisecond
Pressure Output (in 2-cc Volume):	1000 psi
Post-Firing Resistance (Pin/Pin & Pin/Case):	> 5000 ohms

FIGURE 15 - Summary of Measured Performance Capabilities, Pelmeo Model 1353 Initiator

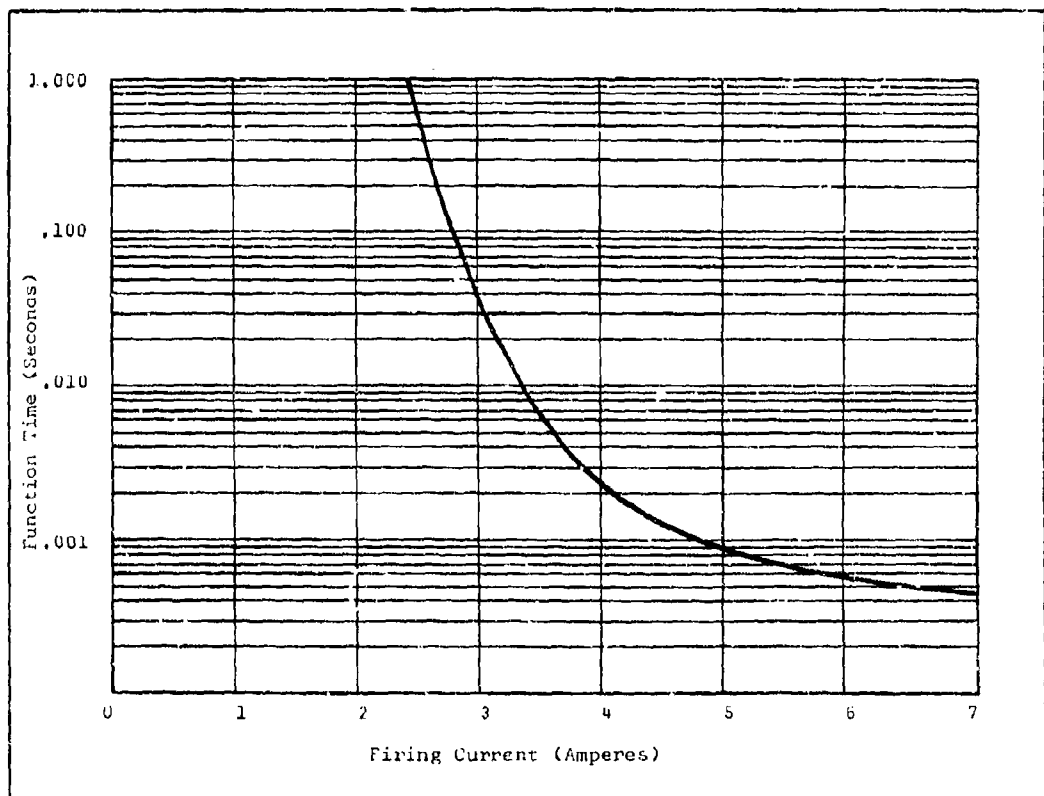


FIGURE 16 - Function Time versus Firing Current, Pelmeo Model 1353 Initiator.

Current (Amps)	Sample No.																								
	1	2	3	4	5	6	7	8	9	10	11	12	13	14	15	16	17	18	19	20	21	22	23	24	25
1.95						X								X		X							X		
1.90					0		X						0		0		X				0		X		X
1.85				0			X					0						X		0				0	
1.80	X		0						X		0									0					
1.75		0									0														

X = Fire, 0 = No-Fire; Bridge Resistance = .38 ± .04 ohm.

50% Probability Point = 1.87 Amperes

99% No-Fire Probability (95% Confidence) = 1.40 Amperes

99% Sure-Fire Probability (95% Confidence) = 2.33 Amperes

FIGURE 17 - Bruceton 5-Minute No-Fire Test, Pelmeo Model 1353 Initiator

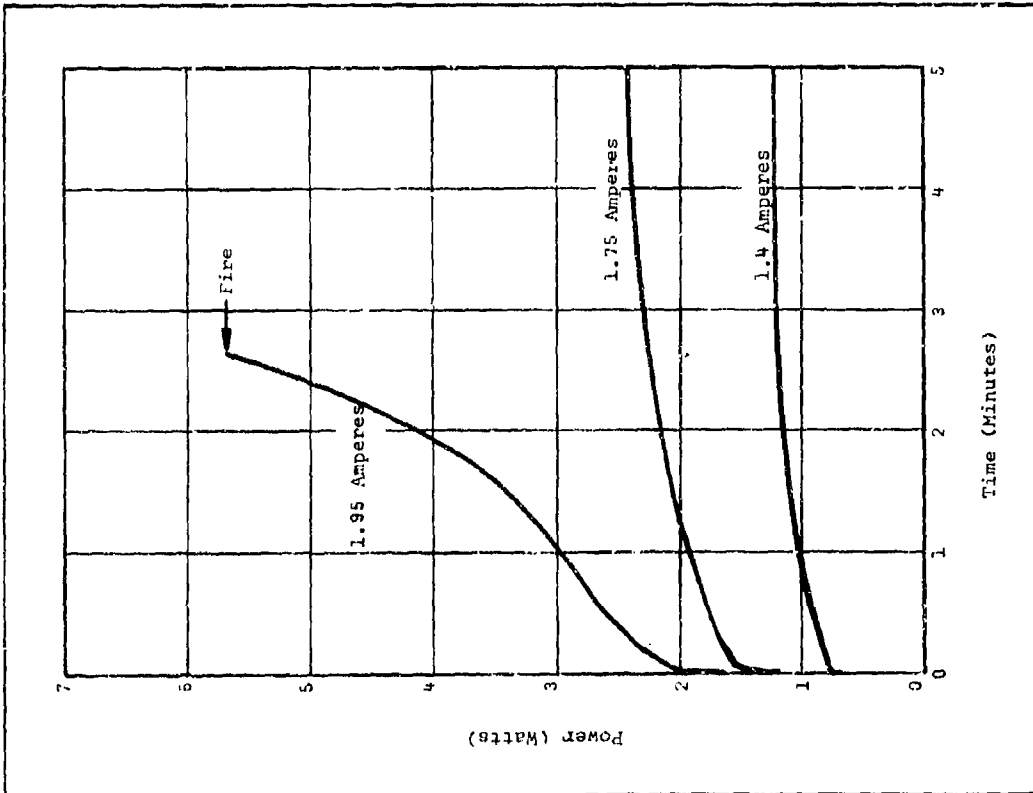


FIGURE 18 - Power Dissipation versus Time at Various Levels of Applied Current for Model 1353 Initiator

## DISCUSSION

The temperature values plotted in the graphs were obtained by monitoring the bridge current and voltage with an oscillograph. From this can be calculated the average bridge temperature. The temperature gradient between pins is not considered. In the notch designs, temperature is not discussed because of the non-uniform pattern.

Since the bridge is bonded directly to the ceramic header, it should pass the shock and vibration tests; however, qualification tests have not been performed as yet.

The bridge is designed so that its open circuit resistance after firing is 15,000 ohms when no pyrotechnic material is used. The final resistance will be lower when a pyrotechnic material is placed adjacent to the bridge. A typical value for a device containing a metal oxide mix and fired in a pressure chamber was 5,000 ohms.

3-6 ELECTRIC DETONATORS WITH "MARKITE" ELECTRICALLY  
CONDUCTIVE PLASTIC BRIDGE ELEMENTS

By R. H. Stresau, R. L. Peterson, S. A. Corren and M. A. Coler  
Stresau Laboratories and Markite Engineering Co.

INTRODUCTION

During the past twenty years, mainly in connection with the development and manufacture of potentiometers of highly controlled characteristics, the Markite Corporation has learned to synthesize and compound plastics with a wide range of precisely predetermined electrical conductivity and other characteristics and to fabricate these materials in a variety of configurations. Means were also found to substantially increase the thermal conductivity of plastics without altering their electrical insulation characteristics.

When concern regarding electromagnetic radiation hazards resulted in the promulgation of lower limits for firing current and power of electroexplosive devices, it became apparent that electrically conductive plastics, in combination with the other capabilities, might be applicable.

Figure 1 is a photograph of two plugs made for Naval Ordnance

Laboratory at White Oak. These units met the 1 ampere, 1 watt, no-fire criterion. They illustrate some of the structural variations that are possible with all-plastic elements. The bridge area in one element is raised while in the other the bridge is in the plane of the plug face.

The silver plated brass terminals, the plastic insulator base, the conductive plastic bridge and the highly conductive contact areas are co-molded into one unitary structure. Units such as these can be tailored to meet specific requirements by varying such parameters as:

1. The specific resistance of the bridge material.
2. The geometry of the bridge.
3. The geometry of the plug.
4. The thermal conductivity and heat capacity of the insulator plastic substrate.

For use in guided missiles, the Naval Ordnance Laboratory at Corona, California has a requirement for an electric detonator which will meet the "one-ampere, one-watt, no fire" criterion but which might be substituted directly for the Mk. 71 detonator without requiring modification of existing firing circuits (which can be relied upon to deliver about 10,000 ergs, in a capacitor discharge). The study of the feasibility of such a detonator has been assigned to the R. Stresau Laboratory by the Naval Ordnance Laboratory (Corona). The use of conductive plastic as a bridge element is one of several approaches which are under consideration.

A joint effort of the R. Stresau Laboratory and the Markite Engineering Company has resulted in the development of the bridged plug shown in Figure 2. Tests indicated that such units could meet the requirements of the Naval Ordnance Laboratory (Corona).

The reticulated design permits the better dissipation of the 1 watt input. This picture illustrates again the design flexibility inherent in the plastic molding technique.

Subsequent experimentation has shown that Markite conductive plastic bridge elements are adaptable to a wide range of applications, including some where miniaturized components with extreme sensitivity are required. Figure 3 is a photograph of an element with an overall diameter of 0.077 inch. The conductive plastic forms a bridge between the metal stem and the metal collar. These units like the others can be made by automated operations. The particular elements shown fired at 1000 ergs with 5 volts or with 2000 ergs at 2 volts.

#### "HIGH POWER, LOW ENERGY" REQUIREMENT:

The combination of relatively high power requirements (one watt) with relatively low energy (10,000 ergs) is theoretically feasible as was shown in "Electrical and Thermal Consideration in the Design of Electroexplosive Devices" by Peterson, Chamberlain, and Stresau, presented in another paper at this meeting. The high power requires that the heat loss factor of the bridge element be large and the low energy requires that its heat capacity be low. In view of the very small range of the volumetric specific heats of solids, the requirement for a small heat capacity ordinarily calls for a small bridge element volume. This leads to the use of microscopically fine wires. It was found, however, that the relationship of heat capacity and firing energy is substantially

altered when conductive plastic bridges are used. When certain critical currents are exceeded local high temperatures are generated which are far in excess of what would be expected from the total volume of bridge material. The V-I characteristics of the conductive plastic are described later.

#### FEASIBILITY EXPERIMENTS

The plugs shown in Figure 2 were incorporated in test initiators, loaded with lead styphnate and tested. The threshold pulse firing energy (discharge from a 0.5 microfarad condenser) was between 11,000 and 12,000 ergs and was not significantly affected by exposure to one watt or one ampere for five minutes. If cased in heat sinks of sufficient thermal conductivity, their threshold firing power was close to five watts. These results showed that a comparatively substantial bridge of electrically conductive plastic on a substrate of comparatively high thermal conductivity had promise of meeting the Navy guided missile requirement.

#### PRELIMINARY EVALUATION TESTS

An evaluation of conductive plastic bridged plugs supplied by the Markite Engineering Company was performed by R. Stresau Laboratory, Inc. This was done under contract to the U. S. Naval Ordnance Laboratory, Corona, California.

Three hundred of the units (Type 21166) shown in Figure 4 were sub-

jected to test. The body of the plug conforms to the requirements of the Mk. 71 detonator. The maximum diameter is 0.178 inch and the overall height is 0.230 inch. This includes an integrally molded cup for holding the charge. The black zone is the conductive plastic bridge. Its short dimension (0.040 inch) is the length. The width extends across the face of the plug (0.125 inch). These dimensions, as well as the thickness and specific resistance of the conductive plastic may be varied, depending on the characteristics desired. The remainder of the face is a highly conductive plastic which joins the terminal pins to the bridge. All these elements are co-molded into one integral structure.

The test program was based on MIL-L-23659(WEP) and MIL-STD-322 to establish compliance with the one watt, one ampere, no fire criterion with modifications to allow for using only 300 instead of 1500 samples normally required. The description of the tests and the full results are reported by R. Stresau Laboratory, Inc. under the aforementioned contract in NOLC Report No. 707, dated 1 March 1967.

Figure 5 shows a schematic assembly of the test detonators. Immediately adjacent to the conductive plastic bridge is a layer of normal lead styphnate, milled and pressed at 1,000 psi. This layer is followed by several layers of lead azide and finally 40 mg. of RDX. The cup is stainless steel as used in Primer Mk. 63. The case is sealed to the plug with an epoxy resin.

The pulse firing circuit is shown in Figure 6. The capacitor is discharged through the bridge by activating the relay. With the 0.5 microfarad capacitor a calculated input of 10,000 ergs requires charging to 63.2 volts.



The apparatus for determining sensitivity at extreme temperatures is shown schematically in Figure 7. Note that the detonator fits into an aluminum heat sink. This arrangement was specified by NOIC as corresponding to field conditions.

Details of the "Stop Timing" probe can be seen in Figure 8. The functioning times of the pulse fired units were measured with a Tektronix 517 oscilloscope with sweep rates ranging from five nanoseconds per centimeter to twenty microseconds per centimeter. The sweep was triggered with the firing impulse and displaced by the shorting shims in the "Stop Timing" circuit by the detonator output.

The main features of the test results are summarized in Tables 1, 2 and 3.

Table 1 gives values for mean threshold firing current and power as determined by a Bruceton test procedure. It is at once evident that regardless of the environmental or mechanical exposure the mean amperes and mean watts are well below one. As for the drop, vibration and jolt tests, the detonators tested were able to carry the one ampere, one watt with no failures.

Table 2 shows the effect of the test conditions on the pulse sensitivity of the detonators. The mean firing energy was determined by the Bruceton test procedure. It is apparent that the all-fire pulse energy is appreciably below the 10,000 erg requirement, regardless of the test conditions. The number of test samples is too small for a definitive analysis of the effects of the various tests on the pulse sensitivity or on reliability. These results are analyzed in detail in the Stresau report previously mentioned and the implications are discussed.

The functioning times given were measured incidental to Bruceton tests and were thus for detonators fired with only slightly more than their threshold energies. At 10,000 ergs we expect the functioning times would average about 20 microseconds.

The dent test averages of about 0.015 inch are about what would be expected for items of this size. The actual size is to some extent reduced by the shim studs and air gap of the timing probe.

Table 3 shows the effect of subjecting the detonators to one ampere or one watt for five minutes before subjecting them to various tests. The data indicate an apparent rise in the mean energy to blow for all except the 160°F test. The increased energy, however, is still well within the 10,000 erg requirement.

The test does not require that the units function after the drop, vibration and jolt tests. That the units did function after the drop and vibration tests is an indication of the ruggedness of the structure.

#### VOLT-AMPERE CHARACTERISTICS

Some of the electrical characteristics of the Markite conductive plastic appear to be intrinsically different from the more conventional types of bridge material.

Bridge materials were compared by means of the circuit shown in Figure 9. The AC voltage, Variac-controlled, is passed through the material to be tested and a standard resistance, so that the abscissa reads current while the ordinate displays the IR drop across the test specimen.

Figure 10 is a drawing of representative curves generated on the oscilloscope when the current is increased from zero to the point at which the conductive plastic blows with visible spark. The resistance wire, representative of metal wire bridges, maintains a simple ohmic relationship. The conductive plastic (Type 21166) bridge material has an initial ohmic range, a short non-linear range, followed by a range in which the current remains substantially constant while the voltage rises rapidly to the destruction of the element. The limiting current, in this case 2.5 amperes, corresponds to a temperature sufficiently high to explode the ordinary primer material. Current inputs up to Point A of Figure 10 do not cause irreversible changes in the material, and the same curve segment can be regenerated again and again. Between Points A and B small irreversible changes occur in the material. If the current is repeatedly raised from zero to Point B, there is a slight increase of resistance with each repetition. When the current is raised beyond Point B, the unloaded material blows with a visible spark. This property of the material permits presumptive testing of the blow characteristics of a detonator without loading.

Figure 11 shows the curve generated by a thin graphite rod in the same resistance range as the conductive plastic of Figure 10. The characteristic of the graphite rod, unlike the conductive plastic, is ohmic at least up to 10 amperes.

Figure 12 shows the behavior of Acheson Dag 440, a resin-containing graphite dispersion. This relatively high resistance material appeared to have a limiting voltage and did not reach a current sufficient to blow in this test.

In Figure 13 is shown the behavior of a film of Aquadag (a water suspension of colloidal graphite). Because of the considerably higher resistance of the Aquadag, the characteristic is not strictly comparable to those of the previous tests, but its non-linear characteristic appears similar to the Dag 440 and certainly different from the conductive plastic.

To observe whether the V-I characteristic of the conductive plastic was merely a heating effect, continuous AC below the critical value was applied to a conductive plastic bridge. Figure 14 shows the result of this test. It will be seen that the ohmic characteristic of the material below the critical current was maintained although the total energy generated was far in excess of that required to blow the equivalent bridge in Figure 10.

#### CONCLUSION

In conclusion we indicate some of the advantages that might be realized from the use of Markite conductive plastic bridged initiators:

1. The plastic structure permits considerable flexibility in design.
2. The unitary molded structure is resistant to vibration and handling damage.
3. The relatively large area of the bridge minimizes the effect of nicks and scrapes.
4. Non-destructive pretesting for IA-1W is possible.
5. It is possible to test presumptively for firing characteristics

without loading.

6. The properties of the bridge can be varied by varying the specific resistance of the bridge material.
7. The properties of the bridge can be varied by varying the thermal conductivity, heat capacity and current leakiness of the insulator body.
8. These plugs have cost advantages inherent in molding processes when large quantities are involved.
9. There is the possibility of including circuitry within the body of the molded plug.
10. The conductive plastic bridge requires no skilled hand labor such as for spot welding wire.
11. Miniature units can be made by automated procedures.
12. The conductive plastic bridge can be made to encompass a broad range of stable resistances.

Acknowledgement:

The material in this paper is based in part on work performed for the U. S. Naval Ordnance Laboratory, Corona, California, under Contract No. N123(62738)5350A(X).

DISCUSSION

The shelf life of the plastic bridges is not known.

It is believed that the Markite plastic can withstand the temperature required for sterilization.



FIGURE 1

Markite Conductive Plastic Bridged Plugs  
One Ampere - One Watt, No Fire



FIGURE 2

Markite Conductive Plastic Bridged Plugs  
One Ampere - One Watt, No Fire

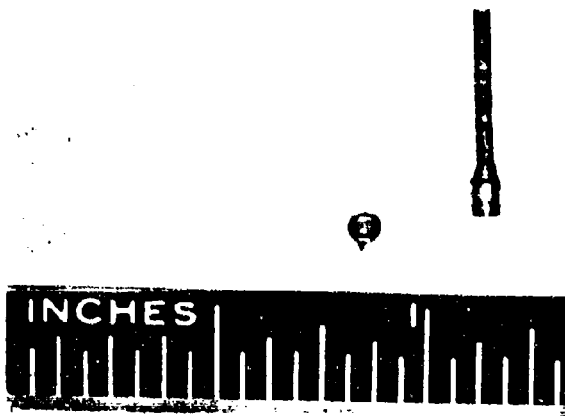


FIGURE 3

Markite Conductive Plastic Bridged Plugs  
Miniature



FIGURE 4

Markite Conductive Plastic Bridged Plugs  
Type 21166

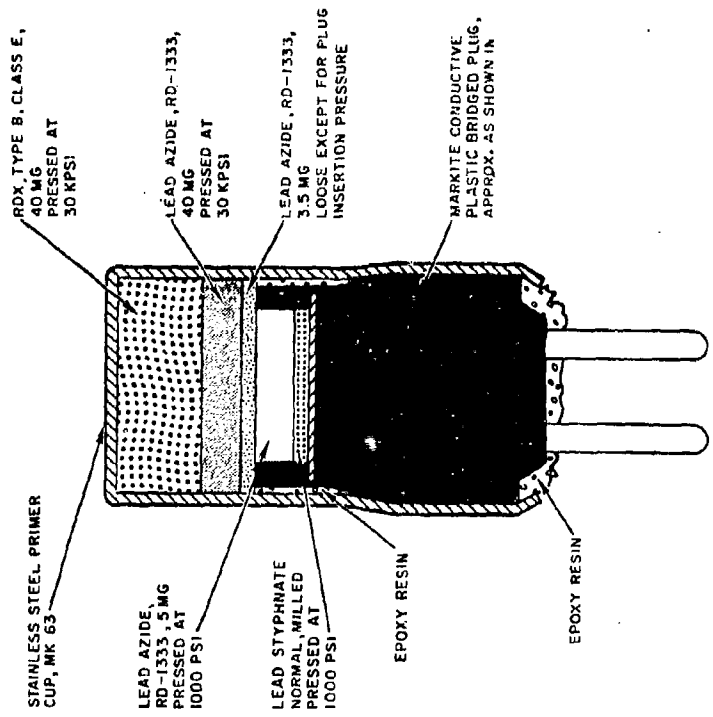


FIGURE 5. Experimental Electric Detonator With Markite Conductive Plastic Bridged Plug

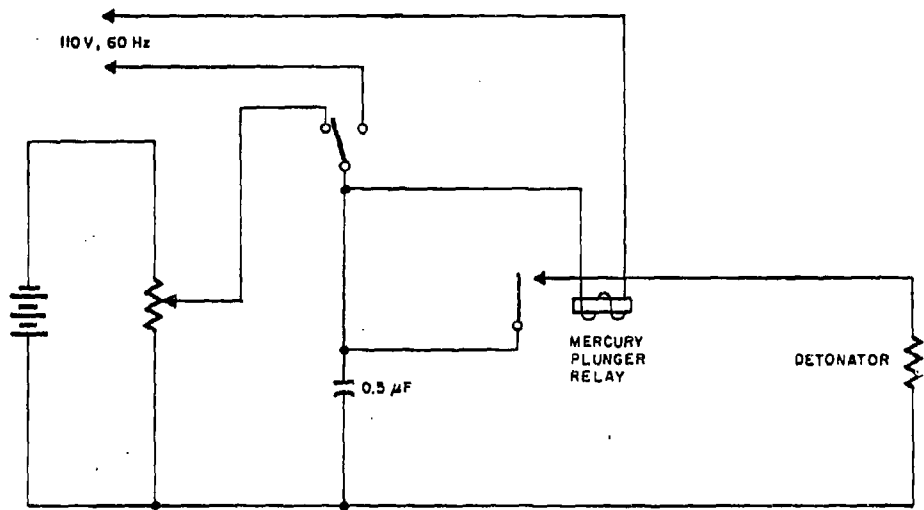


FIGURE 6. Circuit for Pulse Firing Test



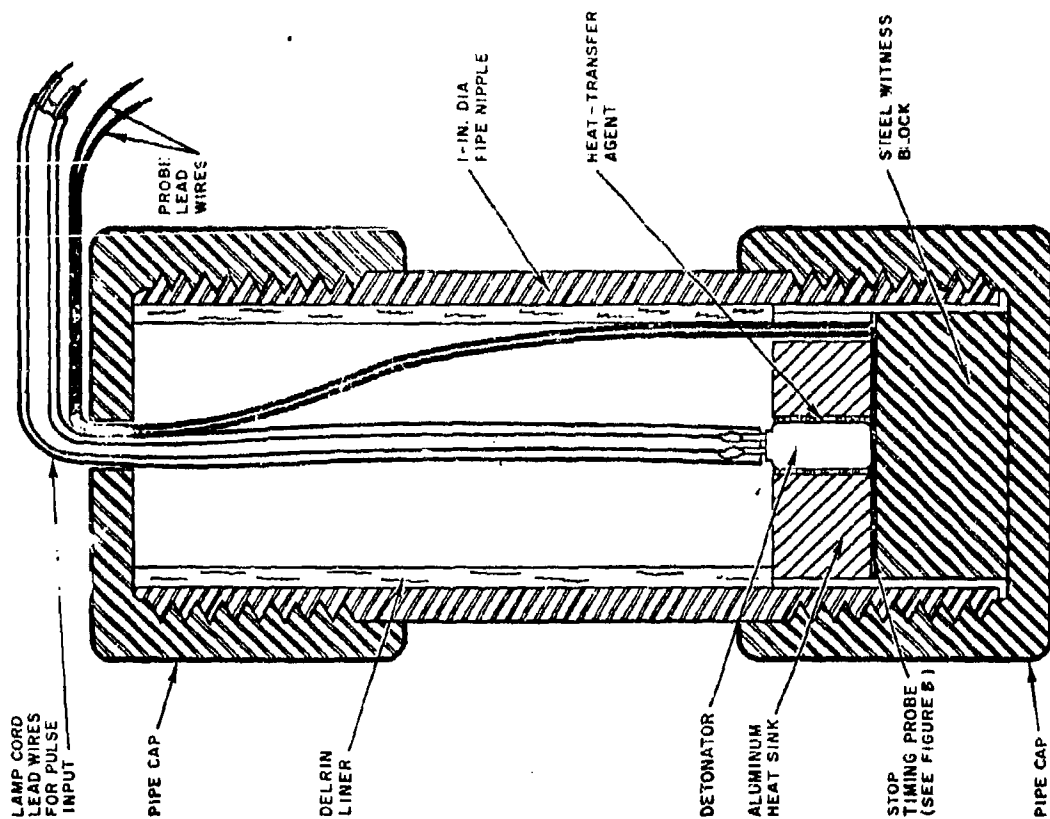


FIGURE 7. Test Apparatus for Sensitivity at Extreme Temperatures

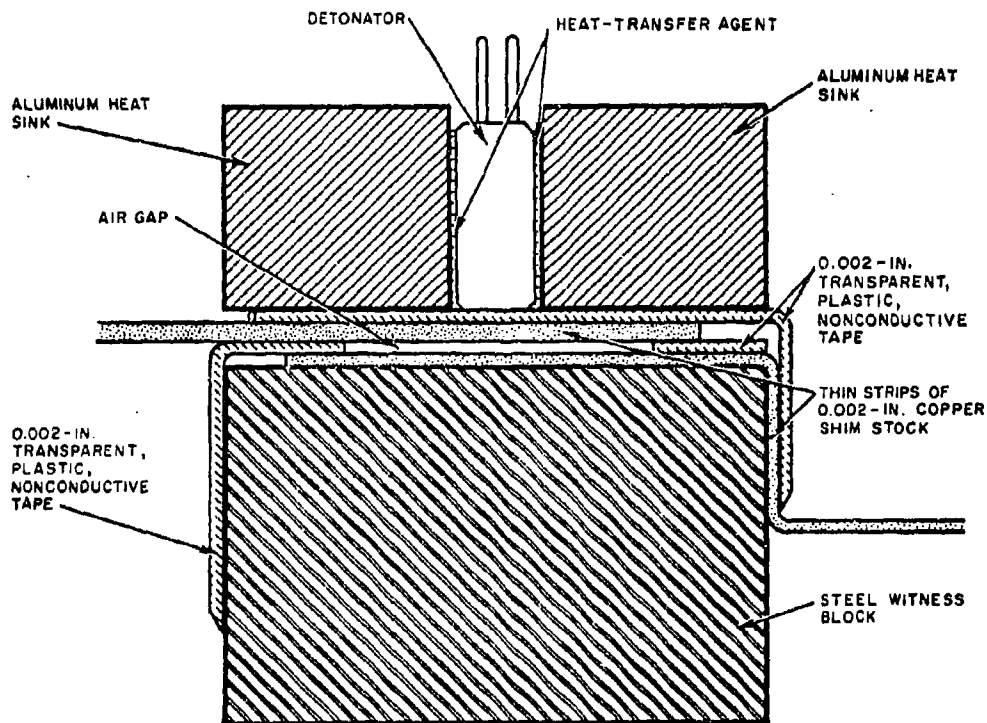
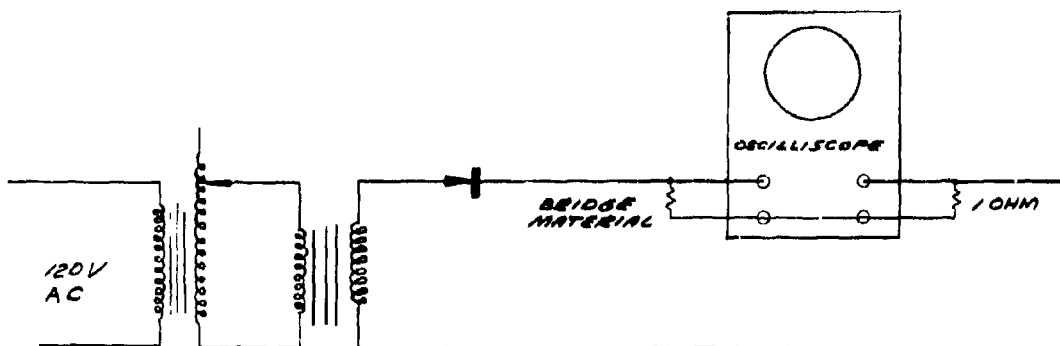
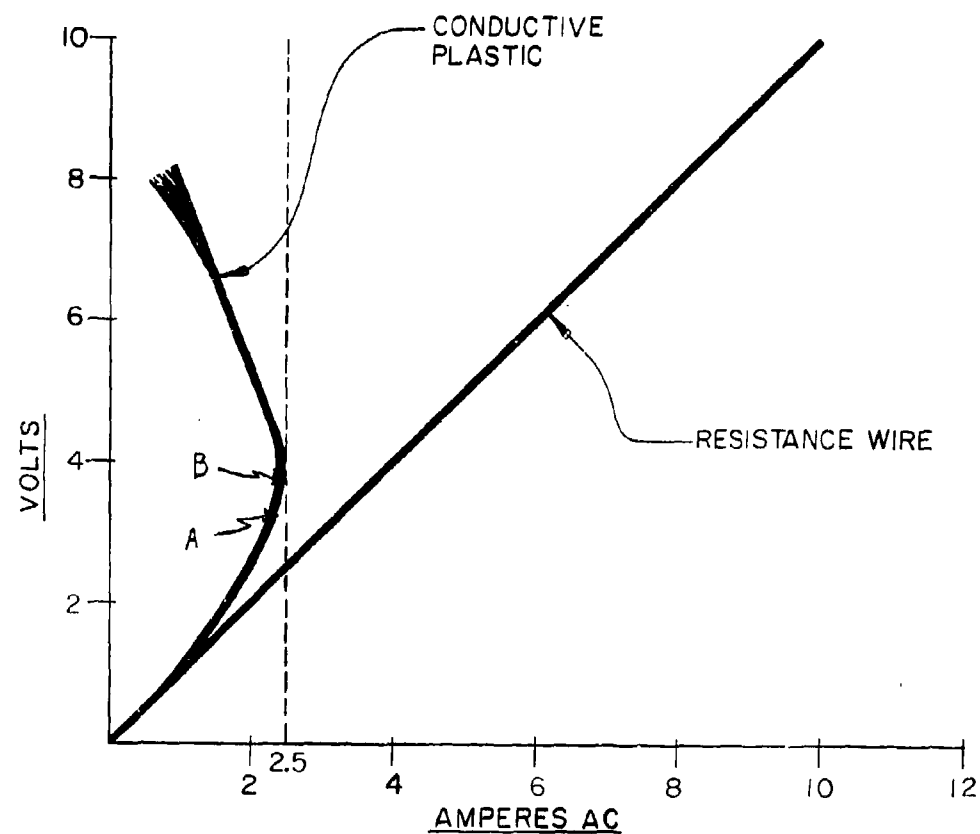


FIGURE 8. Probe Design Used for Determining Functioning Time



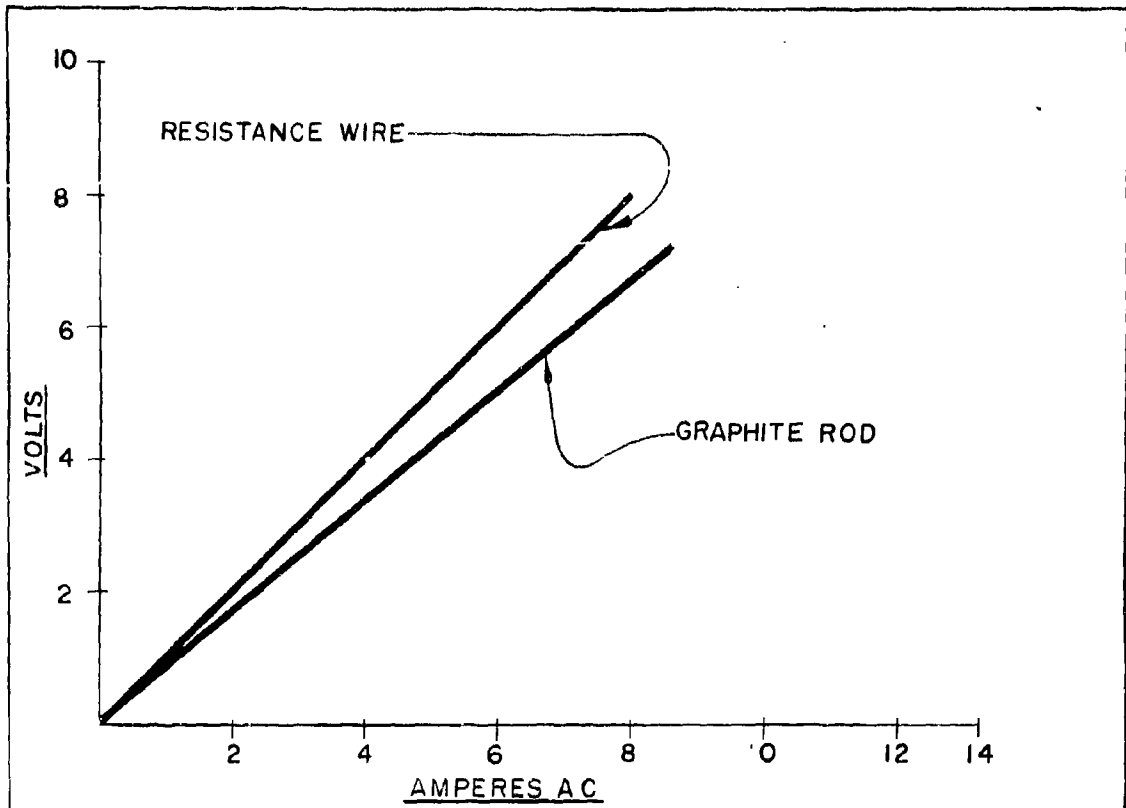
CIRCUIT FOR  
OBTAINING V-I CHARACTERISTICS

FIGURE 9



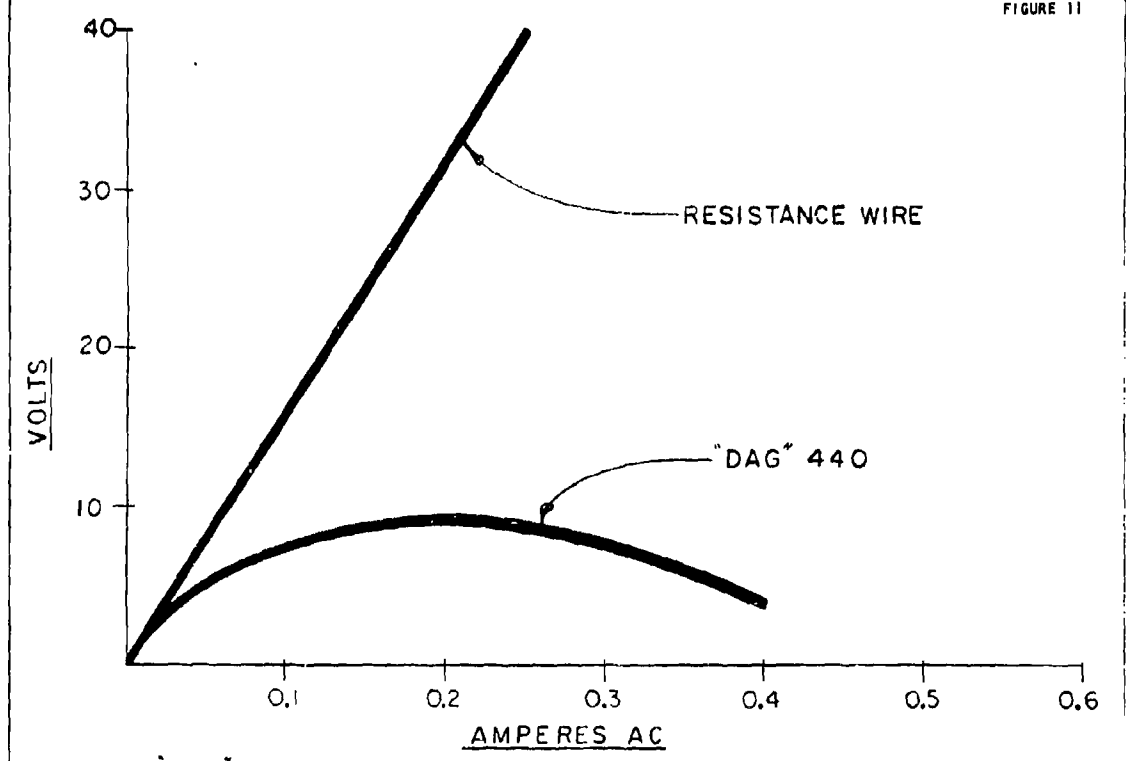
MARKITE CONDUCTIVE PLASTIC VS. RESISTANCE WIRE

FIGURE 10



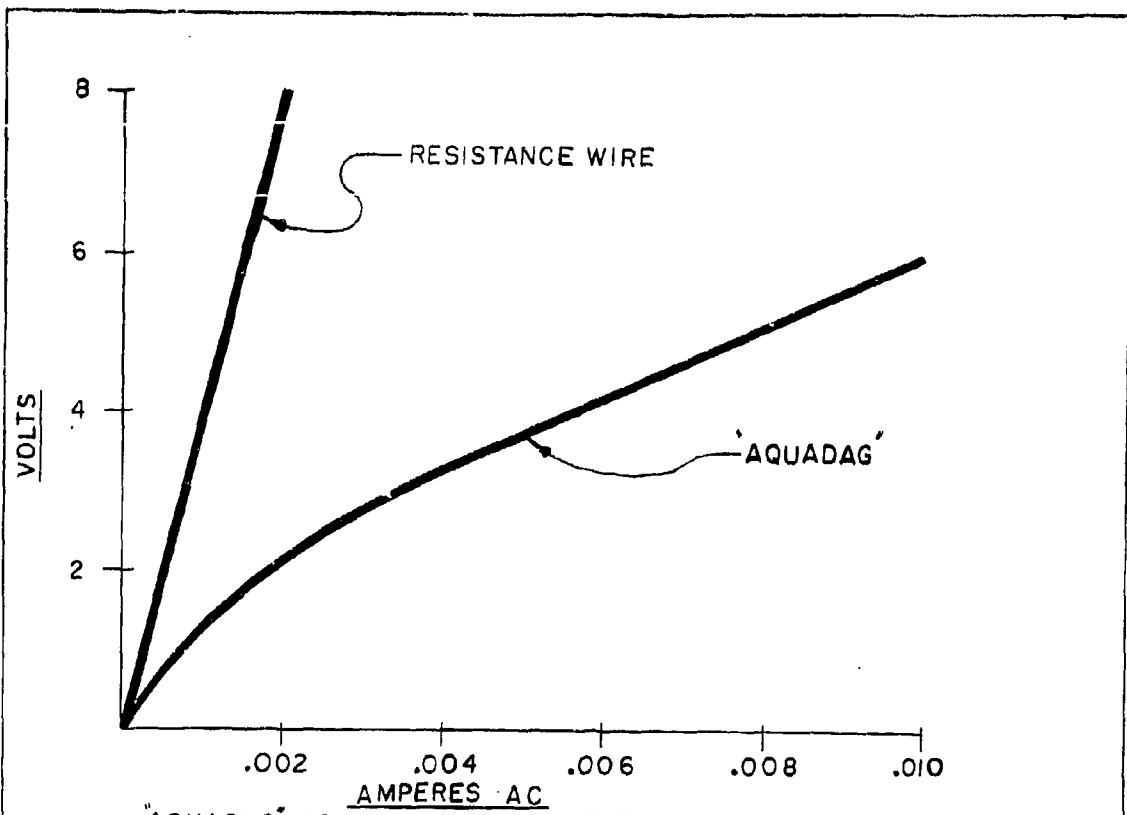
GRAPHITE ROD VS RESISTANCE WIRE

FIGURE 11



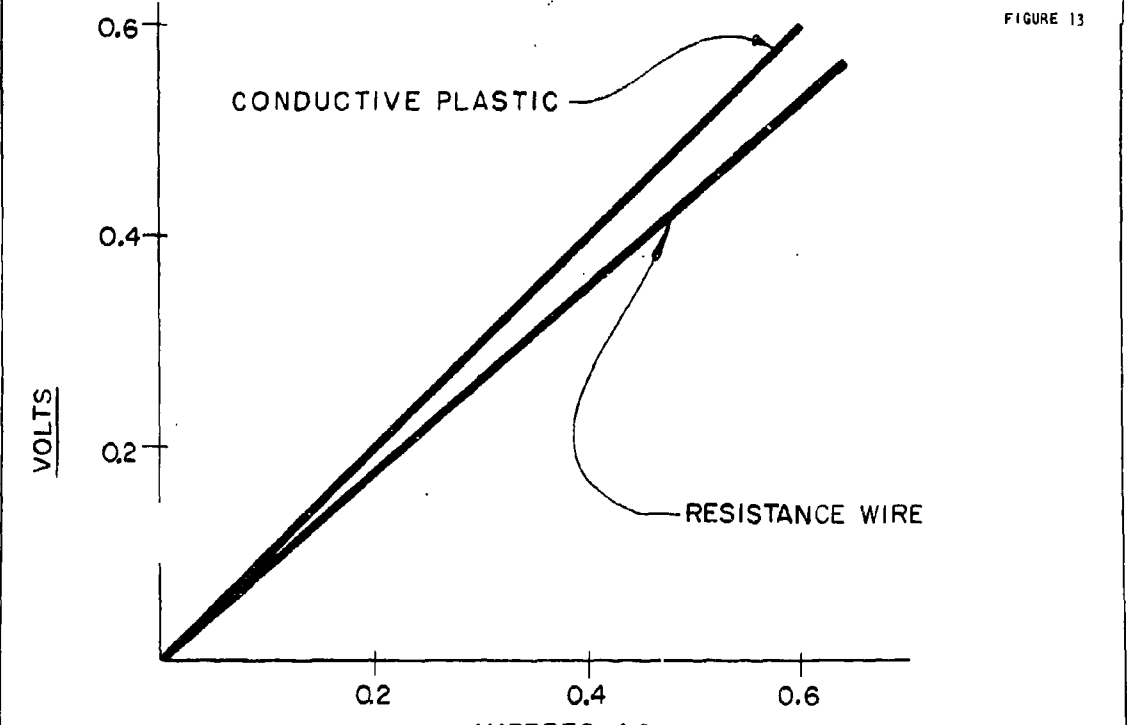
"DAG" 440 VS RESISTANCE WIRE

FIGURE 12



"AQUADAG" VS RESISTANCE WIRE

FIGURE 13



CHARACTERISTICS:  
CONDUCTIVE PLASTIC & RESISTANCE WIRE LONG HEATING BELOW  
CRITICAL CURRENT.

FIGURE 14

TABLE 1 CURRENT-POWER SENSITIVITY

EXPOSURE BEFORE TEST	AS LOADED	JAN. TEMP. HUMD. CYCLE	HIGH TEMP. STORAGE	CONDITIONED TESTED AT		FORTY FOOT DROP TEST	VIBRATION TEST	JOLT TEST
				160°F	-65°F			
NO. OF DETONATORS	25	20	12	10	10			
AMPS MEAN	1.78	1.71	1.89	1.88	1.79	0/5@1.0	0/4@1.0	0/3@1.0
DENT SIZE AVERAGE INCHES	0.017	0.013	0.018	0.017	0.012			
WATTS MEAN	2.22	2.43	3.80	1.87	1.27	0/5@1.0	0/4@1.0	0/3@1.0

TABLE 2 PULSE SENSITIVITY AS LOADED

EXPOSURE BEFORE TEST	AS LOADED	JAN. TEMP. HUMD. CYCLE	HIGH TEMP. STORAGE	CONDITIONED TESTED AT	
				160°F	-65°F
NO. OF DETONATORS	29	20	11	10	9
ERGS MEAN	4630	4200	7140	4220	7650
FUNCT. TIME MICRO SECS. AVERAGE	27	51	49	26	34
DENT SIZE AVERAGE INCHES	0.014	0.014	0.017	0.018	0.015

TABLE 3 PULSE SENSITIVITY AFTER ONE WATT - ONE AMP.

EXPOSURE BEFORE TEST	AS LOADED	JAN. TEMP. HUMD. CYCLE	HIGH TEMP. STORAGE	CONDITIONED TESTED AT		FORTY FOOT DROP TEST	VIBRATION TEST	JOLT TEST
				160°F	-65°F			
NO. OF DETONATORS	25	17	12	10	10	5	4	3
ERGS MEAN	5670	8850	8410	6000	7130	5/5@ 10,000	4/4@ 10,000	0/3@ 10,000
FUNCTIONING TIME MICRO SEC. AVER.	26	50	46	20	64	23	23	
DENT SIZE AVERAGE INCHES	0.016	0.016	0.017	0.016	0.014	0.020	0.017	

3-7P HIGH TEMPERATURE RESISTANT  
CONDUCTIVE PRIMING MIXES

Allen F. Schlack

William E. Perkins

Chemistry Research Laboratory  
Frankford Arsenal, Phila., Pa. 19137

INTRODUCTION

This presentation deals with work directed toward the development of an electric ignition element for a specific application, namely, a bomb ejector cartridge. The requirements established for this cartridge and tight time schedule which had to be met influenced many of the decisions which were made throughout the development phase of this program.

Some of the major requirements for this electric ignition element were:

1. be capable of withstanding a minimum of one ampere direct current and/or one watt of D.C. power for five minutes without firing or duding.
2. be capable of being actuated from a D.C. pulse of five amperes in less than 25 milliseconds
3. be operable at and after extended conditioning at 350°F.
4. be operable at and after extended conditioning at -65°F.
5. be non-case grounded

6. be insensitive to a static discharge of 150,000 ergs from a 500 micromicrofarad condenser

7. be an open circuit or exhibit a resistance of 20 ohms or more as a result of firing.

These requirements were listed in the purchase request<sup>1\*</sup> received from the Air Force Weapons Laboratory, Kirtland Air Force Base, Albuquerque, New Mexico for the development of a bomb ejector cartridge.

The most severe requirement for this electric ignition element is that it must be capable of withstanding conditioning at 350°. For the past few years electro-explosive devices (EEDs) are being used in more applications where they may be exposed to elevated temperatures. These temperature requirements have put an added burden on the design engineer in that he must find explosive mixtures which, in themselves, are stable at these temperatures and also are compatible with the metallic components which are to contain them.

#### APPROACH

Two approaches were considered to meet these requirements; one, use of a bridgewire element with a built-in bridgewire destroyer, and the other, use of a conductive mix element which inherently produces an open circuit when fired. Both approaches required that a high

---

\* See references

temperature ignition mixture be developed. Use of a conductive mix element was chosen for this program because the design and manufacture of this type element seemed simpler.

Initially, an electric ignition test element was designed to study promising mixtures. The basic design shown in Figure 1 contains the following:

1. Simplified construction for ease of manufacture.
2. Body and electrode constructed of stainless steel to withstand the high conditioning temperature without being affected adversely by the priming mixture.
3. Insulator made from ceramic to withstand high conditioning temperature and high pressures produced during its actuation.
4. A steel support cup which is crimped into place to maintain the compression on the conductive charge to stabilize the resistance and provide an adequate degree of confinement at actuation.
5. A cavity for placing a supplemental charge to adapt the element to a wider variety of applications without affecting its basic sensitivity.
6. Magnesium discs to provide an adequate degree of confinement for the conductive mixture and supplemental charge. These are consumed during ignition.

The next consideration was choosing the mixture compositions to be evaluated in these ignition elements. Previous studies<sup>2,3</sup> on high



temperature stable percussion primers provided two promising mixtures capable of withstanding conditioning at elevated temperatures. Table I shows the composition of these mixtures. FA 989 mixture consists of calcium silicide, antimony sulfide and potassium chlorate. Primers

Table 1  
Compositions of High Temperature Stable  
Percussion Priming Mixtures

Ingredients	Mixtures	Per Cent Composition	
		FA 989	FA 968
Calcium Silicide		17	
Antimony Sulfide		30	
Potassium Chlorate		53	
Phosphorus, red			27.3
Barium Nitrate			66.0
Glass, ground			6.7

containing this mixture were not adversely affected by conditioning at 400° for several weeks.<sup>2,3</sup> FA 968 mixture consists of red phosphorus, barium nitrate and ground glass. Primers containing this mixture were not adversely affected by conditioning at 350° for several weeks.<sup>2</sup> With the addition of conductive materials to the priming compositions, the mixtures can be made conductive. Therefore, these two basic mixtures were chosen for study.

In studying conductive mixtures, certain conductivity relationships must be considered. The conductive particles are dispersed in a random manner throughout the entire mixture and the resultant

electrical conductivity is a function of the resistivity of the conductive ingredient, length of the most conductive path and the physicochemical characteristics of the composition.

The mechanism of the initiation of conductive mixtures is complex primarily due to the fact that resistance measurements are variable and depend upon the current of the firing circuit. The initiation mechanism has probably been studied in more detail for conductive mixtures containing carbon than any other conductive ingredient.<sup>4</sup> Therefore, carbon was chosen as the conductive ingredient to be used in these mixtures.

It is believed that for some applications carbon could be used in conjunction with other conductive materials to obtain various and possibly unique performance characteristics. However, in this program no conductive materials other than carbon were used in the conductive mixtures in order not to complicate the design which might cause long time delays. The conductivity of the ingredients in each of the basic mixtures was determined. Calcium silicide in the FA 989 mixture was found to be conductive and was deleted from this mixture. Initial studies were performed using a basic mixture of antimony sulfide and potassium chlorate. Table 2 lists the compositions of three mixtures evaluated in these studies. It is noted that the carbon content was increased from 14 to 20 per cent. The range of carbon content in these studies was chosen from results obtained in preliminary studies.

Table 2  
Compositions of Mixtures  
Evaluated in Test Elements

Ingredients	Mixtures	Per Cent Compositions		
		FA 984	FA 986	FA 985
Antimony Sulfide		28	28	27
Potassium Chlorate		58	55	53
Carbon		14	17	20

Since the ignition elements must pass one ampere current for five minutes, their resistance had to be necessarily low, and it was decided that a value of approximately one ohm would suffice. This would limit the power required to approximately one watt. As the resistance of the element increases with constant current, the power drawn by this element increases. Thus, with high resistance large amount of power would be drawn, heating the priming mixture considerably and perhaps igniting or duding the mixture. The resistance of an ignition element is largely affected by the composition of the conductive mixture, the gap width, which is the distance as measured through the mixture between the two electrodes, and the loading pressure of the mixture. These variables were evaluated in the following studies.

Figure 2 shows the effect of gap width on resistance as the carbon content was increased from 14 to 20 per cent. A straight line was obtained when the average resistance was plotted against the logarithm of gap width. As the gap width increased, the average

resistance of the ignition elements increased. Gap widths below .020 inches were not studied because the assembly of the ceramic insulators to the metallic components became too difficult. Based on available data, a gap width of .020 inches was chosen for use in the standard ignition elements. As the carbon content of the mixture increased, the resistance of the elements decreased. With a .020 inch gap width there was no significant difference in the resistances of the elements which were between 1.6 and 2.0 ohms. On the basis of exploratory studies, the mixture containing 17 per cent carbon was chosen for further evaluation. Since the ignition elements must meet the one amp/one watt requirement, it was essential that sufficient carbon be added in order to conduct this input energy without firing. Fourteen per cent carbon did not seem sufficient to meet this requirement safely. The addition of twenty per cent carbon, it was thought, would dilute the output of the primer below that required.

Figure 3 shows the effect of loading pressure on resistance of the ignition elements containing FA 986 mixture (17% carbon). The gap width in this study was .020 inches. A straight line was obtained when average resistance was plotted against the logarithm of loading pressure. As the loading pressure was increased the average resistance of the elements decreased. When the loading

pressure was equal to 1000 psi the resistance of the ignition elements was approximately 2 ohms. At this resistance there was an indication that the ignition elements lacked sufficient electrical sensitivity. It was decided that 800 psi represented a satisfactory compromise for loading pressure.

Having established a gap width and loading pressure, the electrical sensitivity of the FA 986 mixture charged into these ignition elements was next considered. Figures 4 and 5 show the functioning characteristics of the ignition elements. Figure 4 shows the per cent of elements which functioned satisfactorily versus the firing current. In this study an element was considered to have functioned satisfactorily if it fired in less than 25 ms. The curve shows that the current at which no element functioned satisfactorily was approximately 2 amperes and the current at which all elements functioned satisfactorily was approximately 5 amperes.

Figure 5 shows the average functioning time of the elements versus the firing current. The functioning times were quite long (about 1000 ms) using a firing current of 2 amps. The functioning times decreased rapidly as the current was slightly increased. The functioning times averaged less than 25 ms when the firing current was greater than 4 amps.

All of the elements prior to these functioning tests were subjected to one ampere current for five minutes. None of the elements fired. The firing circuit used for these tests is shown

in Figure 6. At the start of each test the switch was turned to position 1 and the voltage was slowly increased until the line current read one ampere. This current was allowed to flow through the ignition element for five minutes. The switch was then turned to position 3. The current was readjusted to read one ampere by changing the resistance of the rheostat to match the resistance of the element. The voltage was next increased until the firing current was obtained. The switch was turned to position 1 applying the firing current to the element. The functioning time of the element was recorded.

From these data the non-case grounded XM 54 electric ignition element, shown in Figure 7, was designed and fabricated. When these elements were charged with 4.0 grains of FA 986 mixture, the following characteristics were exhibited:

1. all resistances, as measured at 1.0 ampere current, were found to be between 2.3 and 4.5 ohms
2. all elements were capable of passing 1.0 ampere current for 5 minutes without firing
3. all elements tested at 2.0 ampere current fired but functioning times were in excess of one second
4. all elements tested at 3.0 amperes current fired, with functioning times averaging under 100 ms.
5. all elements tested at 4.0 amperes current fired with functioning times mostly under 25 ms.
6. all elements tested at 5.0 amperes current fired in less than 10 ms.

High temperature storage tests were performed on the XM54 elements. The elements were conditioned at 400°F for 25 hours and then cooled to room temperature. All elements fired with the application of 5.0 ampere current.

Ten XM 54 elements were subjected to an electrostatic discharge of 300,000 ergs from a 2 micromicrofarad condenser. No elements fired.

At this time the purchase description for the bomb ejector cartridge was changed significantly. The current at which the functioning times of the ignition elements had to be 25 ms or less was changed from 5.0 to 4.0 amperes. Also, a requirement was added that the combustion products of the mixture be non-corrosive.

Since FA 986 mixture produces corrosive products on combustion it could no longer be considered for use in these ignition elements. Under the high temperature percussion primer program<sup>2</sup> the red phosphorus/barium nitrate/ground glass non-corrosive mixture was developed. Using the same technical approach followed to develop the FA 986 conductive mixture, a series of non-corrosive blends using a basic blend of red phosphorus, barium nitrate and carbon were prepared and evaluated in XM 54 components. The ground glass was excluded from the mixture since it was only used in the percussion primer to enhance impact sensitivity which is obviously not required in these ignition elements. Table 3 shows the mixtures evaluated.

Table 3  
Compositions of Non-Corrosive Mixtures Evaluated in  
XM 54 Components

Ingredients	Mixtures	Per Cent Compositions			
		FA 997	FA 998	FA 999	FA 1001
Phosphorus, red		25	22	20	24.0
Barium Nitrate		70	68	65	68.5
Carbon		5	10	15	7.5

The carbon content was increased from 5 to 15 per cent. The electrical sensitivity studies indicated that the mixture designated FA 1001 exhibited the best results. XM 54 ignition elements charged with 3.0 grains of FA 1001 mixture exhibited resistances in the range of 2.5 to 4.5 ohms which were capable of passing one ampere direct current for five minutes without firing or duding and were capable of firing from a 4.0 amp pulse in less than 25 ms.

It was noted during the functioning tests that the resistance of the ignition elements did not adhere to ohms law, but changed significantly as the current in the circuit was increased. This was especially true at the higher current levels. Since this current change is pertinent to electrical sensitivity information an oscillograph was placed in the test circuit as shown in Figure 8, to provide a current versus time curve. A series of curves were obtained showing the average actual firing current versus time as the apparent current in the circuit was increased in increments of .25 amperes from 2.50 to 3.50 amperes. The apparent current is defined



as that current which flows in an equivalent circuit in which a resistor, whose resistance is equal to that of the ignition element at one ampere, is substituted for the element.

Figure 9 shows the results of this study. As shown, the actual firing current is significantly higher than the apparent current applied indicating the resistance of the element decreased as the current of the circuit was increased.

The purchase request required that a Bruceton analysis of these ignition elements be performed based on the firing current being the independent variable. The results of the previous study show that the firing current is not an independent variable; instead the firing current and the resistance of the element are interdependent. It was suggested that the method of conducting the Bruceton analysis be modified to reflect the actual results obtained in this test. Since this suggestion was not favorably received, the test was conducted as close to the original specification as possible using the apparent current as the independent variable. Data obtained in this analysis are contained in Appendix A.

Using the apparent current in the circuit, the electrical sensitivity of the XM 54 electric ignition elements charged with FA 1001 mixture was calculated as follows:

1. Current for 99% confidence level -- 3.82 amperes
2. Current for 95% confidence level -- 3.48 amperes

3. Current for 5% confidence level -- 2.15 amperes

4. Current for 1% confidence level -- 1.81 amperes

High temperature performance tests were conducted on these XM 54 ignition elements. The elements were conditioned at 350°F for 8 hours. A current of one ampere was passed through the elements for 5 minutes with none firing. Subsequently, an apparent current of 4 amperes was passed through the elements and all fired.

Static discharge sensitivity tests were conducted on five XM 54 electric ignition elements. Each was subjected to 10 pulses of 150,000 ergs from a 500 micromicrofarad condenser with none functioning.

Numerous other tests were conducted on the cartridge in which the XM 54 electric ignition element was a part of the performance train. Included in these tests were the shock and vibration, sonic, temperature cycling between -65°F and +350°F, and leakage tests. No malfunctions were obtained that were attributed to the XM 54 electric ignition element.

## CONCLUSIONS AND RECOMMENDATIONS

Under this program two conductive mixtures were developed which exhibit no change in functioning characteristics after exposure to a temperature of 350 to 400°F. Use of these mixtures in other applications where temperature stability is required should be investigated.

Although many of the studies performed in the development of these mixtures were exploratory in nature, the information obtained indicates that a wide range of performance characteristics can be produced with conductive mixtures.

In the past few years EEDs, including bridgewire and exploding bridgewire elements, have become more sophisticated to meet increasingly severe performance specifications. The design changes required to accomplish this have increased the costs of these EEDs such that reliability tests are performed using only small quantities. On the other hand, conductive mix elements can be designed so that they are relatively cheap to manufacture providing large production savings over other types of EEDs. Also, because of these reduced costs, reliability tests can be performed using much larger quantities, therefore, giving more accurate analysis of the performance characteristics of the elements. The conductive mix approach undoubtedly has its limitations, and may not meet every requirement for every EED, but its simplicity in design and versatility should be brought into focus for future considerations.

#### REFERENCES

1. Purchase Request No. 146303 from Air Force Weapons Laboratory, Kirtland Air Force Base, Albuquerque, New Mexico, 15 October 1963.
2. Stevenson, T. and Ciccone, T. Q., "High Temperature Percussion Primers for PAD Systems", presented in Proceedings of Electric Initiator Symposium, held at Franklin Institute, 1963.
3. Johnson, T. B., "High Temperature Percussion Primers", Remington Arms Company, Inc., Report AB-62-10, July 1961 - September 1962.
4. Hutchinson, J. F., "Electric Primer Treatise, Vol. I-III," Remington Arms Company, Inc., May 1962.

APPENDIX A

Data for Brucecon Analysis of the XM 54 Electric Ignition Elements  
Charged With FA 1001 Mixture - Lot 1

No.	Resistance of Element at 1 amp ohms	'Functioning Data'					Funct. Time ms	Actual Line Current amps		Resistance of Element at Firing Current ohms	
		2.25	2.50	2.75	3.00	3.25		3.50	Initial	Final	Initial
1	3.00				X		8.13				
2	3.20			X			6.45				
3	3.35						5.16				
4	2.55		X				119				
5	2.90	0					587	2.85	3.03	1.52	1.30
6	3.30			0			35.60				
7	3.20				0		26.30	3.67	4.03	1.92	1.52
8	3.00					X	21.30	4.52	5.08	1.35	0.96
9	2.80				X		16.80	4.18	4.69	1.82	1.39
10	3.00			X			12.50	3.91	4.18	1.63	1.38
11	3.00			0			62.50				
12	2.80			X			9.35	3.33	3.43	1.70	1.42
13	3.50		X				10.00	3.73	3.93	1.46	1.28
14	2.90	0					1000+	3.82	4.26	1.52	1.13
15	3.05		X				18.10				
16	3.10	0					1183	3.24	3.52	1.83	1.50
17	2.65			0			1000+	2.79	3.24	2.07	1.46
18	2.90						124				
19	3.30			0		X	5.62	3.67	3.94	1.62	1.35
20	4.50			X			4.69	3.55	3.91	2.46	2.02
								3.58	3.76	2.94	2.67

\* Ignition elements which did not function within 25 ms were considered as misfires

APPENDIX A ( cont'd)

Data for Bruceton Analysis of the XM 54 Electric Ignition Elements  
Charged with FA 1001 Mixture - Lot 1

No.	Resistance of Element at 1 amp ohms	Functioning Data*				Func. Time ms	Actual Line Current amps		Resistance of Element at Firing Current ohms	
		2:25	2:50	2:75	3:00		3:25	3:50	Initial	Final
21	2.70		0			83.20	3.06	3.33	1.81	1.47
22	3.00			X		17.80	3.74	3.88	1.61	1.47
23	3.00		0			54.70	3.52	3.89	1.49	1.11
24	3.00					48.70	3.76	4.08	1.58	1.29
25	2.75				0	73.50	4.29	4.71	1.21	0.90
26	2.80					15.60	4.49	4.81	1.41	1.16
27	3.80			X		3.87	4.62	4.80	1.67	1.52
28	3.40				0	42.80	3.21	3.48	2.58	2.20
29	2.50			X		8.07	3.95	4.20	1.35	1.14
30	2.60				0	168.	3.58	3.85	1.48	1.21
31	3.35				X	8.07	4.15	4.52	1.89	1.45
32	3.10				0	61.50	3.76	3.95	1.65	1.49
33	3.40			X		11.80	4.59	4.78	1.44	1.30
34	3.20				0	47.20	3.67	3.94	1.85	1.56
35	2.60				0	56.40	4.34	4.71	1.57	1.28
36	3.60				0	699.	4.46	4.83	1.29	1.00
37	3.00				X	8.13	5.60	5.97	1.40	1.16
38	3.40			X		2.82	4.55	4.92	1.50	1.22
39	3.40				0	31.30	4.59	4.88	1.44	1.21
40	3.20			X		23.30	4.24	4.60	1.94	1.58

\* Ignition elements which did not function within 25 ms were considered as misfires

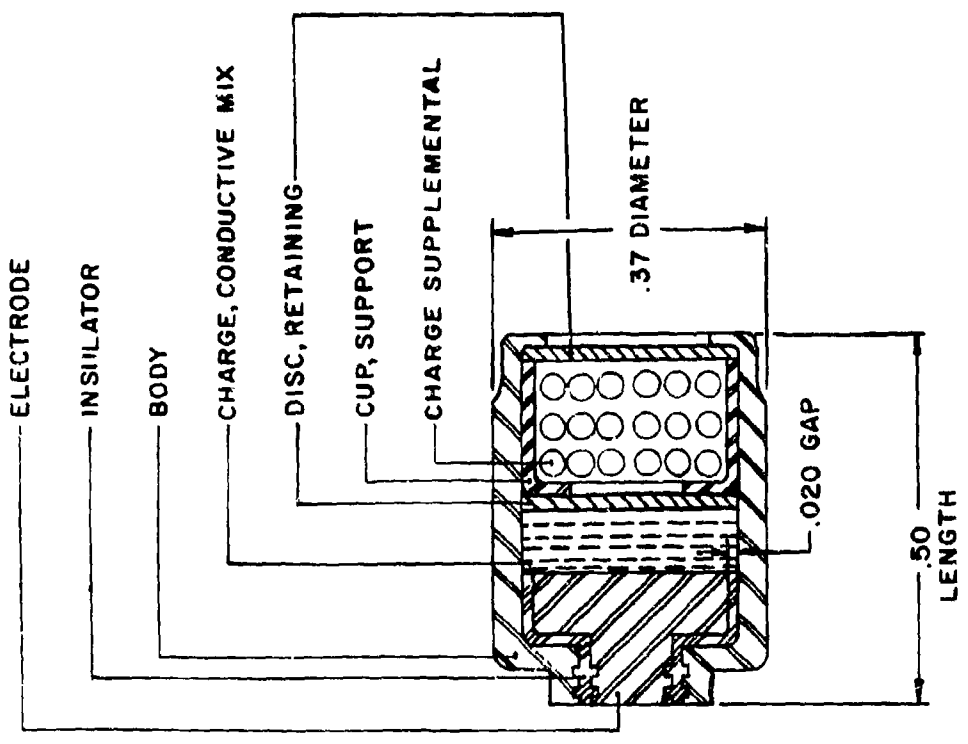
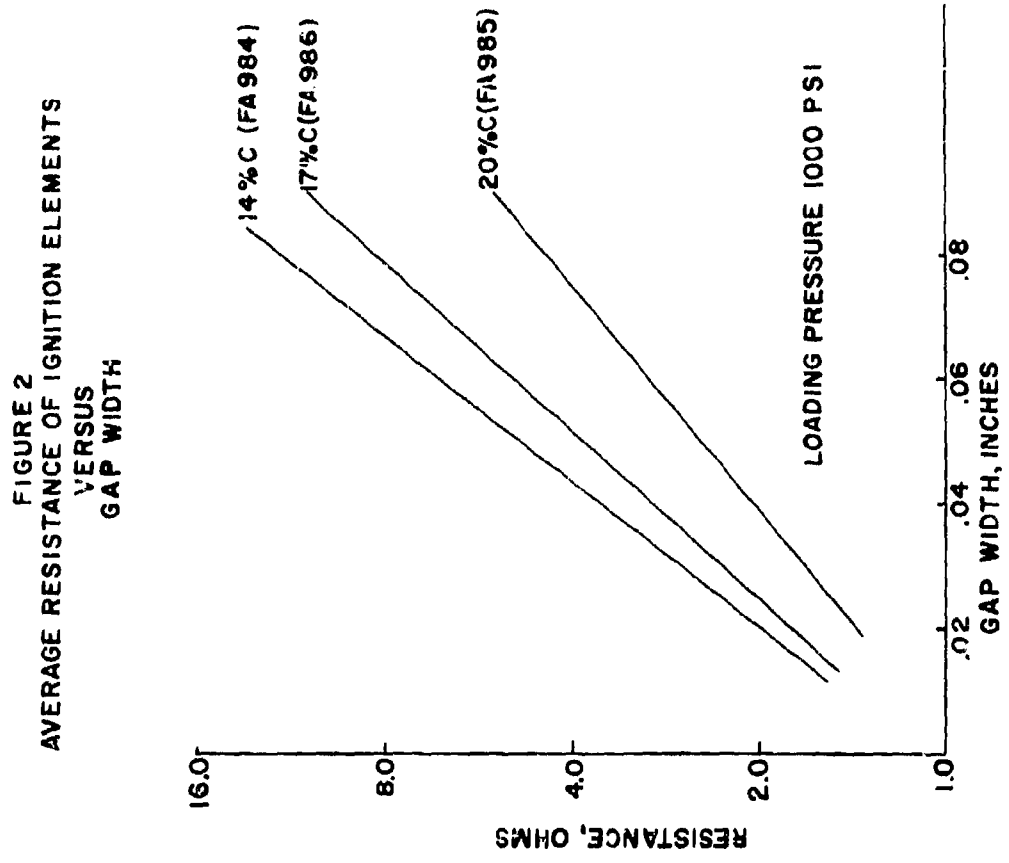


**FIGURE 1. ELECTRIC IGNITION TEST ELEMENT**

**FIGURE 4**  
**PER CENT OF IGNITION ELEMENTS**  
**WHICH FUNCTIONED SATISFACTORILY**  
**VERSUS**  
**FIRING CURRENT**

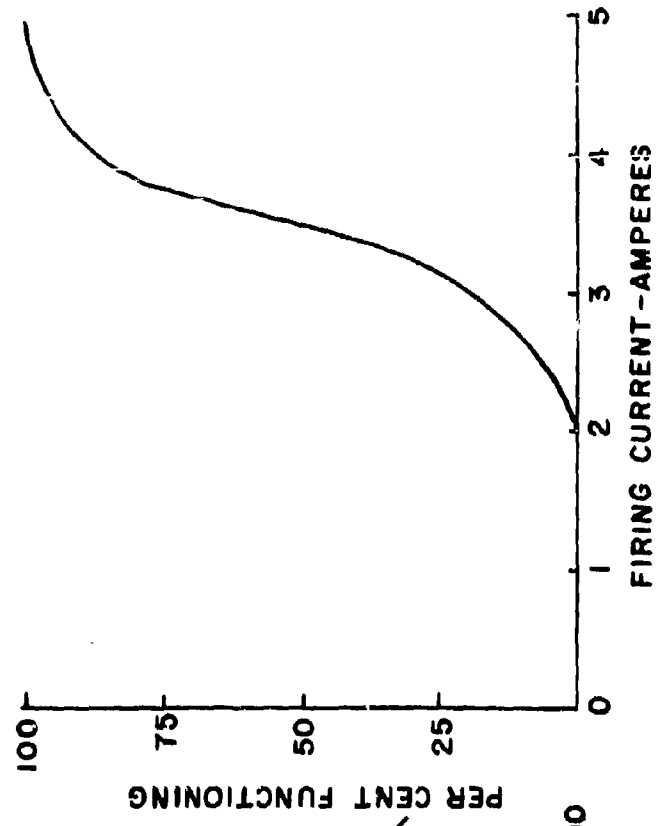


**FIGURE 3**  
**AVERAGE RESISTANCE OF IGNITION ELEMENTS**  
**VERSUS**  
**LOADING PRESSURE**

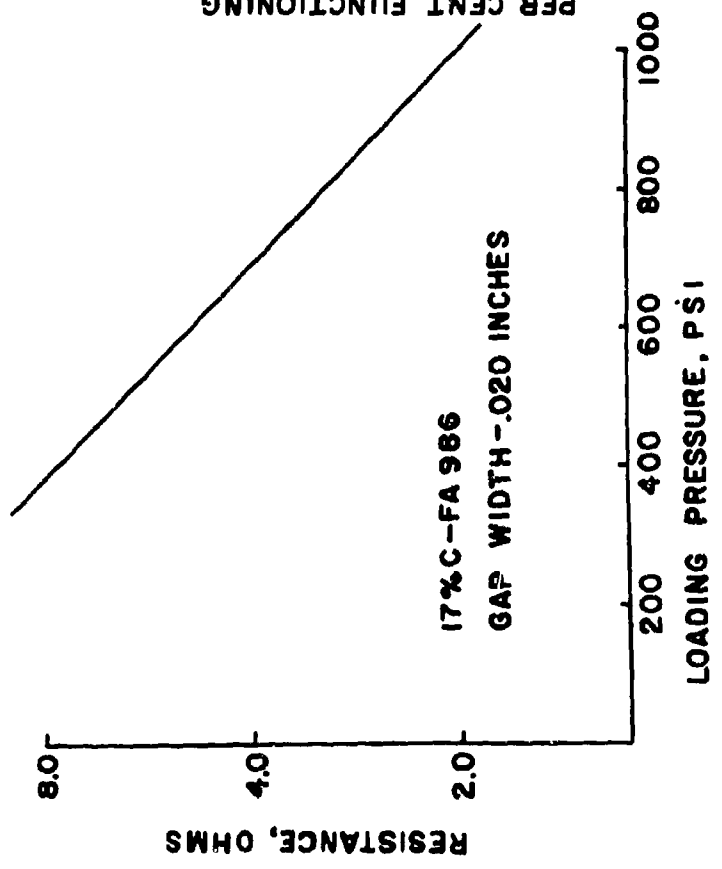




**FIGURE 5**  
**AVERAGE FUNCTIONING TIME OF IGNITION ELEMENTS**  
**VERSUS**  
**FIRING CURRENT**

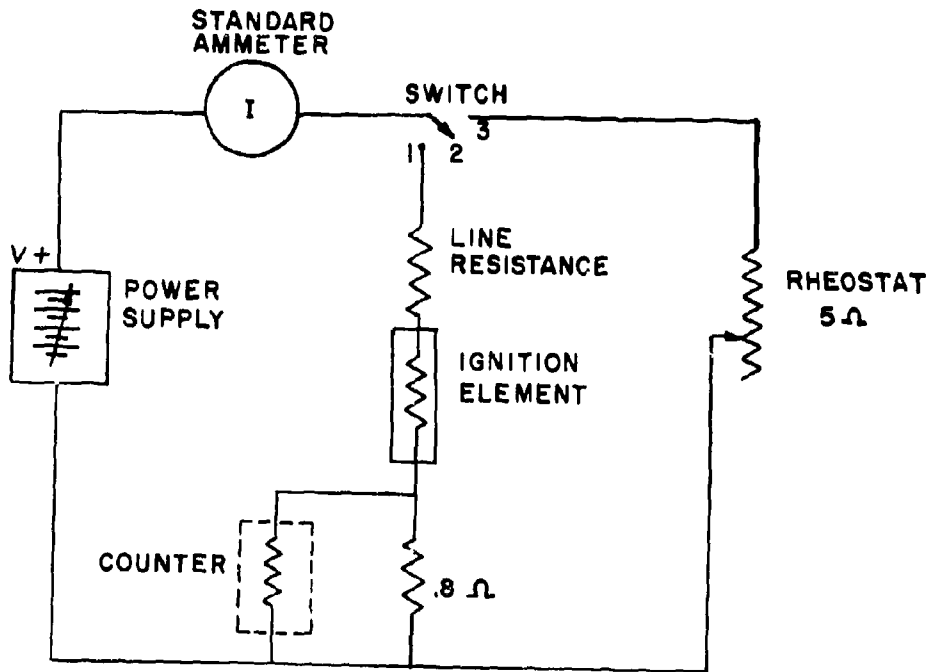
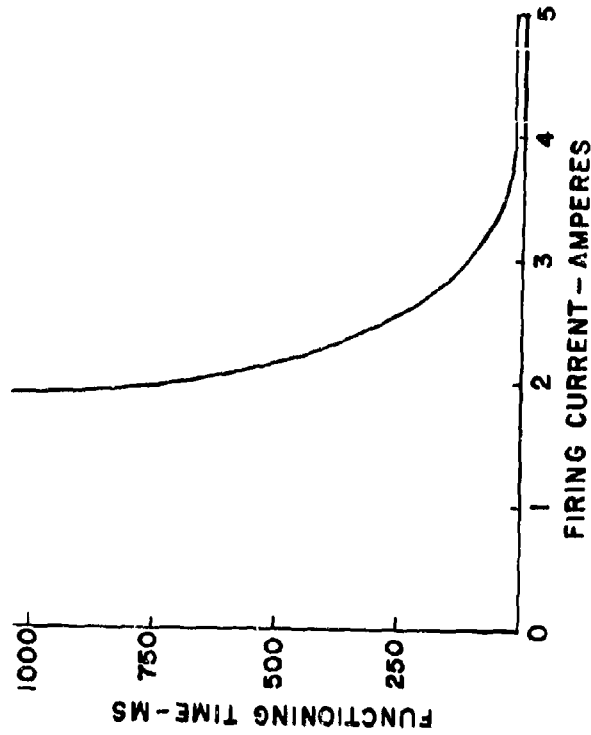


**FIGURE 6. FIRING CIRCUIT FOR ELECTRIC IGNITION**  
**TEST ELEMENTS**

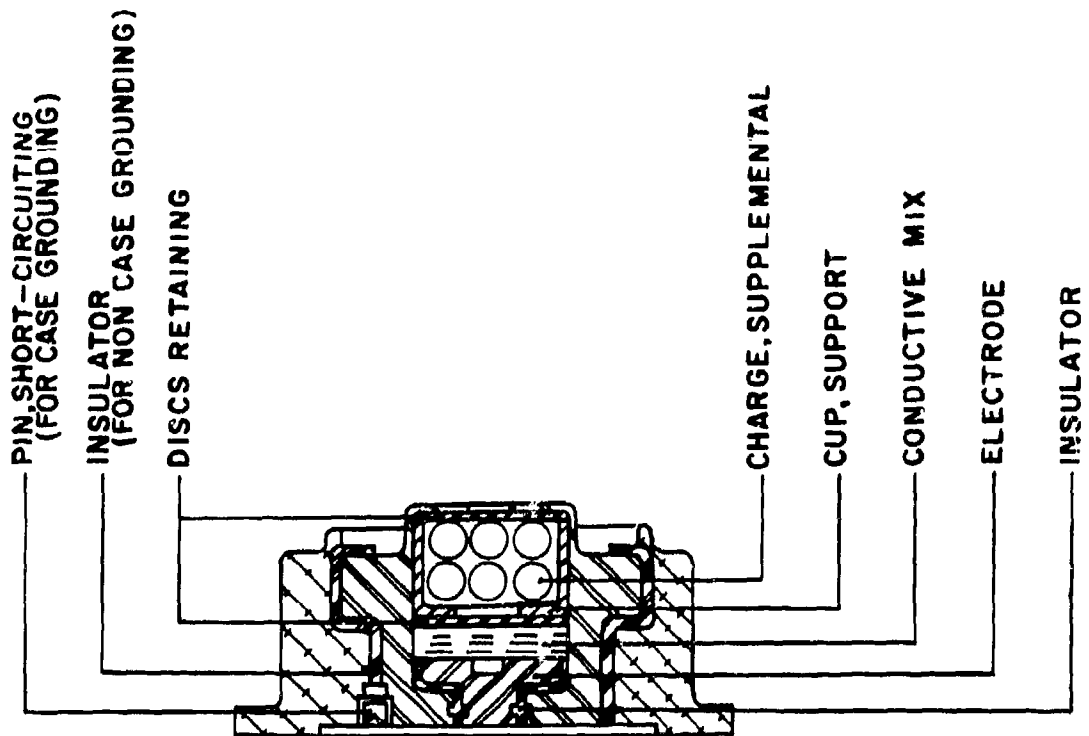


FIGURE 7. XM54 ELECTRIC IGNITION ELEMENT

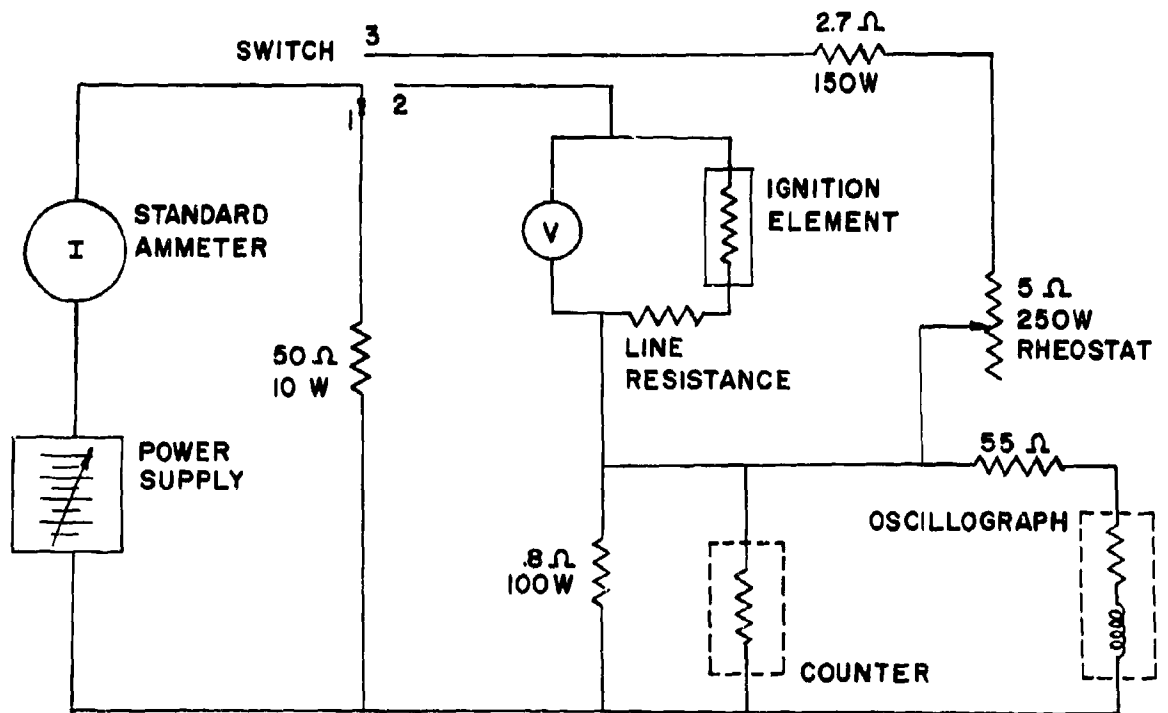
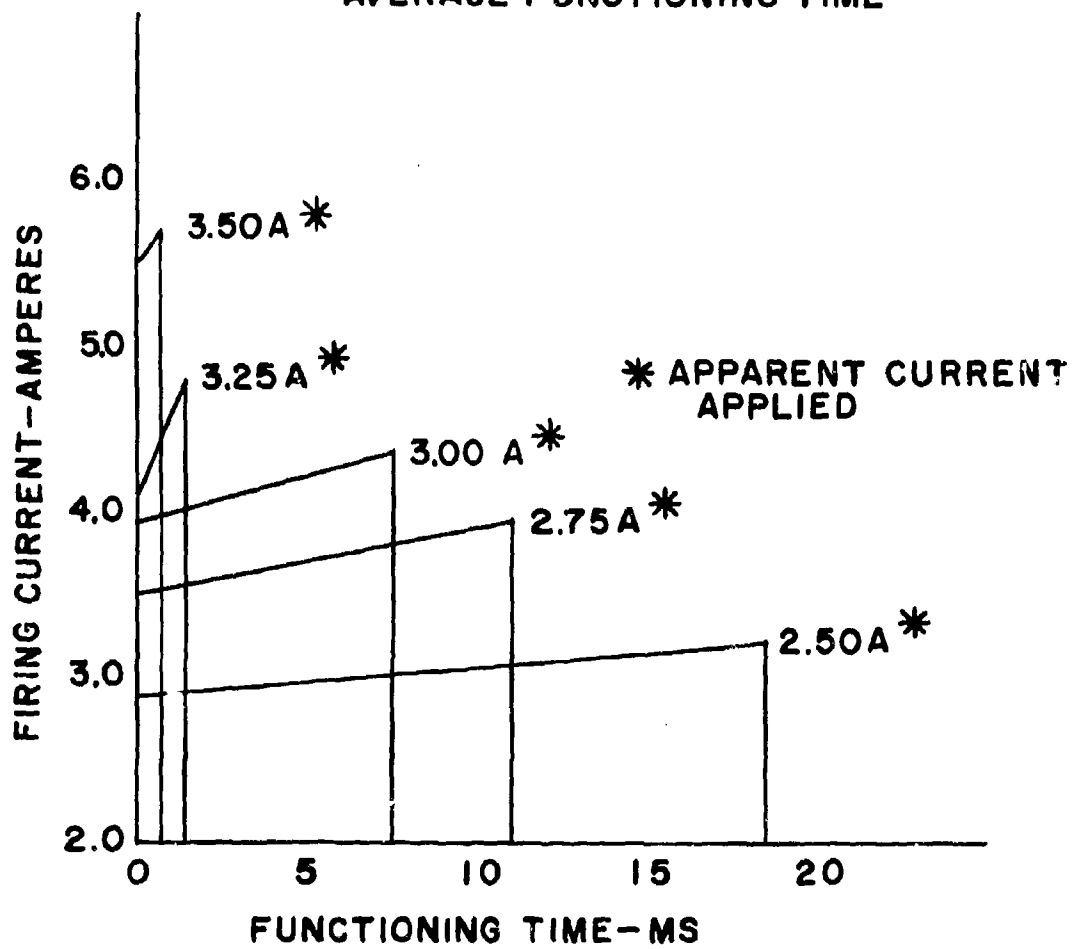


FIGURE 8. FIRING CIRCUIT FOR XM54 ELECTRIC IGNITION ELEMENTS

FIGURE 9  
AVERAGE FIRING CURRENT REQUIRED  
FOR XM54 IGNITION ELEMENTS  
VERSUS  
AVERAGE FUNCTIONING TIME



3-8P A HEAT TRANSFER STUDY OF HOT WIRE IGNITION  
OF A METAL-METAL OXIDE MIXTURE\*

by

J. L. Austing and J. E. Kennedy,  
IIT Research Institute, Chicago, Illinois

and

D. H. Chamberlain and R. H. Stresau,  
R. Stresau Laboratory, Inc., Spooner, Wisconsin

ABSTRACT

Measured values of thermal conductivity and autoignition temperature of an aluminum-tungstic oxide mixture and the electrothermal heat loss factor of a hot bridgewire have been used to calculate the temperature profile history of the bridgewire and surrounding reactant. Experimentally observed ignition characteristics correlate with the calculated thickness of reactant elevated above autoignition temperature.

INTRODUCTION

The hot wire ignition threshold of metal-metal oxide mixtures in contact with bridgewires is controlled by heat transfer processes in and between the bridgewire and the pressed granular bed of reactive solids. In principle, given values of the physical and chemical properties of the bridgewire and the reactive mixture and specifications of the system geometry, one could calculate the response of a device to a given electrical firing pulse.

\*This work was supported by the U.S. Atomic Energy Commission under Contract No. AT (11-1)-578, Task Orders No. 55 and 64.

In practice, analysis of hot wire ignition is usually limited either to study of the bridgewire temperature history, from which estimates of ignition probability or time may be made in certain cases, or to consideration of heat transfer into the reactant and its ensuing reaction through use of a computer. A method is illustrated in this paper which permits calculation of the temperature profile history of the reactant bed by a graphical finite difference solution easily done by hand, and a criterion of ignition is suggested for a reactant for which no kinetic data are available other than autoignition temperature.

An analysis is presented of a system studied experimentally by Austing and Weber<sup>(1)</sup>, specifically the 2/3 stoichiometric aluminum-tungstic oxide mixture\* subjected to constant current firings. Experimentally determined values of the electrothermal heat loss factor of the bridgewire, and of the thermal conductivity and autoignition temperature of the reactive mixture, together with values obtained from handbooks, represented the input for the analysis. Advantage was taken of the fact that values of thermal conductivity of the reactive bed can be derived from experiments in which the heat loss factor is determined; derivation of equations showing this relation is presented.

---

\*This mixture is formulated from H-3 spherical grade aluminum and TO-2 grade tungstic oxide. The term 2/3 stoichiometric implies aluminum deficiency.

The bridgewire temperature history was calculated up to and beyond the wire's melting temperature by use of the electrothermal equation studied extensively by Rosenthal<sup>(2)</sup>. This bridgewire temperature history was then used as the interior boundary condition in calculating radial heat conduction from the wire into the reactive bed. A parameter determined from the temperature profile histories thus calculated for the reactive bed was plotted against experimentally determined ignition times to provide an "ignition threshold" curve from which ignitability and ignition times may be predicted for untested conditions. The calculated parameter chosen as a criterion of ignition was the heating of a critical thickness of bed to a temperature in excess of the autoignition temperature.

#### BRIDGEWIRE TEMPERATURE HISTORY

The differential equation that describes the heating of a bridge system with heat losses under constant-current conditions is<sup>(2)</sup>:

$$C_p \frac{d\theta}{dt} + \gamma\theta = I^2 R_0 (1 + \alpha\theta) \quad (1)$$

where

- $C_p$  = heat capacity of the bridge
- $\theta$  = temperature rise above ambient temperature
- $t$  = time
- $\gamma$  = electrothermal total heat loss factor
- $I$  = current
- $R_0$  = resistance of the bridge at ambient temperature
- $\alpha$  = temperature coefficient of resistivity.

As expressed in Equation (1), the heat loss factor,  $\gamma$ , is a lumped type of coefficient meant to include all modes of heat transfer from the bridge, namely, conduction, convection, and radiation.

The solution to the Equation (1) is:

$$\theta = \frac{I^2 R_0}{\gamma - I^2 R_0 \alpha} \left[ 1 - \exp\left(-\frac{\gamma - I^2 R_0 \alpha}{C_p} t\right) \right] \quad (2)$$

if  $\alpha$  and  $\gamma$  are not function of temperature. For Evanohm (the bridgewire material used in ignitability experiments<sup>(1)</sup>, the temperature coefficient of resistivity,  $\alpha$ , is quoted to be  $\pm 0.00002/^\circ\text{C}$ <sup>(3)</sup>, a value that justifies assuming  $\alpha=0$ . Equation (2) thus simplifies to:

$$\theta = \frac{I^2 R_0}{\gamma} \left[ 1 - \exp\left(-\frac{\gamma}{C_p} t\right) \right] \quad (3)$$

Equation (3) was used to calculate the bridgewire temperature histories at selected current levels and several values of the heat loss factor,  $\gamma$ . As illustrated in Figure 1, the solution involves a portion in which the wire is below its melting point of  $1325^\circ\text{C}$ , a constant temperature plateau during which the wire melts, and a region in which the wire is molten but is assumed to maintain its shape. The heat capacity of molten Evanohm was assumed to be nearly double that of the solid Evanohm, as is the case with most metals. Equation (3) was applied for

solution of both regions in which temperature rose with time; an appropriate delay time was entered into the solution in the molten region, to account for the time required to melt the wire.

The value of  $\gamma$  was determined by conducting steady state experiments at low currents, insufficient to cause initiation; at steady state, the bridgewire temperature remains constant, hence Equation (1) reduces to

$$\gamma\theta = I^2R_0(1 + \alpha\theta) = I^2R_T \quad (4)$$

where

$R_T$  = resistance at steady state temperature. A bridge of platinum, which has a high value of  $\alpha$ , was used in heat loss factor experiments to that the steady state resistance of the wire could be used to imply its temperature.

#### Axial and Radial Partitioning of Heat Loss

The steady state temperature attained by a bridgewire is an equilibrium condition in which the total heat loss is equal to the ohmic heating. The total heat loss factor  $\gamma$  may be partitioned into axial and radial components wherein

$$\gamma = \gamma_a + \gamma_r \quad (5)$$

where

$\gamma_a$  = axial heat loss factor

$\gamma_r$  = radial heat loss factor



Since radial gradients in the wire and axial flow in the surrounding media can be ignored because of the very large ratio of thermal conductivities of the two media in most systems of practical interest, we may assume that heat flow can be divided into axial flow along the bridgewire and radial flow into the surrounding reactive bed. The steady state situation in a differential length,  $dL$ , of wire can be represented by the equations:

$$\frac{I^2 \rho_e dL}{A} = dq + \theta k_r dL$$

or 
$$\frac{dq}{dL} = \frac{I^2 \rho_e}{A} - \theta k_r \quad (6)$$

and 
$$q = -k_w A \frac{d\theta}{dL} \quad (7)$$

where

$\rho_e$  = electrical resistivity of wire metal

$A$  = cross-sectional area of wire

$q$  = axial heat flow at any point in the wire

$k_r$  = radial heat loss factor per unit length, and

$k_w$  = thermal conductivity of the wire.

Equations (6) and (7) may be combined,

$$\frac{dq}{dL} = \frac{dq}{d\theta} \cdot \frac{d\theta}{dL} = \frac{q}{k_w A} \frac{dq}{d\theta} = \frac{I^2 \rho_e}{A} - \theta k_r$$

and rearranged

$$q dq = (A k_w k_r \theta - I^2 \rho_e k_w) d\theta \quad (8)$$

Through integration and application of the boundary conditions that  $q = 0$  and  $\theta = \theta_m$  (maximum temperature rise) at the midpoint of the wire,

$$q^2 = 2I^2 \rho_e k_w (\theta_m - \theta) - Ak_w k_r (\theta_m^2 - \theta^2) \quad (9)$$

By setting  $\theta = 0$  as at either end of the bridgewire, the heat flow through the wire at each end,  $q_e$ , may be determined. Since by definition

$$\gamma_a = \frac{2q_e}{\theta_m},$$

$$\gamma_a = \left[ \frac{8I^2 \rho_e k_w}{\theta_m} - 4Ak_w k_r \right]^{1/2} \quad (10)$$

The total heat loss factor,  $\gamma$ , is by definition the quotient of the total electric power by the maximum temperature rise.

$$\gamma = \frac{I^2 \rho_e L}{A\theta_m} \quad (11)$$

Since  $\gamma_r = Lk_r$  and combining with Equation (5),

$$\frac{I^2 \rho_e}{\theta_m} = \frac{A}{L} \gamma_a + Ak_r \quad (12)$$

Equation (10) can be substituted into Equation (12) to eliminate  $\theta_m$ , which is not readily determined experimentally, to derive

$$\gamma_a = \frac{4Ak_w \pm 2\sqrt{4A^2 k_w^2 + Ak_w k_r L^2}}{L} \quad (13)$$

The radial component of the heat loss factor,  $\gamma_r$ , is given by:

$$\gamma_r = \frac{k_r \int \theta dL}{\theta_m} = \frac{k_r \theta_{av} L}{\theta_m} \quad (14)$$

Rather than derive a rigorous but cumbersome expression for temperature as a function of position along the bridgewire, an estimate of the ratio  $\theta_{av}/\theta_m$  based on similarity is suggested, in the form

$$\frac{\theta_{av}}{\theta_m} = 1 - \frac{c\theta_m/L}{(d\theta/dL)_e} \quad (15)$$

where the subscript e denotes the end of the bridgewire, and c is a constant. The value of c can be shown to be approximately  $\frac{8}{3}$  by comparison of heat loss factors and temperature distributions of "short" bridgewires<sup>(4)</sup>. By substituting expressions from Equations (7), (10), and (14) into Equation (15), we derive:

$$\gamma_r = k_r \left[ L - \frac{8Ak_w}{3\gamma_a} \right] \quad (16)$$

The value of  $k_r$  is dependent upon the configuration of the surrounding boundaries as well as the thermal conductivities of the media. For a cylindrically symmetric system,

$$k_r = \frac{2\pi k_f}{\ln(D_f/D_b)} \quad (17)$$

where

$k_t$  = effective thermal conductivity of the material surrounding the bridgewire

$D_f$  = inside diameter of a surrounding heat sink, and

$D_b$  = bridgewire diameter

#### Experimental Measurements of Heat Loss

The above equations imply that measurement of values of the axial and radial heat loss factors also provides the data for calculation of thermal conductivity of the surrounding media. The experimental arrangement for determining heat loss factors consisted of a Glasseal glass skirted flange header with pins set 0.250-inch apart. The pins and glass were ground and polished flat and the bridgewire was soldered to these pins. The header was then epoxied into an aluminum charge holder with an internal diameter of 0.404-inch. The aluminum-tungstic oxide mixture was pressed into this holder and onto the bridgewire at the loading pressure (or density) of interest. Heat loss factors and thermal conductivities presented in Table 1 were derived from data obtained in steady state experiments using this hardware. To calculate the apparent thermal conductivity of the glass/reactant surround of the bridgewire, Equation (17) was solved simultaneously for each pair of data sets acquired for a given reactant composition loaded at a given loading pressure at each of two bridgewire diameters. The value of the equivalent heat sink diameter,  $D_f$ , was also obtained for this calculation.

The thermal conductivity of the surround was found to vary from approximately  $1 \times 10^{-3}$  to  $1.5 \times 10^{-3}$  cal/sec cm °C as loading pressure on the aluminum-tungstic oxide mixture was increased from 4,800 to 20,000 psi. Because these values are very close to those of glass (which ranges from 1.5 to  $2. \times 10^{-3}$  cal/sec cm °C), we may accept the measured values as representing the thermal conductivity of the reactant mixture.

The partitioning of heat loss between axial heat losses, which are not useful in ignition, and radial heat losses which flow into the reactant is apparent from Table 1. The observation that thermal conductivity of a granular bed increases with loading pressure (as particles are pressed closer together) is in agreement with work reported by Kistler and Caldwell<sup>(5)</sup>.

The thermal conductivity of the  $\frac{2}{3}$  stoichiometric aluminum-tungstic oxide mixture was checked independently in a more standard cell for determination of thermal conductivity. The results were in agreement with the values in Table 1<sup>(6)</sup>.

#### TEMPERATURE PROFILES IN REACTANT

A comparison between calculated bridgewire temperature histories and ignition times for hot wire ignition of aluminum-tungstic oxide mixtures demonstrates clearly that the bridgewire temperature can far exceed the measured autoignition temperature of 825°C<sup>(1)</sup> for aluminum-tungstic oxide for many milliseconds before ignition occurs. This point clearly indicates that a

significant radial thickness of bed reaches or exceeds auto ignition temperature and therefore presumably reacts at a substantial rate prior to initiation of a propagating reaction wave. Because no reaction kinetics data are known to have been determined for the aluminum-tungstic oxide mixture, an analysis was made of the temperature profile induced in the reactive bed as a function of time, omitting consideration of chemical reaction. The thickness of bed that had exceeded autoignition temperature at the time of experimentally observed ignition was estimated for each of several constant firing currents. Upon these calculated data is based a hypothesized "ignition threshold" from which ignitability and ignition times may be predicted.

#### Finite Difference Solution

The partial differential equation describing conductive heat transfer to an inert bed (since reaction can not be treated quantitatively) from an infinitely long cylindrical bridgewire is<sup>(7)</sup>:

$$\frac{\partial \theta}{\partial t} = \frac{k_f}{\rho c_p r} \frac{\partial}{\partial r} \left( r \frac{\partial \theta}{\partial r} \right) \quad (18)$$

where:  $\rho$  = bulk density of reactive bed,  
 $c_p$  = specific heat of bed, and  
 $r$  = radial position measured from the wire axis,

with the boundary condition:

$$\theta = \theta(t)^* \text{ according to Figure 1 or equivalent,} \\ \text{at } r \leq R_{\text{wire}} \text{ for } t \geq 0,$$

and the initial condition:

$$\theta = 0 \text{ at all } r \text{ at } t = 0.$$

The rather complex expression for bridgewire temperature history imposed as the interior boundary condition and the fact that a temperature plateau occurs during melting in the midst of the bridgewire heating cycle make analytical solution of Equation (18) cumbersome. The interior boundary condition is handled easily, however, by a finite difference method of solution.

Let us introduce the substitution  $Z = \ln(r/R_{\text{wire}})$ , as suggested by Peck<sup>(8)</sup>, which produces the transformed equation

$$\frac{\partial \theta}{\partial t} = \frac{k}{\rho c_p r^2} \frac{\partial^2 \theta}{\partial Z^2}, \quad (19)$$

where  $\theta = \theta(Z, t)$ . To express Equation (19) in finite difference form, write Taylor series to provide expressions for  $\frac{\partial \theta}{\partial t}$  and  $\frac{1}{2} \frac{\partial^2 \theta}{\partial Z^2}$ <sup>(9)</sup>. The value of  $\theta$  at the  $m^{\text{th}}$  increment of  $Z$  and the  $n^{\text{th}}$  increment of  $t$  is denoted by the symbol  $\theta_{m,n}$ . The series

$$\theta_{m,n+1} = \theta_{m,n} + \frac{\partial \theta}{\partial t} (t_{n+1} - t_n) + \dots$$

\*Bridgewire temperature history was calculated using total heat loss factor  $\gamma$  (rather than  $\gamma_r$ ) because this was believed to lead to the most accurate value of temperature history near the center of the bridgewire.

can be arranged to obtain

$$\frac{\partial \theta}{\partial t} = \frac{\theta_{m,n+1} - \theta_{m,n}}{t_{n+1} - t_n}$$

Similarly Taylor series in  $Z$  about  $\theta_{m,n}$  for estimates of  $\theta_{m+1,n}$  and  $\theta_{m-1,n}$  are solved simultaneously, by elimination of  $\frac{\partial \theta}{\partial Z}$ , for  $\frac{1}{r^2} \frac{\partial^2 \theta}{\partial Z^2}$ . The series

$$\theta_{m+1,n} = \theta_{m,n} + \frac{\partial \theta}{\partial Z} (z_{m+1} - z_m) + \frac{\partial^2 \theta}{\partial Z^2} \left( \frac{z_{m+1} - z_m}{2} \right) + \dots$$

and

$$\theta_{m-1,n} = \theta_{m,n} + \frac{\partial \theta}{\partial Z} (z_{m-1} - z) + \frac{\partial^2 \theta}{\partial Z^2} \left( \frac{z_{m-1} - z_m}{2} \right) + \dots$$

and use of a substitution  $r\Delta Z = \Delta r$  lead to

$$\frac{1}{r^2} \frac{\partial^2 \theta}{\partial Z^2} = \frac{z \left[ (z_m - z_{m-1}) \theta_{m+1,n} + (z_{m+1} - z_m) \theta_{m-1,n} \right]}{(\Delta r)^2 (z_{m+1} - z_{m-1})} - \frac{2\theta_{m,n}}{(\Delta r)^2}$$

The full finite difference form of Equation (19) denoting  $(t_{n+1} - t_n)$  by  $\Delta t$ , is

$$\theta_{m,n+1} - \theta_{m,n} \left[ 1 - \frac{2k_f \Delta t}{\rho c_p (\Delta r)^2} \right] = \frac{2k_f \Delta t}{\rho c_p (\Delta r)^2} \left[ \frac{(z_m - z_{m-1}) \theta_{m+1,n} + (z_{m+1} - z_m) \theta_{m-1,n}}{z_{m+1} - z_{m-1}} \right] \quad (20)$$



The coefficient  $2k_f \Delta t / \rho c_p (\Delta r)^2$  is the modulus of the equation. Imposing the arbitrary constraint

$$\frac{2k_f \Delta t}{\rho c_p (\Delta r)^2} = 1, \quad (21)$$

the coefficient of  $\theta_{m,n}$  vanishes and Equation (20) simplifies to

$$\theta_{m,n+1} = \frac{(z_m - z_{m-1})\theta_{m+1,n} + (z_{m+1} - z_m)\theta_{m-1,n}}{(z_{m+1} - z_{m-1})} \quad (22)$$

In making calculations at equal time intervals such that  $\Delta t$  is constant,  $\Delta r$  must also be constant in accordance with Equation (21). With  $\Delta r$  constant,  $\Delta Z$  must vary as a function of  $r$  as

$$\Delta Z = \frac{\Delta r}{r} = \frac{\Delta(r/R_{\text{wire}})}{r/R_{\text{wire}}} \quad (23)$$

Equation (22) is applicable for the case of differing as well as constant values of  $\Delta Z$ .

A graphical construction for solving Equation (22) is a linear plot of  $\theta$  versus  $Z$ , with  $Z$  intervals marked off per Equation (23). Equation (22) is an algebraic statement of the "lever rule," indicating that the value of  $\theta_{m,n+1}$  can be read at the intersection of a straight line drawn between  $\theta_{m-1,n}$  and  $\theta_{m+1,n}$  with the vertical line  $Z_m$ . Since  $Z = \ln(r/R_{\text{wire}})$ , semi-logarithmic graph paper can be used with  $\theta$  on the linear scale and  $r/R_{\text{wire}}$  on the log scale. This facilitates the reading

of temperature rises at various radial positions. The calculation proceeds from the bridgewire surface (at which  $Z = 0$ , since  $r/R_{\text{wire}} = 1$ ) into the bed.

An example of the graphical finite difference solution is shown in Figure 2. After arbitrarily selecting a value of  $\Delta t$  to be 1 msec for that calculation and setting the modulus equal to unity, the value of  $\Delta r/R_{\text{wire}}$  is calculated per Equation (21) to be 0.354. The equal increments of  $\Delta r/R_{\text{wire}}$  are laid out on the graph, then connecting lines are drawn for successive time increments in accordance with Equation (22). The first non-trivial connecting line is drawn for a time of 2 msec between temperatures existing at the bridgewire surface ( $r/R_{\text{wire}} = 1.000$ ) at 1 msec per Figure 1 and at the second increment to the right ( $r/R_{\text{wire}} = 1.708$ ) at 1 msec. The value of  $\theta(Z_1, 2 \text{ msec})$  can be read at the intersection of this line with  $Z_1$ , and this point is used as an end-point for construction of a line for  $t = 3 \text{ msec}$ , as seen in Figure 2. As the graphical calculation proceeds to subsequent time intervals, additional increments in  $Z$  enter into it, signifying temperature rises at increasing distances from the bridgewire. After several time increments, estimates of temperature rise at alternate increments of  $Z$  (e.g.,  $Z_1, Z_3, Z_5, \dots$ ) are available at a given time increment, in addition to knowledge of the temperature at  $Z_0$ , which is the wire surface.

Temperature profile histories calculated in this way for different values of current level, and bridgewire diameter, are presented as Figures 3 and 4. In each case the value of  $\Delta t$  used in the calculations was much smaller than the time increments displayed as parameters in the graphs. The value of  $\Delta t$  used in each calculation was selected so as to be small in comparison with the observed or anticipated ignition time for a given set of conditions.

It should be noted that it is possible in this finite difference method to make quantitative use of reaction kinetics data when such is available for the reactant. The extent of reaction at each location during each time increment could then be calculated since each local temperature is known. Heat release (or absorption) accompanying the calculated degree of reaction can be appropriately accounted for by adjustment of each local temperature before proceeding with the next incremental calculation.

#### Hypothesized Ignitability Criterion

From plots of the temperature profile histories such as in Figure 3, the calculated thickness of reactant bed heated above autoignition temperature may be determined as a function of heating time at constant current. It is reiterated that these plots were made omitting consideration of chemical reaction. In particular, the thickness of critically heated bed was calculated for each of four current levels for which ignition times

had been experimentally measured<sup>(1)</sup>, for a constant Evanohm bridgewire diameter of 5 mils and reactant density of about 3.5 g/cc. These data, listed in Table 2, are plotted in Figure 5 to form the solid "ignition threshold" curve.

The thickness of the reactant zone which exceeds auto-ignition temperature prior to ignition is approximately 0.001 to 0.002 in., depending upon current level, heat loss factor, and heating time. This thickness represents a linear distance equivalent to ten to twenty 3- $\mu$  particle diameters. The fact that the zone of growing reaction is many particles deep lends some justification to our implicit assumption, through use of the heat conduction equation, of a bed of constant properties at all locations.

It is hypothesized that ignition will occur (1) whenever calculation neglecting chemical reaction indicate that the thickness of bed exceeding autoignition temperature is greater than the threshold curve of Figure 5 at any time, and (2) that it will occur at the time at which the threshold curve is reached. Although the threshold curve was constructed from data obtained in constant current firings of units with 5-mil bridge-wires and 3.5 g/cc reactant density, it is suggested that the curve may be used to estimate behavior (i.e., ignitability and ignition time) for untested conditions different from the above, e.g., at different bridgewire diameters, reactant densities, or current waveforms. Indeed an analytical criterion such as offered in Figure 5 is of substantial value only if it will serve to describe various sets of conditions of interest.

To test the generality of the ignition threshold curve, predictions of ignition times were made for two variations in the input data. Comparisons of the predictions with the results of experiments are given in Table 3. First, initiators containing Inconel-glass headers bridged with 2-mil diameter Tophet-C wire were loaded with the 2/3 stoichiometric mixture of H-3 aluminum and TO-2 tungstic oxide, and were fired at 5 amperes. This current is the design all-fire current for these initiators, which have a 1-amp, 1-watt no-fire capability. Three experimental firings indicated an ignition time of 3.5 msec, which was in fair agreement with the value of 4.6 msec predicted from Figure 5.

Secondly, had been observed<sup>(1)</sup> that an increase in reactant density caused an increase in ignition time. An attempt was made to determine whether the analysis would agree with this observation. An aluminum-tungstic oxide density of 4.0 g/cc density inferred a different value of thermal conductivity ( $1.5 \times 10^{-3}$  cal/sec cm °C, measured experimentally) and a different value of heat loss factor  $\gamma$  (0.022 watts/°C, extrapolated from values in Table 1) which affect the calculation. The high value of  $\gamma$  in particular effects a substantial reduction in the equilibrium bridgewire temperature, which is closely approached during the pre-ignition period. The calculated value of 27 msec for ignition time at 4.0 g/cc, 15 amperes, and 5-mil bridge diameter is in very good agreement with the observed value of

29 msec; these values differ sharply from the value of 14 msec at 3.5 g/cc, 15 amperes, and 5-mil bridge diameter, which was used as one of the datum points in constructing the ignition threshold curve. Thus the analysis appears to account satisfactorily for the effect of density upon ignition time, principally through recognition of the effect of density upon the value of  $\gamma$ .

On the basis of these results it is suggested that ignition threshold calculations as described may be applicable both in cases where reaction rate information is available, and where it is lacking.

#### REFERENCES

1. Austing, J.L., and Weber, J.P., "Constant Current Ignition of Metal-Metal Oxide Mixtures," Proc. of Fifth Symposium on Electroexplosive Devices, Franklin Institute, Phila., June 13-14, 1967.
2. Kabik, I., Rosenthal, L.A., and Solem, A.D., "The Response of Electro-Explosive Devices to Transient Pulses," NOLTR 61-20, June, 1961.
3. Alloy Handbook, Wilbur B. Driver Co., Newark, N.J.
4. Stresau, R.H., "Electrical and Thermal Consideration in the Design of Electro-Explosive Devices," R. Stresau Laboratory Report 64-11-1, Spooner, Wisc., 23 Dec. 1964.
5. Kistler, S.S., and Caldwell, A.G., "Thermal Conductivity of Silica Aerogel," Ind. Eng. Chem. 26, 658-62, 1934.
6. Austing, J.L., and Kennedy, J.E., "Determination of Physical Chemical Characteristics of Metal-Metal Oxide Mixtures," Report No. SC-CR-66-2019, Sandia Corp., Albuquerque, 1966.
7. Carslaw, H.S., and Jaeger, J.C., "Conduction of Heat in Solids," Oxford, Clarendon Press, 1959.
8. Peck, R.E., private communication at Illinois Institute of Technology, Oct., 1957.
9. Leipziger, S., private communication regarding Taylor series derivation, August, 1965.

Table 1

## HEAT LOSS FACTOR AND THERMAL CONDUCTIVITY OF REACTANT\*

Loading Pressure psi	Density g/cc	Bridgwire D mils	L mils	Heat Loss Factors mw/°C			$k_r$ mw/mil °C	Thermal Conductivity $k_f$ cal/sec cm °C
				$\gamma$	$\gamma_a$	$\gamma_r$		
4,800	3.61	1	434	7.01	0.314	6.70	0.0154	0.00118
4,800	3.74	1	400	5.72	0.296	5.42	0.0136	0.00104
4,800	3.69	1.94	473	8.10	0.628	7.47	0.0158	0.00105
4,800	3.69	1.94	496	8.03	0.614	7.42	0.0150	0.00094
4,800	3.39	1.94	218	6.61	0.844	5.77	0.0264	0.00105
20,000	4.04	1.94	220	8.92	0.970	7.95	0.0361	0.00151
4,800	3.50	4.67	250	11.18	2.58	8.60	0.0344	0.00100
20,000	3.76	4.67	250	16.37	3.02	13.35	0.0534	0.00152
4,800	3.62	5	478	11.15	1.93	9.22	0.0193	0.00098

NOTE:  $\gamma$ ;  $k_r$ ;  $k_f$  values derived by noting electrical resistance changes in platinum bridgwire at steady state in temperature range 100°C to 450°C.

\*2/3-Stoichiometric H-3 aluminum + T0-2 tungstic oxide.

Table 2  
IGNITION THRESHOLD DATA\*

Shot Number (1)	Current, amps	Ignition Time, msec	Radial Thickness of Bed Above Autoignition Temp., in.
323	35	2	0.0009
219	25	5	0.00145
167	15	14	0.0019
106	11	28	0.0016

\*2/3-Stoichiometric H-3 aluminum + TO-2 tungstic oxide, nominally 3.5 g/cc, heated by 5-mil Evanohm bridgewire, for  $\gamma = 0.012$  watt/°C.

Table 3  
PREDICTED AND OBSERVED EFFECTS OF CHANGES  
IN DENSITY AND WIRE DIAMETER ON IGNITION TIME

Reactant Density (g/cc)	Current (amps)	Bridgewire Diameter (mils)	Observed Ignition Time (msec)	Calculated Ignition Time (msec)
3.5	15	5	14	*
4.0	15	5	29	27
3.5	5	2	3.5	4.6

\*Datum point used in constructing "ignition threshold" curve.



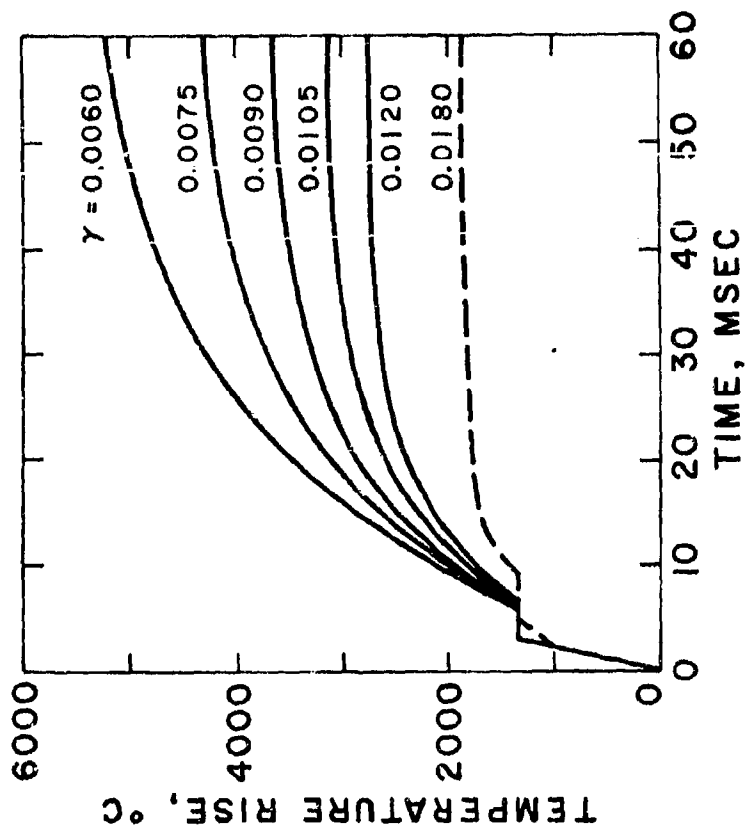


Figure 1 CALCULATED TEMPERATURE HISTORY OF  
5-MIL EVANOHM BRIDGEWIRE

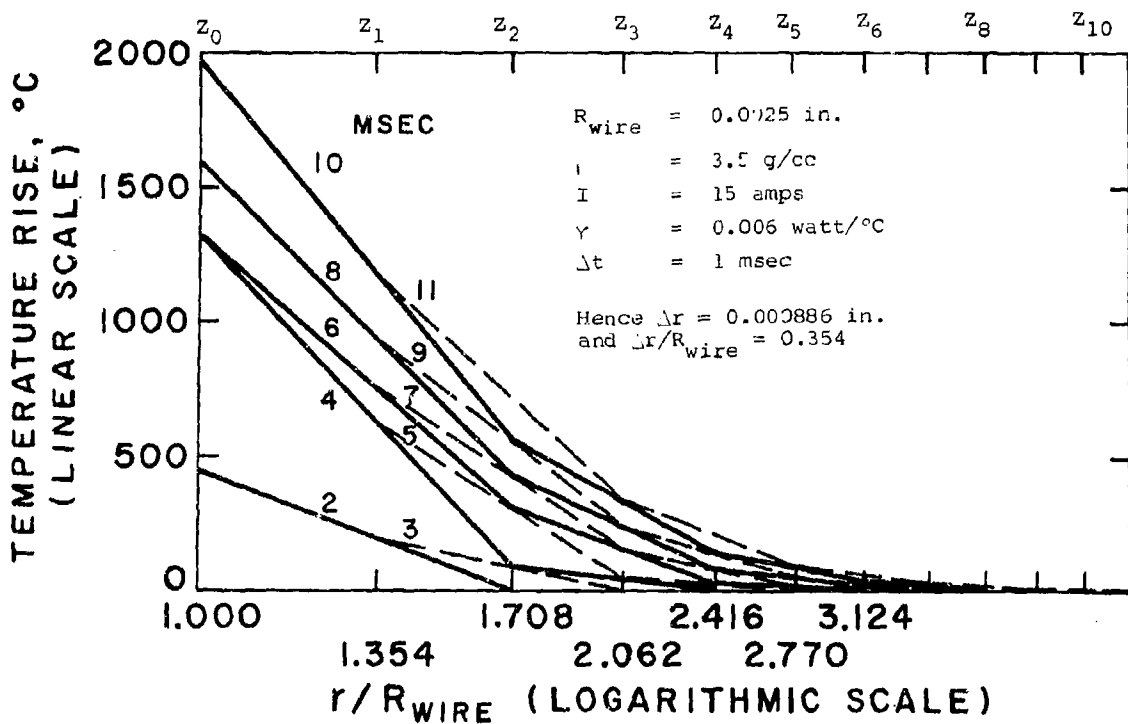


Figure 2 EXAMPLE OF GRAPHICAL FINITE DIFFERENCE SOLUTION FOR  
REACTANT TEMPERATURE PROFILE HISTORY

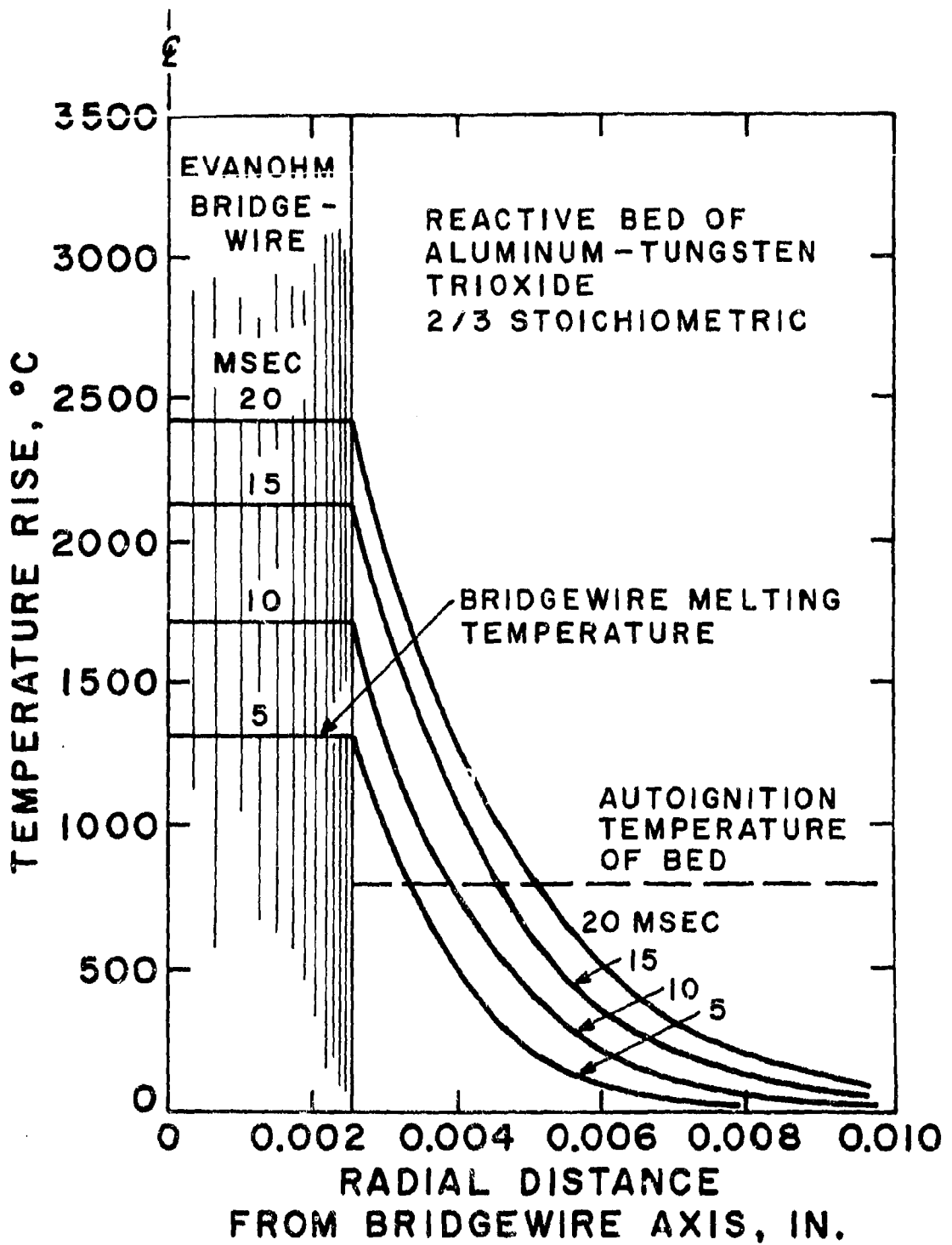


Figure 3 CALCULATED TEMPERATURE PROFILE HISTORY  
 AT 15 AMPERES CONSTANT CURRENT FOR  $\gamma = 0.012$  WATT/°C

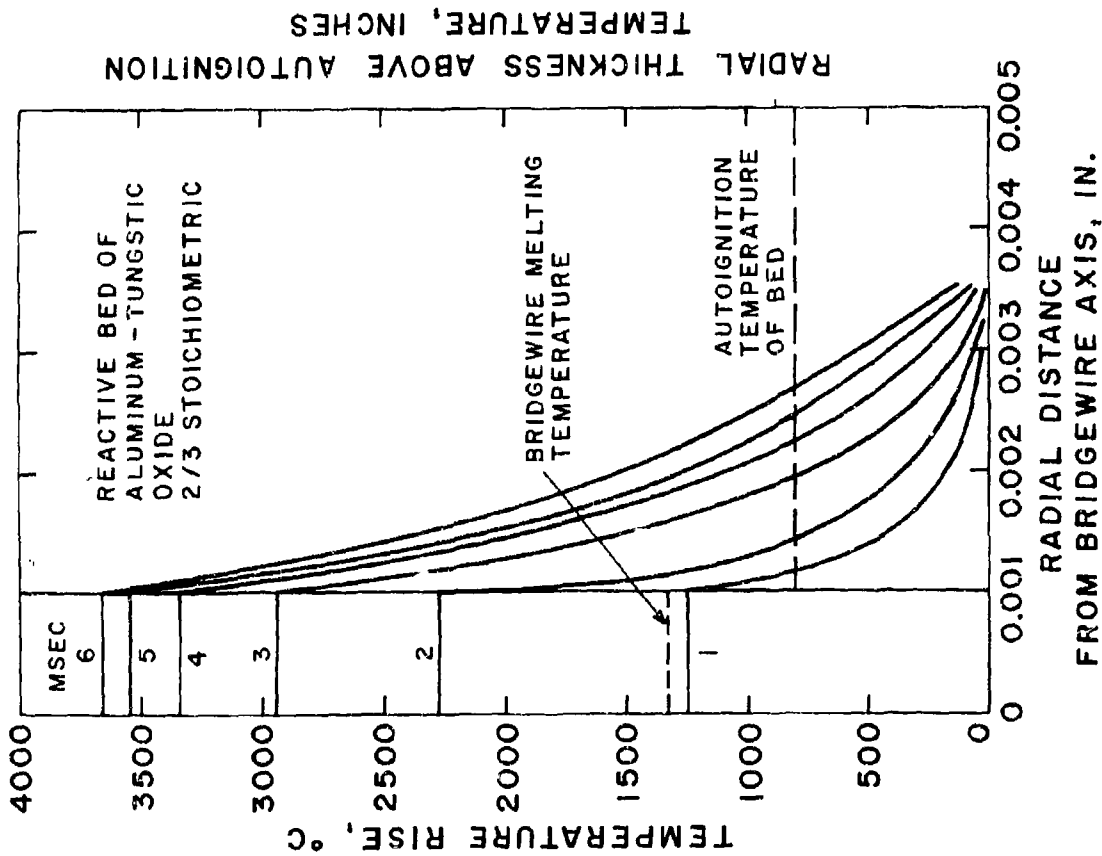


Figure 4 CALCULATED TEMPERATURE PROFILE HISTORY AT 5 AMPERES CONSTANT CURRENT IN TOPHET - C BRIDGEWIRE FOR  $\gamma = 0.009$  WATT/°C

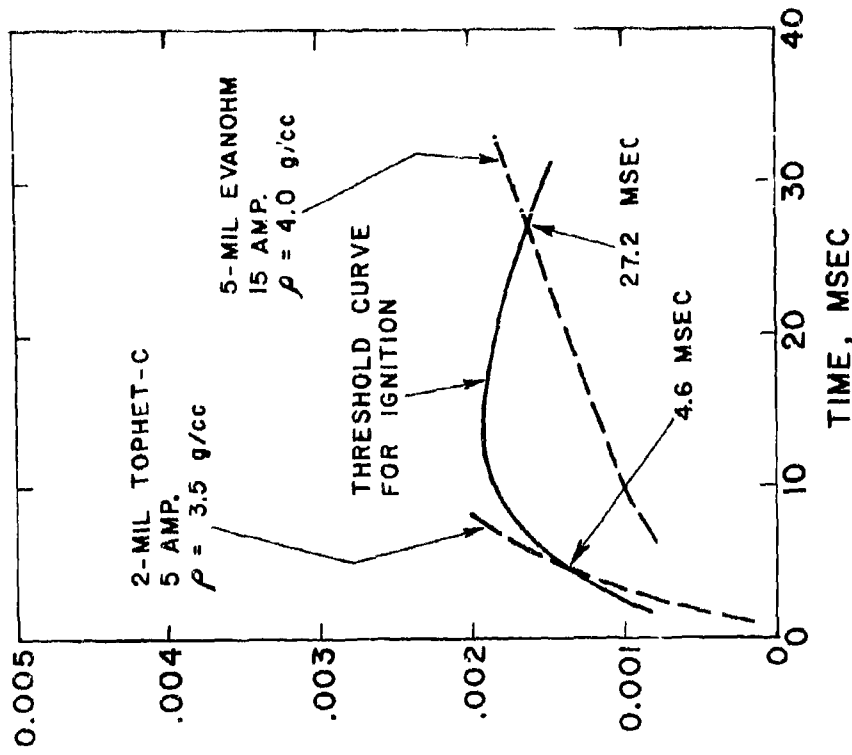


Figure 5 IGNITION THRESHOLD CURVE AND HEATING CROSS-CURVES FOR PREDICTION OF IGNITION TIMES

3-9P ELECTRICAL AND THERMAL CONSIDERATIONS IN THE DESIGN OF  
ELECTRO-EXPLOSIVE DEVICES

By R. H. Stresau, R. Peterson, and D. Chamberlain  
R. Stresau Laboratory, Inc. Spooner, Wisconsin

INTRODUCTION

Widespread concern regarding hazards of premature initiation of electroexplosive devices as the result of electromagnetic or electrostatic conditions inherent in ordnance applications has led to the promulgation of a number of specifications<sup>1</sup> and standards limiting the sensitivity of EEDs. General application of some specifications intended for general use<sup>1</sup> would result in the disqualification of practically all EEDs in current use in fuzes. A more serious effect would be the disqualification of existing firing circuits, designed for use with the relatively sensitive EEDs in current use and the need to replace them with larger and heavier units necessary for the less sensitive EEDs which meet these recently established criteria. However, more detailed consideration of the characteristics and limitations of firing circuits in current use and of the criteria set forth in recent documents indicates that they are not necessarily incompatible. Many firing circuits in current use are essentially pulse generators capable of quite substantial output of instantaneous current and power but somewhat limited amounts of energy per pulse,

while the recently established criteria place lower limits of power and/or current required to fire with no reference to energy sensitivity. In principle, as will be shown, power sensitivity and energy sensitivity are subject to independent control by the designer's choice of materials and dimensions.

The input characteristics of thermal EEDs (as distinguished from exploding bridgewire devices) are determined by the interaction of resistive heating, heat transfer, and reaction kinetics. A complete and rigorous analysis of even the simplest EED in these terms would require an extensive (and expensive) computer program as well as data which are not available. However, thermal EEDs have been found to be particularly susceptible to analyses in terms of simplified models which have been found to be extremely useful (within their intended ranges of application) in the design of EEDs to meet specified input requirements and in the prediction of performance and behavior of existing designs. The analyses presented herein are based on such simplified models of designs which have been suggested to comply with the requirements of Reference 1 and yet fire from the output of existing circuits. In addition to the analyses, this report includes experimental data which are in general agreement with one of the analyses.

#### GENERAL PRINCIPLES

As with any explosive initiation system, the threshold condition for initiation is that at which heat is liberated by the explosive decomposition faster than it is dissipated from the

nucleus of reaction. This, of course, results in a temperature increase and (in view of the exponential relationship between reaction rate and temperature) an exponential increase in reaction rate. If the explosive is assumed to be a continuous solid medium in which the dominant heat transfer process is conduction and which reacts in accordance with the Arrhenius equation, it is possible to express this process in a differential equation which can be (and has been<sup>2</sup>) solved numerically to yield critical temperatures for various reaction nucleus dimensions<sup>2</sup>. However, the assumptions mentioned are so unrealistic in their representation of granular solid explosives that the numbers obtained are meaningless<sup>3</sup>. On the other hand, if the magnitudes are ignored, the relationships predicted by such calculations have been verified by any number of experiments<sup>3, 4, 5, 6</sup>. In Reference 4, it was pointed out that such solutions indicated that the inverse of the threshold temperature should vary with the logarithm of the reaction nucleus dimension. Experimental data for hot wire EEDs gave straight lines when inverse critical temperatures were plotted versus logarithms of bridgewire diameters<sup>4</sup>. Moreover, activation energies obtained from the slopes of these lines were in excellent agreement with those obtained by other investigators using very different techniques<sup>5</sup>.

Although the considerations discussed above indicate that the threshold temperature for initiation of an EED varies as an inverse function of the bridgewire diameter (and also of the time the temperature is sustained), this variation in temperature over the usual range of EED designs is small enough that

the assumption of a single "ignition temperature" for each explosive material can be very useful. Kabik, Rosenthal, and Solem<sup>7</sup> combining this assumption with the equation:

$$C_p \frac{d\theta}{dt} + \gamma \theta = P(t) \text{ --- (1)}$$

where

$C_p$  is the heat capacity of the bridge system

$\theta$  is the temperature rise above ambient

$t$  is time

$\gamma$  is a heat loss factor

and  $P(t)$  is time dependent power input

have, after experimentally determining  $C_p$  and  $\gamma$  for an existing EED (as well as  $\theta_m$ , the threshold temperature for initiation) predicted with precision the response to a wide variety of complex input signals.

If Equation (1) is solved for a pulse so short that losses may be neglected, the relationship:

$$C_p \theta = \int P dt = E \text{ --- (2)}$$

where

$E$  is the energy delivered by the pulse to the bridge-wire can be combined with the assumption of a constant "ignition temperature" to obtain the relationship that the firing energy requirement is proportional to the bridgewire volume (since volumetric specific varies rather little from one metal to another). For a rather large range of bridgewire dimensions, the threshold firing energy is given by the empirical equation:

$$E_t = 25 + 450 D \frac{2L}{b} \text{ --- (3)}$$

### Convenient Units and Conversion Factors

Since

10 ergs = one microjoule = one watt-microsecond  
the energy (E) in ergs stored in a capacitor of (C) microfarads  
capacitance, charged to (V) volts becomes:

$$E = 5CV^2 \text{ - - - - - (5)}$$

and the energy of a pulse becomes:

$$E = 10 \int P dt \text{ - - - - - (6)}$$

where

E is the energy in ergs

P is the power in watts

and t is time in microseconds.

For bridgewires, a convenient unit of volume is the cylindrical mil, which is defined as the volume enclosed in a cylinder of one mil diameter by one mil length. A rather accurate estimate of the heat capacity of a bridge ( $C_p$ ) can be made by multiplying the specific heat by the specific gravity and applying the conversion:

$$1 \text{ calorie/ml}^\circ\text{C} = 0.54 \text{ ergs/cylindrical mil}^\circ\text{C} \text{ - - - - (a)}$$

For non-cylindrical bridges, the cubic mil may be a more convenient unit of volume.

$$1 \text{ calorie/ml}^\circ\text{C} = 0.687 \text{ ergs/cubic mil}^\circ\text{C} \text{ - - - - (b)}$$

For resistance calculations it is convenient to convert handbook values to ohm mils or ohm circular mils/mil:

$$\begin{aligned} 1 \text{ microhm centimeter} &= 0.000394 \text{ ohm mils - - - - (c)} \\ &= 0.501 \text{ ohm circular mils/inch (d)} \end{aligned}$$



Heat transfer coefficients are most convenient in watts/mil°C.

$$1 \text{ calorie/second cm } ^\circ\text{C} = 0.0106 \text{ watts/mil}^\circ\text{C} \text{ - - - - - (e)}$$

#### Relationship of Electrical and Thermal Conduction

Since both thermal and electrical conductivity are proportional to the area of the conductor at right angles to the path of flow and inversely proportional to the length of the path.

Thus, for any conductor:

$$P_f/\theta = k\rho/R \text{ - - - - - (7)}$$

where

$P_f$  is the rate of heat flow between two points,

$\theta$  is the temperature differential between the points

$R$  is the electrical resistance between the points

$k$  is the thermal conductivity of the material

and  $\rho$  is its electrical resistivity.

for EED design calculations, it is convenient to express the product ( $k$ ) in ohm watts/°C. Published heat transfer data are often expressed in terms of calories per second, which may, of course, be converted to watts by multiplying by 4.185.

#### Relevant Properties of Materials Used in EEDs

The properties given in the tables (1,2) are taken from handbooks<sup>8, 9</sup>, manufacturers' descriptions, and other sources. They have been combined and converted to the convenient units mentioned above.

Thermal properties of electrical insulators which have been used or might find application in EEDs are given in Table 2. A glance at the heat capacity data given in Tables 1 and 2 will reveal that the volumetric heat capacities of all materials,

metallic and insulators, vary rather little from one to another. The search for a heat sink medium with an unusually large heat capacity has rather dim prospects. In metallic conductors, there is a tendency for high resistance alloys to have low thermal conductivities but this tendency is insufficient to compensate for the increase in electrical resistivity and maintain the nearly constant value of the product ( $\rho k$ ) which applies to the pure metals and alloys of medium resistivity. In general, this tendency continues for insulators in that most electrical insulators are also reasonably effective thermal insulators. A notable exception is beryllium oxide, which is comparable with pure metals as a thermal conductor. It may be noted that the ceramics listed have thermal conductivities about ten times those of the plastics listed. Of course, plastics can be varied in many of their properties by the addition of fillers. One maker of specialized plastics has stated<sup>10</sup> that plastics with thermal conductivities approaching one-tenth of that of metallic aluminum are possible.

#### Gross Heating of an EED

Most considerations of heat accumulation and dissipation in an EED are concerned with the bridgewire and its immediate surroundings. It is of some interest to consider these matters as they apply to the whole EED considered as a lumped thermal mass. Equation (1) is as applicable to such considerations as to the bridgewire system.

A reasonable estimate of the heat capacity of a typical EED can be made rather easily in view of the fact, which can be checked

by reference to Tables 1 and 2, that the volumetric heat capacities of materials used in EEDs vary rather little from one to another. Assuming the average to be 0.3 erg/°C cyl. mil., the heat capacity (Cp) of a detonator the size of the Mk.71 (0.195" dia by 0.5" long) is about 5,700,000 ergs/°C 0.57 joules/°C Cp. If such a detonator were thermally isolated (that is to say,  $\gamma = 0$ ), the solution of Equation (1) for the one watt five minute test would be:

$$C_p \theta = P t \text{ - - - - - (8)}$$

$$.57 \theta = 300$$

$$\theta = 527^\circ\text{C}$$

which would be hot enough to initiate most explosive materials.

Of course, such thermal isolation is impossible and can be approached only by such extreme measures as a Dewar flask. However, this calculation serves to illustrate the importance of heat transfer from the detonator to its surroundings. If we consider a detonator of this kind hanging in free air, the heat loss factor ( $\gamma$ ) may be seen to be the sum of the heat loss factor due to convection and that due to conduction along the lead wires. Reference 9 gives, for the surface coefficient of heat transfer for ordinary surfaces in still air 1.65 BTU/sq. ft. hr. °F which is equal to 0.0063  $\frac{\text{Watt}}{\text{sq. in. } ^\circ\text{C}}$ .

Since the surface area of a detonator of the size mentioned above is about 0.36 square inches, the heat loss factor for loss to the air is 0.00227 watt/°C. The heat loss through the lead wires can vary enormously over the range of materials and sizes used for lead wires in current practise. Two examples of commonly

used combinations of materials and dimensions are 26 gage stainless steel and 20 gage copper, each four inches long. Solving Equation (7) for the stainless, the heat loss through each wire turns out to be about 0.00001 watt/°C, a nearly negligible contribution to the total heat loss factor. On the other hand, the heat loss through each of the copper leads is 0.00215 watt/°C. Adding the surface losses to the lead-wire losses, the heat loss factors ( $\gamma$ ) are 0.00229 watt/°C for the EED with the stainless steel lead wire and 0.00657 watt/°C with the copper leads. Equilibrium temperatures for the two detonators with steady power input of one watt while hanging free in still air are ~~465°~~ 465° and 153° above ambient respectively. Thermal time constants ( $C_p/\gamma$ ) for the two detonators are 255 seconds and 87 seconds respectively. These time constants, of course, are very much larger than those of any bridgewire systems of practical interest. Thus, for steady state conditions, the temperature rise ( $\theta$ ) of the detonator considered as a lumped thermal mass must be added to that of the bridgewire system as calculated using Equation (1) in its usual context.

Although it would be possible to combine Equation (1) for the bridgewire system with the same equation for the EED as a lumped thermal mass to obtain a somewhat more realistic prediction of its behavior, such an equation, in addition to being a bit cumbersome, would be an oversimplification of the true situation. A rigorous representation would have to consider temperature distribution within the EED and in surrounding media in terms of distributed parameters. In view of the complex

configuration of initiator components and the variety of design, a general formulation for such consideration does not seem possible. A more profitable pursuit would seem to be the consideration of each general design as a unique system.

The condition assumed in the foregoing analysis, that of a detonator hanging free in still air, is unlike any anticipated condition of use in a weapon. As used in weapons, EEDs are usually inserted in relatively snug fitting holes in metal fuze components. Under these conditions, the heat loss factor is somewhat difficult to assess because of its dependence on clearance, fuze body materials, surface finishes, etc. but it is safe, in general, to assume that it will be large enough that the equilibrium temperature rise of the detonator body will be negligible. However, a test for compliance with the "one watt, one-ampere no-fire" criterion, in the absence of specified procedures or test fixtures is unlikely to be performed under service installation conditions and may be performed under the free hanging conditions assumed above. A designer forced to design for such conditions has two alternatives: (1) Increasing the heat capacity ( $C_p$ ) sufficiently that the 300 joules causes a manageable temperature rise. (2) Increasing the heat loss factor ( $\gamma$ ) enough to limit the equilibrium temperature rise to a reasonable value. In view of the small range of volumetric heat capacities of solids (see Tables 1 and 2), the first of these alternatives is possible only by increasing the volume to several times that of the Mk. 71 Detonator (a change which would be quite unpopular with fuze designers). The second alternative can be attained by the use of sufficiently conductive lead wires. The 20 gage by

four inch copper leads assumed above would be nearly sufficient. However, it should be pointed out that this calculation is based on the assumption that the ends of the lead wires are held at "ambient" temperature. It is probable that such an assumption is probably quite valid for most test arrangements since relatively large clips are the most convenient and durable means of connecting for test purposes. However, the compact, isolated electrical systems which are preferred in many designs to reduce electrical hazards may be relatively poor dissipators of heat. Thus a detonator designed to dissipate heat through its case to surroundings might fail a "one-amp, one-watt no-fire" test yet be appreciably safer in a fuze installation than another which passes the test because it was designed to dissipate heat through the lead wires. A third alternative, which is useful in some situations, is the use of radiation to dissipate heat from an initiator. The high temperature (400°C - 500°C) needed to dissipate a watt from the square centimeter or so area of a detonator, (even if it is black) imposes limitations in the choice of materials and design. If the initiator designer is given sufficient voice in conditions of use to assure that it will be mounted in firm contact with a "heat sink" of adequate heat capacity, detonators much smaller than the Mk. 71 can be designed to comply with Ref. 1.

To assure adequate levels of safety against environmental electrical hazards and avoid expensive delays resulting from conflicting interpretations, a document such as Reference 1 should include unambiguous criteria defining thermal characteristics

of mountings and electrical circuits used in both use and testing of EEDs for compliance with "one watt, one ampere no-fire" or similar requirements.

#### DESIGN CONCEPTS AND ANALYSIS

All of the designs which will be considered herein involve a "bridge", a small electrically conductive element which is heated by the passage of electricity to a temperature sufficiently high to ignite a "flash charge" of explosive or pyrotechnic material with which it is in intimate contact. General types of bridges to be considered include "long" bridgewires, both round and flat, "short" bridgewires, and "film bridges".

##### Long Bridgewires

For purposes of this discussion, a "long" bridgewire is defined as a bridgewire long enough that end effects are negligible in determining heat loss factors. Because metals are so much better conductors of heat than explosives or pyrotechnics "long" bridgewires, in this sense, are exceptional. In most EEDs, the bridgewires are of "intermediate" length in that both end and radial heat losses are significant. In most cases, radial losses to the flashcharge explosive are greater than end losses.

If it is assumed that the heat flow pattern about a bridgewire is cylindrically symmetrical, the flux through any cylindrical surface is given by:

$$P_r = -2\pi r l k_r \frac{dT}{dr} \text{ - - - - - (9)}$$

where

$P_r$  is the total heat flux through the surface  
 $r$  is the radius of the cylindrical surface  
 $L$  is the length of the cylinder (and the bridgewire)  
 $k_f$  is the thermal conductivity of the flash charge material  
and  $dT/dr$  is the temperature gradient at the particular section

Rearranging and integrating:

$$P_r/\theta = \gamma_f = \frac{2\pi Lk}{\ln D_2/D_b} \text{ --- (10)}$$

where

$\theta_r$  is the temperature difference between a bridgewire of diameter  $D_b$  and a concentric cylindrical heat sink of internal diameter  $D_2$

and  $\gamma_f$  is a "heat loss factor" which can be used in Equation (1)

(1) Of course, rather few, if any practical initiators approximate the cylindrically symmetrical configuration to which Equation (10) applies, however, for any given design, it is possible to estimate an approximate effective value of  $D_2$ , or if experimental data are available relating steady state power sensitivity to bridgewire diameter for a given combination of hardware and flash charge material, the data may be substituted in Equation (10) to obtain an estimate of the effective  $D_2$  and the thermal conductivity ( $k$ ) of the flash charge explosive.

A number of investigators<sup>11, 12</sup> have assumed that the heat loss factor of a bridgewire with a given explosive surrounding it can be characterized in terms of a surface coefficient of heat transfer, which can be multiplied by a temperature to obtain a bridgewire surface heat flux density for "no-fire", "mean", or



"all-fire" conditions. Designs based on such assumptions have not always performed as desired<sup>12</sup>. In at least one such case, Equation (10) was found to fit the data of other experimenters. Equation (10) has been verified experimentally in the work reported in Reference (13).

No calculations are necessary to show that current "long" bridgewire designs with explosives and loading practices in current use will not produce a detonator which will comply with Reference 1 and still be usable with currently used guided missile fuze firing circuitry. Any number of examples can be cited of such detonators which have firing energy requirements several times that available from fuze circuits and yet will fire on a fraction of a watt. A glance at Equation (10) and Table 2 will reveal that, of the factors which affect power dissipation, that subject to the widest variation is the thermal conductivity ( $k$ ) of the flash charge. Unfortunately, data relating thermal conductivities of explosive materials to state of aggregation are not readily available. Data culled from the literature<sup>14</sup> reduce to thermal conductivities of lead azide and mercury fulminate of 0.00164 and 0.00117 mw/°C respectively at unstated states of aggregation. Assuming that these values are for powdered materials at relatively low loading densities, an effort was made to determine the increase possible as the crystal densities of primary explosives were approached. Lead and silver azide and basic and normal lead styphnate were pressed around bridgewires at 150,000 pounds per square inch. Because of the dimensions of the wires, which made it difficult to

separate radial and axial heat flow and may have introduced a variable related to the relative size of the particles of explosive and the wire diameter, some interpretation difficulties were experienced. However, the thermal conductivities seem to range from about 0.005 or 0.006 mw/°C for normal lead styphnate, to 0.010 or 0.012 mw/°C for silver azide. Unfortunately, these values are still too low for the explosive to transmit sufficient heat to obtain the "one-watt, one-amp no-fire" level which is often required. However, it was found that the addition of flake aluminum (25% to 50% by weight) increases the thermal conductivities of these materials by a factor of 10 or more, which is sufficient<sup>15</sup>.

It has been shown<sup>16</sup> that it is feasible to meet the requirements of Reference 1 in a detonator of conventional design, wherein a substantial part of the heat loss factor is attributable to radial heat flow from the bridgewire to the flash charge explosive. An objection to all such designs is that such radial heat flow depends upon firm and intimate contact between explosive and bridgewire. Such contact may be lost as the result of relative movement of explosive and bridgewires due to environmental temperature changes, vibrations, or accelerations, shrinkage of a "beaded" explosive charge due to loss of solvent, local thermal decomposition or melting as the result of "no-fire" currents or pulses, or gradual relief of residual loading stresses. Such loss of contact can result in substantial decrease of the heat loss factor and hence of the "no-fire" power or current. If a specification such as Reference (1) is to be relied upon

to assure safety against premature functioning as the result of environmental radiofrequency, perhaps more positive and reliable heat flow paths should form the basis of the "no-fire" conditions specified.

#### Flattened Long Bridgewires

The assumption that the heat loss from a bridgewire to the flash charge explosive can be characterized in terms of a surface coefficient of heat transfer suggests the use of a flat wire or ribbon to increase the surface area for a given cross-section. There is no question that such systems can substantially increase heat loss factors without increasing the heat capacity of a bridge system, but it is safe to predict that the increase will generally be less than would be calculated on the basis of the surface coefficient assumption. The complexity of the heat flow pattern about such a bridge discourages analysis at this time, but it is clear that the reduction in the divergence of the flow will result in a reduction of the effective surface coefficient. In itself, the flattening of a bridgewire seems an unlikely solution to the problem with which this report is primarily concerned. It might turn the trick if it was found possible to increase the thermal conductivity of a flash charge material almost to the point where a long round wire met the requirements. A flat bridgewire bonded to a thermally conductive substrate would be the equivalent of the "film" bridge discussed in a later paragraph.

### Short Bridgewires

A "short" bridgewire is defined as a bridgewire short enough that radial losses are negligible in determining heat loss factors. Like long bridgewires, short bridgewires in these terms are exceptional in current practice.

In a "short" bridgewire, as defined above, only axial heat flow need be considered. The axial flow at any point in a wire is given by the expression:

$$p = -k_p A dT/ds \text{ - - - - - (11)}$$

where

$p$  is the local rate of heat flow

$k_p$  is the thermal conductivity of the bridgewire material

$T$  is the temperature at any point

and  $s$  is a given length of wire.

If it is assumed that the ends of the bridgewire are connected to effective heat sinks at the same temperature, the temperature distribution will be obviously symmetrical and the thermal gradient and hence heat flow is zero at the center. The heat flow through any cross-section at a distance  $s$  from the center is equal to:

$$p = sP_a/L \text{ - - - - - (12)}$$

where

$P_a$  is the total power dissipated in the bridgewire

and  $L$  is the total length of the bridgewire.

Combining Equations (11) and (12) and integrating:

$$k_b A dT/ds = -P_a \frac{r}{L}$$

$$dT = -\frac{P_a r ds}{k_b A L}$$

$$T_e = T_c - \frac{P_a}{k_b A L} \int_0^{L/2} r ds = T_c - \frac{P_a}{k_b A L} (L^2/8)$$

$$T_c - T_e = \theta_m = \frac{P_a L}{8k_b A} \quad \text{--- (13)}$$

$$P_a/\theta_m = \gamma_a = \frac{8k_b A}{L} = \frac{2\pi D^2 k_b}{L}$$

where

$\gamma_a$  is the heat loss factor

$T_c$  is the temperature at the center of the wire

$T_e$  is the temperature at the ends

and  $\theta_m$  is the maximum temperature rise

Of course, the electrical resistance of the wire is given by:

$$R_b = \rho L/A \quad \text{--- (14)}$$

where

$R_b$  is the resistance of the bridgewire

and  $\rho$  is the resistivity of the metal

Combining Equations (13) and (14):

$$\theta_m = P_a R_b / 8k_b \rho \quad \text{or} \quad \gamma_a = 8k_b \rho / R_b \quad \text{--- (15)}$$

Equation 15 can be a useful design tool since thermal conductivities and electrical resistivities are readily available data for all bridgewire materials and ignition temperatures can be estimated from available data, or determined experimentally.

It should be noted that in Equation (13) the power requirement is proportional to the length, while, in Equation (3) the

energy requirement is nearly proportional to the bridgewire volume. Thus with a given wire, the power requirement is increased and the energy requirement decreased by reducing the length of the bridgewire. The power and energy sensitivities of "short" bridgewire initiators may thus be controlled by the designer quite independently of one another. Given the desired values, they may be substituted in Equations (3) and (13) or (3), (14), and (15) which may be solved simultaneously to obtain the bridgewire dimensions needed. Suppose, for example, that a detonator is required with a one-watt "no-fire" condition and a fifty percent firing energy of about 4500 ergs. From Equation (3):

$$D_b^2 L = 10.$$

and from Equation (13), assuming a tungsten bridge:

$$e_m = 300 = \frac{(1)(L)(4)}{(8.0)(0.0037)D_b^2}$$

$$D_b^2/L = 0.144$$

combining:

$$\frac{D_b^2 L}{D_b^2/L} = L^2 = \frac{10}{0.144} = 69.5, L = 8.35 \text{ mils}$$

$$\text{and } D_b^2 = \frac{10}{8.35} = 1.20, D_b = 1.1 \text{ mils}$$

The foregoing example illustrates on the one hand, the simplicity of designing "short Bridgewire" initiators, and on the other, the fabrication problems which may be encountered. The resistance of such a bridgewire would be about .015 ohm.

"Short bridgewire" initiators have the advantages of positive heat dissipation and independence between energy and power sensitivity. However, the determinate relationship between power requirement and resistance makes it impossible for a

"short bridgewire" initiator using available alloys as bridge-wires and primary explosive flash charges to meet the requirements of Reference (1). The development of higher temperature flash charge materials might alleviate this difficulty. Another possibility is the insertion of a thermal barrier, such as a disc of mica, between the bridgewire and the flash charge.

#### Short Bridgewire with Series Resistance

In the foregoing section, one of the most serious difficulties noted was that, when the resistance of a short bridgewire is low enough to raise the no-fire power to one watt, the no-fire current is over five amperes. Another is that the resistances are so low as to result in rather difficult dimensions, from a fabricator's viewpoint. Low resistances are also difficult to deal with electrically and may introduce new hazards. All of these problems suggest a rather simple solution, that of designing a bridgewire with a "no-fire" current of one ampere and adding sufficient series resistance to raise the overall resistance to one ohm. The no-fire input power of such a combination will, of course, be one watt.

If, in Equation (15), power is expressed in terms of current and resistance:

$$P = I^2 R_b = 8k_p \theta / R_b$$

$$I = \sqrt{\frac{8k_p \theta_m}{R_b}} \text{ --- (16)}$$

where

I is the current which will result in a temperature rise  $\theta$ . Substituting values for gold in Equation (16) the IR product, which, incidentally, has the dimensions of voltage and indicates

that, for short bridgewires, firing voltage is independent of bridge resistance, is 0.14 for 350°C, 0.17 for 500°C and 0.24 for 1000°C. It would seem that a gold bridgewire should have a resistance close to one-eighth of an ohm to attain a one ampere no-fire condition. Because of the small range of the products of electrical resistivity and thermal conductivity for pure metals (and alloys of medium resistivity) the relationship of peak temperature to the IR product is nearly independent of bridge-wire material.

A few experiments have been performed to verify the calculations above and to develop design data applicable to a detonator to comply with Reference (1). In a preliminary attempt to fabricate a group of initiators with 0.3 mil gold bridgewires with resistances close to one-tenth of an ohm resulted in a group with quite variable resistances ranging from less than one-tenth to over two-tenths of an ohm. Tests of these (with basic lead styphnate flash charges) indicated that the threshold value of the product of resistance and current is close to 0.13 ohm-amperes. The items with resistances between 0.08 and 0.11 ohms were apparently unaffected by exposure to one ampere for five minutes.

A larger group, made with similar materials, was sorted into two categories. Those with resistances above 0.11 ohms were subjected to a steady current test, using the Bruceton technique, in which the test variable was the product of the measured cold resistance and the applied current. The mean threshold firing condition was 0.123 ohm-amperes with a standard



deviation of 0.047 log units. (A threshold temp. of 270°  
 (Equation (16).)

These data tend to verify Equation (16) and indicate that a practical solution to the problem of developing a detonator of reasonable input energy requirement which complies with Reference 1 may be a short bridgewire with series resistance. As pointed out above, a bridgewire-flash charge combination with a one ampere no-fire characteristic, combined with sufficient series resistance to raise the total to one ohm, becomes a "one ampere-one watt no-fire" device. Of course, the series resistance increases the total energy requirement in proportion to the resistance increase, but, as has been pointed out, the energy and power or current requirements of short bridgewire initiators can be adjusted independently. The validity of this principle and its feasibility as a practical solution has been demonstrated experimentally<sup>15</sup>.

#### Bridgewires of Medium Length

In a bridgewire in which both the axial and radial components of the heat loss factor are significant  $\gamma_a$  can be represented by the equation:

$$\gamma_a = \frac{4AK_w \pm 2\sqrt{4A^2K_g^2 + AK_wK_rL^2}}{L} \text{ --- (17)}$$

where

A is the cross section area of the wire

$K_w$  is the thermal conductivity of the wire metal at any point along the wire

$K_r$  is the radial heat loss factor per unit length

L is the length of the wire

and  $\gamma_a$  is the axial component of the heat loss factor

The radial component of the heat loss factor ( $\gamma_r$ ) can be represented by the equation:

$$\gamma_r = K_r \left( L - \frac{8AK_w}{2\gamma_a} \right) \text{--- --- --- --- ---} \quad (18)$$

Equation 18 has been simplified for tractibility but Reference 18 shows it to be applicable and also gives the derivation of Equations (17) and (18).

#### Film Bridges on Thermally Conductive Substrates

The formation of bridgewires by depositing an electrically conductive film on an insulating substrate has been the subject of wide interest for many years. Films have been deposited by vacuum evaporation and sputtering techniques, chemical, electrochemical, "writing", and as paints, glazes, "dags", and inks. Stencils, masks, and photographic techniques have been used to control the pattern of the film.

If the heat flow from a limited area on the surface of a relatively large mass is considered, it is quite plain that the flow will tend to approach spherical divergence. In spherically divergent flow, the flux through any spherical surface is given by:

$$P_s = -k_p A \frac{dT}{dr} = -k_p 4\pi r^2 \frac{dT}{dr}$$

rearranging and integrating:

$$4\pi k_p dT = -P_s \frac{dr}{r^2}$$

$$4 k_p \theta_s = P_s \int_{r_1}^{r_2} \frac{dr}{r^2} = P_s (1/r_1 - 1/r_2)$$

but since  $r_2$  is much greater than  $r_1$ , its reciprocal becomes

negligible so:

$$P_s = 4\pi k_p \theta r_1$$

where

$P_s$  is the total heat flux in a spherically divergent flow  
 $\theta$  is the temperature drop from a small spherical surface of radius  $r_1$  to a much larger, concentric spherical surface of radius  $r_2$ , or, more generally, the difference in temperature between a point at distance  $r$  from the center and a remote point.

The heat flux per unit area ( $p$ ) is given by:

$$p = \frac{4\pi\theta k_p r_1}{4 r_1^2} = \frac{k_p \theta_s}{r_1} \text{ - - - - - (19)}$$

Of course, the heat flow in a substrate very close to a heat-emitting film is quite complex and the spherical flow is an approximation. However, if it is assumed that the effective center of the spherical flow from a film of square outline is at a distance from the corners equal to the side ( $s$ ) of the square, the temperature  $\theta_v$  at the corners is given by:

$$\theta_v = \frac{P_s}{k_p s}$$

but the center of such a flat surface is closer to the center of the sphere than the corners (in this case the distance at the center,  $h = s \sqrt{2}$ ) so the temperature rise  $\theta_c$  at the center of the film with respect to remote points in the substrate is:

$$\theta_c = \frac{P_s}{\sqrt{2} k_p s}$$

and, since the effects of variations of film configuration may

be expected to be reasonably self compensating if the configuration is not too radically different from square, a reasonable approximation of the maximum temperature rise  $\theta_m$  of a film of area A is given by:

$$\theta_m = \frac{P_s}{k_p \sqrt{2A}} \text{ --- (20)}$$

and the heat loss factor:

$$P_s/\theta_m = \gamma_s = k_p \sqrt{2A} \text{ --- (21)}$$

Assuming a safe "no-fire" temperature of 300°, Equation (20) can be converted to a design formula for "one watt no-fire":

$$A = \frac{P_s^2}{2k_p^2 \theta^2} = \frac{(1,000)^2}{2 k_p^2 (300)^2} = \frac{5.55}{k_p^2} \text{ --- (22)}$$

Power is expressed in milliwatts so that thermal conductivities given in Table 2 may be used directly. To design a bridge which will also fire reliably on 10,000 ergs (from Equation (3) assuming the same relationship between volume and energy requirement in film bridges as wire bridges and also assuming that the "all-fire" energy is twice the fifty per cent point), the volume should be limited to about 8 cubic mils. To make the one-ampere level coincide with the one-watt level, a resistance of one ohm is desirable. Table 3 gives some film bridge dimensions, calculated using the foregoing considerations, which should result in initiators which comply with Reference (1) and could be substituted in many currently used guided missile fuze systems. As is illustrated in Table (3), the squaring of the thermal conductivity of the substrate material in Equation (22), in combination with the wide range over which thermal conductivities vary

(Table 2) limits the choice of substrate materials to a relative few. At the one extreme, beryllia is such a good thermal conductor that it is questionable that a film bridge of reasonable dimensions would fire a flash charge on five watts. The dimensions of the film on alumina are quite compatible with those of detonators in current use. Film bridges on alumina substrates have been shown to quite feasible solutions to the stated problem<sup>16</sup>.

Table 3. Dimensions of Film Bridges (all in mils)

Substrate	Film Area	Film Thickness	Gold Films Width	Gold Films Length	Platinum Films Width	Platinum Films Length
Alumina	22.2	0.36	0.244	91.5	0.49	45.4
Beryllia	0.2	40.	- - - - - this is ridiculous!			
Mullite	2222.	0.0036	24.4	91.5	49.	45.4
Glass (max $k_p$ )	9650.	0.00083	105.	91.5	197.	45.4
Nylon	165,000.	0.0000484	1800.	91.5	3680.	45.4

The area necessary for films on glass substrates is close to the maximum which could fit into a detonator of usual dimension. It probably violates the assumption upon which the derivation of Equation (22) is based that the film is of small extent compared with the substrate, which may increase its heat loss factor and, hence, its "no-fire" power and current.

The dimensions necessary for a film bridge on a nylon substrate were included mainly to illustrate the uselessness of unmodified plastics for this application. In Table 2 it may be noted that most plastics have appreciably lower conductivities than nylon, so much larger contact areas would be needed.

#### Plug and Terminal Design and Materials

In the foregoing discussion of film bridge initiators, the

thermal conductivity of the plug was shown to be the most critical variable. For other types of initiator, the relationship is somewhat less direct, but still quite important. In a "short" bridgewire, the calculations are based on the assumption that the terminals are effective "heat sinks" which remain at ambient temperature. The validity of this assumption rests on the implied assumption that the heat loss factor from the inner ends of the terminals is sufficiently large to keep the temperature at least reasonably close to ambient. The second order differential equation relating this heat loss factor to dimensions and conductivities of plugs and terminals is not difficult to solve, but satisfactory insertion of boundary conditions has not been accomplished at the time of this writing.

The temperature drop between the inner face of the terminal and the case of the detonator can be approximated by assuming it to be the sum of the drop through that portion of the terminal (or lead) wire which is molded into the plug (which may be calculated by means of Equation (7)) and the radial drop from the wire to the case through the plug (which may be calculated using Equation (10)). Applying this approach to the plug used in the Mk. 71 detonator, assuming that a half-watt is carried off in each terminal, the temperature drop through the bridgewire is  $50^{\circ}$  and that through the plug (assuming its thermal conductivity to be  $0.01$  milliwatts/mil $^{\circ}$ C) turns out to be about  $100^{\circ}$ . This  $150^{\circ}$  must be subtracted from the no-fire temperature of the explosive to obtain the permissible temperature differential between the center and ends of the bridgewire. An increase in thermal

conductivities of plugs and terminals would make it possible to design for higher temperature drops in the bridgewire and allow somewhat higher bridge resistances. If the thermal conductivity of the plug is reduced sufficiently and a good thermal contact established between the terminal and the plug, the terminal wire might serve quite usefully as the series resistance with a short bridgewire.

In a "long bridgewire," the effect of the plug is still more indirect, but the plug undoubtedly contributes significantly to the heat loss factor, particularly in a "flush bridged" initiator like the Mk. 71 detonator. A "long bridgewire," flush bridged on a plug of high thermal conductivity (such as alumina or the carbonyl iron which has been employed as an RF attenuator) is an interesting possibility for the applications considered herein, particularly if used with an explosive of good thermal conductivity.

#### Choice of Flash Charge Explosive and Loading Conditions

As has been stated earlier in this report, the assumption of a more or less fixed "ignition temperature" as a property of a particular explosive is an approximation which greatly simplifies calculations such as those given herein. However, this approximation should not be relied upon too quantitatively<sup>3</sup>. For instance, if the heat capacity of the bridge system is considered to be that of the bridgewire itself, the threshold firing temperature of lead styphnate (under pulse firing conditions) as implied by Equation (3), which is based upon performance data for a number of detonators, is over 1000°, while steady current

firing data imply a much lower threshold temperature. In terms of the more basic consideration that initiation results when the sum of the input power and the rate at which it is dissipated, in combination with chemical kinetics, the threshold temperature for pulse firing should be higher than that for steady state firing. It might be argued that the success of Equation (1) in predicting behavior of initiators to which it has been applied in extensive experiments tends to support the supposition that a fixed initiation temperature is a real property of an explosive. However, adjustment of the heat capacity and heat loss factor to fit experimental data could mask this difference, so that Equation (1) could be a highly successful empirical relationship without representing the true situation. Although a quantitative analysis will not be undertaken at this point, it is quite clear that this difference in temperatures would be expected to vary greatly with the thermal properties of the initiator system and the kinetic properties of the flash charge material. It is suspected that the choice of the Mk. 1 squib for the extensive experiments in the application of Equation (1)<sup>7</sup> was fortuitous in this respect. Initiators of the characteristics which would comply with Reference 1 and yet fire on a pulse of reasonable energy content might be expected to have larger differences in these temperatures since the combination of a small heat capacity and a large heat loss factor would result in very short cooling times. This difference would be further increased in such systems as short bridgewires and film bridges, in which most of the heat loss is to inert parts rather than the explosive.



Explosives of high activation energy increase their reaction rates more sharply with rising temperatures so that their effective "ignition temperatures" vary less with conditions. Of the commonly used primary explosives, normal lead styphnate has an unusually high activation energy. From this point of view it might be the ideal explosive for use in short bridgewire and film bridges initiators of the kind discussed herein.

It is quite probable that heat transfer considerations account for at least some of the effects which have been related to reaction kinetics. It has been observed<sup>17</sup> that energy requirements for pulse firing of initiators loaded with both lead and silver azide decreased progressively as the loading pressure was increased, so that the average value for explosives pressed at 90,000 pounds per square inch was about one-third of that for the materials pressed at 3,300 pounds per square inch in otherwise identical devices. The only reasonable explanation which occurs to the writer is that the higher thermal conductivity resulting from the higher loading pressure cause a large fraction of the energy delivered to the bridgewire to be transferred to the explosive rather than back to the terminals. It has been shown<sup>15</sup> experimentally that both the increased current requirement and decreased pulse energy requirement which are desirable for purposes with which this report is concerned can be obtained by the use of explosives with high thermal conductivities. The investigation of the effects of explosive composition and loading techniques upon thermal conductivities of primary explosives may be expected to yield data of value in the development and design of improved EEDs.

## SUMMARY

It is possible, by the application of heat transfer considerations as discussed herein, to design electroexplosive devices with a wide range of input characteristics. The relationship between threshold firing power is by no means direct and, in fact, for some circumstances it may be inverse. The full application of the design techniques outlined herein will depend upon the accumulation of more complete data regarding heat transfer properties of primary explosives and the development of techniques for the fabrication of initiators of materials and dimensions indicated by the calculations.

## REFERENCES

- <sup>1</sup>MIL-I-23659(WEP) "Military Specifications, Initiators, Electric, Design and Evaluation of," March, 1963.
- <sup>2</sup>Bowden, F. P., and Yoffe, A. D., "Initiation and Growth of Explosion in Solid Explosives," The Syndics of the Cambridge University Press, Bentley House, London.
- <sup>3</sup>Stresau, R. H., "The Sensitivity of Explosive Initiators," The Journal of the JANAF Fuze Committee," (Joint Army, Navy, Air Force), Serial No. 13.0 dated 13 February, 1958.
- <sup>4</sup>Kabik, I., Stresau, R. H., and Hampton, L. D., "Firing Characteristics of Electric Initiators Made by the Spraymetal Process," NOLM 10771, U. S. Naval Ordnance Laboratory, White Oak, Silver Spring, Maryland, dated 30 March 1952.
- <sup>5</sup>Henkin, H., and McGill, R., "Thermal Sensitivity of Explosives," J. Ind. and Eng. Chem. 48, 1090 (1956).
- <sup>6</sup>Wenograd, Joseph, "The Behavior of Explosives at Very High Temperatures," Proceedings of Third Symposium on Detonation, (Princeton University) ONR Symposium Report, ACR-52, Vol. 1, p. 61, 26-28 Sept, 1960.
- <sup>7</sup>Kabik, I. B., Rosenthal, L. A., and Solem, A. D., "The Response of Electroexplosive Devices to Transient Electrical Pulses," Paper No. 18, Proceedings of Electrical Initiator Symposium, 1960, held at the Franklin Institute, Philadelphia, 29,30 November, 1960, (F-A2446).

- <sup>8</sup>Handbook of Chemistry and Physics (41st Edition, 1959), Chemical Rubber Publishing Co., Cleveland.
- <sup>9</sup>Eschbach, O. W., "Handbook of Engineering Fundamentals," John Wiley & Sons, New York.
- <sup>10</sup>Coler, M., Markit Corporation, 155 Waverley Place, New York, New York, private communication.
- <sup>11</sup>Kabik, I., Chapter on Electric Initiators, Fuze Explosive Train Designers Handbook, NOLR 1111, U. S. Naval Ordnance Laboratory, White Oak, Silver Spring, Maryland.
- <sup>12</sup>Lynch, R. W., and Allen, R. C., "Increased No-Fire Safety with Film Resistor Initiators," Paper No. 7, Proceedings of Electric Initiator Symposium, 1960.
- <sup>13</sup>Austing, J. L., Kennedy, J. E., Stresau, R. H., and Chamberlain D. H., "A Heat Transfer Study of Hot Wire Ignition of Metal-Metal Oxide Mixtures," Paper for Fifth Symposium on Electro-explosive Devices, 1967.
- <sup>14</sup>Melesky, B., and Kabik, I., "The Physical Properties of Explosives and Inert Materials - - -," The Journal of the JANAF Fuze Committee, Serial No. 17.0.
- <sup>15</sup>Stresau, R. H., "Electric Detonators for Navy Guided Missile Applications Experimental Studies of Four Concepts," for the U. S. Naval Ordnance Laboratory, Corona, Calif., 18 Oct. 1966.
- <sup>16</sup>"McDanel Industrial Ceramics, Physical Properties," Bulletin No. D661, McDanel Refractory Porcelain Co., Beaver Falls, Pa.
- <sup>17</sup>Stresau, R. H., and Rowe, M. H., "Observations of the Effects of Loading Density on the Initiation and Growth of Detonation in Azides," NOLTR 61-134, U. S. Naval Ordnance Laboratory, White Oak, Silver Spring, Maryland, 7 December 1961 (Also Paper No. 17, "Proceedings of Electric Initiator Symposium, 1960").

Table 1

## Properties of Metals Used in Bridgewires and Other Components

Metal	Volumetric Specific Heat*		Electrical Resistivity(p)#		Thermal Conductivity(k)	Electro-Thermal (p)microhm watts/°C
	$\frac{\text{ergs}}{\text{°C}} \frac{\text{cu. mil}}{\text{cu. mil}}$	$\frac{\text{ergs}}{\text{°C}} \frac{\text{cyl. mil}}{\text{cyl. mil}}$	milliohm <sup>a</sup> -circ. mils	milliohm <sup>a</sup> -circ. mils/mil	$\frac{\text{milliwatts}}{\text{mil}} \frac{\text{°C}}{\text{°C}}$	
Aluminum	0.534	0.422	1.11	1.46	5.3	5.84
Constantan	0.611	0.481	19.3	24.6	0.57	10.73
Copper	0.672	0.529	0.678	0.862	9.24	6.55
Evanohm <sup>c</sup>	0.597	0.469	52.8	67.2	0.30	20.3
Gold	0.424	0.334	0.96	1.22	7.4	7.2
Inconel	0.600	0.479	39.4	50.1	0.403	15.85
Manganin	0.547	0.431	17.75	22.6	0.55	9.75
Platinum	0.514	0.405	3.94	5.02	1.76	6.93
Pt/Ir, 90/10	0.503	0.397	9.45	12.05	0.79	7.43
Silver	0.432	0.341	0.64	0.817	10.7	6.83
Stainless Steel (309)	0.768	0.603	36.3	46.0	0.73	26.5
Tungsten	0.452	0.356	2.08	2.76	3.7	8.07
Carbon	0.618	0.486	314.0	402.0	0.127	42.7

\*Specific heats given are estimated averages for the range from 0-1000°C

#Resistivities are at 20°C

<sup>a</sup>Resistivity values are given in milliohm mils and milliohm circular mils per mil because the numbers are close to one. For calculations in the suggested units, they should be converted to ohms.

<sup>b</sup>Thermal conductivity values are given in milliwatts/mil because numbers are close to one. For calculations in suggested units, convert to watts.

<sup>c</sup>Evanohm is a proprietary alloy of the Wilbur Driver Company containing 74.5% Nickel, 20.00% Chromium, 2.75% Aluminum and 2.75% Copper. Data from 'Evanohm' booklet prepared by Wilbur B. Driver Company-Newark, New Jersey.

Table 2. Thermal Properties of Some Electrical Insulators

Material	Volumetric	Thermal	Temp. (°C) Melting or Distortion <sup>c</sup>	Max. Cont. <sup>d</sup>	Refer- ences
	Heat Capacity Ergs °C cu. mil	Conductivity Milliwatts mil°C			
Alumina (Al <sub>2</sub> O <sub>3</sub> )	0.46	0.5	2050	1500	9,12
Beryllia (BeO)	0.528	5.3	2530		9
Delrin <sup>r</sup> acetal	0.34	0.0058	160 c	100	14
Epoxy	0.2-0.3	0.004-0.04	120 c	80	9,18
Mica	0.4	0.019			9
Mullite <sup>a</sup>		0.05	1770	1650	9,12
Mylar <sup>r</sup>		0.0038	250 c	150	13,14
Nylon	0.3	0.0058	180 c	150	14
Glass app.	0.35	0.011-0.024		400-500	9
Polyethylene	0.35	0.0085	40-50 c	100	14
Polystyrene	0.32	0.003	70 c	70	14
Phenolics	0.27-0.4	b	160 c	200	9
Porcelain	0.42	0.04		1000	12
Quartz (cryst.)	0.34	0.338 <sup>e</sup>	1756		9
Silica (SiO <sub>2</sub> )	0.27	0.026	1670	1620	9
Silicones	0.27-0.4	0.004		260	9
Teflon <sup>r</sup>	0.37	0.0064	120 c	290	14

<sup>a</sup>Mullite - 3Al<sub>2</sub>O<sub>3</sub>:2SiO<sub>2</sub>, a ceramic available in tubing and other forms

<sup>b</sup>Properties of phenolics depend upon filler

<sup>c</sup>Distortion temperatures are based on arbitrary test conditions. It is difficult to assess their pertinence to EED design.

<sup>d</sup>Maximum continuous service temperatures are based on judgement of persons unknown. They are included, as are the distortion temperatures, for comparison purposes.

<sup>e</sup>Thermal conductivity is given, for quartz, along the "c" axis, highest value in this direction.

3-10 OBSERVATIONS ON THE INITIATION OF  
SECONDARY EXPLOSIVES BY EXPLODING WIRES

Howard S. Leopold

U. S. Naval Ordnance Laboratory  
White Oak, Silver Spring, Maryland

INTRODUCTION

PETN (pentaerythritol tetranitrate) is one of the most commonly used explosives in EBW devices. However, it has limitations as the explosive choice for initiators in some of the new weapon systems. It has fairly low thermal stability (m.p. 141°C) and is considered by some as too sensitive to be used in an in-line fuze train. Therefore, there is increasing interest in the possible use of other insensitive explosives, especially those with good thermal stability and radiation resistance properties.

Explosive characteristics of prime importance to EBW designers are the sensitivity of the explosive to EBW initiation and the explosive's build-up to detonation characteristics. The anticipated increase in voltage necessary for initiation of less sensitive explosives is important since engineering difficulties increase rapidly with rising voltages. The growth to detonation pattern of the explosive should permit use within the limited dimensions characteristic of electrical initiators. Secondary considerations in the

choice of the explosive would naturally include those for any explosive application - that is the safety, reliability, and performance characteristics.

This paper gives preliminary results on some of the considerations necessary for the initiation of secondary explosives other than PETN. Stresau, Hillyer, and Kennedy<sup>1</sup> have demonstrated that the initiation energy can be markedly reduced for the EBW initiation of secondary explosives by the judicious use of confinement. The experiments described in this paper were made to determine what explosives would be practical with an initiator of conventional size in which propagation is mainly dependent upon the stimulus intensity and only to a small degree upon the confinement.

#### EXPERIMENTAL METHODS

The test explosive was loaded in the fixture shown in figure 1. The fixture permits streak camera observation of the growth of explosion along the surface of the explosive in contact with the transparent plastic, as seen through the camera slit. Though the fixture pieces are relatively massive, the confinement is still considered to be relatively weak.

Various firing circuits were employed for different voltage levels in the experiments described. Care was taken to minimize the circuit inductance and resistance for the different units and a 0.6 meter long coaxial transmission cable was used to connect the pulser unit to the test fixture. A streak photograph and oscillogram were taken of each shot to help in the interpretation of the results.

#### EXPERIMENTAL RESULTS

Sensitivity - To start a sensitivity survey, the assumption was initially made that conditions favorable for the initiation of PETN (i.e., bridgewire dimensions, density, small particle size, etc.) would also apply to other secondary test explosives. A capacitor of 1 microfarad<sup>\*</sup> charged to 4000 volts was the energy source for firing. The voltage, though higher than that used in current ordnance units, is still within a reasonable practical working level. As a starting basis, an initial survey was made to determine the EBW sensitivity of various test explosives. Table 1 gives selected properties of the test explosives and table 2 gives the survey results. Out of the explosives

---

\* This size capacitor is used in many practical EBW firing circuits.



tested, eight including PETN could be initiated high order at 4000 volts. When tested at 2000 volts under the same conditions, six of the eight explosives were initiated high order.

Previously, a 2-mil diameter, 75-mil length gold bridge-wire was found optimum with a 1-microfarad capacitor for initiating PETN. When this size wire was used at 4000 volts, the wire exploded during the early portion of the current pulse, making inefficient use of the available energy. Therefore, further tests were run with other wire sizes and some partial results are shown in figure 2. Note that PETN has a voltage minimum with the 2-mil diameter bridgewire. Note also that tetryl which could not be initiated at 4000 volts with the 2-mil diameter bridgewire can now be initiated at lower voltages with larger wires. This shows that the initial assumption that bridgewire dimensions found optimum for PETN are also optimum for other explosives is not valid. Diameter effects of this type have also been reported by Kennedy, Bergmann, and Stresau<sup>2</sup>. EDNA was observed to also have a minimum voltage requirement with the 4-mil diameter bridgewire. Explosives less sensitive than EDNA required voltages too high to be practical. For example, HNS has a minimum 50% firing voltage of 13,000 volts with the 4-mil

diameter bridgewire. DNPN, TACOT, and the five most insensitive explosives tried could not be initiated high order using voltages up to 17,500 volts with a 1-microfarad capacitor.

Since the capacitor-voltage relationship curve for EBW's shown in figure 3, is of the same general shape as it is for hot wire items, the firing voltage if critical can be partially reduced by the use of larger capacitors until the voltage asymptote is reached. Lower voltages, however, will increase the time to burst of the exploding wire. If the amount of stored energy is critical, a burst current<sup>3</sup> can be determined for a specific wire-explosive-confinement combination and Chare's formula<sup>4</sup> can be used to determine the capacitor-voltage-relationship for firing. This relationship can then be used to calculate the capacitance-voltage combination that will require the least amount of stored energy.

The firing voltages can be used as an indication of practicality and should be applicable to firing circuits with similar circuit values. If the circuit capacitance, inductance, or resistance are quite different from the values used herein, the voltage values lose their meaning as a means of comparison.

Growth to Detonation Characteristics - In recent years, the Bruceton test with sample sizes of 100 or less has been shown to give a good mean, but a relatively poor standard deviation.<sup>6</sup> A prevalent practice is to use as a rule of thumb a + 4 or + 5 standard deviation extrapolation from the Bruceton mean as an estimation of the so called "all fire point". While this might be satisfactory for a primary explosive, it should be used with caution with secondary explosives since an "all fire point" may not also give the desired build-up to detonation characteristics. Figure 4 shows the growth to detonation of tetryl at different voltage levels. Bruceton testing of this particular batch of tetryl gave for a 1-microfarad capacitor, a mean of 2,960 volts and a standard deviation of 42 volts. At a test voltage of 3,200 volts which is + 5.5 standard deviations from the mean, the build up to detonation is still typical of what is observed using a marginal initiation stimulus. This build up consists of an initial reaction, not apparent photographically, which undergoes an abrupt transition to a higher velocity at approximately 5-7 microseconds after the wire burst. The other build-up curves show the effect of increasing voltage. The length of the initial reaction in granular explosives varies inversely with the strength of the stimulus. The results

are not peculiar to the EBW stimulus alone, having been found to apply also to other types of initiation.<sup>7</sup>

Figure 5 shows the growth characteristics of HNAB at the 2000- and 4000-volt levels. Although occurring later in time, the reactive wave induced by the weaker stimulus (2.0 kilovolts) reached steady detonation velocity at a shorter distance from the bridgewire than did the wave induced by the 4.0-kilovolts pulse. Although experimental confirmation was not tried, this raises the interesting possibility that if one were measuring output at a distance of 5 to 6 mm from the bridgewire, the more weakly initiated item might possibly have had greater output.

Density Considerations - It is well known that reactions can be more easily established in porous low density charges than in high density charges. The reason appears to be that particles of explosive react by surface burning rather than by homogenous thermal decomposition during the initial stages of propagation.<sup>8</sup> The density used for PETN ( $\sim 0.9 \text{ g/cm}^3$ ) in EBW devices appears to be a compromise between that necessary for resisting practical handling and launching forces and that needed for suitable sensitivity. Since most of the secondary organic explosives have crystal densities similar to that of PETN (usually within  $\pm 0.1 \text{ g/cm}^3$ ) the density used for PETN

appears to be a reasonable value to use for the more insensitive explosives as well. Figure 6 shows the 50% firing voltage-density curve for tetryl. It is similar to that of PETN, indicating that the density assumption is probably applicable to other organic high explosives. The shape of the curve indicates that slight increases in sensitivity can be effected by the use of a lower packing density. Whether or not such lower density charges are still capable of resisting mechanical forces is not known.

When the bulk density is determined by permitting a powdered material to flow freely under standardized conditions into a volumetrically calibrated container, the bulk density decreases with decreasing powder size. Since smaller explosive particles also give faster growths to detonation, the use of finer particles originally appeared to be an attractive means for obtaining a lower packing density. However, as shown in Figure 7, there is an optimum size for the greatest sensitivity. This particle size also required the least amount of energy at densities of 0.7 and 1.1 g/cm<sup>3</sup>. This limits the use of size reduction as a means of increasing EBW sensitivity. Decreasing sensitivity with decreasing size has been reported by Seely,<sup>9</sup> Dinegar, Rochester, and Millican<sup>10</sup> and is believed to be due to changes in size of the interstitial spaces. It appears that changes in crystal habit might provide a more remunerative method of reducing the initiation energy requirement.

## SUMMARY

Several of the more sensitive secondary explosives can be initiated by EBW's without the use of confinement using voltages which appear reasonable for ordnance application. The voltage used should be sufficient to ensure a satisfactory growth to detonation for the desired application. Conditions such as particle size and density found optimum for EBW initiation of PETN appear to also apply to less sensitive explosives. However, the optimum bridgewire size can change with the explosive.

## REFERENCES

1. Stresau, R. H., Hillyer, R. M., and Kennedy, J. E., "Confinement Effects in Exploding Bridgewire Initiation of Detonation", The Fourth Symposium on Detonation, U. S. Naval Ordnance Laboratory, White Oak, Silver Spring, Md., Oct 1965.
2. Kennedy, J. E., Bergmann, E. P., and Stresau, R. H., "Initiation of Insensitive Explosives", TR No. ATL-TDR-64-44, IIT Research Institute, Oct 1964.
3. Tucker, T. J., "Exploding Wire Detonators: The Burst Current Criterion of Detonator Performance" in Exploding Wires, Vol. 3, edited by W. G. Chace and H. K. Moore (Plenum Press, New York, 1964) p 175.

4. Cnare, E. C., "Exploding Wire Detonators: An Approximate Method of Predicting Exploding Wire Detonator-Capacitor Discharge System Performance" in Exploding Wires, Vol. 3, edited by W. G. Chace and H. K. Moore (Plenum Press, New York, 1964) p 185.
5. Hampton, L. D., Ayres, J. N., and Kabik, I., "Estimation of High and Low Probability EED Functioning Levels", Proceedings of Electric Initiator Symposium, Franklin Institute, Oct 1963.
6. Martin, J. W., and Saunders, J., "Bruceton Tests: Results of a Computer Study on Small Sample Accuracy" Proceedings of Electric Initiator Symposium, Franklin Institute, Oct 1963.
7. Jones, E., and Mitchell, D., "Spread of Detonation in High Explosives", Nature 161, 98, 1948.
8. Macek, A., "Sensitivity of Explosives", Chemical Reviews Vol. 62, No. 1, Feb 1962.
9. Seely, L. B., "A Proposed Mechanism for Shock Initiation of Low-Density Granular Explosives", Proceedings of Electric Initiator Symposium, Franklin Institute, Oct 1963.
10. Dinegar, R. H., Rochester, R. H., and Millican, M. S., "Effect of Specific Surface on the Shock Sensitivity of Pressed Granular PETN", Symposium on Explosives and Hazards and Testing of Explosives, Division of Fuel Chemistry, 145th National Meeting of American Chemical Society, New York, 1963.

#### DISCUSSION

Changes in the crystal habit of tetryl can produce a considerable change in its sensitivity.

Table 1 SELECTED PROPERTIES OF TEST EXPLOSIVES

Symbol	Name	Melting Point (°C)	Crystal Density (g/cm <sup>3</sup> )	50% Impact Ht. <sup>1</sup> (cm)
PETN	pentaerythritol tetranitrate	141	1.77	12
TNETB	trinitroethyl trinitrobutyrate	93	1.78	20
RDX	cyclotrimethylene trinitramine	204	1.82	74
DNPN	dinitropropylnitramine	188d	1.73	9-32
HNAB	hexanitroazobenzene	222	1.7	27
DINA	diethylnitramine dinitrate	54	1.70	27
BTNES	bis-trinitroethyl succinate	125	1.68	30
HNH	hexanitroheptane	132	1.70	28-34
HMX	cyclotetramethylenetetranitramine	273	1.90	32
EDNA	ethylenedinitramine	175d	1.71	33
Tetryl	methyltrinitrophenylnitramine	130	1.73	40
HNS	hexanitrostilbene	316	1.74	39-48
DNPTB	dinitropropyl trinitrobutyrate	95	1.68	28-250
TACOT <sup>2</sup>	tetranitrodibenzotetraazapentalene	410d	1.85	85
TNB	trinitrobenzene	121	1.69	103
DIPAM	dipicramide	298	1.79	132
TNT	trinitrotoluene	81	1.65	210
Exp D	ammonium picrate	265d	1.72	235
TATB	triaminotrinitrobenzene	440d	1.94	~320
NQ	nitroguanidine	232	1.72	~320

<sup>1</sup> 2.5 Kg. Wt.

<sup>2</sup> Trade name, E. I. duPont Co.

d = decomposition



Table 2 RESULTS OF EXPLOSIVE SURVEY

Explosive	Particle Size (microns)	Test Density (g/cm <sup>3</sup> )	% of TMD	4000 Volts	2000 Volts
PETN	<44	0.9	51	H.O.	H.O.
TNETB	<44	0.9	51	H.O.	H.O.
RDX	<44	0.9	49	H.O.	H.O.
DNPN	<44	0.9	52	L.O.	-
HNAB	<44	0.9	53	H.O.	H.O.
DINA	<44	0.9	53	H.O.	H.O.
BTNES	<44	0.9	54	H.O.	H.O.
HNH	<44	0.9	53	H.O.	L.O.
HMX	<44	1.1	58	H.O.	L.O.
EDNA	<44	0.9	53	L.O.	-
Tetryl	<44	0.9	53	L.O.	-
HNS	<44	0.9	52	L.O.	-
DNPTB	<44	0.9	54	L.O.	-
TACOT	<44	0.9	49	L.O.	-
TNB	<44	0.9	53	L.O.	-
DIPAM	<44	0.9	50	L.O.	-
TNT	<44	0.9	55	L.O.	-
Exp D	<44	0.9	52	L.O.	-
TATB	<44	0.9	46	L.O.	-
NQ	Unscreenable	0.5, 0.9	29, 52	L.O.	-

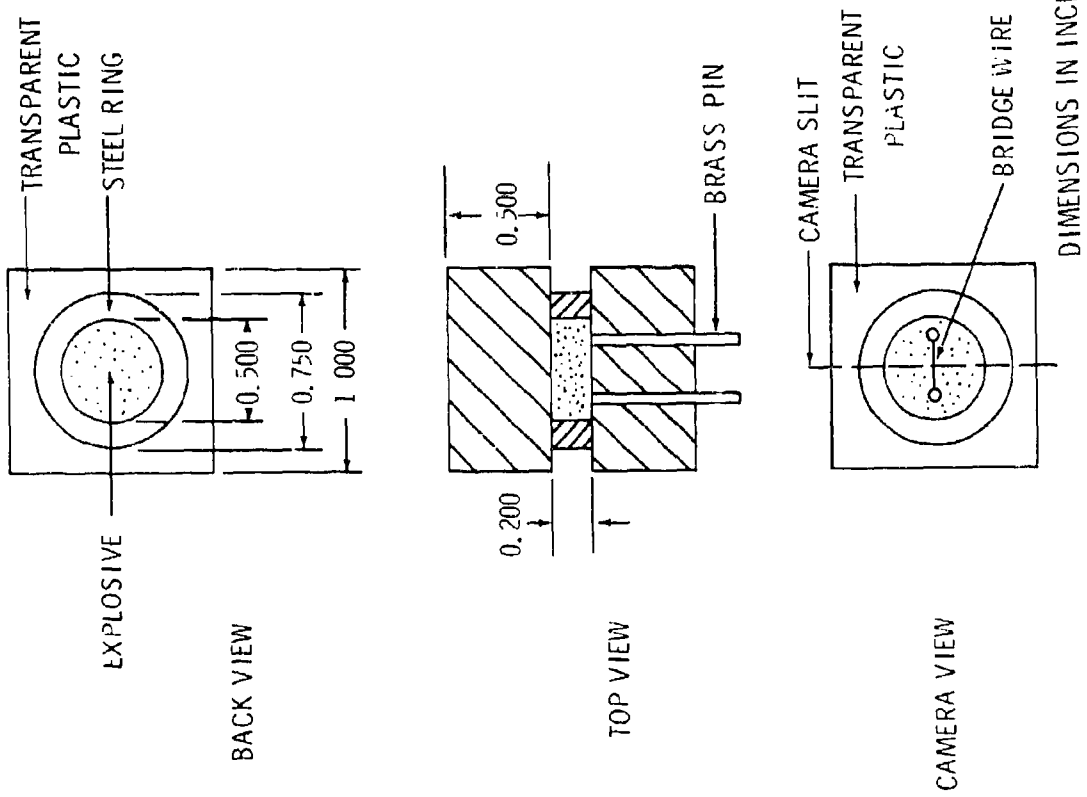
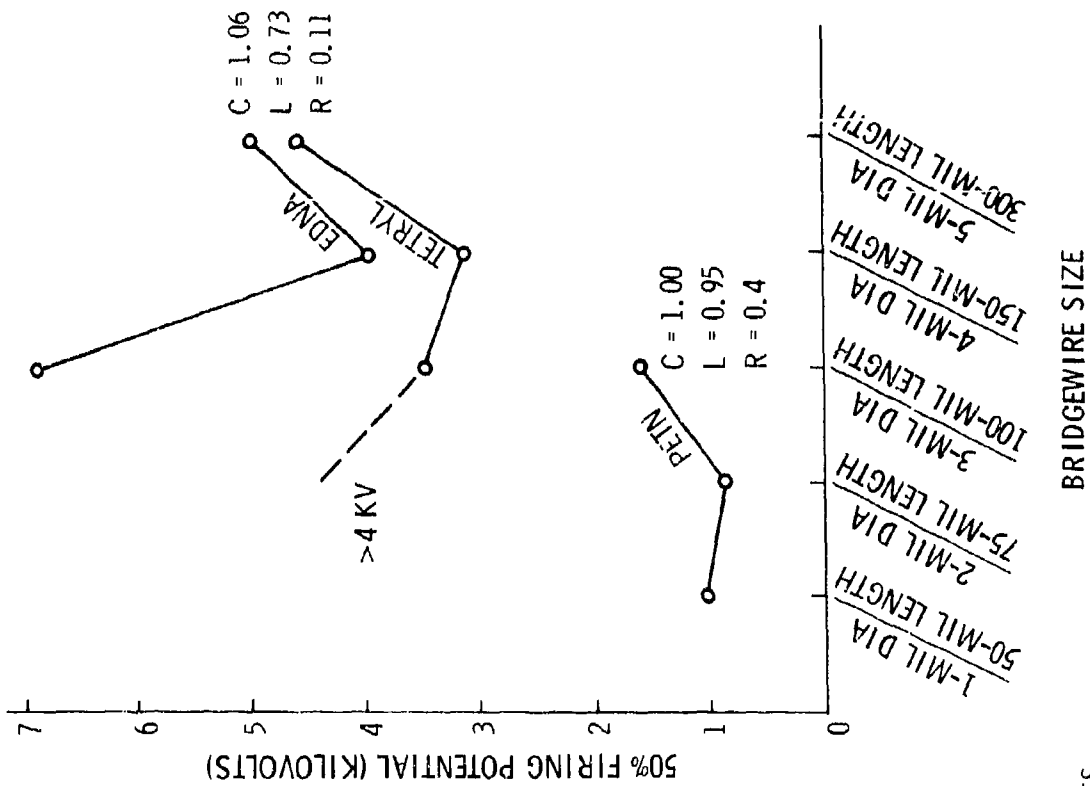


FIG. 2 POTENTIALS NEEDED FOR 50% FIRING WITH A 1-MICROFARAD CAPACITOR

FIG. 1 TEST FIXTURE

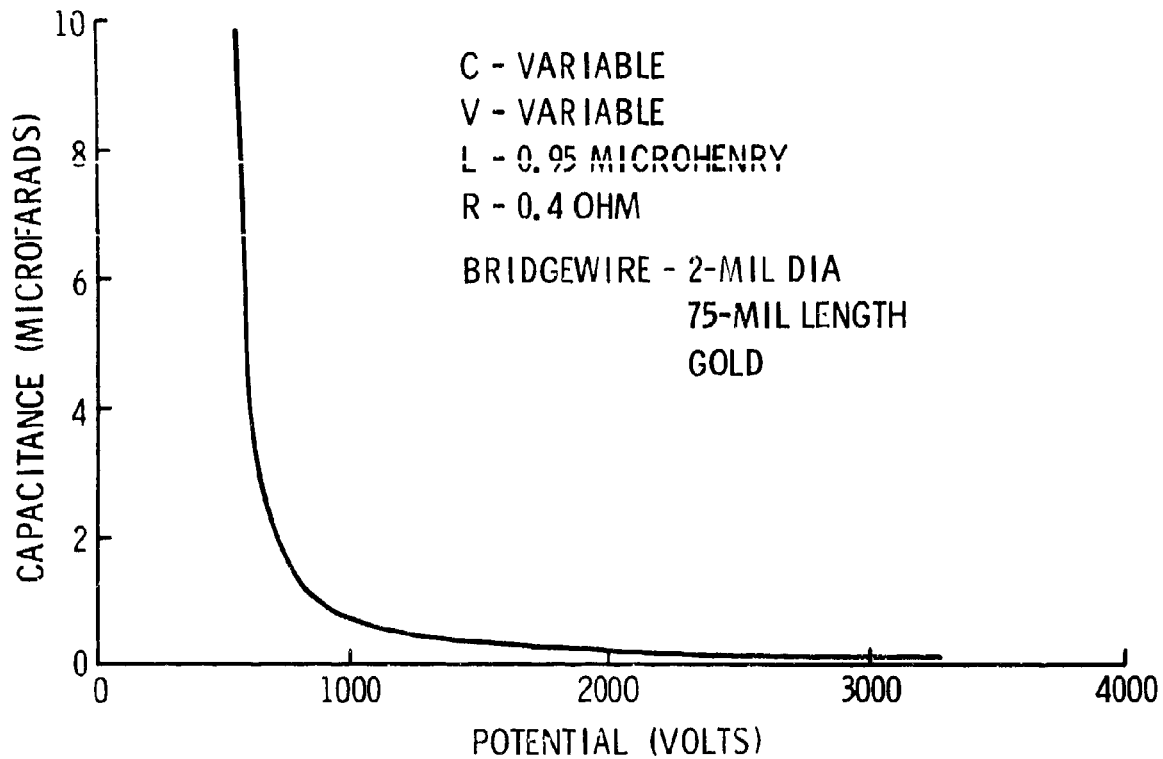


FIG.3 CAPACITANCE-VOLTAGE RELATIONSHIPS FOR 50% FIRING OF PETN

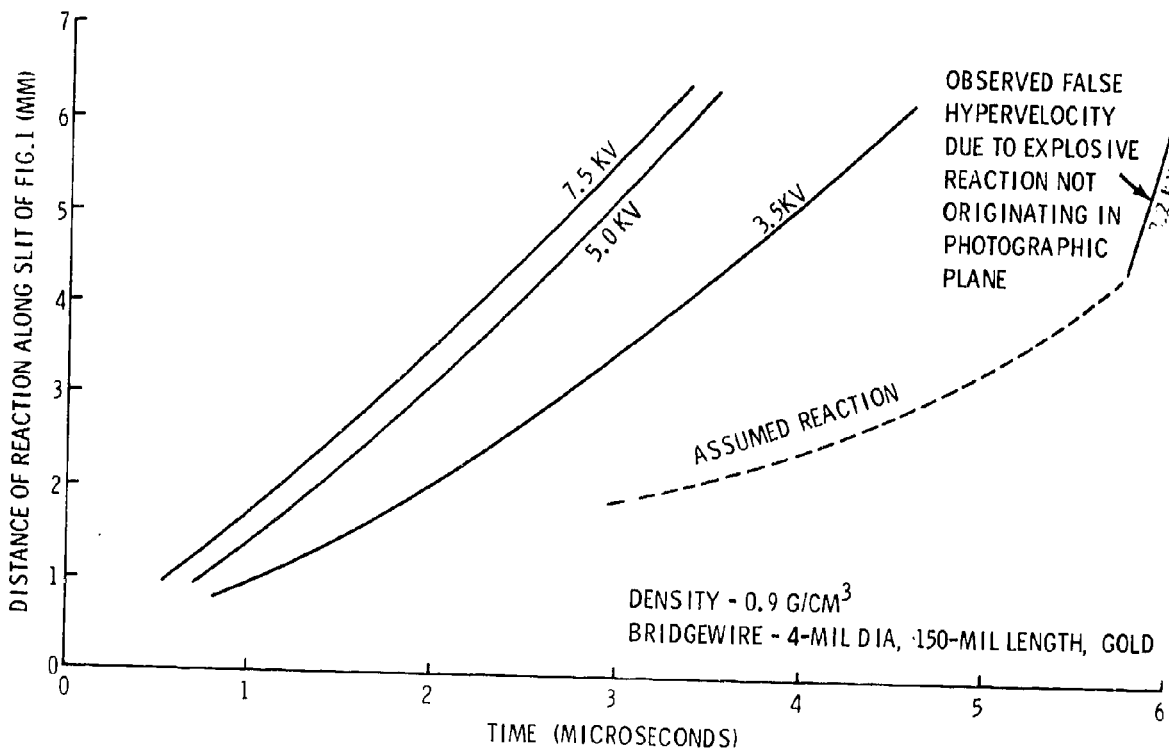


FIG.4 GROWTH OF DETONATION IN TETRYL

3-11 AN APPLICATION OF A THERMAL EXPLOSION CRITERION TO THE  
INITIATION OF EXPLOSIVES BY RAPIDLY HEATED WIRES\*

M.H. Friedman and R.L. McCally

Applied Physics Laboratory, The Johns Hopkins University, Silver Spring, Maryland

The mechanism by which explosives are initiated by embedded exploding wires is complex. The wire transfers both mechanical and thermal energy to the EED charge. One approach to determining which, if either, energy transfer mechanism controls the initiation process is to assume that only one of these mechanisms is operative and to compute an initiation delay on this basis. If the computed delay is significantly longer than that measured experimentally, this would be strong evidence that the alternate energy transfer mechanism cannot be ignored.

In such an analysis, the chemical decomposition kinetics inevitably enter the formulation of the hydrodynamic or thermal transfer equations, which then must be solved numerically. Recently, a relatively simple thermal explosion criterion has been developed<sup>(1)</sup> which obviates recourse to a computer. The purpose of this paper is to present this criterion for the information of the EED community and to illustrate its use in application to EBW initiators.

In the absence of reactant depletion, and transport phenomena other than thermal conduction, the heat equation for an exothermic material which decomposes by an Arrhenius-type process is

---

\* This work supported by the Naval Ordnance Systems Command, Dept. of the Navy under Contract NOW 62-0604-c.

$$C_e \rho_e \frac{\partial T_e}{\partial t} = k_e \nabla^2 T_e + \rho_e Q Z \exp(-E/RT_e) \quad (1)$$

I                      II                      III

where  $C$  = heat capacity,  $\rho$  = density,  $T$  = temperature,  $t$  = time,  $k$  = thermal conductivity,  $Q$  = exothermicity,  $Z$  = frequency factor,  $E$  = activation energy,  $R$  = gas constant,  $\nabla^2$  = Laplacian with respect to the coordinate  $\vec{r}$  and the subscript "e" denotes the explosive. The physicochemical properties of the explosive and the explosion products are taken to be equal and constant. When Term I [II, III] is dropped from Equation (1), the solution for  $T(\vec{r})$  [ $T(t)$ ,  $T(\vec{r}, t)$ ] is the steady-state [adiabatic, inert] solution. When Term III is retained, the solutions thus obtained are usually approximate; the inert solution can frequently be obtained exactly.

The adiabatic solution can be developed for  $RT/E \ll 1$  as (2)

$$t_{o,1} \approx \frac{CRT_o^2}{QZE} \exp(E/RT_o) \left[ 1 + O(RT/E) \right] \Big|_{T=T_1}^{T=T_o} \quad (2)$$

where  $t_{o,1}$  is the time required for the explosive to self-heat from  $T_o$  to  $T_1$ . The "adiabatic explosion time" ( $t_{ad}$ ) can be defined as that time at which  $T_1$  becomes much greater than  $T_o$ ; then the lower limit of the integral becomes negligible and

$$t_{ad}(T_o) \approx \frac{CRT_o^2}{QZE} \exp(E/RT_o) \quad (3)$$

For the given set of initial and boundary conditions which define a particular thermal explosion problem, let the inert solution be  $T_1(\vec{r}, t)$ . Let the uninterrupted duration for which  $T_1$  (the "inert" temperature) exceeds an arbitrary temperature  $T_a$ , at  $\vec{r}$ , be  $t_a(T_a, \vec{r})$ . The function  $t_a$  is normally single valued in  $T_a$ ; though it need not be. The criterion for thermal explosion that was proposed is the satisfaction of Equation (4) at some point  $\vec{r}_a$  within the explosive and for some value of  $T_a$ .

$$t_a(T_a, \vec{r}_a) \geq t_{ad}(T_a) \quad (4)$$

Let  $t_{ra}(T_a, \vec{r})$  be the time required for the "inert" temperature at  $\vec{r}$  to reach  $T_a$ . The "inert" temperature at  $\vec{r}$  remains at  $T_a$  or above until  $t_{ra} + t_a$ ; the explosion time is given by

$$t_e = \min_R [t_{ra} + t_{ad}(T_a)] \quad (5)$$

where  $R$  is the region in  $(T_a, \vec{r})$  - space in which Equation (4) is satisfied.

#### THE HOT WIRE PROBLEM

The problem considered is the following: the region  $0 \leq r \leq b$  is occupied by a metal electrical conductor, and the region  $r > b$  is explosive. Wire end effects are neglected so that the problem is one-dimensional and axially symmetric. At time  $t = 0$ , the metal and explosive are at the same uniform temperature  $T_0$ . At  $t = 0$ , current begins to flow in the metal, heating it at the rate  $B(t)$  calories per cubic centimeter per second. Since the metal diffusivity  $\left( K_m = \frac{k_m}{\rho_m C_m} \right)$  is typically several hundred times as large as the explosive diffusivity, it is assumed that the metal is a perfect heat

conductor. It is also assumed that the metal and explosive are in perfect thermal contact and no phase changes or radiation effects are considered. Then, the time to explosion is found by solving the governing differential equation (1), subject to the following initial and boundary conditions:

$$T_m(0) = T_e(r,0) = T_0 \quad r \geq b \quad (6a)$$

$$T_m(t) = T_e(b,t) \quad t \geq 0 \quad (6b)$$

$$\rho_m C_m \frac{\partial T_e}{\partial t} = B(t) + \frac{2k_e}{b} \frac{\partial T_e}{\partial r} \quad r = b, t \geq 0 \quad (6c)$$

$$\lim_{r \rightarrow \infty} \frac{\partial T_e}{\partial r} = 0 \quad (6d)$$

Explosion occurs when the temperature at some point inside the explosive begins to increase very rapidly because the heat generated by the chemical reaction cannot be conducted away fast enough. This "thermal runaway" is illustrated in Fig. 1. A computer program has been written<sup>(3)</sup> to solve Equation (1) subject to conditions (6) for any explosive-metal combination and any heating function B(t).

To apply the thermal explosion criterion to exploding wire problems, it is necessary in principle to know the complete inert solution  $T_i(r,t)$  to Equations (1) (less Term III) and (6). However, two features of exploding wire heating simplify the problem. First, in consequence of the form of the heating function,  $T_i(b,t) > T_i(r,t)$  for  $t > 0$ ,  $r > b$ , so attention need be directed to only  $T_i(b,t)$ . That is, the thermal explosion criterion predicts

that initiation will always take place at the wire-explosive interface. Second, because the Fourier number  $K_e t/b^2$  at explosion is small, the wire temperature is always nearly identical to that which would obtain were the wire adiabatic. The adiabatic wire temperature is

$$T_{m,ad}(t) = T_0 + \frac{1}{\rho_m C_m} \int_0^t B(\tau) d\tau \quad (7)$$

From the above observations and boundary condition (6b), it is concluded that a satisfactory solution to Equation (5) can be obtained by replacing the function  $T_i(r,t)$  by the considerably simpler  $T_{m,ad}(t)$ .

If the heating function  $B(t)$  is such that the inverse function  $t_{ra}(T_{m,ad})$  is explicit, Equation (5) yields an algebraic equation for  $t_e$ . Usually,  $t_{ra}(T_{m,ad})$  cannot be found explicitly, but the explosion delay can still be determined graphically. For the heating functions characteristic of EBW's, the latter approach is usually required and will be employed here.

A typical exploding wire circuit can be approximated by a series RLC circuit. If a capacitor is charged to a voltage  $V_0$  and allowed to discharge the current in the circuit is

$$i(t) = i_0 e^{-\alpha t} \sin \omega_d t \quad (8)$$



where 
$$i_o = \frac{V_o}{\omega_d l} \quad (8a)$$

$$\omega_d^2 = \omega_o^2 - \alpha^2 \quad (8b)$$

$$\alpha = \frac{R}{2L} \quad (8c)$$

$$\omega_o^2 = \frac{1}{LC} \quad (8d)$$

Then

$$B(t) = \frac{\rho' i_o^2}{JA^2} e^{-2\alpha t} \sin^2 \omega_d t \quad (9)$$

where  $\rho'$  is the resistivity of the wire,  $R = \rho' l/A$  is the resistance,  $l$  the length,  $J = 4.1854$  Joules per calorie and  $A$  is the cross-sectional area. From Eq. (7) the adiabatic wire temperature is

$$T_{m,ad} = T_o + \frac{\rho' i_o^2}{4\rho_m C_m J \omega_o^2 A^2} \left\{ \omega_d^2 \left[ 1 - e^{-2\alpha t} \right] - \left[ 2 \alpha e^{-2\alpha t} \right] \times \left[ \sin \omega_d t \left( \alpha \sin \omega_d t + \omega_d \cos \omega_d t \right) \right] \right\} \quad (10)$$

This obviously cannot be solved explicitly for  $t$ .

The explosion time has been calculated by two methods for a typical EED system consisting of a 2 mil diameter platinum wire 0.10 inch long embedded in pressed PETN. (See Table I for the physical parameters). The first method is rigorous. Equation (1) is integrated numerically subject to the conditions (6) and the heating function (9). This solution will be called the complete solution. The second method is approximate and uses the explosion criterion (5) with the adiabatic wire temperature (10). Figure 2 shows the graphical (approximate) solution for explosion temperature.

The results for explosion time are:

$$\text{Complete } t_e = 2.99 \times 10^{-7} \text{ sec}$$

$$\text{Approximate } t_e = 2.74 \times 10^{-7} \text{ sec.}$$

The two values agree to 8%.

### Discussion

The explosion criterion as applied to the hot wire problem generally predicts explosion times that are shorter than those predicted by the complete solution. The principal reason for this is contained in the definition of adiabatic explosion time. The adiabatic explosion time (3) is the time required for a thermal runaway to occur in an insulated mass of explosive initially at a uniform temperature. In applying the explosion criterion to the hot wire, the adiabatic explosion time for the explosive at  $r = b$  is used. This infinitesimally thin region of explosive is not insulated from its cooler surroundings, in this case the entire mass of explosive not in contact with the wire. In fact, explosion results when the self-heating in a region near the wire overcomes the heat loss to the explosive further from the wire. This obviously requires more time than an adiabatic explosion. The thermal runaway occurring near the wire is shown clearly in Figure 1.

The assumption of an adiabatic wire increases the difference between the approximate and rigorous explosion times because the adiabatic wire temperature is always slightly greater than the interface temperature given by the inert solution. The explosion time based on the inert solution was found

to be  $2.79 \times 10^{-7}$  seconds, which is only 2% greater than the explosion time found when assuming an adiabatic wire.

Finally these calculations consider only the mechanism of heat conduction. The explosion time calculated is the thermal explosion time; i.e., the onset of thermal runaway. It is not the time to detonation, the calculation of which is extremely complex and must involve hydrodynamics. The functioning time of exploding wire detonators is of the order of micro-seconds; <sup>(11)</sup> the calculated thermal explosion time is approximately  $0.3 \mu$  sec. Therefore, no conclusion can be drawn regarding the roles of the thermal and mechanical mechanisms in the initiation process. Certainly, the thermal mechanism cannot be rejected. Further studies are needed. For example, some questions that should be answered are:

1. Does the thermal model predict the observed dependence of explosion time on wire and circuit parameters?
2. What is the effect of thermal contact resistance at the wire-explosive interface?
3. What is the effect of phase changes in the wire and reaction in the explosive, and the consequent variation of electrical and physical parameters with time?
4. How fast and by what mechanism does a thermal explosion grow to detonation?

It is hoped that the techniques presented here will be helpful in answering some of these questions.

#### REFERENCES

1. M.H. Friedman, Comb. and Flame, in press.
2. G.M. Muller and D. Bernstein, "Initiation of Explosives by Internal Heating," Stanford Res. Inst. Rept. 007-60, August 1960.
3. R.L. McCally, Section 111/11b, Research and Development Programs Quarterly Report, July-Sept. 1965, APL/JHU U-RQR/65-1.
4. Ordnance Engineering Design Handbook, RDP 20-177, U.S. Ordnance Corps, 1960.
5. W.R. Tomlinson, Jr., "Properties of Explosives of Military Interest," Picatinny Arsenal Tech. Report 1740. (1958).
6. F.P. Bowden and A.D. Yoffe, Fast Reactions in Solids, Butterworths Scientific Publications, London, 1958.
7. D.L. Ornellas, et. al., Rev. Sci. Instr., 37, 907, (1966).
8. J.A. Brown, Esso Research & Engineering, Private Communication, May 1967.
9. Handbook of Chem. and Physics, 37th Ed. Chemical Rubber Pub. Co., Cleveland, 1955.
10. R. Hultgren, R.L. Orr, P.D. Anderson and K.K. Helly, Selected Values of Thermodynamic Properties of Metals, John Wiley and Sons Inc., 1963.
11. Aerospace Ordnance Handbook, Prentice Hall Inc., Englewood Cliffs, N.J. 1966.

TABLE I  
PHYSICAL PARAMETERS

EXPLOSIVE	-	PETN	REFERENCE
$\rho_e$	=	1.7 gm/cm <sup>3</sup>	(4)
$C_e$	=	0.26 cal/gm - °K	(5)
$k_e$	=	$6.0 \times 10^{-4}$ cal/cm-sec - °K	(6)
Q	=	1490 cal/gm	(7)
Z	=	$3.437 \times 10^{10}$ sec <sup>-1</sup>	(8)
E	=	31.474 kcal/mole	(8)
T <sub>o</sub>	=	300°K	
WIRE	-	PLATINUM	
$\rho_m$	=	21.37 gm/cm <sup>3</sup>	(9)
$C_m$	=	0.0339 cal/gm - °K [300 - 1000°K]	(10)
$\rho'$	=	$25.15 \times 10^{-6}$ ohm - cm [300 - 1000°K]	(9)
b	=	$2.54 \times 10^{-3}$ cm.	
l	=	0.254 cm.	
CIRCUIT			
V <sub>o</sub>	=	2600 volts	(11)
L	=	$0.75 \times 10^{-6}$ henries	
C	=	$0.50 \times 10^{-6}$ farad	

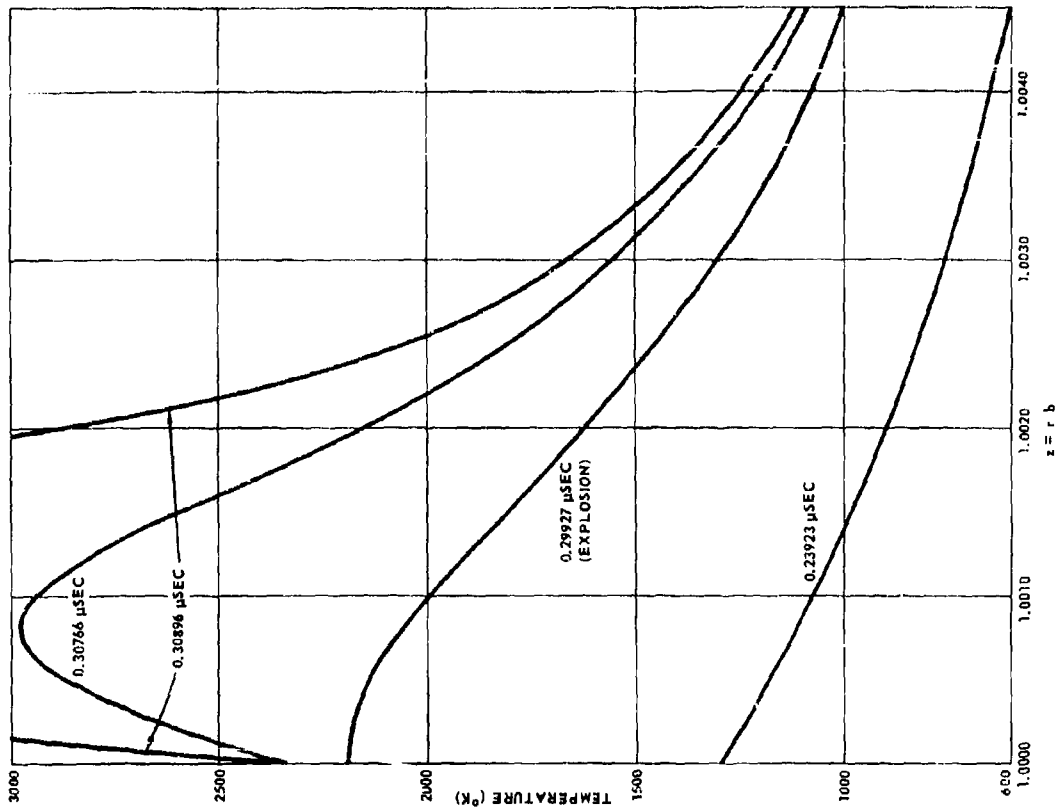


Fig. 1 TEMPERATURE PROFILES FROM COMPLETE SOLUTION

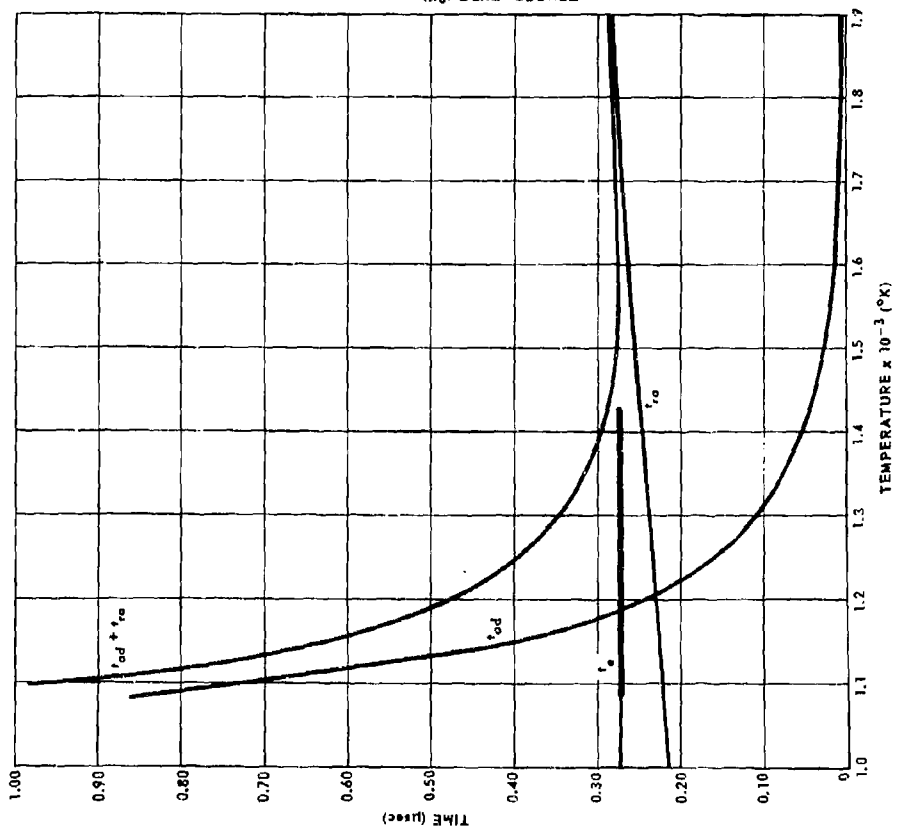


Fig. 2 GRAPHICAL SOLUTION FOR EXPLOSION TIME  $t_e = 0.274 \mu$ SEC

## DISCUSSION

Mr. Stresau: I would like to compliment you on being one of the first people in a long time to apply the thermal explosion theory to EED's. Incidentally, I think in 1954 there was some pretty good quantitative verification of the applicability of this theory to primary explosives. The question is, in these organic (crystalline) explosives as used in EBW applications, what is it that keeps the heat contributed by the reaction from slipping out through all those big interstices that you have in the low density stuff?

Mr. McCally: First of all, this was a simplified mathematical model in which we assumed a rather high density, in fact a pressed density. We did not assume a low density, and we did assume a material, at least for this mathematical model, to be of a constant uniform density.

Mr. Stresau: But the problem is that you cannot make those go off with an exploding wire.

Mr. McCally: I think you can probably at least get charring to occur and this is really the thermal explosion. As I say, we did not study the transit problem. We were studying the initiation problem.

3-12 EBW FIRING UNIT AND DETONATOR  
COMPATIBILITY INVESTIGATION

John M. Reuter  
General Laboratory Associates, Inc.  
Norwich, N. Y.  
and  
Raymond G. Amicone  
Franklin Institute Research Laboratories  
Philadelphia, Pa.

INTRODUCTION

The Saturn IB and Saturn V launch vehicles each use 22 EBW Firing Unit - EBW Detonator systems to perform such function as retro motor ignition, ullage motor ignition and jettison stage separation and destruct. (Slide - Figure 1). The purpose of this joint investigation of FIRL and GLA was to compare the output of the firing unit to the input required by the detonator to determine the reliability that can be expected by the random pairing of production units.

The General Laboratory Associates, Inc. P/N 41496 - 41503 EBW Firing Unit is a solid state electronic device which charges a  $1.0 \pm .1 \mu\text{f}$  capacitor to  $2300 \pm 100$  volts on application of a  $28 \pm 4$  volt DC arming signal. A  $28 \pm 4$  volt DC signal to the trigger circuit discharges this stored energy through a three point spark gap as an exponentially damped sine wave. Output current and time to the first sinusoidal peak must fall within the outline described by Figure 2. (slide). This figure forms part of the NASA specification for the Firing Unit, and was originally obtained by individually varying the lumped R, L, C and voltage parameters of the firing unit output circuit through the full range of their specification tolerances. To determine the firing unit reliability, NASA specified a mean time to failure of 250 hours at a 90% confidence level and a one firing per 15 minute duty cycle. They also specified environmental



conditions, input and output limits, and various other parameters for acceptance and for qualification.

The associated McCormick-Selph P/N 805630 detonator is a 1.4 grain, PETN loaded device with a  $900 \pm 300$  volt protective spark gap in series with a .002" diameter, 0.17 ohm, Secon 443 bridgewire. Functioning time, firing energy, no-fire and all-fire input conditions, operating and storage environments, and other parameters for acceptance and for qualification are specified by NASA. Reliability is specified for this detonator as a 0.1 and a 99.9% all-fire voltage level established at 90% confidence by a Bruceton Test.

Although the detonator and the firing unit are made to meet specified tolerances, this is no guarantee of a specific reliability for the total system unless the tolerances bear some known relevance to the performance criterion.

To give you a ridiculous example - my car is 6 ft. wide and my garage doors are 9 ft. wide. Tolerances on these measurements are tight, considering the dimensions given, but I have lost count of the number of car parking system malfunctions my wife has demonstrated.

Since it was necessary for the establishment of system reliability, a quantitative measurement of firing unit - detonator interface compatibility was required.

#### TEST EQUIPMENT

Aside from normal electrical and mechanical measuring devices, six pieces of equipment were used: steel witness blocks, a variable energy firing unit, an explosion chamber, a low temperature test chamber, a 28 volt DC power supply and a shunt isolator. To obtain quantitative output data, detonations were measured as dents in cold rolled steel (AISI-C1010-B70 to B98 Rockwell) witness blocks.

The variable energy firing unit, shown in Figure 3 (slide), used the same circuitry as a production unit, except that output tank voltage and inductance were variable to give a range of 0.56 to 2.4  $\mu$  second time to peak current and 340 to 7000 peak amperes. This variable energy unit enables us to produce any combination of peak current and time-to-peak that could possibly be delivered by production firing units. This unit, in fact, can produce currents and times well in excess of the above for the extrapolations of this test.

The explosion chamber, also shown in Figure 3, or firing fixture was welded up from 1/4" and 3/8" cold rolled steel, to contain the products of explosion, reduce back pressure on the firing unit cable and to act as a mount for positioning the detonators against the witness blocks.

The low temperature test chamber, shown in Figure 4 (slide), was maintained at  $-65 \pm 1^\circ\text{F}$  and continually purged with dry nitrogen at 0.15 to 0.2 cfm to prevent influx of moisture laden air. This chamber is necessary to comply with a decision to perform the test at the worst case specified temperature condition of  $-65^\circ\text{F}$ .

The 28 volt input was from a 28 volt, 12 ampere battery supply, also on Figure 4, with desirable negligible ripple.

A GLA P/N 42063 shunt isolator was used as a current measuring device for calibration of output at each level. This device consists of a non-inductive .001 ohm load resistor and a transformer converting output current to volts at a 500 amp/volt ratio.

## TEST PROCEDURE

The sensitivity of approximately 800 detonators was tested at  $-65^{\circ}\text{F}$  at four discrete pulse times to peak, 0.57, 0.8, 1.6 and 2.4 microseconds. The detonators were individually mounted on 1/4 inch thick steel plates within the explosion chamber. The detonators were positioned within the chamber so that they butted against the witness block with relatively constant pressure. All detonators, blocks, fixture, etc. soaked at  $-65^{\circ}\text{F}$  for a minimum of 2 hours to stabilize temperature before firing. A stream of dry nitrogen was directed at the cable connector to insure a moisture free fitting.

Approximately 200 detonators were fired at each pulse condition. Five devices were used to zero-in on a voltage reading near the expected 50% firing probability level. This information was used to design a 20 firing Brucceton Test, the results of which were used as a guide for testing at higher voltages to estimate the current for 99.9% all fire at 95% confidence. The Brucceton test, as outlined in the Brucceton Report<sup>1</sup> had pulse condition fixed in four separate tests, with stimulus either raised or lowered by a fixed logarithmic increment of current, depending upon whether the preceding observation was a non-fire or a fire. These results (mean and estimated standard deviation) were used as a guide in selecting test levels for higher firing probability.

Approximately 175 detonators were fired at higher current levels, divided as outlined by Hampton, Ayres and Kabik<sup>2</sup>, to keep the product  $np(1-p)$  approximately constant where (n) is the number of detonators to be fired at the (p) estimated probability level. Where necessary, revisions were made to refine the estimates as the tests proceeded.

Throughout the tests, pulse amplitude and time-to-peak were checked by oscilloscope current photographs and used to calibrate the firing unit panel voltmeter. The current measuring device was a shunt isolator cable termination having a transformation ratio of 500 amperes/volt and a shunt impedance simulating the detonator.

The depth of dent produced in the steel witness blocks was measured with a dial indicator.

### RESULTS

This testing program accumulated data to measure sensitivity in terms of current input to the detonators at four discrete pulse times. This sensitivity was measured as detonator output, which was assessed by observing the depth of dent made in a steel witness block. A large variability was noted in these measurements, which ranged from no measurable dent to .025 inches. The average dent was .018 inches, if those blocks with no dent were disregarded. The skewed distribution of this data, as seen in Figure 5 (slide), makes one question the ability of the detonator to initiate the next element in the explosive train, mild detonating fuse (MDF), when less than all-fire stimuli are used. Some differences are to be expected. Based on the patterns observed with similar devices<sup>3</sup>, we would expect a mean dent depth of .019 inches and a standard deviation of .002 inches to be reasonable values. This assumption would place all those depths .013 inches or less beyond that to be expected from the inherent variation of the detonator, thus we chose to define these no-fires, since there is a possibility that they may not perform the intended function. We cannot guarantee that dent depths .014 inches or greater will always produce the desired result

without a further investigation to correlate dent depth with reliability of initiating the required MDF. The actual output required of the detonator may well be less than .014 inches, also. Further justification for this cut-off point is based on the assumption that all detonator outputs within the range of normal variation will do the job, but anything less than the lower limit of this range will be unsatisfactory.

Two separate estimates of the 99.9% and the 0.1% functioning probability were made, one by the logit<sup>4</sup>, and one by the probit<sup>5</sup> method. Fit of calculated values to experimental data was tested for both methods of analysis and chi square values were comparable, showing no pronounced advantage in either method other than the chi square test for the probit method is based on one more degree of freedom.

An equation for each analysis and for each probability level was written by means of a least squares regression analysis. These equations express the relationship of peak current (I) required for a given probability as a function of time to peak (T), as follows:

#### Probit Analysis

Functioning Probability	Regression Equation
0.1% (95% Conf.)	Log I = 7.052 - 1.341 Log T
50%	Log I = 6.408 - 1.065 Log T
99.9% (95% Conf.)	Log I = 5.867 - 0.828 Log T

#### Logit Analysis

0.1% (95% Conf.)	Log I = 7.215 - 1.404 Log T
50%	Log I = 6.449 - 1.079 Log T
99.9% (95% Conf.)	Log I = 5.682 - 0.754 Log T

The curves resulting from these equations were plotted on the firing unit output diagram as Figure 6 (slide). You will note from the diagram that the logit analysis is more conservative, and because of this, the logit values are used in our

conclusions.

#### CONCLUSIONS AND RECOMMENDATIONS

As Figure 5 (slide) demonstrated, there was a large variability in witness block dent depth and there was a considerably skewed distribution of dent depths, with a large number of low order firings. A possible explanation for this behavior may be that the EBW detonator is inherently dependent on high order detonation of the bridgewire for reliable initiation of its secondary explosive. Electrical stimuli that produce marginal detonation of the wire may result in a wide range of output, depending upon the order of detonation finally achieved in the PETN charge. Since the largest currents in our test were less than the estimated 99.9% all fire current and output does improve as current increases, it may be that there is no cause for concern with respect to detonator output, but data to substantiate reliability of output should be obtained. We have recommended that a study be made of: (1) the output that can be expected as a function of detonator input current over a current range which includes the all-fire level, and (2) the output required to initiate the next element in the explosive train, MDF.

As the all-fire curves of Figure 6 (slide) demonstrated to us, the logit derived 99.9% all-fire line appears near the center of the firing unit output diagram (demonstrate with pointer). This line is actually above 45% of the area in the cited diagram, thus indicating only a 55% probability of finding a production firing unit which will fire 99.9% of the detonators. At least, this is the implication if the full specification tolerances are indicative of production firing units. In fact, however, a data search on all production firing units delivered to the customer, NASA, demonstrated that 95% of them fall above the 99.9% all-fire curve. In addition, both the

firing units and the detonators are used in redundant installations. Conditions were recommended, however, to shift the firing unit output outline up and to the right in the diagram. These included a minor increase in stored voltage and/or in capacitance.

#### ACKNOWLEDGEMENTS

This paper is a summarization of FIRL Report No. F-B2357 and GLA Report No. 349, "EBW Firing Unit - Detonator Compatibility Test", prepared for NASA under Contract No. NAS8-14004, by Raymond G. Amicone, Victor W. Goldie and John M. Reuter.

We gratefully acknowledge the assistances of Messrs. E. E. Hannum, Manager of FIRL Applied Physics Laboratory, Ronald Palmer and Roland Brand of the GLA Electrical Engineering Staff and A. J. O'Connor of the NASA - MSFC Astrionics Laboratory.

#### REFERENCES

1. "Statistical Analysis for a New Procedure in Sensitivity Experiments", July 1, 1944. Prepared by the Statistical Research Group, Princeton University (SRG Report No. 40) for the Applied Mathematics Panel NRDC and Redesignated AMP Report 101.R.
2. "Estimation of High and Low Probability EED Functioning Levels", L. D. Hampton, J. N. Ayres, I. Kabik, U. S. Naval Ordnance Laboratory, White Oak, Silver Spring, Md. Presented at the Electric Initiator Symposium at the Franklin Institute, Philadelphia, Pa., October 1, 1963.

3. "Evaluation of Detonators and Primers", R. G. Amicone and V. W. Goldie, FIRL, Prepared for U. S. Naval Ordnance Laboratory, Corona, California, November 1961, under Contract No. N123 (62738) 23268A.
4. "A Statistically Precise and Relatively Simple Method of Estimating the Bio Assay with Quantal Response, Based on the Logistic Function", J. Berkson, Journal of the American Statistical Association, September, 1953.
5. "Probit Analysis, A Statistical Treatment of the Sigmoid Response Curve", D. J. Finney, Cambridge Press, 1947.

#### DISCUSSION

In reply to a question, the author stated that the study technique was similar to one previously used at McDonnell-Douglas except that the test range was extended to higher output levels and that tests were conducted at  $-65^{\circ}\text{F}$  and that the input values were extended to higher levels. The electrical circuit used was similar to that used in the McDonnell-Douglas test in all measurable parameters. The time to peak was varied by varying inductance and cable length.

In the case of a non-fire, in some instances an attempt was made to determine if the bridge wire had been burned out; in most cases no attempt was made.



EBW FIRING UNIT SATURN APPLICATIONS

SATURN IB		SATURN V	
S-IB	S-IC		
2 - DESTRUCT	2 - DESTRUCT		
8 - S-IB RETRO IGN.	2 - S-IC RETRO IGN.		
2 - S-IB/IVB SEPARATION	2 - S-IC/S-II SEPARATION		
		S-IVB	
S-IVB	S-II		
2 - DESTRUCT	2 - DESTRUCT	2 - DESRTRUCT	
6 - ULLAGE IGNITION	2 - S-II RETRO IGN.	2 - S-IV ULLAGE IGN.	
2 - ULLAGE JETTISON	2 - S-II ULLAGE IGN.	2 - S-IV ULLAGE JETT	
22 TOTAL SATURN IB	2 - S-II/S-IVB SEPARATION		
	2 - S-II SKIRT SEPARATION		
			22 TOTAL SATURN V

FIGURE 1

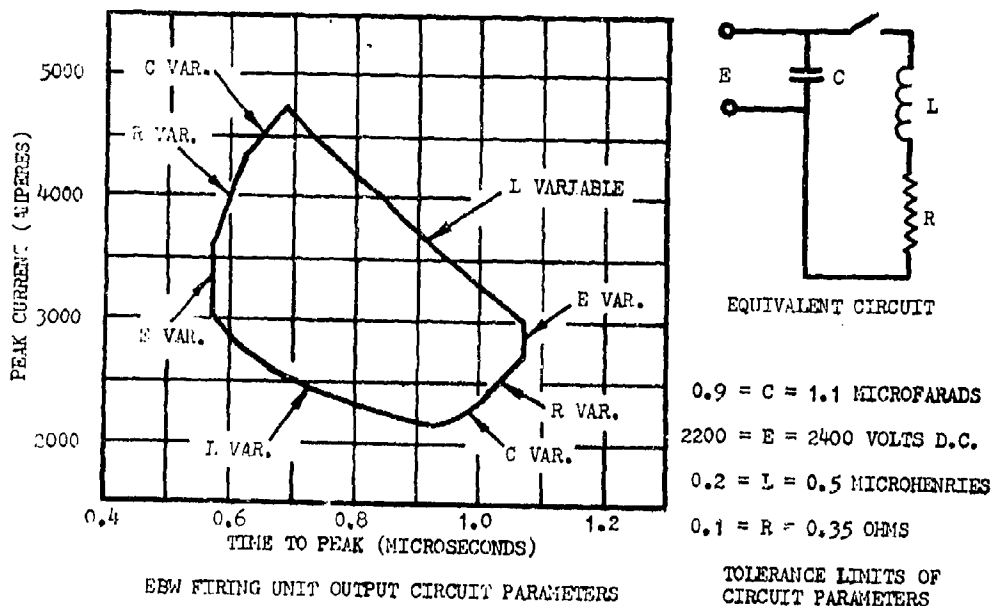


FIGURE 2

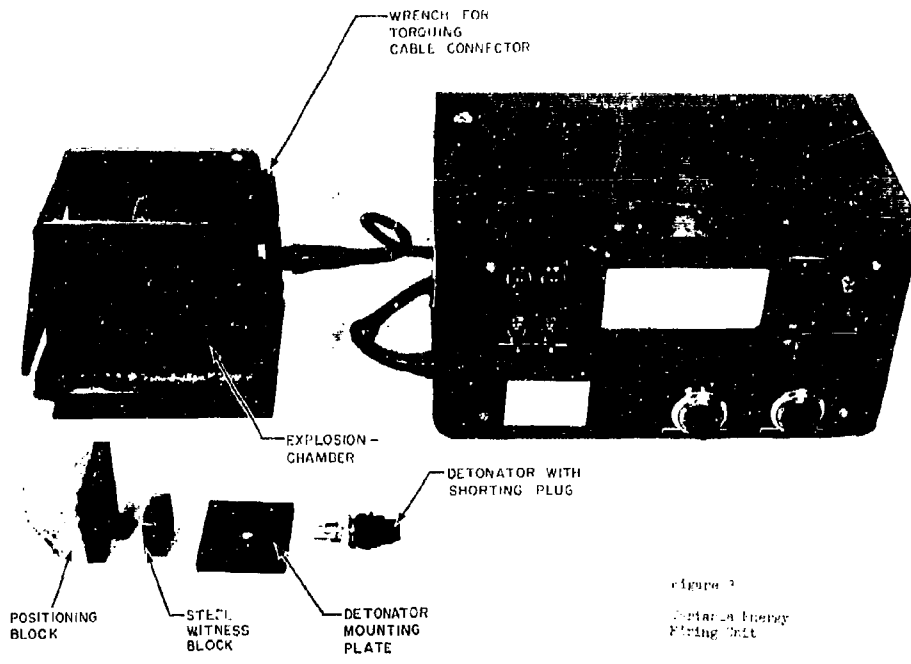


Figure 3  
 Detail of Energy Firing Unit

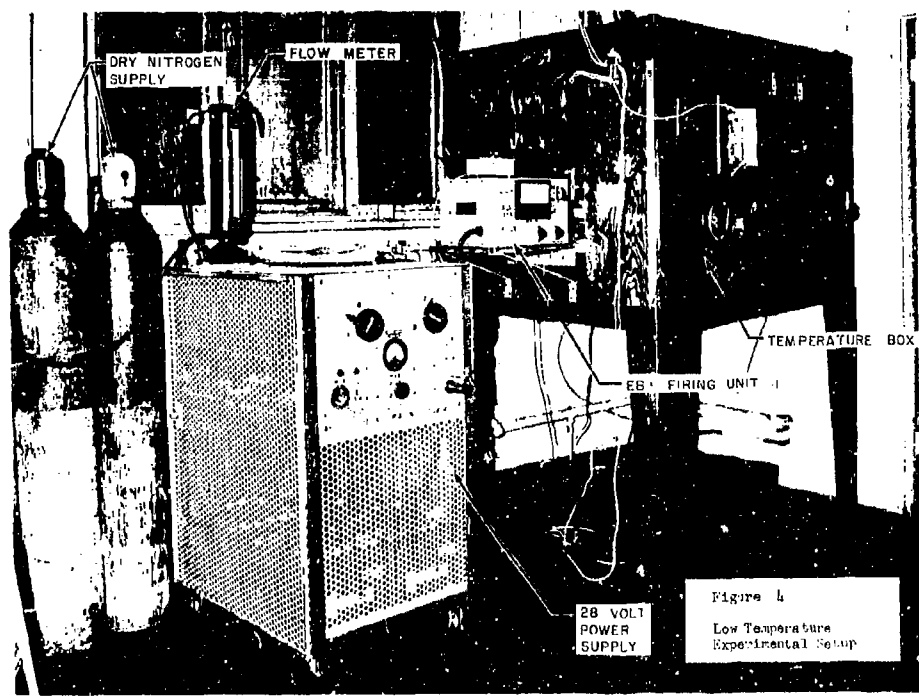


Figure 4  
 Low Temperature Experimental Setup

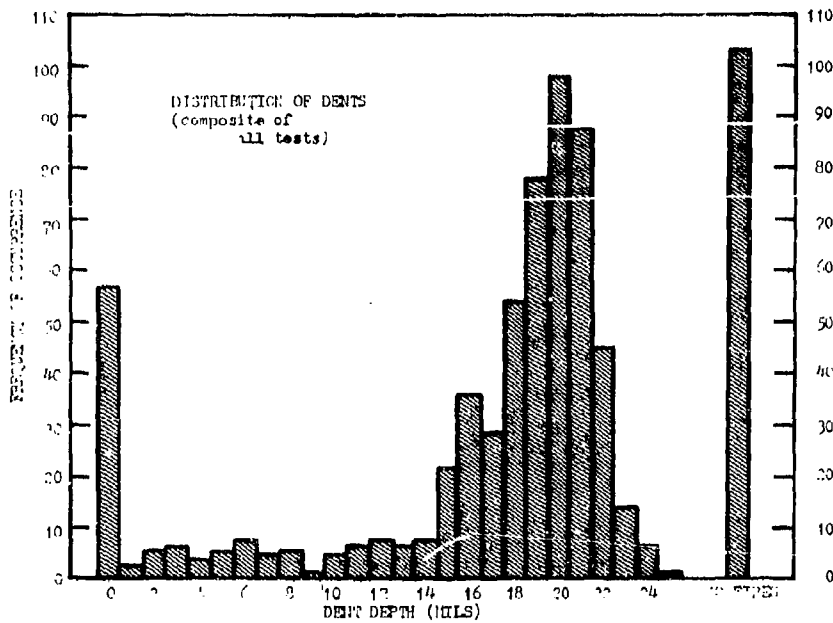
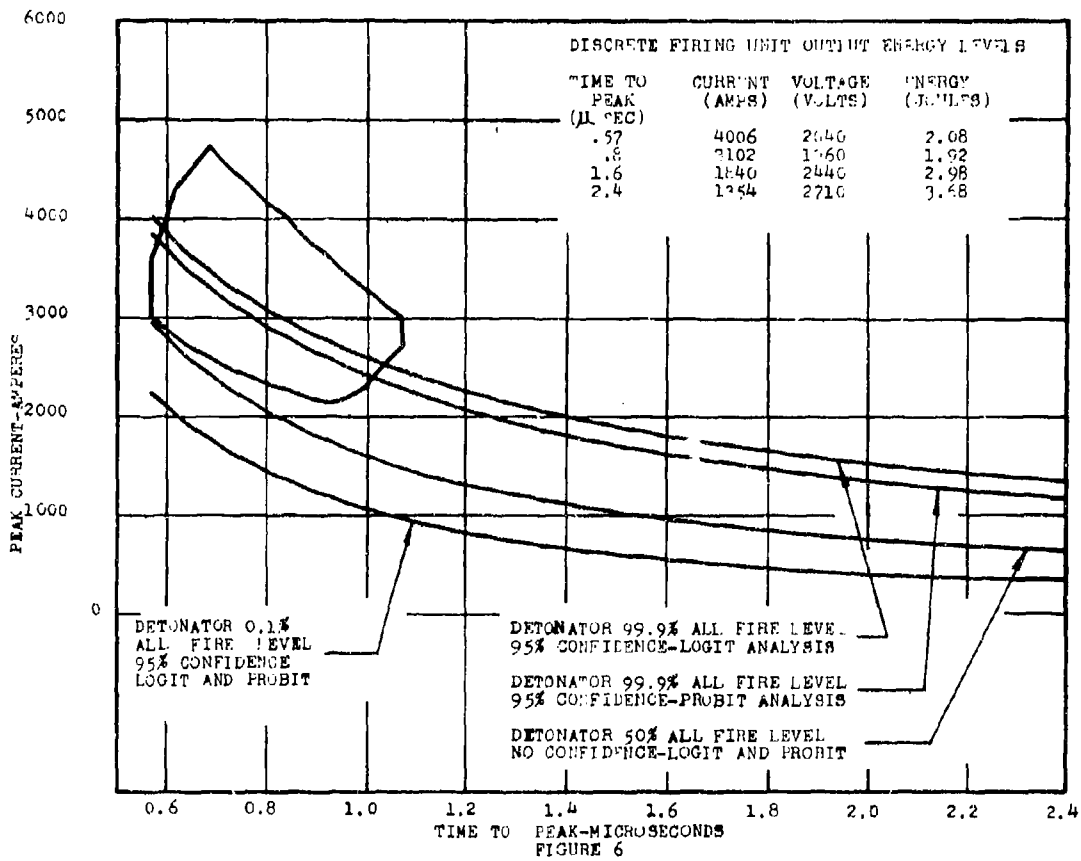


FIGURE 5



ABSTRACTS SESSION FOUR

4-1 The Outlook for Nondestructive Electrothermal Parametric Measurements on Wire-Bridge EED's

J. N. Ayres  
C. W. Goode  
I. Kabik  
L. A. Rosenthal

Numerous techniques have been developed over the years for measuring the thermal time constant heat capacity and heat loss factor of wire-bridge EED's. We find that measurements of these parameters give an understanding of the response of such EED's to various firing signals. However, our hopes that parametric measurements would yield a simple method for classifying EED's from a single production batch into distinct groups of high, intermediate, and low sensitivity have not been realized fully. A more profitable avenue for application of these techniques is during the process of EED manufacture.

4-2 Reactivity of Organic Nitro Compounds

E. E. DeMaris

There is a Military Standard for guiding the mechanical engineer in selecting metals for construction. There is no similar standard for guidance of the explosive train design engineer. This survey of a wide range of organic chemistry defines distinct categories of chemical reactions that must be avoided in the selection of materials for use in stable explosive systems.

4-3P The Design of Sterilizable Pyrotechnic Devices

N. J. Rowman  
E. F. Knippenberg

The use of temperatures in the vicinity of 130 to 145° C for biological sterilization of space vehicles traveling to other planets has resulted in a need to study the ability of explosive devices to withstand the temperature and exposure time of explosive devices to these temperatures. A number of devices currently in use have failed temperature cycles required for sterilization and a number of others have survived the cycle. Materials comprising the electroexplosive devices were examined as well as construction techniques, and certain conclusions are reached concerning their influence on heat sterilizable electroexplosives.

4-4P Information Sources for EED's

Gunther Cohn

Problems with technical information have been with us for some time but they have recently become more acute. This is due to the prolific amount of information recently generated (information explosion). Information centers help a lot but, alas, still none exists for EED's.

For this reason, this paper reviews briefly the useful information sources for EED's. Included are: (1) library tools, (2) mission houses, (3) technical manuals, (4) Engineering Design Handbook series, (5) symposium proceedings, (6) FIRC reports, (7) commercial publications, and (8) reports in publication.

4-5P Instrumentation for Research, Evaluation, and Quality Control of Electroexplosives

C.T. Davey  
W.S. Weiss  
W.J. Dunning

The characteristics of specialized instrumentation for the testing and evaluation of electric initiator sensitivity is presented. Testing from constant current, constant voltage and capacitor discharge is possible with the equipment that is briefly described.

4-6 Comments Relating to Confidence-Reliability  
Combinations for Small-Sample Tests of  
Aerospace Ordnance Items

A. J. Benedict

Analysis epitomized by the widely-used equation " $\gamma$  equals 1 minus R to the nth" is shown to be reasonably appropriate for small-sample tests of aerospace ordnance items; high-reliability, low-confidence combinations are discussed.

4-7 Lot to Lot Variations in Explosive Properties and Their  
Consequences in Explosive Component Development and  
Production

Richard A. Whiting  
James N. Ayres  
Richard H. Stresau

Failure in production functioning tests of items which had been demonstrated to be highly reliable (in design proof tests) is a recurring problem. Such failures are attributable to various factors among which lot to lot variability of explosive properties is among the most difficult to forestall. By economic and logistic necessity specifications must include tolerances in composition and particle size distribution. Only rarely does a specification include requirements regarding sensitivity or output as evidenced by detonation transfer.

4-8 Reliability Assessment of Ordnance Components from  
Variables Performance Parameters

S. Demskey  
V. Goldie  
M. West

The traditional and most widely accepted methods for determining reliability estimates involves the application of the binomial distribution to attribute (go/no go) performance data. Since the variables data is ordinarily recorded, this type of statistical analysis is relatively inefficient.

This report provides a statistical procedure which yields system estimates with multidimensional ordnance components and defines the most widely accepted performance parameters for various types of ordnance components. This in turn provides the means for reducing sample sizes and costs.

4-9 A Mathematical Analysis of Ordnance Circuitry to  
Determine the Susceptibility to Stray RF Fields

Jon E. Klima

This paper presents highlights of a mathematical analysis used to determine the RF ordnance susceptibility of an EED when installed and connected to its firing circuitry. The analysis is applicable to both pin to pin and pin to case modes and provides an upper limit to the RF power delivered to the EED from its firing circuitry. The analysis results can then be compared to EED firing levels and the margin of safety computed.

4-10 Experimental Distribution of Bruceston Test Statistics

Herbert D. Peckham

A set of statistics from sixty-one Bruceston Tests conducted against a particular EED are analyzed. The means of the Bruceston Test are tested for the expected normal distribution. The standard deviations from the Bruceston Tests are observed to have a positively skewed distribution which supports the generally accepted tendency of the Bruceston Test to underestimate the standard deviation. The data, representing hard experimental results, are given more credulity than data generated on computers which may, or may not, represent a true simulation.

4-1 THE OUTLOOK FOR NONDESTRUCTIVE ELECTROTHERMAL  
PARAMETRIC MEASUREMENTS ON WIRE-BRIDGE EED's

J. N. Ayres  
C. W. Goode  
I. Kabik  
L. A. Rosenthal

U. S. Naval Ordnance Laboratory, White Oak, Maryland

1. The following paper is an extension as well as a summary of work that has been carried out under a program to develop a basic understanding of the nature of EED's (electroexplosive devices). Reports and papers by NOL personnel in this and related fields are described in the bibliography, page 18. The work has been limited to non-EBW wire-bridge EED's.

A wire-bridge EED (Figure 1) can be described physically as a thin strand of metal (the bridge wire) attached at each end to support posts and surrounded by an explosive composition. The cross-sectional area of the support posts is much greater than that of the bridge wire, and the wire may or may not be in contact with the substrate or plug structure. An EED is a transducer, transforming an electrical input to an explosive output. It converts electrical energy into heat which raises the bridge temperature. At some critical temperature elevation the explosive will be initiated.

2. Part of the transducer action can be expressed quantitatively using what we term "Electro-Thermal Parameters". These parameters are combined in a simplified lumped-constant model<sup>2</sup>. The model can be expressed as a differential equation:

$$C_p \frac{d\theta}{dt} + \gamma\theta = P(t) \quad (1)$$

3. Whenever a bridgewire is raised above the initial (ambient) EED temperature ( $T_0$ ) by ohmic heating we assume that the support posts and the EED outer boundary will act as semi-infinite heat sinks and will stay at temperature  $T_0$ . The temperature elevation of the bridge wire above ambient,  $T_H - T_0$ , is expressed by  $\theta$ .

4. Heat flows away from the bridge axially into the support posts and radially into material(s) in contact with the bridge wire surface — explosive, air, plug, or substrate. It can easily be shown that heat loss by radiation can be ignored at the temperatures that are apt to be encountered in this type of EED. We use, therefore, the Fourier law of heat conduction — that the rate of heat flow is proportional to the driving temperature (temperature difference,  $\theta$ ). The flow rate proportionality constant is designated by  $\gamma$  and is usually expressed in units of microwatts/ $^{\circ}$ C. In our work we refer to  $\gamma$  as the "Heat Loss Factor". Under steady-state heating conditions (where  $\theta$  is constant and  $\frac{d\theta}{dt}$  disappears) the differential equation reduces to

$$\gamma\theta = P(t) \quad (2)$$

which is a restatement of the First Law of Thermodynamics, i.e., that the (electrical) energy flowing into the system —  $P(t)$  — must be equal to the (heat) energy flowing away —  $\gamma\theta$ .

5. The heat capacity of the bridge wire (including a certain quantity of any substance in contact with the bridge surface) is represented by  $C_p$ . Under adiabatic heating conditions — when the electrical energy goes in so rapidly that the conduction heat losses can be ignored — Equation (1) reduces to

$$C_p \frac{d\theta}{dt} = P(t) \quad (3)$$

If we integrate over the energy-input time,  $t$ , and solve for

$$C_p \text{ we obtain } C_p = \frac{\int_0^t P(t) dt}{\theta} = \frac{E}{\theta} \quad (4)$$

where  $E$  denotes the input energy.  $C_p$ , as defined above, has the dimensions of  $\frac{\text{energy}}{\text{temperature}}$ , and is usually expressed in electrical units — microjoules/ $^{\circ}\text{C}$  or microwatt-seconds/ $^{\circ}\text{C}$ .

6. Since Equation (1) is a simple conduction heat flow equation, we would expect an exponential change of temperature when the input power is applied or removed as a step function. Consider, for instance, the system from the time the power is cut off instantaneously. The bridge wire will be at a temperature elevation  $\theta_0$ , and the heat flow equation will now be

$$C_p \frac{d\theta}{dt} + \gamma\theta = 0 \quad (5)$$

The solution to this equation is

$$\theta = \theta_0 \exp\left[\frac{-t}{\frac{C_p}{\gamma}}\right] = \theta_0 \exp\left(\frac{-t}{\tau}\right) \quad (6)$$

the cooling time constant,  $\tau$ , being equal to the expression  $\frac{C_p}{\gamma}$ .

7. A number of methods have been developed for measuring  $C_p$ ,  $\gamma$ , and  $\tau$ , without damaging the bridge wire/explosive system.\* All of the measurement methods depend on the fact that the bridge wire temperature elevation is deduced from its change in resistance.

$$R_H = R_0 [1 + \alpha(T_H - T_0)] \quad (7)$$

\*See References 2, 3, 7, 15, 20, 21, 27, 30, 32, and 35



When  $T_0 = 0^\circ\text{C}$  [and  $R_0$  and  $\alpha$  have both been measured at  $T_0$ ] this becomes

$$R_H = R_0 [1 + \alpha \theta] \quad (8)$$

Here  $\alpha$  has the units of ohms/ohm/ $^\circ\text{C}$  and is a property of the composition and of the mechanical and thermal history of the wire material.

8. It can easily be shown<sup>13</sup> for any  $T_0$  that the product,  $\alpha R_0$ , is constant for a given EED provided  $\alpha$  and  $R_0$  are both determined at  $T_0$ . Equation (7) can be rewritten as

$$R_H = R_0 + M(T_H - T_0), \text{ or} \quad (9a)$$

$$M = \frac{R_H - R_0}{T_H - T_0} = \frac{\Delta R}{\Delta T} \quad \text{where} \quad (9b)$$

$$M = \alpha R_0 = \alpha R_0. \quad (9c)$$

From the equations we see that  $M$  is the slope of the straight-line graph of resistance vs temperature. We find that  $M$  is an individual EED parameter varying from unit to unit of a batch of EED's in much the same way that  $R_0$ ,  $C_p$ ,  $\gamma$ , and  $\tau$  vary.

#### RESOLUTION AND ACCURACY

9. The resolving power of any of the non-destructive methods for measuring  $\alpha$ ,  $M$ ,  $\gamma$ ,  $C_p$ , and  $\tau$  depends upon the magnitude of the resistance change compared to the detection sensitivity of the equipment. The resistance change depends upon the bridge wire material and the temperature swing. For non-destructive testing it is desirable to limit the upper temperature to about  $75^\circ\text{C}$  (the upper limit of MIL-STD-304). To increase the temperature

swing it is possible to set the lower limit below normal room temperature by use of a cold box. As a consequence the usable  $\Delta T$  is normally in the order of 50 to 80°C.

10. Figure 2 presents the relationship between resistance change, wire bridge material, and  $\Delta T$ . For example, an 80°C temperature change ( $\Delta T$ ) will produce, in a platinum iridium alloy of the type used in the Mk 1 Squib ( $\alpha \approx 1000 \mu\text{ohms}/\text{ohm}/^\circ\text{C}$ ), a resistance change ( $\Delta R/R$ ) of 0.08. That is, the signal ( $\Delta R$ ) will be 8% of the ambient EED bridge resistance.

11.  $M$  and  $\alpha$  are determined by measuring  $R_H$ ,  $T_H$ ,  $R_0$ , and  $T_0$ . If  $M$  and  $\alpha$  are going to be determined to  $\approx 3\%$  accuracy, the temperatures must be measured to two or three tenths of a degree and the resistances to one part in a thousand or better for platinum-iridium. For tungsten the accuracy of the resistance measurement could be relaxed to three parts in a thousand, and for a nichrome wire such as is used in the M-100 Match the accuracy would need to be bettered to about one part in three thousand. We have found that the determination of  $M$  and  $\alpha$  is by far the most difficult of any of the electrothermal parameters, requiring very careful laboratory procedures<sup>21</sup>.

12. A number of methods for the determination of  $\gamma$ ,  $C_p$ , and  $\tau$  have been developed which depend upon measuring a transient  $\Delta R$ . The absolute value of  $R_H$  (or  $R_0$ ) is either not needed as precisely or else not needed at all. In general  $\gamma$ ,  $C_p$ , and  $\tau$  are more easily measured than  $M$  and  $\alpha$ . Replicate measurements have been made both on Mk 1 Squibs and M-100 Matches. They showed that the

experimental error was about 3% for both  $\gamma$  and  $C_p$  for the Mk 1 Squib; and about 6% for  $\gamma$  and 3% for  $C_p$  for the M-100 Match. Because  $\alpha$  is so much higher for the Mk 1 Squib than for the M-100 Match, the errors for the latter would be surprisingly low except that an improved<sup>90</sup> low-frequency thermal follow bridge with better resolution had been developed by the time this work was undertaken.

13. We have noted a trend towards bridge wires with very low values of  $\alpha$ , such as Evenohm and Constantan. Apparently the designer's intent is to come up with an EED whose load on the firing circuit will be constant until firing occurs. With such materials there is no chance of sensing the bridge wire temperature change since the resistance change will be negligible. We suggest that in order to exploit these non-destructive measurements of the electrothermal parameters, the EED should be optimized to facilitate such measurements. One direction for design optimization is to choose high  $\alpha$  materials, such as tungsten or other pure refractory or noble metals. (In general alloying of a metal will sharply reduce its  $\alpha$ .)

14. But even with the present EED designs determinations of  $C_p$ ,  $\gamma$ , and  $\tau$  can be made simple enough to perform on a routine basis. By such sophistications as servo circuits, digital conversion, and shared-time digital computer links it is possible to make a single instrument which would measure and compute the above parameters (assuming a fixed M) within a few seconds after the EED is connected to the instrument.

## APPLICATIONS

Three ways of using electrothermal parameters have been studied:

- a. Predicting EED response to a specific input.
- b. Sorting a group of EED's into sensitivity categories.
- c. Quality control techniques.

### Prediction

15. The response of a particular type of EED to a specific electrical input can be predicted by use of Equation (1). An example will show how the technique is used.

WILL A MK 1 SQUIB AT AMBIENT TEMPERATURE BE FIRED

BY A 20-MICROSECOND, 13-AMPERE CONSTANT CURRENT PULSE?

Typical data for the Mk 1 Squib are:

$$R_0 = 1 \text{ ohm}$$

$$\tau = 8 \text{ milliseconds}$$

$$M = 950 \text{ } \mu\text{ohms}/^\circ\text{C}$$

$$C_p = 7 \text{ } \mu\text{joules}/^\circ\text{C}$$

$$T_0 = 20^\circ\text{C}.$$

We know by experiment for a pulse input short compared to the EED thermal time constant that the bridge resistance will increase

linearly with time. Consequently the effective resistance is

$\frac{R_0 + R_H}{2}$ . Equation (1) becomes

$$C_p \frac{d\theta}{dt} + \gamma\theta = I^2 \frac{R_H + R_0}{2}. \quad (10)$$

Also we know that conduction heat losses in such a short time\* can be ignored. Cancelling the middle term, separating variables,

\*The maximum per cent error introduced by this assumption will be  $\frac{100t}{\tau}$  where  $t < 0.1\tau$ .

and integrating between zero and t gives

$$\theta C_p = I^2 \left( \frac{R_H + R_0}{2} \right) t \quad (11)$$

arranging the expression

$$M = \frac{\Delta R}{\Delta T} = \frac{R_H - R_0}{\theta}, \text{ and substituting it into Equation (9) gives}$$

$$\theta = \frac{I^2 R_0 t}{C_p - \frac{1}{2} I^2 M t} \quad (12)$$

$$\theta = \frac{(13)^2 (1) (20 \times 10^{-8})}{7 \times 10^{-8} - 0.5 (13^2) (950 \times 10^{-8}) (20 \times 10^{-8})}$$

$$= 626^\circ \text{C.}$$

Both by applying Bowden's "hot spot theory" and from actual experiment we find that  $\theta$  necessary for firing will be in the order of 450 to 500°C. The answer to the question is, therefore, yes with a high probability.

16. The denominator of Equation (12),  $C_p - \frac{1}{2} I^2 M t$ , incorporates a heat feed-back term,  $\frac{1}{2} I^2 M t$ . The effect of this can be seen by repeating the above computations with everything the same except halving the time to 10 microseconds;  $\theta$  comes out to be 272°C rather than 313 which would be expected in a linear relationship.

#### Sorting

17. We can measure M,  $C_p$ , and  $\gamma$  on individual units of a group of EED's. We can then apply the prediction techniques just mentioned to compute the temperature to be expected for each EED when subjected to a specific input. The units with the highest predicted temperatures should be the most sensitive of the group to the specific input signal\* Merely by classifying according to

\*An EED with the highest sensitivity to a given input signal is not necessarily the most sensitive to a different input signal.

the predicted temperatures it should be possible to sort the group into sub-groups of differing sensitivities.

18. We tried to sort both Mk 1 Squibs and M-100 Matches<sup>21</sup>. Out of 210 Mk 1 Squibs three groups were selected for sensitivity testing under a constant current input of long duration. The two extreme groups were fired with a fail being defined as a non-response after 10 seconds at the test level. The results were:

Group	Prediction	Linear-Logistic Firing Points		No. of Units Fired
		%	Milliamperes	
a	Greater Sensitivity (Less current)	5	259.1	51
		50	266.8	
		95	274.4	
b	Lesser Sensitivity (More current)	5	271.5	30
		50	277.0	
		95	282.5	

19. The probability that such a shift in the mean could have been observed, had the two groups been taken from a single population, is only 1 in 200. We can therefore say that a statistically significant sorting was achieved. From an engineering standpoint this sorting would not be particularly useful since the difference between the two means is less than 5% and because the upper and lower distributions are not distinct from each other.

20. The remaining Mk 1 Squibs were subdivided into three groups on the basis of response to an adiabatic input and fired with a

50 microsecond variable amplitude constant current input. The energy delivered into each EED was measured from the oscilloscope records. The most sensitive group (23 units) had a sensitivity of 1.30 millijoules; the least (23 units) 1.44 millijoules. However, the standard deviations were so large that, statistically, there was no significant difference between the groups. While disappointing, this answer was not wholly unexpected with such small sample sizes.

21. A constant current sorting and long duration firing was tried with M-100 Matches. There were  $\approx$  32 units per subgroup. In addition an unsorted sample of EED's from the parent group was also fired as a control.

Group	Prediction	Test Results (milliamperes)	
		50% Point	
L	Least sensitive	352	7.1
M	Intermediate	350	6.8
H	Most sensitive	347	5.4
-----		-----	
	Control	348	14.1

22. The sensitivity trend of the sorted groups is in the right direction. But the standard deviations are so large that there is no real difference between any of the groups. Perhaps the really notable result here is that the sorted groups have significantly smaller standard deviations than the parent group. This seems a reasonable outcome.

23. The ultimate goal of this effort was to isolate a subgroup of EED's made up of the very sensitive portion of normal EED's. With EED's as they are currently made this objective does not seem to be attainable. The inherent variability of well-made EED's is not apt to be very great — a standard deviation being just a few per cent of the mean. In order to make a definitive sort and in order to minimize misclassification (i.e. including a unit that should have been excluded, or vice versa) the total experimental error should be less than 1/10th of the standard deviation of the parameter's distribution. For the Mk 1 Squib this would mean that the experimental error should not exceed 0.3 to 0.8%. However, (based on such indications as drift of  $R_0$  with time) the squib may have inherent dimensional instability which would make such accuracy impossible.

24. One of the intended uses for sorting of EED's into sensitivity groups was that the most sensitive group could be used in Go/No-Go systems tests such as exposure to radar fields. The reasoning here is that if the very sensitive units were not initiated then the tactical units would most certainly not be initiated. The logic is valid. However, to obtain Go/No-Go system test results which will give an indication of how much margin of safety there is, it is necessary to test with EED's which are considerably more sensitive (by a factor of three, or five, or ten). This large a sensitivity ratio is needed to compensate for uncontrollable variations in system circuitry, components, and environment. From the Mk 1 Squib firing data we can only expect that the sensitivity



ratio might be only 1.1 or 1.15 instead of the desired 3.

#### Quality Control

25. Since the electrothermal parameters measure factors which relate directly to the sensitivity of EED's it is quite obvious that they should be useful in improving uniformity of product during manufacture. Bridge wire resistance has been the only measurable parameter which in any way reflected the nature of the bridge wire. But even this measurement cannot be interpreted unequivocally. A high resistance can arise either from "too long" or "too thin" a bridge. Conversely, a low resistance can indicate either "too short" or "too fat" a bridge. It is possible to have a whole family of bridges of identical resistance which would be either (a) both larger in diameter and longer, or (b) else both smaller in diameter and shorter. Case (b) would give rise to a more sensitive EED (adiabatically because the mass is less, and at steady state because cross-section and surface areas are less) while (a) would be less sensitive.

26. Our approach is to measure  $R_0$ ,  $\gamma$ , and  $C_p$  before loading and then measure  $\nu$  and  $C_p$  with material in contact with the bridge wire.  $C_p$  is primarily a function of the mass of the bridge wire -- increasing with increasing bridge length and/or diameter.  $\gamma$  is a function of the surface and cross-section areas of the bridge and, particularly after loading, of the thermal conductivity of the material in contact with the bridge. Instead of controlling  $R$  only, a more uniform bridge wire will be obtained by controlling  $C_p$  and  $\gamma$  as well. This is so because variations in diameter and

length (whether occurring individually or simultaneously) will affect the three parameters in different ways. There is no way that the diameter and length can be out of control if all three parameters are used to set acceptance limits.

27. But the best is yet to come. The electrothermal parameters can be used to detect the presence of the explosive on the bridge wire. This statement is based in part on the experimental results<sup>20,24</sup> described below:

Ten Mk 1 Squibs were tested on the Low Frequency Thermal Follow Bridge (at 10 Hertz) measuring  $C_p$ ,  $\gamma$ , and  $\tau$  under the following sets of conditions:

- a. As received condition; 100 milliamperes.
- b. Explosive dissolved away from bridge wire; 100 milliamperes.
- c. Bridge wire covered with distilled water; 100 milliamperes.
- d. Same as step (b) except current is adjusted until bridge wire resistances (and therefore dynamic equilibrium temperatures) are the same as in step (a).
- e. Same as step (c); currents adjusted to match step (a) resistances.

28. The results were:

(see next page)

Treatment	Power (milliwatts)	$\gamma$ ( $\mu$ watts/ $^{\circ}$ C)	$C_p$ ( $\mu$ wattsec/ $^{\circ}$ C)	$\tau$ (millisec)	Environment
a	10.38	1430	6.96	4.86	Explosive
b	10.66	330	4.07	12.38	Air
c	10.18	5660	20.95	3.71	Water
d	5.11	312	4.10	13.39	Air
e	58.1	6164	20.74	3.37	Water

Here it can be seen that both  $\gamma$  and  $C_p$  increase as we go from an air environment to explosive to water. The shift in  $\gamma$  is particularly marked and is in the right direction.  $C_p$  also increases which is also in accordance with theory. Note that the change in  $\tau$  does not follow the same pattern.

29. That the shifts in  $\gamma$  and  $C_p$  are not only large but also clearly discernible under the three environments can be seen from the observed limits for the data at 100 milliamperes through the bridge wire.

	$\gamma$			$C_p$		
	min	avg	max	min	avg	max
air	316	330	347	3.84	4.07	4.32
explosive	1287	1430	1569	6.31	6.96	7.27
water	5335	5660	5900	17.41	20.95	25.70

This leads to the idea of following the values of  $\gamma$  and  $C_p$  during manufacture in three steps:

- a. Bare bridge (in air)
- b. Bare bridge (in vacuum or in water)
- c. Loaded bridge (after thorough drying of the bridge structure if step b is done in water).

From these three sets of values it appears possible to come up with enough simultaneous equations<sup>21</sup> to make a first-order approximation of the thermal conductivity of the explosive. Such a computation would be of interest to serve as a check on the process but would not very likely be useful in a quality control procedure.

30. The general quality control scheme that we would recommend is as follows:

- a. From a pilot group of EED's determine an average  $M$  (or average  $\alpha$ ). Also determine average  $R$ ,  $\gamma$ , and  $C_p$  and their standard deviation on the bare bridge, and then in the loaded state\*.
- b. From the observed means and standard deviation on  $R$ ,  $\gamma$ , and  $C_p$  compute acceptance bands for testing all EED's in the different conditions using the  $M$  (or average  $\alpha$ ) obtained on the control group.

31. Undoubtedly the setting of the acceptance bands will have to be a cut-and-try process, at least at first. If the bands are set too close nothing will get through. But information can be obtained which will help in deciding whether or not the acceptance bands are properly set; those falling outside the limits are presumably less reliable or at least differ from the desired norm. The rejects should be collected and fired under conditions appropriate to the reason for rejection.

---

\*Whether or not a third condition such as bare bridge in vacuum or in water will give information worth the extra effort is a moot point.

32. Certainly the above quality control testing program would not be economically feasible for 10-cent detonators. But there has been some utilization of these techniques on a production-line 100% inspection basis, the readings being taken by ordnance workers trained to operate the equipment. And, if as has been previously suggested, the measurements can be fully automated, the effort to carry out this phase of a quality control program would not be very large when compared to all the other operations that are now customary in the inspection of the more sophisticated EED's.

33. Word has come to us of independent work being carried out at another laboratory where groups of EED's have been run through the thermal-follow bridge and then given a standard firing signal. Most of the units had values for the electrothermal parameters that fell closely together. The ones with abnormal readings fell outside of the acceptable firing time limits.

#### CONCLUSIONS

34. This is a sketchy presentation of our findings and current views. Detailed descriptions of our experimental work and instrumentation can be found in the works referenced in the bibliography.

35. We find that electrothermal parameter measurements can be used as a tool in the design of EED's and in systems analysis of EED's and EED firing circuits. Sorting of EED's does not seem to be a profitable venture. It may be that refined designs of EED's wherein resistance drift and dimensional instabilities have been minimized would make sorting feasible. But again, the precise

laboratory techniques that would have to be used might negate any real advantage in this type of work.

36. The most promising application is the use of these measurements during EED manufacture to detect anomalous bridge structures and to assure uniformity of explosive loading. In times past we have encountered supposedly high-quality EED's which never would have fired — no flash charge in one case, and water in the first-fire mix in another instance. Such gross defects would have been detected by these techniques. Whether or not loading with the wrong explosive or an inert material could be detected is rather doubtful but should not be discounted altogether.

37. Finally, we would propound the idea of designing EED's which are optimized for making electrothermal parameter measurements. We suspect that such optimization may, in some instances, lead directly to better EED designs. In any case, it would make simpler the application of these measurement techniques to the production of EED's with the goals of obtaining a higher quality EED and demonstrating that it has the higher quality.

REF ID: A66666

BIBLIOGRAPHY OF NOL-AUTHORED DOCUMENTS

Copies of reports listed below may be requested from the Defense Documentation Center, Cameron Station, Alexandria, Va. 22314 by citing the AD number, where provided.

- (1) NAVORD Report 4322 AD 120180 "A Discussion of the Mechanism of Initiation of Electrically Fired Explosive Devices by Electro-Magnetically Propagated Energy", by James N. Ayres, 28 Jun 1956.
- (2) NAVORD Report 6684 AD 230917 "Electro-Thermal Equations for Electro-Explosive Devices", by L. A. Rosenthal, 15 Aug 1959.
- (3) NAVORD Report 6691 AD 231918 "The Harmonic Generation Technique for the Determination of Thermal Characteristics of Wire Bridges used in Electro-Explosive Devices", by L. A. Rosenthal, 9 Sep 1959.
- (4) NAVORD Report 6826 "Characterization of the Mk 1 Mod 0 Squib: Impedance Measurements in the Frequency Range 50-1500 Megacycles", by R.M.H. Wyatt, 31 May 1960.
- (5) NAVWEPS Report 7308 AD 253541 "Characterization of Squib Mk 1 Mod 0: Capacitor Discharge Sensitivity Instrumentation", by J. N. Ayres, 10 Jan 1961.
- (6) NAVWEPS Report 7309 AD 252791 "Characterization of Squib Mk 1 Mod 0: 5 Megacycle RF Burst Sensitivity", by L. Green, C. Goode, 16 Dec 1960.
- (7) NAVWEPS Report 7313 AD 252372 "A Cooling Curve Generator and Its Application to Electro-Explosive Device Studies", by L. A. Rosenthal, 15 Dec 1960.
- (8) NAVWEPS Report 7347 AD 254516 "Characterization of Squib Mk 1 Mod 0: Determination of the Statistical Model", by L. D. Hampton, J. N. Ayres, 30 Jan 1961.
- (9) NAVWEPS Report 7354 AD 255723 "A Radio-Frequency Burst Source for Electro-Explosive Device Testing", by L. A. Rosenthal, 27 Jan 1961.

- (10) NOLTR 61-20 AD 262719 "The Response of Electro-Explosive Devices to Transient Electrical Pulses", by I. Kabik, L. A. Rosenthal, A. Solem, 17 Apr 1961.
- (11) NOLTR 61-24 AD 262720 "Characterization of Squib Mk 1 Mod 0: 5 Megacycle RF Sensitivity for Long Duration Pulses", by C. Goode, I. Kabik, 24 Apr 1961.
- (12) NOLTR 61-108 AD 267876 "Characterization of Squib Mk 1 Mod 0: Thermal Stacking from Radar-Like Pulses", by L. D. Hampton, J. N. Ayres, 15 Sep 1961.
- (13) NOLTR 61-154 AD 277792 "Comments on the Temperature Coefficient of Resistance as Used in Wire Bridge Electro-Explosive Device Analysis", by J. N. Ayres, 1 Nov 1961.
- (14) NOLTR 62-77 AD 293846 "Characterization of Squib Mk 1 Mod 0: Sensitivity to 9 KMC Radar Pulses", by I. Kabik, C. Goode, 31 Aug 1962.
- (15) NOLTR 62-205 AD 409852 "Non-Linear Bridge for Measuring Electro-Thermal Characteristics of Bridge Wires", by L. A. Rosenthal, 5 Mar 1963.
- (16) NOLTR 63-133 AD 426466 "The Prediction of Very Low EED Functioning Levels", by J. N. Ayres, L. D. Hampton, I. Kabik, 4 Sep 1963.
- (17) NOLTR 63-266 AD 434821 "Estimation of High and Low Probability EED Functioning Levels", by L. D. Hampton, J. N. Ayres, I. Kabik, 3 Feb 1964.
- (18) NOLTR 64-117 AD 451120 "Characterization of Squib Mk 1 Mod 0: Sensitivity to 9 GC Radar in the Near Field", by G. P. Carver, 28 Sep 1964.
- (19) NOLTR 64-238 AD 622199 "Maximum Likelihood Logistic Analysis of Scattered Go/No-Go (Quantal) Data", by L. D. Hampton, G. D. Blum, 26 Aug 1965.
- (20) NOLTR 66-113 "A Low-Frequency Thermal Follow Bridge for Measuring the Electro-Thermal Parameters of Bridge Wires", J. N. Ayres, L. A. Rosenthal, R. A. Maio, 17 Mar 1967.
- (21) NOLTR 66-114 "Interpretation of Electro-Thermal Measurements on Wire Bridge Electro-Explosive Devices (EED's)", by J. N. Ayres, to be published.
- (22) NOLTR 66-117 "Monte Carlo Investigations of Small-Sample Bruceton Tests", by L. D. Hampton, 17 Feb 1967.
- (23) NOLTR 66-129 "Logistic Analysis of Bruceton Data", by L.D.Hampton, G. D. Blum, J. N. Ayres, to be published.
- (24) NOLTR 66-182 "Approximation Method for Fixing Wire Bridge EED's at Constant Power", J. N. Ayres, 3 Feb 1967.



- (25) "Ergometer Measures Burst of Energy", by L. A. Rosenthal. Published in Electronics, June 1958.
- (26) 4th Navy Science Symposium on Naval Problems in Electro-Magnetic Radiation", ONR-6, Vol. 1, AD 320772. "The Response of Electro-Explosive Devices to Transient Electrical Pulses", by I. Kabik, L. A. Rosenthal, A. D. Solem, Mar 1960.
- (27) "Generator Delivers Constant Current or Voltage Pulses", by L. A. Rosenthal, published in Electronics, September 1960.
- (28) Proceedings of Electric Initiator Symposium, 1960. Prepared by The Franklin Institute. AD 323117. "The Response of Electro-Explosive Devices to Transient Electrical Pulses", by I. Kabik, L. A. Rosenthal, A. D. Solem, November 1960.
- (29) Proceedings of HERO Congress, 1961. Prepared by The Franklin Institute. AD 326263. "Characterization of Wire Bridge Electro-Explosive Devices", by I. Kabik, J. N. Ayres, A. D. Solem, May 1961.
- (30) "Thermal Response of Bridgewires used in Electro-Explosive Devices", by L. A. Rosenthal, published in The Review of Scientific Instruments, Vol. 32, No. 9, September 1961.
- (31) Proceedings of Second HERO Congress, 1963. Prepared by The Franklin Institute. AD 420595. "The Prediction of Very-Low EED Firing Probabilities", by J. N. Ayres, L. D. Hampton, I. Kabik, Apr-May 1963.
- (32) "Electro-thermal Measurements of Bridgewires used in Electro-Explosive Devices", by L. A. Rosenthal, published in IEEE Trans. on Instrumentation and Measurement, Vol. IM-12, No.1, June 1963.
- (33) Proceedings of Electric Initiator Symposium, 1963. Prepared by The Franklin Institute. AD 440764. "Estimation of High and Low Probability EED Functioning Levels", by L. D. Hampton, J. N. Ayres, I. Kabik, October 1963.
- (34) Proceedings of the Tenth Conference on the Design of Experiments in Army Research Development and Testing, November 1964; sponsored by the Army Mathematics Steering Committee on behalf of the Office of the Chief of Research and Development. "Explosive Safety and Reliability Estimates from a Limited Size Sample", by J. N. Ayres, L. D. Hampton, I. Kabik, pp.261 to 281.
- (35) "Nonlinear Bridges for Electro-thermal Measurements", by L. A. Rosenthal, published in the Review of Scientific Instruments, Vol. 36, No.8, 1179-1182, August 1965.

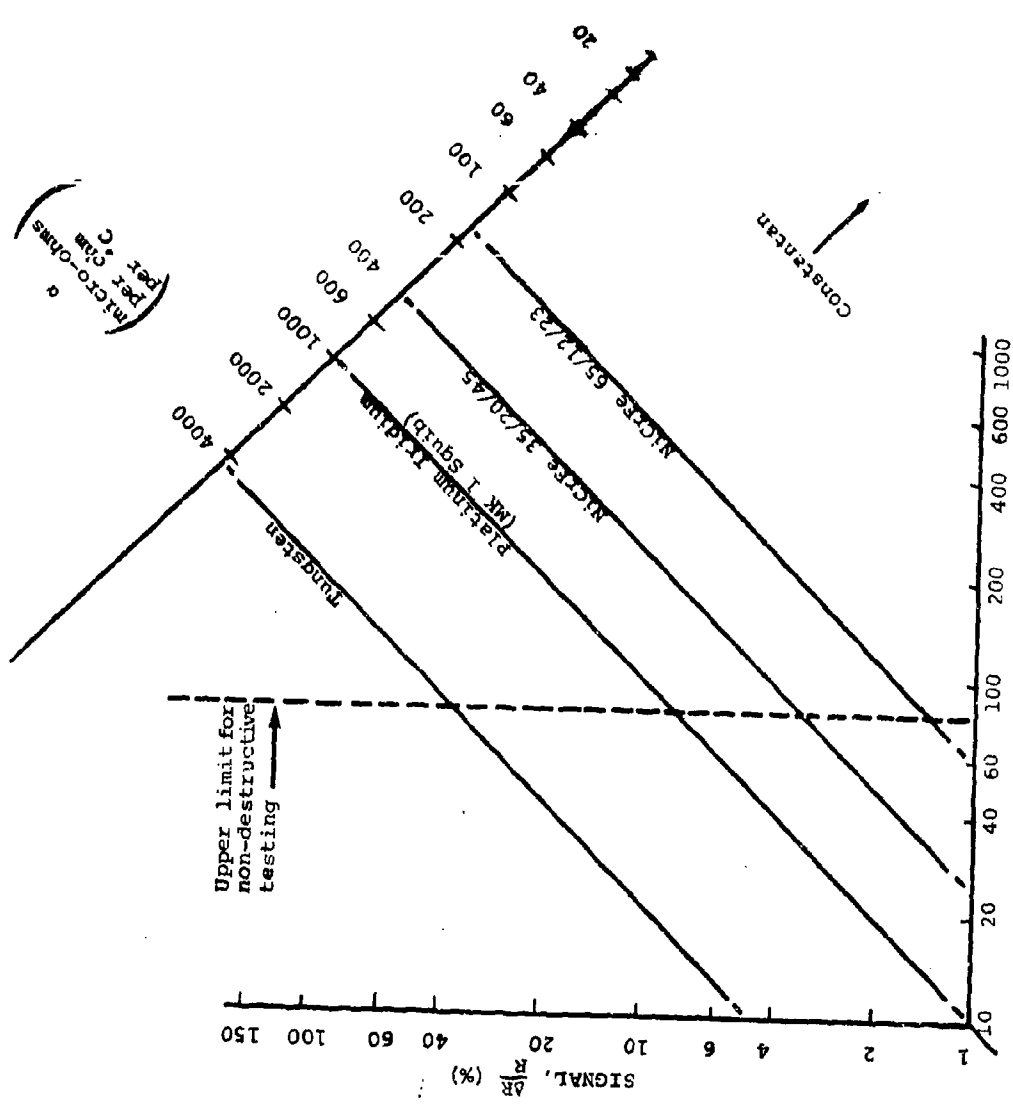


FIG. 2 SIGNAL SIZE AS A FUNCTION OF TEMPERATURE SWING AND BRIDGE WIRE TEMPERATURE COEFFICIENT OF RESISTIVITY.

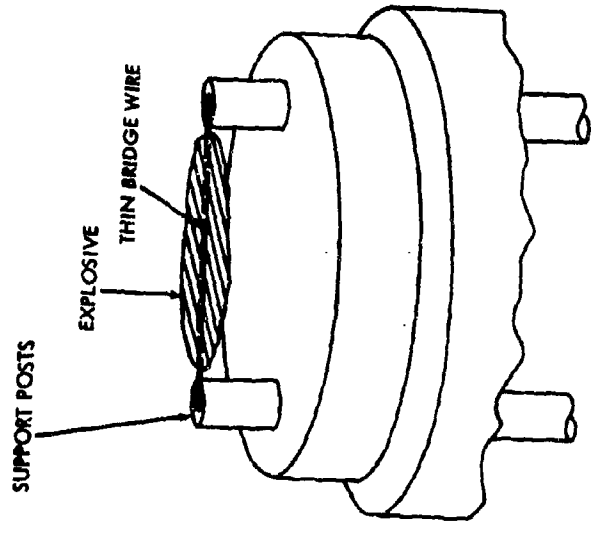


FIG. 1 SCHEMATIC OF BRIDGE WIRE FEED

## DISCUSSION

The author agreed that devices sorted in the manner advocated in this paper probably had a truncated distribution, and that the performance of the lot could not thereafter be described by the distribution parameter. The advantage of the proposed system is that it will permit rapid detection of those unusual defects which are not normally a part of the production process.

When straight primary explosives are loaded and fired by capacitor discharge, this method of analysis permits prediction of the firing time with good accuracy. When the initiators are loaded with some of the metal oxidant type mixtures, the firing time prediction is expected to be more difficult.

In the formulas, the expression  $c_p$  is used to indicate the heat capacity of the type of EED being evaluated. This expression is a property of that particular geometry.

## 4-2 REACTIVITY OF ORGANIC NITRO COMPOUNDS

By: E. E. DeMaris

GENERAL ELECTRIC COMPANY  
RE-ENTRY SYSTEMS DEPARTMENT  
Philadelphia, Pa.

### ABSTRACT

There is a Military Standard for guiding the engineer in selecting compatible metals for construction. There is no similar standard for guidance of the explosive train design engineer. This survey of a wide range of organic chemistry defines distinct categories of chemical reactions that must be avoided in the selection of materials for use in stable explosive systems. Both elevated temperature and extended storage stability can be designed into a device when reactive combinations of materials are avoided.

### I. PHYSICAL MEASUREMENTS

The underlying reasons for the reactivity of organic nitro compounds can best be seen by examining the physical constants of simple nitro compounds. The dipole moments give a good quantitative indication of the electron withdrawing character of the nitro group.

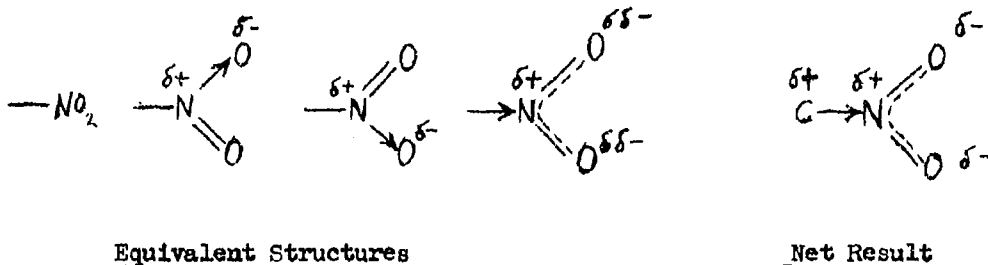
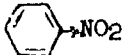
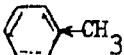
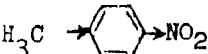
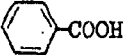
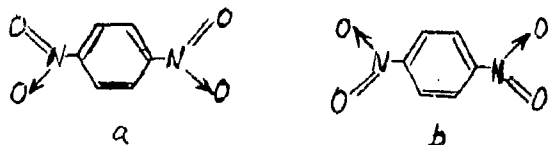


TABLE I

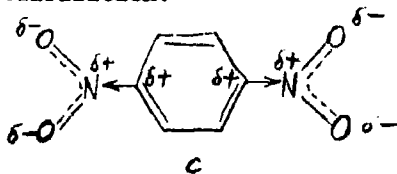
DIPOLE MOMENTS OF SUBSTITUTED BENZENE (1) AND ALIPHATICS (2)

<u>Substituted Benzene</u>	<u>Dipole Moment</u>
	3.97 (4.27) <sub>gas</sub>
	0.41
	4.40
	1.0
<u>Aliphatic Compounds</u>	
$\text{CH}_3 \rightarrow \text{NO}_2$	3.44
$\text{C}_4\text{H}_9 \rightarrow \text{NO}_2$	3.59

The  $\text{NO}_2$  group is accepted as being symmetrical about the N atom since paradinitro benzene has a dipole moment of 0.0.



The true structure is a resonance hybrid intermediate (c) between the structures a and b with internal polarization.

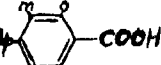
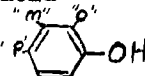


4-2.2

Further evidence of the influence of nitro groups on reactivity can be found in the acid strength of different compounds in solution.

TABLE II

DISSOCIATION CONSTANTS OF (1)  
AROMATIC AND ALIPHATIC ACIDS (1) (3)

	$\frac{K}{P}$	$\frac{K}{K}$	$\frac{[H]^+}{[H]^+} ** \left( \frac{[H]^+}{[H]^+} = .0000001 \right)$ Water @ 25°C
p toluic acid	4.36	$436 \times 10^{-5}$	.0066
benzoic acid 	4.19	$645 \times 10^{-5}$	.0081
o nitro benzoic acid	2.16	$6.9 \times 10^{-3}$	.083
m nitro benzoic acid	3.47	$3.4 \times 10^{-4}$	.0184
p nitro benzoic acid	3.41	$3.9 \times 10^{-4}$	.0198
aci - nitro ethane 23°C	4.4	$4.0 \times 10^{-5}$ (4)	.0063
acetic acid	4.75	$1.78 \times 10^{-5}$	.0042
phenol 	9.89	$1.29 \times 10^{-10}$	.0000114
o - nitrophenol	7.17	$6.75 \times 10^{-8}$	.00027
op dinitrophenol	40	$1 \times 10^{-4}$	.01
trinitrophenol (picric acid)	0.38	$4.17 \times 10^{-1}$	.6
Oxalic acid	1.23	$5.9 \times 10^{-2}$	.24

\*\* acid concentration of 1 molar solution of the compound in water.

The nitro group has the strongest effect on the ortho position in benzene derivatives. The electron withdrawing effect is cumulative as can be seen from the mono, di, and tri nitro phenols. Picric acid is a strong acid ionizing almost completely in water solutions. Because of this acidity its use is now generally avoided.

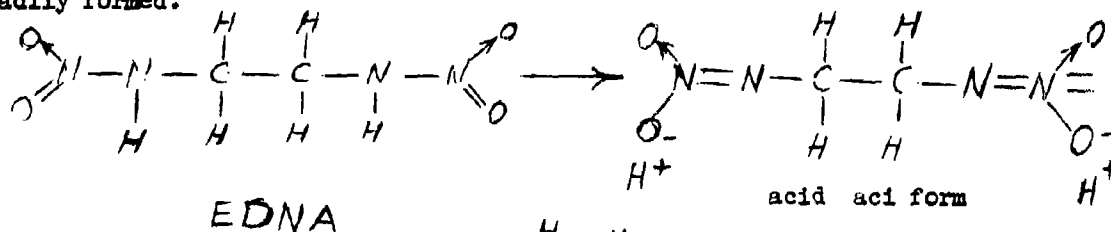


The instability of the aliphatic nitro compounds has been attributed to the "aci" form to the extent that it has been suggested that a trace of acid be added to nitro-aliphatics to increase their stability. (6)

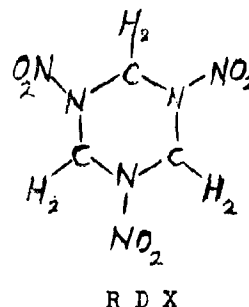
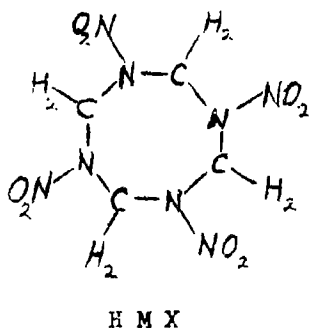
The alkalinity or basicity of glassware which can usually be ignored causes rapid "aci" conversion. The "aci" readily disproportionates into decomposition products (7). One of the decomposition products, an aldehyde is a reducing agent which can be oxidized by normally stable nitro-compounds to form other decomposition products of low stability. A chain reaction of degradation can be initiated by small percentages of contamination by acidic isomers of nitro compounds.

Aci-nitro salts can be converted to the aliphatic nitro compound only with dilute acetic acid or CO<sub>2</sub> without excessive decomposition at the C - N bond.

When water is present, ethylene dinitramine corrodes several metals extensively. (8) This indicates that the acid form of nitro-amines can be readily formed.



The evidence (9) indicates that  $\begin{array}{c} \text{H} \\ | \\ \text{C} - \text{N} - \text{NO}_2 \\ | \\ \text{H} \end{array}$  is present during the synthesis of HMX and RDX which themselves have no H on the N attached to the nitro group.

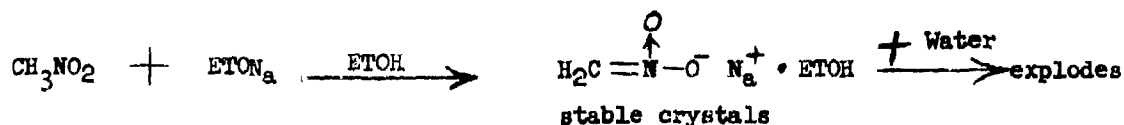




The acidity of RDX permitted by Military Specification MIL R-398C may be condensation products of the  $-CH_2NHNO_2$  group of a range of molecular weights and not nitric acid remaining from the reaction medium. Permissible acidity should be a measure of the improved thermal stability that has been demonstrated by repeated recrystallization. (10) The method of titration would have to be improved and cautiously designed for this to be applicable.

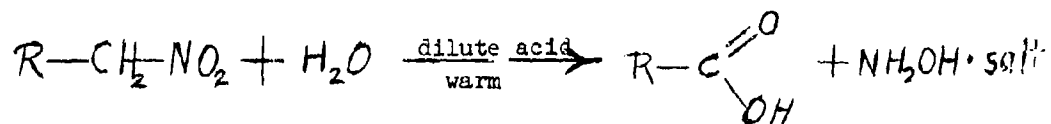
### III ALIPHATIC NITRO COMPOUND REACTIONS

Nitromethane exhibits unique condensations with bases. In anhydrous medium with alkali ethoxides a stable crystalline solvate is formed which explodes on being wet with water.

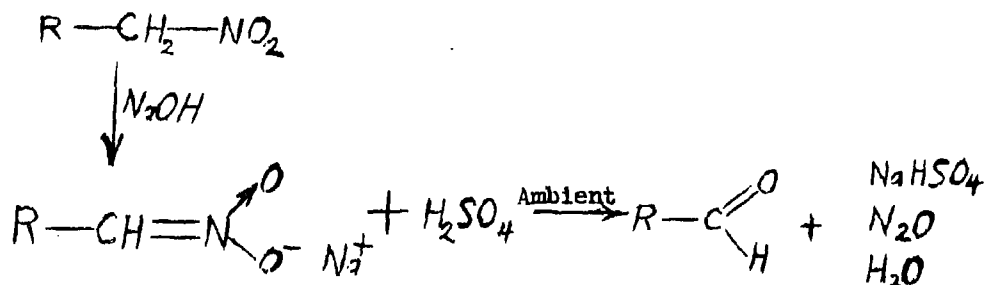


The violent reaction is attributed to the formation of fulminic acid. Mercury fulminate  $\overset{+}{C}NOHg\overset{-}{O}NC$  is an insoluble salt of fulminic acid and a sensitive explosive. Nitro ethane does not lose water to form fulminates in a basic solution.

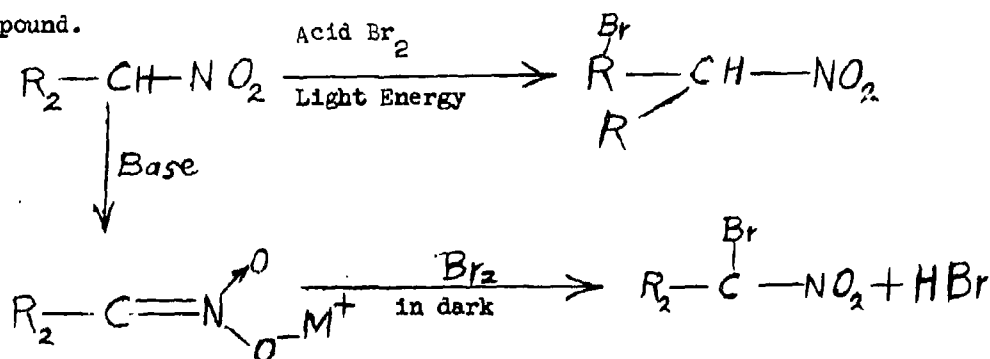
Reaction of nitro compounds with acid yields different products when the starting material is in the "aci" - nitro form.



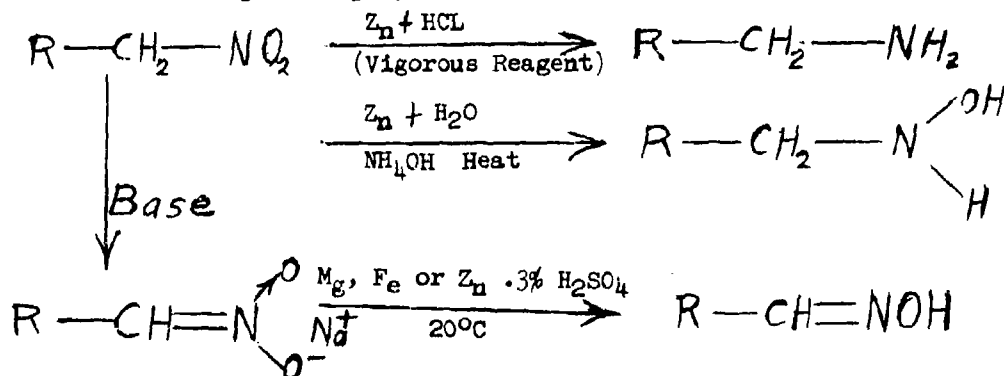
Reaction of nitro compounds with acid yields different products when the starting material is in the "aci" - nitro form.



Halogenation products also depend on the form of the starting nitro compound.

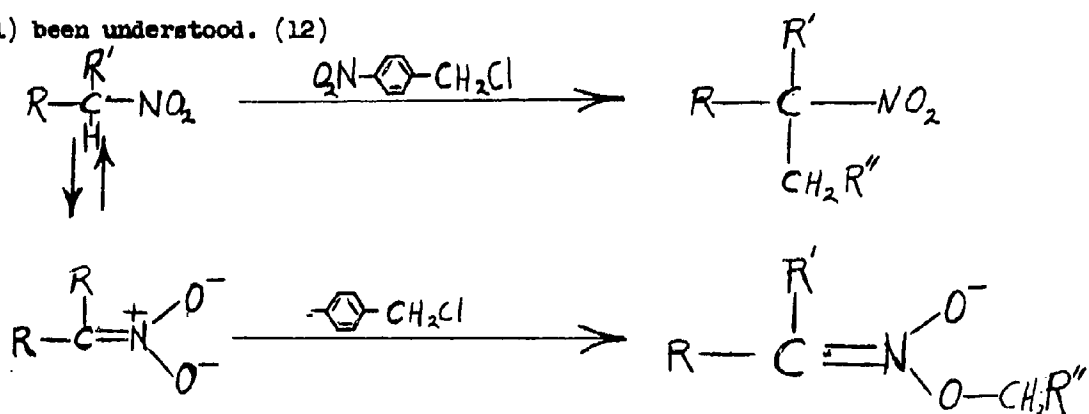


The reduction products, too, are influenced by the isomer that is reduced and the reagents employed.

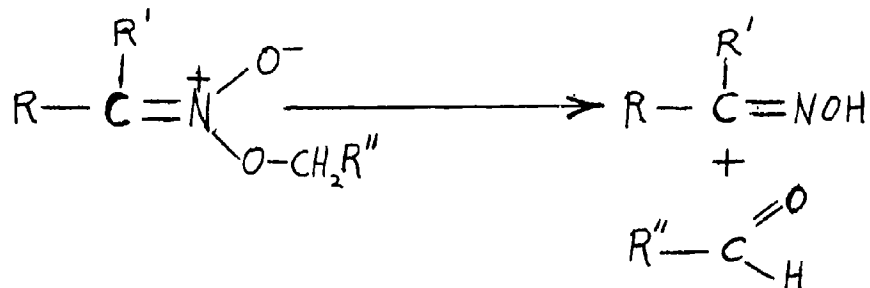


Catalytic reduction can be accomplished with hydrogen and Raney nickel. Thorough agitation, low temperatures and vigorous reducing agents are necessary to avoid condensation of products with the reactants. (11) The complex condensation products make it extremely difficult to determine the source of the original reducing agent in the decomposition products of explosives.

The anion of aliphatic nitro compounds can be alkylated at either the -NO<sub>2</sub> carbon atom or the oxygen atom by condensation with alkyl halides. The determining factors controlling oxygen or carbon alkylation have only recently (1961) been understood. (12)

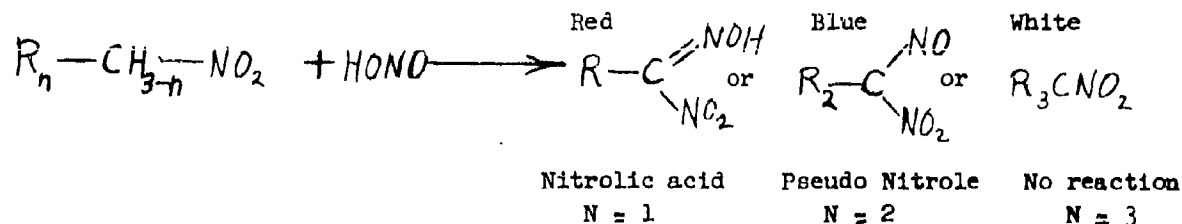


The oxygen alkylation product is unstable and breaks down thus:

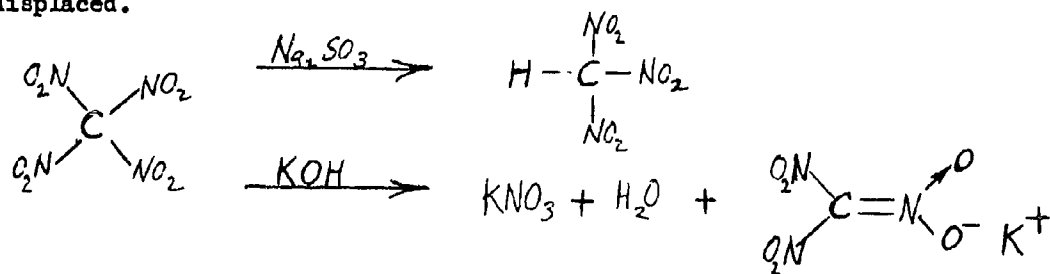


Since oxygen alkylation normally predominates the specific factors effecting carbon alkylation may contribute to the understanding of large number of substitution reactions.

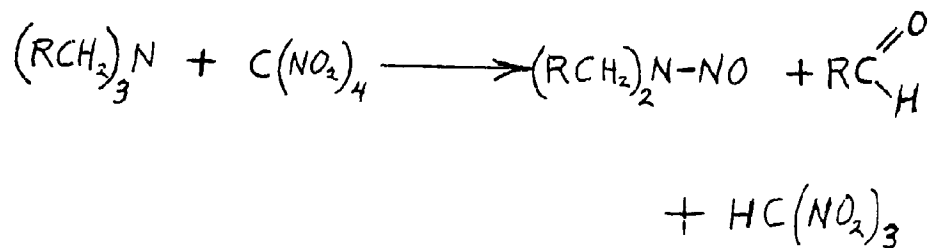
Primary, secondary and tertiary nitro paraffins can readily be identified by the "red, white and blue" reaction of nitrous acid on the nitro-paraffin.



Poly nitro aliphatics are somewhat unstable and NO<sub>2</sub> groups are readily displaced.



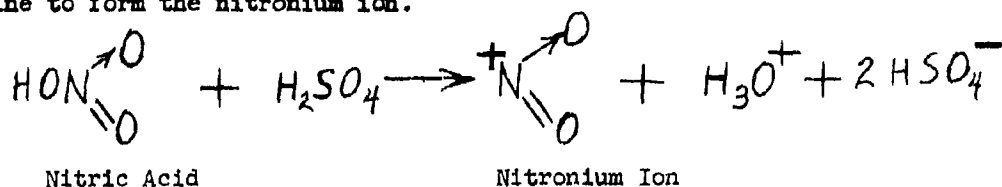
Tetra nitro methane is reactive and forms explosive complexes with aromatic hydrocarbons. These reactions result from the cumulative inductive effects of 4 nitro groups on 1 carbon atom and are not caused by one nitro group being different structurally (dipole moment of C(NO<sub>2</sub>)<sub>4</sub> is 0.0). Tetra-Nitro-methane can be used as an oxidizing agent for amines.



#### IV. AROMATIC NITRO COMPOUNDS

##### A Synthesis

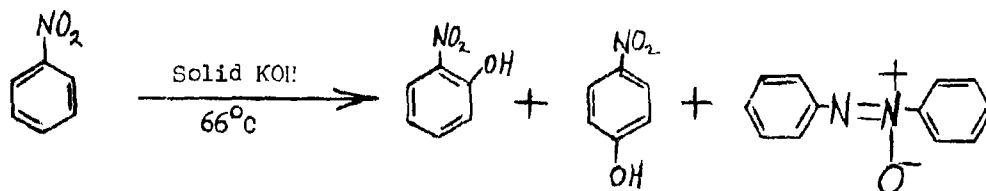
The nitration of aromatic compounds proceeds via a substitution mechanism. The most widely used reagents are sulfuric and nitric acids (mixed acid) which combine to form the nitronium ion.



The mono nitrated benzene can be obtained in yields approaching 98% by the action of mixed acids at 50-55°C on benzene. More rigorous conditions are required to add the second nitro group (fuming HNO<sub>3</sub> conc'd. H<sub>2</sub>SO<sub>4</sub> 95°C) and yields of only 88% are realized. The trinitrobenzene (TNB) can only be obtained by using large excesses of fuming acids and 110°C for 5 days to produce yields of only 45%. The electron withdrawing nature of the NO<sub>2</sub> group greatly deactivates the ring to further electrophilic attack. When the second and third nitro groups are introduced they are located meta to the NO<sub>2</sub> already present. The activating effect of the methyl group (electron donating) on the benzene ring enables the formation of trinitrotoluene (TNT) in yields of 85% under much milder conditions than those required for producing TNB. Nitration of phenols is usually preceded by sulfonation to deactivate the benzene ring and make it less susceptible to oxidation by the mixed acids. During nitration the sulfonic acid groups are replaced by nitro groups.

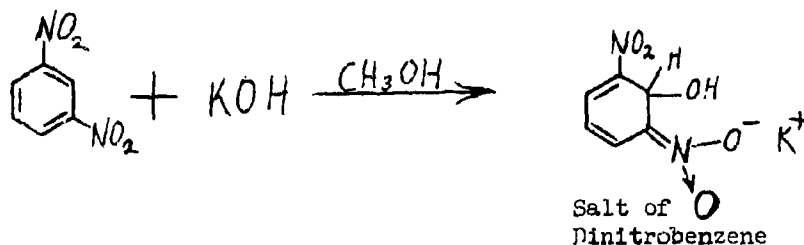
## Reactions

The reactions of mono-nitrated benzene with bases proceed only at elevated temperatures to produce a mixture of products.



The reaction is a diproportionation proceeding in the absence of oxygen and is moderately reminiscent of the Cannizzaro reaction. Para nitro-toluene under prolonged heating with alcoholic alkali suffers dehydrogenation of the methyl group to form the dimer p p' dinitrostilbene. Neither of the above reactions involve disruption of the aromatic ring or the C-N bond.

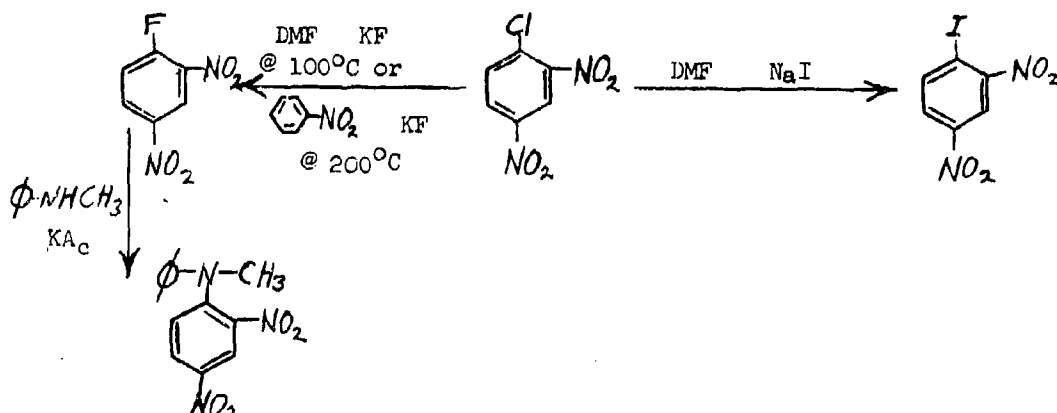
Dinitro benzene is more susceptible to nucleophilic attack, particularly when the nitro groups are meta to each other. The mutually ortho position is subjected to the cumulative electron withdrawing effects of the NO<sub>2</sub> group.



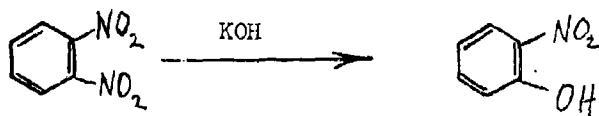
By chilling and acidifying the salt and treating with acetyl chloride the

presence of  $\begin{array}{c} \text{OH} \\ | \\ -\text{N} \\ | \\ \text{O} \end{array}$  group has been confirmed. It should be noted that the

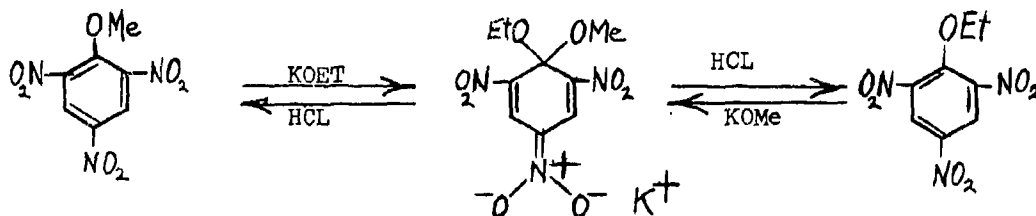
alkoxide addition products of aromatic nitro compounds are reported as being sensitive explosives. The position o, p to the two nitro groups is susceptible to displacements.



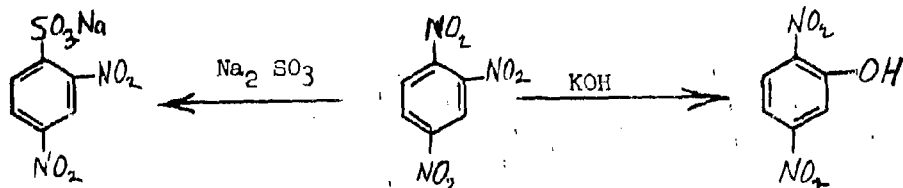
If the first two nitro group are o or p to one another they are more readily displaced by basic reagents. (14)



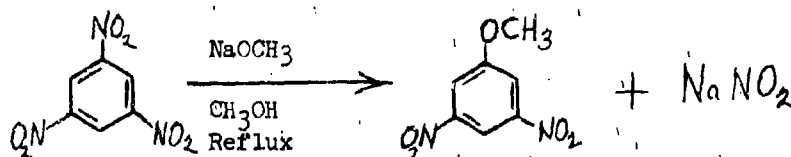
The trinitro benzenes are even more susceptible to basic attack than the dinitro compounds and more stable salts are formed with bases.



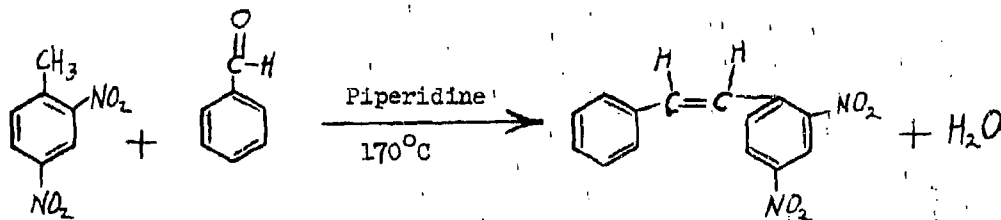
Other than symmetrical trinitro benzenes have a nitro group displaced easily by sodium sulfite or other bases.



Even the symmetrical TNB is converted to 3, 5 dinitroanisole when refluxed with sodium methoxide in methanol.



The methyl group of dinitro toluene is activated to the extent that condensations occur with aldehydes in the presence of secondary amines to produce water. TNT reacts similarly.



The methyl group of TNT can be oxidized to the carboxyl group by acidic dichromate. Decarboxylation of the product results in TNB in high yields.

Nitro aromatic compounds can be reduced rapidly by strong reducing agents to amines (aniline) or by milder reagents to the intermediate hydroxylamines.



Nitroso compounds are intermediates more susceptible to reduction than the parent nitro compound and cannot be obtained by direct reduction. All of the intermediate reduction products are typically less stable than the parent nitro-compound. The reduction products will condense with the original nitro compound to form more of the less stable compounds.

Nitrobenzene acts as an oxidizing agent in aqueous alkali at elevated temperatures.

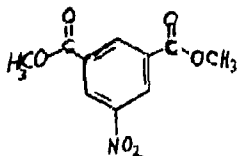


Nitro-compounds are effective in vulcanizing unsaturated elastomers. (15)  
 Nitro compound explosives will cause excessive hardening and sometimes crumbling of rubbers under prolonged contact in storage.

In addition to the activation of methyl hydrogen on carbon atoms attached to the benzene ring of polynitro compounds, hydrogen attached to a nitrogen atom can be made acidic under some circumstances. Diphenylamine is weakly basic but hexanitro diphenylamine (dipicrylamine) is definitely acidic forming ammonium salts (aurantine) (16) and causing extensive skin irritation. Carbazole is also very weakly basic forming (17) salts with perchloric acid. Tetranitrocarbazole is acidic and can be readily titrated with sodium methoxide reagent in a quantitative determination of purity. (18)

## V MOLECULAR COMPLEXES (19)

When two or more electron withdrawing nitro or other similar groups are on a single benzene ring, crystalline complexes are formed with electron rich aromatic and poly-aromatic hydrocarbons. A single nitro group alone is



not enough to cause formation of stable complexes but 2 nitro-meta dimethyl phthalate does form complexes. The poly nitro benzene is a " $\pi$ acid"

i. e. the  $\pi$  orbitals of the aromatic ring are deficient in electrons and will try to align (20) with electron rich aromatic rings substituted with electron donar groups. The picrate complex of carbazole melts at 185°C while the TNB complex melts at 166°C. Since the TNB complexes normally melts higher than picrates (21) there is some indication that acid-base or proton transfer to carbazole in the picrate-carbazole complex (i.e. salt formation) is increasing the melting point. Tetranitromethane forms analogous complexes with isolated ethylenic linkages. These complexes have been extensively characterized and are useful in detecting and identifying aromatic hydrocarbons or conversely identify explosives.

## VI STABILITY OF EXPLOSIVE COMPOSITIONS

The reactions cited earlier proceed at a rapid rate under the conditions specified. They define some of the simple reaction routes for the well defined decompositions of simple nitro compounds. Similar conditions of reactions are used for the destruction of waste explosives. Concentrated sodium hydroxide or sodium thiosulfite (bases and reducing agents) are prescribed for laboratory destruction of small quantities (22) of nitro explosives.

The stability of the C-NO<sub>2</sub> bond is rather high (23) but because the energy released encourages rearrangements of the nitro group it is difficult to measure. The activation energies (24) required for decomposition of high explosives are much lower than that required for the C-N bond alone. The poly-nitro organic compounds that perform well as high explosives (25) have high internal dipoles. The cumulative effect of the internal dipoles increases the tendency to react when a reaction route of low activation energy is present. Impurities or additives may lower the activation energy when a new route of reaction (mechanism) is introduced. This most likely contributes to the difference of values at one temperature reported in ref. (24). The change of mechanism or reaction route will change the activation energy. These facts are widely recognized in the literature and must be acknowledged when stability tests of a given system are planned to avoid misleading test results by change of mechanism.

Contaminates do not always decrease stability even at greatly elevated temperatures (26). In the case of organic nitrates stabilizers are added which combine with decomposition product so that they do not promote (catalyze) more rapid decomposition. If there is decomposition of the additive it will generally react with the explosive via reduction or condensation reactions of the types cited earlier.

A phase change, in itself does not cause decomposition (27), however, it may mobilize reactive pairs that would not meet at lower temperatures so that they can react. Generally, melting will increase the rate of deterioration proportional to the liquid phase via rearrangements and auto oxidation of the energetic molecules in solution. Extensive testing of explosives and materials of construction has been performed by government arsenals. (28) (29). When the chemical

structures of the additive are known it can be anticipated at what temperature reaction rates will be appreciable. Reactions that proceed readily can be avoided by careful material selection. The mobility of the reactive pairs also greatly effects the rate of reaction (30).

1. L. F. Fieser and M. Fieser ADVANCED ORGANIC CHEMISTRY  
Reinhold Publishing Corp. N.Y. 1961.
2. C. D. Hodgman HANDBOOK OF CHEMISTRY AND PHYSICS  
45th Edition Chemical Rubber Co. 1964.
3. R. D. Topsom EQUATION GIVES RESONANCE EFFECT VALUES  
Chemical and Engineering News Vol. 43 No. 30 26 Jul. 1965.
4. M. J. Astle INDUSTRIAL ORGANIC NITROGEN COMPOUNDS  
Reinhold Publishing Corp. N. Y. 1961.
5. E. F. Degering AN OUTLINE OF ORGANIC NITROGEN COMPOUNDS  
University Lithoprinters 1950.
6. N. V. Sidgwick THE ORGANIC CHEMISTRY OF NITROGEN  
Oxford Press, London 1937.
7. E.E. Rochow, D.T. Hurd & R. N. Lewis  
THE CHEMISTRY OF ORGANOMETALLIC COMPOUNDS  
John Wiley and Sons New York 1957,
8. PROPERTIES OF EXPLOSIVES OF MILITARY INTEREST, ENGINEERING  
DESIGN HANDBOOK AMCP 706-177  
U S ARMY MATERIAL COMMAND August 1963.
9. Castorina, T. C. and Autera, J. R. NITROGEN - 15 TRACER STUDIES  
OF THE NITROLYSIS OF HEXAMETHYLENETETRAMINE, INDUSTRIAL AND  
ENGINEERING CHEMISTRY - PRODUCT RESEARCH AND DEVELOPMENT. Vol. 4 No. 3  
J70 September 1965.
10. N. J. Bowman, and E. F. Knippenberg "A DEVELOPMENT PROGRAM TO PROVIDE  
CRITERIA FOR THE DESIGN AND MANUFACTURE OF THERMALLY STABLE FLEXIBLE  
LINEAR SHAPED CHARGE SYSTEMS" CCN 9 Contract No. AFO4(694)-475 29 Oct.  
1965 AD473171,
11. E. F. Riley NITRO PARAFFINS CHEMICAL REVIEWS 32 373-421 1943.
12. N. Kornblum RADICAL ANIONS PLAY ROLE IN SUBSTITUTION REACTIONS  
CHEMICAL AND ENGINEERING NEWS 43 , 22 101 31 May 1965.
13. A. H. Blatt COMPILATION OF DATA ON ORGANIC EXPLOSIVES OSRD # 2014  
29 February 1944.
14. Fieser and Fieser ORGANIC CHEMISTRY 3rd Edition Reinhold Publishing  
Corp. N.Y. 1956.

15. C. C. Davis and J. T. Blake, CHEMISTRY AND TECHNOLOGY OF RUBBER Reinhold Publishing Corp. N. Y. 1937.
16. S. L. Stadler and E. C. Lathrop, ALLENS COMMERCIAL ORGANIC ANALYSIS Vol III Blakiston Corp. 1948.
17. W. C. Sumpter and F. M. Miller, HETEROCYCLIC COMPOUNDS WITH INDOLE AND CARBAZOLE SYSTEMS. Interscience Publishers Inc. 1954.
18. MIL - T - 13723A MILITARY SPECIFICATION FOR TETRANITROCARBAZOLE.
19. L. Andrews, AROMATIC MOLECULAR COMPLEXES, CHEMICAL REVIEWS 54 713 1954.
20. R.G. Pearson SOFT AND HARD ACIDS AND BASES, Chemical and Engineering News. 43 22 90 31 May, 1965.
21. Staff Authors, ORGANIC REAGENTS FOR ORGANIC ANALYSIS Chemical Rubber Publishing Co. Cleveland, Ohio 1946.
22. DEPARTMENT OF THE ARMY TECHNICAL MANUAL TM - 9 - 1910 MILITARY EXPLOSIVES April 1955.
23. T. L. Cottrell, THE STRENGTHS OF CHEMICAL BONDS, Butterworths Scientific Publications, London 1954.
24. M. A. Cook and M. T. Abegg, ISOTHERMAL DECOMPOSITION OF EXPLOSIVES Industrial and Engineering Chem. 1956 48 1090.
25. W. C. Lothrop and G. E. Handrick RELATIONSHIP BETWEEN PERFORMANCE AND CONSTANTS OF PURE ORGANIC EXPLOSIVE COMPOUNDS Chemical Reviews 44 419 - 445 1949.
26. E.E. DeMaris, C. D. Forrest, and G. A. Noddin (To EIDupont De Nemours and Co.) U.S. Pat. 3089, 796 (1963).
27. E. E. DeMaris (To EIDupont De. Nemours and Co.) U.S. Pat. 3, 140, 212 (1964).
28. B. J. Zlotucha, M. Baer THE REACTIVITY OF EXPLOSIVES METALS AND PROTECTIVE FINISHES TR 2288<sup>5</sup> May 1956 Picatinny Arsenal Dover, N. J. AD 94318.
29. ORDNANCE EXPLOSIVE TRAIN DESIGNERS HANDBOOK, Naval Ordnance Laboratory Report 1111. April 1952.
30. Anderson, H. C. EFFECTS OF AMINE CURED EPOXIES ON THE STABILITY OF TNT USNOL, SPE JOURNAL Nov. 1960.

## DISCUSSION

The author was asked to identify some of the sources of the contaminants discussed. The two chief classes of these compounds are bases and reducing agents. Some of these are found in the materials of construction. As such, their tendencies to react are tolerated. There is some tendency to react in any explosive, especially those which are mixtures such as Torpex, a mixture of TNT, RDX, and aluminum. In this instance, the aluminum in the mixture tends to act as a reducing agent thus decreasing the stability of the mixture.

4-3P THE DESIGN OF STERILIZABLE PYROTECHNIC DEVICES

by

Dr. N. J. Bowman, Consulting Engineer, and  
E. F. Knippenberg, Development Engineer (1)

Introduction

Vehicles that land on the other planets of the solar system should be sterilized to prevent contamination with earth bacteria. Among the methods that have been suggested for this are:

1. Dry heat
2. Chemical methods
3. Radiation
4. Ultra sonics

Of these only the first two appear practical at present. Chemical methods will be useful in fabricating individual components but for a complete vehicle only dry heat is adequate to sterilize with a high degree of certainty. The Jet Propulsion Laboratory has studied sterilization with dry heat and at the time this study was undertaken they had established 145°C for 36 hours, three successive times as the standard criteria. Since that time there has been established, a range of temperature-time relationships that will accomplish sterilization. Of these the standard procedure at present is 6 cycles at 135°C for 56 hours each time. Because of physical deterioration of the non-explosive components, particularly plastic materials, this latest procedure should be somewhat less severe on pyrotechnics than the older procedure used in this work involving a higher temperature.

The pyrotechnic devices that will be required on interplanetary landers are among the most sensitive components of the vehicle. The reasons this study

---

(1) Re-Entry Systems Department, General Electric Company,  
3198 Chestnut Street, Philadelphia, Pennsylvania



was undertaken are several. First we wished to establish, insofar as was possible, a list of explosives that in themselves would withstand sterilization conditions and which, therefore, were suitable for use in devices. Second, we sought to find a comprehensive range of pyrotechnic devices, available commercially, that would withstand sterilization. Thirdly, we hoped to establish which of the various possible designs were satisfactory by analysis of the devices that did not pass sterilization. The first of these objectives was largely satisfied by a literature search although some testing was done.

#### Literature Survey

All the available data on properties of a wide range of explosives was tabulated with the object of attempting to determine which ones were of sufficient thermal stability to be sterilizable. There were 4 types of data which were particularly helpful. These were:

#### Five Second Explosion Temperature

As this is one of the standard tests made on explosives, data was available on most explosives. While 5 seconds is about 4 orders of magnitude shorter than the time in which we are interested, a correlation between deflagration time and temperature was made using literature curves available on RDX and PETN. Consideration of this data led to the conclusion that any explosive that would withstand  $285^{\circ}\text{C}$  for 5 seconds would be satisfactory. Similarly, if it deflagrates in 5 seconds at temperatures below  $210^{\circ}\text{C}$ , it would not be acceptable. This gives a temperature range of  $75^{\circ}\text{C}$  in which the suitability of an explosive is questionable.

#### High Temperature Gas Evolution

This is a standard test run on explosives. The temperatures at which it is run vary somewhat, but  $100^{\circ}\text{C}$  is a standard temperature at which much of the

work on this property has been done. A value of 1% weight in 48 hours was taken, more or less arbitrarily, as the dividing line.

#### Vacuum Stability

This is another test that is widely run on explosives and considerable information is available, most frequently at 120°C. A gas evolution rate above 1cc in 48 hours was chosen as the dividing line between what was acceptable and what was not. This again was more or less arbitrarily based on the observed fact that when all the data was tabulated, the vast majority of explosives fell in two general categories. One category had gas evolution rates of a few tenths of a cubic centimeter and the other rates of several cubic centimeters up.

#### Melting Point

The final criteria was the melting point of the explosive. In general any explosive melting at less than 145°C was rejected. If melting occurred it could lead to reaction with other materials which would contribute to non-uniformity and erratic behavior. This is not a hard and fast criteria and depends upon the design. For example TNT melts at 80°C and so was ruled out. However, it is possible that a device might be designed with TNT as the main charge, but completely contained and separated from the initiation charge. In this design the TNT would melt during sterilization but, if separated from the other parts of the system, would probably be quite acceptable. It is recognized that TNT is one of the most stable explosives from a thermal standpoint.

When taken separately these criteria were often not definitive. There was however, very few explosives whose probable ability to withstand sterilization temperatures was in doubt if all criteria were considered. In some cases, of course, data on high temperature stability was available making use of these criteria unnecessary.

Over 150 explosives were surveyed and a list of the ones that appeared acceptable prepared. These are shown in Table I. Also shown are 3 important explosives on which there was insufficient data available to make a decision.

#### Tests on Explosives

Because these important explosives were in the doubtful class, they were tested for gas evolution at 150°C using a modified isoteniscope (Figure 1). This instrument consists of a block of aluminum about 4 inches in diameter and 6 inches high. In the top are bored holes for a test tube, thermometer and thermocouple. These holes go to a depth of about 4 inches. Approximately 0.5 grams of explosive are placed in a test tube filled with glass beads, and placed in the block. A rubber stopper with a capillary tube carries the evolved gas to a 10 ml gas burette with a leveling bulb where the gas is collected over mercury and measured. The capillary tube and glass beads are used to reduce the volume of the system and improve both the accuracy and sensitivity of the measurement. The block is placed on a hot plate which is connected to a source of electric power through a temperature controller.

With this instrument 6 materials were tested, including lead mononitro resorcinol and black powder which were on the questionable list. Several materials that were known to be satisfactory were checked by this method, such as the 3 types of boron-potassium nitrate pellets available commercially. The exact composition of these is given below.

B/ $\text{KNO}_3$ pressed powder	18/82%
B/ $\text{KNO}_3$ /laminac	23.7/70.7/5.6%
B/ $\text{KNO}_3$ /Tetranitro carbazol	15/70/15%

The sixth material was magnesium-teflon ignition material.

The sample of LMNR was placed in the isoteniscope and heated for 4 days at 150°C with no gas evolution. Black powder contains 8 to 10% of sulfur which melts from 112°C to 120°C, depending on the allotropic form, and is quite volatile above 70°C. According to the criteria mentioned above, black powder should

have been eliminated because of the low melting point of the sulfur. However, the sulfur is a minor constituent and it was decided that a test should be made. It was found to evolve no gas in 3 days at 150°C and several black powder devices passed sterilization as will be shown later in this paper.

The boron-potassium nitrate mixtures and magnesium-teflon were tested in the same manner and found to evolve no gas in 4 days. In the case of the boron-potassium nitrate-laminac material, some deterioration in physical properties was found. The pellets were much more easily crushed after sterilization.

Lead styphnate, the remaining material on the questionable list, was available in the form of a charge pressed over a flush bridge wire in an ignition element that had been prepared for General Electric by the Hanley Co. Since these were available it was decided to test them rather than rely on gas evolution of lead styphnate itself. This was particularly fortunate as the decomposition products of lead styphnate would be largely non-volatile materials. The ignition elements were subjected to 3 cycles of 36 hours each at 145°C. A total of 24 were tested and fired subsequently without failure. Lead styphnate was also used in several specific devices that passed sterilization and these two facts establish it as being a satisfactory explosive for use.

It was concluded from these experiments that all 6 of the materials were satisfactory as ingredients of a sterilizable device.

#### Specific Devices

Catalogues from all the major vendors were examined for devices that contained only explosives on the list of those satisfactory for sterilization purposes. It was immediately apparent that, of the thousands of devices listed, only a few were acceptable for our purpose. Most of them used unacceptable explosives for the proposed tests.

The specific devices were placed in a heavy-wall bomb with a screw top and placed in an oven. To make temperature control as accurate as possible, the oven was attached to a temperature controller, timer and temperature recorder. A thermocouple from the controller was placed inside the bomb through a hole in the screw top. The devices were heated to 145°C, as recorded by the thermocouple inside the bomb, and the timer was started when the temperature reached 143°C. The oven was turned off automatically after 36 hours and took 3 to 8 hours to come to room temperature. This time varied depending on whether the time period ended at night or during the day when the bomb could be removed from the oven. The samples were subjected to 3 cycles of 36 hours each with variable periods at room temperature in between.

Devices that failed to fire are shown in Table II and those that fired satisfactorily in Table III. Many of the devices that would not fire had obvious deterioration externally. Typical examples included several cases where the potting compound deformed badly or melted, others where the plastic covering of the lead wires fused and at least one where the case itself was deformed. Many of the devices that would not fire were not affected visibly and had to be cut open with a lathe operated by remote control. In this manner, an insight was obtained to the affect of internal design on sterilizability.

There are four widely used designs for pyrotechnic devices. These are illustrated in Figure 2. Drawing 2A shows an ignition bead, on a free standing bridge wire, which is separated from the main charge by a small air gap; 2B is ignition bead on a bridge wire, where the combination is surrounded and supported by a second explosive; 2C shows a pressed charge with a flush bridge wire design; finally, 2D shows a hybrid type consisting of a bridge wire with ignition bead close to the ceramic or plastic support. Over this is pressed a small amount of ignition charge and there is the main charge loosely contained.

It was found that the devices constructed according to method 2A always failed under sterilization conditions and conversely those of type 2C always passed. Those of types 2B and 2D varied, with some passing and some failing. In some cases of devices of type 2D the failure was traced to a chemical deterioration. For example, several of these used dextrinated lead azide which deteriorated badly, whereas pure lead azide did not. There were also several cases where the ignition bead was physically deteriorated despite the charge pressed over it. On the other hand type 2B, where the ignition bead was only supported by a loose charge and not close to the ceramic header, failed with few exceptions. These data indicate that any device with an ignition bead, rather than pressed ignition charge, is not reliable. Also, of those with an ignition bead, design type D is better than B which in turn is better than A. Figures 3 through 7 illustrate various types of failures encountered.

In summary, it is established that the best design type, both from a mechanical and thermal standpoint, is a welded, flush-mounted bridge wire with a pressed ignition charge. The doped, brushed-on or dipped bead mixes are inherently unsuitable, since they must use some form of volatile carrier and there is no adequate control of the amount of material remaining on the bridge wire. Its physical properties also may vary drastically from batch to batch. A deposited bridge is an acceptable design concept, but it is not recommended because the design needs further development and testing.

It should be emphasized at this point, that this was only a preliminary screening and in no sense a qualification test. Large numbers of devices would have to be shown to be sterilizable, without failure or deterioration of output under a range of conditions, to constitute a qualification test. The deterioration in output, if any, was not measured in these experiments since it would have made the screening too long and expensive. However, we have narrowed the range of potentially usable devices from several thousand to about a dozen types. It will be noted that the explosives contained in the devices potentially satis-

factory, are from a very small list. Many of the newer high temperature explosives in Table I have never been used in devices on more than an experimental basis.

#### Design of an Igniter for Rocket Motors

We had originally hoped to find available, a complete range of devices. In this we were disappointed. The types of devices that were unavailable included shaped charges, percussion primers, and time delay devices. Perhaps the most serious lack, from our standpoint, was an igniter suitable for use in a rocket motor. For this reason we undertook to design a sterilizable rocket igniter by applying the results obtained in this program. There are two main types of rocket igniter designs, those using pyrotechnic "matches" and those having an integral construction. The first type has the so-called matches inserted in the main charge through holes in the base of the device. There are, insofar as we know, no sterilizable matches. They all contain explosives that either have too low an auto ignition point or that show physical deterioration on heating. Most of them contain binders that crumble or lose their physical properties on heating to sterilization temperatures.

The other type utilizes a bridge wire surrounded by an initiation explosive which sets off the main charge. We propose a variation of this type as shown in Figure 8. It consists of a welded, flush-mounted bridge wire with a pressed charge of basic lead styphnate or pure lead azide as the initiation element. The bridge wire ignites the styphnate which in turn ignites the main charge consisting of boron-potassium nitrate pellets and granules. The pellets increase the duration of burning and the granules make it easier to ignite. The basic elements of this system have been tested separately with excellent results. The pressed ignition nitrate pellets have been tested in several forms, both by themselves and in devices. We feel that this design has a very high probability

of being successful without modification. We have not as yet had such a device fabricated. Sometime after the project was completed, we were given two rocket igniters which we found to be sterilizable. These were both of the same general design that we proposed. These are reported in Table III.

#### Discussion and Conclusions

Commercially available pyrotechnic devices were tested for sterilizability using the JPL criteria. It should be emphasized that none of the devices tested were originally developed for the purpose of withstanding sterilization and hence their failure is no reflection on their manufacturers. As a criterion for acceptability, we used the ability to fire after being subjected to sterilization. In general, we ceased testing after the first failure as it is obvious that the device was inadequate from a reliability standpoint.

The preliminary screening survey showed a number of important things. First, it indicated that a moderately wide range of explosives, capable in themselves of withstanding sterilization temperatures, are available for use. It also showed that very few of these explosives have been used in devices. Many on the list are new and some even classified as to structure and specific properties.

Among the thousands of off-the-shelf pyrotechnic devices, better than 98% are not sterilizable. Except in the case of pressure cartridges there are only a handful of available squibs, initiators, and detonators which are sterilizable. In the case of pressure cartridges a few suppliers have developed cartridge designs which can tolerate sterilization conditions. In general these cartridges contain zirconium and potassium perchlorate or other metal/oxidant mixtures. In these designs the initiation charge is pressured over a flush mounted bridge wire and metal-to-glass seals are used. In most cases the cartridges are available as a series of devices in which the only difference is in physical dimensions and in the quantity of explosive used.



We also established that certain designs are much better than others from the standpoint of sterilization. The best design is clearly a welded, flush-mounted bridge wire with a pressed charge over it. No device with an ignition bead can be considered reliable. Sealants and materials of construction are also important. Welding is preferred to soldering and high temperature plastics should be used, both in the device and for insulation of the lead wires (if any). Glass or ceramic seals are preferred to plastic wherever possible.

One of the main devices found to be lacking was an off-the-shelf rocket igniter that was sterilizable. Utilizing the criteria outlined above, we designed such a device as shown in Figure 8. We feel that it will be sterilizable and have a high degree of reliability.

#### References

1. Montgomery, L.C., "Sterilization of Solid Propellants", Space Programs Summary No. 37-20, Vol. IV, pp. 58-60, Jet Propulsion Laboratory, Pasadena, Calif., April 30, 1963.
2. Benedict, A.G., "Development of Sterilizable Pyrotechnic Devices", Space Program Summary No. 37-32, Vol. IV, pp. 112-114, Jet Propulsion Laboratory, April 30, 1965.
3. Bowman, N. J. and Knippenber, E.F., "The Sterilization of Pyrotechnic Devices", Report No. 65SD992, General Electric Company, Missile & Space Division, Philadelphia, Pa., December 23, 1965.

TABLE I

EXPLOSIVES THAT PROBABLY WILL STAND STERILIZATION CONDITIONS

ABH	NONA
Ammonium pictrate	ONT
DAT(N)B	TACOT
DIPAM	TAT(N)B
EL-511	Tetranitro carbazol
Hexite	1, 2, 3, 5 tetranitro benzene
$\beta$ -HMX	TNN
HNO	TNO
KDNBF	Trinitro naphthalene
LDNR	Metal powder/ oxidant mixtures such as B/NKO <sub>3</sub> , Zr/KC10 <sub>4</sub> , etc.
Lead Axide (Pure)	Magnesium and teflon
Nitro guanidine	

INDETERMINENT WITHOUT TESTING

Black powder

LNR

Lead styphnate

TABLE II

## PYROTECHNIC DEVICES THAT FAILED STERILIZATION

DESIGNATION/TYPE/ MANUFACTURER*	IGNITION MIX	MAIN CHARGE	DESIGN TYPE	NO. TESTED/ NO. FAILED	REASON FOR FAILURE
SD-36A0/delay/H	Pb/Se	PbO <sub>2</sub> /B	2D	6/6	deterioration of initiator
D53A1/detonator/H	dextrinated lead azide	lead azide/HKX	2D	3/1	deterioration of initiator
RXL502/squib/A	LHR/KC10 <sub>4</sub>	LHR/KC10 <sub>4</sub>	2A	3/2	deterioration of initiator
NN-S-N2/squib/NF	KC10 <sub>4</sub> /PbSCN/C/Egyptian laquer		2E	5/5	physical deterioration
F3A0/actuator/H	dextrinated lead azide	lead azide	2D	3/1	deterioration of initiator
DM-25H1/dimple motor/H	lead styphnate	LHR/black powder	2D	2/2	deterioration of initiator
S45Q0/squib/H	lead styphnate	Fe <sub>2</sub> O <sub>3</sub> /Zr	2D	2/2	deterioration of main charge
X311G/initiator/D	S4	lead azide	2A	2/2	deterioration of S4 initiator
S75H1/squib/D	S4	black powder	2E	19/17	deterioration of S4 initiator
S84/squib/D	S4	black powder	2E	7/3	deterioration of S4 initiator

43.12

## \* Code To Manufacturers

A = Atlas Powder Co.  
 B = Bernite Powder Co.  
 D = Dupont Co.

H = Hercules Powder Co.  
 HS = Hi Shear Co.

MS = McCormick Selph Co.  
 NF = Northern Flare Div.  
 of Atlantic Research Co.  
 U = Unidynamics

TABLE III

## PYROTECHNIC DEVICES FOUND TO BE STERILIZABLE

DESIGNATION/TYPE/ MANUFACTURER *	IGNITION MIX	MAIN CHARGE	DESIGN TYPE	NUMBER TESTED
---/ignition elements/Hanley Co.	basic lead styphnate	none	2C	24
RXL517B/squib/4	lead styphnate	lead azide	---	3
D45A1/detonator/H	lead azide	lead azide	2D	3
E86/detonator/D	S4	lead azide	2B	10
EM55 mod 5/squib/MS	Zr/BaCr <sup>0</sup> <sub>4</sub>	B/KClO <sub>3</sub>	---	6
No. 1554/initiator/MS	Zr/BaCr <sup>0</sup> <sub>4</sub>	B/KMnO <sub>3</sub>	2B	6
S135A0/squib/H	Zr/BaCr <sup>0</sup> <sub>4</sub>	Pb/Se	2D	6
S205A0/squib/H	Zr/KClO <sub>4</sub>	black powder	2D	3
S11A2/squib/H	lead styphnate/ PbO <sub>2</sub> /B	black powder	2D	6
PC12/pressure cartridge/HS	Zr/KClO <sub>4</sub> /SI rubber	TiH <sub>2</sub> /KClO <sub>4</sub>	2C	12
PC31/pressure cartridge/HS	Zr/KClO <sub>4</sub> /SI rubber	TiH <sub>2</sub> /KClO <sub>4</sub>	2C	3
8225D0/squib/H	Al/KClO <sub>4</sub>	lead azide	2D	6
MK 5 mod 0/driver/H **	lead styphnate	lead styphnate	2D	10
S239A0/squib/H	lead styphnate/ PbO <sub>2</sub> /B	Mg/KClO <sub>4</sub>	2D	16
UH-1097E/igniter/U	B/CaCrO <sub>4</sub>	Mg/Teflon	2C	10
Igniter/B	Zr/KClO <sub>4</sub>	B/TiN03	2C	6

\*\* Carbon bridge

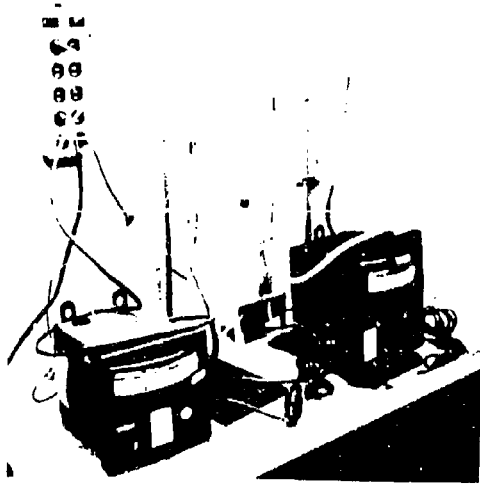


Figure 1. Isoteniscope

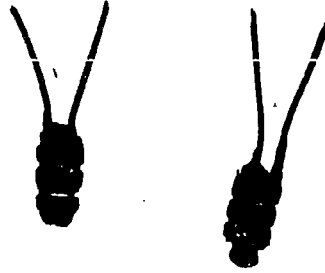


Figure 5. S-84 Squib



Figure 3. RXL-502 Squib

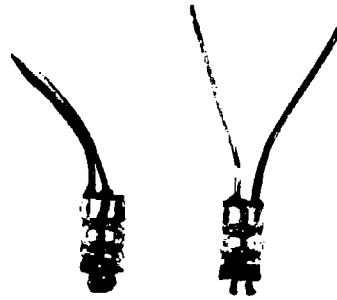


Figure 6. X-311-G Initiator



Figure 4. DM-25-N1 Dimple Motor

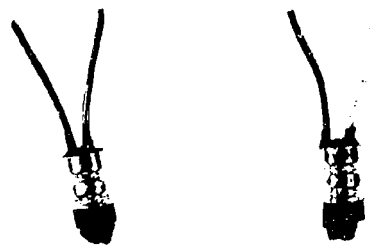


Figure 7. X-75-M1 Squib

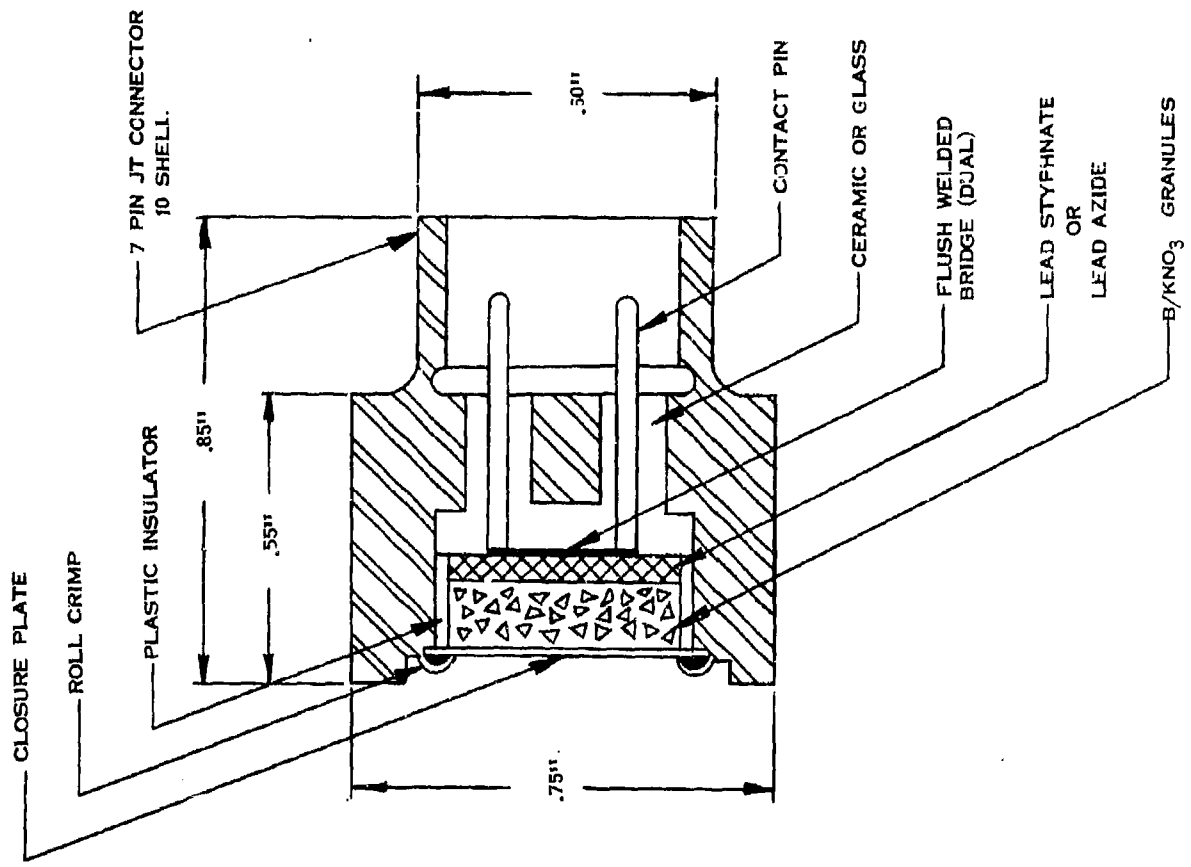
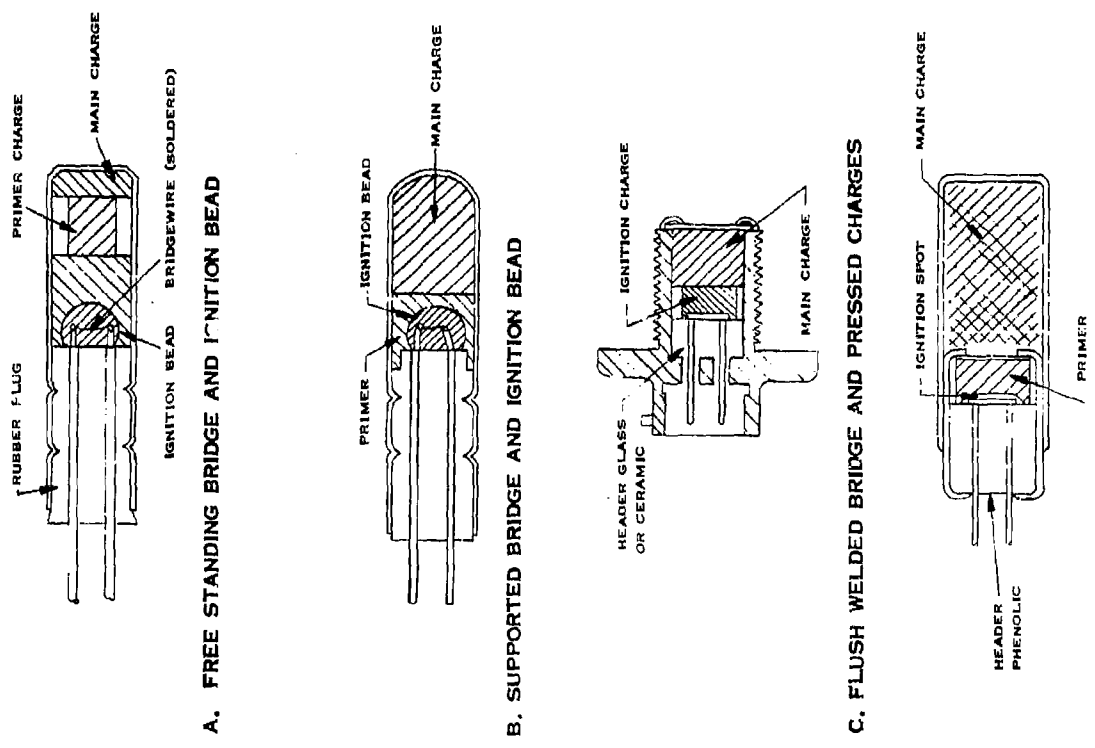


FIGURE 8.  
STERILIZABLE ROCKET IGNITER



A. FREE STANDING BRIDGE AND IGNITION BEAD

B. SUPPORTED BRIDGE AND IGNITION BEAD

C. FLUSH WELDED BRIDGE AND PRESSED CHARGES

D. FLUSH BRIDGE, PRESSED PRIMER, LOOSE MAIN CHARGES

FIGURE 2. TYPICAL ELECTROEXPLOSIVE DEVICES

4-4P INFORMATION SOURCES FOR EED'S  
by Gunther Cohn  
The Franklin Institute Research Laboratories

Problems with technical information have been with us for some time but they have recently become more acute. This is due to the prolific generation of information (information explosion). Information centers help a lot but, alas, still none exists for EED's.

For this reason, this paper reviews briefly the useful information sources for EED's. I have selected a review by sources because of its more general application, even though the type of information they furnish is mixed: some furnish data, some publish documents, some answer questions. The reader may find it rewarding to become familiar with any of the sources listed that he has not dealt with in the past. This is not only a good way to learn of what is currently available but also to keep abreast of new publications.

#### 1. Library Tools

Your librarian is the best starting point. She is most likely familiar with all of the standard sources and should know ordering procedures. Try the indexes of DDC, NASA, and Clearinghouse and order their publications. For the first two you need a contract. All you need for Clearinghouse is \$3 per document. The librarian should also be able to direct you to the information centers: DoD's 22, BuStd's 28, AEC's 26, and NASA's regional 8, as well as the 4 reference centers. If your library does not have this kind of information, search it out at one of the mission houses.

#### 2. The Mission Houses

By mission houses I mean those government agencies whose mission calls for research or development on the item of interest. NASA, AEC, Army, Navy, and Air Force all have agencies that are responsible for a particular piece of hardware or for research in the area of EED's. The advantage of going to a mission house is that they (1) have people who can answer a question or who can direct you to a place where the information can be found, (2) have good technical libraries stocked with documents in their

field, and (3) publish reports, catalogs, indexes and other documents of current interest. A complete listing of these agencies is beyond the scope of this paper but note three sample publications of recent date:

- "Initiators and Initiating Compositions: A Literature Survey," by Alfred M. Ansalone, Picatinny Arsenal, Feltman Research Labs., Technical Report 14, September 1960, Secret.

This literature search resulted in the compilation of almost 1000 abstracts on initiators and initiating compositions. Included are reports by Picatinny Arsenal, its contractors, OSRD and other reports distributed to Picatinny. Subject coverage is broad; there are excluded only artillery primers, igniters, and fuzes. Volumes I (U) and II (S) contain abstracts and Volume III (U) is a coordinate index.

- Explosive Components, Information Pertaining to Fuzes, Volume IV, S. Ordierno, Picatinny Arsenal, September 15, 1964 (AD-451 450).

This volume lists physical and performance characteristics of fuze explosive components such as detonators, primers, relays, leads, and boosters as well as die sizes for booster pellets.

- Security Classification Guide for Explosives, Department of the Navy, NAVORD Instruction 5511.4, ORD-9152, December 12, 1966.

This document contains the most recent Navy position on security classification of explosives.

### 3. Technical Manuals

All services publish a number of formal manuals for their material. The Army has TM's, the Navy OP's, the Air Force TO's. In addition, specifications and standards contain relevant information. All of these can be searched through their indexes that are updated periodically. The two basic manuals in the field are:

- Military Explosives, Department of the Army Technical Manual TM9-1910, April 1955 (Now being revised as TM9-1300-214).

This comprehensive manual is a useful reference for general and technical information on military explosives and propellants. Among the subjects covered are descriptions, properties, tests, handling methods, theory, and use.

- Military Pyrotechnics, Department of the Army Technical Manual TM9-1370-200, December 1958.



Description, use, operating instructions, safe handling, and destruction procedures are given for military pyrotechnics of all types. Included is a 14-page table of data on specific items.

#### 4. Engineering Design Handbook Series

The Army Materiel Command, under contract with the Engineering Design Handbook Office at Duke University, publishes military design manuals. Written by various agencies and contractors, some 75 titles have been published so far. They are listed on the inside back cover of each manual. Military agencies obtain these through their publications office while contractors order them through the contracting officer. Among the handbooks are those on pyrotechnics, statistics, fuzes (currently being revised), propellants, and various ammunition items. The three handbooks pertaining to explosives follow:

- AMCP 706-177, Properties of Explosives of Military Interest, May 1960.

This report contains data sheets on 81 explosive compounds or mixtures. Tabulated data include input sensitivity, performance characteristics, and physical and chemical properties of the explosive. A method of preparation, synthesis, or manufacture is included for each type of explosive.

- AMCP 706-178(C) Properties of Explosives of Military Interest(U), May 1960.

This is a companion volume to the above for some 40 classified explosives.

- AMCP 706-179, Explosive Trains, March 1965.

This text on explosive trains was written as an aid to ammunition designers. It covers fundamental principles of explosive reactions and theory, design considerations of all the diverse explosive elements including main charges, and related considerations of environment, fabrication, and evaluation. Glossary, references, index.

#### 5. Symposium Proceedings

To date we have held at The Franklin Institute four symposia on Electric Initiators and two HERO Congresses on (Hazards of Electromagnetic Radiation to Ordnance). These meetings were sponsored by various military agencies and each was attended by over 300 representatives of government and industry. Their proceedings serve as a review of the state of the art. Copies of the proceedings may be obtained from the Defense Documentation Center, Cameron Station, Alexandria, Va. 22314. Information for ordering copies is as follows:



- "Electric Initiator Handbook(U)," Third Edition, by The Franklin Institute, prepared for Picatinny Arsenal, Contract DA-36 024 501-ORD-3115RD, November 1960, Confidential (AD-319 980). First Supplement, April 1962, Confidential (AD 328-852).

This handbook contains basic data to characterize the performance of 25 electric detonators, primers, and squibs. In addition to a data sheet for each initiator, there are curves that describe functioning time and input sensitivity for various stimuli. The methods and the equipment used (standard test sets, the FILITS) are described in detail. The handbook is meant to serve the initiator field as the RCA tube handbook serves electronic industry.

- "Study of the Design Parameters of Explosive Initiators With Respect to Space Environments," by Raymond G. Amicone and Paul F. Mohrbach, The Franklin Institute Research Laboratories, Report F-B2333, Contract No. NAS 9-4042, December 1965, NASA: CR-65325.

This report summarizes information on possible environmental conditions to which manned spacecrafts may be subjected. These will be the environmental extremes which explosive devices must survive. With the possible exception of the Venus atmosphere, there appear to be no problems.

## 7. Commercial Publications

In recent years, manufacturers' catalogs have improved greatly. They now contain worthwhile technical information, performance data, and other useful notes. Catalogs are available from the manufacturer for the asking. Why not send for them?

Note also that this industry has a relatively new trade association: EPOMA (Explosive and Pyrotechnic Ordnance Manufacturers' Association). Write to Mr. Hugo Lizza, President, Bermite Powder Co., 2216 West Soledad Canyon Rd., Saugus, California.

## 8. Reports in Publication

Here is an advance announcement of some documents in this field that are now being written. All of them should be published by next year. Look for them through their publication sources:

- AMCP-706-235, Hardening Weapon Systems Against RF Energy.

This Engineering Design Handbook is concerned with design techniques that will help protect the weapon systems against radio frequency energy, static electricity, and lightning. Design techniques for various subsystems, examples, glossary, index.

- NASA, Technology Survey of Explosives and Explosive Devices.

A critical review of NASA's literature pertaining to explosives, EED's, and related circuitry that may be of interest to industry.

- MIL-HDBK 219 (Proposed), Military Standardization Handbook, Characteristics and Statistical Data for EED's, Confidential.

A catalog listing specifications, performance data, and characteristics of over 1000 initiators.

#### 4-5P. INSTRUMENTATION FOR RESEARCH, EVALUATION AND QUALITY CONTROL OF ELECTROEXPLOSIVE INITIATORS

C. T. Davey, W. S. Weiss, and W. J. Dunning  
The Franklin Institute Research Laboratories

To make effective use of an electroexplosive device (EED) it is necessary to know the functioning characteristics well. Input characteristics are generally determined by applying different levels of the stimulus under consideration (constant current, constant voltage, or capacitor discharge) to a sample lot of the EED. The test plan used is usually a Bruceton or Probit, depending upon previous knowledge of the type of device under test. Analysis of the test results leads to an expression of central tendency and dispersion that tells the designer how many items can be expected to fire from a given quantity under excitation from a particular level of stimulus.

This information becomes extremely valuable in assessment of system performance. If, for example, a common power source is used in a system containing an EED, troubles can be encountered. A 28-volt source may no longer be 28 volts because of other loading on the power source. If the devices have been tested at 28 volts only, this information is of little use in planning a course of action in the face of a lower exciting signal. The value of precise and accurate statistical data on EED performance cannot be overemphasized.

In the process of testing the EED, unexpected or conflicting data are often obtained that cast doubt upon the value of test results.

These problems can often be traced to the lack of accuracy and precision of the equipment used and to the testing and analytical techniques. Such problems usually arise in the initial phases of equipment development and lead to modification, redesign, and retrofit.

The Franklin Institute has developed a number of test sets for use in our laboratories, missile development facilities, and Government laboratories. Since 1953 well over one-half million electroexplosive devices have been tested in our laboratories. Most of the instrumentation required for these tests was designed and constructed by The Franklin Institute. This was necessary due to the unique and unprecedented requirements of the equipment.

All of the equipment provides accurate and repeatable measurements of all the parameters the apparatus was designed to measure. Provisions for self checking and standardization are incorporated; giving a high level of confidence in the acquired data.

In multi-purpose equipment the transition from one function to another is accomplished readily. Controls are placed for ease of operation, accuracy, minimized human error and safe functioning.

Components and circuitry are incorporated that represent the most advanced state of the art at the time of design of a given piece of equipment. Since this equipment is designed on a custom basis according to the specific needs of the user, who may be our own laboratories or those of an agency outside, it will be modern and up to date.

If required, or requested, the instrumentation is installed in the field by our personnel, and instruction is given to the operators. Subsequent servicing and consultation can be performed.

The initial resistance of the device under test, the sensitivity, and the functioning time are usually of vital interest to those using electroexplosive devices for functions on missiles and spacecraft.

Each of these characteristics can be measured precisely and easily with the equipment that is to be described in greater detail. In addition, there is the built-in facility for examining the dynamic resistance of the initiator, that is, its variation in resistance during the application of a stimulus. This is important in the analysis of the response of the initiator as an electrical circuit element.

Table 1 indicates the kinds of equipment that we have designed and built; they are in operation at Army, NASA and contractor facilities throughout the country as well as in the Applied Physics Laboratory of The Franklin Institute.

Following are pictures and descriptions of many of its instruments constructed by the Franklin Institute Applied Physics Laboratory.

Figure 1 shows the FILUP 3, whose major electrical characteristics are given in Table 2. This equipment provides pulses of constant current from 1 microsecond to several seconds in duration with amplitudes up to 50 amperes. Constant voltage pulses can be provided over the same range of duration, with amplitude dependent to a considerable extent upon the load resistance. The voltage can be as high as several hundred volts for high-resistance loads and a few volts for very low resistance loads. An oscilloscope, a timer, and a digital voltmeter are used to show the test conditions, and their controls are at the fingertips of the operator. All output information may be fed at command to the digital printer. The print-out can include full identification of test data: item, date, operator and other salient information of the test. Current or voltage amplitude, pulse application time, and functioning time can also be fed into the printer at command.

All instruments and power sources are controlled from the front panel of the equipment and setup can be completed in a few seconds. Dummy load resistors near the value of the device being tested can be switched into the circuit for precise adjustment of amplitude.

FILUP 2 is almost identical in appearance to FILUP 3. There is no facility for printing the information, which is made available to the operator in a digital display. FILUP 2, although not FILUP 3, can make capacitor discharge tests of conventional explosive devices as well as EBW devices. In addition it provides a constant slope current pulse for conventional devices with resistances of about ten ohms or less.

Figure 2 shows FILITS 4, which includes capacitor discharge testing of electric initiators, including EBW. It features resistance measurements by digital methods with safe currents, a capacitor bank for conventional hot-wire and carbon bridge initiators, and a capacitor bank for EBW devices. It has built-in monitors to check the energy transfer efficiency of the firing unit. Functioning time and charge voltage on the capacitors are indicated digitally.

Figure 3 shows the FILREP, a generator that simulates the pulses from radar without the added complication of the carrier frequency. It permits determination of the sensitivity of initiators to a train of constant current pulses. It also permits determination of thermal time constant and assessment of the effects of thermal stacking.

Figure 4 shows a firing chamber (protective barricade) used with each of the instruments described. The chamber is designed to withstand the repeated firing of initiators including detonators, squibs and igniters. A safety switch makes an electrical connection to the initiator only when the chamber door is closed; before the door can be opened, the switch must be set so that the initiator is shorted. The chamber is lined with foam rubber to reduce noise and collect fragments.



The bottom of the chamber is baffled and vented to permit the removal of gases through an exhaust connection at the top of the chamber. The box at the left of the chamber contains a flash detector, which stops the timer when measuring functioning time, upon sensing the flash of the initiator.

Figure 5 shows the Static Electricity Tester used for determining the sensitivity of EEDs to personnel-borne static charges. Figure 6 shows the basic circuit that simulates the human being as a source of static electricity. The development of this circuit is described in Franklin Institute Monograph APL-65-1, Electrostatic Hazard to Explosive Devices from Personnel-Borne Charges.

Figure 7 shows the Exploding Bridgewire Tester (also included in FILITS 4). This equipment features an Ignitron firing switch capable of passing thousands of amperes with little loss. It can be used repeatedly hundreds of thousands of times without significant change in its characteristics. Low loss firing cable and choice of firing capacitors and charging voltage make this equipment ideal for research, development and quality control testing of exploding bridgewire devices. Wave forms are monitored on the oscilloscope and photographed for record by means of a Polaroid camera.

Figure 8 shows a modified version of "AIRME" or Apollo Initiator Resistance Measuring Equipment."

Nine of the "AIRME" units are in use in various NASA and contractor facilities. This equipment measures to four significant figures the resistance of bridgewires in the apollo standard initiator, or in the case of the modified unit illustrated, any type of bridgewire initiator.

The leakage resistance from bridgewire to bridgewire, or bridgewires to case can also be determined.

For both measurements the potentials and currents are at low, safe, values. These potentials and currents are applied in the initiator for a predetermined period of time, usually about ten seconds, which is highly repeatable.

The "AIRME" equipment has built in standard resistors of high accuracy, and if desired a dummy initiator can be supplied that checks the operation of the equipment out to the end of the replaceable adapter that fits the actual initiator.

These adapters are normally supplied with "AIRME" to fit the connectors on the initiator. The adapters are replaced after a certain amount of use when wear on the adapter connector becomes excessive.

Table 1  
OPERATIONAL CHARACTERISTICS OF FRANKLIN INSTITUTE INITIATOR TEST EQUIPMENT

Equipment Name	Nature of Stimulus	Operating Ranges		Other Features and Functions
		Capacity of Time	Amplitude	
FILITS 2	Capacitor Discharge	0.0001 to 1 MFD	to 1000 volts	Resistance, Functioning Time
FILITS 3	Capacitor Discharge	0.001 to 1.6 MFD	to 1000 volts	Resistance, Functioning Time
FILITS 4	Combines characteristics of FILITS 3 and EEW tester. Features digital read-out of resistance.			
FILUP	Rectangular Pulse	1 microsec or longer	to 50 amperes to 800 volts	Resistance, Functioning Time
FILUP 2	Adds constant-current slope capability of FILUP in addition to digital read-out of resistance, also full capability of FILITS 3 and EEW tester.			
FILUP 3	Adds digital print-out of all variables to FILUP.			
FILREP	Repeated Rectangular Pulses	1 to 10 microsec trains	to 20 amperes to 2000 volts	Controlled Application Time
Lockheed Tester	Capacitor Discharge, Rectangular Pulse	to 100 MFD	to 1000 volts	Resistance, Functioning Time, Flame Length
EEW Tester	Capacitor Discharges	7 millisecc or longer	to 10 amperes to 160 volts	Current shunt Monitor jacks
Static Safety Tester	Capacitor Discharges	1,2,10 MFD	to 3000 volts	Simulate Personnel-borne Static Electricity
ALIME	Resistance measuring	500 PFD and others	to 25,000 volts	Leakage measuring
		.1 ohms	to 150 megohms	

Table 2

## CHARACTERISTICS OF FILUP

Generator Time Range	Current Range		Time of Pulse (max.)	Amplitude (max. volts)	Voltage Range	
	Amplitude (max. amps)	Load Resistance (max. ohms)			Load Resistance (min. ohms)	Current (max. amps)
Thyatron Discharge (TDG) 1 to 100 $\mu$ sec	16.0	1.0	100 $\mu$ sec	300		500
	4.0	4.0	100 $\mu$ sec			
	.8	10.0	100 $\mu$ sec			
Silicon Controlled Rectifier (SCR) 100 $\mu$ sec to 10 sec +	30.0	0.1	1000 $\mu$ sec	160		50.0
	20.0	1.0	8 millisee	10		50.0
	8.0	5.0	10 sec +			50.0

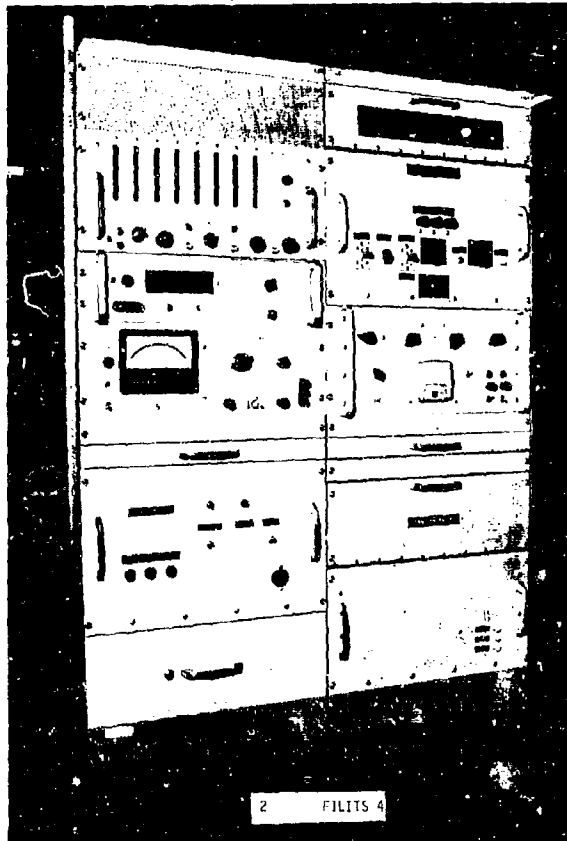
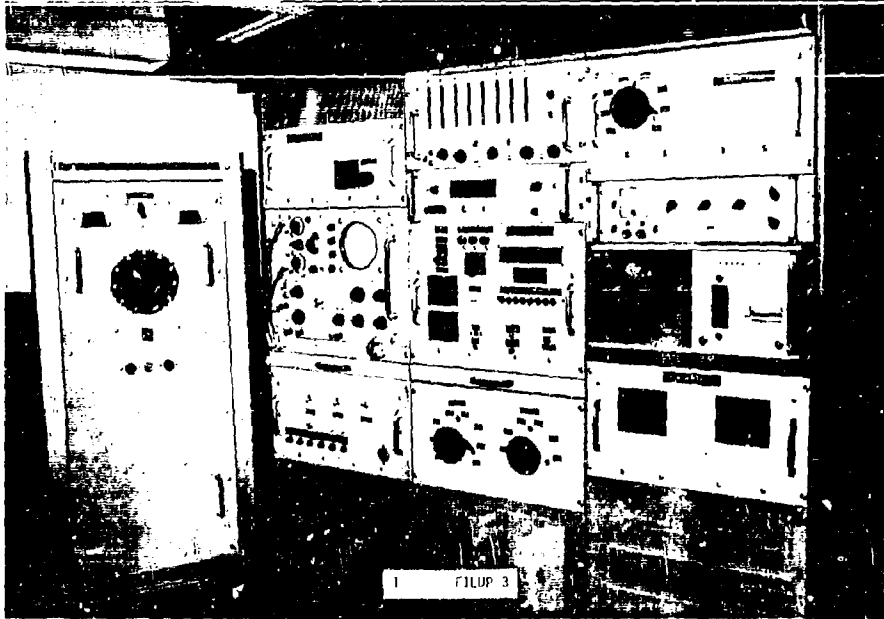
## NOTES:

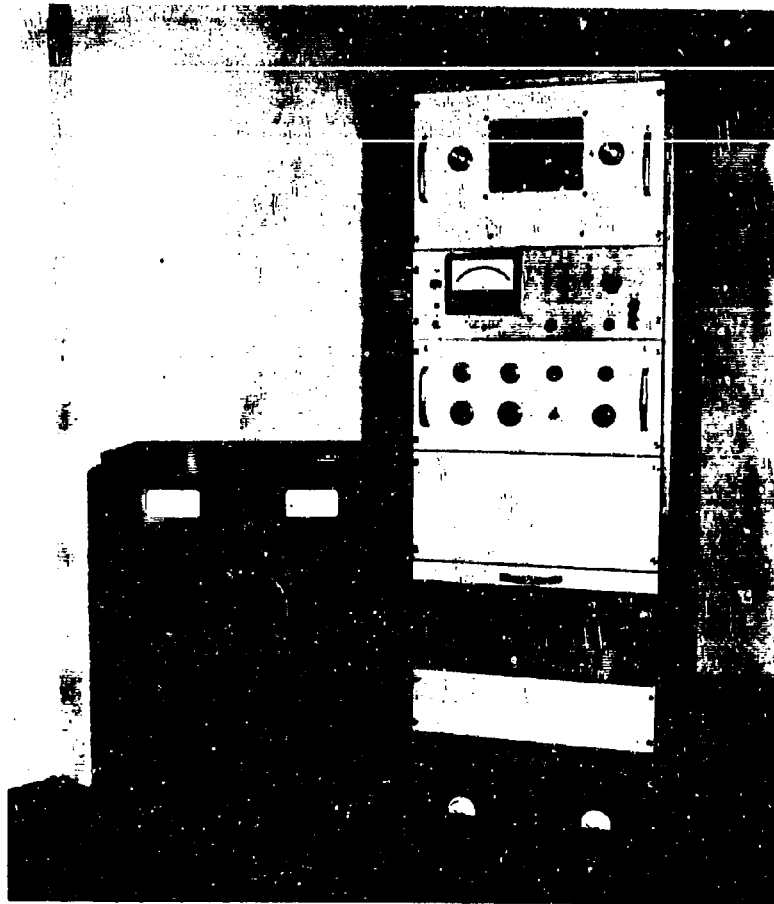
Rise Time: TDG - Less than 5% of set pulse time (5% to 95% of peak voltage) into resistive load.

SCR - Less than 2% of set pulse time (5% to 95% - voltage) into resistive load.

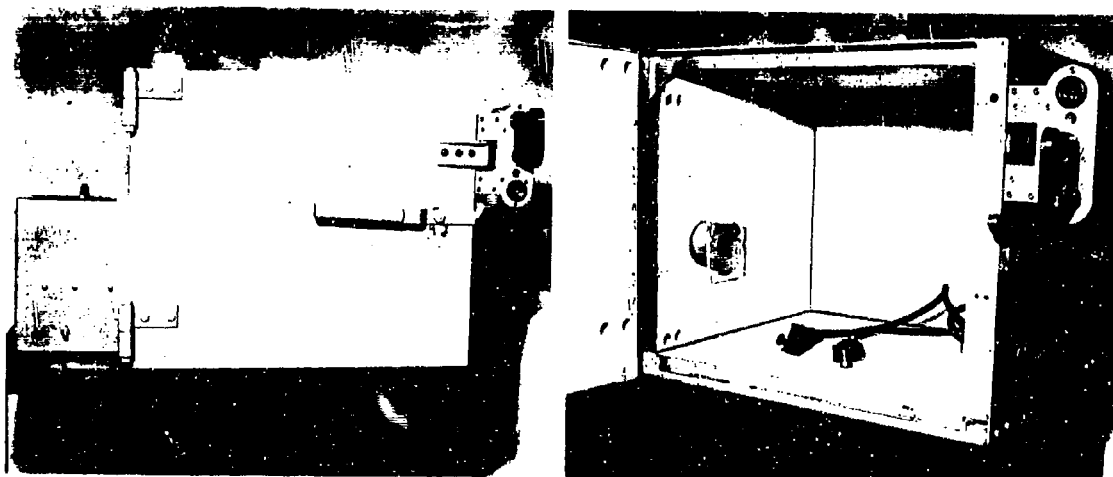
Pulse Time Setting: TDG - to within 5% of total pulse time at half-power points.  
SCR - to within 1% of set time.

Amplitude: To within 3% of desired pulse amplitude.





3 Franklin Institute Laboratories Repetitive Pulser (FILREP)

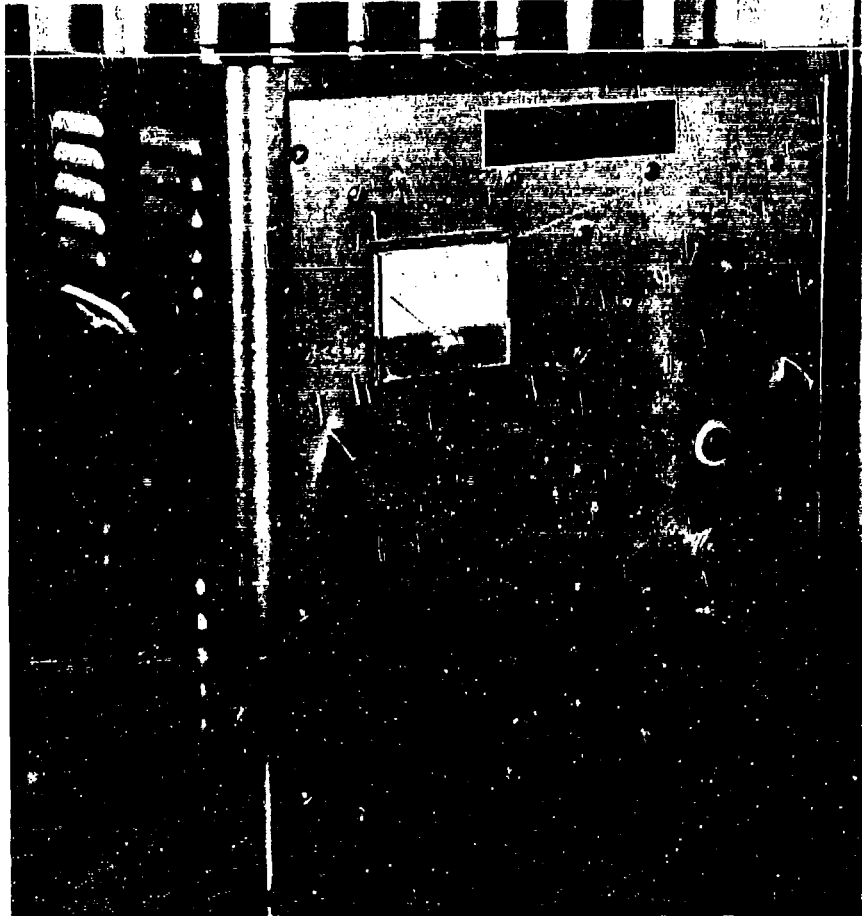


(a) - Door Closed

(b) - Door Open

4 Firing Chamber

4-5.10



5 Franklin Institute Research Laboratories Initiator Static Tester

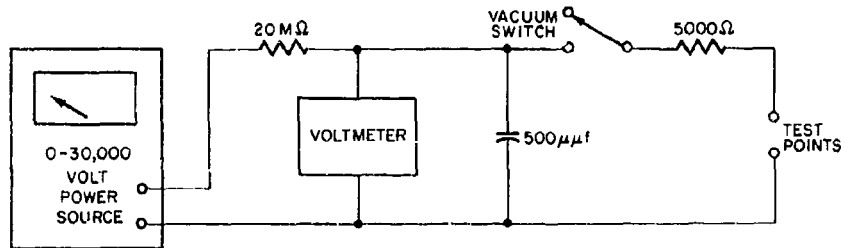
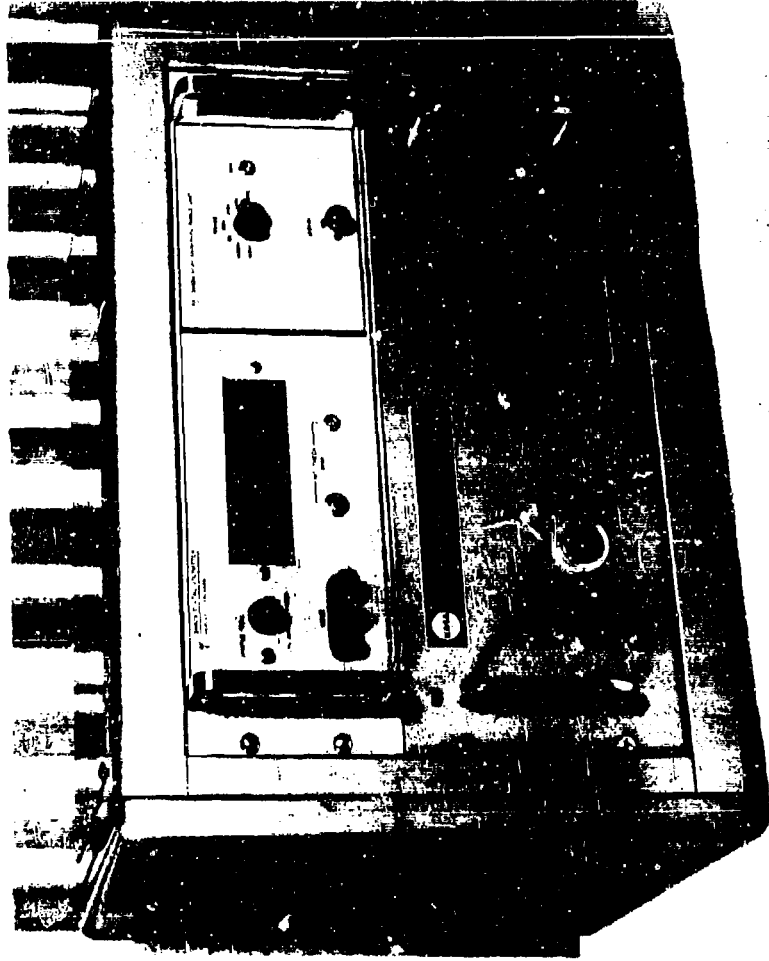


Fig. 6 Static Discharge Test Circuit



7 Exploding Bridgewire Test Set



8 Apollo Standard Initiator Resistance Measuring Equipment (AIRME)



4-6 COMMENTS RELATING TO CONFIDENCE-RELIABILITY

COMBINATIONS FOR SMALL-SAMPLE TESTS

OF AEROSPACE ORDNANCE ITEMS

by

A. G. Benedict

Jet Propulsion Laboratory

California Institute of Technology

ABSTRACT

Analysis epitomized by the widely-used equation

$$Y = 1 - R^n$$

is shown to be reasonably appropriate for small-sample tests of aerospace ordnance items; high-reliability, low-confidence combinations are discussed.

INTRODUCTION

For a complex aerospace system to have even a 50% chance of performing its intended function, the chances of failure in any one subsystem component must be extremely low.

In evaluation of the reliability of aerospace ordnance components, it is common to find--

1. The items are expensive, limiting the number of samples available.
2. The items are of a special design, with no past history to suggest their "likely" reliability.
3. The target reliability approaches unity so that evaluation should really be directed at fail rates rather than reliability.<sup>①</sup>

---

① A decrease of less than 1% in reliability, from 99.9% to 99%, would represent a tenfold increase in fail rate--from  $\frac{1}{1000}$  to  $\frac{1}{100}$ .

4. The items to be tested are "single-shot" and, unlike solenoid relays (for example), cannot be operated non-destructively; items operated in test cannot be used in flight.
5. Tests by both attributes and variables may be appropriate but the frequency distribution for tests by variables is unknown.<sup>②</sup>
6. There will be some uncertainty (if not confusion) in selection of a reliability-confidence combination to best express the results of the evaluation.

Evaluation of small-sample aerospace ordnance tests today follows along lines developed in the mid-twenties by Western Electric and Bell Telephone engineers<sup>③</sup> and is epitomized by the equation

$$\sum_{j=0}^{j=F} \binom{n}{j} f^j (1-f)^{n-j} = \sum_{j=0}^{j=F} \binom{n}{j} (1-R)^j R^{(n-j)} = (1-\gamma) \quad \text{Equation 1}$$

where  $n$  = Number of pass/fail tests

$F$  = Number of fails detected

$$\binom{n}{j} = \frac{n!}{(n-j)! j!}$$

$R$  = Assumed reliability

$f$  = Assumed fail rate

$\gamma$  = Lower confidence limit on  $R$ ,

= upper confidence limit on  $f$ .

② Log-normal or comparable distributions are often assumed, simply as a convenient economy. Although actual test results involving only small samples may prove to be consistent with some arbitrary distribution, use of such a pre-selected distribution for extrapolation to extreme percentiles may be grossly misleading.

③ See Sampling Inspection Tables, Single and Double Sampling page 1, H. F. Dodge and H. G. Romig, John Wiley and Sons, Second Edition, 1959.

which reduces, for a series of  $n$  tests with no failures, <sup>(4)</sup> to

$$(1-f)^n = \frac{\gamma}{n} = 1-\gamma \quad \text{Equation 2}$$

Both equations allow the results of any particular test program to be expressed as indicating any of an infinite number of reliability-confidence combinations. For example, a 5-sample, no-fail test could be interpreted as indicating any one of as many combinations as one wished, including those shown in Table 1

<u>RELIABILITY, R</u>	<u>CONFIDENCE, <math>\gamma</math></u>	<u>MAX. FAIL RATE, <math>f</math></u>
<u>%</u>	<u>%</u>	<u>%</u>
99	5	1
90	41	10
87	50	13
80	67	20
70	83	30
60	92	40
50	97	50
40	99	60

TABLE 1 <sup>(5)</sup>

SOME RELIABILITY-CONFIDENCE COMBINATIONS

FOR A 5-SAMPLE NO-FAIL TEST

(as calculated from Equation 2)

- <sup>(4)</sup> For simplicity, subsequent discussion is limited to no-fail tests; such tests are of particular interest in aerospace ordnance tests, because the number of samples available for test is usually so small that even one failure may imply an intolerably high fail rate.
- <sup>(5)</sup> Note the rapid rise in confidence for a decrease in reliability from 99% to 90% and also that  $\frac{\gamma}{n} \approx f$  for  $\gamma < 50\%$ . It may be shown that, for  $f \approx 0$ ,  
 $\log_{10} (1-\gamma) \approx -.435nf$ .

and the question naturally arises as to which combination, if any, is the most descriptive. For example, if we wanted to use our 5-sample test to judge the quality of a further six items drawn from the same lot, would the 80% reliability-67% confidence combination imply that, of the six samples, five (80%), or four (67%), or three (80% of 67%), would be "passes"--or would none be passes because none are 100% reliable?

Although Equations 1 and 2 relate to tests by attributes, reliability-confidence combinations are also used to express the outcome of tests by variables and the same question arises.

Before proceeding, it is important to note that the original problem faced by the Western Electric and Bell Telephone engineers was that of using small samples to determine whether a particular incoming shipment of components met a quality level which prior shipments had shown the manufacturer to be capable of achieving; if earlier shipments had typically exhibited a "reliability" of 98% or better, with an occasional "bad" lot having a reliability of possibly as low as 80%, the customer might be content with a small-sample receiving inspection scheme which gave him a good chance of detecting lots with less than 98% reliability. By comparison, many aerospace ordnance items involve short-run, one-time production offering no prior history on which to base an "expected" reliability, and the further question arises--is Equation 2 grossly inappropriate in such cases?

#### INHERENT RELIABILITY OF "NO-HISTORY" LOTS

At first glance, it might seem that evaluation of a lot for which all fail rates between 0% and 100% were equally likely would be a much more "pessimistic" process than evaluation of a lot for which fail rates below, say, 70% were assumed to be somewhat unlikely. This is not so, however, because small-sample, no-fail tests quickly cull high fail-rate lots.

CONFIDENCE AND UNEXPECTED FAIL RATES

Although a proportion  $\gamma = 1 - R^{n+1}$  of lots yielding no fails in samples of size  $n$  will contain a proportion  $(1-R) = \frac{1}{n+2}$  or less of faulty items, the remaining fraction  $R^{n+1}$  of the lots will contain a proportion of faulty items larger than  $\frac{1}{n+2}$ ; from these lots will come unexpectedly high and possibly disappointing failure rates. For example, from an 8-sample, no-fail draw the probability of various fail rates can be illustrated as in Table 2.

Reliability <sup>⑧</sup> R	Confidence <sup>⑨</sup> $\gamma$	Most Likely Maximum Fail Rate (1-R)	Approximate Chances of Indicated Fail Rate <sup>⑩</sup>
1	0	0	0
.9	.613	.1	(.613 - 0) .61
.8	.864	.2	(.864 - .613) .25
.7	.959	.3	(.959 - .864) .10
.6	.9897	.4	(.9897 - .959) .03
.5	.9980	.5	(.9980 - .9897) .008
.4	.9997	.6	(.9997 - .9980) .002

TABLE 2

APPROXIMATE CHANCES OF VARIOUS FAIL RATES

FOR A LOT YIELDING NO FAILS IN A SAMPLE OF SIZE 8

- ⑧ .9 is the "inherent" reliability of Equation 5.
- ⑨ Calculated from Equation 6.
- ⑩ These chances strictly relate to ranges of fail rates but are more easily visualized as relating to fails in a lot of size 10.

If we make an n-sample test on a large number K of lots of size L for which all proportions p of passes (P's) between 0 and 1 are equally likely, the chances C of any lot yielding a sample of n P's is given by

$$C = p^n \quad \text{Equation 3} \textcircled{6}$$

and the number of lots M which will yield such samples is given by

$$M = \int_0^1 KC \, dp = \int_0^1 Kp^n \, dp$$

$$\text{from which } M = \frac{K}{n+1} \quad \text{Equation 4}$$

The proportion  $R_1$  of P's in these M lots representing their average quality or "inherent reliability" is given by

$$R_1 = (n+1) \int_0^1 p^n p \, dp = \frac{n+1}{n+2} \quad \text{Equation 5}$$

and the proportion  $\gamma$  of the M lots which will have at least any proportion R of P's is given by

$$\gamma = (n+1) \int_R^1 p^n \, dp$$

$$\text{from which } \gamma = 1 - R^{n+1} \quad \text{Equation 6} \textcircled{7}$$

⑥ True only if samples are returned to the lot as drawn, or if the sample size n is so small by comparison with the lot size L that the removal of the sample has no significant effect on the proportion p of P's remaining.

⑦ Note the similarity between Equation 6 and Equation 2. Equation 6 shows that an isolated lot yielding no fails in a sample of size n will (with confidence  $\gamma$ ) have a comparatively high reliability even if, prior to sampling, all reliabilities between 0 and 1 were considered as being equally likely.

It can be shown that although the inherent reliability approaches 1 as  $n \rightarrow \infty$ , the corresponding  $\gamma$  approaches only the limit  $1 - e^{-1}$ .

From Table 2 it can be seen that an expectation that the fail rate would be 1/10 or less would result in a 25% chance of being disappointed by a factor of 2, and a 10% chance of being disappointed by a factor of 3.

It is obvious that large discrepancies in fail rates will be common unless the chances of excessive fail rates (1- $\gamma$ ) are of the same order as the expected fail rate (1-R). Thus for a meaningful confidence

$$\begin{aligned} \gamma &\approx R \\ \text{but } \gamma &= 1-R^{n+1} \\ \therefore R &\approx 1-R^{n+1} \\ \text{or } n &\approx \frac{\log(1-R)}{\log R} - 1 \qquad \text{Equation 7} \end{aligned}$$

Tabulating n's from Equation 7 for various R's

R	n
.9999	92,000
.999	6,900
.995	1,060
.99	455
.95	57
.90	21
.85	10

TABLE 3

The quantities indicated by Equation 7 are so large for high reliabilities that proof of high reliability of aerospace ordnance components by attribute testing is generally impractical (or unrealistic).

It would seem, however, that tests by variables might allow use of much smaller samples, even if results were evaluated to have matching confidence-reliability combinations, but this would be true only if one is prepared to assume a frequency distribution.

Thus the usual qualification program (involving, typically, no more than one or two hundred test samples) is an anachronism--a carry-over from applications where a limited number of successful tests was considered to demonstrate adequate reliability; a program involving 57 samples, for example, could demonstrate a reliability of only .95<sup>(11)</sup>. At best, small-sample qualification programs of the formalized type will do little more than detect gross fail rates; if test-sample quantities are limited, detection of low potential fail rates depends not on such "qualification" programs, but rather on skillful use of "off-limits" or other comparatively uncommon test techniques, directed toward revealing failure modes rather than toward demonstrating good qualities.

#### CONCLUSIONS

By way of summary--

1. Although strictly not applicable to items with no reliability history, test result analysis techniques epitomized by

$$y = 1 - R^n$$

can continue to be used without introducing serious error.

---

<sup>(11)</sup> See Table 3. This quantity would be required for each parameter; for example, firings at low, medium and high temperature would call for a total of 171 if a .95 reliability was to be demonstrated at each temperature.



2. Low-confidence high-reliability combinations have little practical meaning, but a combination involving equal confidence and reliability will be indicative of the maximum proportion of "fails" which may be expected.
3. Samples of size  $n$  which yield no failures belong to "families" of lots having an inherent reliability  $R_1 = \frac{n+1}{n+2}$  with a confidence  $\gamma = 1 - R^{n+1}$ .
4. Qualification tests are practically useless for demonstrating low failure rates.
5. Small-sample tests by variables are useful for comparative but not absolute evaluation of high reliability.

#### DISCUSSION

It was pointed out during the discussion that the technique described is most adaptable to small lot inspection and that, for large quantity production, only the standard sampling plans are economically feasible.

In presenting the paper, the author commented that the reliability and confidence should be numerically equal. This statement was questioned during the discussion period. The author asked that those wishing to discuss this point contact him on a personal basis.

4-7 LOT-TO-LOT VARIATIONS IN EXPLOSIVE PROPERTIES  
AND THEIR CONSEQUENCE IN EXPLOSIVE COMPONENT  
DEVELOPMENT AND PRODUCTION

by

Richard A. Whiting

Honeywell Inc., Ordnance Division, Hopkins, Minnesota

Richard H. Stresau

R. Stresau Laboratory, Inc., Spooner, Wisconsin

James N. Ayres

U. S. Naval Ordnance Laboratory, White Oak, Maryland

INTRODUCTION

An explosive component that has been performing well in all tests suddenly starts failing. This may happen at any time after the first feasibility tests until the last production lot has been manufactured. If you are involved with explosive components and this has not happened to you, then like the machinist who has never broken a tap, you have not done anything.

Such sudden occurrence of failures may result from several causes: deviations from specifications or drawings, changes in test conditions or procedures, or variation of properties of materials which are either within tolerances or are unspecified. This paper is concerned with this last category of variation and specifically with lot-to-lot variation of those properties of explosives which affect the initiation, growth, and transfer of detonation.

The initiation, growth, and transfer of detonation are complex processes which depend on the interaction of a variety of factors. It is self-evident that these chemical reactions depend on the composition of the explosive. Less obvious and only imperfectly understood are the effects of such physical factors as particle size and shape, particle size distributions, and the microscopic spatial distribution of components of mixtures. There is much experimental evidence to indicate that such physical factors can greatly affect detonation, and can, in fact, make the difference between highly reliable operation and almost certain failure of ordnance items.

## EXAMPLES OF LOT-TO-LOT VARIATION

We all recall instances of difficulties which have been attributed to lot-to-lot variations in explosive properties. Most of these difficulties have been solved by finding a "fix" rather than by definitely determining the cause of the difficulties. It is easier to find examples of variations which could result in problems had they not been detected. Some such examples, categorized in terms of the various functions of an electro-explosive device (EED), are presented below.

### Response to Electrical Stimulus

Figure 1 illustrates the variation of threshold firing energy of electric initiators loaded with dextrinated lead azide <sup>(1)</sup>, of various lots. It should be noted that at the lower loading pressures, the threshold firing energy varied by a factor of more than two. Tungsten bridgewires were used in these experiments: any other metal would probably have burned out without initiating the less sensitive combinations of loading pressure and lot. Thus, particularly if loaded at the relatively low pressures characteristic of the structural limit of many plugs and headers, devices loaded with lead azide from one lot might function reliably, while supposedly identical items loaded with azide from another lot might burn out without firing.

### Growth of Detonation

Reliable propagation across explosive interfaces in an EED or fuze train depends on detonation growth, the total buildup of energy in the detonation head. This includes delays in transition from deflagration to detonation, detonation rate growth, and propagation at less than ideal rates. These phenomena are particularly important for the typical EED situation where the explosive increment length is less than a diameter.

The apparatus shown in Figure 2 has been used by Stresau and Rowe to investigate lot-to-lot variations in the growth of detonation in lead azide <sup>(2)</sup>. Table 1 gives the dent depth in steel witness blocks and dead pressing pressure for various lots of lead azide. In these experiments, dent depth was taken as a measure of the length of explosive column necessary to make a transition from deflagration to detonation. This follows from the geometry of the experiments where column length is less than one diameter. It is also assumed that when the transition takes place in lead azide, it is very abrupt. The range of dent depths is shown to be more than 3:1 for dextrinated lead azide.

In the experiments cited, dead pressing pressure was taken as the point at which a plot of depth versus logarithm of loading pressure descended to half of its peak. The behavior is more clearly illustrated by reference to Figure 3, also taken from the work of Stresau and Rowe. It is particularly important to note the behavior of dextrinated lead azide in the region of 10,000 to 20,000 psi pressing pressure, common for loading EED's. The outputs for some lots of dextrinated lead azide are close to maximum while other lots are approaching minimum output at the same pressure.

Other interpretations of the data presented above are possible. Such factors, including a metastable detonation rate for dextrinated lead azide, were discussed by the experimenters. The implication of these data for present purposes is clear. An EED, developed, tested, and shown to be reliable with one lot of lead azide, may produce consistent duds when loaded with another lot.

#### Stability of Detonation

The explosive increments in an EED or fuze train are often near the critical dimensions for stable propagation of detonation. Experiments with 0.043 inch thick Detasheet C illustrates lot-to-lot variations in critical dimension. The data given in Table 2 show that strips of Detasheet from one lot begin to propagate at 0.04 inch width while strips of the same width from another lot are consistent duds. The particular dimensions are true only for the experimental setup used, but the effect will be encountered in other layouts and with other explosives. The trend toward miniaturization of fuzes will make this a significant problem area in the future. For many, it is a significant problem right now.

The Naval Ordnance Laboratory, White Oak (NOL/WO) has developed a test for measuring the sensitivity of sheet explosive. This test is an adaptation of the NOL small-scale gap test and was developed when it was found that a previously successful explosive device failed to propagate detonation

with a new lot of sheet explosive. The new lot was some twenty or more standard deviations less sensitive than the original explosive. It has since been determined that Du Pont can adjust the sensitivity of sheet explosive within rather wide limits. In sophisticated designs it is necessary to specify the sensitivity required.

#### Detonation Transfer

Only rarely does a specification control the sensitivity or output of an explosive composition. In the case of RDX composition CH-6, where such requirements are included in MIL-R-21723, the initiation requirement has been difficult to maintain in production.

Table 3 gives both the density and sensitivity versus pressing pressure for various lots of RDX Composition CH-6. Reference data for TNT are included. Data given are the mean for twenty measurements.

Attention is directed to the variation in sensitivity at 16,000 psi pressing pressure for lots X344 and X439, respectively 3.984 and 5.479 decibangs (DBg see NOLM 7328 and 7411). At these two points, the standard deviation was calculated and used to predict the percent response versus shock sensitivity shown in Figure 4. In a design requiring a shock sensitivity of 4.7 DBg, lot X344 would be in excess of 99.9 percent reliable while lot X439 would be a consistent dud. The implications for EED design requiring detonation transfer are self-evident.

#### CAUSES OF VARIATION IN EXPLOSIVE PROPERTIES

An EED may unexpectedly exhibit unreliable performance at any point in development or production. The exigency of program schedules seldom permit a detailed investigation of the cause of such failures. A "fix" is

found, generally by overdesign or substitution of explosive. New tests show the item to again be performing properly, and the course of development or production is continued. While the reasons for such behavior are not generally determined, the following are suggested possibilities.

#### Chemical Variables

A cause for variation in explosive performance is the variation, within tolerance, of the composition of mixtures and the purity of compounds.

A case in point is RDX Composition CH-6. This explosive is a mixture of four compounds, each capable of variation within tolerance on weight percent and purity. In combination with factors described below, variations within these tolerances from lot to lot undoubtedly contribute to variations in performance described under Detonation Transfer.

In the case of RDX Type B, the primary impurity is HMX. Military specification MIL-R-398 controls purity primarily by specifying a minimum melting point. Literal interpretation of this specification would allow a wide range of RDX/HMX mixtures. Examination of the melting point curve of Figure 5 makes this amply clear. The effect produced by variations in purity will depend on the particular application, but undoubtedly plays a part in variation in explosive performance. The user must rely primarily on the internal controls of the manufacturer to maintain the purity of this product. It is interesting to note that laboratory analysis of the melting point, with the Fisher John hot stage melting apparatus, of a lot of RDX Type B, Class E from Canadian Industries, Limited, and Holston Defense Corporation both yielded the same result within experimental error: 192°C. The thermograms for the two lots derived by differential thermal analysis also appeared the same. And yet, as will be shown later, these materials have a greatly different particle size and shape, and size distribution.

The percent of lead azide in various lots of several types of azide has been measured <sup>(3)</sup>. Results are given in Table 4. No correlation was observed between lead azide percent and dent depth in the apparatus shown in Figure 2. Such variations in purity undoubtedly effect performance indirectly by changes in density versus loading pressure and may account for some of the variation in threshold firing energy shown in Figure 1.

The military specification for each explosive is unique in the control of purity. Even where minimum purity is specified, such as for HMX and lead azide, the allowed variation is sufficient to result in large variations in reliability in finished ordnance.

#### Loading Pressure versus Density

It is known that the initiation sensitivity of explosives is strongly influenced by density. The difficulty in measuring absolute sensitivity or density casts considerable doubt on comparisons of data obtained in different laboratories. However, relative measurements under controlled conditions in the same laboratory show significant correlation between density and detonation sensitivity of various lots of the same explosive loaded at the same pressure. Such a correlation is evident in the output data for RDX shown in Figure 6 and sensitivity data for RDX Composition CH-6 shown in Figure 7. Although density is not given for lead azide shown in Figure 1, from the trend in the data it is evident that a large portion of the variation between lots is due to lot-to-lot variations in density at constant loading pressure.

In many instances, the unscheduled variation in performance of ordnance items is the result of variations in density at constant loading pressure. Factors which influence obtained density include composition, particle size, particle size distribution, particle shape, moisture content, crystal strength, and loading conditions. Few of these factors are controlled by specification.

## Particle Size

It has been shown for ammonium picrate that a coarse particle size material has a larger critical diameter than a fine material and certain mixtures have a larger critical diameter than either the coarse or fine material<sup>(4)</sup>. The maximum critical diameter occurred at about 75 percent coarse material. There is evidence that RDX mixtures exhibit this same trend<sup>(5)</sup>. The difference in critical dimension, discussed in a preceding section for two lots of Detasheet C, were traced directly to differences in PETN particle size.

A more dramatic example of the effect of particle size can be made by comparing two explosives based on RDX mixtures, namely CH-6 and SPX-2<sup>(6)</sup>. Both explosives exhibit the same sensitivity according to the small-scale gap test<sup>(7)</sup>. However, CH-6 cannot be initiated by 10 grain/foot MDF while SPX-2 is initiated by 1 grain/ft MDF. Composition CH-6 is based on RDX Class A, the particle size of which peaks around 125 microns. Composition SPX-2 is compounded from RDX finer than 44 microns. This illustrates the tremendous difference in sensitivity to initiation by sources of small dimension resulting from gross changes in particle size. It also illustrates the large difference in relative sensitivity that may result from changes of initiation source.

Changes of particle size which affect EED performance are apparent from lot to lot of material. Tables 5 and 6 show the results of sieve analysis for various lots of RDX. Figure 8 shows the difference in particle size, particle size distribution, and particle shape for two lots of RDX Class E. Changes in particle size can also be induced by handling or sampling techniques and should not be confused with intrinsic lot-to-lot variations. For example, sieve analysis of RDX Class C from shipping bags will exhibit variations in particle size not only from lot to lot, but depending on how the test sample is withdrawn. It appears that the coarse material will tend to rise to the top of the bag.



## Crystallographic Factors

Many explosives exhibit polymorphism. For both lead azide and HMX, experimental evidence shows substantial difference in sensitivity between crystalline forms. McCrone<sup>(8)</sup> obtained the impact sensitivity data for HMX given in Table 7. Drop height is shown to vary from 31-32 cm for beta HMX to 7-8 cm for delta HMX. He also found that a small percentage of the sensitive form of HMX would impart its sensitivity to a much larger portion of RDX to which it was added. Under normal circumstances, these observations present little cause for alarm. Beta HMX is stable in the range of normal atmospheric temperatures and precautions are taken to assure that HMX and the HMX content of RDX is of the beta form. However, it is not always possible to learn the complete storage history of an explosive material. Jeffers<sup>(9)</sup> reports that exposure to elevated temperature can result in crystalline transitions which are not always reversed on cooling.

McCrone<sup>(10)</sup> has also found that the sensitivity of HMX can be affected significantly by crystalline strain. It might be expected that other hard crystalline explosives such as RDX and lead azide would also show this tendency. In this respect, there is evidence of substantial residual strain in some lots of PVA lead azide. The strain resulting from twinning has also been suggested as the reason for some of the explosions which occurred in lead azide plants before such control agents as dextrin, polyvinyl alcohol, and carboxymethyl cellulose were used.

Although the specifications for polymorphic explosives are generally written with conscious effort to assure that only the desired crystal form is present, the possibility of recrystallization in storage cannot be ignored. Residual intracrystalline strain is rarely, if ever, considered in specifications. Such factors may account for some lot-to-lot variability.

### State of Association of Mixtures

The intimacy of mechanical mixtures of granular materials is obviously related to the particle sizes of the components. Such mixtures can also be affected by mixing techniques which may cause unintended "balling up" of certain components or conversely grinding or other particle size reductions. Moisture content can be quite critical. Too much moisture can cause some materials to agglomerate. Too little moisture can result in electrostatic effects which greatly alter the properties of a mixture. Mechanical mixtures of materials of dissimilar density or particle size, though quite uniform at manufacture, have been known to segregate under conditions of transportation and handling. The complications from such changes in mixtures have led, in some quarters, to the characterization of the pyrotechnic art as "witchcraft."

Desensitization of RDX by waxy materials seems to be at least partly a lubrication effect. The coating of the RDX in a hot water slurry as in Composition A, or by the precipitation technique used for CH-6, is more effective than mechanical mixing in this respect. In mechanical mixtures containing waxy materials of relatively low melting point, such as stearic acid, exposure to elevated temperature can result in migration of the stearic acid and an effective change from a strictly mechanical mixture to one in which the explosive is coated with the desensitizer. In one recent instance, this has resulted in duds of a component which was highly reliable before such heating.

### CONCLUSION

Lot-to-lot variations in explosives properties which can affect the reliability of EED's or fuze trains have been discussed. It has been demonstrated that such variations are sufficient in many cases to make

the difference between a highly reliable ordnance item and a consistent dud. An aspect which was not discussed, however, is safety. For example, if out-of-line safety is demonstrated with an insensitive lot of explosive in the lead position, later loading of the lead with a sensitive lot of the same explosive could eliminate the safety margin.

The significance of lot-to-lot variations in explosive properties depends on the particular design situation and even on the experience or perceptiveness of the design engineer. A more experienced individual may include in his designs sufficient margin for changes in lot properties. Lacking objective data on lot variations, however, this approach must lead to variable results. The trend toward miniaturization of fuzes and explosive components makes the penalty for overdesign more severe. In this area the development engineer has the greatest problem: an entire development and test program may use only a portion of the material in a shipping container, and it, in turn, may be only an insignificant portion of a lot.

What can be done to offset the effect of lot-to-lot variations as they effect explosive designs? The most productive response would be to incorporate standards for sensitivity and output in specifications. This includes contractor purchase specifications as well as military specifications. In addition, lot variation data could be collected by a larger user, presumably a government arsenal or laboratory, and made available to the explosive designer. Thus, the performance of a wide range of lots could be compared by the explosive designer with the performance of the particular lot available for development testing. Appropriate, but not unnecessary, margins could then be designed into the explosive device.

There are other steps to be taken by the EED designer to avoid problems arising from lot variations in explosive materials. These steps can be taken in the absence of specification-imposed performance controls or

representative performance data for a variety of lots. In a design involving detonation transfer, where the VARICOMP<sup>(11)</sup> testing approach is not used, a much higher level of reliability must be demonstrated than the ordinary 99.5 or 99.9 percent. Where VARICOMP testing is used, an appropriate bandwidth must be allowed between the design output stimulus and receptor sensitivity, somewhat in excess of five standard deviations. As an example of the VARICOMP approach, consider a hypothetical design containing a lead loaded with tetryl, RDX, or HNS. An explosive known to be more sensitive than even the most sensitive lot of the tactical explosive is substituted in the lead. For example the lead is loaded with PETN or lead azide. If the fuze passes out-of-line safety in this circumstance, it can be assumed to be safe with any lot of the tactical explosive. Application of this technique requires considerable care, and a solid background of relevant experience. When used properly, this approach is a powerful tool permitting marked savings in time and material.

Whether the suggestions presented above are implemented, the EED designer will benefit from the material presented if a day-to-day consciousness of lot variations has been created. To be forewarned of lot-to-lot variations in explosive properties is to be forearmed against unexpected consequences.

The authors wish to express their appreciation to the management of their respective organizations for making time and facilities available to prepare this paper. We also wish to thank Mr. Don McClean of Canadian Industries Limited for the data on RDX, and our associates who have contributed experimental data: J. A. Ford and B. W. Kelley, Honeywell Ordnance Division; R. L. Peterson, R. Stresau Laboratory; and C. W. Randall, NOL/WO.

## REFERENCES

- (1) Stresau, R. H. F., and M. H. Rowe, "Observations of the Effects of Loading Density on the Initiation and Growth of Detonation in Azides," U. S. Naval Ordnance Laboratory, White Oak, Maryland, NOLTR 61-134, 1961, p. 18.
- (2) Ibid., p. 13.
- (3) Ibid., p. 11.
- (4) MacDougal, D. P., and R. Messerley, "The Effect of Particle Size on the Detonation Velocity of Ammonium Picrate," OSRD Report 1755.
- (5) R. Stresau Laboratory Report No. 62-5-1, "Design and Development of a Nonelectric Blasting Cap Which Will Detonate Only if Immersed in Water," Spooner, Wisconsin, 31 May 1962.
- (6) For a description of SPX-2 see "Miniaturization of Out-of-Line Explosive Systems," a paper in this Symposium.
- (7) Ibid.
- (8) Authors notes from OSRD reports and private communication from Walter C. McCrone, Cornell University, ca. 1943.
- (9) Jeffers, W., "The Impact Sensitivity of HMX Polymorphs," Proc. of the Gilbert B. L. Smith Memorial Conference on Explosive Sensitivity, NOL White Oak, Maryland, Sept. 16-17, 1957, p. 13-137.
- (10) Private communication from W. C. McCrone, Walter C. McCrone Associates, ca. 1960.
- (11) Ayres, J. N., et al., "VARICOMP, a Method for Determining Detonation-Transfer Probabilities," NAVWEPS Report 7411, 30 June 1961 (AD 263381).

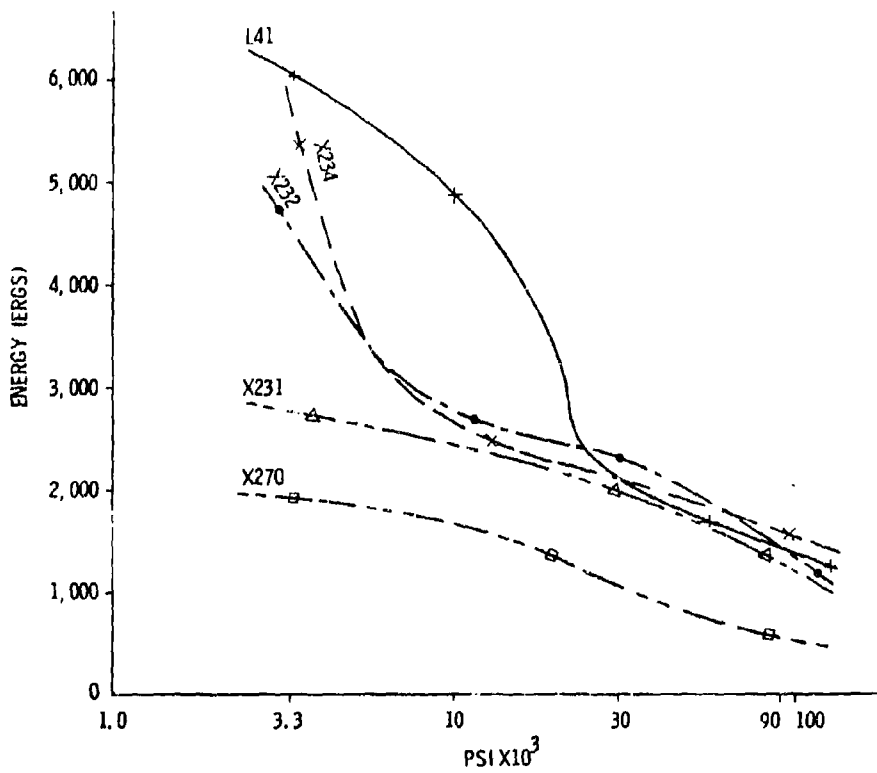


Figure 1 - FIRING ENERGY VS LOADING PRESSURE FOR ELECTRO-EXPLOSIVE DEVICES WITH FLASH CHARGES OF VARIOUS LOTS OF DEXTRINATED LEAD AZIDE.

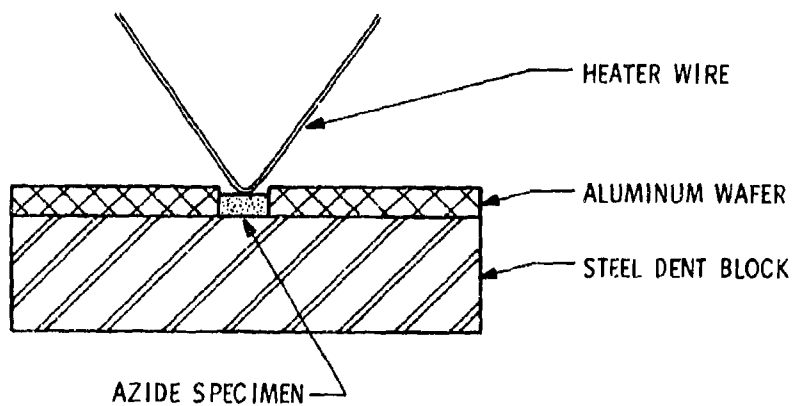


Figure 2 EXPERIMENTAL ARRANGEMENT FOR MICROSCALE PLATE DENT TEST (FROM NOLTR 61-134)

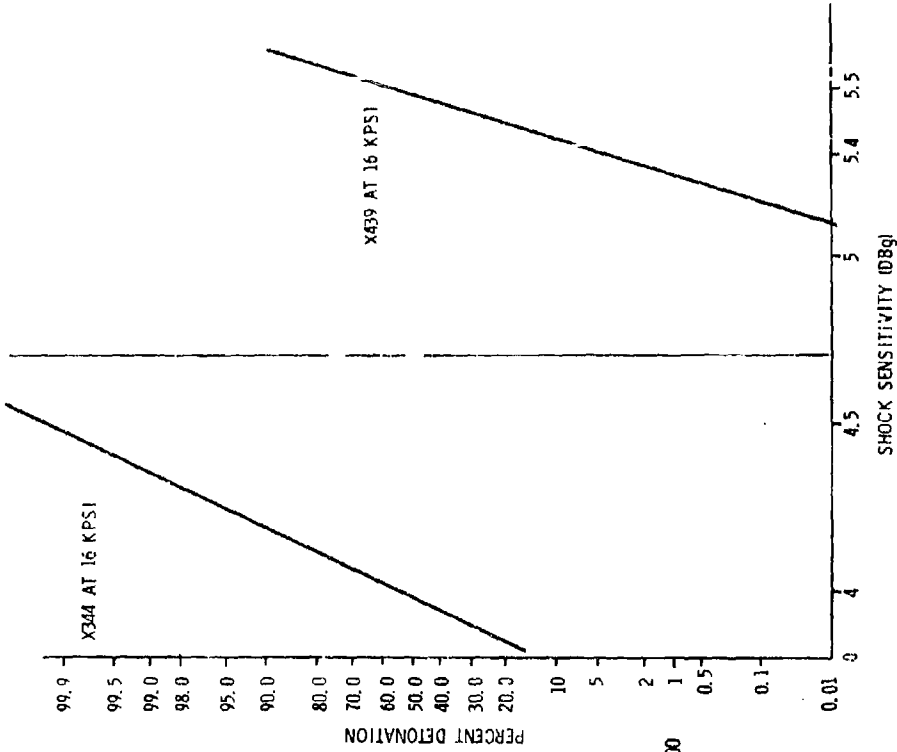


Figure 4 - PERCENT DETONATION VS SHOCK SENSITIVITY FOR 2 LOTS OF CH-6

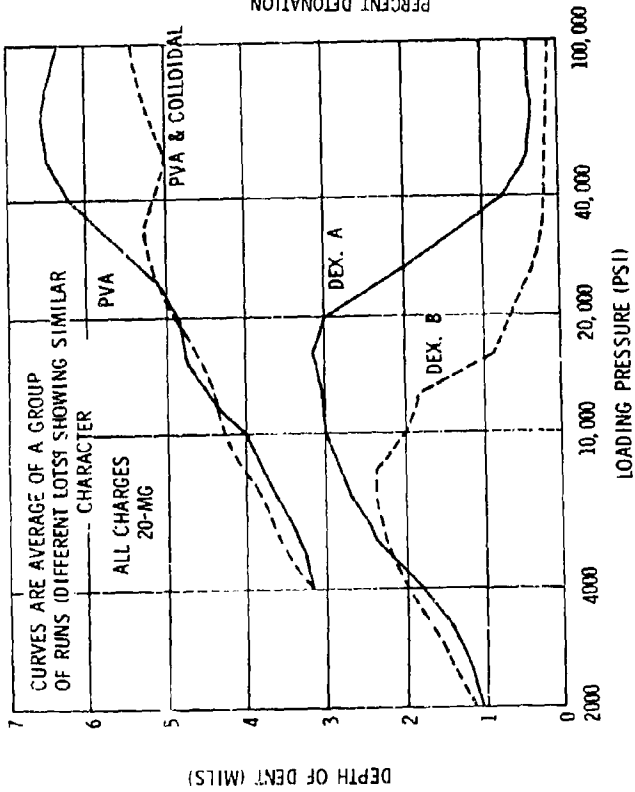


Figure 3 - STEEL PLATE DENT TEST, MICROSACLE (FROM NOLTR 61-134)

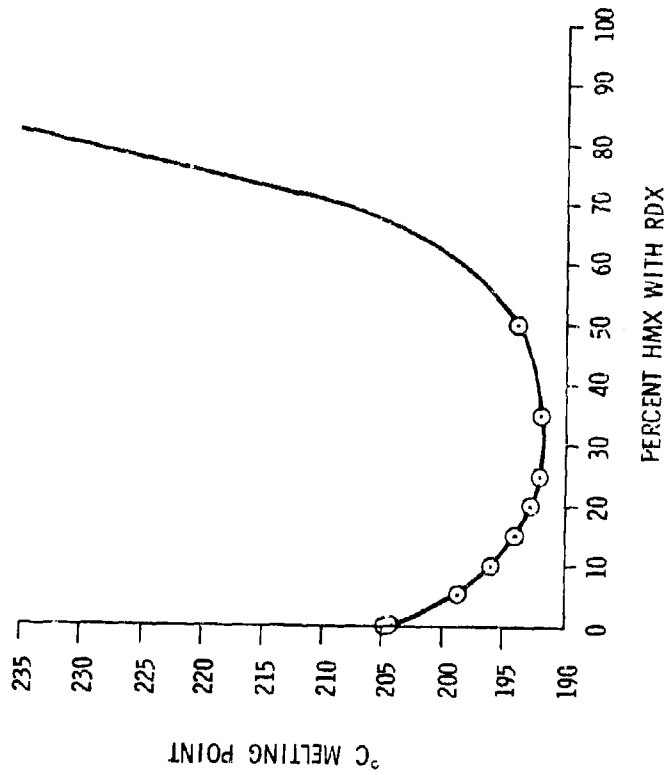


Figure 5 - MELTING POINT OF HMX-RDX MIXTURES

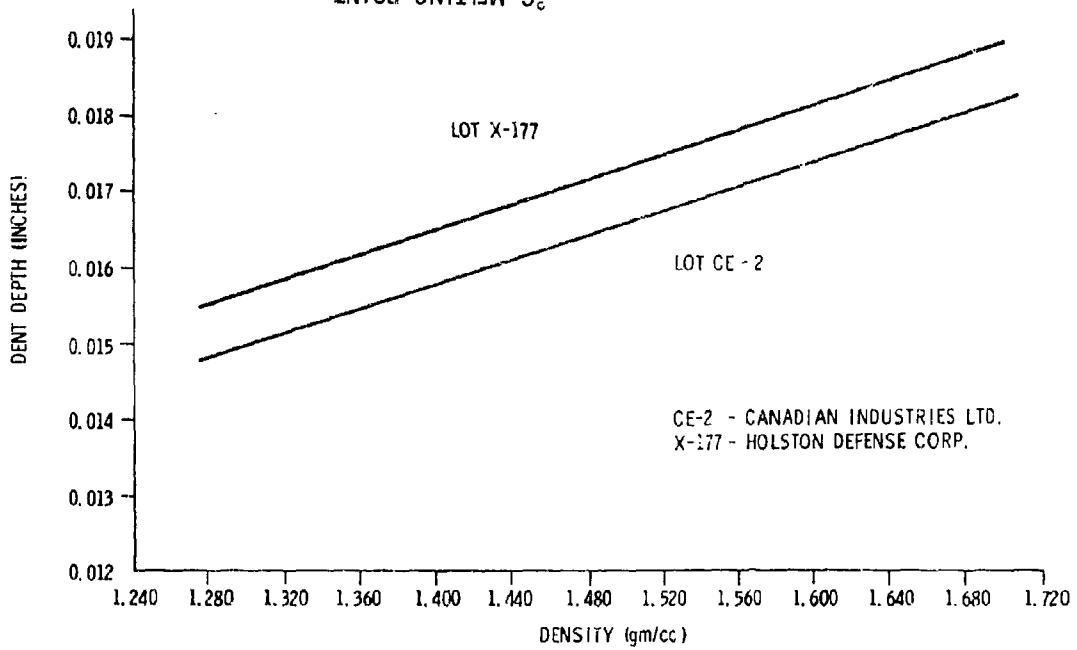


Figure 6 - DENT DEPTH VS. DENSITY FOR TWO LOTS OF RDX CLASS B TYPE E



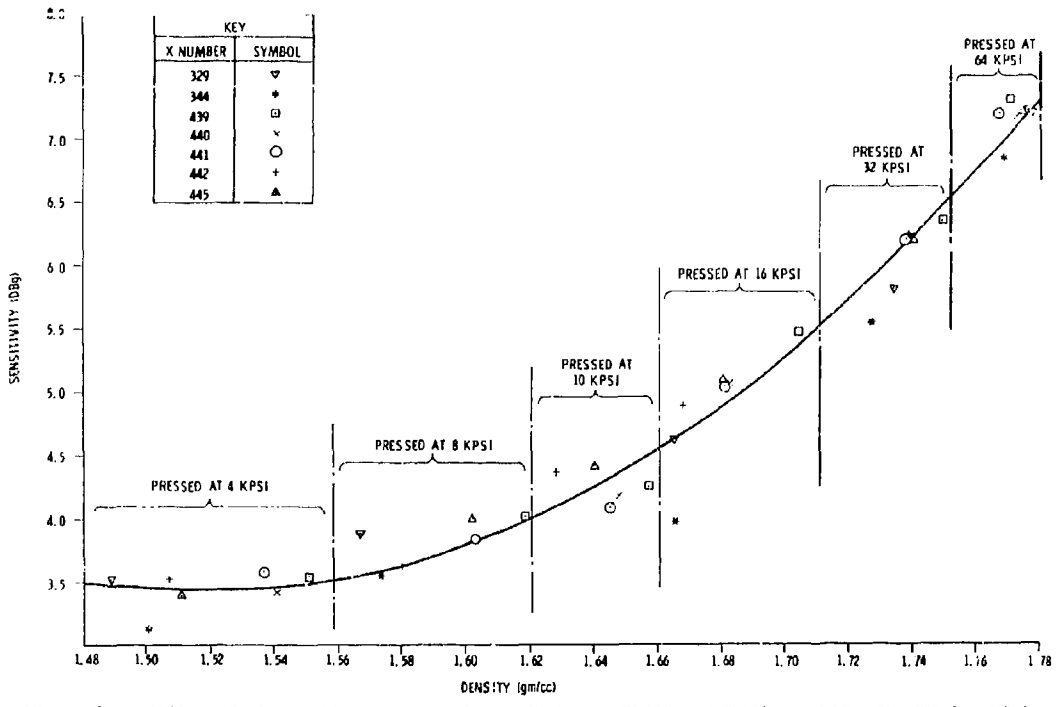
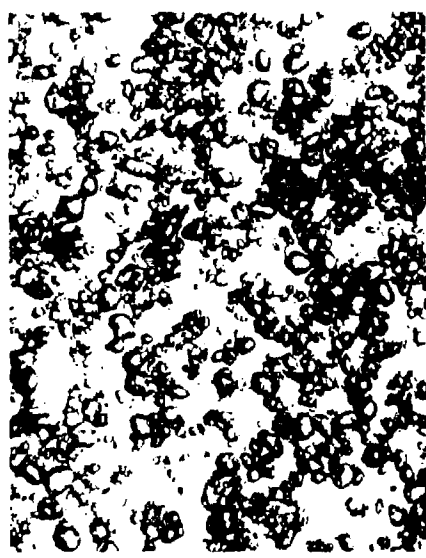
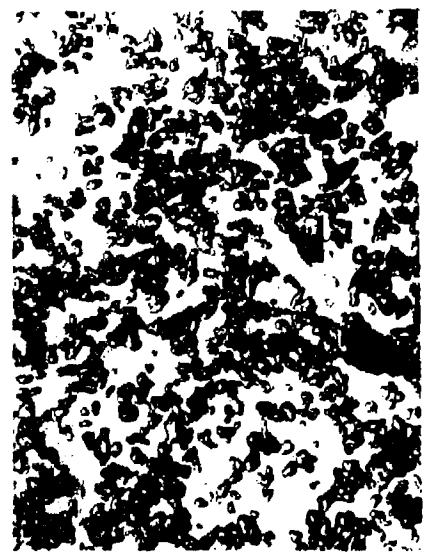


Figure 7 - SMALL-SCALE GAP TEST MEASUREMENT OF SENSITIVITIES OF VARIOUS CH-6'S AS A FUNCTION OF CHARGE DENSITY



PRODUCT OF HOLSTON DEFENSE CORP.



PRODUCT OF CANADIAN INDUSTRIES LTD.

Figure 8 - MICROGRAPH SHOWING TYPICAL POWDER SIZE AND SHAPE FOR TWO LOTS OF RDX TYPE B CLASS E. MAGNIFICATION (250X). TECHNIQUE - BACKLIGHTING THROUGH WATER.

TABLE 1  
 VARIATIONS OF DEAD PRESS PRESSURE AND DENT DEPTH

LOT	AT 10K KPSI DENT DEPTH mils	DEAD PRESS PRESSURE KPSI
DEX L. A.		
X233	0.4	11
X232	0.9	13
X226	0.6	11
X243	0.6	18
X227	0.8	17
X234	0.9	18
X230	1.0	10.8
X225	1.4	14
X239	1.1	14
X235	1.1	14
L41	1.1	34
X240	1.0	25
X231	1.2	18
PVA L. A.		
X228	2.1	125
X238	1.7	> 125
X242	1.8	> 125
X114	2.3	74-125*
X169	2.6	> 40-125*
X241	2.2	> 125

\* BI-MODAL

TABLE 2  
 CRITICAL DIMENSIONS (L) ESTIMATED WITH DEFLATED C  
 0.043 INCH NOMINAL THICKNESS  
 AN EXPERIMENTAL RESULTS LABORATORY

LOT	WIDTH INCHES	NO. OF TRIALS	NO. OF SUCCESSFUL PROPAGATIONS
A	.03	4	2
A	.04	8	7
A	.08	1	1
B	.04	3	0
B	.06	5	2
B	.08	1	1

TABLE 3  
 DENSITY AND SENSITIVITY VS PRESSING PRESSURE  
 FOR VARIOUS LOTS OF CH-6

CH-6 LOT NUMBER								
PRESSING PRESSURE psi	X329	X344	X439	X440	X441	X442	X445	(TNT) X412 REFERENCE
DENSITY, g/cc								
4000	1.489	1.500	1.551	1.541	1.537	1.507	1.511	1.353
8000	1.567	1.573	1.618	1.603	1.603	1.579	1.602	1.446
10000	1.622		1.657	1.648	1.645	1.628	1.640	
16000	1.665	1.665	1.704	1.682	1.681	1.668	1.680	1.549
32000	1.734	1.726	1.749	1.741	1.738	1.738	1.740	1.623
64000	1.777	1.767	1.770	1.772	1.767	1.776	1.774	1.651
SENSITIVITY, DECIBANGS								
4000	3.503	3.131	3.532	3.439	3.580	3.523	3.481	5.067
8000	3.876	3.541	4.006	3.824	3.833	3.627	4.001	5.316
10000	4.197		4.250	4.206	4.090	4.368	4.417	
16000	4.620	3.984	5.479	5.056	5.045	4.915	5.157	5.878
32000	5.812	5.544	6.355	6.243	6.218	6.245	6.236	6.703
64000	7.207	6.838	7.308	7.184	7.203	7.257	7.227	8.066

TABLE 4  
 PURITY OF VARIOUS LOTS OF LEAD AZIDE

LOT NO.	TYPE OF LEAD AZIDE	% LEAD AZIDE BY ANALYSIS
X225	DEXTRINATED	93.4
X226	DEXTRINATED	93.4
X227	DEXTRINATED	91.4
X230	DEXTRINATED	93.4
X231	DEXTRINATED	92.6
X232	DEXTRINATED	92.2
X233	DEXTRINATED	93.5
X234	DEXTRINATED	93.4
X235	DEXTRINATED	93.9
X239	DEXTRINATED	93.1
X240	DEXTRINATED	92.3
X243	DEXTRINATED	91.6
X228	PVA	95.1
X238	PVA	90.0
X241	PVA	95.6
X242	PVA	94.1
X229	COLLOIDAL	98.9
X236	COLLOIDAL DEXTRINATED	90.0
(NaN <sub>3</sub> STANDARD)		99.6

TABLE 5  
 GRANULATION DATA ON SOME BATCHES OF TYPE B,  
 CLASS A RDX PRODUCED AT DE SALABERRY WORKS,  
 CANADIAN INDUSTRIES LTD.

BATCH NO.	PERCENT THROUGH		AVERAGE PARTICLE SIZE	
	U.S. STANDARD NO. 325 SIEVE	BY FISHER SUB-SIEVE (MICRONS)	U.S. STANDARD NO. 325 SIEVE	BY FISHER SUB-SIEVE (MICRONS)
A 971	100.0	100.0	81.3	12.4
A 972	100.0	100.0	78.4	9.5
A 973	100.0	100.0	77.4	26.8
A 974	100.0	100.0	82.9	29.7
A 975	100.0	100.0	77.2	4.9
A 976	100.0	100.0	78.0	8.1
A 977	100.0	100.0	77.0	11.1
A 978	100.0	100.0	76.7	9.9
A 979	100.0	100.0	71.7	17.7
A 980	100.0	100.0	77.1	10.0
A 981	100.0	100.0	82.1	5.8
A 982	100.0	100.0	76.7	6.3
A 983	100.0	100.0	74.5	8.8
A 984	100.0	100.0	79.4	8.6
A 985	100.0	100.0	78.6	6.7
A 986	100.0	100.0	78.2	10.8
A 987	100.0	100.0	81.5	12.2
A 988	100.0	100.0	71.1	11.1
A-1041	100.0	97.9	74.5	7.0
A-1042	100.0	99.9	80.0	6.9
A-1043	100.0	97.5	88.8	6.5
A-1044	100.0	99.9	76.9	7.7
A-1045	100.0	99.8	74.0	6.7
A-1046	100.0	100.0	71.9	7.4
A-1047	100.0	97.9	74.5	7.7
A-1048	100.0	99.9	74.5	6.4
A-1049	100.0	99.8	79.8	6.7
A-1050	100.0	99.9	65.5	11.5
A-1051	100.0	99.9	77.7	6.6
A-1052	100.0	99.9	67.5	9.2
A-1053	100.0	99.9	71.6	7.7
A-1054	100.0	99.9	75.4	6.5
A-1055	100.0	99.9	78.7	9.6
A-1056	100.0	99.9	74.4	11.2
A-1057	100.0	99.9	70.1	6.7
A-1058	100.0	99.9	78.0	6.7

TABLE 6  
 GRANULATION AND PARTICLE SIZE DATA ON SOME BATCHES OF TYPE B  
 CLASS E RDX PRODUCED BY DE SALABERRY WORKS,  
 CANADIAN INDUSTRIES LTD.

BATCH NO. RDX	PERCENT THROUGH U. S. STANDARD NO. 325 SIEVE	AVERAGE PARTICLE SIZE BY FISHER SUB-SIEVE (MICRONS)
E-3	97.8	12
E-9	98.1	13
E-11	99.2	12
E-25	98.9	13
E-32	97.6	12

## DISCUSSION

In reply to a question, the author stated that he did not mean to infer that the crystal strength of a given explosive would vary from lot to lot.

4-8 RELIABILITY ASSESSMENT OF ORDNANCE COMPONENTS  
FROM VARIABLES PERFORMANCE PARAMETERS

S. Demskey

V. Goldie

M. West

General Electric Company  
Re-entry Systems Department  
Philadelphia, Pennsylvania

1.0 ABSTRACT

Even as probability/confidence requirements for aerospace equipment continue to climb, industry still clings to analysis of attribute (go/no-go) test data for providing probability confidence estimates. One justification for this is that the problems faced in alternative approaches are multi-parameter and multi-dimensional, and a recently developed multivariate tolerance procedure is still complex in calculating system performance. The method outlined in this paper, VAEP (Variables/Attributes/Error Propagation), offers a solution which is simple to calculate.

In order to overcome the large sample size associated with application of the binomial analysis, the VAEP procedure utilizes critical variables and performance parameters. Although the analysis is somewhat more complex than a binomial attribute analysis, the advantages outweigh the disadvantages.

The steps followed in providing Probability/Confidence (P/C) estimates based on variables data are as follows:

- 1) Identification of the critical, performance parameters.
- 2) Definition of the test plan
- 3) Statistical analysis

These activities have been and are followed today but not for the purpose of providing Probability/Confidence (P/C) estimates. Step 1 is routinely used in equipment design and Step 2 is used for solving R&D, qualification, and production problems. The statistical analysis, however, does have a new application of an old principle. The two essential statistical methods are statistical tolerance limits and error propagation.

It is the integrated use of these two methods which should suffice until a simple multi-variate tolerance limits method is developed. The concept of error propagation is used to answer the problem of combining confidence levels. Simply, the answer is that we do not combine confidence levels, but this is discussed in more detail in the body of this paper

## 2.0 DEFINITION OF VARIABLES PARAMETERS

Since more than one variables parameter will be used in making P/C estimates for systems, it is apparent that the traditional definition cannot be used because it is concerned primarily with the life parameter. Thus, the use of variables parameters requires knowledge of the intended use in order to correctly identify the critical performance parameters.

Probability is a measure of hardware performance, and, statistically, it is the estimated percentage of units which will fall within assigned specification limits, under real or simulated environments as predicted from experimental data.

Confidence is a measure of data performance, which is an estimate of the number of repeated samplings of the same sample size which will yield the same reliability estimate.

When variables data are to be used, it should be emphasized that both Probability and Confidence are a function not only of sample size but also of data reproducibility (i.e., standard deviation). For two samples with the same mean, sample size and measured against the same specification limit, the sample with the smaller standard deviation yields the higher P/C estimate. Therefore, the sample size to meet any required Probability/Confidence levels is generally smaller than that required for attribute or go/no-go data.

This concept may be appreciated by considering the two diagrams which follow and which represent two sets of results of performance data (e.g., peak pressure) relative to their specification limits:



By considering the data in attribute form, the binomial estimates for 0 failures in six units

Case	Confidence	
	50	95
A	0.8909	0.6070
B	0.8909	0.6070

Both estimates are exactly the same! Yet if any engineer were to be asked which is the better performing unit, the answer would and has been — Design B. A statistical analysis of the variables data would parallel the engineering response.

## 2.1 WHY VARIABLES

The previous paragraph suggests, of course, the primary reason why variables data is used, namely, reduced sample size. The value and effectiveness, to some degree, is suggested by the issuance of MIL-STD-414.



- 1) Reduced sample size, however, is not the only benefit to be realized from an analysis of the variables performance parameters.

As a result of the smaller sample sizes, system testing will be encouraged. For example, a standard being recommended for rockets requires the testing of a large number of igniters, chambers, propellant, etc., and the rocket system estimate will be obtained by a binomial system method. With VAEP, a small number of whole rocket systems could be tested. An exact system test with real hard data is certainly preferred to a group of approximate subsystem tests with subsystem data.

- 2) Analysis of variables data forces the designer into identification and measurement of the pertinent, performance parameters, thereby aiding him in comprehending underlying physical processes.
- 3) The parameters provide criteria for controlling lot-to-lot performance. More productive results can be obtained by exerting control where we know what to control, then worrying about the so called "random" failure.
- 4) Analysis of variables data could prevent pushing the "panic" button by evaluation of instrumentation variation through the use of duplicate instrumentation. No studies have been made as to differences in costs between the instrumentation required for attribute measurements versus that for variables measurements; it is not expected that, even if incremental costs for additional variables instrumentation existed, it would be larger than the positive incremental cost of attribute sample size. If not in a single program, amortization of instrumentation costs over several programs is certainly reasonable.

In the case of static rocket testing, replicate time-thrust traces are taken but the information is not used; the data is averaged and often only a single datum for each parameter is presented to the statistician.

- 5) Inadequate or marginally performing devices can be detected earlier as a result of smaller sample size and more detailed evaluation of the performance.

- 6) A variables analysis permits a more objective appraisal of the performance capability against the specifications so that more reasonable tradeoffs may be made between component and subsystem requirements, as well as between safety margins between various components.
- 7) One situation where the variables approach is more apt to yield an accurate answer, as well as additional information for corrective action, is an ordnance component which has both a lower and an upper specification for operating time (that is, life). Since these devices are of the "one-shot" type, one may decide to use three units simultaneously so as to reduce initiation failure probabilities. The initial P/C estimates computed on an attribute basis is more likely to be based on performance within specifications for every parameter as well as a three way parallel configuration. Although initiation may indeed be estimated as a parallel configuration, the operating time may not. Only one of the three units need operate prior to the upper limit to perform within specifications, but all three must perform after the lower specification limit to perform the function as planned; even one unit operating prior to the lower specification unit fails or pre-matures the function. Thus, the three units are in parallel against the upper specification limit but in series against the lower specification limit.

## 2.2 WHY NOT VARIABLES

If variables are apparently so desirable why is there such resistance to their more frequent use? In addition to the lack of multi-variate tolerance limits, there are other reasons:

- 1) Questions as to the model and whether the correct kind and/or correct number of performance parameters are being used. The engineer must design his equipment to meet design performance parameters. Thus, the solution of variables performance parameters is analagous to the selection of "black boxes", i.e., parts, components, etc., in the customary analysis of a system model. If agreement can be reached regarding selection of the "black boxes", then certainly agreement can be achieved regarding the selection of variables performance parameters.

- 2) The next most important reason for preferring attributes is that the larger sample size would catch the "random" failure. It is this writer's contention that the term "random" failure is confusing; the failures called random are actually due to an uneconomically detectable cause. Attributes analysis not only does nothing to identify the cause but actually encourages further testing to meet the reliability requirement with a failure incurred in the first test group.
- 3) The last reason given is that the data is not normal. It is true that the example given in Section 4.1.1 does use a normal deviate, but this does not imply that estimates based on normal deviates are applicable. References 5 and 6 provide tables for P/C estimates based on the exponential distribution. From this writer's experience, however, the normal distribution has been satisfactory in most cases. If the observed data has not been normal, then a suitable transformation, log, reciprocal square root, etc. has normalized the data. In many cases, distribution tests, e.g., values of the symmetry and peakedness indices, have been very close for the normal, log-normal, and reciprocal-normal distributions.

### 2.3 CONCLUSION

The obvious disadvantages of variables analysis are: a moderate increase in analytical cost, and time for completion of the analysis (both of which are being offset today by increased computer application), and greater detail that is required in planning tests. The advantages to be derived far outweigh the disadvantages in terms of dollars and "sense".

### 2.4 HOW TO SELECT VARIABLES

In accordance with the statement given in the Introduction to MIL-STD-414, "It is important to note that variables sampling plans are not to be used indiscriminately, simply because it is possible to obtain variables measurement data." The best place to start, therefore, is with the design parameters selected by or for the designer. To a large degree, therefore, the problem is one of engineering.

A generalization is made, as follows:

In addition to operating time, the variables approach requires that an analysis be made of some work (or energy) parameter which performs the job and is the reason the equipment has been designed in the first place. The equipment has not been designed merely to exist, and operating time merely defines the time specification within which the work must be performed. Where the component is of the "one shot" type and is routinely subjected to sensitivity tests (e. g. , Bruceton, Probit), then the failure probabilities associated with initiation should also be included in the overall component estimate.

Thus, there are a minimum of two critical parameters (four when sensitivity tests are performed) which reflect launch-to-impact performance and reliability. Other performance parameters may be and should be included if critical. A procedure which can suggest additional, critical parameters is to examine a Failure Mode and Effects Analysis and measure a parameter which would be indicative of a given failure mode. For example, continuity (resistance) measurements are indicative of at least two failure modes in a squib delay switch, i. e. , either a broken bridgewire or dirt jamming the contacts.

The corollary to this approach is that Engineering's objective must be not only to design equipment to do the job, but also that each critical performance parameter be capable of being measured in test, directly or indirectly, prior to use.

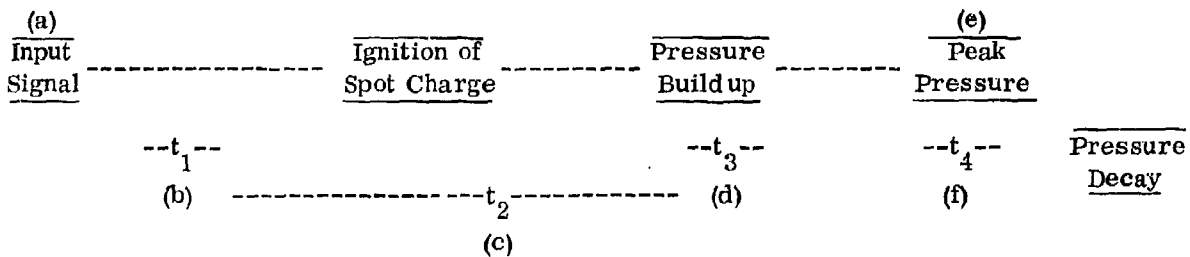
### 3.0 Test Plan

The major topics of test planning involve the statistical design of experiments and definition of performance parameters. Since the former is covered adequately in statistical texts, we will concern ourselves with only the definition of performance parameters for generic types of ordnance devices.

In order to apply the variables test techniques so that an over-all performance reliability can be predicted, it is necessary to know all of the pertinent parameters that influence component performance. Quite often it is difficult to separate the individual parameters dynamics associated with each phase of operation of a component, but our main intent is in the operational reliability of a device and this can be achieved by defining the necessary input to start the action which will result in an output related to a work function with characteristic parameters that can be measured.

#### 3.1 Performance Parameters -

3.1.1 Pressure Cartridge - A typical initiating device used to perform many functions in a space vehicle is a gas generating cartridge. Upon initiation, gaseous products build up and actuate a piston which may cut a bolt, pull a pin, etc. Parameters of interest occur in the following sequence:



- a) Input Signal ("all Fire") (af)
- b) Ignition Time of Spot Charge ( $t_1$ )
- c) Time to Start of Pressure Buildup ( $t_p$ )
- d) Time to peak Pressure ( $t_{pp}$ )
- e) Peak Pressure ( $P_p$ )
- f) Time to Pressure Decay ( $t_{pd}$ )

1. The required input signal (Firing sensitivity) obtained from quantal response data (Bruceton, Probit, etc.) provides a measure of the firing reliability of the device.
2. Ignition time of the spot charge provides us with a measure of the ability of the bridge system to ignite the pyrotechnic mix surrounding the wire element. This parameter could be measured by observing an abrupt change in voltage across the bridgewire, due to sudden heating on ignition of the pyrotechnic mix.
3. Peak Pressure and related times are detected by firing in a closed volume and monitoring pressure with suitable transducer systems.
4. Pressure Decay - Not necessarily a measure of performance, since the rate that the pressure decays is largely a function of the seal of the pressure vessel; and thermal conductivity of the bomb; but could be used as a comparative indicator of the goodness of confinement from test to test.

One exception is using Sensitivity tests for establishing "all-fire" stimula (specifically for low current - long time application) do not necessarily provide for a reliable estimate. For example, it is quoted that a device will have a firing reliability of 99.9% with 95% Confidence for a bridge wire current of (X) amps for an (X) time duration. No limit has been set on the maximum current that may be applied. Unfortunately application of too high a current could reduce rather than add to the reliability. Marginal design of the bridge wire system or the use of exotic materials for heat sinking may contribute to burnout of the bridge before sufficient heat has been absorbed by the explosive to cause ignition. It is recommended that over testing be executed in order to verify ignition for the application of excessive stimuli.

3.1.2 Rocket Igniters, Squibs, and Detonators - The characteristics input response of these devices may be treated in the same manner as that described for the pressure cartridge. Output, on the other hand, is considerably different. In the case of flame producing elements, such as Rocket Igniters, the dominant "ignition" mechanism is heat or more specifically heat-time. The variables of interest here might be; peak temperature, temperature as a function of flame length, or temperature as a function of time. On a relative basis it may suffice to measure total caloric output in a calorimeter, assuming of course, that this parameter can be associated with performance tolerance limits.

Reliability associated with detonator output presents a challenge with absolute if not with relative measurements. Many techniques for measuring relative output have been devised and have fallen in and out of favor over the years. These techniques would include, but not necessarily be limited to;

- (a) Bent nail
- (b) Sand Bomb
- (c) Lead Disc
- (d) Steel Dent
- (e) Gap type tests

These tests will define, under existing conditions, destructive forces on a relative basis. The dominant mechanism(s) which represent useful work output are not easily isolated; and may be a combination of temperature, shock pressure, and impinging particles. The parameter which contributes most, seems to be the pressure wave; as substantiated by the initiation of explosives through barriers and bulk heads. It is not out intent in this paper to specify the exact parameters to be measured, since this will mainly be dictated by the needs of the system, and should be specified by the cognizant personnel. Once the parameter(s) associated with the job has been defined, either relative or absolute, then working limits must be set in order to predict reliability.

3.2 Non Performance (Safety) Reliability - At the other end of the performance spectrum we have the non-fire characteristics of an EED. Premature ignition or degradation of a pyrotechnic device could result in personnel hazards, equipment damage, or in the case of degradation, loss of performance reliability and possible mission failure.

To define the "no-fire" reliability of a component; we must consider the specific areas that relate to the particular system in questions in general we would consider the following;

- (a) Application of specified "no-fire" current
- (b) Application of Electro static discharge
- (c) Susceptibility to RF, etc.

### 3.1.3 Flexible Linear Shaped Charge

The variables approach can also be used to determine the change in performance of flexible linear shaped charge. The analysis of development test data provides the information for baseline testing and statistical methods for analysis of future test data. The criteria for performance of FLSC is to establish a relationship between detonation velocity, jet penetration or depth of cut and the probability of severing the target. Detonation velocity or jet penetration may be affected by various changes such as:

1. Decrease in density
  - a. From handling or flexing the material
  - b. Temperature cycling of materials with different coefficient of expansion.
2. Loss of confinement of the explosive caused by generation of gas within the FLSC resulting in inflating the lead sheath.
3. Change in crystal size of the primary explosive through crystal growth.

As a result, a quantitative relationship between jet penetration in a target resulting from shaped charge action and the probability of severing the target can be obtained. This relationship can be useful in predicting the present and future performance of FLSC used in a system. Test results can be reduced and compared with the initial baseline test data to try to detect performance trends that are life indicators. An analysis of significant trends can be performed to determine when boundary conditions might occur. Logistics will be able to use this data to determine the effect of changes on the FLSC in terms of operational readiness and flight performance.

Engineering specification limits should be established and "no-fire" reliability based on test programs could be specified; except that "all-fire" or performance reliability should be re-established after exposure to these environments to reflect possible degradation.

It would seem reasonable to develop or define a variable associated with initiation for electro initiators in order to avoid the sensitivity testing presently required.



#### 4.0 STATISTICAL ANALYSIS

If a single variables performance parameter were to realistically reflect the total performance of a system the estimate obtained from the application of statistical tolerance limits would be generally acceptable. Since evaluation of two or more parameters is more realistic, the problem resolves into that of merging the individual parameter estimates into a composite, or system estimate. If all parameter probability estimates are high, one intuitively feels that the overall estimate is low. To quantify this intuition in terms of a nominal, statistical system estimate with a confidence interval is the problem to be solved. Since no simple multivariate tolerance procedure is available for estimating system performance, there is no generally accepted statistical procedure for providing system estimates at high confidence levels with economical sample sizes. (Reference 6 and 7). It is believed that the VAEP method will fill the gap. Although the entire gamut of statistical techniques may be used, e. g., regression analysis, analysis of variance, etc. the combination of statistical tolerance limits and error propagation comprise the unique part of this estimation procedure.

##### 4.1 STATISTICAL PROCEDURE (VAEP)

(1) Set up the system equation using the standard combinatorial probability formula; it appears that this generally will be the product (or series) formula. For example, in terms of the example in Section 4.1.1

$$P_S = P_1 \cdot P_2 \cdot P_3 \cdot P_4 \cdot P_5$$

where:

$P_S$  is the probability estimate for the system, i. e., gas generator

$P_1 - P_5$  are the probability estimates for the performance parameters, as follows:

1. Initiation or "all-fire" probability
2. Initiation Time
3. Time to start of pressure buildup
4. Time to peak pressure
5. Peak Pressure

(Note: The calculations in the example illustrate VAEP calculations, but an accurate system estimate is not made; the reason is that a series is assumed although there is some dependence between  $P_1$  and  $P_2$ ,  $P_1$  and  $P_3$ ,  $P_4$  and  $P_5$ .

(2) Estimate the probability of performing within specifications for each performance parameter at the nominal confidence level through the application of statistical tolerance limits. Essentially, the statistical tolerance limit estimate translates performance into a probability, thereby transforming the multi-dimensional parameters into the single probability dimension. In accordance with the theory of error propagation, this is done at mean, 50 percent confidence level for each of the parameters. In other words, the Probability calculated at 50 percent confidence is the value that one would expect to observe from test data if he were using attribute data. The relationship between the variables and attribute estimates is shown in Figure 1. Also calculated is the probability at the required, confidence level for the system (e. g., 0.95).

In determining these two estimates, the VAEP method is calibrated to obtain the same answer that would be obtained by Statistical Tolerance Limits for a single parameter system.

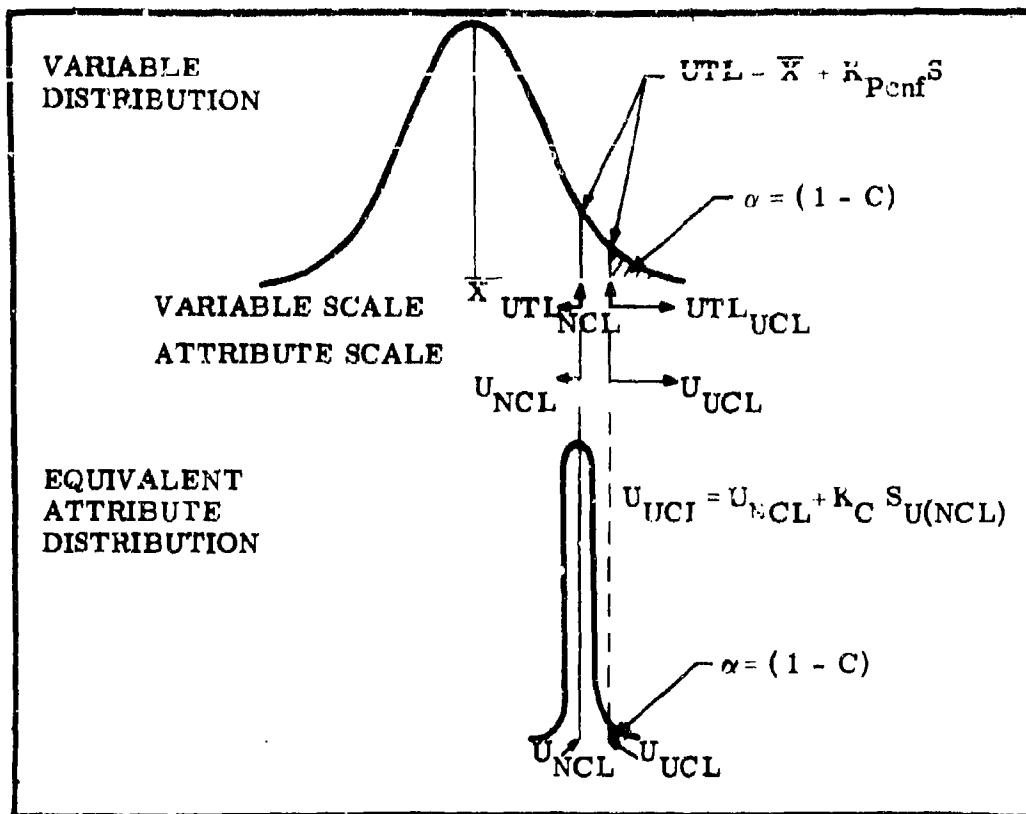


Figure 1. VAEP Calibration of Statistical Tolerance Limits to Equivalent Attribute Limits (Single Sided Case)

- (3) By substituting these parameter estimates in the product equation a nominal system estimate is obtained and a single confidence interval around the system estimate may be calculated, which is the parameter of primary interest.
- (4) The error propagation formula for a product (and in this application the error propagation of a fraction) is used to obtain the variance of the product or system probability (in terms of  $U = 1 - P$ ).
- (5) The system estimate at a high confidence level is calculated by the normal approximation to the binomial.

Appendices A, B, and C provide details on the foregoing steps and provide references pertinent to the specific topic. Appendix A is a discussion on tolerance limits. For those who have reservations about using tolerance limits at the 50 percent confidence level, it is worth emphasizing that the  $K_{P_{cnf}}$  factor converges down to the familiar

normal K factor at an infinite sample size. Therefore, those who customarily use a factor of 3 (in  $3\sigma$  interval) for a two-sided 0.9973 probability will find they are here using a factor larger than 3 because of the small sample sizes.

Appendix B is a discussion of error propagation. Although this concept has been applied, the critical difference in application is the substitution in the attribute error propagation formula for the equivalent sample size. In all the references except B 9 some dependent parameter is a function of other independent parameters, all of which are based on variables data. In Reference B.1 (9) error propagation is used to provide systems estimates from component probability estimates which are based on observed attribute data.

Appendix C discusses the derivation of VAEP which combines the P/C estimates based on statistical tolerance limits with the system variance based on error propagation. Also included are the derivation of the equivalent sample size, and the effects of dependence on the system variance estimate.

The foregoing steps are now applied to the example of Section 4.2.

#### 4.2 SAMPLE PROBLEM

Two sets of formulas for VAEP P/C estimates, which are a little different, are given. Mod I is given in Reference C.5 (8) as well as Appendix E. The preferred method, Mod II, is given in Appendix C. Although both methods yield the same answer, Mod I has some disadvantages: (a) it requires a specific reliability goal which, in turn, requires the calculation of a nominal confidence level which, in turn, leads to calculations from odd confidence levels of statistical tolerance limit tables, e. g. , 0.78; (b) it requires an equivalent sample size formula which often yields very large values; (c) it uses the Poisson approximation to the binomial (Reference C.5 (8) but not Appendix E of this paper).

On the other hand, the Mod II formulas: (a) are more flexible, as only the confidence level is necessary to make an estimate of the reliability or vice versa, (b) use an equivalent sample size formula which, in Appendix C yield a deflated equivalent sample size, as compared with that of Mod I.

TABLE 1a): Variable Data,  $\bar{X}$ , S and Tolerance Deviate Calculation

S/N	$t_l$ (ms)	$t_p$ (ms)	$t_p^P$ (ms)	$P_p$ (ms)
1	1.8	4.30	1.53	3700
2	2.0	4.50	1.61	4200
3	2.0	4.53	1.65	4200
4	1.9	4.42	1.70	4100
5	2.0	4.44	1.73	4000
6	2.2	4.50	1.62	4100
7	1.7	4.00	1.81	4000
8	2.0	4.46	1.57	4300
9	2.4	4.60	1.92	3900
10	2.2	4.58	1.72	4200
11	1.7	4.23	1.86	4200
12	2.0	4.46	1.67	4400
13	2.0	4.50	1.75	4300
14	2.3	4.80	1.78	3900
15	2.0	4.64	1.87	4000
$\bar{X}$	2.0	4.46	1.72	4100
$\bar{X}$ (log)	0.3019	-	0.2345	-
LSL	3.6 max	5.46 max	3.0 max	3000 min
LSL (log)	0.5563	-	0.4771	-
d	0.2554	1.00	0.2421	1100
S	-	0.1858	-	185.2
S (log)	0.043	-	0.0289	-
$K_{Pcnf}$	5.92	5.38	8.39	5.94

TABLE 1b): Bruceton Data, Calculations and Results

Data	
Amps	$n_f$
4.0	1
4.2	3
4.4	5
4.6	12
4.8	2
-----	
23	

	Calculations		
	$\bar{X}$	4.596	n
M	0.9452	d	0.2
S'	1.58	S	0.316 (=S'd)
G	0.955	$G^2$	0.9120
H	1.69	$H^2$	2.8224
$Z_p$	3.29	$Z_p^2$	10.8241
$L_c$	1.717	$L_c S$	0.543

Results

Limit		Value	Comment
P	C		
.9995	0.50	5.640	after standard Bruceton calculation
.9995	0.95	6.275	" " " " " "
.999999	0.95	7.000	Interpolation on probability
~1.0	0.50	7.000	plots

TABLE 2. Sample Problem Calculations

Param #	$K_{Penf}$	$\frac{U}{p(c. 95)}$ ( $1 \times 10^{-6}$ )	$\frac{U}{p(c. 50)}$ ( $1 \times 10^{-6}$ )	$\left( \frac{U}{p(c. 95)} - \frac{U}{p(c. 50)} \right)$ $d =$	$d^2$ ( $1 \times 10^{-12}$ )	$\frac{p^2}{p(c. 50)}$	$\frac{d^2/p^2}{(1 \times 10^{-12})}$	$P$ $p(c. 50)$
1	5.92	28	~ 0	0.000028	784	0.999944	784	0.999972
2	5.38	129	~ 0	0.000129	16641	0.999742	15645	0.999871
3	8.39	0	~ 0	0.000000	~ 0	1.000000	0	1.000000
4	5.94	26	~ 0	0.000026	676	0.999948	676	0.999974
5	-	1	~ 0	0.000001	1	0.999998	1	0.999999
Total		(184)	~ 0				18106	
$\left[ \frac{\sum(d^2/p)}{p} \right]^{1/2} = K_c S_u S$								
$P_s \left[ \frac{\sum(d^2/p)}{p} \right]^{1/2} = K_c S_u S$								
$U_{s(c. 50)}$								
$U_{s(c. 95)}$								
$P_{s(c. 95)}$								

## 5.0 COMPARISON OF VAEP WITH OTHER METHODS

As stated previously, there is no simple method Multivariate Tolerance Limits known to this writer, nevertheless, two comparisons may be made which indicate the reasonable estimates to be made with the VAEP formulas.

### 5.1 SYSTEMS ESTIMATES FOR ATTRIBUTE DATA

In Appendix C system estimates using error propagation of attribute data (AEP) are compared with estimates made by other methods (in ref. D.3. (1); the latter are classified as exact and approximate. AEP estimates are close to the estimates of the approximate methods and more optimistic than the recommended exact method although negligibly for the case  $n = 100$ . A continuity correction factor is used which reduces the difference between this and the exact method. It should be noted that most of the methods discussed in Reference D.3(1) require computers, whereas error propagation requires only a desk calculator. Furthermore, the differences between the "exact" methods are larger than the differences between approximate methods. It would seem therefore that a general exact method for systems estimation is still not available.

### 5.2 VAEP VERSUS AN EXTENSION OF A LLOYD-LIPOW FORMULA

Perhaps the most convincing argument for VAEP is the comparison of VAEP estimates with those made by an error propagation extension of a Lloyd-Lipow formula. In reference D.3 (2) the author, DRNAS, reports the use of statistical tolerance limits for estimating the reliability of battery voltage performance at a lower 95% confidence level. As a secondary method, a formula due to Lloyd and Lipow (see reference D.3 (3)) is given for sample sizes of 50 or greater. For sample sizes less than 50, another statistical procedure is given and is described "... more accurate (but not exact) than the procedure...", (referring to the Lloyd-Lipow formula). He continues, "The method is quite cumbersome in that a table of the non-central 't' distribution and a table of the Incomplete Beta Function are necessary for calculations."

If error propagation is then applied to the Lloyd-Lipow variance formula, a comparison of the system estimate may be made with that of the VAEP estimate. This is done in Enclosure D.2 and close estimates are obtained. In fact the VAEP estimates are a little

more pessimistic and the reason becomes evident when one examines the original Lloyd-Lipow formula for the variance of R; a constant,  $0(1/n^{3/2})$ , is omitted from the calculation. Thus it would be expected that VAEP should yield a slightly more pessimistic estimate.

Furthermore, when a VAEP estimate is compared to the DRNAS small sample method, again remarkably close estimates are obtained. See Enclosure D.3 (2). One reason for this closeness is the fact that the derivation of the single sided tolerance limit involves the non-central 't' distribution.

We may infer therefore that (1) the criterion of calibrating statistical tolerance limits estimate of probability to a binomial estimate through the medium of an equilibration sample size, though pragmatic, yields reasonable estimates (2) VAEP is useful not only for large sample sizes but also for small sample sizes and certainly more convenient, and (3) is very easily calculated.

#### 6.0 CONCLUSION

It will become evident that VAEP is applicable to systems estimates from component data. Other areas where application is contemplated are targeting analysis (two and three dimensions) and the sequence of events in a flight analysis. Although this method is applicable in most hardware areas, the most useful area is the one concerned with destructively tested units, e. g., ordnance hardware; it is in this area that GE-RSD has been concentrating its efforts.

Just as accountants years ago substituted performance objectives for pencils and paper clips in their budgets, the time has come when those in reliability should start replacing "black box" failure rates with performance parameters.



## APPENDIX A

### STATISTICAL TOLERANCE LIMITS

#### A.1 TOLERANCE LIMITS ANALYSIS

A technique known as statistical tolerance limits is applied for estimating hardware performance; it may be used independently for homogeneous groups of data or may be combined with regression analysis for heterogeneous but related groups of data.

The calculated limits within which a predicted proportion of the population (i. e. , reliability or probability) will fall is defined by the formula:

$$TL's = \bar{X} \pm K_{PCnf} S$$

Where,

TL's	are the tolerance limits
$\bar{X}$	is the calculated sample mean
S	is the calculated sample standard deviation
K	is the tolerance probability deviate
P	probability or reliability
c	confidence level
n	sample size
f	degrees of freedom

The formula is related to the familiar formula of  $\bar{X} \pm K\sigma$  for confidence limits in that the  $K_{PCnf}$  for tolerance limits converges to the familiar K for confidence limits of an infinitely large sample size.

If desired, reliability/confidence levels may be estimated against given specification limits by the formula

$$K_{PCnf} = \frac{SL - \bar{X}}{S}$$

where SL refers to the specification limits.

Tables of two-sided tolerance limits are given in References A1 and A4 for the normal distribution and Reference A6 for the exponential distribution. Tables of one-sided tolerance limits are given in Reference A3 for the normal distribution and Reference A5 for the exponential distribution.

Two useful, approximate formulae are given by Hald (Reference A2) for determining the tolerance factor for the normal distribution.

For the Two Sided Case:

$$K_{PCnf} = \left[ \left( 1 + \frac{1}{2n} \right) K_p \right] \sqrt{f/X_c^2}$$

where,

$K_{PCnf}$  is the normal deviate for 'P' Probability or 'R' reliability at  
at C confidence

$X_c^2$  is the chi square probability deviate for f degrees of freedom

$K_p$  is the normal deviate for P Probability

n is the sample size

f are the degrees of freedom, (in most problems (n-1))

By appropriate selection of the  $X_c^2$  value the probability at any confidence value may be calculated by solving for  $K_p$

$$K_p = \frac{K_{PCnf}}{\left( 1 + \frac{1}{2n} \right) \sqrt{f/X_c^2}}$$

For the One-Sided Case:

$$K_{PCnf} = \frac{K_p + K_c \left[ \frac{(1/n) \left( 1 - \frac{K_c^2}{2f} \right) + \left( \frac{K_p^2}{2f} \right)}{\left( 1 - \frac{K_c^2}{2f} \right)} \right]^{1/2}}$$

$K_{PCnf}$  is the normal deviate for 'P' Probability or 'R' Reliability at  
at C confidence

$K_p$  is the normal deviate associated with the required reliability level

$K_c$  is the normal deviate associated with the required confidence level

n is the sample size

f are the degrees of freedom, (in most problems (n-1))

By appropriate selection of the value for  $K_C$ , the probability at any confidence value may be calculated by solving for  $K_P$

$$K_P = K_{PCnf} - K_C \sqrt{\frac{1}{n} + \frac{K_{PCnf}^2}{2f}}$$

## A.2 OTHER DISTRIBUTIONS

The present discussion has been limited to data which is normal, log normal, Poisson or reciprocal normal in nature and which is applicable in most of the day to day problems. The latter three distributions are used in conjunction with the normal tolerance limit factors by simple transformations. A log-transformation of the data will permit reliability and confidence estimates for data log normal distributions; a square root transformation will normalize data from a Poisson distribution. When data is obtained from an exponential distribution, then tolerance factors for this data may be obtained from References 5 and 6 and the computations would differ from the procedures given for the normal distribution. When the Weibull Distribution is appropriate, estimates may be made by the method of Reference 7.

## A.3 REFERENCES

- (1) Statistical Research Group, Columbia University, "Selected Techniques of Statistical Analysis" ed C. Eisenhart, M. W. Hastary and W. A. Wallis, McGraw Hill 1947.
- (2) A. Hald, "Statistical Theory with Engineering Applications", J. Wiley, July 1957.
- (3) D. B. Owen, "Factors for One-Sided Tolerance Limits and for Variables Sampling Plans", Sandia Corporation (and Office of Technical Services of the U.S. Dept. of Commerce), 1963.
- (4) A. Weissberg and G. H. Beatty, "Tables of Tolerance Limit Factors for Normal Distribution" either Technometrics, Nov. 1960 or Battelle Memorial Institute, 1959.

- (5) B. Epstein, "Tolerance Limits Based on Life Test Data Taken from an Exponential Distribution", Industrial Quality Control, August 1960.
- (6) L. A. Goodman and A. Madansky, "Parameter Free and Non-parametric Tolerance Limits: The Exponential Case" in Technometrics, Vol. 4, No. 1, February 1962.
- (7) G. J. Lieberman, "Weibull Estimation Techniques" Fifth Reliability and Maintainability Conference (AIAA/SAE/ASME) July 1966. Journal of the American Statistical Association, Volume 61, Number 315, September 1966.
- (8) V. Chew, "Confidence, Prediction, and Tolerance Regions for the Multivariate Normal Distribution. Journal of the American Statistical Association, Volume 61, No. 315, September 1966.

#### A.4 Bruceton Analysis

The statistical methods underlying the Bruceton analysis are not discussed here as they are quite extensive and would only repeat the information given in references 1-5 of E A.5. The method in which the estimates are used with VAEP, parallel the estimates obtained with statistical tolerance limits. The probability estimates against the specifications are calculated at 50% and for example 95% confidence. Although the standard formula may be used for 50% confidence, the mathematical solution for 95% would be too complex. The simplest procedure for the upper confidence level, e.g. 95%, is to calculate the upper confidence level at 95% confidence for varying probability levels e.g. 99%, 99.9%, 99.99%, until the upper specification limit is surrounded by at least two values. All these 95% confidence values are then plotted on probability paper, and the probability estimate against this upper specification limit is then obtained by interpolation.

#### A.5 References on Bruceton Analysis

- 1) Statistical Research Group, Princeton University "Statistical Analysis for a New Procedure in Sensitivity Experiments" 1944
- 2) W.J. Dixon and F. J. Massey, Jr. "Introduction to Statistical Analysis" McGraw Hill 1957
- 3) E. Crow, F. Davis, M. Maxfield "Statistics Manual" Dover Publications 1960
- 4) M. G. Natrella "Experimental Statistics" NBS Handbook 91, U.S. Government Printing Office

## APPENDIX B

### THE PROPAGATION OF ERROR

If  $f$  is a function of  $x$ ,  $y$  and  $z$ , the linear term in Taylor's series can often be used to express with sufficient accuracy the effect of a smaller error in  $x$ ,  $y$  and  $z$  on  $f$ .

"The differential method has the advantage of giving results even when the distributions of  $x$ ,  $y$ , and  $z$ , and the functions are not known; but because the higher powers of  $X$  (etc.) are neglected, it has the disadvantage for non-linear functions in giving results whose validity is sometimes difficult to calculate. In spite of the approximate character of the derivation for non-linear functions, the Taylor series differential nevertheless often gives remarkably good results for most of the functions and the sample sizes met in practice. This happens, for example, when  $x$ ,  $y$ ,  $z$  are means of samples and  $\Delta x$ ,  $\Delta y$ ,  $\Delta z$  are statistical fluctuations above and below the "expected values of  $x$ ,  $y$ ,  $z$ ." (Reference B2, pages 130, 1.)

B2 for a product:  $f = xyz$

$$C_f^2 = C_x^2 + C_y^2 + C_z^2 + 2r_{xy} C_x C_y + 2r_{xz} C_x C_z + 2r_{yz} C_y C_z$$

(Reference 1, page 133)

The adequacy of the linear term in estimating the dependent function is stated not only in reference 1, but also in reference 3 which is specifically concerned with this problem.

#### B.1 GENERAL FORMULA

For systems composed of mixtures of series and redundant components (or parameters) etc., the generalized formula will be more convenient.

For a system of  $K$  units

$$y = f(x_1, x_2, \dots, x_K)$$

$$S_y^2 = (\partial y / \partial x_1)^2 S_{x_1}^2 + (\partial y / \partial x_2)^2 S_{x_2}^2 + \dots + (\partial y / \partial x_K)^2 S_{x_K}^2 + 2r_{12} S_1 S_2 (\partial y / \partial x_1) (\partial y / \partial x_2) + \dots + 2r_{K-1, K} S_{K-1} S_K (\partial y / \partial x_{K-1}) (\partial y / \partial x_K)$$

## B.2 REFERENCES

- (1) Deming, W. E. "Some Theory of Sampling" J. Wiley, 1950
- (2) Villars, D.S. "Statistical Design and Analysis of Experiments for Development Research" Wm. C. Brown Co.
- (3) Tukey, J. W. "Propagation of Errors, Fluctuations and Tolerances. Basic Generalized Formulas", Technical Report No. 10, Princeton University, 1958.
- (4) Hald, A. "Statistical Theory with Engineering Applications", J. Wiley.
- (5) Davies, O. L. (editor) "Statistical Methods in Research and Production" Hafner Publishing Co.
- (6) A. H. Bowker and G. J. Lieberman "Engineering Statistics" Prentice-Hall, 1960.
- (7) W. Volk "Applied Statistics for Engineers" McGraw Hill, 1958.
- (8) E. Crow, F. Davis, and M. Maxfield "Statistics Manual" Dover Publications.
- (9) H. DeCicco "Note on a Control Procedure for the Reliability of Systems Based on Component Test Data Alone" IEEE Transactions on Aerospace-Support Conference Procedures.
- (10) B. L. Baird and W. N. McLead "Estimates of Error for Design Reliability" Proceedings of the 10th National Symposium on Reliability and Quality Control, January 1964.
- (11) M. Morreale, C. Noel, and C. Potter "Propagation of Error Technique as Applied to Electronic Circuit Design" Fourth National Symposium on Reliability and Quality Control, 1960.
- (12) E. Haugen "Statistical Methods for Structural Reliability Analysis" 10th National Symposium on Reliability and Quality Control, 1964.

## APPENDIX C

### COMBINED STATISTICAL TOLERANCE LIMITS ESTIMATES WITH ERROR PROPAGATION FOR SYSTEMS ESTIMATION

#### C.1 ESTIMATE OF SYSTEM MEAN AND VARIANCE

(1) System Model

$$P_S = P_1 \cdot P_2 \cdot \dots \cdot P_{p-1} \cdot P_p$$

where,

$P_S$  is the system probability estimate

$P_1$  thru  $P_p$  are the probability estimates for each performance parameters - 1 . . . p-obtained from a statistical tolerance limits at a nominal confidence level.

In this first step, the nominal confidence level (NCL), 50 percent is used; this is the level upon which the error propagation formulas are derived.

(2) The error propagation formula for a product, assuming independence, will be used to estimate the standard deviation of  $P_S$ .

$$C_S^2 = C_1^2 + C_2^2 + \dots + C_{p-1}^2 + C_p^2$$

where,

$C$  is the coefficient of variation

$C^2$  is the rel-variance

$C^2$  is  $(U/nP)$  for a binomial attribute

$$S^2 = P^2 C^2$$

$U$  is  $(1-P)$  or the failure probability



(3) Therefore:

$$\frac{U_S(NCL)}{n_S(a) P_S(NCL)} = \frac{U_1}{n_1(a) P_1} + \frac{U_p}{n_p(a) P_p} - \sum_{i=1}^p \frac{U_{p(NCL)}}{n_{p(a)} P_{p(NCL)}}$$

where,

$n(a)$  is the attribute sample size

$U_p$  is a failure probability for 'p' performance parameter

NCL is the nominal or 50% confidence level

(4) Since the variables/tolerance limit estimates will customarily (but not necessarily) be higher than a binomial/attribute estimate, an equivalent attribute sample size will have to be used for  $n_{p(a)}$ . This is derived in paragraph C.2 and is given as  $n = \left( K_c^2 U_{p(NCL)} P_{p(NCL)} \right) / \left( U_{p(UCL)} - U_{p(NCL)} \right)^2$  which is substituted:

$$\begin{aligned} C_s^2 &= \sum_{i=1}^p \frac{U_{p(NCL)}}{\left[ \frac{K_c^2 U_{p(NCL)} P_{p(NCL)}}{\left( U_{p(UCL)} - U_{p(NCL)} \right)^2} \right] P_{p(NCL)}} \\ &= \sum_{i=1}^p \left[ \frac{\left( U_{p(UCL)} - U_{p(NCL)} \right)^2}{K_c^2 P_{p(NCL)}^2} \right] \\ &= \frac{1}{K_c^2} \sum_{i=1}^p \left[ \frac{\left( U_{p(UCL)} - U_{p(NCL)} \right)^2}{P_{p(NCL)}^2} \right] \end{aligned}$$

and since  $S_s^2 = P_s^2 C_s^2$  for a Binomial estimate or

$$S_s^2 = P_s^2 \frac{1}{K_c^2} \sum_{i=1}^p \left[ \frac{\left( U_{p(UCL)} - U_{p(NCL)} \right)^2}{P_{p(NCL)}^2} \right]$$

and,

$$S_s = P_{S(NCL)} \frac{1}{K_c} \frac{p}{\sum_{i=1}^p} \left[ \frac{(U_{p(UCL)} - U_{p(NCL)})^2}{P_p^2(NCL)} \right]^{1/2}$$

or, the confidence interval of  $U_{S(NCL)}$

$$K_c S_s = P_{S(NCL)} \left[ \frac{\sum_{i=1}^p (U_{p(UCL)} - U_{p(NCL)})^2}{P_p^2(NCL)} \right]^{1/2}$$

(5) The normal distribution is now used to estimate the approximate upper confidence limit of the failure probability

$$U_{S(UCL)} = U_{S(NCL)} + K_c S_s$$

$$U_{S(UCL)} = U_{S(NCL)} + P_s \left[ \frac{\sum_{i=1}^p (U_{p(UCL)} - U_{p(NCL)})^2}{P_p^2(NCL)} \right]^{1/2}$$

$$= U_{S(NCL)} + P_s \left[ \frac{\sum_{i=1}^p d^2}{P_p^2(NCL)} \right]^{1/2}$$

where,

$U_S$  is the estimate of the system failure probability

UCL is the upper confidence level

NCL is the nominal, 50% confidence level

$$d = U_{UCL} - U_{NCL}$$

$K_c$  is the normal deviate at an upper confidence level or c or 1 minus the risk level.

$$(6) P_{S(UCL)} = 1 - U_{S(UCL)}$$

### C.2 EQUILIBRATION ATTRIBUTE SAMPLE SIZE

Given: Values of the failure probability U at 50 percent and some upper/required confidence levels which are computed by the method of statistical tolerance limits.

Find: The equivalent attribute sample size,  $n_{(a)}$ , to equilibrate the normal approximation to the binomial to the  $U_{C.50}$  and  $U_{(UCL)}$  obtained by statistical tolerance limits.

$$U_{UCL} = U_{C.50} + K_c \left[ \frac{P_{C.50} U_{C.50}}{n_{(a)}} \right]^{1/2}$$

$$\left[ \frac{P_{C.50} U_{C.50}}{n_{(a)}} \right]^{1/2} = \frac{U_{UCL} - U_{C.50}}{K_c}$$

$$n_{(a)} = \frac{K_c^2 U_{C.50} P_{C.50}}{(U_{UCL} - U_{C.50})^2}$$

### C.3 EFFECT OF DEPENDENCE (WORST CASE)

The effect of dependence between parameters on the system variance estimate is taken into consideration by the error propagation formula is

$$C_s^2 = C_1^2 + \dots + C_p^2 + 2r_{12} C_1 C_2 + \dots + 2r_{p-1,p} C_{p-1} C_p$$

Now the worst case estimate would exist if all  $5C_2$  or 10 combinations of two factors probability estimates were to be completely related.

If all the two factor combinations are related, then  $r_{ij} \rightarrow 1$ , and

$$C_s^2 = \sum_{i=1}^p C_p^2 + \left[ 2(1) C_1 C_2 + \dots + 2(1) C_{p-1} C_p \right]$$

$$= \sum_{i=1}^p C_p^2 + 2 \left[ C_1 C_2 + \dots + C_{p-1} C_p \right]$$

$$= \sum_{i=1}^p \frac{U_{p(NCL)}}{n_{p(a)} P_{p(NCL)}} + 2 \left[ \sum_{i=1}^p \left( \frac{U_{(p-1)(NCL)}}{n_{(p-1)(a)} P_{(p-1)(a)}} \cdot \frac{U_{(p)(NCL)}}{n_{(p)(a)} P_{(p)(NCL)}} \right)^{1/2} \right]$$

$$= \frac{1}{K_c^2} \sum_{i=1}^p \left[ \frac{(U_{p(UCL)} - U_{p(NCL)})^2}{P_p^2(NCL)} \right]$$

$$+ \frac{2}{K_c^2} \sum_{i=1}^p \left[ \frac{(U_{(p-1)(UCL)} - U_{(p-1)(NCL)})^2}{P_{(p-1)(NCL)}^2} \times \frac{(U_{p(UCL)} - U_{p(NCL)})^2}{P_p^2(NCL)} \right]^{1/2}$$

define

$$d = U_{(UCL)} - U_{(NCL)}$$

then

$$C_s^2 = \frac{1}{K_c^2} \left\{ \left[ \sum_{i=1}^p \frac{d^2}{P_p^2} \right] + 2 \left[ \sum_{i=1}^p \frac{d_{(p-i)}}{P_{(p-1)}} \times \frac{d_p}{P_p} \right] \right\}$$

and

$$S_s^2 = \frac{P_s^2}{K_c^2} \left\{ \left[ \sum_{i=1}^p \frac{d_p^2}{P_{(p)}^2} \right] + 2 \left[ \sum_{i=1}^p \frac{d_{(p-1)}}{P_{(p-1)}} \times \frac{d_{(p)}}{P_{(p)}} \right] \right\}$$

$$S_s = \frac{P_s}{K_c} \left\{ \left[ \sum_{i=1}^p \frac{d_{(p)}^2}{P_{(p)}^2} \right] + 2 \left[ \sum_{i=1}^p \frac{d_{(p-1)}}{P_{(p+1)}} \times \frac{d_{(p)}}{P_{(p)}} \right] \right\}^{1/2}$$

It would appear that the effect of the dependency portion of the equation should not be too large since (a) all the r's will not be statistically significant and those that are should not be equal to unity, (b) it does not appear reasonable to expect a physical relationship for every combination of parameters (c) since some r's will be negative as well as positive, thereby providing some compensation in the net effect.

#### C.4 VAEP APPLIED TO MISCELLANEOUS SYSTEMS ESTIMATES

Two other problems have arisen which can be solved by VAEP. The first is the case where the calculated average is statistically different from the nominal or midpoint value, relative to a two-sided specification. The second case is wherein testing has been conducted at two extremes of an environment (e. g. , low and high temperature) and an over-all P/C estimate is required for the hardware.

##### C.4.1 Case I - $\bar{X} \neq$ Specification Nominal

$$1) U_S = U_L + U_H$$

$$2) S_{U_S}^2 = S_{U_L}^2 + S_{U_H}^2 + 2r_{12} S_{U_L} S_{U_H}$$

- 3) Error propagation is being used because observed average,  $\bar{X}$ , is not centrally located at nominal position between specification limits. It is apparent that as the average moves in the direction of a given specification limit, the failure probability in that direction will increase and that the failure probability estimate for the other side must decrease. It is reasonable, therefore, to assume a negative coefficient of correlation approaching minus one.

$$4) \text{ Since } S^2 = \frac{PU}{n}$$

$$5) \text{ and } n = \frac{K_c^2 PU}{d^2} \text{ where } d^2 = (U_{UCL} - U_{NCL})^2$$

$$S^2 = \frac{PU}{\frac{K_c^2 PU}{d^2}} = \frac{d^2}{K_c^2}$$

$$S = \frac{d}{K_c}$$

$$\begin{aligned}
\therefore S_{U_S}^2 &= \left(\frac{d_L}{K_c}\right)^2 + \left(\frac{d_U}{K_c}\right)^2 - 2(1) \frac{d_L}{K_c} \frac{d_U}{K_c} \\
S_{U_S}^2 &= \frac{1}{K_c^2} (d_L^2 + d_U^2 - 2d_L d_U) \\
S_{U_S} &= \frac{1}{K_c} (d_L^2 + d_U^2 - 2d_L d_U)^{1/2} \\
&= \frac{1}{K_c} [(d_L - d_U)^2]^{1/2} = (d_L - d_U) \\
KS_{U_S} &= (d_L^2 + d_U^2 - 2d_L d_U)^{1/2} \\
&= (d_L - d_U)
\end{aligned}$$

#### C. 4. 2 Case II - Overall Estimate for Test at Extreme Levels

If tests are conducted at two ends of a scale (e. g. , high and low temperature), it is still necessary to obtain an over-all P/C estimate for the equipment. In the absence of mission environmental information, it is reasonable to obtain an average of the two failure probabilities and weighting each of the estimates equally. The procedure for computing this at nominal level and confidence interval is as follows: --

$$\begin{aligned}
U_S &= W_1 U_1 + W_2 U_2 \\
S_{U_S}^2 &= (W_1 S_{U_1})^2 + (W_2 S_{U_2})^2 + 2r_{12} W_1 W_2 S_{U_1} S_{U_2}
\end{aligned}$$

since:

$$S^2 = PU/n$$

and:

$$n = \frac{K_c^2 PU}{d^2}$$

where:

$$d = (U_{UCL} - U_{NCL})$$

$$S^2 = \frac{PU}{K_c^2 PU/d^2} = \frac{d^2}{K_c^2}$$

therefore:

$$S_{U_S}^2 = \frac{1}{4} \frac{d_1^2}{K_c^2} + \frac{1}{4} \frac{d_2^2}{K_c^2} + 2r_{12} \frac{1}{2} \cdot \frac{1}{2} \cdot \frac{d_1}{K_c} \cdot \frac{d_2}{K_c}$$

$$S_U^2 = \frac{1}{4K_c^2} (d_1^2 + d_2^2 + 2rd_1d_2)$$

$$S_U = \frac{1}{2K_c} (d_1^2 + d_2^2 + 2r_{12}d_1d_2)^{1/2}$$

if  $r = 0$ , then:

$$S_{U_S}^2 = \frac{1}{4K_c^2} (d_1^2 + d_2^2)$$

$$S_{U_S} = \frac{1}{2K_c} (d_1^2 + d_2^2)^{1/2}$$

or:

$$KS_{U_S} = 1/2 (d_1^2 + d_2^2)^{1/2}$$

if  $r = +1$ , then:

$$S_{U_S}^2 = \frac{1}{4K_c^2} (d_1^2 + d_2^2 + 2d_1d_2) = \frac{1}{4K_c^2} (d_1 + d_2)^2$$

$$S_U = \frac{1}{2K_c} (d_1 + d_2)$$

$$KS_U = \frac{1}{2} (d_1 + d_2)$$

if  $r = -1$ , then:

$$S_{U_S}^2 = \frac{1}{4K_c^2} (d_1^2 + d_2^2 - 2d_1d_2) = \frac{1}{4K_c^2} (d_1 - d_2)^2$$

$$S_{U_S} = \frac{1}{2K_c} (d_1 - d_2)$$

$$KS_{U_S} = \frac{1}{2} (d_1 - d_2)$$

## C.5 REFERENCES

- (1) "Statistical Procedures for Evaluating Simultaneity and Related Timing Functions as Series, Redundant and Series/Redundant Configurations from Variables Data" GE-RSD, PIR 8432-501, May 24, 1965.
- (2) "Battery 47E186818 - Probability/Confidence Estimates of Cell Performance Data" GE-RSD, PIR, May 10, 1965.
- (3) "Reliability Demonstration of MK 12 Initiators by Evaluation of Variables Performance Parameters" GE 65SD558P, April 20, 1965 and Supplement.
- (4) "Statistical Analysis of Battery (Dwg. No. 47D167047) Development Tests" GE-RSD, PIR 8432-444, January 22, 1965.
- (5) DeCicco, H. "Note on a Control Procedure for the Reliability of Systems Based on Component Test Data Alone" IEEE Transactions on Aerospace - Support Conference Procedures.
- (6) N. E. Golovin - "Systems Reliability in the Space Program" Industrial Quality Control, Vol. XX, No. 11, May 1964.
- (7) R. D. Cruickshank "Reply 1-65, Problems Department" Industrial Quality Control, January 1965.
- (8) S. Demskey "Systems Estimation from Performance Parameters" Fifth Reliability and Maintainability Conference (AIAA/SAE/ASME), July 1966.
- (9) S. Demskey "Systems Estimation from Variables Performance Parameters" GE-TIS 66SD342, 30 November 1966.



## APPENDIX D

### COMPARISON OF SYSTEM ESTIMATION METHODS

#### D.1 COMPARISON OF AEP WITH OTHER METHODS

In Reference D. 3 (1) several estimation methods for serial systems are compared, and are classified as exact, approximate, and asymptotic.

First the theory is discussed and then most of these methods are applied to three sample problems involving observed, attribute data. Error propagation, therefore, may be applied directly (i. e. , AEP for attributes/error propagation).

In view of the application of the normal approximation to binomial estimates, error propagation (AEP) would be considered an approximate solution. The first estimate, identified as "no continuity correction" yields higher success estimates, although the difference is negligible in Case I where  $n = 100$ , which is to be expected.

A correction for continuity (CC),  $1/2n$ , is then applied. This correction recommended by Hald in such situations to yield more conservative estimates. The results, AEP with CC of  $1/2n$  yields results which are close to the other approximate methods. This suggested that the CC of  $1/2n$  be used for each contributing  $R_i$  or a continuity correction of  $N/2n$ , where  $N$  is the number of contributing reliability estimates and  $n$  is the sample size upon which each is based. For the sample examples  $N/2n = 2/2n = 1/n$ . This procedure yielded results which again reduced the difference between AEP and the exact method preferred by the authors of Reference C. 4 (8). Some further work in determining the correct continuity correction is necessary. Assuming that the system estimate is binomial and that  $N_S = N_1 = N_2$ , then the binomial estimates are close to the approximate estimates.

COMPARISON OF AEP WITH OTHER SYSTEM ESTIMATION METHODS

TYPE		NAME	CASE I	CASE II	CASE III
A	A				
x	x		$N_1=N_2=100$ $M_1=97, M_2=95$ $C=0.90$ $R_s=.9215$	$N_1=N_2=20$ $M_1=18, M_2=19$ $C=.90$ $R_s=.8550$	$N_1=N_2=10$ $M_1=M_2=9$ $C=.90$ $R_s=.81$
x		LIPOW	0.826	0.475	0.280
x		LIPOW	.870	.866	.468
x		LIPOW	.876	.716	.607
x		SPRINGER-THOMPSON	.8662	.6728	.510
	x	LINDSTRON-MADDEN	.872	.712	.550
	x	GARNER-VAIL	.883	.725	.575
	x	NISHIME	.883	.704	.570
	x	CONNER-WELLS	.8759	.702	.557
	x	MADANSKY	.859	.550	.404
	x	AEP; CC = 1/2N	.882	.728	.593
	x	AEP; BINOMIAL ( $N_s = N_1 = N_2$ )	.390	.725	.600
	x	NAVWEPS OD29034 W BETA W/O BETA	.877	.714	.583
			.882	.735	.620

COMPARISON OF ESTIMATES BY AEP FOR CASES I, II, and III

	Case I			Case II			Case III		
	$n_1 = n_2 = 100; m_1 = 97, M_2 = 95; P_g = .9215$			$n_1 = n_2 = 20; m_1 = 18, m_2 = 19; P_g = .8550$			$n_1 = n_2 = 10; m_1 = m_2 = 9; P_g = .81$		
	$P_1 = .97, P_2 = .95; U_g = .0785$			$P_1 = .90, P_2 = .95; U_g = .1450$			$P_1 = P_2 = .9; U_g = .19$		
	No. Cont. Corr.		Continuity Correction (CC)	No. Cont. Corr.		Continuity Correction (CC)	No. Cont. Corr.		Continuity Correction (CC)
	Binomial	$\frac{1}{2n}$		Binomial	$\frac{1}{2n}$		Binomial	$\frac{1}{2n}$	
$C^2 = \frac{U_1}{n_1 P_1} + \frac{U_2}{n_2 P_2}$	.03	.05	$\frac{.03}{100(.97)} + \frac{.05}{100(.95)}$	.10	.05	$\frac{.10}{20(.90)} + \frac{.05}{20(.95)}$	.10	.10	$\frac{.10}{10(.90)} + \frac{.10}{10(.90)}$
$s_{U_g}^2 = P_g^2 C^2$	.0008	.000837	.000837	.00819	.00819	.0222	.0222	.0222	.0222
$s_{U_g}$	-	.000710	.000710	.00590	.00590	.0146	.0146	.0146	.0146
$t_{.90C}$	.0283	.0266	.0266	.0768	.0768	.121	.121	.121	.121
$t_{.90C} s_{U_g}$	1.282	1.285	1.285	1.328	1.328	1.383	1.383	1.383	1.383
$U_{S(NCL)}$	0.0363	.0341	.0341	.102	.102	.167	.167	.167	.167
Continuity Correction (CC)	0.0785	.0785	.0785	.1450	.1450	.190	.190	.190	.190
$U_{S(NCL)}$	-	.005	.01	.025	.025	.05	.05	.05	.05
$U_{S(NCL)CC}$	-	.0785	.0885	.145	.145	.19	.19	.19	.19
$U_g(.90C)$	0.1148	0.1126	0.1176	0.247	0.247	0.297	0.297	0.297	0.297
$P_g(.90C)$	0.8852	0.8874	0.8924	0.753	0.753	0.703	0.703	0.703	0.703

**D. 2 VAEP VERSUS AN EXTENSION OF LLOYD-LIPOW FORMULA AND THE INCOMPLETE BETA ESTIMATE**

An approximate formula for the variance of R is given in Ref. 3 of D. 3 -

$$\text{Var. } R \sim \frac{K_o^2}{n} \left( 1 + \frac{K^2}{2} \right)$$

where:  $K = \frac{(SL-X)}{S} = \frac{\text{Spec Limit} - \text{Mean}}{\text{Standard Deviation}}$

$K_o$  is the ordinate of normal curve at K

n is the sample size

Using error propagation for obtaining a system variance as given in Enclosure C. 1

$$S_s^2 = P_s^2 C_s^2 = P_s^2 \left[ \sum_{u=1}^p \frac{K_o^2}{n} \left( 1 + \frac{K^2}{2} \right) / P_p^2 \right]$$

and the system estimate for the upper confidence level of U, using the normal approximation is:

$$U_{S(UCL)} = U_{S(NCL)} + K_c P_s \left[ \sum_{u=1}^p \frac{K_o^2}{n} \left( 1 + \frac{K^2}{2} \right) / P_p^2 \right]^{1/2}$$

Now let us take some example given References D. 2 (2) and (3) and compare them with estimates obtained by VAEP.

Comparison #1 - Reference (3)

Given Problem:  $\bar{X}$  = 1500 hours      C = 0.90  
                   s    = 100 hours        n = 50  
                   LSL = 1200 hours

Compare: L/L approximate estimate of P/C. 90 with that of VAEP.

Direct estimate by Statistical Tolerance Limits  $P = 0.9949$  at  $0.90C$ .

L/L Approximation	VAEP
$S_R$ given as 0.00147 $R_L$ , C. 90 given as 0.9968	For a single parameter system $S_R = \frac{U_{(C.90)} - U_{(C.50)}}{K_c}$ $= \frac{0.00375}{1.282} = 0.00292$ $U_{C.90} = U_{C.50} + K_c S$ $= 0.00135 + 1.282(0.00292)$ $U_{C.90} = 0.0051$ $P_{C.90} = .9949$

Result: It is apparent in this problem with  $n = 50$  that VAEP yields the same answer as that given by Statistical Tolerance Limits whereas the Lloyd and Lipow approximation yields an optimistic estimate of  $P$  due to the deflated estimate of the standard deviation.

Comparison #2 - Reference 2

Given: LSL = 30,200                      S = 300  
 USL = 31,730                              n = 16  
 $\bar{X}$  = 31,010                                C = 0.90 (one sided)

Compare: Incomplete Beta estimate of P/C. 90 with that of VAEP.

Incomplete Beta	VAEP
Given: $U_{U,C.50} = 0.0038$	$U_{U,C.50} = 0.008198$
$U_{L,C.50} = 0.0008$	$U_{L,C.50} = 0.003467$
$U_{S,C.50} = 0.0046$	$U_{S,C.50} = 0.011665$
$P_{S,C.50} = 0.9954$	$P_{S,C.50} = 0.988335$
$P_{S,C.90} = 0.9545$	$P_{S,C.90} = 0.961506$

Result: For a case with  $n = 16$ , VAEP yields with much less effort, an estimate very close to the Incomplete Beta method which Drnas described "... but not exact ...".

Actually, this writer would not have calculated the P/C estimate as the sum of two one-sided estimates. A 't' significance test of the average against the specification midpoint yields a 't' of 0.6 which could hardly be interpreted as statistically significant. A P/C estimate could be made directly, therefore, using the two-sided tolerance limit deviate directly. The estimate obtained from this approach is 0.952852P/0.90C. The L/L approximation formula yields an estimate of 0.9814P/0.90C.

Comparison #3 - (Hypothetical System Examples)

Given: A three parameter system with Probability estimates of 0.99, 0.995, and 0.999 at C. 50 associated  $K_{pcnf}$  values for  $n = 10, 50, \text{ and } 100$ .

P C. 50	$K_{pcnf} = (SL-X)S$		
	n =		
	10	50	100
0.990	2.310	2.341	2.334
0.995	2.650	2.590	2.580
0.999	3.205	3.111	3.100

Compare: System P/C. 95 estimates based on the error propagation of L/L Approximation formula with that of VAEP.

n	P/C. 95	
	VAEP	L&L
10	0.8792	0.9580
50	0.9642	0.9706
100	0.9697	0.9743

Results: The estimates are close down to  $n = 50$ , but at  $n = 10$ , VAEP yields a more conservative and more accurate answer, for the same reason given in comparison #1.

Based on the three foregoing comparisons, VAEP yields estimates quite close to those yielded by the other methods relative to recommendations for use with specific sample size ranges. On the other hand, VAEP is applicable to all sample sizes because of its calibration to the Statistical Tolerance Limit estimate. Furthermore, the calculations are much simpler when small sample sizes are used as compared with the Incomplete Beta Method. Until a simple multivariate tolerance procedure is developed, VAEP is recommended for providing reasonable estimates with economical sample sizes.

#### D.3 REFERENCES

- (1) G. Schick and R. Prior "Reliability and Confidence of Serially Connected Systems" Third Space Congress - March 1966, Canaveral Councils of Technical Societies.
- (2) T. Drnas "Methods of Estimating Reliability" Industrial Quality Control, September 1966.
- (3) D. Lloyd and M. Lipow "Reliability: Management, Methods and Mathematics" Prentice Hall Inc. 1962.

## APPENDIX E

### COMBINED STATISTICAL TOLERANCE LIMITS ESTIMATES WITH ERROR PROPAGATION FOR SYSTEMS ESTIMATION (ALTERNATIVE METHOD)

#### E. 1 ESTIMATE OF SYSTEM MEAN AND VARIANCE

(1) System Model

$$P_S = P_1 \cdot P_2 \cdots P_{p-1} \cdot P_p$$

where,

$P_S$  is the system probability estimate

$P_1$  thru  $P_p$  are the probability estimates for each performance parameters  
-1 . . . p-obtained via statistical tolerance limits at a nominal confidence level.

In this first step, the nominal confidence level (NCL), 50 percent is used; this is the level upon which the error propagation formulas are derived.

(2) The error propagation formula for a product, assuming independence, will be used to estimate the standard deviation of  $P_S$ .

$$C_S^2 = C_1^2 + C_2^2 + \cdots + C_{p-1}^2 + C_p^2$$

where,

$C$  is the coefficient of variation

$C^2$  is the rel-variance

$C^2$  is  $(U/nP)$  for a binomial attribute

$$S^2 = P^2 C^2$$

$U$  is  $(1-P)$  or the failure probability

(3) Therefore:

$$\frac{U_S(NCL)}{n_{S(a)}^P S(NCL)} = \frac{U_1}{n_{1(a)}^P P_1} + \frac{U_p}{n_{p(a)}^P P_p} = \sum_{i=1}^p \frac{U_{p(NCL)}}{n_{p(a)}^P P_p(NCL)}$$

where,

$n(a)$  is the attribute sample size

$U_p$  is a failure probability for 'p' performance parameter

NCL is the nominal confidence level



- (4) Since the variables/tolerance limit estimates will customarily (but not necessarily) be higher than a binomial/attribute estimate, and equivalent attribute sample size will have to be used for 'n<sub>p(a)</sub>' in Equation 2. This is derived in Paragraph D.3 and is given as  $n = 0.693/U_{p(NCL)}$  which is substituted:

$$C_s^2 = \sum_{i=1}^p \frac{U_{p(NCL)}}{\left[ \frac{0.693}{U_{p(NCL)}} \right] P_{p(NCL)}} = \sum_{i=1}^p \left[ \frac{U_{p(NCL)}^2}{0.693 P_{p(NCL)}} \right]$$

$$= \frac{1}{0.693} \sum_{i=1}^p \left[ \frac{U_{p(NCL)}^2}{P_{p(NCL)}} \right]$$

and, since  $S_s^2 = P_s^2 C_s^2$  for a binomial estimate or,

$$S_s^2 = P_s^2 \frac{1}{0.693} \sum_{i=1}^p \left[ \frac{U_{p(NCL)}^2}{P_{p(NCL)}} \right]$$

and,

$$S_s = \frac{P_s}{0.8325} \sum_{i=1}^p \left[ \frac{U_{p(NCL)}^2}{P_{p(NCL)}} \right]^{1/2}$$

- (5) The normal distribution is now used to estimate the approximate upper confidence limit of the failure probability

$$U_{s(UCL)} = U_{s(NCL)} + K_c S_s$$

where,

$U_s$  is the estimate of the system failure probability

UCL is the upper confidence level

$K_c$  is the normal deviate at an upper confidence level or c or 1 minus the risk level

- (6)  $P_{s(UCL)} = 1 - U_{s(UCL)}$

## E.2 EFFECT OF DEPENDENCE (WORST CASE)

The effect of dependence between parameters on the system variance estimate is taken into consideration by the error propagation formula (and using subscripts 1, 2, 3, 4, 5 instead of the six parameter symbols is)

$$C_c^2 = C_1^2 + \dots + C_6^2 + 2r_{12}C_1C_2 + \dots + Cr_{56}C_5C_6$$

Now the worst case estimate would exist if all 5C<sub>2</sub> or 10 combinations of two factors probability estimates were to be completely related; this is somewhat extreme, but let us see the effect on the estimate.

If all the two factor combinations are related, the  $r_{ij} = 1$ , and

$$\begin{aligned} C_p^2 &= \Sigma C_p^2 + [2(1)C_1C_2 + \dots + 2(1)C_5C_6] \\ &= \Sigma C_p^2 + 2[C_1C_2 + \dots + C_5C_6] \\ &= \frac{\Sigma U_p^2}{0.693} + 2 \left[ \left( \frac{U_1}{N_1} \cdot \frac{U_2}{N_2} \right)^{1/2} + \dots + \left( \frac{U_5}{N_5} \cdot \frac{U_6}{N_6} \right)^{1/2} \right] \end{aligned}$$

Substituting  $N = 0.693/U$

$$\begin{aligned} C_s^2 &= \frac{1}{0.693} \sum \frac{U_p^2}{P_p} + 2 \left[ \left( \frac{U_1^2}{P_1 \cdot 0.693} \cdot \frac{U_2^2}{P_2 \cdot 0.693} \right)^{1/2} + \dots + \left( \frac{U_5^2}{P_5 \cdot 0.693} \cdot \frac{U_6^2}{P_6 \cdot 0.693} \right)^{1/2} \right] \\ C_s^2 &= \frac{1}{0.693} \sum \frac{U_p^2}{P_p} + \frac{2}{(0.693)^2} \left[ \left( \frac{U_1^2}{P_1} \cdot \frac{U_2^2}{P_2} \right)^{1/2} + \dots + \left( \frac{U_5^2}{P_5} \cdot \frac{U_6^2}{P_6} \right)^{1/2} \right] \\ C_s^2 &= \left\{ \left[ \frac{1}{0.693} \sum \frac{U_p^2}{P_p} \right] + \left\{ (4.16) \left[ \sum \left( \frac{U_p^2}{P_p} - \frac{U_{p-1}^2}{P_{p-1}} \right)^{1/2} \right] \right\} \right\} \end{aligned}$$

Since  $S_s^2 = P_s^2 C_s^2$

$$S_s^2 = P_s^2 \left\{ \left[ \frac{1}{0.693} \sum \frac{U_p^2}{P_p} \right] + \left[ 4.16 \left( \sum \left( \frac{U_p^2}{P_p} - \frac{U_{p-1}^2}{P_{p-1}} \right)^{1/2} \right) \right] \right\}$$

It is apparent that the effect of dependency should not be too large since, (a) all the r's will not be statistically significant and those that are should not be equal to unity. (b) physical relationships are not expected for each paired combination of parameters. and (c) a compensating effect will be present due to both positive and negative r's.

### E.3 EQUILIBRATION/ATTRIBUTE SAMPLE SIZE

Given - A computed value of P and U at the 50 percent confidence level, the following method solves the binomial formula to estimate the equivalent, attribute sample size assuming zero catastrophic failures.

Solution

$$\text{Prob} = {}^n C_{n_S} P^{n_S} U^{n-n_S} \quad (1)$$

where,

Prob =  $\alpha$  risk = (1 - confidence level)

n is the sample size required to meet a probability estimate of (1-C) with a given P and zero failures.

$n_S$  is the number of successful units.

P is the unit success probability estimate from a variables method.

U is (1-P)

$$\begin{aligned} (1-C) &= \frac{n!}{0! n_S!} P^{n_S} U^0 \\ &= (1) P^{n_S} (1) \end{aligned} \quad (2)$$

$$\ln (1-C) = n_S \ln P + n \ln U$$

$$n = \frac{-\ln (1-C)}{-\ln P} = \frac{\ln (1-C)}{\ln P} \quad (3)$$

Since an effective 50 percent confidence level will be used for estimating the equilibration attribute, sample size

$$\ln P \approx 1 - P = U$$

$$n = \frac{\ln 0.50}{\ln P} = \frac{-0.693}{-U} = \frac{0.693}{U}$$

#### E. 4 CORRECTION METHOD FOR SMALL SAMPLE SIZES

It is recognized that in the estimation of tail probabilities of a binomial distribution, the normal distribution is not as precise as desired. Furthermore, a correction factor is also necessary to calibrate the VAEP estimate. The criterion used is that the estimates based on the Variables/Attributes/Error Propagation (VAEP) method should provide the correct answer for a single parameter system. The method by which this is done is to calibrate the VAEP answer to that which would be obtained from statistical tolerance limits. This is done by first reducing the multi-parameter formula:

$$U_{S(UCL)} = U_{S(NCL)} + \frac{K_c [\sum U_P^2]^{1/2}}{0.8325} \quad (1)$$

to a single parameter formula:

$$\begin{aligned} U_{S(UCL)} &= U_{P(NCL)} + \frac{K_c U_{P(NCL)}}{0.8325} \\ &= U_{P(NCL)} + \frac{K_c U_{P(NCL)}}{0.8325} \\ &= U_{P(NCL)} \left[ 1 + \frac{K_c}{0.8325} \right] \end{aligned} \quad (2)$$

$$U_{S(UCL)} = U_{P(NCL)} \left[ 1 + \frac{1.645}{0.8325} \right] = 2.975 U_{P(NCL)} \quad (3)$$

therefore,

$$U_{S(NCL)} = U_{P(NCL)} = \frac{U_{S(UCL)}}{2.975}$$

where,

$K_c$  is the one-sided normal K, deviate for 95 percent confidence.

(NCL) refers to a nominal confidence level to be calculated.

For example,

- (1) Given  $n = 127$  and a requirement of  $0.995P/0.95C$
- (2) The normal tolerance deviate (one-sided) associated with the given information is 2.92

(3) Substituting in Equation 3

$$U_{C(NCL)} = 0.005/2.975 = 0.00168$$

$$\sim 0.0017 \text{ or}$$

$$P_{S(NCL)} = 0.9983$$

(4) It may then be observed that, at the 50 percent confidence level,  $K = 2.92$  for  $P = 0.9983$ . This indicates the accuracy of the VAEP equation with the correction. This should not be a surprise as it may be seen in many statistical texts that the normal distribution does a satisfactory job of estimating the binomial even when the sample size is as low as 100.

(5) Let us continue this method for smaller sample sizes.

n	$K_{PCnf}$ 0.995P/0.95C	$U_{S(C.50)}$	C for $K_{PCnf}$ where $U = 0.0017$
127	2.92	0.0017	0.50
100	2.92	0.0017	0.50
75	3.03	0.0015	0.63
50	3.16	0.0008	0.75
25	3.48	0.0003	~0.80

For requirement of 0.995P/0.95C, estimates could be made to a sample size of 100 without any correction, down to 50 with a negligible increase in  $K_{PCnf}$  and down to 24 with a small increase in the tolerance deviate.

## E. 5 SAMPLE PROBLEM

### E. 5.1 Calculation of Nominal Confidence Level

(1) Given:  $n = 15$ , a P/C requirement of 0.995 P/0.95C

(2)  $K_{PCnf}$  (for 0.999 P/0.95C) = 4.607 (1 sided)

$$(3) U_{S(NCL)} = U_{S(NCL)} \left[ 1 + \frac{K_c}{0.8325} \right]$$

## E. 5 SAMPLE PROBLEM

### E. 5.1 Calculation of Nominal Confidence Level

(1) Given:  $n = 15$ , a P/C requirement of 0.999 P/0.95C

(2)  $K_{Pcnf}$  (for 0.999 P/0.95C) = 4.607 (1 sided)

(3)  $U_{S(NCL)} = U_{S(NCL)} \left[ 1 + \frac{K_c}{0.8325} \right]$

$$0.001 = U_{S(NCL)} \left[ 1 + \frac{1.645}{0.8325} \right] = 2.976 U_{S(NCL)}$$

or  $U_{S(NCL)} = 0.001/2.975 = 0.000336$  or  $P_{S(NCL)} \sim 0.999664$

(4) substituting in Hald's equation

$$K_c = \frac{K_{Pcnf} - K_P}{\sqrt{\frac{1}{n} + K^2 \frac{Pcnf}{2f}}} = \frac{4.607 - 3.382}{\sqrt{\frac{1}{15} + \frac{21.22}{28}}} = 1.349$$

$$C = 0.91$$

D.5.2 System Estimate (Assuming Independence)

Sample Problem

PARAMETER - p	$U_p$ (C.91)	$U_p^2$ (C.91)	p	$\frac{U_p^2}{p}$
# $K_{Pcnf}$	$(1 \times 10^{-6})$	$(1 \times 10^{-12})$		
1 5.92	6	36	.999994	36.0
2 5.38	37	1369	.999963	1369.05
8.39	~ 0	~ 0	~1.0000	0
4 5.94	6	36	.999994	36.00
5 --	0	0	~1.0000	
Total	49	1441		1441.05

$$(\sum U_p^2 / P_p)^{1/2} = 38.0 \times 10^{-6}$$

$$P_s / 0.8325 = 1.2011$$

$$S_{u_s} = \frac{P_s}{0.8325} \left[ \sum \left( \frac{U_{p(NCL)}^2}{P_{p(NCL)}} \right) \right]^{1/2} = 45.64 \times 10^{-6}$$

$$K_{.95} S_{u_s} = 1.645 S_{u_s} = 0.000075$$

$$U_s (NCL) = \sum U_p = 0.000038$$

$$U_s (C.95) = .000113$$

$$P_s (C.95) = .999887$$

4-9 A MATHEMATICAL ANALYSIS OF ORDNANCE CIRCUITRY TO DETERMINE  
THE SUSCEPTIBILITY TO STRAY RF FIELDS

Author  
Jon E. Klima

MARTIN-MARIETTA CORPORATION  
Martin Company  
Denver Division  
Denver, Colorado

INTRODUCTION

In order to comply with requirements for the Titan III program, the Martin Company was directed to perform RF susceptibility testing and circuit analyses on Titan III electro-explosive devices (EED) in accordance with the "Interim Standards to Minimize the Hazards of Electro-Magnetic Radiation to Electro-Explosive Devices," dated 1 October 1962.

To facilitate the analysis, Mr. Dennis E. Roark of the State University of New York at Buffalo prepared for the Martin Company a report entitled "Techniques in RF Susceptibility Studies".<sup>1</sup>

This paper presents highlights of Mr. Roark's report and how it was applied to the Titan III circuit analysis. This technique has also been used to determine the RF susceptibility of several Titan IIIC payload circuits.

BASIC APPROACH TO THE ANALYSIS

The purpose of an RF ordnance susceptibility analysis is to determine when ordnance circuitry is exposed to stray RF fields, how much RF energy can be delivered to and absorbed by an EED when installed and connected to its associated firing circuitry.

The technique of transmission matrices has been chosen to serve as a basis for this analysis. This method has the advantage over other methods



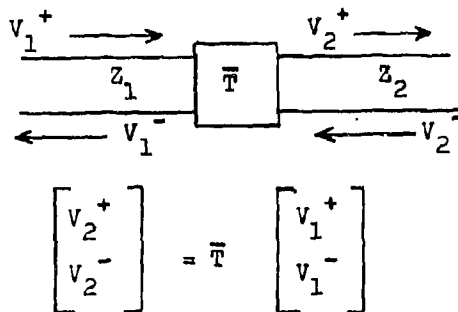
in that a circuit can be broken down into a number of simple parts. Each part may then be represented by a transmission matrix. After each part of the circuit has been assigned a transmission matrix representation, the matrices are multiplied together to form a matrix representing the entire circuit.

The analysis may be separated into two parts. First the antenna characteristics of each segment of wire in the ordnance circuit must be investigated. Second, it must be determined how the signal received by the wire segment is transmitted to the SED.

As in most analyses, certain conservative assumptions must be made, and because of these assumptions, this technique furnishes an upper limit to the power delivered to the SED. These assumptions will be mentioned in the sections where they are applicable.

#### PROPERTIES OF TRANSMISSION MATRICES

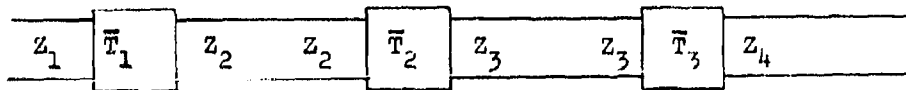
Transmission matrices are linear operators that operate on the parameters  $V_1^+$  and  $V_1^-$  to determine  $V_2^+$  and  $V_2^-$ .



An important relationship to note is that

$$\det \bar{T} = \frac{Z_2}{Z_1} .$$

If a network is given by



the transmission matrix for the over-all network is the product of the matrices for the cascaded components:

$$\bar{T} = \bar{T}_3 \bar{T}_2 \bar{T}_1 .$$

Note that  $\det \bar{T} = \frac{Z_4}{Z_1} .$

#### TRANSMISSION MATRICES USED IN THE ANALYSIS

##### Attenuation Matrix

A signal moving along a transmission line will be attenuated exponentially with an attenuation coefficient  $\alpha$ . The attenuation matrix is represented by <sup>(2)</sup>

$$ATT = \begin{bmatrix} e^{-\alpha l} & 0 \\ 0 & e^{\alpha l} \end{bmatrix}$$

where  $l$  is the length of the cable. For the Titan III transmission cable,  $\alpha$  was determined experimentally and was found not to vary appreciably for different types of wire but was a function of frequency.

Assuming  $l$  is in inches, then the exponents in the attenuation matrix are

$$\pm 0.326 \times 10^{-5} F_{\text{MHz}} l \quad (\text{Pin to Pin})$$

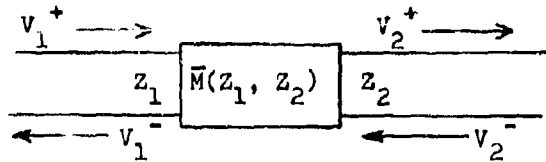
$$\pm 0.527 \times 10^{-5} F_{\text{MHz}} l \quad (\text{Pin to Case})$$

( $F_{\text{MHz}}$  = frequency in megahertz.)

##### Mismatch Matrix

Whenever a wave moving along a line of impedance  $Z_1$  impinges on an

impedance discontinuity, where  $Z_1$  changes to  $Z_2$ , a portion of the wave will be reflected and a portion will be transmitted along  $Z_2$ .



Using the definition of the reflection and transmission coefficient,  $\rho_1$  and  $\tau_1$  respectively, of a wave moving to the right

$$\tau_1 = \frac{2Z_2}{Z_1 + Z_2} \quad \text{and} \quad \rho_1 = \frac{Z_2 - Z_1}{Z_1 + Z_2}$$

and  $\rho_2$  and  $\tau_2$  of a wave moving to the left

$$\tau_2 = \frac{2Z_1}{Z_1 + Z_2} \quad \text{and} \quad \rho_2 = \frac{Z_1 - Z_2}{Z_1 + Z_2}$$

the following mismatch matrix can be derived.

$$\bar{M}(Z_1, Z_2) = \begin{bmatrix} \frac{\tau_1 \tau_2 - \rho^2}{\tau_1} & \frac{\rho}{\tau_1} \\ -\frac{\rho}{\tau_1} & \frac{1}{\tau_1} \end{bmatrix}$$

where

$$\rho = \frac{|Z_2 - Z_1|}{Z_1 + Z_2}$$

Since it is impossible to determine the phasing of any standing wave which might exist, only the points of maximum voltage will be considered. Therefore, it is necessary to use  $|\rho|$ , rather than  $\rho_1$  or  $\rho_2$  when calculating the reflected wave.

The mismatch matrix designation  $\bar{M}(Z_1, Z_2)$  shows that the mismatch is from  $Z_1$  to  $Z_2$ .

In considering a signal entering from the left and/or a signal entering from the right, the following matrix equation must be satisfied.

$$\begin{bmatrix} V_2^+ \\ V_2^- \end{bmatrix} = \begin{bmatrix} M_{11} & M_{12} \\ M_{21} & M_{22} \end{bmatrix} \begin{bmatrix} V_1^+ \\ V_1^- \end{bmatrix}$$

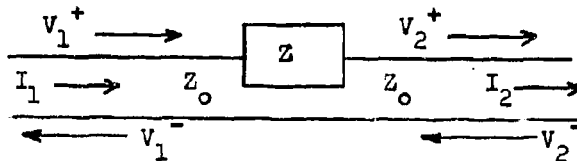
Series Matrix

If an impedance  $Z$  is placed in series with a transmission line of characteristic impedance  $Z_0$ , then the series matrix is

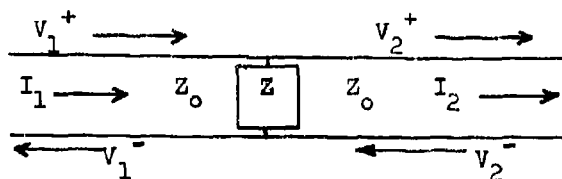
$$\text{SER} = \begin{bmatrix} 1 - \frac{Z}{2Z_0} & \frac{Z}{2Z_0} \\ -\frac{Z}{2Z_0} & 1 + \frac{Z}{2Z_0} \end{bmatrix}$$

As with the mismatch matrix, in considering  $V_2^- = 0$  and/or  $V_1^+ = 0$ , the following matrix equation must be satisfied.

$$\begin{bmatrix} V_2^+ \\ V_2^- \end{bmatrix} = \begin{bmatrix} T_{11} & T_{12} \\ T_{21} & T_{22} \end{bmatrix} \begin{bmatrix} V_1^+ \\ V_1^- \end{bmatrix}$$



Shunt Matrix



If an impedance  $Z$  is placed across a transmission line of characteristic

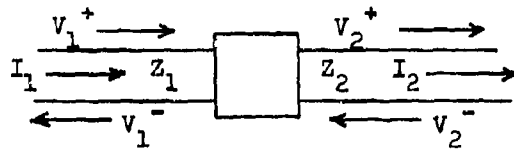
impedance  $Z_o$ , then the shunt transmission matrix is

$$SHT = \begin{bmatrix} 1 - \frac{Z_o}{Z} & \frac{Z_o}{Z} \\ -\frac{Z_o}{Z} & 1 + \frac{Z_o}{Z} \end{bmatrix}$$

The derivation for this matrix is similar to that of the series matrix with the exception that the roles of voltage and current are interchanged.

#### OTHER REQUIRED MATRICES

In many cases, it is impossible to describe various circuit configurations by the preceding transmission matrices. It is therefore necessary to employ several other types of matrices and then convert them to a usable transmission matrix.



$$V_1 = V_1^+ + V_1^-$$

$$V_2 = V_2^+ + V_2^-$$

$$I_1 = \frac{V_1^+ - V_1^-}{Z_1}$$

$$I_2 = \frac{V_2^+ + V_2^-}{Z_2}$$

#### Scattering Matrix

$$\begin{bmatrix} V_1^- \\ V_2^+ \end{bmatrix} = \bar{S} \begin{bmatrix} V_1^+ \\ V_2^- \end{bmatrix}$$

#### Impedance Matrix

$$\begin{bmatrix} V_1 \\ V_2 \end{bmatrix} = \bar{Z} \begin{bmatrix} I_1 \\ -I_2 \end{bmatrix}$$

X-Matrix

$$\begin{bmatrix} V_1 \\ I_2 \end{bmatrix} = \bar{X} \begin{bmatrix} V_2 \\ I_1 \end{bmatrix}$$

Admittance Matrix

$$\bar{Y} = \bar{Z}^{-1}$$

Normalization Matrix

$$\bar{N} = \begin{bmatrix} \frac{1}{Z_1} & 0 \\ 0 & \frac{1}{Z_2} \end{bmatrix}$$

Unit Matrix

$$\bar{U} = \begin{bmatrix} 1 & 0 \\ 0 & 1 \end{bmatrix}$$

The following relationships can be shown to be true.

$$\bar{S} = (\bar{Z} \bar{N} - \bar{U}) (\bar{Z} \bar{N} + \bar{U})^{-1} \quad (1)$$

$$\bar{Z} = (\bar{U} - \bar{S})^{-1} (\bar{U} + \bar{S}) \bar{N}^{-1} \quad (2)$$

$$\bar{Y} = \bar{N} (\bar{U} + \bar{S})^{-1} (\bar{U} - \bar{S}) \quad (3)$$

$$\bar{S} = (\bar{U} - \bar{N}^{-1} \bar{Y}) (\bar{Y} + \bar{N})^{-1} \bar{N} \quad (4)$$

Several other important relationships are the interrelations between the transmission matrix  $\bar{T}$ , and the scattering matrix  $\bar{S}$ , and between the impedance matrix  $\bar{Z}$  and the  $\bar{X}$  matrix.

$$\bar{S} = \begin{bmatrix} \frac{-T_{21}}{T_{22}} & \frac{1}{T_{22}} \\ \frac{\det T}{T_{22}} & \frac{T_{12}}{T_{22}} \end{bmatrix} \quad (5)$$

$$\bar{T} = \begin{bmatrix} \frac{s_{12} s_{21} - s_{11} s_{22}}{s_{12}} & \frac{s_{22}}{s_{12}} \\ -\frac{s_{11}}{s_{12}} & \frac{1}{s_{12}} \end{bmatrix} \quad (6)$$

$$\bar{Z} = \begin{bmatrix} \frac{x_{12} x_{21} - x_{11} x_{22}}{x_{21}} & -\frac{x_{11}}{x_{21}} \\ -\frac{x_{22}}{x_{21}} & -\frac{1}{x_{21}} \end{bmatrix} \quad (7)$$

$$\bar{X} = \begin{bmatrix} \frac{z_{12}}{z_{22}} & \frac{z_{11} z_{22} - z_{12} z_{21}}{z_{22}} \\ -\frac{1}{z_{22}} & \frac{z_{21}}{z_{22}} \end{bmatrix} \quad (8)$$

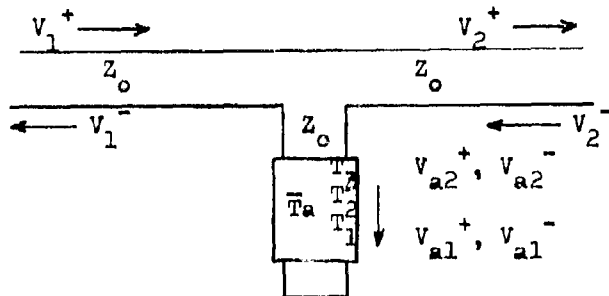
To convert from the  $\bar{Z}$  matrix to the  $\bar{T}$  matrix, use equation (1) to convert the  $\bar{Z}$  matrix to the  $\bar{S}$  matrix, then equation (6) to convert from the  $\bar{S}$  matrix to the  $\bar{T}$  matrix. Reverse the operation to convert from the  $\bar{T}$  matrix to the  $\bar{Z}$  matrix.

Other conversions may be accomplished by similar operations.

#### CASCADE PROCEDURES

With the above equations, it is now possible to show how the transmission matrices of commonly encountered circuit configurations may be formed.

Series Branch



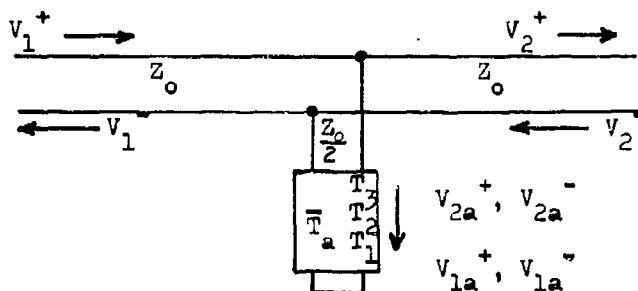
To transform  $T_a$  into the main line, the following matrix transformation is used.

$$\bar{T} = \begin{bmatrix} 1 - \frac{Z_n}{2} & \frac{Z_n}{2} \\ -\frac{Z_n}{2} & 1 + \frac{Z_n}{2} \end{bmatrix}$$

where  $Z_n = \frac{(T_{a21} - T_{a22}) + (T_{a11} - T_{a12})}{(T_{a21} - T_{a22}) - (T_{a11} - T_{a12})}$ .

$T_{a11}$ ,  $T_{a12}$ ,  $T_{a21}$ , and  $T_{a22}$  represent the individual matrix elements of the matrix  $\bar{T}_a$ .

Shunt Branch



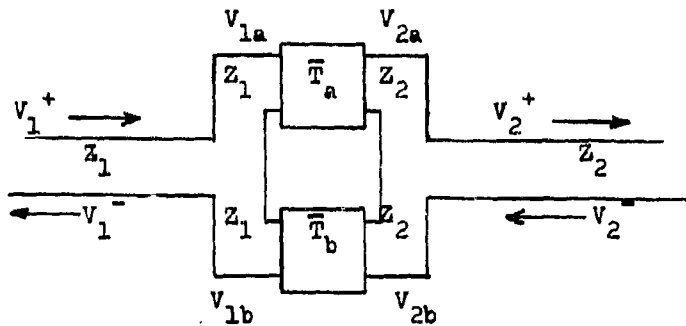
$\bar{T}_a$  may be transformed into the main line by using the following equation.



$$\bar{T} = \begin{bmatrix} \frac{Z_n - 1}{Z_n} & \frac{1}{Z_n} \\ -\frac{1}{Z_n} & \frac{Z_n + 1}{Z_n} \end{bmatrix}$$

where  $Z_n$  is given under the Series Branch section.

Series Multipath



First  $\bar{T}_a$  and  $\bar{T}_b$  are converted to scattering matrices,  $\bar{S}_a$  and  $\bar{S}_b$ .

$$S_i = \begin{bmatrix} -\frac{T_{121}}{T_{122}} & \frac{1}{T_{122}} \\ \frac{Z_2}{Z_1 T_{122}} & \frac{T_{112}}{T_{122}} \end{bmatrix}$$

where  $i = a, b$ .

Next  $\bar{S}_a$  and  $\bar{S}_b$  are converted to impedance matrices using equation (2).

The total impedance matrix  $\bar{Z}$  of the series-multipath configuration is

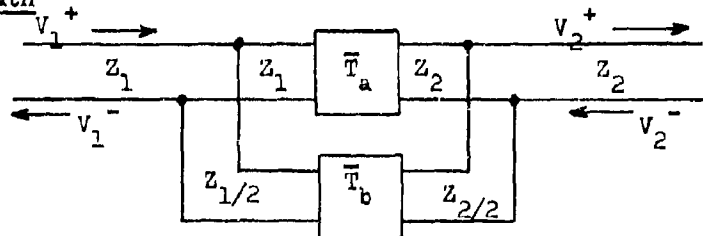
$$\bar{Z} = \bar{Z}_a + \bar{Z}_b.$$

Now using equation (1),  $\bar{Z}$  is converted back to a scattering matrix and then equation (6) is used to get the desired  $\bar{T}$  matrix.

The requirements on  $\bar{T}_a$  and  $\bar{T}_b$  are that their input and output characteristic impedances must be  $\bar{Z}_1$  and  $\bar{Z}_2$  respectively. This is accomplished by placing mismatch matrices on each side of  $\bar{T}_a$  and  $\bar{T}_b$ . Thus, assuming  $\bar{T}_a$  is made up of n individual transmission matrices,

$$\bar{T}_a = \bar{M}(Z_{2a}, Z_n) \bar{T}_n \dots \bar{T}_1 \bar{M}(Z_1, Z_{1a}).$$

Shunt Multipath



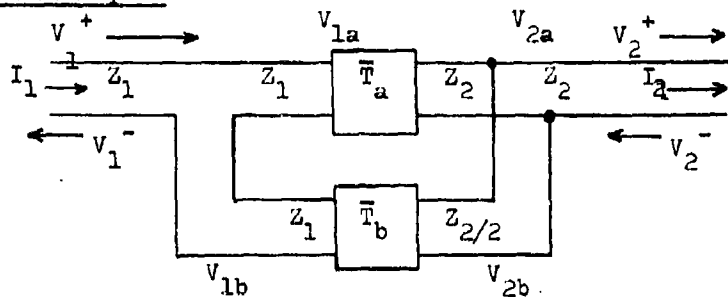
$\bar{T}_a$  and  $\bar{T}_b$  have the matching restrictions as in the Series Multipath case.

The main line transmission matrix is found by first converting  $\bar{T}_a$  and  $\bar{T}_b$  to their equivalent scattering matrices  $\bar{S}_a$  and  $\bar{S}_b$ . The scattering matrices are converted to admittance matrices  $\bar{Y}_a$  and  $\bar{Y}_b$ . The total admittance matrix is

$$\bar{Y} = \bar{Y}_a + \bar{Y}_b.$$

$\bar{Y}$  is then converted to a scattering matrix  $\bar{S}$  and then to the final  $\bar{T}$  matrix.

Series-Shunt Multipath



$\bar{T}_a$  and  $\bar{T}_b$  have the matching restrictions as mentioned in the Series

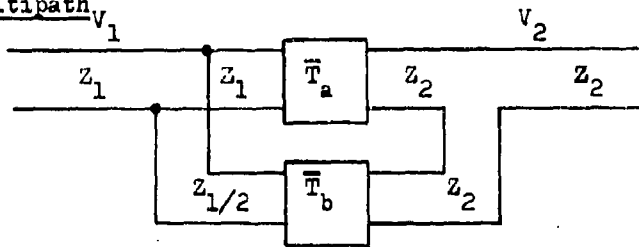
Multipath case.

The main line transmission matrix  $\bar{T}$  is found by first converting  $\bar{T}_a$  and  $\bar{T}_b$  to  $\bar{S}_a$  and  $\bar{S}_b$ .  $\bar{S}_a$  and  $\bar{S}_b$  are then converted to  $\bar{Z}_a$  and  $\bar{Z}_b$  and then to  $\bar{X}_a$  and  $\bar{X}_b$ . The total  $\bar{X}$  matrix is

$$\bar{X} = \bar{X}_a + \bar{X}_b.$$

$\bar{Z}$  is then found from equation (7) and then the scattering matrix  $\bar{S}$  is found from equation (1). Finally the final  $\bar{T}$  matrix is found using equation (6).

Shunt-Series Multipath



This case is most easily handled by using the "reversed transmission matrix". If a circuit is described by a matrix  $\bar{T}$ , it can be "turned around" with the reversed circuit shown to be related to the original matrix  $\bar{T}$  by

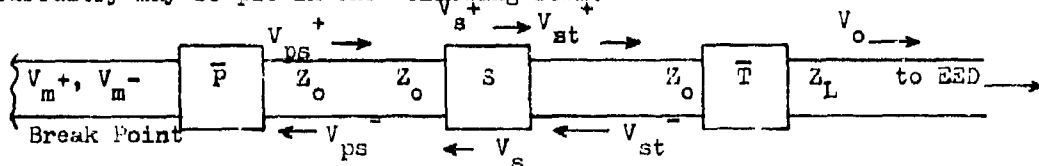
$$\bar{T}^* = \frac{1}{\det \bar{T}} \begin{bmatrix} T_{11} & -T_{21} \\ -T_{12} & T_{22} \end{bmatrix} \quad (9)$$

The reversed matrix of  $\bar{T}$  will be called  $\bar{T}^*$ .

The first step is to follow the same procedure for  $\bar{T}_a$  and  $\bar{T}_b$  as described in the Series-Shunt Multipath section. After the conversions are carried out and  $\bar{T}$  obtained, the reversing matrix is used to obtain  $\bar{T}^*$ .  $\bar{T}^*$  is then the main line transmission matrix.

### TRANSMISSION OF THE RECEIVED SIGNAL TO THE EED

By using the cascading techniques developed in the preceding sections, the circuitry may be put in the following form.



S represents the source (the antenna),  $\bar{T}$  represents the composite matrix of all the circuitry between the antenna and the EED and  $\bar{P}$  represents the composite matrix of all the circuitry considered in the analysis to the left of the antenna. Since it would be impossible to consider all the circuitry to the left of the source (virtually all the vehicle wiring) some arbitrary break point must be chosen. A conservative assumption is made here that any left-moving signal will be completely reflected at the breaking point back toward the EED.

Since it is quite difficult to obtain satisfactory measurements of the EED impedance at the S-Band and higher frequencies, another assumption is made that the EED is perfectly matched to the line, i.e., no reflection will occur and all energy arriving at the EED will be absorbed.

Three final antenna parameters will be described in the following section on Antennas. They are:

$V_s^+$  = source voltage moving to the right

$\sigma$  = symmetry factor =  $\frac{V_s^-}{V_s^+}$

$Z_0$  = characteristic impedance of the antenna

Using these parameters, and the above figure, it is possible to derive the equation for the voltage at the EED.

$$V_o = \left( \frac{V_s^+}{Z_o} \right) \left( \frac{1 + A\sigma}{T_{22} + T_{21}A} \right) Z_L$$

where  $A = \frac{P_{11} + P_{12}}{P_{21} + P_{22}}$ .

$Z_L$  = characteristic impedance of the final transmission line leading to the EED.

There will generally be several antennas for each EED, each contributing a certain voltage as calculated by the above equation. Since it is impossible to determine the phase relationship between each voltage source, the assumption must be made that all voltages add in phase. The total voltage at the EED due to N antennas is

$$V_{\text{total}} = \sum_{i=1}^n |V_{oi}|$$

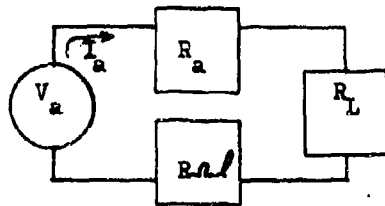
and the total power is

$$P = \left( \sum_{i=1}^n |V_{oi}| \right)^2 / 2Z_L.$$

ANTENNAS

This section on antennas will present the final antenna parameters,  $V_s^+$ ,  $\sigma$ , and  $Z_o$ .  $Z_o$  will be discussed when each individual antenna type is considered.  $V_s^+$  and  $\sigma$  will be generated from several other intermediate parameters derived from initial input parameters.

The equivalent circuit of a receiving system may be shown as:



where  $V_a$  = antenna voltage (amplitude)

$I_a$  = current produced by antenna

$R_a$  = radiation resistance

$R_\Omega$  = ohmic resistance per unit length

$\ell$  = antenna length

$R_L$  = input impedance of the load to which the antenna is connected

It can be shown that the power received is

$$P = \frac{R_L V_a^2}{2 (R_a + \ell R_\Omega + R_L)^2} \quad (10)$$

If the ohmic losses are neglected the effective antenna area is defined as directivity area. <sup>(3)</sup>

$$A_d = \frac{P_{\max}}{|\bar{S}|} \quad (11)$$

where  $\bar{S}$  is the time-average Poynting vector. Assuming a matched condition between the antenna and load (maximum power transfer), i.e.,  $R_L = R_a$ , and  $R_\Omega = 0$  then

$$P_{\max} = \frac{V_a^2}{8R_a}$$

the ratio of  $P$  to  $P_{\max}$  will be defined as  $k$

$$k = \frac{P}{P_{\max}} \quad (12)$$

It can easily be shown that  $P$  is proportional to  $\frac{R_L |\bar{S}|}{2 (R_a + \ell R_\Omega + R_L)^2}$

and also that  $P_{\max}$  is proportional to  $|\bar{S}| / 8R_a$ . Using the definition for  $k$

$$k = \frac{4R_a R_L}{(R_a + \ell R_\Omega + R_L)^2}$$

Using this equation together with equations (11) and (12)

$$P = \frac{4 R_a R_L A_d |\bar{S}|}{(R_a + R_L)^2}$$

Now using equation (10)

$$V_a = \sqrt{8 R_a A_d |\bar{S}|}$$

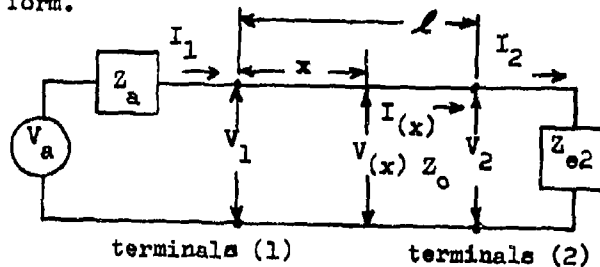
The directivity area is related to the directive gain,  $g$ , by <sup>③</sup>

$$A_d = \frac{\lambda^2 g}{4\pi}$$

The equation for  $V_a$  may now be written as

$$V_a = \lambda \sqrt{\frac{2 R_a g |\bar{S}|}{\pi}}$$

Using Schelkunoff's "end-fire equivalent" the receiving system takes the following form.



at terminals (1)

$$V_1 = V^+ + V^- \quad (13)$$

$$I_1 Z_0 = V^+ - V^- \quad (14)$$

and at terminals (2)

$$V_2 = V^+ e^{-\gamma l} + V^- e^{\gamma l} \quad (15)$$

$$I_2 Z_0 = V^+ e^{-\gamma l} - V^- e^{\gamma l} \quad (16)$$

where  $\gamma = \alpha + i\beta$  (will be discussed later).

$$\text{Also } V_1 = V_a - I_1 Z_a \quad (17)$$

$$\text{and } V_2 = I_2 Z_{e2} \quad (18)$$

By defining the reflection and transmission coefficients:

$$\rho_o = \frac{Z_o - Z_a}{Z_o + Z_a}, \quad \rho_2 = \frac{Z_{e2} - Z_o}{Z_{e2} + Z_o} \quad (19)$$

$$\tau_o = 1 + \rho_o, \quad \tau_2 = 1 + \rho_2 \quad (20)$$

the above equations (13) through (20) may be combined and solved for  $V_2$ .

$$V_2 = \left( \frac{\frac{1}{2} \tau_o \tau_2 e^{j\beta l}}{e^{2j\beta l} + \rho_o \tau_2} \right) V_a$$

$V_2$  is the voltage that will cross the entrance impedance  $Z_{e2}$ .  $V_s^+$  is defined as

$$V_s^+ = \frac{V_2}{\tau_2}$$

$V_s^+$  may now be defined as

$$V_s^+ = \frac{\frac{1}{2} (\rho_o + 1) e^{j\beta l} V_a}{e^{2j\beta l} + \rho_o \rho_2} \quad (21)$$

By replacing  $\rho_2$  by  $\rho_1$

$$V_s^- = \frac{\frac{1}{2} (\rho_o + 1) e^{j\beta l} V_a}{e^{2j\beta l} + \rho_o \rho_1}$$

As defined earlier  $\sigma = \frac{V_s^-}{V_s^+}$

$$\text{or} \quad \sigma = \frac{e^{2j\beta l} + \rho_o \rho_2}{e^{2j\beta l} + \rho_o \rho_1} \quad (22)$$

From equations (21) and (22) both  $V_s^+$  and  $\sigma$  are complex quantities. Also,

$$e^{j\beta l} = e^{\alpha_a l} e^{j\beta l}$$



Because of uncertainties in length  $l$ , the value for  $\beta l$  that gives a maximum voltage at the EED will be used.

The maximizations of  $V_s^+$  and  $\sigma$  are quite lengthy. Therefore only the end results will be shown.

$$\sigma = \sigma_1 \quad \text{if } \sigma_1 \geq \sigma_2$$

$$\sigma = \sigma_2 \quad \text{if } \sigma_1 < \sigma_2$$

where

$$\sigma_1 = \sqrt{\frac{F+B}{C+D}}$$

$$\sigma_2 = \sqrt{\frac{F-B}{C-D}}$$

and

$$B = 2(\rho_0 \rho_2) e^{2\alpha a l}$$

$$C = 4\alpha a l + (\rho_0 \rho_1)^2$$

$$D = 2(\rho_0 \rho_1) e^{2\alpha a l}$$

$$E = 4\alpha a l + (\rho_0 \rho_2)^2$$

Now

$$V_s^+ = \frac{G V_a}{\sqrt{F+H}}$$

where

$$G = \frac{1}{2}(\rho_0 + 1) e^{\alpha a l}$$

$$H = B \text{ if } (\rho_0 \rho_2) \leq 0$$

$$H = -B \text{ if } (\rho_0 \rho_2) > 0$$

#### Intermediate Parameters

Two of the three final antenna parameters have now been defined;  $V_s^+$  and  $\sigma$ . However, before these final parameters can be calculated, several other intermediate parameters must be determined. These are  $|\bar{S}|$ ,  $S$ ,  $\alpha_a$ ,  $R_{a1}$ , and  $R_{a2}$ , and will be discussed in order.

### Time-Average Poynting Vector

The level to which all Titan III ordnance devices are analyzed is 100 watts/meter<sup>2</sup> or  $|\bar{S}_0| = 100 \text{ watts/meter}^2$ . Since it is more convenient to use inches to describe lengths of cable,  $|\bar{S}_0|$  may be expressed as

$$|\bar{S}_0| = 0.0645 \text{ watts/inch}^2.$$

It is occasionally of interest to know how the field is attenuated as it passes through the shield of a shielded cable. This attenuation can be determined experimentally and is called the "extinction coefficient"

$\epsilon$  measured in decibels. The field  $|\bar{S}|$  reaching the center conductors is simply  $|\bar{S}_0|$  reduced by  $\epsilon$ .

$$\epsilon = -10 \log_{10} \left( \frac{|\bar{S}|}{|\bar{S}_0|} \right) = -10/2.3 \ln_e \left( \frac{|\bar{S}|}{|\bar{S}_0|} \right)$$

$$\text{or } |\bar{S}| = |\bar{S}_0| e^{-.23\epsilon} = 0.0645 e^{-.23\epsilon}$$

for 100 watts/meter<sup>2</sup>.

### Directivity

Schelkunoff shows that the directivity of a long antenna is <sup>3</sup>

$$g = 4l/\lambda$$

and of a short current element is

$$g = 1.5.$$

These functions intersect at  $l/\lambda = 0.375$ . Therefore

$$\text{if } l/\lambda > 0.375 \quad g = 4l/\lambda$$

$$\text{and if } l/\lambda \leq 0.375 \quad g = 1.5.$$

### Antenna Attenuation Coefficient

The attenuation coefficient will in general depend on the inductance L, capacitance C, leakage conductance G, and ohmic resistance  $R_{\Omega}$ . The fre-

quencies used in the analysis are sufficiently high

$$\omega L \gg R_{\Omega} \quad \text{and} \quad \omega C \gg G$$

$\alpha'_a$  can thus be defined as <sup>(3)</sup>

$$\alpha'_a = \frac{R_{\Omega}}{2Z_0} + \frac{GZ_0}{2}$$

The assumption that  $G = 0$  will be made, thus reducing to

$$\alpha'_a = \frac{R_{\Omega}}{2Z_0}$$

This assumes that the total voltage is induced at one end of the antenna and the signal attenuated as it propagates down the line. However, in the actual case, the entire cable length receives power and the power received at a distance  $l-x$  will be attenuated only over the distance  $l-x$  and not over the entire length  $l$ .

A more realistic value for the attenuation coefficient can be derived as

$$\alpha_a = \frac{1}{l} \ln_e \left( \frac{\alpha'_a l}{1 - e^{-\alpha'_a l}} \right)$$

The conservative assumption was made that a constant voltage density exists over the line.

#### Types of Antennas

The remaining intermediate parameters  $R_a$  and  $R_{\Omega}$  and the last final parameter,  $Z_0$ , will be discussed under each individual antenna type of which there are four.

1. Straight-wire antenna
2. Twisted-parallel-wire antenna
3. Single-wire shielded antenna
4. Pin-to-case antenna

### Straight Wire Above a Ground Plane

Johnson shows that the characteristic impedance  $Z_0$  of a single wire above a ground plane is <sup>(4)</sup>

$$Z_0 = 60 \ln_e \left( \frac{2d}{a} \right) \text{ ohms}$$

where  $d$  is the distance above the ground plane and  $a$  is the wire radius.

He also shows that the ohmic resistance for a parallel-wire antenna is <sup>(4)</sup>

$$R_{\Omega} = \frac{5.38 \times 10^{-3}}{a} \sqrt{f} \text{ ohms/inch}$$

where  $f$  = frequency in megahertz.

The single wire antenna will behave as a parallel-wire transmission line with the "image wire" located a distance  $2d$  from the single wire. The ohmic resistance can therefore be given for a single-wire above a ground plane as

$$R_{\Omega} = \frac{5.38 \times 10^{-3} d}{a} \sqrt{f} \text{ ohms/inch.}$$

The radiation resistance as given by Ramo and Whinnery for a short antenna ( $l \ll \lambda$ ) as <sup>(5)</sup>

$$R_a = 20 \pi^2 \left( 2 \frac{l}{\lambda} \right)^2 = 20 \pi^2 L^2.$$

Stratton shows that for long antennas <sup>(6)</sup>

$$R_a = 72.45 + 30 \ln_e \left( 2 \frac{l}{\lambda} \right) = 72.45 + 30 \ln_e L.$$

King has shown that a very short antenna a distance  $d$  above a ground plane, the radiation resistance is <sup>(7)</sup>

$$R_a = (20 \pi^2 L^2) \left( 3.2 \pi^2 \frac{d^2}{\lambda^2} \right) \quad (23)$$

provided that  $d \ll \lambda$  and  $d \ll l$ . He also indicates that a good approximation for longer antennas is

$$R_a = (3.2 \pi^2 \frac{d^2}{\lambda^2}) (72.45 + 30 \ln_e L). \quad (24)$$

since equations (23) and (24) intersect at  $L = 0.52$ , equation (23) should be used when  $L < 0.52$  and equation (24) used when  $L > 0.52$ .

#### Twisted-Parallel-Wire Antenna

The values given previously for directivity do not take into account the wire being twisted. The twisted wire used in the TIII vehicle has a twist period of about 0.75 inch. Since the wave lengths used in the analysis are large compared to 0.75 inch, the received power will be proportional to  $\cos^2 \theta$  where  $\theta$  is some angle characteristic of the direction of the incoming wave and the orientation of the parallel line. Since the line is twisted,  $\theta$  will vary continuously over all angles. The average of  $\cos^2 \theta$  is  $\frac{1}{2}$ . Therefore the directivity of a twisted-parallel wire antenna will be  $\frac{1}{2}$  that of a parallel wire antenna or

$$g = 1.5/2 = 0.75 \text{ if } l/\lambda \leq 0.375$$

$$\text{and } g = 4 \cdot 1/2\lambda = 2 \cdot l/\lambda \text{ if } l/\lambda > 0.375.$$

If there are no impedance mismatches, the line will contain a pure traveling wave, and

$$R_a = R_{at}.$$

If a pure standing wave exists

$$R_a = R_{as}.$$

In most cases however, both standing and traveling waves will exist.

Therefore

$$R_a = f_s R_{as} + f_t R_{at}$$

where  $f_s$  varies from 0 to 1 and  $f_t$  varies from 1 to 0 as the signal goes from a pure traveling wave to a pure standing wave.

It can be shown that

$$R_a = f_s R_{as} + \frac{(2 - f_s)}{2} R_{at}$$

where

$$f_s = f_{s1} + f_{s2}$$

and

$$f_{s1} = \begin{cases} 1 - Z_0/Z_{e1} & \text{if } Z_{e1} \geq Z_0 \\ 1 - Z_{e1}/Z_0 & \text{if } Z_{e1} < Z_0 \end{cases}$$

and

$$f_{s2} = \begin{cases} 1 - Z_0/Z_{e2} & \text{if } Z_{e2} \geq Z_0 \\ 1 - Z_{e2}/Z_0 & \text{if } Z_{e2} < Z_0 \end{cases} .$$

$Z_{e1}$  and  $Z_{e2}$  are the entrance impedances at the two ends of the antenna.

$Z_{e1}$  gives rise to  $f_{s1}$  and  $Z_{e2}$  gives rise to  $f_{s2}$ .

$R_{as}$  will be taken as

$$R_{as} = 20 \pi^2 L^2 \text{ if } L \leq 0.52$$

$$R_{as} = 72.45 + 30 \ln_e L \text{ if } L > 0.52.$$

Hund gives the radiation resistance due to a traveling wave along a parallel line as <sup>(8)</sup>

$$R_{at} = 1579 \left( \frac{S}{\lambda} \right)^2 . \quad S = \text{wire spacing in inches}$$

The assumption is made that  $R_{at}$  for a twisted parallel line is equal to that of a parallel line.  $Z_0$  is measured experimentally and is the same impedance that is used when the cable is treated as a transmission line.

The ohmic resistance is

$$R_{\Omega} = \frac{5.38 \times 10^{-3}}{a} \sqrt{f} \quad \frac{\text{ohms}}{\text{inch}}$$

### Single-Wire Shielded Antenna

$Z_0$  is determined experimentally.

$R_a$  is the same as the straight-wire antenna but without the ground plane. Therefore

$$R_a = 20 \pi^2 L^2 \text{ if } L \leq 0.52$$

$$R_a = 72.45 + 30 \ln_e L \text{ if } L > 0.52$$

Johnson shows that the ohmic resistance is given by <sup>(4)</sup>

$$R_{\Omega} = 2.69 \times 10^{-3} \sqrt{f} \left( \frac{1}{a} + \frac{1}{b} \right)$$

where  $a$  = radius of inner conductor in inches

$b$  = radius of shield in inches

$f$  = frequency in MHz.

### Pin-to-Case Antennas

The pin-to-case mode considers energy induced between ground and the pins. It is assumed that the shielding which is grounded at both ends acts as a loop antenna. The antenna transfers a certain portion of its received energy to the inner conductor. The amount of energy transfer is dependent on the extinction factor.

The characteristic impedance is assumed to be the same as the straight-wire antenna above ground plane.

$$Z_0 = 60 \ln_e \left( \frac{2d}{b} \right) \text{ ohms}$$

where  $d$  is the distance between the shield and the ground plane and  $b$  is the radius of the shield.

The ohmic resistance is given as

$$R_{\Omega} = \frac{2.69 \times 10^{-3}}{b} \sqrt{f} \frac{\text{ohms}}{\text{inch}}$$

where  $f = \text{MHz}$

$b = \text{shield radius.}$

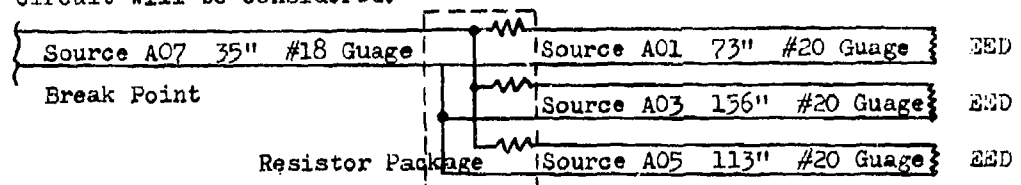
The assumption is made that the loop has the optimum configuration of a circle. For this case, the radiation resistance and directivity are given by <sup>9</sup>

$$R_a = 30 \pi^2 (2L/\lambda)^2 = 296L$$

$$D = 0.68 (L/\lambda) = 0.34L$$

#### EXAMPLE

To demonstrate how the matrix equivalent circuit is set up, the following typical circuit will be considered.



The four voltage sources as identified in the above circuit are as follows:

- Source A01 - 73" #20 gauge wire
- Source A03 - 156" #20 gauge wire
- Source A05 - 113" #20 gauge wire
- Source A07 - 35" #18 gauge wire.

Each source will have two mismatch matrices as shown.



M01 is the mismatch between the characteristic impedance of the circuitry to the left of A01, while M02 is the mismatch between the characteristic impedance of A01 and the circuitry to the right.

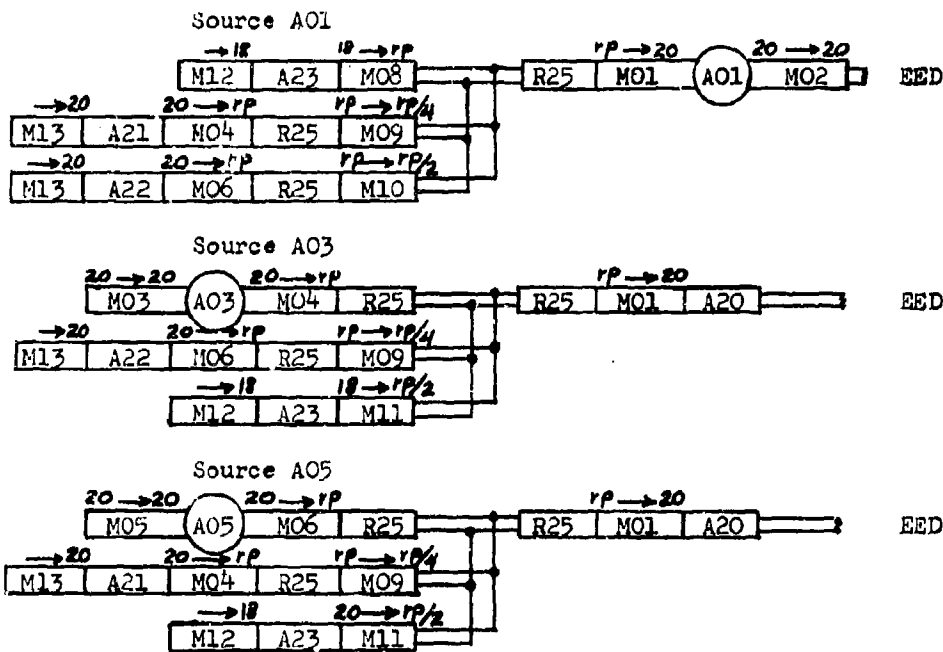


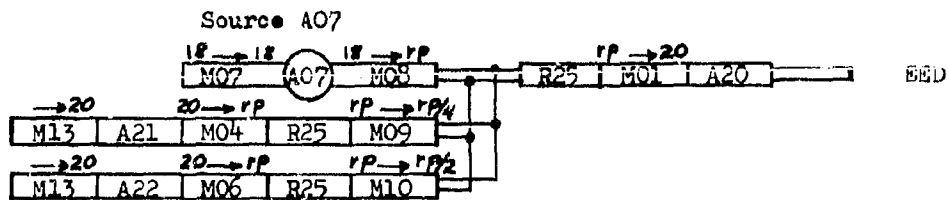
Each voltage source will have a corresponding attenuation matrix as follows:

- A20 = Attenuation for 73" of #20 guage wire
- A21 = Attenuation for 156" of #20 guage wire
- A22 = Attenuation for 113" of #20 guage wire
- A23 = Attenuation for 35" of #18 guage wire.

The resistor package series impedance will be represented by R25. All other matrices in the circuit are mismatch matrices and are used to match different guage wires, the resistor package, and the branch circuits prior to their transformation into the main line feeding the EED.

The matrix equivalent for each voltage source is shown below.





The arrow (  $\longrightarrow$  ) above each mismatch matrix represents the mismatch between the circuit element to the left and the circuit element to the right. For example  $18 \longrightarrow rp$  says the mismatch is between the 18 guage wire and the resistor package.

A computer program has been set up to handle all mathematical operations. Typical instructions to solve for the voltage at the EED from one source are as follows:

For Source A05

- (1) ANT (MO5)
- (2) T70 MUL, MO9, R25, MO4, A21, M13
- (3) T71 SHB, T70
- (4) T72 MUL, T71, M11, A23, M12
- (5) T73 SHB, T72
- (6) T74 MUL, A20, MO1, R25, T73, R25, MO6
- (7) A05 EED (T74) A20

Instruction card (1) identifies which matrix is to the left of the source. Card (2) instructs the computer to multiply matrices  $MO9 \times R25 \times MO4 \times A21 \times M13$  and call the resulting matrix T70. Card (3) instructs the computer to shunt-branch T70 and call it T71. Card (4) instructs the multiplication of  $T71 \times M11 \times A23 \times M12$  calling the resulting matrix T72. Card (5) instructs the computer to shunt-branch T72 and call it T73. Card

(6) instructs the multiplication of  $A_{20} \times M_{01} \times R_{25} \times T_{73} \times R_{25} \times M_{06}$  and call the result  $T_{74}$ . Finally, card (7) identifies the source,  $A_{05}$ , the matrix to the right of the source,  $T_{74}$ , and the matrix next to the EED,  $A_{20}$ .

Similar instruction cards are required for each source. After all instruction cards for all sources are read and the required operations carried out, the source voltages are added and the total power at the EED is calculated.

#### References

- (1) D. E. Roark, Techniques in RF Susceptibility Studies, SSD-CR-66-70, Vol. II of II, Contract AFO4(695)-694, The Martin Company, 1965.
- (2) S. Ramo, J. Whinnery, Fields and Waves in Modern Radio, John Wiley and Sons, 1953, Chapters 10 and 11.
- (3) S. Schelkunoff, H. Friss, Antennas - Theory and Practice, John Wiley and Sons, 1952.
- (4) W. Johnson, Transmission Lines and Networks, McGraw-Hill, 1950.
- (5) Op. Cit., S. Ramo and J. Whinnery, Chapter 12.
- (6) J. A. Stratton, Electromagnetic Theory, McGraw-Hill, 1941.
- (7) R. King, The Theory of Linear Antennas, Harvard University Press, 1956.
- (8) A. Hund, Short-Wave Radiation Phenomena, McGraw-Hill, 1952, p. 524.
- (9) J. Kraus, Antennas, McGraw-Hill, 1950.

## 4-10 EXPERIMENTAL DISTRIBUTION OF BRUCETON TEST STATISTICS

By

Herbert D. Peckham

HOLEX incorporated  
Hollister, California

### ABSTRACT

A set of statistics from sixty-one Bruceton Tests conducted against a particular EED are analyzed. The means of the Bruceton Tests are tested for the expected normal distribution. The standard deviations from the Bruceton Tests are observed to have a positively skewed distribution supporting the generally accepted tendency of the Bruceton Test to underestimate the standard deviation. The data, representing hard experimental results, is given more credulity than data generated on computers which may, or may not, represent a true simulation.

### INTRODUCTION

The current widespread utilization of the Bruceton Test Method in the aerospace industry requires that the closest attention be given to applications, and in particular, misapplications of the method. The high cost of the materiel involved has made it difficult to properly investigate the dangers of the Bruceton Test Method. For this reason, computers have been used to simulate Bruceton testing. Since any simulation is no better than the quality and accuracy of the model utilized in the simulation, and in view of the fact that the precise electro-thermal model

of the electro-explosive device is not well understood, it is very important that a careful examination be conducted of any experimental data which might clarify conclusions reached by computer simulation.

#### BACKGROUND

##### The Bruceton Test

The Bruceton Test Method was designed originally to furnish a relatively simple and precise way of determining the 50% response point of material characterized by a quantal ("go, no-go") response! The method was, is, and probably will be, the most efficient statistical tool to estimate the 50% response point. The problem is that the method has been utilized to measure very high and very low response points. This was not the purpose of the Bruceton Method, and therefore should be the subject of the most strict examination.

As applied, the Bruceton Method is simplicity itself to administer. An increment of the test stimulus is set which separates the predetermined test levels. A part is tested at a given test level. If it responds, the next test is at the next lower test level, if not, at the next higher level. This pattern is maintained throughout the test. As can be seen, the method concentrates the testing about the median response point. There is an important consequence of determining the increment between the test levels in terms of the standard deviation of the material being tested. Improperly chosen, the magnitude of

the test increment can bias the results. The problem is that generally the test increment is selected in ignorance of the standard deviation of the function being determined.

Once the test has been completed, the data is processed to give estimates of the mean and standard deviation of the unknown probability distribution function. Methodology is also available to provide estimates of the variance in the determination of both the mean and standard deviation of the unknown function. This permits estimates of high and low response points to be made at specified confidence levels.

#### Assumption of Normality

If a statistical tool is relatively insensitive to the assumptions implicit in the method it is said to be a "robust" method. The Bruceton Method is critically dependent upon the assumption that the unknown probability distribution being measured is a normal distribution. This is particularly true when high and low response points are being estimated. The Bruceton Method is not, therefore, a "robust" method. When used to determine the mean, the method is, relatively speaking, more "robust." If there is any question to question the normality of the distribution being measured, the Bruceton Method must be used with great care. In addition, as will be shown, even if the underlying assumption of normality is satisfied, the Bruceton Method tends to preclude biased estimates of the standard deviation.

### Computer Simulations of The Bruceton Test

In attempts to learn more of the Bruceton Method computer simulations have been carried out to study the characteristics of the method. Martin and Saunders did a study on the accuracy of small sample Bruceton Tests<sup>2</sup>. Edelman and Prarie did a computer simulation which compared the Bruceton Method to two other methods of sensitivity testing - the One-Shot Method and the Probit Method<sup>3</sup>. Hampton has carried out a computer simulation using Monte Carlo techniques of small sample Bruceton Tests<sup>4</sup>. All these computer simulations have relied upon the computer to replace more costly, and time consuming (and possibly more accurate) tests using live ordnance.

### Predicted Tendencies of The Bruceton Test Method

The computer simulations described above, together with statistical theory can be combined to give some predicted tendencies of the Bruceton Test Method. It will be the main subject of this paper to treat in an experimental fashion the predicted tendencies.

The first trait of the Bruceton Test Method can be predicted from the main body of statistical theory. A fundamental relationship is that the means of samples drawn from an unknown distribution will themselves be normally distributed regardless of the nature of the distribution from which they are drawn. This would require that, if a large number of samples were to be tested by the Bruceton Method, the means as determined by Bruceton Analysis should be normally distributed.



The second characteristic, and the more important as far as the prediction of high and low response points is concerned, is the tendency of the Bruceton Test to underestimate the standard deviation. This bias produces a situation in which the estimates of the standard deviation for a large number of samples will pile up at the low end producing a positively skewed distribution.

#### PRESENT WORK

##### Source of Data

The main body of this paper examines the experimental distribution of a set of statistics gathered from 61 Bruceton Tests conducted against identical bridgewire-prime-body configurations. The statistics of concern are the means and estimates of the standard deviation for the 61 tests. The data was separated and ranked in descending order. The Bruceton Test means are given in Table 1. The Bruceton Test Standard Deviations are given in Table 2.

##### Statistical Examination of Sample Means

A Chi Square "goodness of fit" test was conducted in which a normal distribution was fitted to the experimental data. This test is summarized on Table 3. Column (1) indicates the limits of the zones which comprised the frequency distribution which was used to portray the data. Column (2) is the score that separates the classification zones. The standard deviation of the sample means was 0.0586 amperes, and the mean of the sample means was 0.565 amperes. These figures were used to express the

entries in Column (2) in terms of standard normal scores. These standard scores are listed in Column (3). Column (4) lists the cumulative normal distribution corresponding to the standard scores. Column (5) gives the decimal fraction of the events that would be expected to occur between the standard scores in Column (3). Column (6) is the decimal fraction of the total of 61 events and represents the expected number of occurrences in each zone. Notice that the first 6 entries in Column (6) have been combined to give an expected frequency of 8.01, and the last 2 entries have been combined to give an expected frequency of 7.39. This is because the Chi Squared test requires a minimum expected frequency of 5 in each of the classifications. Column (7) gives the experimental distribution of observed frequencies. Columns (8) and (9) show the calculations necessary to arrive at the Chi Squared statistic for the data. The value for this Chi Squared statistic is 1.429. The final number of data classifications is 6. Two parameters (the mean and standard deviation of the fitted normal distribution) were used in the calculations. Therefore, the number of degrees of freedom is  $6 - 1 - 2 = 3$ . At the .05 level of significance and at 3 degrees of freedom, the critical value of the Chi Squared statistic is 7.185. Since the experimental value of the statistic is less than this, we conclude that the normal distribution is a "good" fit for the experimental data

It is also interesting to measure the skewness of the

distribution. A convenient way to do this is by the Pearson Skewness Coefficient. This is defined as the mean minus the mode, divided by the standard deviation. In the case of the sample means the Pearson Skewness Coefficient is - 0.0256.

#### Statistical Examination of Sample Standard Deviations

The same statistical tests described above were carried out on the sample standard deviations. The results of the Chi Squared test are shown in Table 4. The mean of the sample standard deviations was 0.0363, and the standard deviation was 0.0238. The calculations are carried out in precisely the same way as described above. The result is a Chi Squared statistic of 8.588. In this case the number of degrees of freedom is  $6 - 1 - 2 = 3$ . At the 0.05 level of significance and for 3 degrees of freedom, the critical Chi Squared statistic is 7.815. Since the experimental value of the statistic is greater than the critical value, we must conclude that the normal distribution does not provide a good fit for this data.

In this case, the Pearson Skewness Coefficient is determined to be + 0.737 indicating a highly positively skewed distribution. It should be noted that the distribution of standard deviations is approximately 30 times more skewed than the distribution of means.

#### CONCLUSIONS

The experimental results indicate quite clearly that the distribution of means is normally distributed, and that the distribution of standard deviations is positively skewed. It

is believed that the real significance of these experimental results lies not in their own value but in the confirmation of the computer simulation that has been done. Since it is most likely that the majority of work done in investigating the characteristics of the Bruceton Test Method will be done by computer, it is essential to establish a feeling of confidence in the results. It is hoped that this paper will help in that end.

#### BIBLIOGRAPHY

1. Dixon, W.J. and Mood, A.M., "A Method for Obtaining and Analyzing Sensitivity Data," Journ. Amer. Stat. Assoc. 43 pp. 109-126 (1948).
2. Martin, J.W. and Saunders, J., "Bruceton Tests: Results of a Computer Study on Small Sample Accuracy," International Conference on Sensitivity and Hazards of Explosives," London, 1-3, October 1963.
3. Edelman, D.A., and Prarie, R.R., "A Monte Carlo Evaluation of The Bruceton, Probit, and One-Shot Methods of Sensitivity Testing," Sandia Corporation report SC-RR-66-59, March 1966.
4. Hampton, L.D., "Monte Carlo Investigations of Small Sample Bruceton Tests," NOLTR 66-117.

Rank	$\bar{x}_i$ (amps)	Rank	$\bar{x}_i$ (amps)
1	.668	31	.567
2	.653	32	.565
3	.642	33	.560
4	.638	34	.560
5	.635	35	.555
6	.635	36	.550
7	.625	37	.550
8	.625	38	.550
9	.620	39	.550
10	.620	40	.545
11	.620	41	.545
12	.614	42	.542
13	.610	43	.538
14	.608	44	.535
15	.603	45	.535
16	.600	46	.532
17	.598	47	.530
18	.597	48	.525
19	.595	49	.525
20	.592	50	.525
21	.592	51	.522
22	.592	52	.519
23	.592	53	.515
24	.590	54	.515
25	.586	55	.505
26	.585	56	.500
27	.585	57	.499
28	.580	58	.485
29	.580	59	.472
30	.569	60	.418
		61	.325

Table 1 - Bruceton Test Means

Rank	$s_j$ (amps)	Rank	$s_j$ (amps)
1	.1520	31	.0310
2	.0965	32	.0303
3	.0834	33	.0290
4	.0800	34	.0284
5	.0680	35	.0261
6	.0640	36	.0258
7	.0639	37	.0238
8	.0623	38	.0237
9	.0585	39	.0226
10	.0584	40	.0226
11	.0564	41	.0226
12	.0492	42	.0226
13	.0477	43	.0226
14	.0464	44	.0224
15	.0441	45	.0224
16	.0420	46	.0218
17	.0388	47	.0218
18	.0388	48	.0218
19	.0385	49	.0218
20	.0383	50	.0203
21	.0380	51	.0203
22	.0372	52	.0203
23	.0348	53	.0193
24	.0348	54	.0193
25	.0339	55	.0191
26	.0315	56	.0182
27	.0315	57	.0164
28	.0315	58	.0131
29	.0315	59	.0104
30	.0315	60	.0096
		61	.0024

Table 2 - Bruceton Test Standard Deviations

Limits (amps) (1)	X (2)	Stnd. Normal Scores (3)	Cum. Normal Dist. (4)	Theoret. Freq. (%/100) (5)	$e_i$ (6)	$o_i$ (7)	$(o_i - e_i)^2$ (8)	$\frac{(o_i - e_i)^2}{e_i}$ (9)
0 - .333	.3335	- 3.95	0	0	0	1		
.334 - .366	.3665	- 3.39	.0003	.0003	0	0		
.367 - .399	.3995	- 2.82	.0024	.0021	.13	0	9.060	1.131
.400 - .433	.4335	- 2.24	.0125	.0101	.62	1		
.434 - .466	.4665	- 1.68	.0590	.0465	2.84	0		
.467 - .499	.4995	- 1.12	.1314	.0724	4.42	3		
.500 - .533	.5335	- .54	.2946	.1632	9.96	11	1.082	.109
.534 - .566	.5665	+ .026	.5104	.2158	13.16	14	.706	.054
.567 - .599	.5995	+ .59	.7224	.2120	12.93	14	1.145	.089
.600 - .633	.6335	+ 1.17	.8790	.1566	9.55	10	.203	.021
.634 - .667	.6675	+ 1.75	.9599	.0809	4.93	6		
.667 - .00				.0404	2.46	1	.152	.025
Totals				1.0000	61.00	61		$\chi^2 = 1.429$

Table 3 - Chi Squared "Goodness of Fit" Test for Bruceton Test Means

Limits (amps)	X	Std. Normal Scores	Cum. Normal Dist.	Theoret. Freq. (%/100)	$e_j$	$o_j$	$(o_j - e_j)^2$	$\frac{(o_j - e_j)^2}{e_j}$
(1)	(2)	(3)	(4)	(5)	(6)	(7)	(8)	(9)
0 - .0125	.01255	- 1.00	.1587	.1587	9.68	3	44.622	4.610
.0126 - .0250	.02505	- .47	.3192	.1605	9.79	22	1.491	.152
.0251 - .0375	.03755	+ .052	.5207	.2015	12.29	15	7.344	.598
.0376 - .0500	.05005	+ .58	.7190	.1983	12.10	10	4.410	.354
.0501 - .0625	.06255	+ 1.10	.8643	.1453	8.86	4	23.620	2.656
.0626 - .0750	.07505	+ 1.63	.9484	.0841	5.13	3		
.0751 - .0875	.08755	+ 2.15	.9842	.0358	2.18	2		
.0876 - .1000	.10005	+ 2.67	.9962	.0120	.73	1		
.1001 - .1125	.11255	+ 3.20	.9993	.0031	.19	0		
.1126 - .1250	.12505	+ 3.73	1.0000	.0007	.04	0	1.638	.198
.1251 - .1375	.13755	+ 4.25	1.0000	.0000	.01	0		
.1376 - .1500	.15005	+ 4.78	1.0000	.0000	.00	0		
.1501 - .00				.0000	.00	1		
Totals				1.0000	61.00	61		$\chi^2 = 8.588$

Table 4 - Chi Squared "Goodness" of Fit" Test for Brucceton Test Standard Deviations



ATTENDANCE  
5th EED SYMPOSIUM

Douglas L. Aber	Raymond Eng. Lab.	David A. Colpitts	NOTS
G. Adams	G. T. Schjeldahl	Allen L. Conner	Univ. of Calif.
Richard Adams	Sandia Corp.	Neil Coppola	Quantic Ind.
Robert E. Ainslie	Nav. Air Devel. Center	Charles M. Cormack, Jr.	Nav. Air Sys. Cmd.
Robert C. Allen	McCormick Selph	S. A. Corren	Markite Eng.
R. G. Amicone	Franklin Institute	Loyd Corwin	N. American Aviation
J. E. Ardans	-	W. I. Cote	Hercules
James L. Austing	IIT Res. Inst.	R. B. Cowdell	Genisco Tech.
James N. Ayres	NOL, White Oak	R. J. Crosby	Atlas Chemical
William S. Balderston	Harry Diamond Labs.	Geo. W. Coxeter	Raymond Eng. Lab.
Donald R. E. Barnaby	EIMAC-Div. of Varian	D. E. Davenport	Link Ord. Gen Prec.
Mary Barr	Franklin Institute	C. T. Davey	Franklin Institute
Joseph A. Barrett	Atlas Chemical	Thomas Dean	Franklin Institute
Howard E. Baxter	NASA/JFK	Dr. Peter J. Deas	British Embassy Drds.
Baxter L. Beaton	NASA/LEWIS	E. E. DeMaris	GE Co., RSD
Bill Bell	Space Ord. Systems	Daniel Dembrow	NASA/Goddard
L. J. Bement	NASA/LRC	Sid Demskey	GE Co., RSD
Anthony G. Benedict	Jet. Prop. Lab.	Durwood A. Dereng	NASA/Wallops
Roger Benning	Nav. Civ. Engr. Lab.	R. Deusinger	Picatinny Arsenal
Edward C. Bern	Fairfield Scientific	C. F. Dieter	Nav. Ord. Syst. Cnd.
Robert J. Bishop	Conax Corp.	Louis Dignazio	GE Co., STC
Leo Bloomfield	Atlantic Res.	R. E. Donnard	Frankford Arsenal
Dr. N. J. Bowman	GE Co., RSD	David Dreitzler	Redstone Arsenal
W. M. Boydston	Pace Corp.	James B. Drew	Franklin Institute
Frank H. Bratton	Ensign-Bickford	V. W. Drexelius	McDonnell Douglas
B. Arthur Breslow	NOTS	Cyrus G. Dunkle	-
Henry Brizzalora	Atlas Chemical	W. J. Dunning	Franklin Institute
Merle E. Brown	Magnavox	Daniel E. Elliott	Ensign-Bickford
A. S. Browne	NASA/WTR/JFK	William Ellis	Pyronetics
Paul J. Bryan	Dupont	Eugene E. Elzafon	Atlantic Res.
J. E. Bubser	Atlas Chemical	Melvin Eneman	Bulova Watch
F. B. Burkdoll	Explosive Technology	John H. Evans, Jr.	Atlas Chemical
Joe H. Burson	NASA/MSFC	Mario J. Falbo	NASA/MSC
Dalton E. Burkhalter	Hercules	Norman P. Faunce	Atlas Chemical
Arthur Burns	Mallory Battery	J. R. Feldmeier	Franklin Institute
Frank J. Byrne	Link Ord. Gen. Prec.	K. S. Fertner	Franklin Institute
A. W. Caldwell	Franklin Institute	Werner Field	Picatinny Arsenal
C. E. Campbell	McCormick Selph	Howard C. Filbert *	Miller Res.
C. Patrick Cannong	Atlantic Res.	D. F. Finocchio, Jr.	Quantic Ind.
L. J. Caparoni	Atlas Chemical	Bert Fleming	Avco-Lycoming
Bert Carlson	Lockheed MSC	Bobby J. Flowers	NASA/Wallops
B. W. Carter	Kentron-Hawaii, Ltd.	James A. Ford	Honeywell
Sam Carter	Space Ord. Sys.	Edward A. Fox, Jr.	Atlas Chemical
E. B. Chambers	Northrop/Nortronics	E. W. Frank	Aerospace Corp.
A. W. Cipkins	Franklin Institute	W. B. Freeman	Martin-Marietta
Gunther Cohn	Franklin Institute	M. H. Friedman	Johns Hopkins
Toney Coffey	Nav. Ord. Systems Cmd.	Fred A. Fritz	Hercules
James R. Coge	Aerospace Corp.	John W. Fronabarger	Unidynamics
Dr. Myron A. Coler	Markite Eng.		

\*Registered

Best Available Copy

B. A. Gay  
M. C. Giovanni  
Ken Girkey  
Charles Goddard  
Jim Gohl  
Victor W. Goldie  
V. J. Gordon  
Thomas J. Graves  
D. N. Griffin  
Arthur E. Haefner  
Sigmund Halpern  
E. E. Hannum  
Ralph W. Hanson  
E. W. Hargens \*  
H. H. Harris, Jr.  
Robert G. Harwood  
E. W. Hayford  
S. E. Hedden  
Art Heinz  
Thomas Hennessy  
M. C. Henry  
C. Herschel  
William Higgins  
James T. Hillman  
R. R. Hindle  
John R. Hinves  
Thomas Hoffman  
W. B. Hopson  
Leonard H. Horwitz  
Wm. F. Huseonica  
Charles G. Irish, Jr.  
Charles P. Janis  
Stan Jepson  
L. M. Jercinovic  
E. S. Jeris  
Wm. H. Johnson  
Jerry O. Jones  
Ken Jones  
Robert B. Jones  
Geo. Kaeding  
Ahmed D. Kafadar \*  
Dennis S. Kaisand  
R. J. Kandravich  
Paul Karnow  
Kenneth Kautz  
John H. Kawka  
M. G. Kelly  
J. E. Kilmer  
Jon Klima  
E. F. Knippenberg  
Bohdan Korduba  
Charles LaCarrubba  
Elmer K. Landis

Atlas Chemical  
Avco Missile Systems  
Pan American  
Army Natick Lab.  
Magnavox  
GE Co., RSD  
Franklin Institute  
NASA, MSC  
Quantic Ind.  
Conax Corp.  
RCA, Princeton  
Franklin Institute  
Technical Ordn.  
Franklin Institute  
G. T. Schjeldahl  
GE Co., RSD  
Picatinny Arsenal  
Naval Weapons Lab.  
Olin Mathieson  
Frankford Arsenal  
Army Natick Lab.  
Franklin Institute  
Unidynamics  
Sandia Corp.  
NASA/Wallops  
Nav. Underwater Res.  
EG&G, Inc.  
Jet. Res. Center  
Aerospace Corp.  
NASA/JFK  
Olin-Mathieson  
Aerospace Corp.  
EIMAC. Div. of Varian  
Sandia Corp.  
NASA/LRC  
Magnavox  
NOL, Corona  
Hi-Shear  
Monsanto Res. Lab.  
TRW Systems  
Ord. Eng. Assoc.  
Chamberlain Manuf.  
Atlas Chemical  
Nav. Air Devel. Center  
RCA, Van Nuys  
Norton A.F.B.  
Franklin Institute  
NOL, White Oak  
Martin Marietta Corp.  
GE Co., RSD  
Frankford Arsenal  
Maxson-Macon  
Limited War Lab.

T. E. Landry  
Paul N. Laufman  
Ray Laughlin  
John T. Lee  
Howard Leopold  
Don Lewis  
Herbert N. Lewis  
Jack Lightfoot  
Milton Lipnick  
J. Louie  
L. S. Love  
R. D. Lowe \*  
W. G. MacDonald  
Ernest A. Magyar  
Len Mahler  
Irving Margulies  
David J. Marshall  
Don Masyada  
Edward W. Matthews  
Robert C. May  
Oliver W. Mayes  
Andrea McCabe  
R. L. McCally  
Robert McGirr  
Clinton D. McLaughlin  
Quinton A. McLellan  
Elbert Medcalf \*  
Vincent J. Menichelli  
Roger N. Messier  
Bruce C. Meyer  
George H. Meyer  
Wilbert H. Meyers  
Glen J. Miller  
P. F. Mohrbach  
Louis J. Montesi  
Nowlin A.N.K. Morse  
Sidney A. Moses  
Donald A. Moyant  
D. J. Mullen  
Arthur J. Murphy  
E. Nelson  
Gary R. Nelson  
A. L. Newcomb  
C. R. Newman  
Gerald L. O'Barr  
E. A. O'Brien  
Cecil O'Dear  
J. P. O'Donnell

Avco. Corp.  
Lockheed Prop. Co.  
United Technology  
Atlas Chemical  
NOL, White Oak  
Space Ordn. Systems  
Ballistic Res. Lab.  
Pace Corp.  
Harry Diamond Labs.  
Franklin Institute  
Pace Corp.  
GE Co., STC  
Canadian Forces H.Q.  
Genisco Tech.  
Aerospace Corp.  
Bulova Watch Co.  
Magnavox  
Micro Precision  
NASA/Wallops  
Remington Arms  
McDonnell Douglas  
Franklin Institute  
Johns Hopkins  
Atlas Chemical  
Nav. Torpedo Station  
Harry Diamond Labs.  
Magnavox  
NOL, White Oak  
NASA/MSC  
GE Co., Pleasanton  
Boeing, Kent SC  
Los Alamos Scientific  
Gen. Lab Asscc.  
Franklin Institute  
NOL, White Oak  
Nav. Ammo Depot, Oahu Hawaii  
McDonnell Douglas  
Atlas Chemical  
Franklin Institute  
Jet Prop. Lab.  
Franklin Institute  
Chamberlain Manuf.  
NASA/LRC  
Quantic Ind.  
General Dynamics/Convair  
Unidynamics  
NASA/Lewis  
Hughes Aircraft

Walter Orsiak, Jr.	Nav. Weap. Lab.	William M. Smith	Ensign-Bickford
Rudy L. Ortega	General Dynamics/Convair	Thomas J. Snier *	Jet Prop. Lab.
J. M. Palovchik	Olin Mathieson	Robert H. Spatz	Nav. Ord. Station
Robert Parker	Lawrence Rad. Lab.	J. R. Stahmann	Lightning & Transients Res
John L. Parks, Jr.	NASA/Wallops	William E. Stark	Atlas Chemical
J. Pasamanick	Martin-Marietta	Donald G. Starr	Hi-Shear Corp.
Nancy Pearson *	Franklin Institute	Emil Steinberg	TRW Systems
Herbert D. Peckham	Holox, Inc.	Harry Stern	Hercules
Wm. Perkins	Frankford Arsenal	Franklyn E. Stevens, Jr.	Pyrofuze Corp.
Seymour Perlman	NASA/JFK	Philip M. Stevens	Hercules
Roland L. Peterson	R. Stresau Lab.	Fred Stolte	McCormick Selph
John T. Petrick	Nav. Weap. Lab.	Howard W. Stone	Raymond Eng.
A. E. Pierard	LTV Aerospace Corp.	Richard H. Stresau	R. Stresau Lab.
L. D. Pitts	General Precision	Dr. Zoltan G. Sztankay	Harry Diamond Labs.
Zane Porter	UMC Ind.	Louis N. Tallerico	Sandia Corp.
Robert Price	Nav. Weap. Lab.	Robert Tarpley	McDonnell Douglas
Harold H. Radke	Aerospace Corp.	Boyd Taylor	Ballistic Res. Lab.
R. R. Raksnis	Franklin Institute	Leonard W. Thomas	ECAC
Herbert P. Redman	AVCO Corp.	W. R. Thomas	Hercules
J. M. Reuter	Gen. Lab. Assoc.	R. H. Thompson	Franklin Institute
Richard D. Roach	Jet. Res. Center	Eddie A. Timmons, Jr.	NASA/JFK
Robert L. Robinson	NASA/MSC	John R. Tomlinson	Ballistic Res. Lab.
L. A. Rosenthal	NOL, White Oak	H. T. Tucker	Franklin Institute
Klaus G. Rucker	DuPont	T. J. Tucker	Sandia Corp.
Robert D. Rung	Westinghouse Electric	Earl VanLandingham	NASA/LRC
Fred Sawyer	DuPont	Dave Vaughn	GE Co., MSD
John J. Scanlon	Remington Arms	Harry Vollmer	N. American Aviation
Herbert L. Schaaf	DuPont	F. S. VonderSmith	Navy Dept. Special Proj.
Armond W. Schellman	Fairfield Scientific	Scott Wagner	NASA/LRC
M. L. Schimmel	McDonnell Douglas	Wallace L. Walker	Nav. Ammo. Depot, Crane
Allan Schlack	Frankford Arsenal	S. R. Warren	Quantic Ind.
Dr. Albert E. Schmidlin	General Precision	John D. Warrick	Atlas Chemical
F. B. Schoenberger	NASA/JFK	D. Waxler	Picatinny Arsenal
F. W. Schor	ITT Cannon Electric	DeRoo Weber	Atlantic Res. Corp.
Donald S. Schover	General American Res. Div.	John P. Weber	Sandia Corp.
Christian F. Schroeder, Jr.	Sandia Corp.	H. S. Weintraub *	Marquardt
Sidney B. Schulman	Bulova Watch	W. S. Weiss	Franklin Institute
Calvin L. Scott	NOL, White Oak	B. E. Welstead	McDonnell-Douglas
J. Holland Scott, Jr.	NASA/Wallops	A. E. White	Frankford Arsenal
Eugene M. Serra	Picatinny Arsenal	M. J. White, Jr.	Atlas Chemical
Alfred D. Shea	EG&G Inc.	C. J. Whiting	Franklin Institute
J. W. Sheerin	Space Ordn. Systems	R. A. Whiting	Honeywell
Joseph E. Sidoti	Micro-Precision	Paul P. Wiggins	Nav. Weap. Lab.
Joseph W. Silva	Olin Mathieson	Fred S. Willis	Nav. Weap. Lab.
Bernard Silver	Atlantic Res.	Norman Wilson	Bell Tel. Labs.
David Simonds	Sprague Electric	P. P. Woerner	Ordn. Eng. Ass.
Arthur Singleton	Hi-Shear Corp.	R. F. Wood	Franklin Institute
Robert T. Skelton	NOL, White Oak	Virgil Wood	Bell Tel. Lab.
Orval N. Skousen	Unidynamics	William A. Wood	Philco-Ford
M. R. Smith	Franklin Institute	David E. Wright	TRW Systems
O. Curt Smith	Atlantic Res.	Don N. Yates, Jr.	Holox, Inc.
Ralph Smith	Boeing Co.	Thomas P. Young	General Dynamics/Convair
Robert D. Smith *	Unidynamics	Stephen J. Zardas	Ballistic Res. Lab.
		M. B. Zisfein	Franklin Institute